ADVANCES IN Inorganic Chemistry
44

Edited by
A. G. SYKES

Academic Press

Advances in

INORGANIC CHEMISTRY

Volume 44

Advances in
INORGANIC CHEMISTRY

EDITED BY

A. G. Sykes

Department of Chemistry
The University of Newcastle
Newcastle upon Tyne
United Kingdom

VOLUME 44

ACADEMIC PRESS

San Diego London Boston
New York Sydney Tokyo Toronto

This book is printed on acid-free paper. ♾

Academic Press, Inc.
525 B Street, Suite 1900, San Diego, California 92101-4495, USA
http://www.apnet.com

Academic Press Limited
24-28 Oval Road, London NW1 7DX, UK
http://www.hbuk.co.uk/ap/

International Standard Serial Number: 0898-8838

International Standard Book Number: 0-12-023644-3

PRINTED IN THE UNITED STATES OF AMERICA
96 97 98 99 00 01 BC 9 8 7 6 5 4 3 2 1

CONTENTS

Arsenic and Marine Organisms

KEVIN A. FRANCESCONI AND JOHN S. EDMONDS

The Biochemical Action of Arsonic Acids Especially as Phosphate Analogues

HENRY B. F. DIXON

Intrinsic Properties of Zinc(II) Ion Pertinent to Zinc Enzymes

EIICHI KIMURA AND TOHRU KOIKE

Activation of Dioxygen by Cobalt Group Metal Complexes

CLAUDIO BIANCHINI AND ROBERT W. ZOELLNER

Recent Developments in Chromium Chemistry

DONALD A. HOUSE

This Page Intentionally Left Blank

ADVANCES IN INORGANIC CHEMISTRY, VOL. 44

ORGANOMETALLIC COMPLEXES OF FULLERENES

ADAM H. H. STEPHENS and MALCOLM L. H. GREEN

Inorganic Chemistry Laboratory, University of Oxford, Oxford OX1 3QR, United Kingdom

I. Introduction

A. Aim and Scope

The solid-state and organic chemistries of fullerenes are currently active areas of research with possible applications, for instance, in the field of superconductivity (*1*). As illustrated in Fig. 1, more than 3000 papers now have appeared in refereed journals (*2*). Several excellent reviews summarizing physical (*3*), solid-state (*4*), and organic chemis-

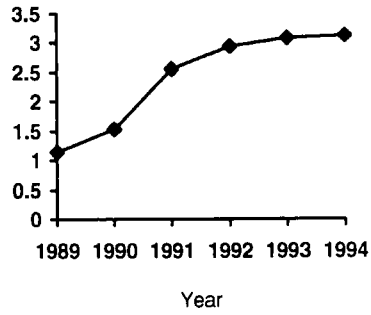

FIG. 1. Log_{10} of the number of C_{60}-related papers published 1989–1994. {As determined by an ACS Chemical Abstracts search on footballen (C_{60}), registry number [99 685-96-8].}

try (*5*) have been published. In contrast, organometallic chemistry remains relatively unexplored (*6, 7*).

This review describes the preparation, characterization, and properties of all nonpolymeric complexes that contain a metal σ- or π-bound to a fullerene. In addition, for the sake of completeness, a number of adducts where the metal is one bond removed from the fullerene also are included. The article does not cover the essentially ionic fullerides M_mC_n (*4*) or the endohedral metallofullerenes M_mC_n (*8*), which have been reviewed previously. The extended fullerenes, or so-called carbon nanotubes, which have hollow centers and can be filled with metal salts, also are not discussed. The majority of complexes involve π-bonds and, apart from alkyl lithium fullerides, the potentially useful synthetic area of σ complexes has not been explored. Table I shows the occurrence of metal-bound adducts across the periodic table.

B. Relevant Physical Properties of Fullerenes

All fullerenes (C_n) are composed of sp^2 hybridized carbon atoms forming a 3-D network of fused $(n - 20)/2$ six-membered and 12 five-membered rings. As enshrined in the Isolated Pentagon Rule (IPR), so far, none of the structures isolated have two pentagons fused together. The curvature of the cage results in some strain, and the three angles around a carbon atom sum to 348° instead of the ideal value of 360° for C_{60}. The [6,6] fusions have most double-bond character and are invariably where complexation occurs. For C_{60} there are 30 such equivalent double bonds. Although all fullerenes comprise alternating single and double CC bonds, there is little π-electron delocalization between the latter. As a result, fullerenes are more reactive than might be expected and behave like giant closed-cage alkenes rather than super arenes.

TABLE I

OCCURRENCE OF FULLY CHARACTERIZED METAL-BOUND FULLERENE COMPLEXES

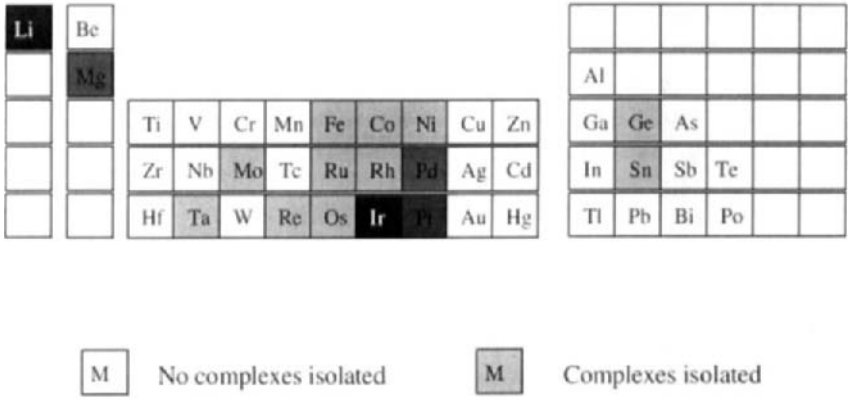

The MO scheme for C_{60}, illustrated in Fig. 2, consists of a fivefold degenerate strongly bonding HOMO (H_u) and an essentially nonbonding LUMO (T_{1u}). The low-lying nature of the triply degenerate LUMO means that it is very easy to populate. In both solution and the solid state, it has been possible to prepare the anions C_{60}^{n-} (n = 1–6) (*4, 9*). C_{60} has a large electron affinity (E_A) ≈ 2.65 eV, comparable with other electron-withdrawing alkenes such as TCNE (E_A = 2.88

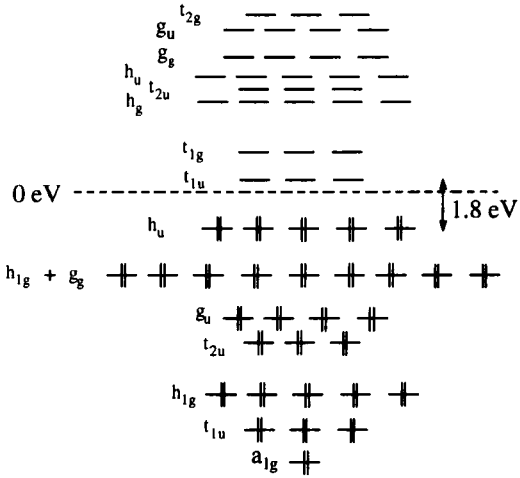

FIG. 2. The partial MO diagram of C_{60}.

eV), and this strongly influences its chemical behavior. Thus, not only does C_{60} react readily with nucleophiles and radicals, but it is also a relatively strong oxidizing agent and has been termed a radical sponge. For the anions in the solid state there is sufficient overlap between adjacent MOs that a band structure can develop, with a band gap estimated to be ≈1.7 eV for an fcc lattice. Its partial occupancy can result in interesting electrical and magnetic properties such as superconductivity.

The low-lying nature of the HOMO of C_{60} (1st ionization potential = 7.6 eV) means that its reducing behavior is very limited. However, electrochemical studies have shown that both C_{60} and C_{70} can be reversibly oxidized to the monocations, at ≈+1.26 V vs Fc/Fc^+ (*10*).

The small HOMO–LUMO band gap and presence of other close-in-energy MOs results in fullerenes being easily polarized. They all give very intense Raman scattering lines and have relatively large χ values useful for NLO applications (*11*). Indeed, C_{60} is one of the best materials known to date for optical limiting.

The MO scheme for the higher fullerenes is similar; for example, C_{70} has a triply degenerate essentially nonbonding LUMO. Anions up to C_{70}^{6-} have been made in both solution and the solid state, although the latter do not show superconducting properties.

Table II lists some of the physical properties of C_{60} and C_{70}.

TABLE II

SUMMARY OF PHYSICAL PROPERTIES OF C_{60} AND C_{70}

Property	C_{60}	C_{70}
Color	Films are mustard. Bulk solid is brown. Solutions are generally purple.	Films and bulk solid are brown. Solutions are deep red.
Density	1.76 g cm^{-3}	1.69 g cm^{-3}
First EA	2.65 eV	≈2.69 eV
First IP	7.54 ± 0.04 eV	≈7.6 ± 0.2 eV
Sublimation Point	≈600°C	≈650°C
ΔH_f°	2327 ± 17 kJ mol^{-1}	2555 ± 12 kJ mol^{-1}
Dimensions	Diameter 7.1 Å. 1.45 Å (C—C). 1.39 Å (C=C).	Diameter 7.8 by 6.9 Å. 1.46 Å (C—C). 1.37 Å (C=C).
Solubility	Soluble in CS_2, aromatics, and low-MW paraffins. Insoluble in ethers, H_2O, and NH_3.	Similar to but often slightly higher than that of C_{60}.

C. Chemical Properties of Fullerenes

The chemistry of all fullerenes is dominated by their ability to react as poorly conjugated and electron-deficient 2π alkenes; they show very few properties typical of dienes or arenes (*5*). In addition, because of the high cage stability, they never undergo substitutions. C_{60} shows behavior similar to that of a monosubstituted alkene such as vinyl chloride or acrylate. All fullerenes readily add to electron-rich species such as nucleophiles, bases, radicals, or reducing agents. They are, for example, perfect dienophiles for Dieles–Alder reactions. The types of reactions undergone by fullerenes are illustrated in Scheme 1.

It is a considerable challenge to isolate a pure adduct. One of the unique features of fullerene chemistry is the large number of products that sometimes result from addition of even one mole eqivalent of reagent. Owing to its relatively high abundance, most fully characterized complexes are for C_{60}, but the behavior of higher fullerenes is broadly similar. The availability of only small amounts of higher fullerenes, coupled with the inequivalency of some of the double bonds, introduces additional complications.

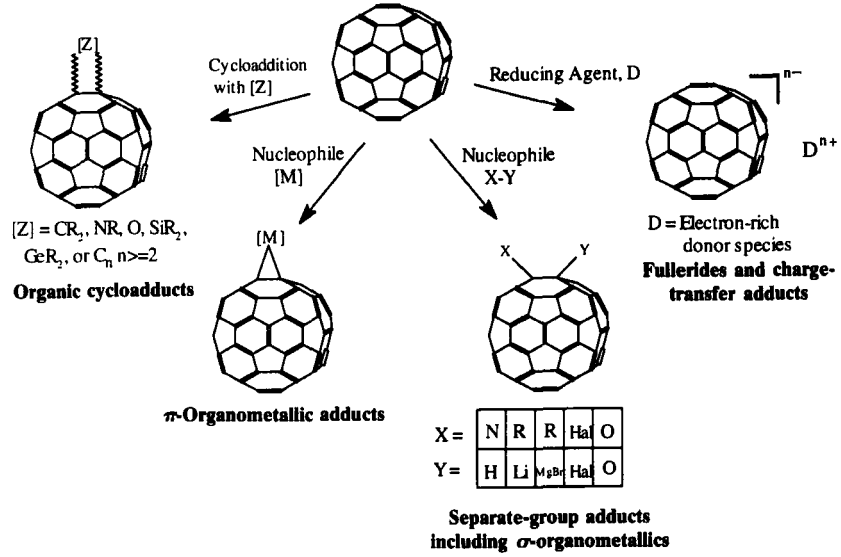

SCHEME 1. Schematic illustration of the general types of reactions undergone by C_{60} (and higher fullerenes).

D. Classes of Organometallic Fullerene Adducts

We now present an exhaustive survey of all the fully characterized metal π or σ complexes reported to date. The survey also includes adducts where the metal is one bond removed from the fullerene, such as $C_{60}O_2OsO_2(4\text{-}Bu^tC_5H_4N)_2$ and $C_{60}S_2Fe_2(CO)_6$. Adducts in which the metal is bound at a more distant site on the organic side chain are not discussed.

In contrast to the great variety of known organic adducts, there is a relative paucity of metal-containing fullerene complexes. Tables III and IV list (in yearly order of appearance in the literature) all the fully characterized π (*6, 7*) and many of the known σ complexes.

For some of the complexes listed, analogous adducts are also quoted in the paper, but the spectroscopic evidence for them is much less. For instance, in addition to the listed complexes $[Mo(\eta\text{-}C_5H_4Bu^n)_2(\eta^2\text{-}C_{60})]$, $[Os_3(CO)_{11}(\eta^2\text{-}C_{60})]$, and $[Pt(P(OPh)_3)_2(\eta^2\text{-}C_{60})]$, the compounds $[Mo(\eta\text{-}C_5H_5)_2(\eta^2\text{-}C_{60})]$ (*22*); $[Os_3(CO)_{10}(L)(\eta^2\text{-}C_{60})]$ (L = MeCN or PPh_3) and $[Os_3(CO)_9(PPh_3)_2(\eta^2\text{-}C_{60})]$ (*34*); and $[C_{60}\{M(P(OR)_3)_2\}_n]$ (M = Pt, Pd or Ni; R = Ph, Bu, or Et; n = 1 or 2) (*37*) also have all been prepared and partly characterized. The reaction of C_{60} with $Pd_2(dba)_3$ or $Pt(dba)_2$ has been reported to give brown amorphous solids $C_{60}M_n$ (M = Pd, n = 1–3; M = Pt, n = 1–2) (*25, 31, 40*), in which the value of n was found to vary depending on temperature and ratio of reactants. Although no proof of the structure was presented, it was assumed to consist of a 3-D C_{60}–M polymer. Reaction of C_{60} anions with $FeCl_2$ produced an amorphous solid that is claimed to be $C_{60}Fe$ (*41*).

The gas-phase reaction of C_{60} with various metal ions has been monitored by mass spectrometry and reported to give MC_{60}^+ [M = V, VO, Fe, Co, Ni, Cu, Rh, La, Ni(C_{60}) and $Fe(CO)_4$] (*42, 43, 44, 45*). The presence of a peak corresponding to $[Ru(C_5Me_5)(C_{60})]^+$ in the positive-ion FAB mass spectrum of $[\{Ru_2(\mu\text{-}Cl)(\mu\text{-}X)(\eta\text{-}C_5Me_5)_2\}(\eta^2\text{-}, \eta^{2'}\text{-}C_{60})]$ (X = Cl, H) was taken as evidence for the formation of an η^6-C_{60} bond in the gaseous phase (*35*).

As for the π complexes, there are additional σ adducts that are only partially characterized. The multiple addition analogues $C_{60}\{S_2Fe_2(CO)_6\}_n$ (n = 2–3) (*53*) are known, and Wudl prepared $C_{60}(H)(Li)$ by reaction of C_{60} with $LiBHEt_3$ (*56*). An organometallic radical, $C_{60}Ag^{\cdot}$, was prepared and analyzed using matrix isolation and ESR techniques (*57*).

Although fulleride lithium and Grignard adducts have often been used as synthetic intermediates, only $C_{60}(Bu^t)(Li)$ has been isolated pure and fully characterized. Many alkyl lithium fullerides, such as

TABLE III

FULLY CHARACTERIZED π-BONDED METAL–FULLERENE COMPLEXES[a]

Compound	X-ray structure	^{13}C NMR data	References
$[Pt(PPh_3)_2(\eta^2\text{-}C_{60})]$[b]	√		*12*
$[\{Ru(\eta\text{-}C_5Me_5)(CH_3CN)_2\}_3(C_{60})]^{3+}$ $(O_3SCF_3^-)_3$			*12*
$[Ir(CO)(PPh_3)_2(\eta^2\text{-}C_{60})Cl]$	√		*13*
$[Ir(CO)(PPh_3)_2(\eta^2\text{-}C_{70})Cl]$	√		*14*
$[Ir(\eta^5\text{-}C_9H_7)(CO)(\eta^2\text{-}C_{60})]$			*15*
$[C_{60}\{M(PEt_3)_2\}_6]$ (M = Ni, Pd, Pt)	√	√	*16*
$[M(PEt_3)_2(\eta^2\text{-}C_{60})]$ (M = Ni, Pd, Pt)			*17*
$[\{Ir(CO)(PMe_2Ph)_2Cl\}_2(\eta^2,\eta^{2'}\text{-}C_{70})]$	√		*18*
$[Ir(CO)(bobPPh_2)_2(\eta^2\text{-}C_{60})Cl]$[c]	√		*19*
$[\{Ir(CO)(PMe_2Ph)_2Cl\}_2(\eta^2,\eta^{2'}\text{-}C_{60})]$	√		*20*
$[\{Ir_2(\mu\text{-}Cl)_2(1,5\text{-}C_8H_{12})_2\}_2(\eta^2\text{-},\eta^{2'}\text{-}C_{60})]$	√		*21*
$[Fe(CO)_4(\eta^2\text{-}C_{60})]$		√	*22*
$[Mo(\eta\text{-}C_5H_4Bu^n)_2(\eta^2\text{-}C_{60})]$[b]		√	*22*
$[Ta(\eta\text{-}C_5H_5)_2(\eta^2\text{-}C_{60})H]$			*22*
$[Pd(PPh_3)_2(\eta^2\text{-}C_{60})]$	√		*23*
$[Rh(CO)(PPh_3)_2(\eta^2\text{-}C_{60})H]$	√		*22, 24*
$[Pd(PR_3)_2(\eta^2\text{-}C_{60})]$[d]		√	*25, 17*
$[Ru(CO)_4(\eta^2\text{-}C_{60})]$		√	*26, 27*
$[Ir(CO)(PPh_3)_2(\eta^2\text{-}C_{84})Cl]$	√		*28*
$[Ir(CO)(PPh_3)_2(\eta^2\text{-}C_{60}O)Cl]$	√		*29*
$[Rh(acac)(3,5\text{-}Me_2C_5H_3N)_2(\eta^2\text{-}C_{60})]$[b]	√		*30*
$[Pt(PR_3)_2(\eta^2\text{-}C_{60})]$ (R = Ph, Et, OMe)		√	*31*
$[Ir(CO)(PPh_3)_2(\eta^2\text{-}C_{60})H]$			*32*
$[\{Ir(CO)(PR_3)_2Cl\}_2(\eta^2\text{-},\eta^{2'}\text{-}C_{60})]$ (R = Me, Et)	√		*33*
$[Os_3(CO)_{11}(\eta^2\text{-}C_{60})]$[b]		√	*34*
$[\{Ru_2(\mu\text{-}Cl)(\mu\text{-}X)(\eta\text{-}C_5Me_5)_2\}(\eta^2\text{-},\eta^{2'}\text{-}C_{60})]$ (X = Cl, H)	√		*35*
$[Ir(CO)(PPh_3)_2(\eta^2\text{-}C_{60}O_2)Cl]$	√		*36*
$[Pt(P(OPh)_3)_2(\eta^2\text{-}C_{60})]$[b]		√	*37*
$[C_{70}\{Pt(PPh_3)_2\}_4]$[b]	√		*38*
$[Ir(CO)(AsPh_3)_2(\eta^2\text{-}C_{60}O)Cl]$	√		*39*

[a] For some complexes, there are no ^{13}C NMR or crystallographic structural data, but there are sufficient other spectroscopic details, such as elemental analysis, ^{31}P or ^{1}H NMR, IR, UV, and/or MS, to warrant their inclusion.

[b] In these cases, other structurally related adducts are also mentioned in the references, but with considerably less spectroscopic data quoted.

[c] bobPPh$_2$ = $PhCH_2OC_6H_4CH_2PPh_2$.

[d] PR_3 = PPh_3, PEt_3, PMe_2Ph, PPh_2Me, $P(OMe)_3$ or ½dppe.

$C_{60}(Li)(C{\equiv}CTMS)$ (*58, 59*), $C_{60}(Li)(PPh_2BH_3)$ (*60*), and $C_{60}(Li)(Me)$ (*52*) have been prepared and quenched *in situ* with the electrophiles H^+ or R^+. Grignards that were prepared and reacted *in situ* include $C_{60}(MgHal)(CH_2SiMe_2Y)$ (Y = H, Me, Ph, $CH{=}CH_2$ and OPr^i) (*61*),

TABLE IV

FULLY CHARACTERIZED σ-BONDED METAL–FULLERENE COMPLEXES[a]

Compound	X-ray structure	^{13}C NMR data	References
$C_{60}O_2OsO_2(4\text{-}Bu^tC_5H_4N)_2$	√	√	*46, 47*
$C_{60}(O_2OsO_2(4\text{-}Bu^tC_5H_4N)_2)_2$		√	*48*
$C_{60}(Bu^t)(Li)$		√	*49*
$C_{60}\{Re(CO)_5\}_2$			*50*
$C_{70}O_2OsO_2(4\text{-}Bu^tC_5H_4N)_2$		√	*51*
$C_{60}(SnBu_3)(H)$			*52*
$C_{60}S_2Fe_2(CO)_6$		√	*53*
$C_nO_2OsO_2(L^b)_2$ (n = 76, 78, 84)			*54*
$C_{60}Ge(Dis)_2$[c]			*55*
$C_{60}(Ge(Dis)_2CH_2CH_2)$[c]			*55*

[a] For some complexes, there are no ^{13}C NMR or crystallographic structural data, but there are some other data, such as elemental analysis, ^{31}P or ^1H NMR, IR, UV, and/or MS, to warrant their inclusion here.

[b] L is the optically active Sharpless cinchona alkaloid ligand.

[c] Dis = $CH(SiMe_3)_2$.

$C_{60}(MgHal)(Et)$ (*62*), and $C_{70}(MgHal)(Ph)$ (*52*). As is discussed in Section V, the extent of covalent σ bonding between C_{60} and Li or Mg is debatable, and there is much evidence for charge delocalization. The adduct of Schwartz's reagent and C_{60}, $C_{60}\{(Zr(\eta\text{-}C_5H_5)_2Cl)(H)\}_n$ (n = 1–3), also has been described and reacted *in situ* with *N*-bromosuccinimide, *m*-chloroperbenzoic acid, or HCl (*63, 64*).

II. Synthesis

The most widely used method for the synthesis of π metal fullerene adducts involves the standard procedure of displacement by the fullerene of a ligand that is weakly bound to the metal. The ligand may be PPh_3, an alkene, or even CO under favorable conditions (Scheme 2). Also, reductive elimination of H_2 has been used.

The effective generation *in situ* or direct reaction of a coordinatively unsaturated species with the fullerene has also been used [Eqs. (1)–(4)]. In the first two reactions outlined, NaOH effectively eliminates HCl from the precursor, and the latter then reacts with C_{60} [Eqs. (1) and (2)] (*32*).

$$[Ir(CO)(PPh_3)_2(\eta^2\text{-}C_{60})H] \xleftarrow[[Ir(CO)(PPh_3)_2ClH_2]]{NaOH} C_{60} \xrightarrow[[Pt(PPh_3)_2ClH]]{NaOH} [Pt(PPh_3)_2(\eta^2\text{-}C_{60})] \quad (1,2)$$

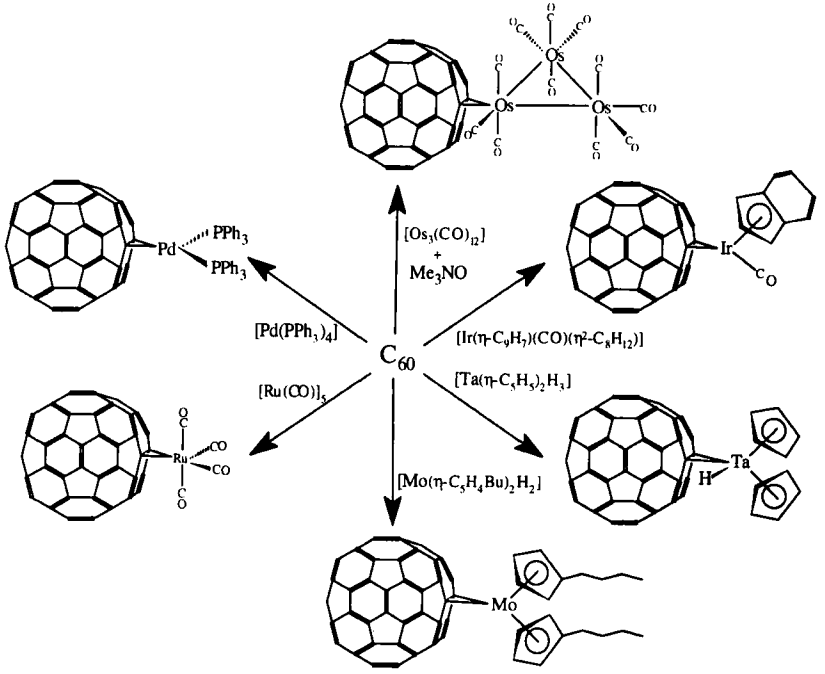

SCHEME 2. Synthetic routes to some fullerene organometallics by displacement of weakly bound ligands.

$$[Fe(CO)_4(\eta^2\text{-}C_{70})] \xleftarrow{C_{70}} [Fe_2(CO)_9] \xrightarrow{C_{60}} [Fe(CO)_4(\eta^2\text{-}C_{60})] \qquad (3,4)$$

In the case of Vaska-type compounds, $(Ir(CO)(PR_3)_2Cl)$, it has proved possible to form different adducts by varying either the fullerene or phosphine used [Eqs. (5)–(7)] (*13, 14, 28, 29, 33*):

$$C_{60} \xrightarrow{[Ir(CO)(PR_3)_2Cl]} [\{Ir(CO)(PR_3)_2Cl\}_2(\eta^2\text{-},\eta^{2'}\text{-}C_{60})] \qquad (5)$$
$$R = Me, Et$$

$$C_n \xrightarrow{[Ir(CO)(PPh_3)_2Cl]} [Ir(CO)(PPh_3)_2(\eta^2\text{-}C_n)Cl] \qquad (6)$$
$$n = 60, 70, 84$$

$$C_{60}O \xrightarrow{[Ir(CO)(PPh_3)_2Cl]} [Ir(CO)(PPh_3)_2(\eta^2\text{-}C_{60}O)Cl] \qquad (7)$$

Use of an excess of metal precursor often produces a multimetallic adduct (Scheme 3) (*33, 38*):

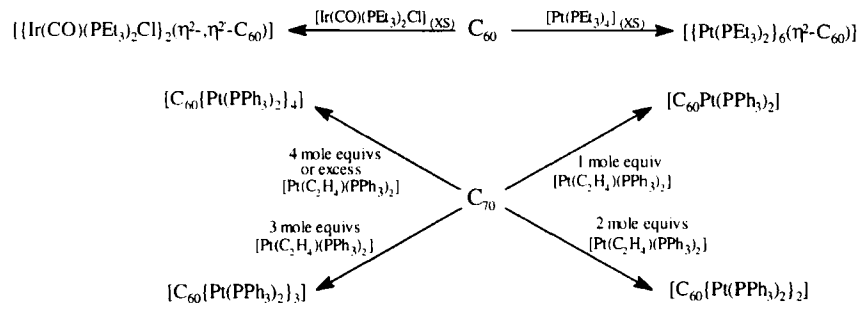

SCHEME 3. Synthetic routes to some multimetallic fullerene organometallics.

Photolysis also has been used as in the preparation of $C_{60}\{Re(CO)_5\}_2$ and $C_{60}S_2Fe_2(CO)_6$ [Eqs. (8) and (9)] (*50, 53*). Care must be taken to deoxygenate any solvents used, as the triplet excited C_{60} ($^3C_{60}$) produced reacts very readily with O_2.

$$C_{60}Fe_2S_2(CO)_6 \xleftarrow[h\nu]{[Fe_2S_2(CO)_6]} C_{60} \xrightarrow[h\nu]{[Re_2(CO)_{10}]} [C_{60}\{Re(CO)_5\}_2] \qquad (8,9)$$

σ-Organometallics have all been prepared by the effective addition of [M]-R into a fullerene double bond (Scheme 4).

Slow addition at low temperatures of ≈1.2 mole equivalent of RLi is preferable, as this minimizes multiple additions. For the less reactive (i.e., bulky) alkyl lithiums and for all Grignards (*52*), $[Zr(\eta\text{-}C_5H_5)_2HCl]$ (*63, 64*), and Bu_3SnH (*52*), then an excess of nucleophile is necessary. The reaction can be monitored by removing aliquots, quenching with dilute acid, and using an HPLC to analyze for products. Changing the solvent can have important consequences, and Nagashima found that

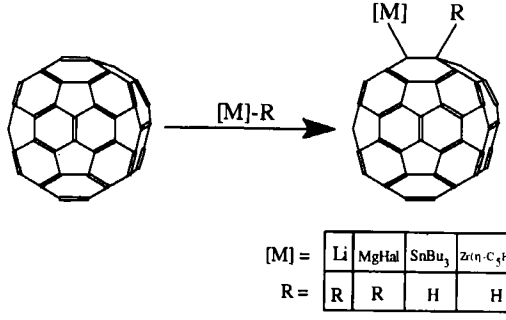

SCHEME 4. Synthetic routes to some σ-fullerene organometallics.

a reaction run in thf or toluene favored the formation of a mono- or diadduct, respectively (*61*).

Two germanium-containing compounds were prepared using the route analogous to the standard route for silylene derivatives [Eq. (10)] (*55*):

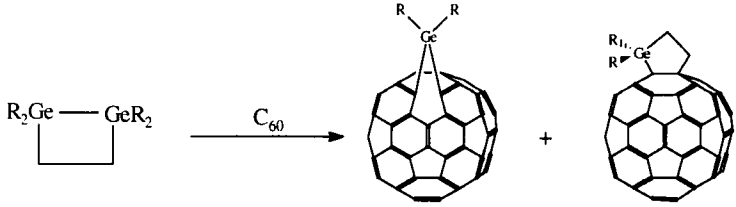

R = $CH(SiMe_3)_2$

As far as the practical work-up procedure is concerned, the adducts possess many of the physical and chemical properties typical of air-sensitive compounds. However, because all the adducts tenaciously retain solvent molecules, which can prove troublesome in elemental analyses and in ^{13}C NMR, it is worth outlining a procedure, found highly useful by the authors, which circumvents the problem:

1. A concentrated solution of the unique compound is prepared using an appropriate solvent with the aid of sonication. Low-boiling-point solvents are preferable.
2. A large excess (≈×5–10 volume) of pentane is added and the resulting precipitate allowed to settle. Sometimes it is necessary to filter using either glass or Whatman 50 filter papers, as natural settling takes too long. Ordinary Whatman 1 filter paper allows through many of the finer particles of product.
3. The precipitate is washed up to three times with pentane aided by sonication for ≈30-s periods, which breaks down the particle size.
4. Finally, the solid is dried *in vacuo* for ≈4 hours.

III. Characterization

A. General Points

Fullerene compounds have been characterized by typical spectroscopic techniques including ^{13}C NMR, IR, UV-vis, electrochemical methods, mass spectrometry (MS), and X-ray diffraction. Each of these methods is discussed here in relation to specific points arising from the

presence of a fullerene moiety in the molecule. Any problems arising from the characterization of the remainder of the molecule are discussed as warranted.

It is first worth mentioning some general problems of fullerene characterization. Not only can a mixture of various multiple adducts result from a given reaction, but also each of them may exist as a mixture of regioisomers that can often only be separated by HPLC. In addition, there is often a poor signal-to-noise ratio for many spectroscopic techniques owing to the use of only small amounts of relatively high molecular mass and low solubility.

B. ^{13}C NMR Spectroscopy

By far the most powerful tool for analysis of fullerene compounds is solution ^{13}C NMR spectroscopy, as the number, positions, and relative intensities of resonances often provide unambiguous evidence for a particular structure. The molecular point group of about 300 fullerene compounds has been identified using ^{13}C NMR spectroscopy.

However, obtaining an adequate signal-to-noise ratio is often problematic. In addition to the complications of instability, low solubility, and ^{13}C isotopic abundance, there are also difficulties associated with the presence of only quaternary carbon atoms. Such carbon atoms have long relaxation times, and polarization transfer or NOE enhancement pulse sequences cannot be applied. Several groups of workers have added relaxation reagents such as $Cr(acac)_3$ in the hope of shortening the T_1 relaxation times. However, no qualitative or quantitative information has been reported concerning their effectiveness, nor have any ^{13}C longitudinal T_1 relaxation times been quoted. For all the intensity arguments that follow, it is assumed that the fullerene carbon atoms do not relax at significantly different rates from each other. The solvent of choice is most commonly an aromatic or THF, but CS_2 also has been occasionally used.

Of the few cases of reported scalar couplings between C_{60} and a metal moiety, the value was comparable with analogous metal–alkene molecules.

1. Identification of the Point Group

By observing the number and relative intensity of ^{13}C resonances it is possible to identify to which point group an adduct belongs. For C_{60}, with I_h symmetry, all 60 carbon atoms are equivalent, giving rise to a single sharp line at 143.3 ppm in C_6D_6. Complex formation causes a reduction in symmetry, and the fullerene carbon atoms become in-

TABLE V

NUMBER AND INTENSITY OF $\delta(^{13}C)$ FULLERENE RESONANCES IN DIFFERENT SYMMETRY ENVIRONMENTS

Point group	Total no. of resonances	No. of sp^2 resonances	No. of sp^3 resonances	Example	Reference
T_h	3	2 (I = 24)	1 (I = 12)	$[C_{60}\{Pt(PEt_3)_2\}_6]$	*16*
C_{2v}	17	13 (I = 4) 3 (I = 2)	1 (I = 2)	$[Fe(CO)_4(\eta^2\text{-}C_{60})]$	*22*
C_s (‖)[a]	32	28 (I = 2) 2 (I = 1)	2 (I = 1)	$C_{60}(Li)(Bu^t)$	*49*
C_s (⊥)[a]	32	27 (I = 2) 4 (I = 1)	1 (I = 2)	$[Co(NO)(PPh_3)_2(\eta^2\text{-}C_{60})]$	*27*
C_1	60	58 (I = 1)	2 (I = 1)	$C_{60}(CHOMe)(C_7H_6)$[b]	*65*

[a] C_s (‖) refers to the mirror plane running through the $C(sp^3)$—$C(sp^3)$ bond. C_s (⊥) refers to the mirror plane bisecting the $C(sp^3)$—$C(sp^3)$ bond.

[b] No fullerene organometallics have been made yet with the C_1 point group.

equivalent, with more peaks appearing for a lower symmetry. Table V shows the expected number of peaks for various common point groups, and Fig. 3 illustrates some relevant structures. Not all the resonances have equal intensity, as some carbon atoms lie on a mirror plane.

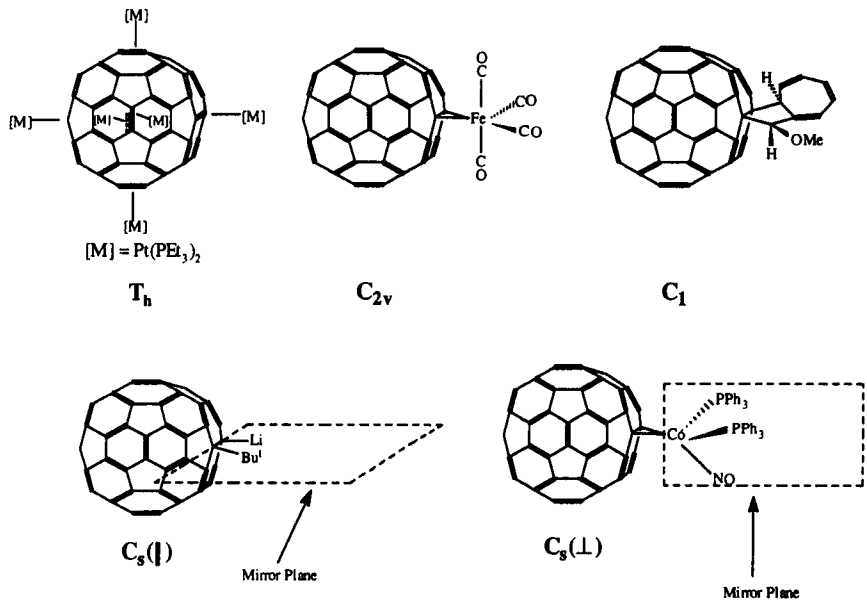

FIG. 3. Examples of some of the various symmetries possible for C_{60} complexes.

Even for a given molecular formula, a number of structures are possible. For instance in the cases of organic carbene or nitrene adducts, addition can occur at the [6,6] or [6,5] ring junction of the fullerene, and each gives rise to a different symmetry product (*66*). Organometallic additions have been found to occur only at the thermodynamically more favorable [6,6] junction. For C_{70} and the higher fullerenes, the [6,6] bonds are no longer all equivalent, and mixtures of regioisomers are possible, each often with a different point group.

For di- and higher adducts, the number of regioisomers resulting is even larger. Only in a few cases, such as $[C_{60}\{Pt(PEt_3)_2\}_6]$, have they been successfully isolated and spectroscopically characterized (*16*).

2. *Assignment of Individual Fullerene Resonances*

The chemical shifts of the fullerene sp^2 and sp^3 carbon atoms are typically in the regions 155–135 ppm and 80–50 ppm, respectively. However, in cases where the latter carbon atoms are bound to an especially electronegative heteroatom, then they resonate at much lower fields, e.g., for $C_{60}O$ $\delta(Csp^3)$ = 91 ppm (*67, 68*).

Assignment of individual sp^2 carbon atom resonances to particular carbon atoms of the framework has proved very difficult. A full analysis was reported for $C_{60}O_2OsO_2(4\text{-}Bu^tC_5H_4N)_2$, achieved using ^{13}C 2-D INADEQUATE on a ^{13}C-enriched sample (*46*). Green and co-workers successfully assigned most of the resonances in $[Co(NO)(PPh_3)_2(\eta^2\text{-}C_{60})]$ by 2-D EXSY (*27*). Nevertheless, through observation of scalar couplings to the heteroatom X, it occasionally has proved possible to identify the sp^2 carbon atoms adjacent to the sp^3 ones (henceforth referred to as the C2 carbon atoms) (*49, 52, 60, 69, 70*). In all these cases, as

TABLE VI

NUMBER OF C2 FULLERENE RESONANCES FOR DIFFERENT SYMMETRIES

Structure[a]	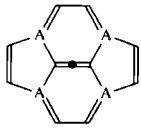	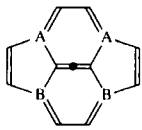	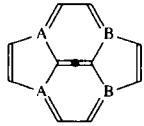	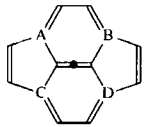
Symmetry	C_{2v}	C_s (⊥)	C_s (∥)	C_1
No. of C2 resonances	1	2	2	4
Examples	$[Fe(CO)_4(\eta^2\text{-}C_{60})]$	$[Rh(NO)(PPh_3)_2(\eta^2\text{-}C_{60})]$	$C_{60}(Li)(Bu^t)$	$C_{60}(CHOMe)(C_7H_6)$

[a] The letters A, B, C, and D refer to different chemical environment for the C2 carbon atoms relative to the central metal complexed double bond.

well as for $C_{60}O_2OsO_2(4\text{-}Bu^tC_5H_4N)_2$ and $[Co(NO)(PPh_3)_2(\eta^2\text{-}C_{60})]$, these sp^2 carbon atoms resonate at uniquely low fields, typically >150 ppm. This useful generality also can help with the structural identification of other C_{60} monoadducts. Often it is difficult to deduce the point group from analysis of all the peaks, as they are often overlapping or are lost in the baseline (especially true of the sp^3 carbon atoms). Use of this generality means that the symmetry can be tentatively deduced just from counting the number of C2 resonances present.

For simple organometallic monoadducts with the point groups C_{2v}, C_s or C_1, there will be one, two, or four chemical environments for the C2 carbon atoms, respectively, and a corresponding number of especially low-field peaks in the ^{13}C NMR spectrum. Some examples are illustrated in Table VI and Fig. 4.

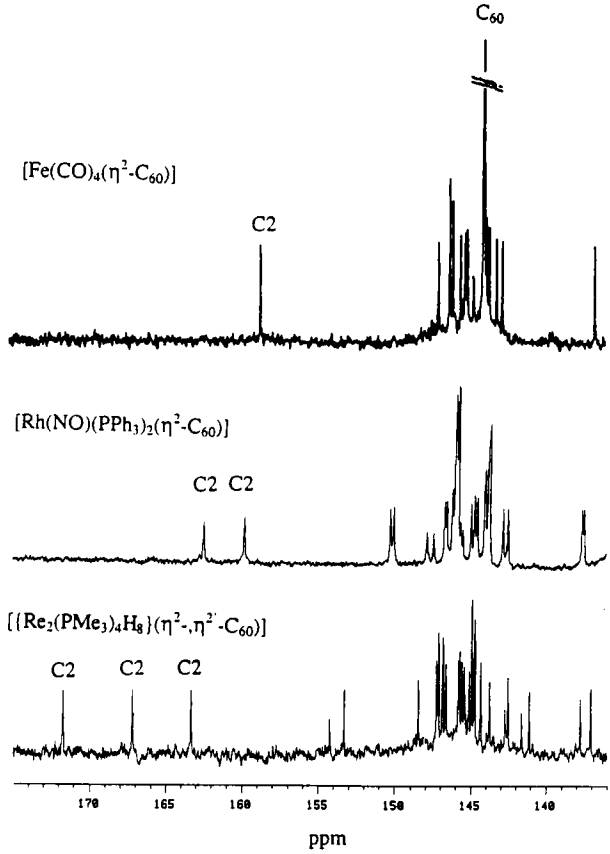

FIG. 4. The ^{13}C NMR of $[Fe(CO)_4(\eta^2\text{-}C_{60})]$ (in CS_2/C_6D_6), $[Rh(NO)(PPh_3)_2(\eta^2\text{-}C_{60})]$ (−90°C in C_4D_8O) and $[\{Re_2(PMe_3)_4H_8\}(\eta^2\text{-},\eta^{2'}\text{-}C_{60})]$ (in C_4D_8O) in the fullerene sp^2 C region.

Furthermore, this generality also holds for practically all organic closed [6,5] or [6,6] and separate group monoadducts (*46, 71, 72*). It also is useful in the analysis of mixtures and multiple adducts; indeed, the dimetallic adduct $[\{Re_2(PMe_3)_4H_8\}(\eta^2\text{-},\eta^{2'}\text{-}C_{60})]$ has three types of C2 carbon atoms and, as expected, three low-field signals appear in the ^{13}C NMR. Higher fullerene adducts also often show especially low-field signals whose number seems to be consistent with the generality, such as for the compound $C_{70}(H)(Me)$ (*52*).

Although it generally has not proved possible to assign further fullerene carbon atoms, most organometallics and many organic adducts also show one fullerene sp^2 resonance that is a little separated to high field from the rest. For instance, as shown in Fig. 4, these occur at 136.2 ppm for $[Fe(CO)_4(\eta^2\text{-}C_{60})]$ and at 137.0 and 136.9 ppm for $[Rh(NO)(PPh_3)_2(\eta^2\text{-}C_{60})]$. For both $C_{60}O_2OsO_2(4\text{-}Bu^tC_5H_4N)_2$ and $[Co(NO)(PPh_3)_2(\eta^2\text{-}C_{60})]$, the corresponding high-field signals have been assigned to one type of sp^2 carbon atoms that are adjacent to the C2 ones, henceforth referred to as the C3 carbon atoms. Furthermore, just as for C2 resonances, the number of C3 sites generally equals the number of these slightly high-field signals.

C. Vibrational Spectroscopy

Excluding local-site and solid-state effects, C_{60} has 174 degrees of vibrational freedom. Only four of these vibrations (T_{1u}) are IR active and occur at 526, 577, 1184, and 1429 cm^{-1}, with those above and below 900 cm^{-1} expected to involve predominantly tangential and radial displacements, respectively (*3, 73*). All monoadducts also show diagnostically strong bands in these regions. However, the lower symmetry of an adduct causes a loss in degeneracy of the T_{1u} modes and often results in the bands being either broad or split. For instance, the IR spectrum of $[Ta(\eta\text{-}C_5H_5)_2(\eta^2\text{-}C_{60})H]$, shown in Fig. 5, contains bands at 572, 562, 529, and 518 cm^{-1}, compared with just two for uncomplexed C_{60} at 576 and 526 cm^{-1}. Similar behavior was observed for $[Os_3(CO)_{11}(\eta^2\text{-}C_{60})]$ (*34*). Despite the reduction in symmetry, no additional bands have ever been unambiguously assigned to internal fullerene active vibrations. For multiple addition adducts, the severe disruption to the cage structure results in a markedly different spectrum.

The $\nu(CO)$ stretch for metal carbonyls is a useful way of assessing the relative electron-withdrawing power of fullerenes. For $[M(CO)_4(\eta^2\text{-}C_{60})]$ (M = Fe or Ru) and $[Ir(CO)(PR_3)_2(fullerene)Cl]$, values of $\nu(CO)$ suggest that fullerenes are similar to monosubstituted alkenes such as methyl acrylate or acrylonitrile. For instance, for $[Ru(CO)_4$

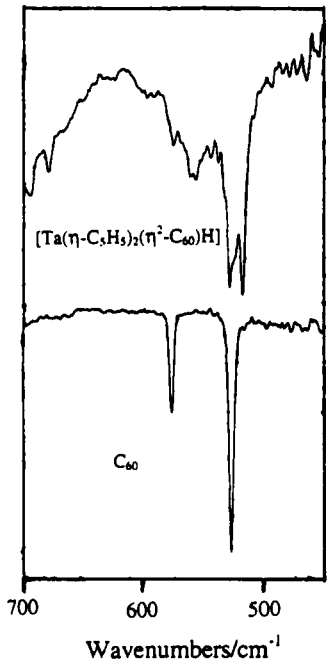

FIG. 5. Part of the IR spectrum of $[Ta(\eta\text{-}C_5H_5)_2(\eta^2\text{-}C_{60})H]$ and C_{60} in Nujol mull.

$(\eta^2\text{-}C_{60})]$ and $[Ru(CO)_4(\eta^2\text{-}CH_2CHCN)]$, the two highest ν(CO)s are at 2125, 2056, and 2123, 2055 cm^{-1}, respectively (*26, 27*). These conclusions are in consonance with other studies such as cyclic voltammetry or NMR.

Raman spectroscopy has proved a valuable tool not only for discussions of bonding but also, more interestingly, for structural elucidation. This is because intense Raman scattering lines are generally observed as a result of the relatively large polarizable nature of the fullerene core. In a similar way to the IR spectrum, complexation causes loss of degeneracy of the Raman active modes (8 H_{1g} and 2 A_{1g}) and the appearance of new previously silent modes. Both of these effects have been observed for $[M(PR_3)_2(\eta^2\text{-}C_{60})]$ (M = Ni, Pd, Pt; R = Ph, Et) and $[\{M(PEt_3)_2\}_6(C_{60})]$ (M = Ni, Pd, Pt) (*17*). Indeed the fivefold degenerate mode at 772 cm^{-1} (H_{1g}) in C_{60} is split into the expected five components for the C_{2v} complex $[Pt(PPh_3)_2(\eta^2\text{-}C_{60})]$. Similar results have been found in the surface-enhanced Raman spectrum of $[Ir(\eta^5\text{-}C_9H_7)(CO)(\eta^2\text{-}C_{60})]$ (*74*). Metal complexation causes a slight weakening of the bonds, as a result of π back-donation into the fullerene π^* MOs, and a concomitant shift to lower frequencies is observed.

There are few IR and Raman studies of the higher fullerene adducts, but the conclusions drawn are similar (*52*).

D. UV-VIS SPECTROSCOPY

On complexation, the fullerene structure is not significantly altered electronically and as a result the spectrum is similar to the unbound form. In the case of C_{60}, the following features are common to both the free ligand and to all its monoadducts:

1. Two very intense bands at ≈220 nm, ≈255 nm.
2. One moderately intense band at ≈330 nm.
3. A broad, featureless weaker band between 450 and 600 nm.

Figure 6 shows the UV-vis spectra of C_{60} and $[Ru(CO)_4(\eta^2\text{-}C_{60})]$.

By reference to the MO scheme in Fig. 2, the bands at $\lambda < 400$ nm have been assigned to sharp and intense parity-allowed transitions between occupied (bonding) and empty (antibonding) MOs. Such excitations include $h_u(\text{HOMO}) \rightarrow t_{1g}(\text{LUMO} + 1)$ and $h_g \rightarrow t_{1u}(\text{LUMO})$. Optical transitions between the HOMO(h_u) and LUMO(t_{1u}), which are electric dipole forbidden, occur via excitation of a vibronic state with appropriate u parity symmetry and account for the broad and low intensity band at $\lambda > 400$ nm.

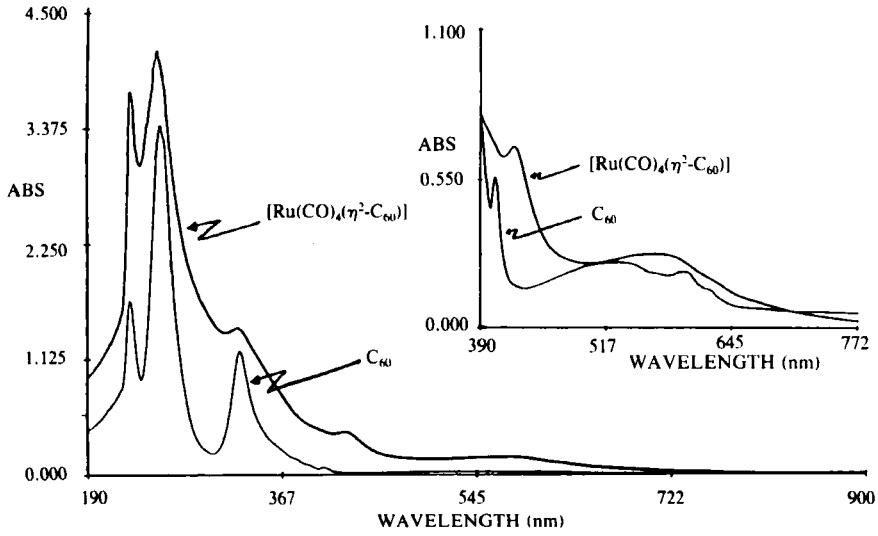

FIG. 6. The UV-vis spectra of C_{60} and $[Ru(CO)_4(\eta^2\text{-}C_{60})]$ in CH_2Cl_2.

In addition, many monoadducts including π- and σ-organometallics exhibit a weak diagnostic peak at $\approx$430 nm. For [Ir(η^5-C_9H_7)(CO)(η^2-C_{60})], spectrochemical UV-vis studies showed that this peak was invariant upon reduction to the anion, consistent with it being an intraligand transition that is only symmetry allowed in a reduced symmetry complex (*75*). For organic compounds, its presence or absence is a useful guide as to whether the structure is [6,6]-closed or [6,5]-open, respectively (*76, 77*). This is presumably because the fullerene chromophore is less electronically perturbed in the latter. For multiple adducts, the electronic structure of the cage is often sufficiently altered that only some of the preceding features are observed (*37, 78*). Some monoadducts also show a very weak peak at $\approx$700 nm (*79*).

UV-vis studies on C_{70} and higher fullerene adducts are scarce. However, the similarity in features between the free and bound fullerenes, such as for C_{70} and $C_{70}(SiMes_2)_2CH_2$, has allowed analogous structural conclusions to be drawn (*80, 81*).

Assuming that no other strongly absorbing chromophores are present, then the organic C_{60} adducts tend to be intensely red, whereas the organometallic adducts tend to be intensely green or red. The extinction coefficients (ε) have values comparable to those of uncomplexed C_{60}, with the more intense color arising because of small shifts in the 450–600 nm band.

Only the fulleride anions C_{60}^{n-} (n = 1–6) show broad (diagnostic) peaks in the near-IR (NIR) spectrum (*82, 83*).

E. Electrochemical Studies

All C_{60} adducts have low-lying LUMOs that can easily be populated by electrochemical methods. For C_{60} itself, six reduction couples have been observed by cyclic voltammetry (CV) or square-wave voltammetry (SWV), and as many as four reduction couples have been found for many organometallics (*9, 84*). Most of the studies have been performed in thf or acetonitrile at lower temperatures, which increases the size of the potential window. Table VII lists the half-wave potentials for some metal complexes, and Fig. 7 shows the cyclic voltammogram for [Co(NO)(PPh_3)$_2$(η^2-C_{60})].

The reduction couples are thought to be C_{60}-based rather than metal-based owing to their very similar, but slightly more negative, values (*84*). This slight shift of ≈ -0.3 V indicates that the complexes are harder to reduce and is due to perturbations in the electron affinity of the fullerene cage arising from metal complexation. Shapley performed spectrochemical IR studies on [Ir(η^5-C_9H_7)(CO)(η^2-C_{60})] and found only

TABLE VII

ELECTROCHEMICAL HALF-WAVE POTENTIAL VALUES FOR SOME π-ORGANOMETALLICS[a]

Complex	$E^\circ_{(ox)}$ (V)	$E^\circ_{(0,-1)}$ (V)	$E^\circ_{(-1,-2)}$ (V)	$E^\circ_{(-2,-3)}$ (V)	Reference
$[Ni(PEt_3)_2(\eta^2\text{-}C_{60})]$	+0.08	−1.20	−1.74	−2.32	*84*
$[Pd(PEt_3)_2(\eta^2\text{-}C_{60})]$	+0.20	−1.18	−1.69	−2.23	*84*
$[Pt(PEt_3)_2(\eta^2\text{-}C_{60})]$	+0.33	−1.20	−1.73	−2.27	*84*
$[Pt(PPh_3)_2(\eta^2\text{-}C_{60})]$	+0.42	−1.21	−1.75	−2.23	*84*
$[Co(NO)(PPh_3)(\eta^2\text{-}C_{60})]$	−0.29	−1.17	−1.72	−2.25	*27*
$[Rh(NO)(PPh_3)_2(\eta^2\text{-}C_{60})]$	+0.35	−1.14			*27*
$[Ru(NO)(PPh_3)_2(\eta^2\text{-}C_{60})H]$		−1.12	−1.70	−2.29	*27*
$[\{Re_2(PMe_3)_4H_8\}(\eta^2\text{-},\eta^2\text{-}C_{60})]$	−0.34	−1.05	−1.53		*27*
C_{60}		−0.86	−1.48	−2.08	*84*
$[Ir(\eta^5\text{-}C_9H_7)(CO)(\eta^2\text{-}C_{60})]^b$	+0.72	−1.08	−1.43	(−1.94)	*75*
$[Ru(CO)_4(\eta^2\text{-}C_{60})]^b$		−1.13	−1.50		*27*
$C_{60}{}^b$		−1.00	−1.39	−1.81	*75*

[a] All couples are quoted relative to the Fc/Fc^+ couple with $E^\circ_{(+1,0)} = 0.00$ V and are recorded in thf/0.1 or 0.2 *M* Bu_4NPF_6.

[b] Recorded in CH_2Cl_2/0.1 *M* Bu_4NPF_6 .

very small shifts ($\Delta \approx 10\ cm^{-1}$) in ν(CO) on reduction to the mono and dianion, consistent with the reductions being essentially C_{60}-based (*75*). Metal complexation effectively removes one double bond from the fullerene π-system, thus raising the energy of the LUMO and decreasing

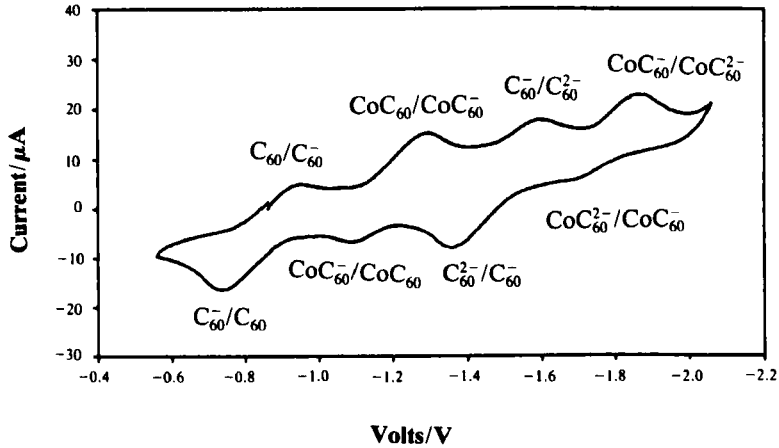

FIG. 7. The cyclic voltammogram of $[Co(NO)(PPh_3)_2(\eta^2\text{-}C_{60})]$ in thf/0.1 *M* Bu_4NPF_6. (Referenced to Fc/Fc^+ with $E^\circ = 0.0$ V.)

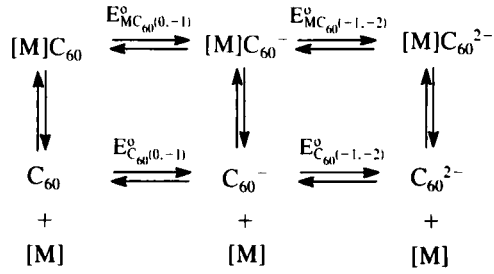

SCHEME 5. Equilibria present in the cyclic voltammogram of π-organometallics.

the electron affinity of the cage. Nevertheless, metal complexation does not always fully "decouple" this double bond, and instead allows some residual interaction betwen the metal center and the fullerene π-system. Thus, changes in the metal electronegativity may account for the slight differences in the E° values. In the reduced species, the additional electrons are accommodated in a LUMO that is derived from the remaining 29 double bonds of C_{60}, as well as a component of metal–C_{60} antibonding character. For the more highly reduced anions, there is increased occupancy of this LUMO, and so the metal–fullerene bond becomes weaker and causes increased metal dissociation. This accounts for the relatively smaller and larger areas of successive couples in the CV for the complex and for free C_{60}, respectively. Scheme 5 illustrates the most important equilibria present in solution.

Oxidation waves associated with the metal moiety often are observed.

F. OTHER TECHNIQUES

1. Elemental Analysis

Although elemental analysis is useful as a probe to stoichiometry, there are two special problems associated with fullerene compounds: incomplete combustion and the tenacious propensity of fullerene compounds to retain solvent, which can both lead to confusing results. The first effect can be circumvented either by burning with a catalyst such as V_2O_5 or by performing the analysis with an abnormally small amount of sample. The second problem can often be overcome by using the procedure described in Section II, which involves precipitation using a highly volatile solvent.

2. *Mass Spectrometry*

The usefulness of this technique is somewhat restricted owing to the ease of dissociation of the fullerene moiety in the mass spectrometer. As a result, for many complexes only the unbound fullerene peak is observed (e.g., at 720 amu for C_{60}) when using electron impact (EI) or laser desorption (LD) techniques. However, with milder ion generation techniques, such as matrix-assisted laser desorption/ionization (MALDI), fast atom bombardment (FAB), or field desorption (FD), then molecular ions are often observable, such as for $[Ir(\eta^5\text{-}C_9H_7)(CO)(\eta^2\text{-}C_{60})]$ (*15*), $[Os_3(CO)_{11}(\eta^2\text{-}C_{60})]$ (*34*), and $[\{Re_2(PMe_3)_4H_8\}(\eta^2\text{-},\eta^{2'}\text{-}C_{60})]$ (*27*). The even milder ion generation technique of electrospray ionization (ESI) has been used very successfully on charge-separated organic adducts; furthermore, the progress of reactions, such as methoxylation, easily can be monitored (*85, 86*).

3. *X-Ray Diffraction*

The first reported fullerene crystal structure was for $C_{60}OsO_4(4\text{-}Bu^tC_5H_4N)_2$ (*47*), and there are now many more structures, with over 50 deposited at the Cambridge Crystallographic Database. Tables III and IV list all the fullerene organometallics for which there are published crystal structures. No special techniques are required, although low temperatures and Cu radiation are preferable.

Successful crystal growth is nontrivial and highly serendipitous. Fagan grew the first fullerene metal complex by the tried and tested method of leaving an NMR tube standing around the lab for several weeks (*7*). In general, most X-ray quality crystals have been grown by the slow diffusion together of reactant solutions.

4. *Mössbauer Studies*

The ^{193}Ir and ^{57}Fe Mössbauer spectra have been reported for $[Ir(CO)(PPh_3)_2(\eta^2\text{-}C_{60})Cl]$ (*87*) and $[Fe(CO)_4(\eta^2\text{-}C_{60})]$ (*88*), respectively. In each case, the isomer shift and quadrupole splitting were consistent with C_{60} being a weakly π-accepting ligand. For $[Fe(CO)_4(\eta^2\text{-}C_{60})]$, the isomer shift was found to vary linearly with temperature and yielded a value of $\approx$120 g mol^{-1} for the Fe center "effective vibrating mass." This is $\approx$15% of the formula weight (888) and suggests that the iron atom only interacts with a small portion of the fullerene ligand. A plot of the temperature dependence of $\ln(A)$, where A = area under the doublet, was linear with temperature and had a large gradient. This implies that there is coupling between one or more low-lying librational

or lattice modes of C_{60} with one or more appropriate symmetry normal modes of the Fe center in $[Fe(CO)_4(\eta^2\text{-}C_{60})]$.

IV. Structure

A. π-Bonded Complexes

1. Hapticity of Complexes

X-ray diffraction and NMR studies have shown that metal fragments add exclusively across the [6,6] fusions to give η^2-type adducts. In contrast, organic derivatives add either to the [6,6] to form a closed adduct, or to the [6,5] fusions to form either an open or closed adduct (*66*). The ease with which some metal fragments dissociate off and on to the cage, in contrast to the organic derivatives, may explain the exclusive formation of the thermodynamically most stable [6,6]-adducts.

There are no known examples of η^n- ($n \geq 3$) coordination of C_{60}, and indeed reaction with $[Ru(\eta\text{-}C_5Me_5)(CH_3CH)_3]^+$ $O_3SCF_3^-$, a reagent known to readily bind η^6- to polyenes such as styrene, resulted in only η^2-coordination, as shown in Fig. 8 (*7*). This behavior has been rationalized in terms of the relative disposition of the carbon *p* orbitals in C_{60} and in arenes and the relative energies of their MOs (*89, 90*). Studies have shown that for electron-rich metal centers it is energetically more favorable to form η^2-bonds between M and C_{60} than between M and small ligands, and furthermore there are net electron–electron repulsions for higher hapticity metal–C_{60} bonding. Although for hard metal centers, such as Ag^+, any form of interaction between the metal and C_{60} is less favorable, there is less difference between the hapticity

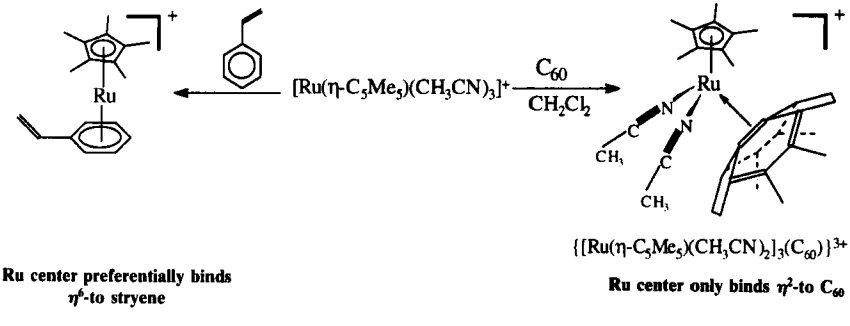

FIG. 8. The reaction of $[Ru(\eta\text{-}C_5Me_5)(CH_3CN)_3]^+$ $O_3SCF_3^-$ with styrene and C_{60}.

forms. Thus, with judicious choice of hard metal center, it might prove possible to produce higher-hapticity adducts. In terms of *p*-orbital disposition, for curved fullerenes the orbitals are tilted away from the center of a particular six-membered ring and so produce weakened interaction when compared with a metal bound to a planar arene. This also will be true for η^n- (n = 3–5) coordination, although the difference in energy between planar and tilted rings is less. Thus, for the reaction of C_{60} with $[Ru(\eta\text{-}C_5Me_5)(CH_3CN)_3]^+$, the acetonitrile is a strong donor and preferentially binds to the Ru center and prevents weak hexahapto bonding occurring between the Ru atom and C_{60} (*7*).

2. Monoadduct Structures

The majority of π complexes are monoadducts in which the metal complexes η^2 at one of the 30 equivalent [6,6] ring fusions. Typical structures and some general details are given in Fig. 9.

For C_{70} and higher fullerenes addition also occurs only at the [6,6] fusions. However, these sites are no longer all equivalent, and a variety of regioisomers can result. For C_{70}, of the four possible products, as illustrated in Fig. 10, addition occurs exclusively at the polar fusion, A (*14*). This is the sterically most accessible site, and energy calculations have shown there is the greatest release of steric strain on complexation (*91*). The equatorial [6,6] fusion, D, has lowest bond order, and correspondingly, no complexations to it have been observed. For C_{84}, complexation with Vaska's compound occurs at the fusion with the highest bond order, as shown by Hückel calculations (*28*).

3. Multimetallic Adduct Structures

In addition to the monoadducts, there are a growing number of multimetallic complexes, of which some are illustrated in Fig. 11. These can be subdivided into those that involve metals binding to adjacent and to more distant C=C bonds.

There are only three examples of the first division, namely $[\{Ir_2(\mu\text{-}Cl)_2(1,5\text{-}C_8H_{12})_2\}_2(\eta^2\text{-},\eta^{2'}\text{-}C_{60})]$ (*21*), $[\{Ru_2(\mu\text{-}Cl)(\mu\text{-}X)(\eta\text{-}C_5Me_5)_2\}(\eta^2\text{-},\eta^{2'}\text{-}C_{60})]$ (X = Cl, H) (*31*), and $[\{Re_2(PMe_3)_4H_8\}(\eta^2\text{-},\eta^{2'}\text{-}C_{60})]$ (*27*). The presence of bridging ligands may partly account for their unusual structure. In addition, $[C_{60}\{Re(CO)_5\}_2]$ has been prepared, and molecular modeling studies have suggested that the two Re atoms are bound in a σ-1,4 fashion (*50*).

Multiple additions that involve complexation at more distant sites have been found for a number of metal fragments, and these are generally prepared using a large excess of the metal precursor. Often a mixture of products results and, apart from serendipitous crystalliza-

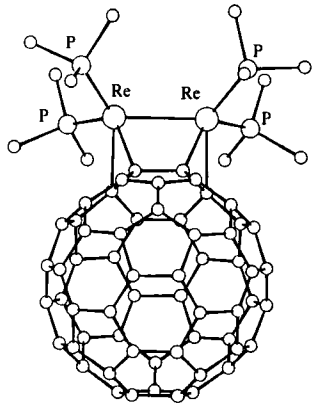

Structure of $[\{Re_2(PMe_3)_4H_8\}(\eta^2\text{-},\eta^{2'}\text{-}C_{60})]$

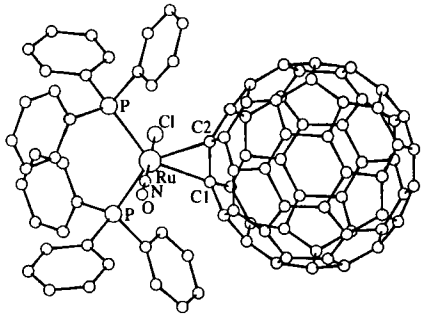

Structure of $[Ru(NO)(PPh_3)_2(\eta^2\text{-}C_{60})Cl]$

[6,6]-Addition (Organometallic addition occurs exclusively here as well as many organic additions)

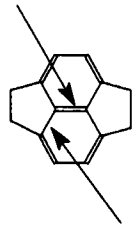

[6,5]-Addition (Some organic additions occur here)

Regiochemistry of addition

FIG. 9. General structural details and typical examples of C_{60}-organometallics.

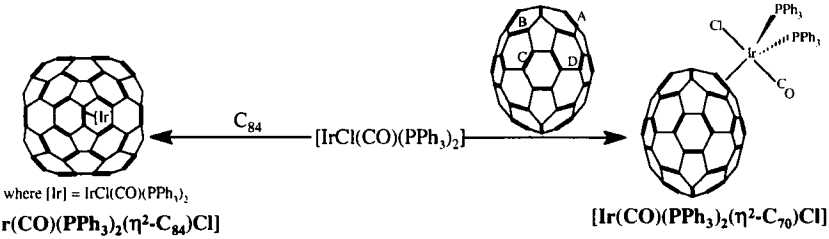

FIG. 10. Structures of $[Ir(CO)(PPh_3)_2(\eta^2\text{-}C_{70})Cl]$ and $[Ir(CO)(PPh_3)_2(\eta^2\text{-}C_{84})Cl]$. (The letters A, B, C, and D indicate different possible sites for [6,6] fusion complexation on C_{70}.)

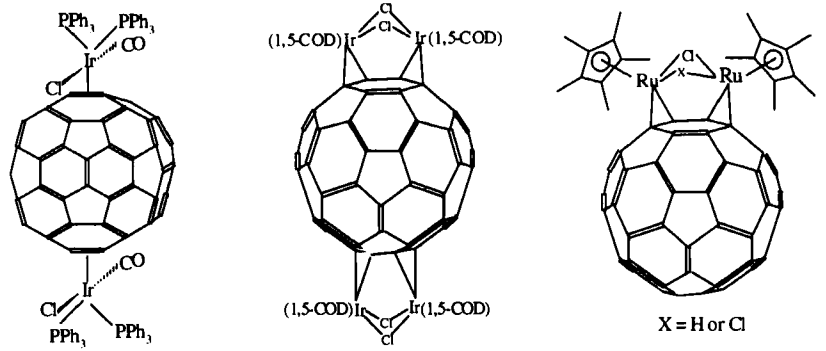

$[\{Ir(CO)(PPh_3)_2Cl\}_2(\eta^2,\eta^{2'}\text{-}C_{60})]$ $[\{Ir_2(\mu\text{-}Cl)_2(1,5\text{-}C_8H_{12})_2\}_2(\eta^2\text{-},\eta^{2'}\text{-}C_{60})]$ $[\{Ru_2(\mu\text{-}Cl)(\mu\text{-}X)(\eta\text{-}C_5Me_5)_2\}(\eta^2\text{-},\eta^{2'}\text{-}C_{60})]$

(X=Cl or H)

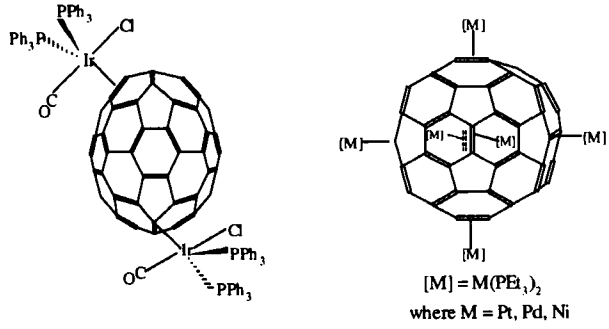

$[\{Ir(CO)(PPh_3)_2Cl\}_2(\eta^2,\eta^{2'}\text{-}C_{70})]$ $[C_{60}\{M(PEt_3)_2\}_6]$

FIG. 11. Some multimetallic fullerene adducts.

tion, the main method of separation is HPLC. This was used to separate out the constituents of $C_{60}\{S_2Fe_2(CO)_6\}_n$ (n = 1–3) (*53*). Distant-site multiple additions involve either two metal moieties that bind at diametrically opposite poles of the fullerene (para adducts) or six metal fragments that form an octahedral array around C_{60}. This contrasts with organic additions, which often result in regioisomeric mixtures of difficult-to-separate mono- to hexaadducts. Examples of para diadducts include those formed between C_{60} or C_{70} and Vaska's compound. Like the corresponding monoadduct, the latter contained Ir centers bound to CC bonds that give the greatest degree of pyramidalization on complexation (type A C=C bonds) (*18*). It is generally believed that these diadducts are intermediates on the pathway to hexaadducts, although further intermediates have so far eluded characterization.

Very recently the first tetrametallic and highest multimetallic adduct of C_{70} has been crystallographically characterized in the form of $[C_{70}\{Pt(PPh_3)_2\}_4]$ (*38*). It was postulated that the high bond order of sites A and B, the resulting steric bulk of a tetra adduct, and the low bond order of site D best explain the observed exclusive addition to sites A and B. Intermediate di- and triadducts were partially characterized and are thought to form through initial binding at two A sites followed by binding to a B site.

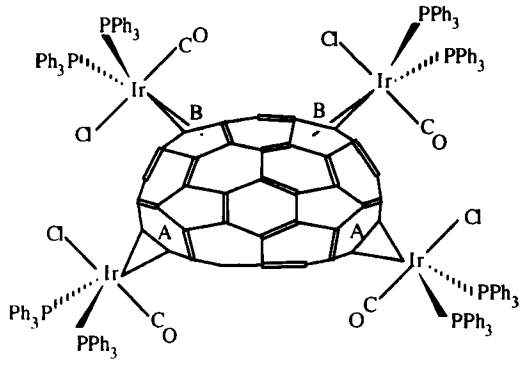

The hexaadducts $[C_{60}\{M(PEt_3)_2\}_6]$ (M = Ni, Pd, Pt) involve an octahedral array of metal moieties in a similar fashion to $C_{60}\{C(CO_2Et)_2\}_6$ and possess the very rare point group T_h (*16*). It is believed that each metal fragment binds to one fullerene C=C bond and sterically blocks the neighboring four, so that six moieties will block all 30 C=C bonds of C_{60}. Hence, π-adducts involving more than six addends are likely to be difficult to prepare.

The only reported examples of a multiple adduct where the addends bind to C_{60} using different atoms are $[Ir(CO)(PPh_3)_2(\eta^2\text{-}C_{60}O_n)Cl]$ (n = 1,2) (*29, 36*) and $[Ir(CO)(AsPh_3)_2(\eta^2\text{-}C_{60}O)Cl]$ (*39*). For both n = 1 and 2, there is disorder with the O occurring in as many as seven different sites. The major forms are shown next and involve the Ir and O centers coordinating to adjacent double bonds. No doubt the oxophilic Ir center is initially attracted to a double bond adjacent to the epoxide O atom.

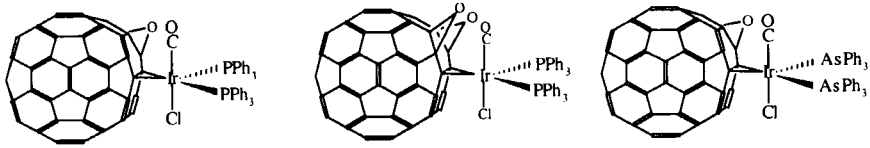

4. *Internal Structure of the Fullerene*

As far as the fullerene internal structure is concerned, there is little change on metal complexation. The metal bound transannular [6,6] bond is elongated relative to the remaining fullerene C=C bonds. It often attains a length (≈1.5 Å) comparable with that of other C—C bonds such as the transannular [6,5] bond or those for an analogous alkene complex. The structure often is described as metallacyclopro-

TABLE VIII

$C(sp^3)$—$C(sp^3)$ BOND LENGTH IN SOME FULLERENE ORGANOMETALLICS

Compound	$C(sp^3)$—$C(sp^3)$ bond length/Å[a]	Reference
$C_{60}OsO_4(4\text{-}Bu^tC_5H_4N)_2$	1.624	*47*
$[Ir(CO)(PPh_3)_2(\eta^2\text{-}C_{60})Cl]$	1.533	*13*
$[Pt(PPh_3)_2(\eta^2\text{-}C_{60})$	1.502	*12*
$[\{Ir(CO)(PMe_3)_2Cl\}_2(\eta^2\text{-},\eta^{2'}\text{-}C_{60})]$	1.51	*33*
$[Ir(CO)(PPh_3)_2(\eta^2\text{-}C_{60}O)Cl]$	1.500	*29*
$[C_{60}\{Pt(PEt_3)_2\}_6]$	1.497	*7*
$[Rh(CO)(PPh_3)_2(\eta^2\text{-}C_{60})H]$	1.479	*24*
$[\{Ir(CO)(PPhMe_2)_2Cl\}_2(\eta^2\text{-}C_{60})]$	1.477	*20*
$[\{Ir_2(\mu\text{-}Cl)_2(1,5\text{-}C_8H_{12})_2\}_2(\eta^2\text{-},\eta^{2'}\text{-}C_{60})]$	1.47	*21*
$[Pd(PPh_3)_2(\eta^2\text{-}C_{60})]$	1.447	*23*
$[Ir(CO)(PPh_3)_2(\eta^2\text{-}C_{70})Cl]$	1.46	*14*
$[\{Ir(CO)(PPhMe_2)_2Cl\}_2(\eta^2\text{-}C_{70})]$	1.523	*18*
$[Ir(CO)(PPh_3)_2(\eta^2\text{-}C_{84})Cl]$	1.457	*28*
C_{60}	1.391[b]	*92*
C_{70}	1.39[b]	

All other fullerene CC bonds are not altered significantly on complexation

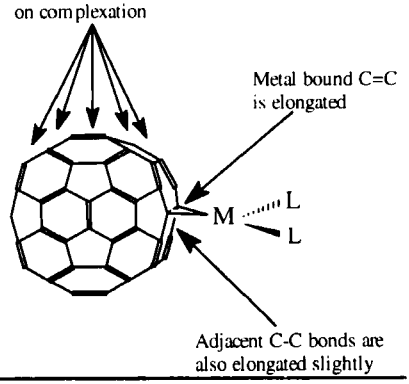

[a] For multimetallic adducts, this corresponds to the average C=C ····· M bond length.
[b] Corresponds to the C=C bond that complexes to the metal.

TABLE IX

θ VALUES FOR SOME Pt–ALKENE COMPLEXES

θ	Compound
31°	C_{60}
41°	$[Pt(PPh_3)_2(\eta^2\text{-}C_{60})]$
0°	Alkenes
22–35°	Most Pt–alkenes

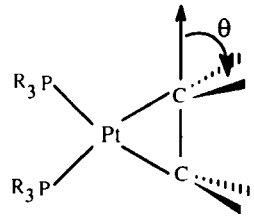

pane and is consistent with the presence of high-field fullerene ^{13}C NMR chemical shifts. The remaining CC bonds are little altered, with the other [6,6] fusions having a length of ≈1.40 Å and the [6,5] fusions of ≈1.45 Å, comparable with those for C_{60} of 1.39 and 1.45 Å, respectively (*92*). The C(sp^2)—C(sp^3) bonds do show some lengthening and increase to a value of ≈1.5 Å.

The two metal bound carbon atoms are also pulled out from the cage, consistent with the change in hybridization to sp^3 (*7*). The degree of "pullout," defined as the angle θ between the C–C axis and the plane containing one of these carbon atoms and its two neighboring sp^2 carbon atoms, is a useful guide to the extent of π back-donation and increases with back-bonding.

5. Dynamic Behavior of the Metal Fragment

The dynamic behavior of the metal moiety on the fullerene surface has only been briefly investigated. However, there is growing evidence that some complexes may be fluxional, with the metal fragment migrating over the surface of the sphere, i.e., globe-trotting, via a dissociative equilibration. Preliminary $^{31}P\{^1H\}$, ^1H, or ^{13}C NMR studies on the multimetallic complexes $[Ru(\eta\text{-}C_5Me_5)(CH_3CN)_2]_3(C_{60})]^{3+}(O_3SCF_3^-)_3$ (*12*), $[\{Ir(CO)(PMe_2Ph)_2Cl\}_2(\eta^2,\eta^{2'}\text{-}C_{70})]$ (*18*), $[\{Ir(CO)(PEt_3)_2Cl\}_2(\eta^2,\eta^{2'}\text{-}C_{60})]$ (*33*), $[C_{60}\{Pt(PEt_3)_2\}_n]$ (n = 2, 6) (*16*), and $[Pd(PR_3)_2(\eta^2\text{-}C_{60})]$ (*25*) showed the presence of mixtures of interconverting regioisomers. For $[\{Ir(CO)(PEt_3)_2Cl\}_2(\eta^2,\eta^{2'}\text{-}C_{60})]$, the equilibria could be slowed down sufficiently at low temperatures to allow spectroscopic detection of both free and bound $IrCl(CO)(PEt_3)_2$ (Fig. 12). In solutions of $[C_{60}\{Pt(PEt_3)_2\}_6]$, Fagan postulated that the ability to trap the $Pt(PEt_3)_2$ by reaction with diphenylacetylene and the fact that mixtures of regioisomeric diadducts only gave rise to one highly symmetric hexaadduct were indicative of a dis-

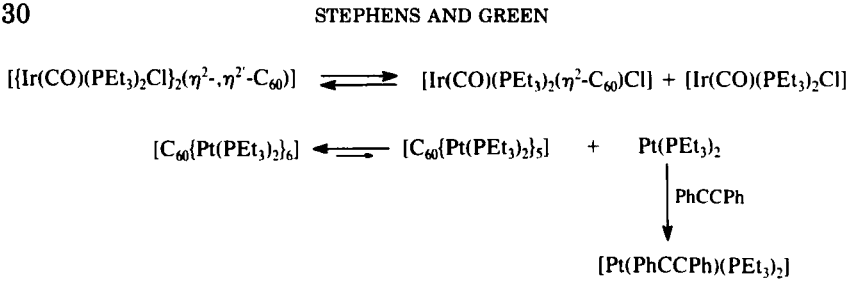

FIG. 12. Examples of metal–fullerene dissociative equilibria.

sociative dynamic equilibrium. In these and other complexes, e.g., $\{Ru(\eta\text{-}C_5Me_5)(CH_3CN)_2\}_3(C_{60})\}^{3+}(O_3SCF_3^-)_3$ and $[\{Ir(CO)(PMe_2Ph)_2Cl\}_2(\eta^2,\eta^{2'}\text{-}C_{70})]$, such a dynamic equilibrium has been invoked to explain the interconversion or preferential crystallization of certain regioisomers. All these systems often involve complicated equilibria in which both the rate and equilibrium constant are very sensitive to temperature.

For $[Pd(PR_3)_2(\eta^2\text{-}C_{60})]$ (PR_3 = PPh_3, PEt_3, PMe_2Ph, PPh_2Me, $P(OMe)_3$, or $\frac{1}{2}$dppe) preliminary ^{13}C NMR studies showed that the metal fragment migrates over the surface of the fullerene via a dissociative process (*25*). In the cases of $[M(NO)(PPh_3)_2(\eta^2\text{-}C_{60})]$ (M = Co or Rh), it is believed that metal migration over the surface of the fullerene also takes place to a small extent via an additional intramolecular route, as shown in Fig. 13. The mechanism was investigated using variable-temperature and 2-D EXSY ^{13}C NMR (*27*). Using the former technique for each complex, the fullerene ^{13}C NMR spectrum underwent a change

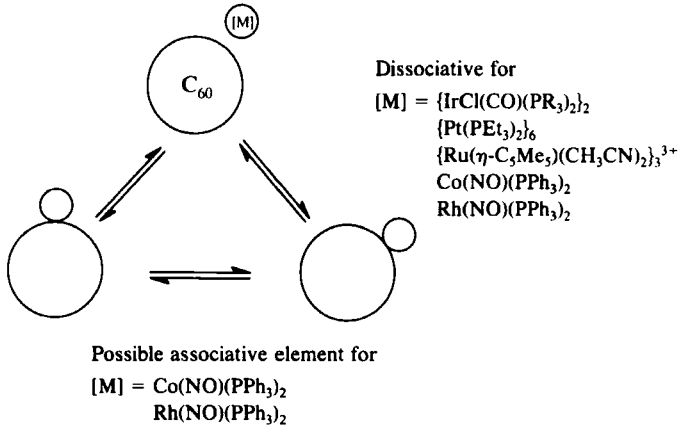

FIG. 13. The fluxional processes present in some fullerene complexes.

from 17 lines (C_{2v} symmetry) to one broad line at above room temperature, which is consistent with all the fullerene carbon atoms becoming equivalent. The 2-D ^{13}C EXSY spectrum of $[Co(NO)(PPh_3)_2(\eta^2\text{-}C_{60})]$ showed cross peaks that were only consistent with a dominant 1,3 shift process: that is, the metal migrating to adjacent double bonds. The cross peak intensities are most consistent with intramolecularity, and furthermore are consistent with a transition state that involves the Co atom binding to two C=C bonds and the nitrosyl temporarily acting as a 1 e^- donor.

Often for double addition reactions, despite the presence of many regioisomers in solution, only one isomer crystallizes out in high yields. This is the para diadduct, which, with its high symmetry and low polarity, exhibits lower solubility (*33*). Preferential crystallization of the high-symmetry tetra- and hexaadducts $[\{Ir_2(\mu\text{-}Cl)_2(1,5\text{-}C_8H_{12})_2\}_2(\eta^2\text{-}, \eta^{2'}\text{-}C_{60})]$ (*21*) and $[C_{60}\{Pt(PEt_3)_2\}_6]$ (*16*) has similarly been accounted for in these terms, with the high yields due to a dynamic equilibration between the various regioisomers.

As fullerenes behave as typical weakly π-electron withdrawing alkenes, it is not surprising that some metal complexes undergo alkene rotation. The observation of only one carbonyl signal in the ^{13}C NMR of $[M(CO)_4(\eta^2\text{-}C_{60})]$ (M = Fe or Ru) (*22, 26*) is consistent with the metal moiety undergoing concomitant metal–fullerene rotation and Berry rearrangement. Furthermore, for $[M(NO)(PPh_3)_2(\eta^2\text{-}C_{60})]$ (M = Co or Rh) and $[Ru(NO)(PPh_3)_2(\eta^2\text{-}C_{60})H]$, the low-temperature ^{13}C NMR spectra show fullerene resonances consistent with C_s symmetry, and hence a static structure, but on warming change to a C_{2v} structure with concomitant fullerene metal bond axis rotation (*22*). Figure 14 shows this change in the ^{13}C NMR spectrum of $[Rh(NO)(PPh_3)_2(\eta^2\text{-}C_{60})]$ between −90°C and +20°C, as well as the process of metal fragment migration over the fullerene surface.

B. σ-Bonded Complexes

Most of the σ-bonded organometallics that have been characterized structurally (mainly by ^{13}C NMR) involve bonding to the fullerene at adjacent carbon atoms, i.e., 1,2 addition. Such is the case for the osmate esters, $C_{60}(Bu^t)(Li)$ (*49*) and $C_{60}S_2Fe_2(CO)_6$ (*53*), which are illustrated in Fig. 15. Occasionally 1,4 addition occurs as for $C_{60}\{Re(CO)_5\}_2$ (*50*) and substitution of Li in $C_{60}(Bu^t)(Li)$ with bulky electrophiles.

For $C_{60}(Bu^t)(Li)$ the Bu^t rotation can be hindered sufficiently at lower temperatures on the ^1H NMR time scale to allow the individual methyl group signals to be resolved (*49*).

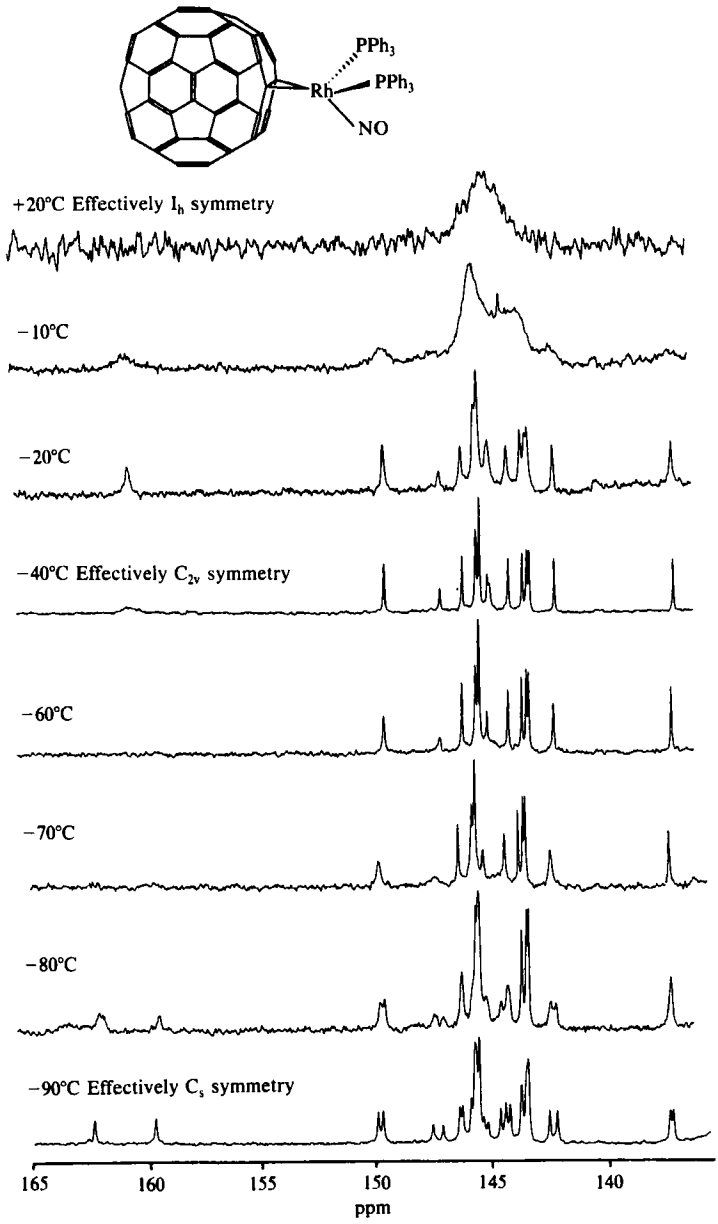

FIG. 14. $^{13}C\{^1H\}$ NMR spectrum in the fullerene sp^2 carbon atom region of [Rh(NO)$(PPh_3)_2(\eta^2\text{-}C_{60})$] between −90 and +20°C in C_4D_8O.

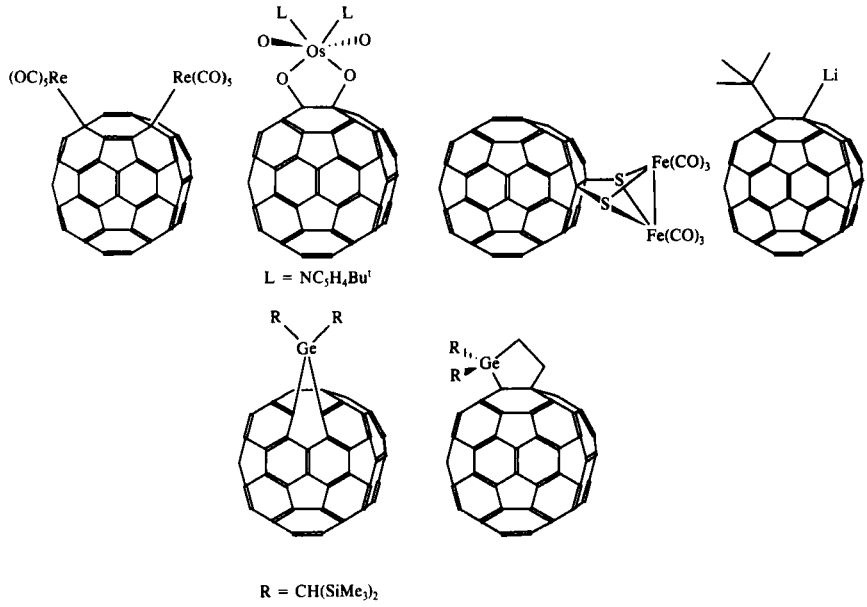

FIG. 15. The structure of some σ-bonded fullerene organometallics.

V. Effects on Bonding of Metal Complexation

This section briefly discusses the effect of metal complexation on the electronic structure of C_{60} and draws together some information that has been presented in previous sections.

In terms of the Dewar–Chatt model of bonding, for π metal complexation one double bond is effectively removed from the fullerene conjugation system due to extensive interaction between metal *d* orbitals and the fullerene HOMO and LUMO (*7*). The remaining 29 double bonds then behave almost identically to uncomplexed C_{60} with their IR, Raman, UV-vis, and ^{13}C NMR spectra showing only slight perturbations, mainly as a result of diminution of symmetry effects. Nevertheless, it is important to state that the fullerene metal interaction is not confined purely to the former's HOMO and LUMO, and that other molecular orbitals are energetically suitable for interaction (*89, 90*). The spectroscopic evidence cited for the preceding statement is as follows:

1. Electrochemical studies: Adducts undergo similar electrochemical processes, with reduction couples shifted to slightly more negative potentials owing to the lower electron affinity of the cage. This is due to

the removal of one double bond from the π system, as well as the metal inductively donating some electron density into the σ-bond framework. Further shifts to even more negative potentials are observed on increasing metal addition for the species $[C_{60}\{M(PEt_3)_2\}_n]$ (M = Ni, Pd, Pt; n = 1–6) (*84*). Shapley monitored changes in the UV-vis spectrum, in the ν(CO) stretch in the IR spectrum, and in the surface-enhanced Raman spectrum for $[Ir(\eta^5\text{-}C_9H_7)(CO)(\eta^2\text{-}C_{60})]$ on reduction to the monoanion and the dianion (*74, 75*). He found only slight shifts on anion formation that were also consistent with the negative charges residing mainly on the fullerene.

2. Raman studies on $[M(PPh_3)_2(\eta^2\text{-}C_{60})]$ and $[C_{60}\{M(PEt_3)_2\}_n]$ (M = Ni, Pd, Pt; n = 1, 6) showed slight shifts to lower wavenumbers, suggesting some M $\rightarrow \pi^*$ back-bonding (*17*).

3. Mössbauer studies on $[Ir(CO)(PPh_3)_2(\eta^2\text{-}C_{60})Cl]$ (*87*) and $[Fe(CO)_4(\eta^2\text{-}C_{60})]$ (*88*) indicated that C_{60} is only slightly perturbed but is a weak π acceptor.

4. Diffraction studies showed only slight changes in fullerene C–C bond lengths and angles.

5. UV-vis spectroscopy showed only small changes on complexation.

Because the fullerene hemisphere not directly involved in metal bonding is little altered by metal complexation, it is not surprising that multimetallic adducts can be formed. However, the strength of fullerene–metal bonding, the size of the addend, and the ease of dissociation also play a part in determining the likelihood of isolating such a species.

Various calculations have shown that fullerenes will form especially strong bonds to electron-rich metal centers. This has been attributed to (a) favorable relief of bond strain and (b) electron-withdrawing fullerene having MOs highly energetically suitable for interaction. For harder metal centers such as Ag^+, calculations have shown that the interaction is much weaker (*89, 90*).

In terms of π complex vs metallocyclopropane formalism, there has been little discussion. However, the $\delta(^{13}C)$ chemical shifts values suggest intermediates tending toward metallocyclopropane behavior.

For σ complexes, similar bonding conclusions concerning the uncomplexed portion of the cage have been drawn. There is debate, however, over the extent of σ covalency between C_{60} and [M] for [M] = Li or Mg. Charge delocalization does occur and explains the formation of 1,4 adducts with bulky electrophiles. Radical center delocalization occurs in many RC_{60} species.

VI. Physical Properties and Chemical Reactivity

All adducts tend to be red/brown or green powders that are moderately and very air sensitive in the solid state and solution, respectively. Generally, they dissolve poorly in aromatic hydrocarbons and sometimes thf to give intensely green or red colored solutions. These are sometimes thermally unstable at room temperature and liberate C_{60} on standing at room temperature.

A. Reactions of π Complexes

The π-organometallics show a reactivity pattern typical of an alkene bound weakly to a metal center. The C_{60} moiety may be displaced easily by a variety of donor ligands such as CO or PR_3 (R = OMe, Ph), and indeed many of the complexes are very air and water sensitive. Reactions can be monitored easily by the color change from the intense red or green of the adduct to the characteristic purple color of the free C_{60} molecule; the other products tend to have much lower extinction coefficients [Eqs. (11) and (12)] (*15, 26*).

$$\underset{\text{deep red}}{[Ru(CO)_4(\eta^2\text{-}C_{60})]} + CO \longrightarrow [Ru(CO)_4(PPh_3)] + \underset{\text{purple}}{C_{60}} \tag{11}$$

$$\underset{\text{deep green}}{[Ir(\eta^5\text{-}C_9H_7)(CO)(\eta^2\text{-}C_{60})]} + CO \longrightarrow [Ir(\eta^5\text{-}C_9H_7)(CO)_2] + \underset{\text{purple}}{C_{60}} \tag{12}$$

The stability of solutions of the complexes varies widely. Some adducts, such as $[Ir(CO)(PPh_3)_2(\eta^2\text{-}C_{60})Cl]$ (*13*) [Eq. (13)], readily revert to starting materials on dissolution in certain solvents or on thermolysis, whereas others, such as $[Os_3(CO)_{10}(PPh_3)(\eta^2\text{-}C_{60})]$ [Eq. (14)] (*32*), are sufficiently robust that other ligands may be preferentially displaced:

$$[Ir(CO)(PPh_3)_2Cl] + C_{60} \underset{CH_2Cl_2}{\overset{C_6H_6}{\rightleftharpoons}} [Ir(CO)(PPh_3)_2(\eta^2\text{-}C_{60})Cl] \tag{13}$$

$$[Os_3(CO)_{10}(PPh_3)(\eta^2\text{-}C_{60})] \xrightarrow{\text{i) } PPh_3 \text{ ii) } Me_3NO} [Os_3(CO)_9(PPh_3)_2(\eta^2\text{-}C_{60})] \tag{14}$$

Weakly basic ligands such as alkenes and acetylenes only occasionally displace the fullerene [Eqs. (15)–(17)]:

$$[Ir(\eta^5\text{-}C_9H_7)(CO)(\eta^2\text{-}C_{60})] + C_2H_2 \longrightarrow \text{No reaction} \quad (15)$$

$$[Mo(\eta\text{-}C_5H_5)_2(\eta^2\text{-}C_{60})] + C_2Ph_2 \longrightarrow \text{No reaction} \quad (16)$$

$$[C_{60}\{Pt(PEt_3)_2\}_6] + C_2Ph_2 \longrightarrow [C_{60}\{Pt(PEt_3)_2\}_5] + [Pt(PPh_3)_2(C_2Ph_2)] \quad (17)$$

Except for the reaction between $[Ir(\eta^5\text{-}C_9H_7)(CO)(\eta^2\text{-}C_{60})]$ and CO, which is associative (*15*), all the other displacements are believed to be dissociative. As discussed in Section IV,A,5, there is much evidence for the equilibrium shown in Eq. (18), which is the first step in such a mechanism:

$$[M]C_{60} \rightleftharpoons [M] + C_{60} \quad (18)$$

For $[C_{60}\{Pt(PEt_3)_2\}_6]$, Fagan trapped the dissociated metal fragment $Pt(PEt_3)_2$ by complexation with diphenylacetylene to give $[Pt(PEt_3)_2(\eta^2\text{-}C_2Ph_2)]$ (*7*). Similarly, ^{31}P NMR studies carried out on the system $[\{Ir(CO)(PEt_3)_2Cl\}_2(\eta^2,\eta^{2'}\text{-}C_{60})]$ (*33*) suggested that the following equilibria exist (Scheme 6).

Nagashima found an unusual route to $M(PR_3)_2(\eta^2\text{-}C_{60})$ (M = Pd or Pt; R = Et, Ph, OMe, etc.) by addition of PR_3 to the insoluble polymeric materials $C_{60}M_n$ (M = Pd or Pt, $n \approx 1$) [Eq. (19)] (*25, 31*).

$$C_{60}M + 2PR_3 \longrightarrow [M(PR_3)_2(\eta^2\text{-}C_{60})] \quad (19)$$
(M = Pd or Pt)
(PR_3 = PEt_3, PPh_3, ½dppe, PMe_2Ph, $PMePh_2$, $P(OMe)_3$)

Attempts to further functionalize the fullerene cage have not proved successful. Surprisingly, there have been no reports of multimetallic adducts involving two different metal moieties. For those reactions investigated, what tends to happen is that the second moiety displaces the first, as in the case of $[Co(NO)(PPh_3)_2(\eta^2\text{-}C_{60})]$ reacting with $[Mo(\eta\text{-}C_5H_5)_2H_2]$ to produce $[Mo(\eta\text{-}C_5H_5)_2(\eta^2\text{-}C_{60})]$ (*27*). Similarly, addition of an organic moiety to a π complex fails, and instead the metal addend

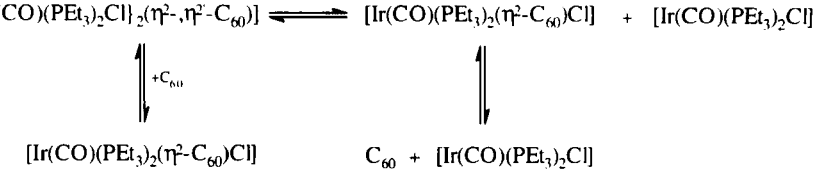

SCHEME 6. Equilibria present in solutions of $[\{Ir(CO)(PEt_3)_2Cl\}_2(\eta^2,\eta^{2'}\text{-}C_{60})]$.

is displaced, with a purely organic fullerene adduct forming. However, it is interesting to note that treatment of a stoichiometric mixture of C_{60}/[$Pd(PPh_3)_4$]/$Ph_2PCH_2CH_2PPh_2$ with $CH_2{=}(CH_2OAc)CH_2SiMe_3$ resulted in the formation of the organic illustrated in Eq. (20). No reaction occurred when C_{60} was mixed purely with the organic or in the presence of a catalytic amount of a Pd catalyst, suggesting that some functionalization of organometallics may be possible (*93*).

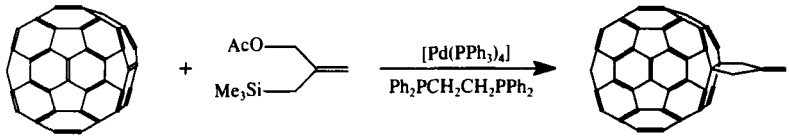

(20)

$C_{60}CMe(OMe)$ has been synthesized by reaction of the Fischer carbene [$Cr(CO)_5$(=CMe(OMe))] with C_{60} and is believed to involve initial η^2 coordination of the Cr center to C_{60} (*94*).

Although several alkene analogues of the π-fullerene organometallics are active catalysts, only for [$Rh(CO)(PPh_3)_2(\eta^2\text{-}C_{60})H$] has catalytic activity been investigated. It was found to have similar activity to [$Rh(CO)(PPh_3)_3H$] for alkene hydroformylation (*95*). The incompletely characterized polymers $C_{60}M_n$ (M = Pd, $n \geq 3$; M = Pt, n = 1,2) showed some activity toward heterogeneous hydrogenation of alkenes and acetylenes (*31, 96*).

B. Reactions of σ Complexes

The chemical reactions of σ complexes can be divided into two types: those that involve substitution of the metal center by an electrophile, and those that involve the reaction of the fullerene core with excess nucleophile.

The first category has proved an increasingly popular route to the initial functionalization of fullerenes, and some reactions are illustrated in Scheme 7. Incoming electrophiles are invariably H^+ or an alkyl group. For instance, acidification of $C_{60}(Bu^t)(Li)$ produces $C_{60}H_2$, whose pK_a shows it to be one of the strongest acids known, composed purely of carbon and hydrogen (*49*). Acidification of $C_{60}(H)(Zr(\eta\text{-}C_5H_5)_2Cl)$ has produced $C_{60}H_{2n}$, n = 1–3 (*63, 64*). An interesting series of phosphine adducts $C_{60}(H)(PRR')$ (R = R′ = chiral alkyl group) have been prepared by reaction of C_{60} with RR′(BH_3)P-Li followed by acidification (*60*). The resulting ligand can complex to BH_3, $PtCl_2$, and $PdCl_2$

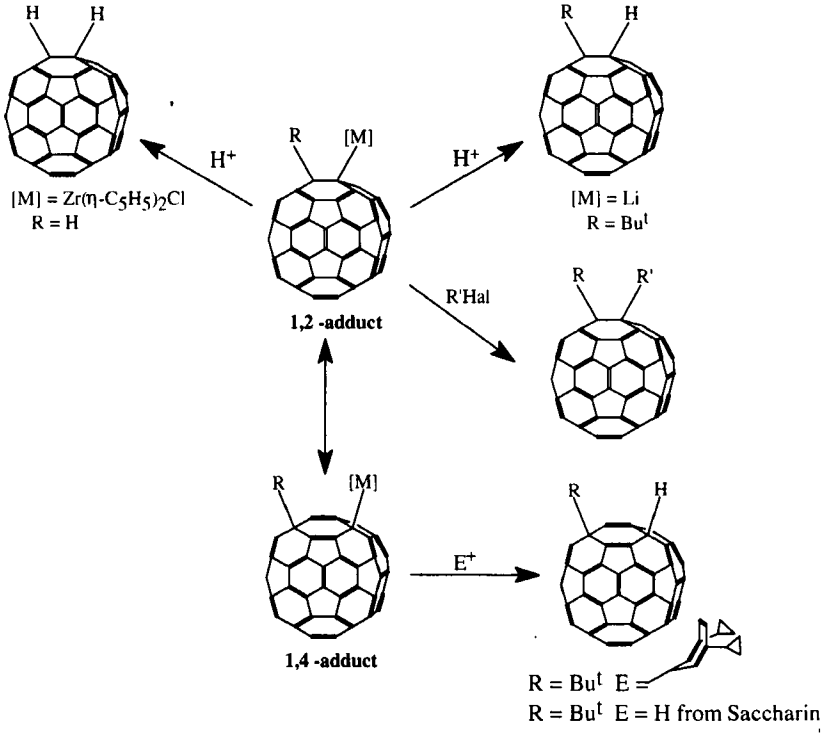

SCHEME 7. Some electrophilic substitution reactions of alkyl fulleride anions.

via its P atom. Most additions tend to be 1,2, but occasionally 1,4 addition can occur, especially with bulky electrophiles.

Although alkyl fulleride anions are a useful synthon, they are sometimes difficult to prepare because of side reactions and are often not as reactive as might be expected. The high electronegativity of fullerenes and resonance stabilization of a radical center over the cage mean that fullerenes are "radical sponges." As such, competing radical side reactions occur in the synthesis of alkyl fullerides because of abstraction of an electron from the incoming nucleophile R^-. Low anion reactivity toward electrophiles is a result of large steric bulk and resonance stabilization of the negative charge. This delocalization also means that mixtures of 1,2 and 1,4 regioisomers often also occur. Some adducts are thermally unstable: $C_{60}\{Re(CO)_5\}_2$ reverts to $[Re_2(CO)_{10}]$ and C_{60} on standing at room temperature (*50*).

The second type of chemical behavior is reaction with excess nucleophile, which can often be a problematic competing side reaction in

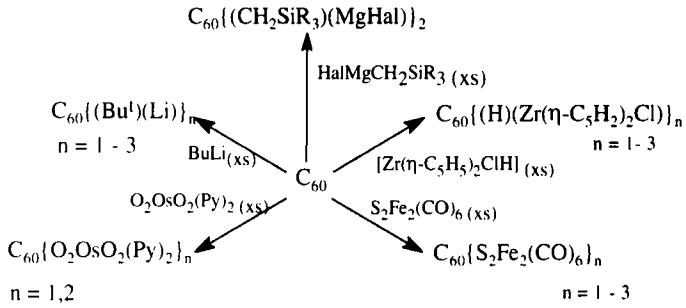

SCHEME 8. Multiple addition reactions of σ-fullerene organometallics.

the synthesis of monoadducts. Only a few multiple adducts have been partially characterized, as shown in Scheme 8, and only for $C_{60}(O_2OsO_2(4\text{-}Bu^tC_5H_4N)_2)_2$ (*48*) is the structure known with any certainty. For the functionalization of the organic side chain, basic/nucleophilic reagents cannot be used, as they preferentially react with the fullerene core.

VII. Conclusion

Overall, fullerenes and especially C_{60} show a chemical reactivity very similar to that of bulky electron-deficient alkenes. They readily react with many electron-rich metal centers to form stable π or σ complexes. With either bulky or less electron-rich centers, they show a reduced reactivity and form much less stable complexes.

Although the π complexes have not yet found any practical uses, they have proved helpful in structural characterization, as well as providing some insight into the dynamical behavior of fullerenes. The σ complexes are a relatively unexplored area, but where they have been prepared, they are useful intermediates in the preparation of organic fullerene adducts.

ACKNOWLEDGMENTS

The authors are grateful to their fellow workers Drs. R. E. Douthwaite, J. F. C. Turner, and W. Bidell and to Lincoln College, Oxford, for a J.R.F. to A.H.H.S.

List of Abbreviations

Ac	Acetyl
acac	2,4-Pentanedionate
COD	Cyclooctadiene
dba	1,5-Diphenyl-1,4-pentadien-3-one
EXSY	Exchange spectroscopy
Fc	Ferrocene
HPLC	High-pressure liquid chromatography
HOMO	Highest occupied molecular orbital
INADEQUATE	Incredible natural abundance double quantum transfer experiment
LUMO	Lowest occupied molecular orbital
NLO	Nonlinear optical
thf	Tetrahydrofuran
TMS	Trimethylsilyl
ΔH_f°	Standard heat of formation

References

1. Hebard, A. F.; Rosseinsky, M. J.; Haddon, R. C.; Murphy, D. W.; Glarum, S. H.; Palstra, T. T. M.; Ramirez, A. P.; Kortan, A. R. *Nature* **1991,** *350,* 600.
2. Braun, T. *Ang. Chem. Int. Ed.* **1992,** *31,* 588.
3. Dresselhaus, M. S.; Dresselhaus, G.; Eklund, P. C. *J. Mater. Res.* **1993,** *8,* 2054.
4. Rosseinsky, M. J. *J. Mater. Chem.* **1995,** *5,* 1.
5. Taylor, R.; Walton, D. R. M. *Nature* **1993,** *363,* 685.
6. Browser, J. R. *Adv. Organometal. Chem.* **1994,** *36,* 57.
7. Fagan, P. J.; Calabrese, J. C.; Malone, B. *Acc. Chem. Res.* **1992,** *25,* 134.
8. Bethune, D. S.; Johnson, R. D.; Salem, J. R.; de Vries, M. S.; Yannoni, C. S. *Nature* **1993,** *366,* 123.
9. Xie, Q.; Pérez-Cordero, E.; Echegoyen, L. *J. Am. Chem. Soc.* **1992,** *114,* 3978.
10. Xie, Q.; Arias, F.; Echegoyen, L. *J. Am. Chem. Soc.* **1993,** *115,* 9818.
11. Tang, N.; Guan, H.; Partanen, J. P.; Hellwarth, R. W. *SPIE Proc.* **1994,** *2143,* 272.
12. Fagan, P. J.; Calabrese, J. C.; Malone, B. *Science* **1991,** *252,* 1160.
13. Balch, A. L.; Catalano, V. C.; Lee, J. W. *Inorg. Chem.* **1991,** *30,* 3980.
14. Balch, A. L.; Catalano, V. C.; Lee, J. W.; Olmstead, M. M.; Parkin, S. R. *J. Am. Chem. Soc.* **1991,** *113,* 8953.
15. Koefod, R. S.; Hudgens, M. F.; Shapley, J. R. *J. Am. Chem. Soc.* **1991,** *113,* 8957.
16. Fagan, P. J.; Calabrese, J. C.; Malone, B. M. *J. Am. Chem. Soc.* **1991,** *113,* 9408.
17. Chase, B.; Fagan, P. J. *J. Am. Chem. Soc.* **1992,** *114,* 2252.
18. Balch, A. L.; Lee, J. W.; Olmstead, M. M. *Ang. Chem. Int. Ed.* **1992,** *31,* 1356.
19. Balch, A. L.; Catalano, V. C.; Lee, J. W.; Olmstead, M. M. *J. Am. Chem. Soc.* **1992,** *114,* 5455.
20. Balch, A. L.; Lee, J. W.; Noll, B. C.; Olmstead, M. M. *J. Am. Chem. Soc.* **1992,** *114,* 10984.
21. Rasinkangas, M.; Pakkanen, T. T.; Pakkanen, T. A.; Ahlgrén, M.; Rouvinen, J. *J. Am. Chem. Soc.* **1993,** *115,* 4901.
22. Douthwaite, R. E; Green, M. L. H.; Stephens, A. H. H.; Turner, J. F. C. *J. Chem. Soc. Chem. Commun.* **1993,** 1522.

23. Bashilov, V. V.; Petrovskii, P. V.; Sokolov, V. I.; Lindeman, S. V.; Guzey, I. A.; Struchkov, Y. T. *Organometal.* **1993,** *12,* 991.
24. Balch, A. L.; Lee, J. W.; Noll, B.C.; Olmstead, M. M. *Inorg. Chem.* **1993,** *32,* 3577.
25. Nagashima, H.; Yamaguchi, H.; Kato, Y.; Saito, Y.; Haga, M.; Itoh, K. *Chem. Letts.* **1993,** 2153.
26. Rasinkangas, M.; Pakkanen, T. T.; Pakkanen, T. A. *J. Organometal. Chem.* **1994,** *476,* C6.
27. Green, M. L. H.; Stephens, A. H. H. Unpublished results.
28. Balch, A. L.; Ginwalla, A. S.; Lee, J. W.; Noll, B. C.; Olmstead, M. M. *J. Am. Chem. Soc.* **1994,** *116,* 2227.
29. Balch, A. L.; Costa, D. A.; Lee, J. W.; Noll, B. C.; Olmstead, M. M. *Inorg. Chem.* **1994,** *33,* 2071.
30. Ishii, Y.; Hoshi, H.; Hamada, Y.; Hidai, M. *Chem. Letts.* **1994,** 801.
31. Nagashima, H.; Kato, Y.; Yamaguchi, H.; Kimura, E.; Kawanishi, T.; Kato, M.; Saito, Y.; Haga, M.; Itoh, K. *Chem. Letts.* **1994,** 1207.
32. Schreiner, S.; Gallaher, T. N.; Parsons, H. K. *Inorg. Chem.* **1994,** *33,* 3021.
33. Balch, A. L.; Lee, J. W.; Noll, B. C.; Olmstead, M. M. *Inorg. Chem.* **1994,** *33,* 5238.
34. Park, J. T.; Cho, J.-J.; Song, H. *J. Chem. Soc. Chem. Commun.* **1995,** 15.
35. Mavunkal, I. J.; Chi, Y.; Peng, S.-M.; Lee, G.-H. *Organometal.* **1995,** *14,* 4454.
36. Balch, A. L.; Costa, D. A.; Noll, B. C.; Olmstead, M. M. *J. Am. Chem. Soc.* **1995,** *117,* 8926.
37. Brady, F. J.; Cardin, D. J.; Domin, M. *J. Organometal. Chem.* **1995,** *491,* 169.
38. Balch, A. L.; Hao, L.; Olmstead, M. M. *Ang. Chem. Int. Ed.* **1996,** *35,* 188.
39. Balch, A. L.; Costa, D. A.; Noll, B. C.; Olmstead, M. M. *Inorg. Chem.* **1996,** *35,* 458.
40. Nagashima, H.; Nakaoka, A.; Saito, Y.; Kato, M.; Kawanishi, T.; Itoh, K. *J. Chem. Soc. Chem. Commun.* **1992,** 377.
41. Pradeep, T.; Kulkarni, G. U.; Kannan, K. R.; Guru Row, T. N.; Rao, C. N. R. *J. Am. Chem. Soc.* **1992,** *114,* 2272.
42. Roth, L. M.; Huang, Y.; Schwedler, J. T.; Cassady, C. J.; Ben-Amotz, D.; Kahr, B.; Freiser, S. J. *J. Am. Chem. Soc.* **1991,** *113,* 6298.
43. Huang, Y.; Freiser, B. S. *J. Am. Chem. Soc.* **1991,** *113,* 9418.
44. Huang, Y.; Freiser, B. S. *J. Am. Chem. Soc.* **1991,** *113,* 8186.
45. Jiao, Q.; Huang, Y.; Lee, S. A.; Gord, J. R.; Freiser, B. S. *J. Am. Chem. Soc.* **1992,** *114,* 2726.
46. Hawkins, J. M.; Loren, S.; Meyer, A.; Nunlist, R. *J. Am. Chem. Soc.* **1991,** *113,* 7770.
47. Hawkins, J. M.; Meyer, A.; Lewis, T. A.; Loren, S.; Hollander, F. J. *Science* **1991,** *252,* 312.
48. Hawkins, J. M.; Meyer, A.; Lewis, T. A.; Bunz, U.; Nunlist, R.; Ball, G. E.; Ebbesen, T. W.; Tanigaki, K. *J. Am. Chem. Soc.* **1992,** *114,* 7954.
49. Fagan, P. J.; Krusic, P. J.; Evans, D. H.; Lerke, S.A.; Johnston, E. *J. Am. Chem. Soc.* **1992,** *114,* 9697.
50. Zhang, S.; Brown, T. L.; Du, Y.; Shapley, J. R. *J. Am. Chem. Soc.* **1993,** *115,* 6705.
51. Hawkins, J. M.; Meyer, A.; Solow, M. A. *J. Am. Chem. Soc.* **1993,** *115,* 7499.
52. Hirsch, A.; Grösser, T.; Skiebe, A.; Soi, A. *Chem. Ber.* **1993,** *126,* 1061.
53. Westmeyer, M. D.; Galloway, C. P.; Rauchfuss, T. B. *Inorg. Chem.* **1994,** *33,* 4615.
54. Hawkins, J. M.; Nambu, M.; Meyer, A. *J. Am. Chem. Soc.* **1994,** *116,* 7642.
55. Ando, W. *Pure Appl. Chem.* **1995,** *67,* 805.
56. Wudl, F. In *Fullerenes Synthesis, Properties and Chemistry of Large Carbon Clusters;* ACS Symposium Series 48, 1992, 161–175.
57. Howard, J. A.; Tomietto, M.; Wilkinson, D. A. *J. Am. Chem. Soc.* **1991,** *113,* 7870.

58. Anderson, H. L,; Faust, R.; Rubin, Y.; Diederich, F. *Angew. Chem. Int. Ed.* **1994,** *33,* 1366.
59. Komatsu, K.; Murata, Y.; Takimoto, N.; Mori, S.; Sugita, N.; Wan, T. S. M. *J. Org. Chem.* **1994,** *59,* 6101.
60. Yamago, S.; Yanagawa, M.; Nakamura, E. *J. Chem. Soc. Chem. Commun.* **1994,** 2093.
61. Nagashima, H.; Terasaki, H.; Nakajima, K.; Itoh, K.; *J. Org. Chem.* **1994,** *59,* 1246.
62. Hirsch, A.; Soi, A.; Karfunkel, H. R. *Angew. Chem. Int. Ed.* **1992,** *31,* 766.
63. Ballenweg, S.; Gleiter, R.; Krätschmer, W. *Tet. Letts.* **1993,** *34,* 3737.
64. Ballenweg, S.; Gleiter, R.; Krätschmer, W., *J. Chem. Soc. Chem. Commun.* **1994,** 2269.
65. Beer, E.; Fuerer, M.; Knorr, A.; Mirlach, A.; Daub, J. *Angew. Chem. Int. Ed.* **1994,** *33,* 1087.
66. Diederich, F.; Isaacs, L.; Philp, D. *Chem. Soc. Rev.* **1994,** 243.
67. Creegan, K. M.; Robbins, J. L.; Robbins, W. K.; Millar, J. M.; Sherwood, R. D.; Tindall, P. J.; Cox, D. M.; Smith, A. B.; McCauley, J. P.; Jones, D. R.; Gallagher, R. T. *J. Am. Chem. Soc.* **1992,** *114,* 1103.
68. Elemes, Y.; Silverman, S. K., Sheu, C.; Kao, M., Foote, C. S.; Alvarez, M. M.; Whetten, R. L.; *Angew. Chem. Int. Ed.* **1992,** *31,* 351.
69. Win, W. W.; Kao, M.; Eiermann, M.; McNamara, J. J.; Wudl, F.; Pole, D. L.; Kassam, K.; Warkentin, J. *J. Org. Chem.* **1994,** *59,* 5871.
70. Prato, M.; Lucchini, V.; Maggini, M.; Stimpfl, E.; Scorrano, G.; Eiermann, M.; Suzuki, T.; Wudl, F. *J. Am. Chem. Soc.* **1993,** *115,* 8479.
71. Avent, A. G.; Kirkett, P. R.; Crane, J. D.; Darwish, A. D.; Langley, G. J.; Kroto, H. W.; Taylor, R.; Walton, D. R. M. *J. Chem. Soc. Chem. Commun.* **1994,** 1463.
72. Birkett, P. R.; Avent, A. G.; Darwish, A. D.; Kroto, H. W.; Taylor, R.; Walton, D. R. M. *J. Chem. Soc. Chem. Commun.* **1993,** 1230.
73. Stanton, R. E.; Newton, M. D. *J. Phys. Chem.* **1988,** *92,* 2141.
74. Zhang, Y.; Du, Y.; Shapley, J. R.; Weaver, M. J. *Chem. Phys. Lett.* **1993,** *205,* 508.
75. Koefod, R. S.; Xu, C.; Lu, W.; Shapley, J. R.; Hill, M. G.; Mann, K. R. *J. Phys. Chem.* **1992,** *96,* 2928.
76. Skiebe, A.; Hirsch, A. *J. Chem. Soc. Chem. Commun.* **1994,** 335.
77. Eiermann, M.; Wudl, F.; Prato, M.; Maggini, M. *J. Am. Chem. Soc.* **1994,** *116,* 8304.
78. Isaacs, L.; Haldimann, R. F.; Diederich, F. *Angew. Chem. Int. Ed.* **1994,** *33,* 2339.
79. Zhang, X.; Romero, A.; Foote, C. S. *J. Am. Chem. Soc.* **1993,** *115,* 11024.
80. Smith, A. B.; Strongin, R. N.; Brard, L.; Furst, G. T.; Romanov, W. L.; Owens, K. G.; Goldschmidt, R. J. *J. Chem. Soc. Chem. Commun.* **1994,** 2187.
81. Akasaka, T.; Mitshuida, E.; Ando, W.; Kobayashi, K.; Nagase, S. *J. Am. Chem. Soc.* **14994,** *116,* 2627.
82. Lawson, D. R.; Feldheim, D. L.; Foss, C. A.; Dorhout, P. K.; Elliott, C. M.; Martin, C. R.; Parkinson, B. *J. Electrochem. Soc.* **1992,** *139,* L68.
83. Fullagar, W. K.; Gentle, I. R.; Heath, G. A.; White, J. W. *J. Chem. Soc. Chem. Commun.* **1993,** 525.
84. Lerke, S. A.; Parkinson, B. A.; Evans, D. H.; Fagan, P. J. *J. Am. Chem. Soc.* **1992,** *114,* 7807.
85. Wilson, S. R.; Kaprinidis, N.; Wu, Y.; Schuster, D. I. *J. Am. Chem. Soc.* **1993,** *115,* 8495.
86. Wilson, S. R.; Wu, Y. *J. Am. Chem. Soc.* **1993,** *115,* 10344.
87. Vértes, A.; Gál, M.; Wagner, F. E.; Tuczek, F.; Gütlich, P. *Inorg. Chem.* **1993,** *32,* 4478.
88. Herber, R. H.; Bauminger, E.; Felner, I. *J. Chem. Phys.* **1996,** *104,* 1.
89. Lichtenberger, D. L.; Wright, L. L.; Gruhn, N. E.; Rempe, M. E. *J. Organometal. Chem.* **1994,** *478,* 213.

90. López, J. A.; Lealli, C. *J. Organometal. Chem.* **1994,** *478,* 161.
91. Baker, J.; Fowler, P. W.; Lazzeretti, P.; Malagoli, M.; Zanasi, R. *Chem. Phys. Letts.* **1991,** *184,* 182.
92. David, W. I. F.; Ibberson, R. M.; Matthewman, J. C.; Prassides, K.; Dennis, T.J. S.; Hare, J. P.; Kroto, H. W.; Taylor, R.; Walton, D. R. M. *Nature* **1991,** *353,* 147.
93. Shiu, L.; Lin, T.; Peng, S.; Her, G.; Ju, D.; Lin, S.; Hwang, J.; Mou, C.; Luh, T. *J. Chem. Soc. Chem. Commun.* **1994,** 647.
94. Merlic, C. A.; Bendorf, H. D. *Tet. Letts.* **1994,** *35,* 9529.
95. Claridge, J. B.; Douthwaite, R. E.; Green, M. L. H.; Lago, R. M.; Tsang, S. C.; York, A. P. E.; *J. Mol. Catal.* **1994,** *89,* 113.
96. Nagashima, H.; Nakaoka, A.; Tajima, S.; Saito, Y.; Itoh, K. *Chem. Letts.* **1992,** 1361.

This Page Intentionally Left Blank

ADVANCES IN INORGANIC CHEMISTRY, VOL. 44

GROUP 6 METAL CHALCOGENIDE CLUSTER COMPLEXES AND THEIR RELATIONSHIPS TO SOLID-STATE CLUSTER COMPOUNDS

TARO SAITO

Department of Chemistry, School of Science, The University of Tokyo, Tokyo 113, Japan

I. Introduction

The cluster complexes of the group 6 metals, molybdenum in particular, are very important because of their relationships to higher-dimensional systems such as the superconducting Chevrel phases (*1*) and bioclusters such as nitrogenase (*2*). Since the discovery of the Chevrel phase compounds, their unique and aesthetically pleasing structures have attracted the attention of many inorganic chemists. The structural motifs of the Chevrel clusters, consisting of six molybdenum atoms arranged in an octahedral array with chalcogen atoms capping all the triangular faces, are very similar to those in the historic cluster

compound Mo_6Cl_{12} (*3*). This may be one of the reasons for the special interest in these octahedral cluster complexes. Octahedral cluster compounds have played a great role in filling the gap between the molecular and solid-state inorganic chemistries (*4*). The preparation of molecular analogues of the Chevrel phases and their chromium and tungsten analogues has been a challenging target of cluster synthesis to solve some structural problems and to derive "chromium or tungsten Chevrels" starting from molecular clusters.

Nitrogenase is another big target of cluster synthesis. The X-ray elucidation of the active center of the Fe–Mo cofactor and P-cluster (*5*) has accelerated the efforts to find rational preparative methods of trinuclear or cubane-type clusters containing molybdenum (*6–9*). The raft cores in these cluster complexes are one of the general structural units also in solid-state compounds, and the mutual relationships are very important. A number of review articles are now available on the syntheses, structures, and other properties of metal chalcogenide cluster compounds (*6, 7, 10–24*).

The structural relationship between the molecular and solid-state compounds has been a hot issue in inorganic chemistry for some time (*25–27*). The extrusion (or excision) from preformed solid-state cluster compounds is one of the major synthetic methods of the preparation of cluster complexes (*26*). Use of cluster complexes as precursors to solid-state cluster compounds is the reverse reaction of excision. Both reactions utilize the structural similarity of the metal cluster units. The basic cluster units of polyhedra (deltahedra) or raft structures are triangles, and both molecular and solid-state clusters with octahedral, tetrahedral, and rhomboidal cores have been reported. Similarity of other properties such as electronic structures based on the cluster units is also important. The present review is concerned with the syntheses and structures of the cluster complexes of the group 6 metals and with their relationships to solid-state chemistry.

II. Octahedral Clusters

A. Synthesis

1. Chromium

Steigerwald *et al.* prepared the first octahedral chromium cluster $[Cr_6Te_8(PEt_3)_6]$ by the reaction of either $(C_3H_5)_2Cr(PEt_3)_2$ or (2,4-dimethyl-$C_5H_3)_2Cr$ with $TePEt_3$ and PEt_3. The yield in the latter reaction

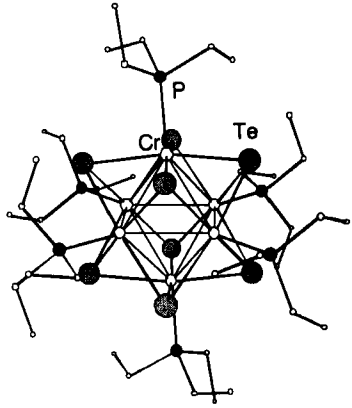

FIG. 1. Structure of $[Cr_6Tc_8(PEt_3)_6]$.

was 38% (*28*) (Fig. 1). This reaction is based on the properties of $TePEt_3$, which releases "atomic tellurium" and triethylphosphine because they are in equilibrium in solution (*29*). The formal oxidation state of chromium is changed from +2 to +2.67 (average).

$$TePEt_3 \rightleftharpoons Te + PEt_3$$

Similar reactions have been used for the synthesis of $[Co_6Te_8(PEt_3)_6]$ (*30*), $[Ni_9Te_6(PEt_3)_8]$, and $[Ni_{20}Te_{18}(PEt_3)_{12}]$ (*31*).

Sulfur and selenium analogues $[Cr_6E_8(PR_3)_6]$ (E = S, PR_3 = PEt_3, PMe_3; E = Se, PR_3 = PEt_3, PMe_3, PMe_2Ph) have been prepared by the reaction of $CrCl_2$ with either NaS_xH or Na_2Se_x in the presence of PR_3 in methanol (*32*). The reactions depend very much on the difference of phosphines, and the best yield (22%) is attained for the combination of sulfur and triethylphosphine. In the case of the sulfur complexes, Na_2S_x is not good, because only insoluble sulfides form. There are no trinuclear chromium chalcogenide complexes suitable for dimerization to form octahedral cluster complexes, and the self-assembly reaction of mononuclear chromium complexes is the only way to accomplish such syntheses at present. Selectivity is the key point for self-assembly reactions, and combinations of appropriate reagents should be necessary to attain good yields.

2. *Molybdenum*

The cluster cores Mo_6E_8 (E = S, Se, Te) are very similar to those of molybdenum dihalides MoX_2 (X = Cl, Br, I), and their derivatives

that have eight face-capping halides on the triangular Mo_3 faces of the Mo_6 octahedron (*3*). The substitution of the capping halides into chalcogenides was attempted starting from MoX_2 [= $(Mo_6X_8)X_2X_{4/2}$] to prepare the Mo_6E_8 cluster compounds, but only one or two of the eight chlorine atoms were substituted into chalcogen atoms (*33–36*). However, McCarley *et al.* accomplished complete substitution by reacting Mo_6Cl_{12} with NaSH and NaOBu in 1-butanol and pyridine to form $Na_{2x}Mo_6S_{8+x}(py)_y$ (*37*). This pyridine-deficient compound was refluxed in neat pyridine to produce $[Mo_6S_8(py)_6]$ as a brown crystalline compound (Fig. 2). Similar reactions in propylamine formed a propylamine derivative, and this in turn has been transformed into pyrrolidine or piperidine derivatives. Excess sulfiding agent was needed to produce a completely sulfur-substituted product. However, the initial product did not contain enough pyridine, and further treatment with pyridine was necessary to attain the right stoichiometry. The preceding reactions suggest that the face-capping halides are fairly inert to substitution into chalcogens and rather forcing reaction conditions are required.

Since the Mo_6E_8 framework is just a face-to-face dimer of the Mo_3E_4 clusters, dimerization of suitable Mo_3E_4 cluster complexes should lead to the octahedral cluster complexes. This type of fragment condensation has been realized by the synthesis of $[Mo_6E_8(PEt_3)_6]$ from $[Mo_3E_4Cl_4(PEt_3)_x(Sol)_{5-x}]$ (Sol = MeOH or thf). When the trinuclear cluster complex was treated with magnesium metal in thf, four terminal chlorine ligands were reductively abstracted and two trinuclear fragments condensed to give a hexanuclear cluster (*38*). The first synthesis used an isolated complex $[Mo_3S_4Cl_4(PEt_3)_4(MeOH)]$ (*39*), but later

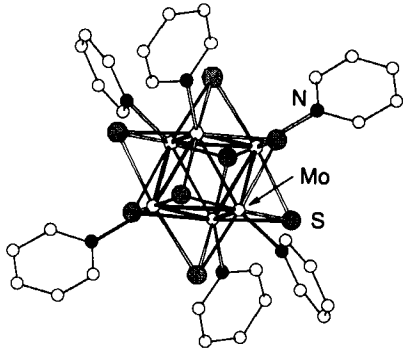

FIG. 2. Structure of $[Mo_6S_8(py)_6]$.

the reaction of a solid-state cluster compound $Mo_3E_7Cl_4$ with triethylphosphine, followed by magnesium reduction without the isolation of the intermediate, was employed (*40*). The yield has been at best 30% based on molybdenum, and by-products have not been identified. Although there is room for improvement in selectivity, fragment condensation using trinuclear building blocks will be useful for the construction of deltahedral cluster skeletons.

3. Tungsten

The first example of the tungsten cluster complexes of the type $[W_6E_8L_6]$ has been synthesized by the reductive condensation of a trinuclear tungsten cluster complex although the intermediate was not fully characterized (*41*). The starting compound was prepared by the reaction of W_6Cl_{12} with sulfur, which is probably $W_3S_7Cl_4$ (*42*). The solid-state cluster compound was excised by triethylphosphine in thf, and the product was reduced by magnesium metal to form $[W_6S_8(PEt_3)_6]$ in 10% yield.

More recently the substitution of the face-capping chloride into sulfide was achieved by Zhang and McCarley (*43*) and DiSalvo and coworkers (*44*). McCarley reacted W_6Cl_{12} with NaSH and NaOBu in refluxing pyridine for 2 days. The insoluble product was exhaustively extracted with methanol to give a dark red powder of $[W_6S_8(py)_6]$. DiSalvo used essentially the same combination of reactants and heated the mixture at 115°C for 4 days to obtain the same compound in 43% yield. A 4-*tert*-butylpyridine derivative (Fig. 3) was likewise prepared by using W_6Cl_{12}, KSH, KOBu, and 4-*tert*-butylpyridine in DMF at

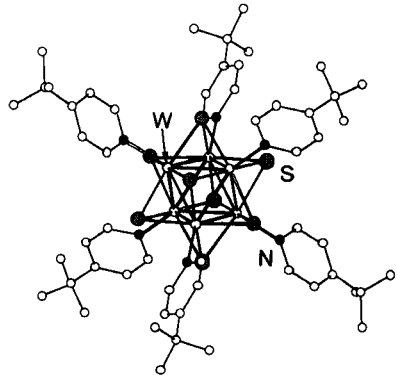

FIG. 3. Structure of $[W_6S_8(t\text{-Bupy})_6]$.

25°C for 6 days. The cluster complex is a little more soluble than the pyridine derivative.

B. Molecular Structure

1. Chromium

The chromium cluster complexes $[Cr_6E_8(PR_3)_6]$ (E = S, Se, Te) have the Cr_6E_8 cluster unit, consisting of a Cr_6 octahedron and eight face-capping chalcogen atoms (*28, 32*). One trialkylphosphine ligand coordinates to each chromium atom. The overall structures of the cluster cores are essentially octahedra with small distortions depending on the chalcogen and alkyl groups of the phosphine. The average Cr–Cr and Cr–E interatomic distances are listed in Table I.

Although the cluster units are not much different from those of the similar cluster $[M_6E_8(PR_3)_6]$ (M = Mo, W, Fe, Co) (*45*), some different features are clearly distinguishable. The differences are the metal–metal bond order and the distortion of the octahedra from a regular octahedron. Table II shows the Pauling bond order n, which is calculated by the equation $d(n) = d(1) - 0.6\log n$, where $d(n)$ refers to the average M–M distance and $d(1)$ to the single-bond distance calculated

TABLE I

Interatomic Distances (Å) in Octahedra of Metal and Ligating Atoms

Compound	M–M	Δ(M–M)	L–L	Δ(L–L)	Ref.
$[Cr_6S_8(PMe_3)_6]$	2.649–2.710	0.061	5.668–6.371	0.703	*32*
$[Cr_6S_8(PEt_3)_6] \cdot 2C_6H_6$	2.592–2.596	0.004	5.925–6.035	0.110	*32*
$[Cr_6Se_8(PMe_3)_6]$	2.723–2.787	0.064	5.784–6.435	0.651	*32*
$[Cr_6Se_8(PEt_3)_6]$	2.676–2.683	0.007	6.086–6.133	0.047	*32*
$[Cr_6Se_8(PMe_2Ph)_6]$	2.684–2.67	0.083	5.745–6.487	0.742	*32*
$[Cr_6Te_8(PEt_3)_6]$	2.896–2.953	0.057	6.258–6.456	0.198	*28*
$[Mo_6S_8(PMe_3)_6]$	2.635–2.637	0.002	5.875–6.470	0.595	*48a*
$[Mo_6S_8(PEt_3)_6]$	2.662–2.664	0.002	6.179–6.291	0.112	*40*
$[Mo_6S_8(PMe_2Ph)_6]$	2.678–2.694	0.016	6.005–6.602	0.596	*48a*
$[Mo_6Se_8(PEt_3)_6]$	2.701–2.708	0.007	6.190–6.402	0.218	*40*
$[PPN][Mo_6S_8(PEt_3)_6]$	2.664–2.677	0.013	6.028–6.522	0.494	*40*
$[PPN][Mo_6Se_8(PEt_3)_6]$	2.703–2.718	0.015	6.122–6.555	0.433	*40*
$[Mo_6S_8(py)_6] \cdot 2py$	2.640–2.647	0.007	5.871–6.047	0.176	*37*
$[Mo_6S_8(pip)_6] \cdot 7pip$	2.637–2.658	0.021	5.751–6.070	0.319	*37*
$[Mo_6S_8(pyrr)_6] \cdot pyrr$	2.635–2.672	0.037	5.543–6.013	0.470	*37*
$[W_6S_8(PEt_3)_6]$	2.678–2.681	0.003	6.174–6.310	0.136	*41*
$[W_6S_8(py)_6]$	2.654–2.667	0.013	5.748–5.932	0.184	*43, 44*
$[W_6S_8(t\text{-Bupy})_6] \cdot 6C_6H_6$	2.656–2.667	0.011	5.789–5.917	0.128	*44*

TABLE II

M–M BOND ORDER AND PBO/*e*

Compound	*d*(*n*)/Å (M–M av.)	Bond order n[a]	PBO/*e*[b]	Ref.
$[Cr_6S_8(PEt_3)_6]$	2.594	0.445	0.53	*32*
$[Cr_6Se_8(PEt_3)_6]$	2.680	0.320	0.38	*32*
$[Cr_6Te_8(PEt_3)_6]$	2.935	0.120	0.14	*28*
$[Mo_6S_8(PEt_3)_6]$	2.663	0.845	1.01	*40*
$[Mo_6Se_8(PEt_3)_6]$	2.703	0.724	0.87	*40*
$[W_6S_8(PEt_3)_6]$	2.680	0.841	1.01	*41*

[a] $d(n) = d(1) - 0.6 \log n$; $d(1)$ = 2.383 Å (Cr), 2.619 Å (Mo), 2.635 Å (W) (*46*).
[b] PBO/$e = n \times 4/(20/6)$.

from the M–M distance in bulk metals (*46*). When the ligands are sulfur and triethylphosphine, the bond order of the chromium cluster (0.445) is much smaller than those of molybdenum (0.845) or tungsten (0.841), but larger than that of cobalt (0.150). This indicates that the metal–metal bonding interaction in the chromium cluster complexes is much weaker than in the molybdenum or tungsten cluster analogues. Also, selenium and tellurium derivatives have still weaker bonding interaction. This is important for estimating the cause of the distortion of the Cr_6 cluster cores, which is discussed later.

The selected interatomic distances and angles for the chromium complexes are listed in Table I. The Cr—Cr bond lengths are considerably different among the six complexes, and the virtual symmetry of the Cr_6 octahedra is O_h in the PEt_3, D_{3d} in the PMe_3, and D_{2h} in the PMe_2Ph complexes (Fig. 4). In the PEt_3 complexes, the differences in intramolecular Cr–Cr distances are <0.02 Å, and the Cr_6 octahedra have pseudo-O_h symmetries. In contrast, the Cr_6 cores are antitrigonal prisms (D_{3d}) in the PMe_3 complexes, and the differences in intratriangle and intertriangle Cr–Cr distances are more than 0.06 Å both in sulfide and selenide PMe_3 complexes. The molecules of the PMe_2Ph complex have a crystallographically imposed inversion center, and there are six crystallographically independent Cr–Cr distances with 0.08 Å difference. A pair of the Cr–Cr distances is significantly longer than other five pairs, and the Cr_6 octahedron has D_{2h} symmetry in the PMe_2Ph complex.

The structures of the Cr_6 core are affected by the terminal phosphine ligands. The variation of the chromium octahedra contrasts with molybdenum clusters, which always have almost regular octahedral geometry. In a crystal, the structure of a molecule is influenced by steric

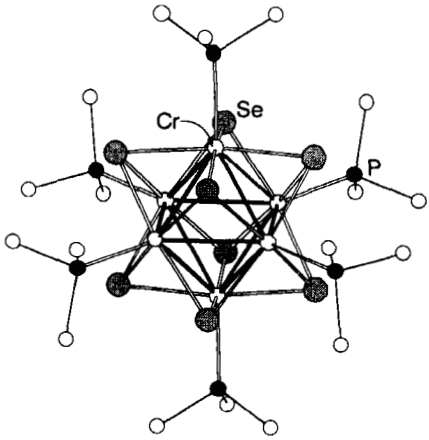

FIG. 4. Structure of $[Cr_6Sc_8(PMe_3)_6]$.

demand between neighboring molecules. The peripheral ligands play an important role in determining the whole structure of a molecule (*47, 48*). These chromium cluster complexes contact with each other through the alkyl groups of the phosphine ligands. The direct effects of crystal packing should be reflected in the positions of phosphorus atoms. Since the six phosphine ligands are at the terminal positions of the Cr_6 octahedron, they form a P_6 octahedron around the Cr_6 octahedron (Fig. 5). The P–P distances are listed in Table I. In all these compounds, the P_6 octahedron has the same virtual symmetry as the Cr_6 octahedron. By comparison of the Cr_6 and P_6 octahedra, it has become apparent that the distortion of the Cr_6 octahedra parallels the distortion of the surrounding P_6 octahedra, which is caused by the

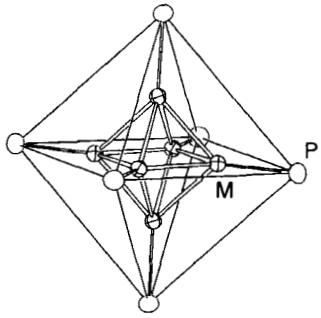

FIG. 5. Geometrical relation of the metal and phosphorus octahedra in $[M_6E_8(PR_3)_6]$ complexes.

crystal packing effect (*32*). Although the Cr_6 octahedra are affected by the P_6 octahedra, the Mo_6 octahedra in $[Mo_6E_8(PR_3)_6]$ are not much influenced by the crystal packing. As listed in Table I, the distortions of the P_6 octahedra in molybdenum derivatives with PMe_3 or PMe_2Ph are comparable to those of the chromium clusters (*48a*). Nevertheless, the Mo_6 octahedra in those complexes are as regular as in the PEt_3 derivative. This seems to imply that the Mo—Mo bonding is stronger than the Cr—Cr bonding, and that the Mo_6 octahedra are free from crystal packing distortion of the ligands.

2. Molybdenum

The Mo–Mo distances in the 20-electron clusters $[Mo_6E_8L_6]$ are nearly equal, and the cluster frameworks are regular octahedra (Table I). As these compounds form molecular crystals, the ranges of interatomic distances between the coordinating atoms forming coordination octahedra are included in the table to aid in estimating the nonbonding interaction of cluster molecules in the crystals. The figures in the table indicate that the molybdenum octahedra show little distortion even for complexes with considerable distortion of the coordination octahedra of the ligands. As described earlier, the Cr_6 octahedra in the chromium analogues are more susceptible to distortion because of the weakness of the Cr—Cr bonds. Therefore, the regular octahedra in the Mo_6 skeletons are characteristic of the 20-electron Mo_6E_8 clusters and are derivable from the electronic structure.

If the Mo—Mo bond order of the 24-electron Mo_6 clusters with 12 Mo—Mo bonds is taken to be unity, the bond order of the Mo—Mo bonds in the 20-electron clusters becomes 20/24 = 0.833 by a simple calculation. If $d(0)$ is 2.619 Å (*23*) in the Pauling bond order equation $d(n) = d(1) - 0.6 \log n$ (*49*), $d(20/24) = 2.619 - 0.6 \log (20/24) = 2.667$ Å, which is very close to the observed values for $[Mo_6E_8L_6]$ complexes in Table I. The bond orders are calculated by using the observed Mo–Mo distances and given in Table II. The Mo–Mo distance (average) in the 24-electron cluster $[(Mo_6Cl_8)Cl_4(PBu_3)_2]$ is 2.616 Å (*50*), showing that $n \approx 1$ and the bonds are two-center, two-electron single bonds. Although the Mo–Mo distances in the 21-electron clusters $[PPN][Mo_6E_8(PEt_3)_6]$ should be reduced judging from this simple electron–bond order relationship, the actual values (2.670 Å (av)) are somewhat larger than those of the 20-electron clusters. It may be possible to understand this situation from the Mo—Mo slightly antibonding nature of the LUMO in the $[Mo_6E_8(PH_3)_6]$ (*51*) (see Section II,C,2). It is very interesting to know the trend of bond distances for the further reduced clusters in case they are to be isolated and structurally characterized.

The comparison of the Mo–Mo distances in the sulfur and selenium complexes shows that the selenium analogues have longer (ca. 0.04 Å) distances. This can be explained by the larger intracluster matrix effect of selenium. This contrasts with the shorter average Mo–Mo distances for the selenium compounds in the solid-state Chevrel phases (*52*).

The bond order between a molybdenum atom and the coordinating atom of the exo ligands becomes smaller in the order P > S > N (*37*). The bond orders for the nitrogen ligands are about 0.5, showing that the bonds are fairly weak and the ligand displacement reactions are the easiest for the clusters with nitrogen ligands.

The infrared and Raman spectra of the $[Mo_6S_8L_6]$ complexes have been reported (*37*) (Table III). The infrared spectra have an Mo—S stretching band at 378–390 cm^{-1}, and the Raman spectra show a distinguishing sharp peak at 411–418 cm^{-1} that can be attributed to the A_{1g} totally symmetric Mo—S stretching mode. The broad band at 836 cm^{-1} in the piperidine complex is most likely the first overtone of the band at 411 cm^{-1}. The ligand-deficient propylamine and pyridine cluster complexes exhibit a broadened Mo—S band at 448 cm^{-1} that is described as due to the loss of the octahedral symmetry by loss of ligands (*37*).

The proton NMR spectra have been used for distinguishing coordinated and free ligands in crystals, and the spectra of the piperidine cluster complex have been analyzed in detail (*37*) and the peaks of each proton on the piperidine rings assigned using both 1-D and 2-D spectra. Conformational exchange between the boat and chair forms of the ligands was not observed.

TABLE III

VIBRATIONAL SPECTRA[a]

Compound	Infrared ν (M–S)	Raman ν (M–S) A_{1g} mode
$[Mo_6S_8(PEt_3)_6]$	390	416
$[Mo_6S_8(tht)_6]$	389	416
$[Mo_6S_8(pip)_6]$	382	411
$[Mo_6S_8(pyrr)_6]$	381	415
$[Mo_6S_8(PrNH_2)_{6-x}]$	384 (br)	418
$[Mo_6S_8(py)_6]$	378	418
$[W_6S_8(py)_6]$	378	

[a] In cm^{-1} (*37*).

3. *Tungsten*

The cores of the W_6 clusters are very similar to those of the Mo_6 analogues, and they are composed of the regular octahedra of six tungsten atoms capped by eight sulfur atoms (*41, 43, 44*). The W–W distances are almost the same, and difference in terminal ligands has little effect on the geometry (Table I). Only in the case of *tert*-butylpyridine complexes has a very small compression of the octahedron been observed in the *c*-axis direction (*44*). The bond order for the W—N bonds in the pyridine complexes is much weaker than that for the triethylphosphine analogue (*43*).

The strongest band at 378 cm^{-1} in the infrared spectrum of $[W_6S_8(py)_6]$ has been assigned to the T_{1u} W—S stretching mode of the W_6S_8 unit. The second bond at 231 cm^{-1} is attributed with some uncertainty to another set of T_{1u} modes involving either W—W or W—N stretching or W—S bending vibrations (*43*).

C. Electronic Structure

1. *Chromium*

The average Cr–Cr distance in PMe_3 complexes is longer than in the corresponding PEt_3 complexes (Table I). The DV (discrete–variational)-Xα calculations (*53–55*) on $[Cr_6S_8(PH_3)_6]$, which is a model compound of $[Cr_6S_8(PR_3)_6]$, have revealed that the molecular orbital levels are very sensitive to Cr–Cr distance (*32*). Energy levels have been calculated by changing the Cr–Cr distance and the Cr_6 symmetry for these four cases: (a) d(Cr–Cr) = 2.59 Å in O_h, (b) d(Cr–Cr) = 2.59 Å in D_{3d}, (c) d(Cr–Cr) = 2.69 Å in O_h, and (d) d(Cr–Cr) = 2.69 Å in D_{3d} (Fig. 6). The average Cr–Cr distance is 2.59 Å in $[Cr_6S_8(PEt_3)_6]$ and 2.69 Å in $[Cr_6S_8(PMe_3)_6]$. If the Cr–Cr distance is long (2.69 Å), a structure deformed in D_{3d} symmetry is favorable. The distortion of P_6 to D_{3d} symmetry required by crystal packing effects is transmitted to the Cr_6 to result in the distortion of the Cr_6 core in D_{3d} symmetry, and MO calculations indicate that the D_{3d} symmetry requires the elongation of the average Cr–Cr distance to gain some electronic energy. Similar calculations on the molybdenum congener have shown that a change in Mo–Mo distances does not cause any favorable effect on the change of the symmetry from O_h to D_{3d}, even with Mo–Mo distances 0.1 Å longer, and the cluster can always be in the low-spin state.

2. *Molybdenum*

The superconductivity of the Chevrel phases $M_xMo_6E_8$ has been attributed mainly to Mo_6E_8 cluster units, and M_x influences the critical

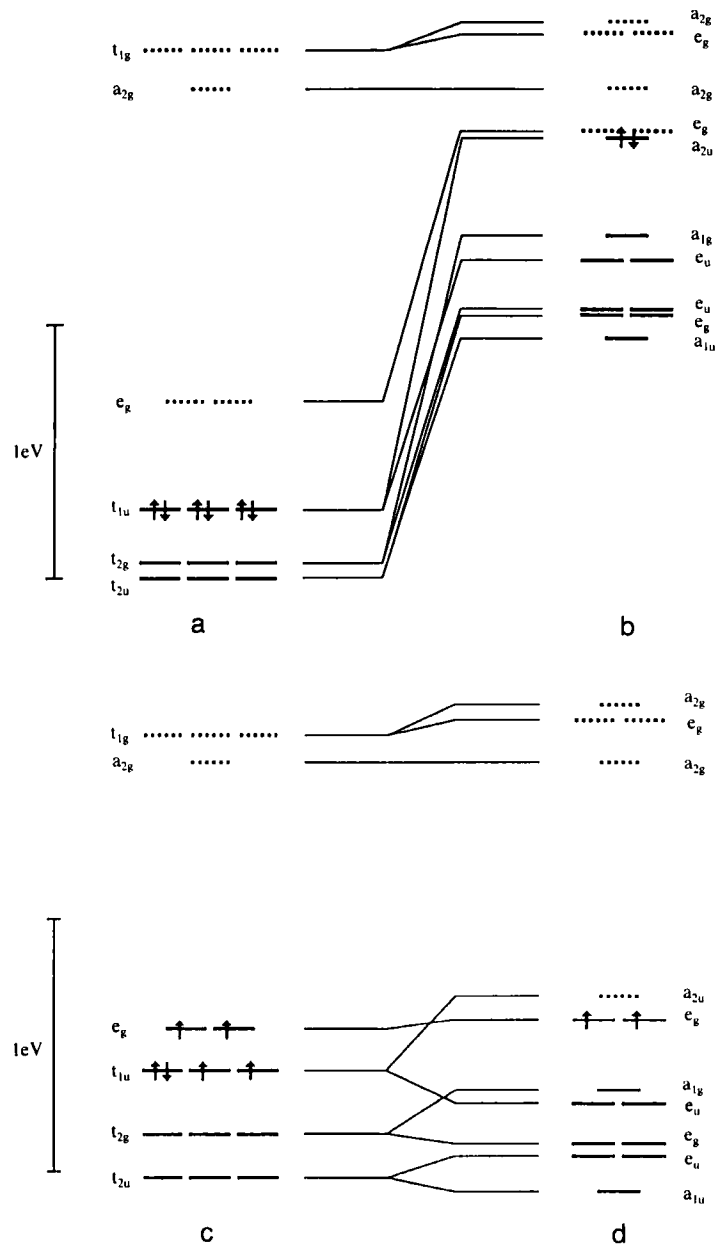

FIG. 6. MO of $[Cr_6S_8(PH_3)_6]$ for different Cr–Cr distance and symmetry. (a) d(Cr–Cr) = 2.59 Å, O_h; (b) d(Cr–Cr) = 2.59 Å, D_{3d}; (c) d(Cr–Cr) = 2.69 Å, O_h; (d) d(Cr–Cr) = 2.69 Å, D_{3d}.

temperature only indirectly (*56*). The Mo_6E_8 unit consists of an octahedron of six molybdenum atoms with eight chalcogen atoms capping the Mo_3 faces. The eight chalcogen atoms form a cube, and the molybdenum atoms are located in the center of each square face of the cube. In order to reduce the nonbonded repulsion between the chalcogen atoms of different cluster units, the chalcogen cubes are rotated about 26° (*57*). In this geometry, a face-capping chalcogen atom bonds to the molybdenum atom of the adjacent Mo_6 cluster unit (Fig. 7). Consequently each molybdenum atom has a square pyramidal coordination with five chalcogen atoms. The intracluster and intercluster Mo–E distances are almost identical (*52*). Because the Mo_6E_8 clusters are separated, the electronic structure of the cluster units is closely related to that of the solid-state Chevrel phases (*58*). MO calculation of the Mo_6S_8 cluster has been the subject of many studies (*51, 57, 59–65*). The molecular cluster complexes $[Mo_6E_8L_6]$ have structures with the exo positions blocked by neutral ligands L instead of the chalcogen atoms of the adjacent cluster units (*37, 40*) (Fig. 8).

Imoto has reported calculations of the electronic structures of the model compounds $[Mo_6E_8(PH_3)_6]$ (E = S, Se) by the DV Xα method (*53–55, 66*). O_h symmetry is assumed for the Mo_6 cluster. Stepwise calculations beginning from the Mo_6 cluster, followed by the inclusion

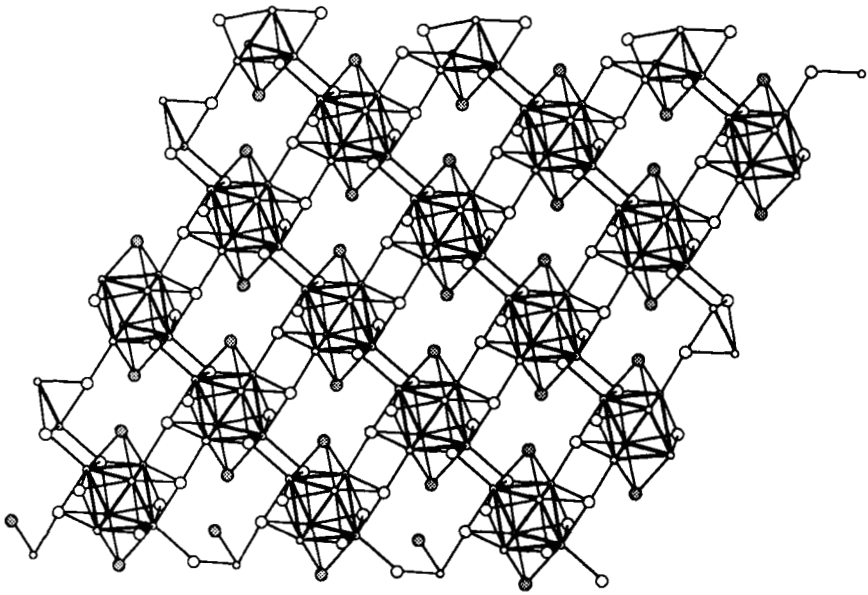

FIG. 7. Structure of Mo_6S_8.

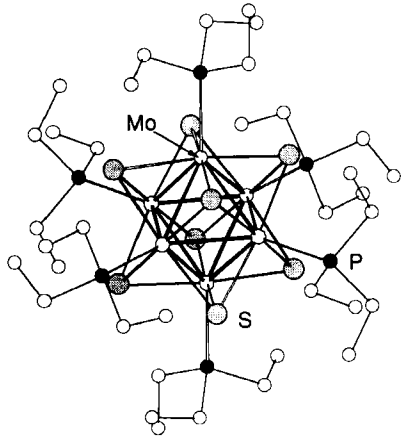

FIG. 8. Structure of $[Mo_6S_8(PEt_3)_6]$.

of E_8 and $(PH_3)_6$ are performed. As the Mo(4*d*) and S(3*p*) energy levels are close, they are well mixed in the molecular orbitals. The principal factors in determining the relative energies of the valence orbitals are the three types of interatomic interactions, and their order is Mo–E > Mo–Mo > E–E. The electronic levels and overlap populations of $[Mo_6S_8(PH_3)_6]$ and $[Mo_6Se_8(PH_3)_6]$ are shown in Figs. 9 and 10. As they are very similar, only the important molecular orbitals of the sulfur compound are described.

The LUMO of this 20-*e* cluster is a $17e_g$ orbital consisting mainly of Mo(4*d*) and S(3*p*) orbitals and having a weak Mo—S antibonding nature. The dominant component of the HOMO ($27t_{1u}$) is the S(3*p*) orbitals. The second HOMO ($15t_{2g}$) has a larger contribution from Mo(4*d*) orbitals, though its major component is also the S(3*p*) orbitals. The third HOMO ($10t_{2u}$) contains about 80% Mo(4*d*) orbitals. In the previous study for the 24-*e* system $[Mo_6S_8]^{4-}$ with EHMO (*63*) or the 22-*e* system $[Mo_6S_8]^{2-}$ with SCF MS Xα (*64*), the HOMO is the e_g orbital, and the t_{2u} is the second HOMO. Therefore the order of the energy levels in the t_{1u}, t_{2g}, t_{2u} orbital block is different. The Mo(4*d*) contributions to these orbitals are comparable to those in the calculations of Le Beuze *et al.* (*64*). The S(3*p*)–S(3*p*) interactions are not negligible and are responsible for the matrix effects between the sulfur atoms (*23*).

The molecular cluster complexes $[Mo_6E_8(PEt_3)_6]$ have characteristic bands in the UV-vis spectra at around 10,000 and 20,000 cm^{-1} (*40*) (Figs. 11 and 12, Table IV). Imoto *et al.* calculated oscillation strengths for the electronic transitions in $[Mo_6E_8(PH_3)_6]$ and assigned the peaks in the spectra of the real cluster complexes $[Mo_6E_8(PEt_3)_6]$ (*51*). The

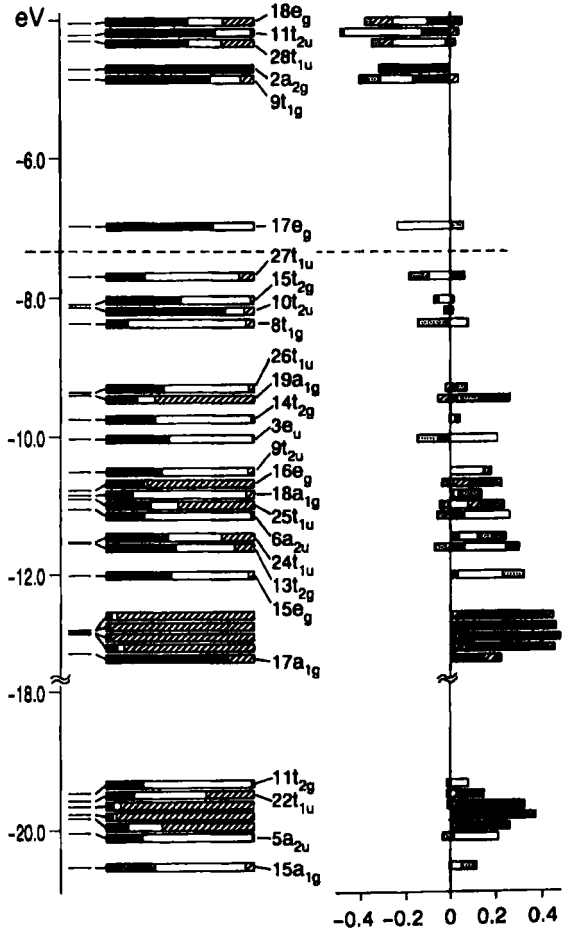

FIG. 9. Electronic levels and overlap populations of $[Mo_6S_8(PH_3)_6]$. [Reprinted with permission from (*51*). Copyright 1995, American Chemical Society.]

lower-energy bands are assigned to $10t_{2u} \rightarrow 17e_g$ (E = S) and $13t_{2u} \rightarrow 20e_g$ (E = Se) and the higher-energy bands to $26t_{1u} \rightarrow 17e_g$ (E = S) and $32t_{1u} \rightarrow 20e_g$ (E = Se). Both the initial and the final MOs of these transitions consist mainly of Mo($4d$) orbitals; they are charge-transfer transitions from metals to metals. The agreement between the calculated and observed transitions above 25,000 cm^{-1} is not very satisfactory.

XPS (X-ray photoelectron spectra) (*67*, *68*) and UPS (ultraviolet photoelectron spectra) (*69*) have been used to show that solid-state Chevrel

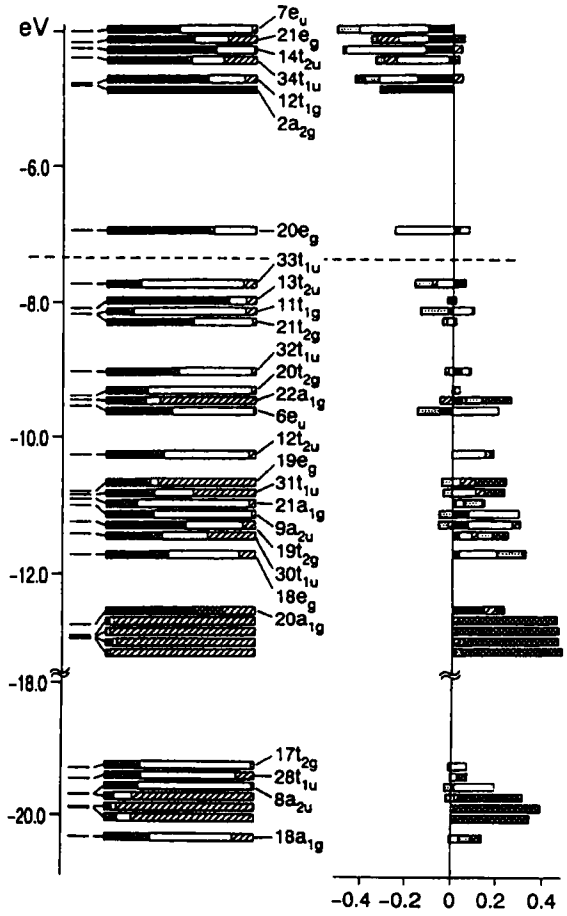

FIG. 10. Electronic levels and overlap populations of $[Mo_6Sc_8(PH_3)_6]$. [Reprinted with permission from (*51*). Copyright 1995, American Chemical Society.]

phases and their molecular analogues have similar Mo($3d_{5/2}$, $3d_{3/2}$) and S($2p_{3/2}$, $2p_{1/2}$) binding energies, indicating the cluster-like properties observed in the solid phases (*56*) (Table V). XPS and UPS of $PbMo_6S_8$ and $SnMo_6S_8$ have the common features of a valence bandwidth of about 7.0 eV and the presence of a steep and narrow peak at 1.0 eV, a valley at 2.5 eV, and a broad peak between 3.0 and 7.0 eV. The steepness at the leading edge is considered to reflect the magnitude of DOS at the Fermi level, which has a good correlation with the superconducting transition temperatures T_c (*65*).

According to the calculations of Arratia-Pérez (*59*), the splitting Mo($3d_{5/2}$–$3d_{3/2}$) value for the cluster model $Mo_6S_8H_6^{6-}$ amounts to 3.3

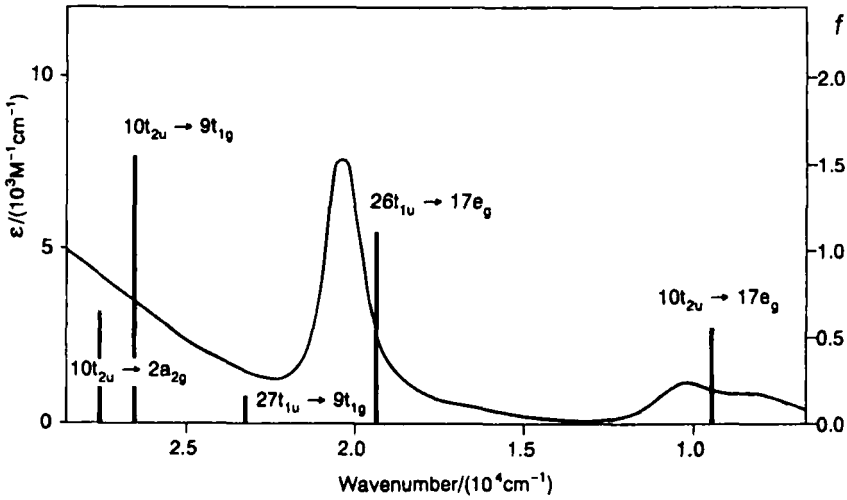

FIG. 11. UV-vis spectrum of $[Mo_6S_8(PEt_3)_6]$ and assignments of bands from calculations on $[Mo_6S_8(PH_3)_6]$. [Reprinted with permission from (*51*). Copyright 1995, American Chemical Society.]

eV, which is comparable to the corresponding values for AMo_6S_8 (A = Pb, La, Ag, In)(3.1–3.5 eV) (*67*) and for $[Mo_6S_8(PEt_3)_6]$ (3.2 eV) (*40*). The calculated valence local DOS of $Mo_6S_8H_6^{6-}$ shows broadening of the valence bandwidth to ca. 6.0 eV with the presence of a steep and narrow

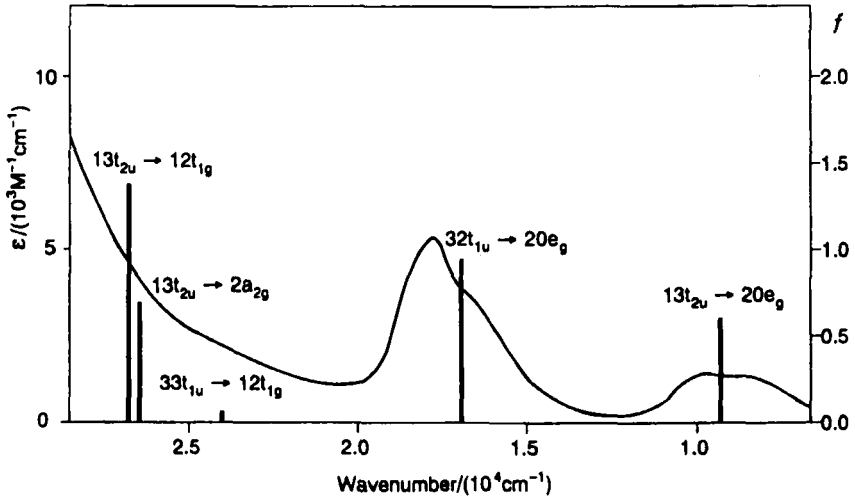

FIG. 12. UV-vis spectrum of $[Mo_6Sc_8(PEt_3)_6]$ and assignments of bands from calculations of $[Mo_6Se_8(PH_3)_6]$. [Reprinted with permission from (*51*). Copyright 1995, American Chemical Society.]

TABLE IV

UV-VIS SPECTRA

Compound	λ_{max}/nm (ε/$M^{-1}cm^{-1}$)	Ref.
$[Cr_6S_8(PEt_3)_6]$	400 (1.5×10^4), 570 (4×10^3), 850 (1×10^3)	*32*
$[Mo_6S_8(PEt_3)_6]$	491 (8.1×10^3), 991 (1.2×10^3), 1200 sh	*40*
$[Mo_6Se_8(PEt_3)_6]$	556 (5.5×10^3), 1034 (1.4×10^3), 1152 sh	*40*
$[W_6S_8(PEt_3)_6]$	409 (8.7×10^3), 882 (2.5×10^3), 964 sh	*41*

peak at near 1.0 eV from E_F, a valley at near 2.0 eV from E_F, and a broad peak of about 3.8 eV. The major contributions to the Fermi level are the spinors $4d_{5/2}$ and $4d_{3/2}$. A strong hybridization between Mo ($4d_{5/2}$, $4d_{3/2}$)–μ_3-S ($3p_{1/2}$, $3p_{3/2}$) and –H ($1s_{1/2}$) is observed in the region between –1.8 and –6.0 eV. The contributions from S ($3s_{1/2}$) are located in the leftmost region of the DOS curve (Fig. 13). DOS of the cluster model is consistent with those observed for the Chevrel phases and supports the conclusion that their superconducting behavior is mainly due to the $4d$ electrons of Mo_6 octahedra with small contributions from the intercluster bonding interactions.

XPS data on $[Mo_6S_8L_6]$ (L = pip, pyrr, py, $PrNH_2$, PEt_3, tht) exhibit Mo $3d_{5/2}$ between 227.6 and 227.8 eV and Mo $3d_{3/2}$ between 230.7 and 230.9 eV; S $2p_{3/2}$ between 160.6 and 161.0 eV; and S $2p_{1/2}$ between

TABLE V

XPS BINDING ENERGY/eV

Compound	Mo $3d_{5/2}$	Mo $3d_{3/2}$	Mo $3p_{3/2}$	Mo $3p_{1/2}$	S $2p_{3/2}$	S $2p_{1/2}$	S $2s$	Ref.
Mo_6S_8	228.0	231.5	394.1	412.1				*52*
$AgMo_6S_8$	227.7	230.9	393.9	411.5				*52*
$PbMo_6S_8$	228.2	231.5	394.1	411.8				*52*
$LaMo_6S_8$	227.7	230.9	393.7	411.5				*52*
Mo_6Se_8	227.7	231.2	394.1	412.1				*52*
$LaMo_6Se_8$	227.5	230.7	393.5	411.3				*52*
Mo_6Te_8	227.2	230.4	393.2	410.9				*52*
$[Mo_6S_8(PEt_3)_6]$	227.8	231.0			161.1	162.1	130.6[a]	*40*
$[Mo_6S_8(PEt_3)_6]$	227.8	230.9			161.0	162.1	225.1	*37*
$[Mo_6S_8(pip)_6]$	227.7	230.8			160.7	161.9	224.9	*37*
$[Mo_6S_8(pyrr)_6]$	227.7	230.8			160.6	161.8	225.4	*37*
$[Mo_6S_8(py)_6]$	227.6	230.7			160.6	161.8	225.0	*37*
$[Mo_6S_8(PrNH_2)_{6-x}]$	227.7	230.9			160.6	161.8	225.3	*37*
$[Mo_6S_8(tht)_6]$	227.7	230.9			160.7	161.8		*37*
$[Mo_6Se_8(PEt_3)_6]$	227.8	230.8			53.8[b]		130.6[a]	*40*

[a] P $2p$.
[b] Se $3d$.

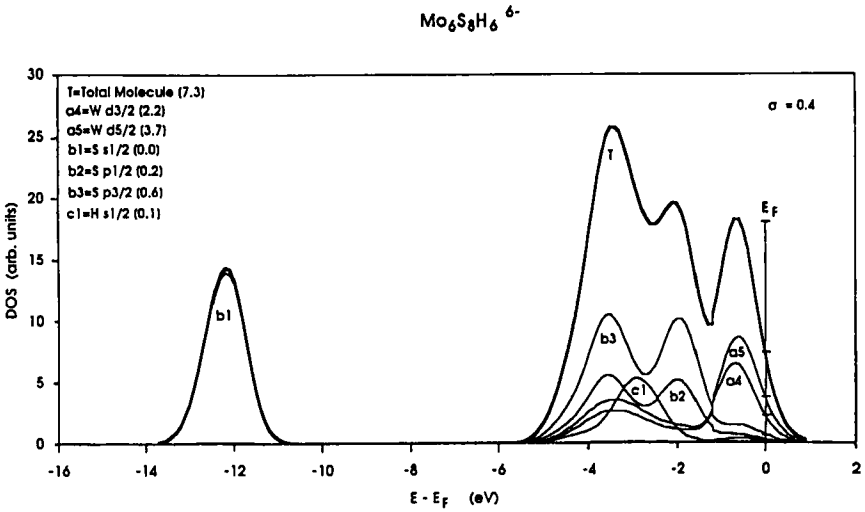

FIG. 13. Calculated DOS for $Mo_6S_8H_6^{6-}$. [Reproduced from (*59*) with permission.]

161.8 and 162.1 eV (*37*). These values are very close to the ones for $[Mo_6S_8(PEt_3)_6]$ (*40*) (Table V), indicating that the axial ligands have very small effects on the binding energies and the electronic structures should be essentially the same. It is to be noted that the calculated energies of the levels for the ground state of the model compounds $[Mo_6E_8(PH_3)_6]$ (E = S, Se) are within 1.3 eV of the observed binding energies for $[Mo_6E_8(PEt_3)_6]$ (*51*).

D. DIMERS OF OCTAHEDRAL CLUSTERS

Dimers of octahedral clusters can be regarded as the model embryo of the Chevrel phases. Only two real compounds have been reported. One is $[Co_{12}S_{16}(PEt_3)_{10}](TCNQ)_2$ (*70*), which was obtained from the mother solution of the synthesis of $[Co_6S_8(PEt_3)_6](BPh_4)$, and the other is $[Cr_{12}S_{16}(PEt_3)_{10}]$ (*71*), formed by removal of a PEt_3 from $[Cr_6S_8(PEt_3)_6]$ (*32*) (Fig. 14).

Hughbanks has calculated the molecular orbitals of a hypothetical 25-*e* $[Mo_6S_8L_5]$ cluster and discussed their dimerization (*72*). The $2e_g$ and $2t_{1u}$ σ-acceptor orbitals lie above the manifold of 12 metal–metal bonding orbitals, which include some *s* and *p* hybridization acting to accentuate their projection outward from the cluster. These orbitals are strongly destabilized when the cluster is capped by donor ligands to form the dative exo M—X bonds. There remains one $2e_g$ (z^2) acceptor

orbital on the last exposed Mo atom of the cluster, which is used for the intercluster Mo—Mo bonding. The preferred formal cluster electron count is 25 for each cluster to fill the bonding orbital, and the HOMO–LUMO gap becomes 1.17 eV. The model does not take the intercluster μ_3-S → Mo interactions into account, and the linking mode of two octahedral cluster units is different from that of Chevrel phases. In Chevrel-type bonding, the last exposed Mo atom is also capped by a sulfur atom of the adjacent cluster unit, and the $2e_g$ (z^2) is used for bonding. Because the vector between the two molybdenum atoms is not colinear to the z direction, the $1t_{1u}$ bonding or $2t_{2u}$ antibonding orbitals are likely to be used for the intercluster Mo—Mo bonding.

The first example of a dimer of octahedral clusters of Chevrel type has been reported by Cecconi and others (*70*). This cluster complex $[Co_{12}S_{16}(PEt_3)_{10}](TCNQ)_2$ was obtained as a by-product of the synthesis of $[Co_6S_8(PEt_3)_6](BPh_4)$ (*73, 74*). The linkage between the two Co_6S_8 cores (Co–Co 2.639 Å, Co–μ_4-S 2.148 Å) is significantly shorter than the mean distances (Co–Co 2.840 Å, Co–S 2.221 Å) within each Co_6S_8 unit. The geometry of the octahedral core shows only minor variation upon dimerization of the Co_6 cores, but the Co–Co separations in the triangular face bridged by the μ_4-S appear significantly larger (ca. 0.06 Å) than in all the others. In a recent theoretical study of the dimeric cluster performed at the extended Hückel level, Mealli and Orlandini have suggested that dimerization of the 37-*e* $[Co_6S_8(PEt_3)_6]^+$ upon loss of one terminal phosphine is facilitated by localization of the unpaired electron largely at the metal that is involved in the Co-μ_4-S bonding (*75*). They have also argued that the condensation of the two clusters is favored by the spin coupling between the two metal radicals, leading to a Co—Co bond with bond order close to a single bond.

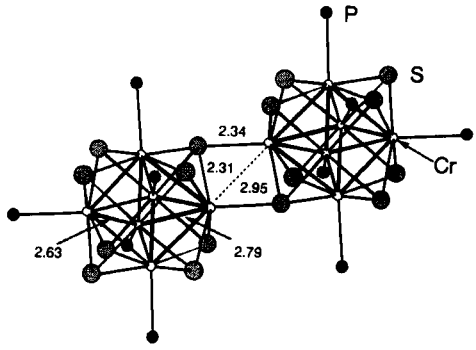

FIG. 14. Structure of $[Cr_{12}S_{16}(PEt_3)_{10}]$.

Dimerization of the 20-*e* $[Cr_6S_8(PEt_3)_6]$ units leads to $[Cr_{12}S_{16}(PEt_3)_{10}]$ with an intercluster Cr–Cr distance of 2.95 Å (*71*). This distance is significantly longer than the average Cr–Cr intracluster distance of 2.59 Å in the monomer. In solid-state Mo_6S_8, the similar intercluster Mo–Mo distance is 3.084 Å, as compared with an intracluster distance of 2.780 Å (average) (*52*). The intercluster M–M distance seems to be determined by the position of the metal atom relative to the plane of the sulfur atoms. Namely, when intracluster M–M distances are long because of the weakness of the M—M bond, the metal atom is above the surface of the sulfur cube, and the intercluster M–M distance becomes necessarily shorter than the intracluster M–M distance to keep the intercluster M–μ_4-S distances normal. Figure 15 shows the relationship between the intercluster M–M distance MM, the intracluster M–S distance MS, and the distance *d* of the metal atom from the plane of the S_8 cube, assuming that the intracluster and intercluster M–μ_4-S distances are the same and that the angle ∠M–S–(center of the S_4 square plane) is 90°. Table VI shows *d* for the M_6 cluster compounds, and *d* and θ calculated for the linked clusters by using Eqs. (1) and (2) in Fig. 15. *d* for the Co_6 cluster is much longer than for the chromium and molybdenum clusters, and this seems to be reflected in the shortness of the intercluster Co–Co distance. This trend is also observed in $M_xMo_6E_8$, where a stretching of the Mo—Mo intercluster bonds in isoelectronic compounds correlates with a shortening of the Mo—Mo intracluster bonds (*76*). It is an interesting problem whether the shortness of the intercluster M–M distance leads to more effective M–M interaction in case a pair of electrons are available for such a bond,

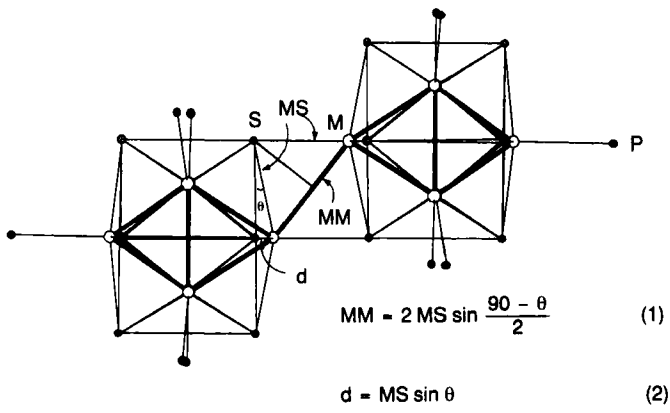

FIG. 15. The geometrical relationship between the position of the metal atoms and the length of the M—M bond in $[M_{12}E_{16}(PEt_3)_{10}]$.

TABLE VI

GEOMETRICAL RELATIONSHIP OF METAL AND CHALCOGEN ATOMS

Compound	Diagonal M–M (Å)	S–S (Å)	θ (deg)	d (Å)	Intercluster M–M (Å)	Intercluster M–S (Å)	Ref.
$[Co_6S_8(PEt_3)_6]BPh_4$	3.95	3.10		0.43			*74*
$[Cr_6S_8(PEt_3)_6]$	3.67	3.29		0.19			*32*
$[Mo_6S_8(PEt_3)_6]$	3.77	3.45		0.16			*40*
$[Co_{12}S_{16}(PEt_3)_{10}](TCNQ)_2$			14.2[a]	0.53[b]	2.64	2.15	*70*
$[Cr_{12}S_{16}(PEt_3)_{10}]$			11.8[a]	0.48[b]	2.95	2.34	*71*
Mo_6S_8			11.3[a]	0.48[b]	3.08	2.43	*52*

[a] Calculated using Eq. (1) in Fig. 15.
[b] Calculated using Eq. (2) in Fig. 15.

since the distances are correlated with the T_c in superconducting Chevrel phases (*56*).

The matching of t_{1u} orbitals in any one of the Co, Cr, or Mo clusters is similar, and if other conditions are satisfied, such intercluster M—M bonding interaction may be favored. Magnetic measurements will give us some clue to the solution of the problem.

E. RELATIONSHIP TO SOLID-STATE CLUSTER COMPOUNDS

1. Structure of Chevrel Phases

The incentive for synthesis of molecular cluster complexes with the cluster cores M_6E_8 (M = Cr, Mo, W; E = S, Se, Te) has been to solve some of the structural problems in the Chevrel phases (*40*) and to find solution chemistry to prepare "chromium or tungsten Chevrels" (*28, 77*).

There are two basic structures in octahedral clusters: M_6X_{12} and M_6X_8 types (*19*). The Chevrel-phase compounds belong to the latter type, with eight chalcogen atoms capping the M_3 triangular faces (*20, 78–83*). In the solid-state Chevrel compounds $M_xMo_6E_8$ (E = S, Se, Te), the Mo_6E_8 cluster units are linked by the bonding of the capping chalcogen atom to the apical molybdenum atoms of the adjacent cluster units. Namely, chalcogen atoms have a μ_4-bridging mode that generates an additional intercluster Mo—Mo bonding interaction (Fig. 16). The intercluster Mo–Mo distance (3.08–3.67 Å) depends on the size, location, and charge of the cation M_x. M_x is in the cavity made by the eight chalcogen atoms of eight Mo_6E_8 cluster units. Therefore, larger cations are likely to exert a more sterically demanding influence on the separation of the cluster units.

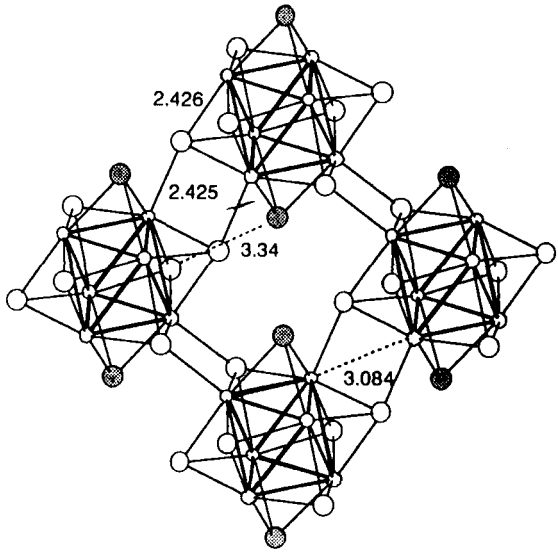

FIG. 16. Four cluster units and connectivity in Mo_6S_8.

The relationship between the trigonal distortion of the octahedra of Mo_6 in the Chevrel phases and the oxidation states (number of cluster valence electrons) of Mo_6E_8, the difference of chalcogens, the oxidation states, and the sizes of M have been repeatedly discussed (*84*). The main issues can be summarized as follows.

1. Mo–Mo distances in the triangles of Mo_3 perpendicular to the threefold axis are almost constant, and Mo–Mo distances between the triangles become longer for the more oxidized clusters. Therefore, the distortion of the Mo_6 octahedra is largest for the binary phases Mo_6E_8 (20 *e*).
2. The change of chalcogen atoms from sulfur to selenium and tellurium diminishes the intertriangle distances and the distortion of Mo_6 octahedra.
3. The metal atoms M are classified according to position in the cavity of eight chalcogen atoms from different cluster units; large atoms (Ag, Sn, Pb, La, Ca, Eu, Sr, Ba, etc.) located at the origin of the rhombohedral unit cell with 6 + 2 coordination by chalcogens; 5-coordinate In or 4-coordinate Cu, Ni, or Fe at the sixfold equivalent crystallographic positions. The larger distance from the origin and the E2 atoms (on the threefold axis) is related to the larger intercluster Mo–Mo distances.

In order to make these points clearer, interatomic distances in representative compounds are listed in Table VII. The distortion of Mo_6 should be caused by electronic effects from the individual cluster units and/or steric effects due to the linkage of the clusters. At one time the electronic effects were considered more important based on the band calculations (*58, 84*). The strong e_g Mo *d*-bonding character of the conduction band causes contraction of the Mo octahedron, and the filling of the $t_{1u}(O_h) \rightarrow e_u$ (S_6) and t_{2u} (O_h) $\rightarrow a_u$ (S_6) band is related to the smaller intratriangle distance. Namely, the larger shift of electrons from M_x and chalcogen atoms to the molybdenum atoms is related to smaller distortion of the Mo_6 octahedra.

The distortion was measured by the difference between intra- and intertriangle Mo–Mo distances in the octahedra. A cation with larger formal charge and less electronegative chalcogen atoms put more electrons to the cluster. When the cluster core is more reduced as the result of the electron transfer, the octahedron tends to contract and become more regular.

If steric effects in solid-state cluster compounds could be eliminated by the isolation of discrete molecules with the same cluster units as Chevrel phases, a part of the preceding problem would be solved. The structures of the cluster molecules in the isolated state free from the crystal packing effects are most suitable for such discussion. The geometry of free molecules in vacuum cannot be known from X-ray structure determination, and usually it is difficult to measure crystal packing effects in molecular crystals. In the case of metal complexes with sym-

TABLE VII

INTERATOMIC DISTANCES (Å) IN $M_xMo_6E_8$ (E = S, Se, Te)

Compound	Mo–Mo intratriangle	Mo–Mo intertriangle	Mo–Mo intercluster	Mo–μ_4-E intercluster	Origin–E2[a]	M covalent radius[b]	Ref.
Mo_6S_8	2.698	2.862	3.084	2.425	2.362		*52*
Mo_6Se_8	2.684	2.836	3.266	2.598	2.385		*52*
Mo_6Te_8	2.700	2.722	3.674	2.837	2.425		*52*
$SnMo_6S_8$	2.688	2.737	3.232	2.550	2.741	1.40	*52*
$PbMo_6S_8$	2.679	2.732	3.262	2.561	2.796	1.47	*52*
$LaMo_6S_8$	2.667	2.707	3.238	2.590	2.823	1.69	*52*
$CaMo_6S_8$	2.667	2.724	3.222	2.510	2.715	1.74	*86*
$EuMo_6S_8$	2.666	2.717	3.277	2.508	2.830	1.85	*86*
$SrMo_6S_8$	2.666	2.712	3.300	2.505	2.841	1.91	*86*
$BaMo_6S_8$	2.667	2.703	3.409	2.498	2.968	1.98	*86*

[a] Origin of the rhombohedral unit cell and E2 atoms on the threefold axis.

[b] Ref. Sanderson, R. T. *Inorganic Chemistry;* Reinhold: New York, 1967.

metrical ligand arrangements, the positions of ligating atoms can be a good probe for estimating the packing effect due to the contact of the outer portions of the ligands. The molecular cluster complexes $[Mo_6E_8(PR_3)_6]$ provide excellent specimens for such examination because the P_6 octahedron can be used as such a probe. The X-ray structures of the complexes $[Mo_6E_8(PR_3)_6]$ have indicated almost regular octahedral geometry of the Mo_6 core, although the P_6 octahedra are not always regular because of packing effects (see Section II,B,1). Triethylphosphine derivatives have especially regular cluster cores. It is very likely that packing effects in crystals do not affect the geometry of the Mo_6 core because of strong Mo–Mo bonding interaction. It has been found that the selenium derivative has a larger cluster core, indicating a stronger intracluster matrix effect to enlarge the Se_8 cube and Mo_6 octahedron. It has become evident that full occupation of the triply degenerate HOMO does not lead to any Jahn–Teller type distortion for the 20-*e* clusters. Lack of distortion in the 20-*e* cluster molecules strongly suggest that the principal cause of the distortion of the Mo_6 in Mo_6E_8 is unlikely to be electronic. The contraction and diminished distortion in $M_xMo_6E_8$ are probably due to insertion of the M_x cation in the E_8 cavity, which elongates intercluster Mo—Mo bonds and diminishes intercluster matrix effects.

Corbett did not agree with the electronic explanation and has argued that the matrix effects of chalcogen atoms give rise to the distortion (*23, 85*). As the cluster units are firmly bound to each other and metal cations are inserted in the chalcogen cubes, introduction of matrix effects of chalcogen atoms becomes necessary (Fig. 16). Corbett emphasizes the close intercluster contacts of chalcogen atoms, which cause elongation of the cluster core along the threefold axis because it appears the only possible alternative to lengthening the apparently strong intercluster bonds (Fig. 17). He states that elusive electronic effects do not seem necessary to account for both the contraction and diminished distortion of the octahedra in more electron-rich clusters (*85*).

The steric explanation emphasizes the importance of the intercluster bonding because the molecular cluster $[Mo_6E_8(PEt_3)_6]$ with the smallest CVE (20 *e*) shows only negligible distortion (*40*). However, as Table VII indicates, the larger chalcogen atoms with stronger matrix effects are accompanied by smaller distortion of the Mo_6 octahedron. It seems more natural to consider that matrix effects are not directly responsible for elongation of the intertriangle distances, but the larger chalcogens cause the elongation of intercluster Mo–Mo distances. As the sum of the Mo–Mo bonding interaction within and between the cluster units should be constant for a particular bond order sum, the increase in

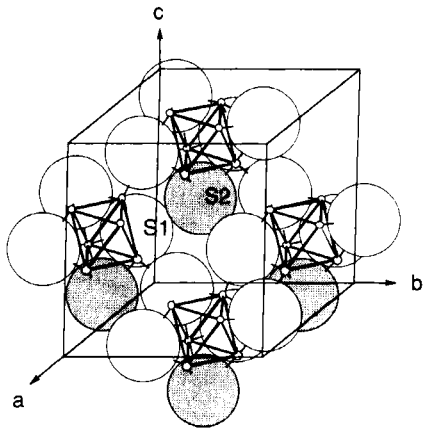

FIG. 17. Representation of the intercluster matrix effect between S1 and S2 atoms in Mo_6S_8. The radius of the sulfur atoms is set to 1.7 Å.

intercluster distance causes a decrease in intracluster distances. Yvon also has presented a mechanical spring model to explain the situation (*84*). Table VII also shows that the introduction of larger M results in an increase in intercluster Mo–Mo distances and a decrease in distortion (*86*).

Structure determinations of $[M_{12}S_{16}(PEt_3)_{10}]$ (M = Cr, Co) (*71, 70*) have shown that dimerization of $[M_6S_8(PEt_3)_6]$ by displacing a PEt_3 ligand and forming μ_4-S → M bonds distorts the cluster framework to a considerable extent. Such cluster linkages should be very important in Chevrel phase compounds, leading to the distortion.

Nevertheless, we cannot neglect the change in band structure as a result of contraction or distortion of the cluster octahedra. The misleading thing was the assumption that primarily electronic effects determine structure. It seems better if the relation is reversed: namely, steric constraints have a decisive influence on structure, and the resultant structure coupled with the number of CVE is responsible for particular band structures.

2. *Attempts to Prepare Chevrel-Type Solid-State Compounds*

All Chevrel phases are molybdenum compounds, and no chromium or tungsten analogues have been prepared. Preparative conditions using high temperatures (900–1300°C) result in the formation of thermodynamically more stable Cr_3Te_4 or WS_2 (*28, 77*). Consequently, preparation of "chromium or tungsten Chevrels," as well as of known molybdenum Chevrels at lower temperatures starting from preformed M_6E_8 cluster complexes has been attempted.

Thermolysis of $[Cr_6Te_8(PEt_3)_6]$ in an evaculated tube at 315°C for 19 hr removed the ancillary ligands to form Cr_3Te_4, which was identified by powder X-ray (*28*). The structure of this compound is a distorted metal-deficient NiAs type, and the Cr–Cr distance is 3.09 Å, indicating very weak Cr–Cr interaction. The Cr–Cr distance in the octahedral molecular cluster is also long (2.94 Å), and the Cr–Cr interaction is inferred to be weak in a Chevrel-type Cr_3Te_4. Therefore, even if a Chevrel-type Cr_3Te_4 is formed during pyrolysis, it would convert to the known NiAs-type compound. The initial stages of the growth of β-CoTe by the pyrolysis of a similar telluride cluster $[Co_6Te_8(PEt_3)_6]$ have been considered to be the conversion of an octahedral Co_6 array to a trigonal prism one of the NiAs structure (*30*). Removal of the ligands must be carried out at lower temperatures to reach a Chevrel-type Cr_3Te_4. It is interesting to note that differential scanning calorimetry (DSC) showed a broad endotherm between 210 and 250°C (*28*).

As molybdenum Chevrel compounds are thermodynamically stable phases, it would be worth trying to prepare the same compounds by low-temperature methods using molecular cluster compounds with Mo_6E_8 cores in order to gain an insight into the preparation of "chromium or tungsten Chevrels" by precursor methods. McCarley's group has attempted to remove neutral ligands from $[Mo_6S_8L_6]$ by thermolysis or by using phosphine acceptors such as $Co_2(CO)_8$, $Mo(CO)_6$, or CuCl when L is tertiary phosphines (*87*). The thermal de-ligation experiments combined with EXAFS, Raman, FTIR, and XPS techniques support retention of the Mo_6S_8 core up to 500°C, and there is no indication of cluster decomposition to form MoS_2 and Mo (*87*). High-yield preparations of the amorphous ternary salts $Na_{2x}(Mo_6S_8)S_x.yMeOH$ (x = 1.0 to 1.5; y = 4 to 5) have been devised by reaction of Mo_6Cl_{12} with NaSH and NaOBu in BuOH followed by extraction with methanol (*77*). The salts were converted into $M^{n+}_{2x/n}(Mo_6S_8)S_x.yMeOH$ (M = Sn, Co, Ni, Pb, La, Ho) by ion exchange. After removal of bound methanol from the sodium salt *in vacuo* at 500°C, further annealing at 800°C formed $NaMo_6S_8$. Annealing at 900°C resulted in much better crystallinity of the product. When the tin salt was heated at 700–1000°C under flowing H_2, crystalline $SnMo_6S_8$ formed.

Attempts to remove the pyridine ligands from $[W_6S_8(py)_6]$ by thermolysis *in vacuo* did not give W_6S_8 (*43*). At temperatures up to 250°C, the W_6S_8 core is retained but at higher temperatures formation of WS_2 is observed. Pyrolysis of the mixture of the pyridine cluster with tin or lead at low temperature leaves the metals unreacted. The use of pyridine acceptors such as CF_3SO_3H, $AlCl_3$, or BF_3 is also unsuccessful (*43*). The reaction of W_6Cl_{12} with NaSH and NaOEt in acetonitrile at

refluxing temperature for 3–4 days gave $Na_{2.1}(W_6S_8)S_{1.05}(MeOH)_{5.4}$ after extraction with methanol (*77*). The sodium salt was converted into $Sn_x(W_6S_8)S_x$ by ion-exchange reaction. After the sodium salt was heated at 130°C *in vacuo* for 3 days, the compound retained the W_6S_8 cluster unit, but after heating at 300°C for 1 day it decomposed to form WS_2 and W. Heating at 200°C under flowing H_2 also formed W and WS_2. The tin salt did not convert to the Chevrel-type phase after heating at 200°C under H_2.

Reports by Chevrel and others (*88*) of a new low-temperature synthesis of $PbMo_6S_8$ by the insertion of Pb into Mo_6S_8 at 440°C under H_2 flow using PbS as a lead source are interesting in showing that Chevrel phases can be prepared at a much lower temperature than those usually employed (>900°C). Although "chromium or tungsten Chevrels" have not been prepared yet by either high-temperature or low-temperature methods, progress in the complex chemistry of M_6E_8 clusters may shed light on the very narrow path toward formation of potentially important compounds.

III. Tetrahedral Clusters

A. Synthesis and Structure

Since the work of Dahl on synthesis and structural characterization of $[Cp_4Mo_4S_4]$ (*89*), many cubane-type complexes with Mo_4S_4 cores have been reported and reviewed (*10, 14, 15*). They have the general formula $[Mo_4S_4L_{12}]$ (Fig. 18), where L denotes ligating atoms with either neutral

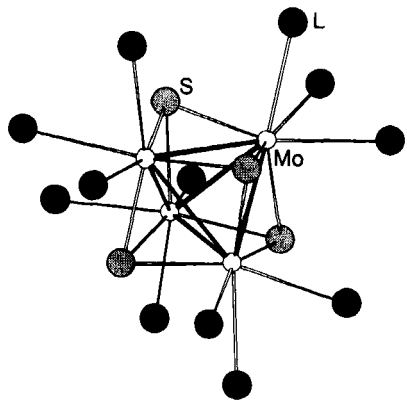

FIG. 18. General structure of $[Mo_4E_4L_{12}]$ cluster molecules.

or anionic ligands and the charge on the cluster units depends on the charge of the ligands. The oxidation states of the Mo_4 core vary from +12 to +20, namely 4 × Mo(III) to 4 × Mo(V). The Mo–Mo distances range from 2.732 to 2.904 Å (*15*).

Main preparative routes are dimerization of Mo_2 complexes and condensation of Mo_3 complexes with $Mo(CO)_6$ (*10, 14*). Self-assembly routes from $Mo(CO)_6$ or $[MoCl_3(CH_3CN)_3]$ have been developed (*90*).

The electronic structures of the Mo_4E_4 cubane systems have been analyzed (*91, 92*). Three sets of bonds, including Mo—Mo bonds, Mo—μ_3-E bonds, and Mo—L bonds, must be taken into account. The Mo—Mo bonds are weakest among the three, and they are considered separately (*91*). In the Mo—Mo bonding levels ($a_1 + e + t_2$), the energy order is $t_2 > e > a_1$ and the HOMO is considered to be weakly Mo—Mo bonding or nonbonding (*93*). In the electron count, 12 CVEs (cluster valence electrons) correspond to the six Mo—Mo bonds of the cubane structures.

Reduction of $[W_4S_6Cl_2(PMe_2Ph)_6]$ (see Section IV,A) with excess Na/Hg in thf at room temperature gives $[W_4(\mu_2\text{-}S)_6(PMe_2Ph)_4]$ in 10% yield (*94*). The structure consists of an almost regular tetrahedron of W(III) atoms with each edge bridged by a μ_2-S atom (Fig. 19). The six

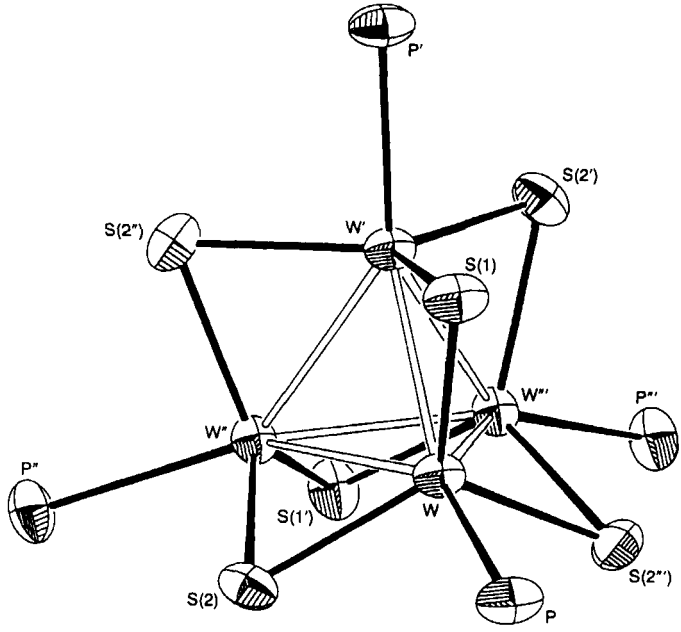

FIG. 19. Structure of $[W_4S_6(PMe_2Ph)_4]$. (Reproduced from (*94*) with permission.)

W–W distances (2.634(3) Å) are significantly shorter than those in the rhombus cluster and consistent with 12 CVE. The W_4S_6 framework may be regarded as an adamantanoid core, but the coordination geometry around the tungsten atoms is distorted from a regular tetrahedron. This reductive core rearrangement of sulfide clusters is unique and will open a preparative pathway to similar clusters.

B. Relationship to Solid-State Cluster Compounds

Solid-state molybdenum compounds MMo_4E_8 (M = Al, Ga, E = S; M = Ga, E = Se) (*95, 96*) and MoSX (X = Cl, Br, I) (*97*) with characteristic cubic structures have been reported. They contain Mo_4E_4 cubane cluster units, and the molybdenum atoms are octahedrally coordinated by six chalcogen atoms or three chalcogen and three halogen atoms (Fig. 20). The gallium or aluminum is tetrahedrally coordinated by four chalcogen atoms. The MMo_4S_8 compounds can be regarded as having deformed spinel structures with half of the A atoms in AB_2O_4 lacking, as molybdenum atoms are at (x, x, x) and $(x, -x, -x)$ positions, different from the positions of the B atoms $(\frac{5}{8}, \frac{5}{8}, \frac{5}{8})$ and $(\frac{5}{8}, \frac{7}{8}, \frac{7}{8})$ in spinels. The Mo–Mo distance in the cubane clusters in $GaMo_4S_8$ is 2.82 Å, and the intercluster Mo–Mo distance is 4.06 Å. The cubane clusters are linked by sharing S atoms among three cluster units, and the compositions are described as $M(Mo_4S_4^i)S_{12/3}^{a\text{-}a}$. The compounds MoSX have similar connectivity of $(Mo_4S_4^i)X_{12/3}^{a\text{-}a}$; the intracluster Mo–Mo distances are 2.80

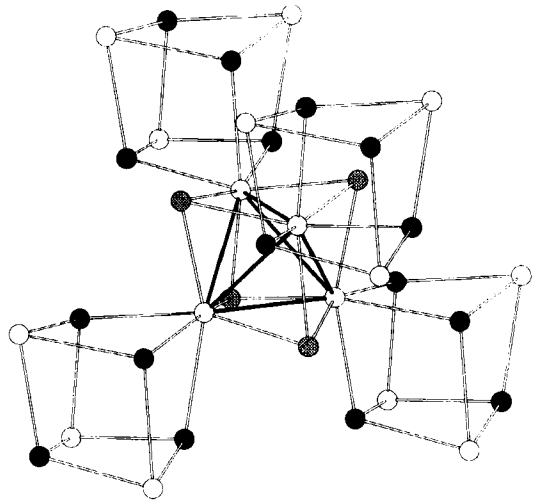

FIG. 20. Partial structure of MMo_4E_8 or MoSX. Black spheres represent E or X.

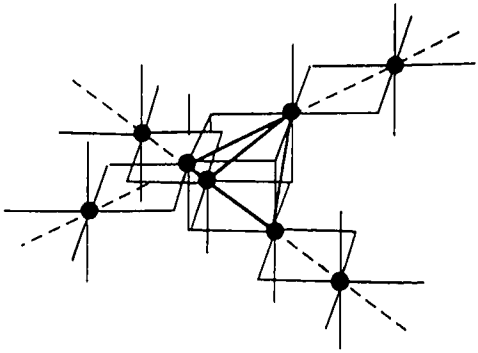

FIG. 21. Crossing of two $MoS_2S_{4/2}$ chains to form a Mo_4S_4 tetrahedral cluster unit by the Jahn–Teller effect. (Reproduced from (*98*) with permission.)

Å and intercluster Mo–Mo distances are 4.24 Å. The centers of the X_4 tetrahedra are vacant. The cluster units are therefore very much like those of the molecular cluster compounds $[Mo_4S_4L_{12}]^{n+}$, and the structural analogy between the two types of compounds is apparent.

The number of cluster valence electrons in $GaMo_4S_8$ is 11, and the compound is paramagnetic with an unpaired electron located in the cluster (*96*). The CVE is 12 for MoSX cluster compounds, a number consistent with six Mo—Mo single bonds in the tetrahedral cluster units. We notice that the tetrahedral units are somewhat enlarged in the 11-electron clusters. Formation of the tetrahedral clusters has been analyzed by EHMO as the result of the crossing of two infinite chains of $MoS_2S_{4/2}$ (Fig. 21), which is the expression of a multidirectional Peiers distortion leading to the stabilization of Mo_4 clusters in $GaMo_4S_8$ (*98*).

IV. Rhomboidal Clusters

A. Synthesis and Structure

A few cluster complexes with fused triangles of molybdenum or tungsten have been reported. They are tetranuclear and hexanuclear cluster complexes, which may be viewed also as having fused incomplete cubanes of M_3E_4.

The cluster $[Mo_4(\mu_3\text{-}S)_2(\mu_2\text{-}S)_4(SH)_2(PMe_3)_6]$ has been prepared by the reaction of $(NH_4)_2[Mo_3S_{13}]$ with trimethylphosphine in a mixed solvent of butylamine and thf at room temperature followed by reflux in 14% yield (*99*). The SH ligands can be replaced by halogens in reac-

tions with SnX_2, and the reaction of $[Mo_4S_6Br_2(PMe_{)6}]$ with Na[dtc] (dtc = diethyldithiocarbamate) forms $[Mo_4(\mu_3\text{-}S)_2(\mu_2\text{-}S)_4(dtc)_2(PMe_3)_4]$ (*100*) (Fig. 22).

The tetranuclear cluster complex $[Mo_4(\mu_3\text{-}S)_2(\mu_2\text{-}S)_4(SH)_2(PMe_3)_6]$ contains four molybdenum atoms arranged in a rhombus geometry. A twofold axis passes through Mo(1) and Mo(1′). The Mo(1)–Mo(2) distance is 2.825(1), and the Mo(1)–Mo(1′) distance 2.845(1) Å. The two Mo_3 triangles are capped by a sulfur atom, and they are on the opposite sides of the Mo_4 plane. Each peripheral Mo–Mo edge is bridged by a sulfur atom, and the structure of the cluster molecule is a fusion of two Mo_3S_3 units along one edge or a fusion of two Mo_3S_4 incomplete cubanes. The molybdenum atoms Mo(2) and Mo(2′) are bound to an SH ligand. Although the X-ray structure did not reveal the hydrogen atoms, infrared spectra indicated a weak band assignable to ν (SH) at 2516 cm^{-1}.

Hidai *et al.* have reported that treatment of *cis*-$[W(N_2)_2(PMe_2Ph)_4]$ with $(Me_3Si)_2S$ and MeOH in toluene at 50°C for 4 hr under vacuum affords $[W_4(\mu_3\text{-}S)_2(\mu_2\text{-}S)_4(SH)_2(PMe_2Ph)_6]$ in 43% yield, and the reaction of this complex with $SnCl_2$ in thf at reflux forms $[W_4(\mu_3\text{-}S)_2(\mu_2\text{-}S)_4Cl_2(PMe_2Ph)_6]$ in 63% yield (*94*). The tungsten cluster $[W_4(\mu_3\text{-}S)_2(\mu_2\text{-}S)_4(SH)_2(PMe_2Ph)_6]$ has a rhombus structure with somewhat shorter W–W distances (2.8118(6) and 2.8373(8) Å) compared with the corresponding Mo–Mo distances (*99*) (Fig. 23). The ν (SH) is at 2512 cm^{-1}, and ^{31}P NMR spectra indicate two kinds of phosphorus resonances at δ −18.3 ppm for the wing tip PMe_2Ph and at δ −52.6 ppm for the hinge PMe_2Ph.

The average oxidation state of the metals in both molybdenum and tungsten clusters is +3.5, and the number of cluster valence electrons is 10. The number is consistent with five M—M single bonds.

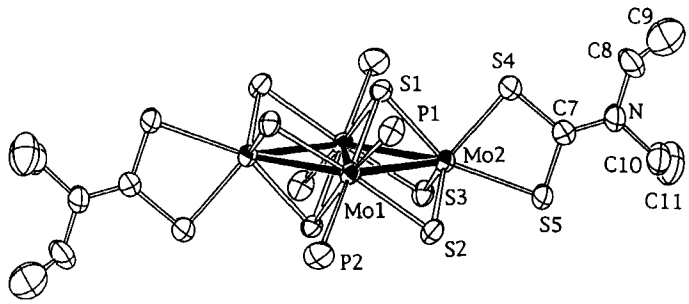

FIG. 22. Structure of $[Mo_4S_6(dtc)_2(PMe_3)_4]$.

A solution of $[Mo_3O_2S_2(H_2O)_9]^{4+}$ in 4M Hpts (pts = *para*-toluene sulfonate) was reacted with indium metal for 24 hr at room temperature and stored in a refrigerator for a few days to form $[Mo_4(\mu_3\text{-}S)_2(\mu_2\text{-}O)_4(H_2O)_{10}](pts)_4 \cdot 10H_2O$ (*101*). The cluster core of $Mo_4S_2O_4$ is similar to those of Mo_4S_6 cluster complexes.

It is difficult to devise simple schemes for the construction of tetranuclear frameworks from the triangular ones, unless decomposition of the mother skeleton into either dinuclear or mononuclear fragments occurs. The facile formation of tetranuclear clusters from either trinuclear or mononuclear complexes suggests that this cluster framework is favorable electronically and sterically. Similar geometry of four metals has been observed for other kinds of tetranuclear complexes such as $[Ti_4(OEt)_{16}]$ (*102*), $[W_4(OEt)_{16}]$ (*103*), $[Mn_4O_2(OAc)_6(bipy)_2]$ (*104*), $[Mn_4(L)_2(O)_2(OAc)_2]$ (*105*), $(NH_4)_2[V_4S_2(SCH_2CH_2S)_6]$ (*106*), or $[Nb_4Cl_{10}(PMe_3)_6]$ (*107*).

The electronic levels of a model compound $[Mo_4S_6Cl_2(PH_3)_6]$ have been calculated by the DV-Xα method (*100*). In a cluster of C_{2h} symmetry, five metal—metal bonding orbitals (two a_g, one a_u, one b_g, and one b_u) are expected. These orbitals are strongly mixed with the ligand orbitals and show large HOMO–LUMO gaps (Fig. 24), which may be the characteristics of the electron-precise clusters with 10 electrons.

When $(NH_4)_4[Mo_3S_{13}]$ was treated with triethylphosphine in thf, $[Mo_6(\mu_3\text{-}S)_4(\mu_2\text{-}S)_6(SH)_2(PEt_3)_6]$ formed in 11% yield (*99*). The cluster

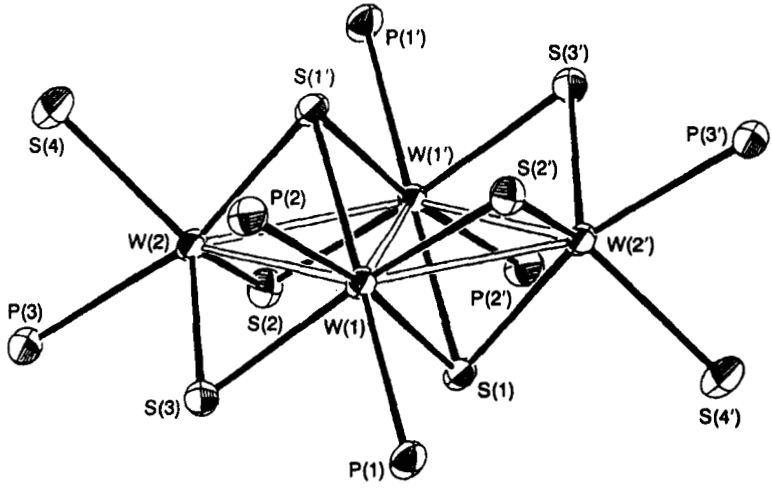

FIG. 23. Structure of $[W_4S_6(SH)_2(PMe_2Ph)_6]$. (Reproduced from (*94*) with permission.)

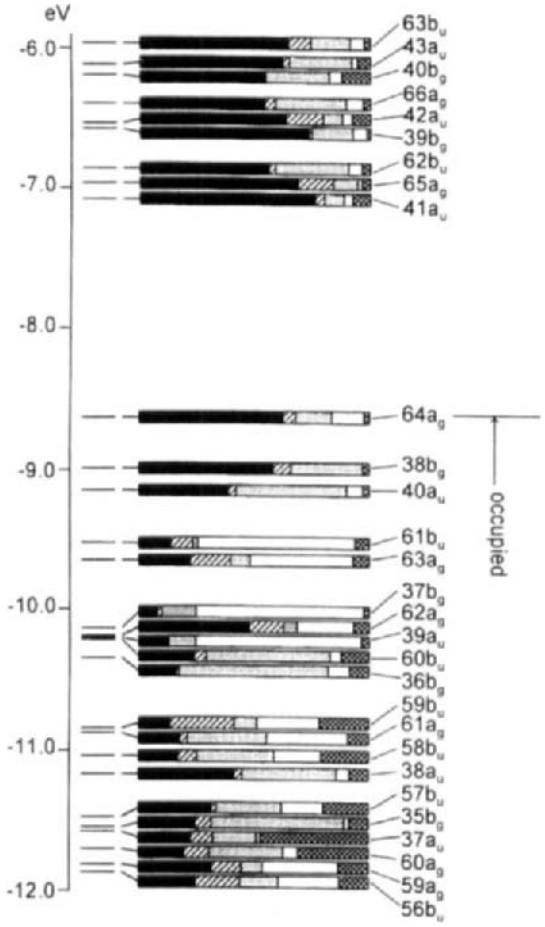

FIG. 24. MO of $[Mo_4S_6Cl_2(PH_3)_6]$.

complex is composed of six molybdenum atoms in a raft geometry of four Mo_3 triangles aligned linearly, sharing the edges (Fig. 25). The Mo–Mo distances range from 2.73 to 3.06 Å, and seven distances can be regarded as those of Mo—Mo single bonds. Each Mo_3 triangle is capped by a sulfur atom, and each peripheral Mo–Mo edge is also bridged by a sulfur atom. The central molybdenum atom (Mo3) is octahedrally coordinated by five sulfur atoms and a triethylphosphine, while Mo1 has a deformed trigonal–bipyramidal coordination with three sulfur atom, an SH, and a triethylphosphine ligand. The coordination geometry of Mo2 is intermediate between a trigonal bipyramid

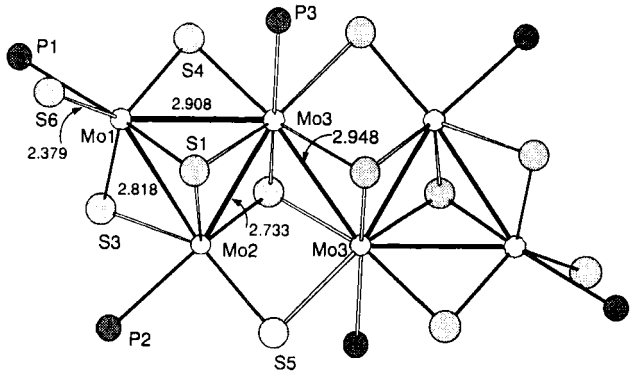

FIG. 25. Structure of $[Mo_6S_{10}(SH)_2(PEt_3)_6]$.

and a square pyramid. The position of the hydrogen on the SH has not been determined, but the infrared spectrum shows ν (SH) at 2497 cm^{-1}.

The compound $Mo_3S_7Cl_4$ was reacted with triethylphosphine in thf at room temperature for 24 hr, and the solution was reduced with magnesium metal at −20°C for 3 hr. After the solvent was removed under reduced pressure, the precipitate was crystallized from benzene to give $[Mo_6(\mu_3\text{-}S)_4(\mu_2\text{-}S)_4(\mu_2\text{-}Cl)_2Cl_4(PEt_3)_6]$ in 26% yield. Similar reac-

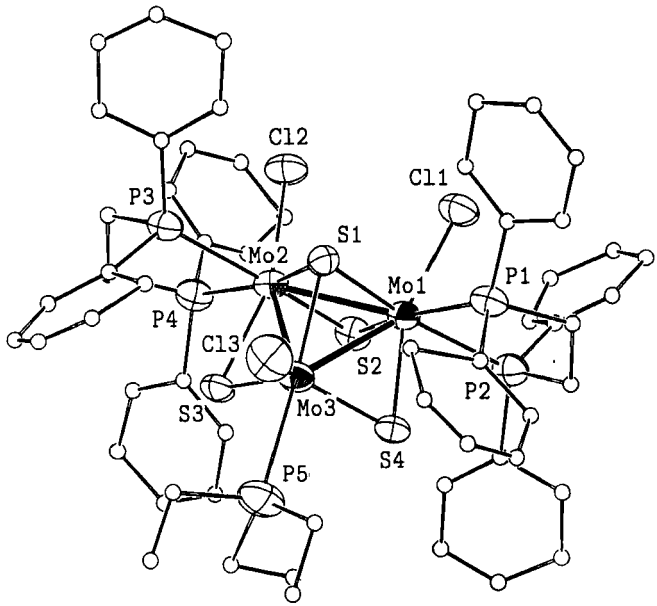

FIG. 26. Structure of $[Mo_3S_4Cl_3(dppe)_2(PEt_3)]$.

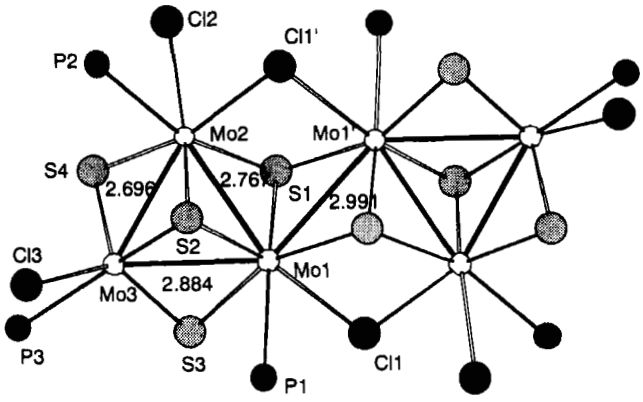

FIG. 27. Structure of $[Mo_6S_8Cl_6(PEt_3)_6]$.

tion starting from $Mo_3Se_7Cl_4$ afforded $[Mo_6(\mu_3\text{-}Se)_4(\mu_2\text{-}Se)_4(\mu_2\text{-}Cl)_2Cl_4(PEt_3)_6]$ in 11% yield (*108*). This reaction is noteworthy because a similar reduction at higher temperature leads to the octahedral clusters $[M_6E_8(PR_3)_6]$ (*40*), which indicates that the formation of metastable seven-electron clusters is a turning point to either horizontal dimerization of the trinuclear clusters or vertical dimerization after further reduction. The structure of a seven-electron cluster stabilized by dppe has been determined (*109*) (Fig. 26).

Six molybdenum atoms in $[Mo_6(\mu_3\text{-}S)_4(\mu_2\text{-}S)_4(\mu_2\text{-}Cl)_2Cl_4(PEt_3)_6]$ are arranged similarly, four fused triangles with capping sulfur atoms (Fig. 27). The edges are bridged by sulfur or chlorine atoms. Among the Mo–Mo distances (2.693(1)–3.556(1) Å), seven (2.693–2.999 Å) are assigned to Mo—Mo single bonds. The selenium analogue $[Mo_6(\mu_3\text{-}Se)_4(\mu_2\text{-}Se)_4(\mu_2\text{-}Cl)_2Cl_4(PEt_3)_6]$ has a similar structure, with Mo–Mo distances ranging from 2.771(1) to 3.683(1) Å (*108*).

The three hexanuclear clusters are mixed valency complexes of two M(III) and four M(IV) centers, and the average oxidation state of the metal is +3.67. The number of cluster valence electrons is 14, which agrees with seven M—M bonds. Relatively short M–M distances for the intra- and intertriangles suggest that the clusters can be viewed as dimers of triangular clusters. Extension of the triangle condensation would lead to higher polymers.

B. Relationship to Solid-State Cluster Compounds

Condensation of discrete triangular metal cluster units in the metal cluster plane is another way of building extended solid-state com-

pounds. There are a few examples of metal halides, oxides, and chalcogenides consisting of triangular or fused triangular (planar rhombus) metal frameworks. For example, $CsNb_4Cl_{11}$ (*110*), $NaMo_2O_4$ (*111*), MMo_2S_4 (*112*), and ReS_2 (*113*) contain planar M_4 rhombuses with face-capping and edge-bridging anions.

The essential structural features of $NaMo_2O_4$ are layer arrangements similar to the CdI_2 structure in which molybdenum atoms are included in octahedral sites of oxygen atoms (*111*). Within MoO_2 layers the Mo atoms are shifted from the center of octahedra toward neighboring Mo atoms, forming infinite chains of fused rhomboidal cluster units. Each Mo atom is bonded to two Mo atoms parallel to the chain direction at 2.893(2) Å and to two other Mo atoms via zigzag bonds at 2.535(2) Å. The CVE of each Mo atom is 2.5 electrons, two of which are used for zigzag bonds and 0.5 for the long bonds in the chain direction. If the rhomboidal units are emphasized, the CVE of 10 electrons is consistent with five Mo—Mo bonds within the cluster unit, but actually the electrons are used for four Mo—Mo single bonds and four Mo—Mo 0.25 bonds for each Mo_4 unit.

The compound $Ba_{1.14}Mo_8O_{16}$ contains similar rhomboidal clusters of Mo_4 in the infinite chains (*114*). One is more regular, with five Mo—Mo bonds in the edge-shared bitriangle (2.578(1)–2.616(1) Å), and another is rather distorted with two long and three short Mo—Mo bonds (2.546(1)–2.847 Å). The CVE is 18.26; this can be divided into 10 for the more regular cluster and 8.26 for the distorted cluster, and the distortion can be understood from the viewpoint of electron deficiency.

Another similar molybdenum oxide, $K_2Mo_8O_{16}$, is also composed of a regular Mo_4 and a distorted Mo_4 rhomboidal cluster (*115*). The compound has 18 CVE, which can be divided into 10 for the regular rhombus (2.551(3)–2.687(2) Å) and 8 for the distorted one (2.527(3)–2.837(2) Å).

The preceding three reduced molybdenum clusters indicate that rhomboidal cluster units are common among this kind of oxide, and the Mo–Mo distances in the cluster units are dependent on CVE assignable to the Mo_4 units. MO calculations on Mo_4 molecular cluster compounds containing 10 CVE and 8 CVE have shown that the 8-electron clusters distort from a second-order Jahn–Teller effect (*116*). Such a distortion has been observed in the 8-electron $W_4(OEt)_{16}$ (*117*).

Solid-state sulfide compounds MMo_2S_4 (M = V, Cr, Fe, Co) contain infinite chains of Mo_4S_6 clusters with intracluster Mo–Mo distances (2.756–2.989 Å) and intercluster distance (2.960 Å) for the cobalt derivative (*112*). As the valence of M is +2, judging from magnetic measurements, and the average oxidation state of molybdenum +3, the CVE for $M_2Mo_4S_8$ is 12. This agrees with five intracluster and one intercluster

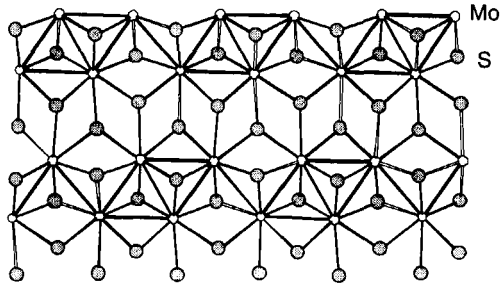

FIG. 28. Partial structure of $CoMo_2S_4$. Cobalt atoms are omitted.

Mo—Mo bonds (Fig. 28). Similar M_4S_6 structures can be recognized also in ReS_2 (*113*), also with 12 CVE for the Re_4S_8 formulation, and in a molecular analogue $[Re_4S_2(SO_2)_4(CN)_{10}]^{8-}$ with 14 CVE (*118*).

The structure of the niobium halide $CsNb_4Cl_{11}$ shows a typical example of the linking of rhombuses of flat butterfly clusters with M_4X_{16} cluster units (*110*). The cluster core is composed of an Nb_4 plane and two capping Cl in the opposite sides of the Nb_4 plane, and four edge-bridging Cl atoms. This cluster is linked to the adjacent clusters by 10 bridging Cl atoms (six terminal Cl to the wing-tip Nb atoms, and four terminal Cl to the hinge Nb atoms). The average oxidation state of niobium is +2.5, and 10 CVE are available for the intracluster Nb—Nb bonds (2.84–2.95 Å). The rhombus also can be regarded as the first member of the extension of incomplete cubanes to form raft-type clusters. For N units of this type, $4 - (6/N)$ electrons have to be supplied to each metal atom to form a full two-electron bond between every adjacent pair of metal atoms (*107*). A molecular cluster complex $[Nb_4Cl_{10}(PMe_3)_6]$ with a very similar cluster framework has been reported (*107*). The Nb–Nb distances range from 2.904 to 2.987 Å, showing that there are five Nb—Nb single bonds, consistent with 10 CVE from four niobium atoms in the oxidation state of +2.5.

V. Triangular Clusters

A. Synthesis and Structure

The $[M_3(\mu_3\text{-}E)(\mu_2\text{-}E)_3L_9]$ (I), $[M_3(\mu_3\text{-}E)(\mu_2\text{-}E_2)_3L_6]$ (II), and $[M_3E_5L_6]$ (III) types of cluster compounds (Fig. 29) are known, and because of the importance of triangular cluster units as building blocks of higher clusters, much effort has been put into the synthesis of such clusters.

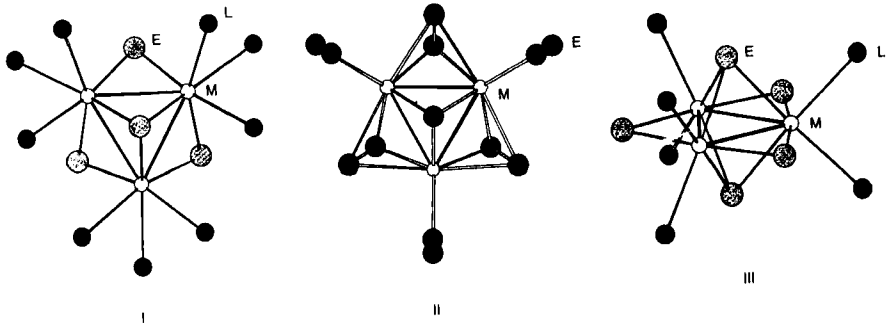

FIG. 29. General structure of $[M_3E_4L_9]$ (I), $[M_3E_7L_6]$ (II), and $[M_3E_5L_6]$ (III) type cluster complexes.

Some new compounds have been reported since the previous review (*10*).

No tellurium derivatives of $M_3E_7X_6$-type compounds had been described until Fedin *et al.* reported the synthesis of $Mo_3Te_{10}I_{10}$ from the reaction of molybdenum, tellurium, and iodine at 398°C for 48 hr in a sealed tube (*119*). The structure (Fig. 30) is composed of $[Mo_3(\mu_3\text{-Te})(\mu_2\text{-}$

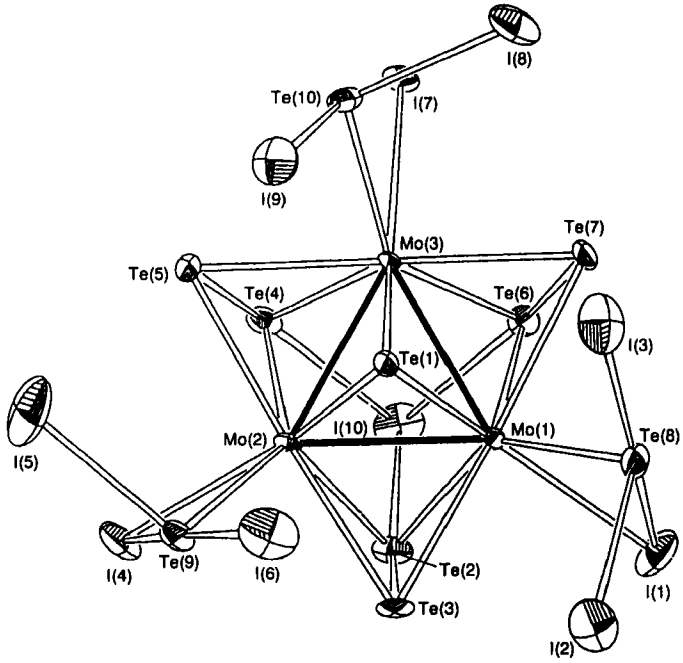

FIG. 30. Structure of $Mo_3Te_{10}I_{10}$. (Reproduced from (*119*) with permission.)

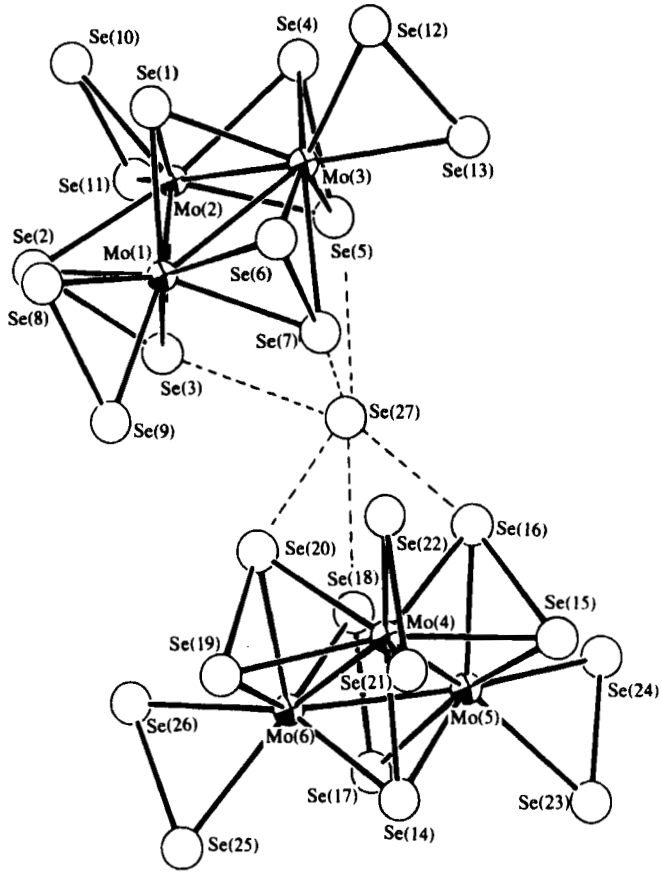

FIG. 31. Structure of $K_6Mo_6Se_{27}$. [Reprinted with permission from (*121*). Copyright 1995, American Chemical Society.]

$Te_2)_3(TeI_3)_3]I$ with an isosceles Mo_3 triangle and novel TeI_3^- ligands. The TeI_3^- ligands coordinate to molybdenum via Te–I. An extra iodine anion has a short contact with the axial Te atoms of the Te_2 bridges. When this compound is reacted with an aqueous KCN solution, $Cs_{2.5}K_2[Mo_3Te_7(CN)_6]I_{2.5} \cdot 3H_2O$, $Cs_3[Mo_3Te_7(CN)_6]I \cdot 3H_2O$, and $Cs_{4.5}[Mo_3Te_7(CN)_6]I_{2.5} \cdot 3H_2O$ are formed (*120*). The Mo–Mo distance in the equilateral Mo_3 triangle is 2.891(2) Å, and the Mo–μ_3-Te distance is 2.696(1) Å. The three axial Te atoms in the Te_2 bridges also have a short contact with an iodine atom as a counteranion. Attempts to prepare $[Mo_3Te_4L_9]$-type clusters by abstracting one of the tellurium atoms in the Te_2 bridges by either CN^- or PR_3 were unsuccessful.

When MoO_3, Na_2Se_2, and Me_4NCl are reacted at 135°C for 3 days under hydrothermal reaction conditions, $(Me_4N)_2Mo_3Se_{13}$ crystallizes out (*121*). The compound is an analogue of $(NH_4)_2Mo_3S_{13}$, which has been known for some time (*122*). The short contact between the μ_3-Se and the three axial selenium atoms of the Se_2 bridges (3.147 Å) suggests that this is a pseudo-solid-state compound that behaves as a semiconductor with a band gap of 1.6 eV due to band formation along the *c*-axis. The compound is sparingly soluble in DMF. The infrared spectrum shows a band at 451 cm^{-1} assignable to (Mo_3—μ_3-Se) vibration. The peak at 165 cm^{-1} is assigned to a Mo—Mo vibration. The reaction using K_2Se_2 as a selenium source in the absence of the ammonium salt formed $K_6Mo_6Se_{27} \cdot 6H_2O$ (*121*), in which two $[Mo_3Se_{13}]^{2-}$ anions are linked via an extra Se^{2-} ion (Fig. 31). Molecular orbital calculations have been performed to explain the anion–anion bonding interaction, which looks anomalous. The results indicate that the axial selenium atoms in the Se_2 bridges possess the least electron density, and the bonding interaction with the anionic Se^{2-} ion is rather natural. It would be very interesting if similar interactions in the number of $[Mo_3E_7]$-type compounds have the same sort of charge distribution to account for the anion–anion short contacts (*123, 124*).

A compound with half of the μ_3-Se replaced by μ_3-O has been obtained in the preceding reaction as another product (*121*). This is formulated as $K_2Mo_3Se_{12.5}O_{0.5}$ and is the first example of the Mo_3 cluster compound with a μ_3-O ligand. The cluster is more closely packed than the ammonium salt because of the smaller size of potassium ion and the replacement of half the μ_3-Se atoms by smaller oxygen atoms.

Details of the MO analysis of $[Mo_3(\mu_3\text{-}S)_2(\mu_2\text{-}S)_3(PMe_3)_6]$ have been reported (*125*). The cluster unit Mo_3S_5 is the first member of the Chevrel cluster $Mo_{3n}S_{3n+2}$, and development of the chemistry of this cluster complex is anticipated (Fig. 32).

B. Relationship to Solid-State Cluster Compounds

A few solid-state compounds of molybdenum and tungsten $M_3(\mu_3\text{-}E)(\mu_2\text{-}E_2)(E_2)_3X_2X_{4/2}$ (M = Mo, W; E = S, Se; X = Cl, Br, I) have been reported (*22, 42, 126–129*). They have the zigzag chain of the $M_3E_7X_2$ units bridged by four halogen atoms (Fig. 33). The Mo–Mo distances for $Mo_3S_7Cl_4$ are 2.741(3), 2.747(3), and 2.748(3) Å (*127*), and the equilateral triangle is a little larger than those in the molecular cluster complexes (2.700–2.734 Å) (*10*). The W–W distances in the isosceles W_3 in $W_3S_7Br_4$ are 2.700 and 2.722(3) Å (*129*). In the ionic cluster $(PPr_4)_2W_3S_7Br_6$, the W–W distances are elongated to 2.735–2.744 Å

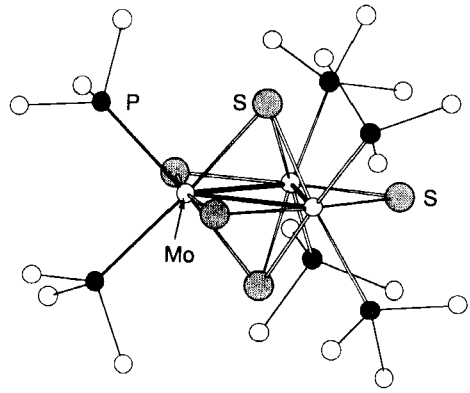

FIG. 32. Structure of $[Mo_3S_5(PMe_3)_6]$.

(*42*). The oxidation state of the metals in these cluster compounds is +4, and the bridges between the cluster units in the solid-state compounds can be cleaved by various reagents to form either μ_2-E_2- or μ_2-E-bridged molecular clusters in the same oxidation state. Since the solid-state triangular cluster compounds can be prepared in high yield and high selectivity, they will be good starting materials for a variety of trinuclear cluster complexes.

In relation to the HDS (hydrodesulfurization) catalysts, Müller has emphasized the structural relationships between MoS_2 and $(NH_4)_2[Mo_3S(S_2)_6]$ (*21, 130*). Both compounds are most stable binary Mo–S compounds with Mo(IV). Removal of the μ_3-S from $[Mo_3(\mu_3\text{-}S)(\mu_2\text{-}S_2)_3(S_2)_3]^{2-}$ rearranges the S_2^{2-} groups symmetrically around the Mo_3 triangles. By some variation of the bond distances (d(Mo—Mo) from 2.72 to 3.15 Å and d(S—S) from 2.0 to 3.6 Å), a complete section of

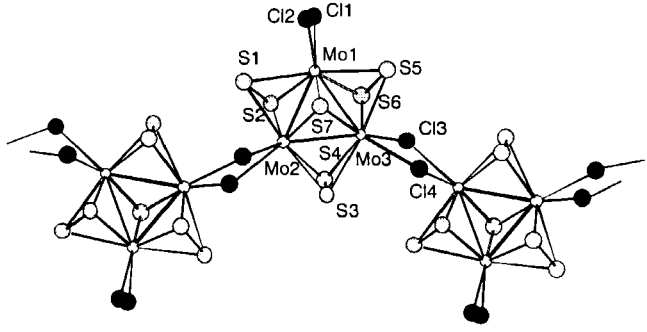

FIG. 33. Structure of $Mo_3S_7Cl_4$.

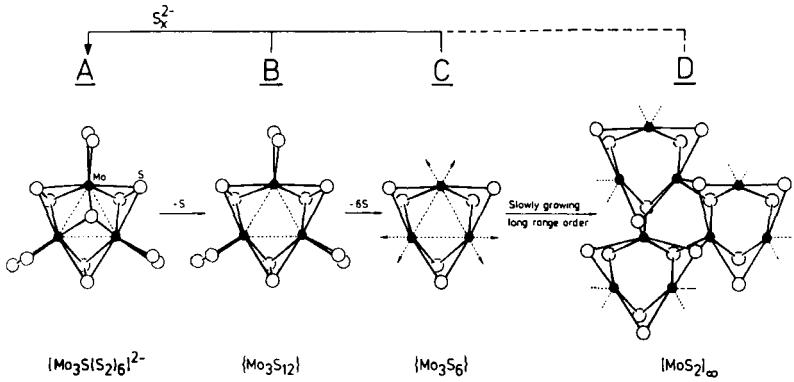

FIG. 34. Thermal decomposition of $(NH_4)_2[Mo_3S_{13}]$ to form MoS_2. [Reprinted from *Polyhedron*, Vol. 5, A. Müller, pp. 323–340, Copyright 1986, with kind permission from Elsevier Science Ltd., The Boulevard, Largford Lane, Kidlington OX5 1GB, UK.]

MoS_2 emerges. Also, the cluster compounds can be regarded as a model for the surface of MoS_2 crystals. The thermal decomposition of $(NH_4)_2[Mo_3S(S_2)_6]$ to yield MoS_2 has been monitored using DTA-TG measurements, and the desulfurization process is expressed as Fig. 34 shows (*21*).

The structural relationships between the solid-state compounds consisting of discrete triangular building blocks and their molecular analogues provide an interesting opportunity to study solid-state properties based on the cluster units in molecular clusters. Also, molecular cluster complexes can be starting materials for preparing the corresponding solid-state cluster compounds by their rational condensation.

REFERENCES

1. Chevrel, R.; Sergent, M.; Prigent, J. *J. Solid State Chem.* **1971,** *3,* 515.
2. Rees, D. C.; Chan, M. K.; Kim, J. *Adv. Inorg. Chem.* **1993,** *40,* 89.
3. Kepert, D. L. "The Early Transition Metals"; Academic Press: London, 1972.
4. Simon, A. *Angew. Chem. Int. Ed. Engl.* **1981,** *20,* 1.
5. Kim, J.; Rees, D. C. *Science* **1992,** *257,* 1677.
6. Holm, R. H. *Adv. Inorg. Chem.* **1992,** *38,* 1.
7. Coucouvanis, D. *Acc. Chem. Res.* **1991,** *24,* 1.
8. Cen, W.; MacDonnell, F. M.; Scott, M. J.; Holm, R. H. *Inorg. Chem.* **1994,** *33,* 5809.
9. Demadis, K. D.; Coucouvanis, D. *Inorg. Chem.* **1995,** *34,* 436.
10. Saito, T. In "Early Transition Metal Clusters with π-Donor Ligands"; Chisholm, M. H., Ed.; VCH: New York, 1995.
11. Dance, I.; Fisher, K. *Prog. Inorg. Chem.* **1994,** *41,* 637.
12. Kanatzidis, M. G.; Huang, S. P. *Coord. Chem. Rev.* **1994,** *130,* 509.

13. Roof, L. C.; Kolis, J. W. *Chem. Rev.* **1993,** *93,* 1037.
14. Shibahara, T. *Coord. Chem. Rev.* **1993,** *123,* 73.
15. Shibahara, T. *Adv. Inorg. Chem.* **1991,** *37,* 143.
16. Pena, O.; Sergent, M. *Prog. Solid State. Chem.* **1989,** *19,* 165.
17. Fenske, D.; Ohmer, J.; Hachgenei, J.; Merzweiler, K. *Angew. Chem. Int. Ed. Engl.* **1988,** *27,* 1277.
18. Zanello, P. *Coord. Chem. Rev.* **1988,** *83,* 199.
19. Perrin, A.; Perrin, C.; Sergent, M. *J. Less-Common Met.* **1988,** *137,* 241.
20. Chevrel, R.; Hirrien, M.; Sergent, M. *Polyhedron* **1986,** *5,* 87.
21. Müller, A. *Polyhedron* **1986,** *5,* 323.
22. Fedorov, V. E.; Mishchenko, A. V.; Fedin, V. P. *Russian Chem. Rev.* **1985,** *54,* 408.
23. Corbett, J. D. *J. Solid State Chem.* **1981,** *39,* 56.
24. Müller, A.; Jostes, R.; Cotton, F. A. *Angew. Chem. Int. Ed. Engl.* **1980,** *19,* 875.
25. Rouxel, J. *Acc. Chem. Res.* **1992,** *25,* 328.
26. Lee, S. C.; Holm, R. H. *Angew. Chem. Int. Ed. Engl.* **1990,** *29,* 840.
27. Sunshine, S. A.; Keszler, D. A.; Ibers, J. A. *Acc. Chem. Res.* **1987,** *20,* 395.
28. Hessen, B.; Siegrist, T.; Palstra, T.; Tanzler, S. M.; Steigerwald, M. L. *Inorg. Chem.* **1993,** *32,* 5165.
29. Steigerwald, M. L.; Sprinkle, C. R. *Organometallics* **1988,** *7,* 245.
30. Steigerwald, M. L.; Siegrist, T.; Stuczynski, S. M. *Inorg. Chem.* **1991,** *30,* 2256.
31. Steigerwald, M. L. *Polyhedron* **1994,** *13,* 1245.
32. Tsuge, K.; Imoto, H.; Saito, T. *Bull. Chem. Soc. Jpn.* **1996,** *69,* 627.
33. Michel, J. B.; McCarley, R. E. *Inorg. Chem.* **1982,** *21,* 1864.
34. Ebihara, M.; Toriumi, K.; Saito, K. *Inorg. Chem.* **1988,** *27,* 13.
35. Ebihara, M.; Isobe, K.; Sasaki, Y.; Saito, K. *Inorg. Chem.* **1992,** *31,* 1644.
36. Ebihara, M.; Toriumi, K.; Sasaki, Y.; Saito, K. *Gazz. Chim. Ital.* **1995,** *125,* 87.
37. Hilsenbeck, S. J.; V. G. Young, J.; McCarley, R. E. *Inorg. Chem.* **1994,** *33,* 1822.
38. Saito, T.; Yamamoto, N.; Yamagata, T.; Imoto, H. *J. Am. Chem. Soc.* **1988,** *110,* 1646.
39. Saito, T.; Yamamoto, N.; Yamagata, T.; Imoto, H. *Chem. Lett.* **1987,** 2025.
40. Saito, T.; Yamamoto, N.; Nagase, T.; Tsuboi, T.; Kobayashi, K.; Yamagata, T.; Imoto, H.; Unoura, K. *Inorg. Chem.* **1990,** *29,* 764.
41. Saito, T.; Yoshikawa, A.; Yamagata, T.; Imoto, H.; Unoura, K. *Inorg. Chem.* **1989,** *28,* 3588.
42. Fedin, V. P.; Sokolov, M. N.; Geras'ko, O. A.; Kolesov, B. A.; Fedorov, V. Y.; Mironov, A. V.; Yufit, D. S.; Slovohotov, Y. L.; Struchkov, Y. T. *Inorg. Chim. Acta* **1990,** *175,* 217.
43. Zhang, X.; McCarley, R. E. *Inorg. Chem.* **1995,** *34,* 2678.
44. Ehrlich, G. M.; Warren, C. J.; Vennos, D. A.; Ho, D. M.; Haushalter, R. C.; DiSalvo, F. J. *Inorg. Chem.* **1995,** *34,* 4454.
45. Bencini, A.; Midollini, S. *Coord. Chem. Rev.* **1992,** *120,* 87.
46. Pearson, W. B. "The Crystal Chemistry and Physics of Metals and Alloys"; Wiley: New York, 1972.
47. Braga, D. *Chem. Rev.* **1992,** *92,* 633.
48. Braga, D.; Grepioni, F. *Acc. Chem. Res.* **1994,** *27,* 51.
48a. Sasahara, J.; master's thesis; University of Tokyo, 1992.
49. Pauling, L. "The Nature of the Chemical Bond"; Cornell University Press: Ithaca, New York, 1960.
50. Saito, T.; Nishida, M.; Yamagata, T.; Yamagata, Y.; Yamaguchi, Y. *Inorg. Chem.* **1986,** *25,* 1111.
51. Imoto, H.; Saito, T.; Adachi, H. *Inorg. Chem.* **1995,** *34,* 2415.

52. Chevrel, R.; Sergent, M. In "Superconductivity in Ternary Compounds I"; Fischer, Ø., and Maple, M. B., Eds.; Springer: Berlin, 1982.
53. Adachi, H.; Tsukada, M.; Satoko, C. *J. Phys. Soc. Jpn.* **1978,** *45,* 875.
54. Satoko, C.; Tsukada, M.; Adachi, H. *J. Phys. Soc. Jpn.* **1978,** *45,* 1333.
55. Adachi, H.; Shiokawa, S.; Tsukada, M.; Satoko, C.; Sugano, S. *J. Phys. Soc. Jpn.* **1979,** *47,* 1528.
56. Fischer, Ø. *Appl. Phys.* **1978,** *16,* 1.
57. Burdett, J. K.; Lin, J. H. *Inorg. Chem.* **1982,** *21,* 5.
58. Nohl, H.; Klose, W.; Andersen, O. K. In "Superconductivity in Ternary Compounds I"; Fischer, Ø., and Maple, M. B., Eds.; Springer: Berlin, 1982.
59. Arratia-Pérez, R. *Chem. Phys. Lett.* **1993,** *213,* 547.
60. Arratia-Pérez, R.; Hernández-Acevedo, L. *J. Mol. Struct.* **1993,** *282,* 131.
61. Mealli, C.; López, J. A.; Sun, Y. *Inorg. Chim. Acta* **1993,** *213,* 199.
62. Wooley, R. G. *Inorg. Chem.* **1985,** *24,* 3519.
63. Hughbanks, T.; Hoffmann, R. *J. Am. Chem. Soc.* **1983,** *105,* 1150.
64. Le Beuze, L.; Makhyoun, M. A.; Lissllour, R.; Chermette, H. *J. Chem. Phys.* **1982,** *76,* 6060.
65. Bullett, D. W. *Phys. Rev. Lett.* **1977,** *39,* 664.
66. Slater, C. J. "The Calculation of Molecular Orbitals"; Wiley: New York, 1979.
67. Yashonath, S.; Hedge, M. S.; Sarode, P. R.; Rao, C. N. R.; Umarji, A. M.; Rao, G. V. S. *Solid State Commun.* **1981,** *37,* 325.
68. Ihara, H.; Kimura, Y. *Jpn. J. Appl. Phys.* **1978,** *17,* 281.
69. Kurmaev, E. Z.; Yarmoshenko, Y. M.; Nyholm, R.; Martensson, M.; Jarlborg, T. *Solid State Commun.* **1981,** *37,* 647.
70. Cecconi, F.; Ghilardi, C. A.; Midollini, S.; Orlandini, A. *Inorg. Chim. Acta* **1993,** *214,* 13.
71. Kamiguchi, T.; Imoto, H.; Saito, T. The 45th Conference on Coordination Chemistry, Japan, Fukuoka, 1995, 1Aα11.
72. Hughbanks, T. *Inorg. Chem.* **1986,** *25,* 1492.
73. Cecconi, F.; Ghilardi, C. A.; Midollini, S. *Inorg. Chim. Acta* **1981,** *64,* L47.
74. Cecconi, F.; Ghilardi, C. A.; Midollini, S.; Orlandini, A.; Zanello, P. *Polyhedron* **1986,** *5,* 2021.
75. Mealli, C.; Orlandini, A. *Gazz. Chim. Ital.* **1995,** *125,* 271.
76. Yvon, K. In "Current Topics in Material Science"; Kaldis, E., Ed.; North-Holland: Amsterdam, 1979.
77. McCarley, R. E.; Hilsenbeck, S. J.; Xie, X. *J. Solid State Chem.* **1995,** *117,* 269.
78. Fischer, Ø.; Odermatt, R.; Bongi, G.; Jones, H.; Chevrel, R.; Sergent, M. *Phys. Lett.* **1973,** *45A,* 87.
79. Chevrel, R.; Gougeon, P.; Potel, M.; Sergent, M. *J. Solid State Chem.* **1985,** *57,* 25.
80. Fischer, Ø.; Maple, M. B., Eds. "Superconductivity in Ternary Compounds I"; Springer-Verlag: Berlin, 1982; Vol. 32.
81. Maple, M. B., Fischer, Ø., Eds. "Superconductivity in Ternary Compounds II"; Springer-Verlag: Berlin, 1982; Vol. 34.
82. Chevrel, R.; Sergent, M. In "Crystal Chemistry and Properties of Materials with Quasi-One-Dimensional Structures"; Rouxel, J., Ed.; D. Reidel Publishing Company: Dordrecht, 1986.
83. Eichhorn, B. W. *Prog. Inorg. Chem.* **1994,** *42,* 139.
84. Yvon, K. In "Superconductivity in Ternary Compounds I"; Fischer, Ø., and Maple, M. B., Eds.; Springer: Berlin, 1982.

85. Corbett, J. D. In "Modern Perspectives in Inorganic Crystal Chemistry"; Parthé, E., Ed.; Kluwer Academic Publishers: Dordrecht, 1992.
86. Kubel, F; Yvon, K. *J. Solid State Chem.* **1988,** *73,* 188.
87. Hilsenbeck, S. J.; McCarley, R. E.; Goldman, A. I. *Chem. Mater.* **1995,** *7,* 499.
88. Rabiller, P.; Rabiller-Baudry, M.; Even-Boudjada, S.; Burel, L.; Chevrel, R.; Sergent, M.; Decroux, M.; Cors, J.; Maufras, J. L. *Mat. Res. Bull.* **1994,** *29,* 567.
89. Dahl, L. F. The VIth International Conference on Organometallic Chemistry, Amherst, 1973.
90. Coyle, C. L.; Eriksen, K. A.; Farina, S.; Francis, J.; Gea, Y.; Greaney, M. A.; Guzi, P. J.; Halbert, T. R.; Murray, H. H.; Stiefel, E. I. *Inorg. Chim. Acta* **1992,** *198–200,* 565.
91. Harris, S. *Polyhedron* **1989,** *8,* 2843.
92. Müller, A.; Jostes, R.; Eltzner, W.; Nie, C. S.; Diemann, E.; Bogge, H.; Zimmermann, M.; Dartmann, M.; Reinsch-Vogell, U.; Che, S.; Cyvin, S. J. *Inorg. Chem.* **1985,** *24,* 2872.
93. Bandy, J. A.; Davoes, C. E.; Green, J. C.; Green, M. L. H.; Prout, K.; Rodgers, D. P. S. *J. Chem. Soc., Chem. Commun.* **1983,** 1395.
94. Kuwata, S.; Mizobe, Y.; Hidai, M. *J. Chem. Soc., Chem. Commun.* **1995,** 1057.
95. Perrin, C.; Chevrel, R.; Sergent, M. *Compt. Rend.* **1975,** *280,* 949.
96. Vandenberg, J. M.; Brasen, D. *J. Solid State Chem.* **1975,** *14,* 203.
97. Perrin, C.; Chevrel, R.; Sergent, M. *Compt. Rend.* **1975,** *281,* 23.
98. Le Beuze, A.; Zerrovki, M. C.; Loirat, H.; Lissillour, R. *J. Alloys Compd.* **1992,** *190,* 1.
99. Tsuge, K.; Imoto, H.; Saito, T. *Inorg. Chem.* **1992,** *31,* 4715.
100. Tsuge, K.; Mita, S.; Fujita, Y.; Imoto, H.; Saito, T. *J. Cluster Sci.* **1996,** *7,* 407.
101. Kobayashi, S.; Sasaki, M.; Sakane, G.; Shibahara, T. The 45th Symposium on Coordination Chemistry of Japan, Fukuoka, 1995, 1AP32.
102. Ibers, J. A. *Nature* **1963,** *197,* 686.
103. Chisholm, M. H.; Huffman, J. C.; Kirkpatrick, C. C.; Leonelli, J.; Folting, K. *J. Am. Chem. Soc.* **1981,** *103,* 6093.
104. Christmas, C.; Vincent, J. B.; Huffman, J. C.; Christou, G.; Chang, H. R.; Hendrickson, D. N. *J. Chem. Soc. Chem. Commun.* **1987,** 1303.
105. Mikuriya, M.; Nakadera, K.; Kotera, T.; Tokii, T.; Mori, W. *Bull. Chem. Soc. Jpn.* **1995,** *68,* 3077.
106. Money, J. K.; Huffman, J. C.; Christou, G. *J. Am. Chem. Soc.* **1987,** *109,* 2210.
107. Cotton, F. A.; Shang, M. *J. Am. Chem. Soc.* **1988,** *110,* 7719.
108. Mizutani, J.; Yamada, S.; Imoto, H.; Saito, T. *Inorg. Chem.* **1995,** *34,*
109. Mizutani, J.; Imoto, H.; Saito, T. *J. Cluster Sci.* **1995,** *6,* 523.
110. Broll, A.; Simon, A.; Schnering, H. G. v.; Schäfer, H. *Z. Anorg. Allg. Chem.* **1969,** *367,* 1.
111. McCarley, R. E.; Lii, K. H.; Edwards, P. A.; Brough, L. F. *J. Solid State Chem.* **1985,** *57,* 17.
112. Chevrel, R.; Sergent, M.; Meury, J. L.; Quan, D. T.; Colin, Y. *J. Solid State Chem.* **1974,** *10,* 260.
113. Murray, H. H.; Kelty, S. P.; Chianelli, R. R.; Day, C. S. *Inorg. Chem.* **1994,** *33,* 4418.
114. Torardi, C. C.; McCarley, R. E. *J. Solid State Chem.* **1981,** *37,* 393.
115. Torardi, C. C.; Calabrese, J. C. *Inorg. Chem.* **1984,** *23,* 3281.
116. Cotton, F. A.; Fang, A. *J. Am. Chem. Soc.* **1982,** *104,* 113.
117. Chisholm, M. H.; Huffman, J. C.; Leonelli, J. *J. Chem. Soc. Chem. Commun.* **1981,** 270.
118. Müller, A.; Krickemeyer, E.; Bögge, H.; Ratajczak, H.; Armatage, A. *Angew. Chem. Int. Ed. Engl.* **1994,** *33,* 770.

119. Fedin, V. P.; Imoto, H.; Saito, T. *J. Chem. Soc., Chem. Commun.* **1995,** 1559.
120. Fedin, V. P.; Imoto, H.; Saito, T.; McFarlane, W.; Sykes, A. G. *Inorg. Chem.* **1995,** *34,* 5097.
121. Liao, J.; Li, J.; Kanatzidis, M. G. *Inorg. Chem.* **1995,** *34,* 2658.
122. Müller, A.; Sarkar, S.; Bhattacharyya, R. G.; Pohl, S.; Dartmann, M. *Angew. Chem. Int. Ed. Engl.* **1978,** *17,* 535.
123. Meienberger, M. D.; Hegetschweiler, K.; Rüegger, H. *Inorg. Chim. Acta* **1993,** *213,* 157.
124. Virovets, A. V.; Podberezskaya, N. V. *J. Struct. Chem.* (*Russian*) **1993,** *34,* 150.
125. Tsuge, K.; Imoto, H.; Saito, T. *Inorg. Chem.* **1995,** *34,* 3404.
126. Opalovskii, A. A.; Fedorov, V. E.; Khaldoyanidi, K. A. *Dokl. Akad. Nauk SSSR* **1968,** *182,* 1095.
127. Marcoll, J.; Rabenau, A.; Mootz, D.; Wunderlich, H. *Revue de Chimie Minerale* **1974,** *11,* 607.
128. Fedorov, V. Y.; Mironov, Y. V.; Kuzmina, O. A.; Fedin, V. P. *Zh. Neorg. Khim.* **1986,** *31,* 2476.
129. Cotton, F. A.; Kibala, P. A.; Matusz, M.; McCaleb, C. S.; Sandor, R. B. W. *Inorg. Chem.* **1989,** *28,* 2623.
130. Müller, A.; Diemann, E. *Chimia* **1985,** *39,* 312.

This Page Intentionally Left Blank

ADVANCES IN INORGANIC CHEMISTRY, VOL. 44

MACROCYCLIC CHEMISTRY OF NICKEL

MYUNGHYUN PAIK SUH

Department of Chemistry Education and the Center for Molecular Catalysis, Seoul National University, Seoul 151-742, Republic of Korea

I. Introduction

Many new Ni(II) complexes of aza-type macrocycles have been synthesized, and their redox chemistries have been explored. In particular, complexes of macropolycyclic ligands and bismacrocyclic ligands have been prepared. Complexes with uncommon oxidation states of nickel (Ni^{III} and Ni^{I} complexes) have also been synthesized by employing a specially designed macrocycle, and their characteristic spectroscopic properties and X-ray structures reported. These nickel(II) complexes

have been used in catalytic reactions such as olefin epoxidation and electrochemical reduction of alkyl halide and carbon dioxide. The uncommon high-valent nickel (Ni^{III} and Ni^{IV}) and low-valent nickel (Ni^{I}) species have been proposed to be involved in the former and the latter reactions, respectively. The Ni(I) macrocyclic complexes in particular have attracted great attention because methane production by F430 has been proposed to involve Ni(I) species (*1, 2*). F430 is a Ni(II) hydrocorphinoid complex that is the prosthetic group of methyl coenzyme M reductase. It catalyzes the reductive cleavage of *S*-methyl coenzyme M to coenzyme M and methane in the final stage of carbon dioxide reduction in methanogenic bacteria.

This review deals with syntheses, properties, structures, and reactions of Ni(II), Ni(III), and Ni(I) macrocyclic complexes that have been reported over the past few years.

II. Nickel(II) Complexes

A. Synthesis

The Ni(II) complexes of aza-type macrocylic ligands were prepared by complexation reaction between presynthesized macrocyclic ligands and the metal ion in solution or by metal-ion-directed template condensation reactions. The advantage of the complexation reaction is that the macrocyclic ligand may be isolated, purified, and characterized prior to the synthesis of the complex and the complexation is readily detectable by physical methods. Metal template synthesis generally offers high-yielding and selective routes to new ligand complexes. It often yields the macrocyclic complexes in one-pot reactions in which all reactants are mixed together in the presence of the metal ion and heated at reflux. The Ni(II) ion was used as the template metal ion more often than any other metal ions, because Ni(II) does not impede ligand-forming reactions by redox or hydrolysis, and Ni(II) complexes are in general insensitive to moisture and oxygen. In many instances, when a macrocyclic ligand complex was prepared by using Ni(II) ion as a template, then the same ligand complex was also obtainable using Cu(II).

It has been known that square-planar Ni(II) complexes are most stable with the 14-membered macrocyclic ligands. The typical 14-membered macrocycle is [14]aneN_4, which is called cyclam. Therefore, many Ni(II) complexes synthesized are those with 14-membered macrocyclic ligands that form 6-5-6-5-membered chelate rings with the metal

ion. Some Ni(II) macrocyclic complexes with different ring sizes have been reported as well.

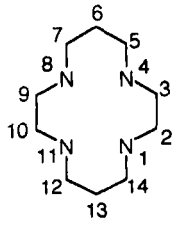

[14]aneN$_4$ (cyclam)

1. Template Condensation Involving Amines and Formaldehyde

Template condensation reactions of amines and formaldehyde are a very simple and convenient way to provide various macrocyclic ligand complexes. The Ni(II) macrocyclic complexes have been prepared by heating amines and formaldehyde in the presence of the metal ion. In cyclization reactions, formaldehyde links two cis-coordinated amine moieties to yield methylenediamine (N—CH_2—N) linkages. Methylenediamine groups are known to be unstable when they contain primary or secondary amines (*3*). Therefore, the nitrogen atoms of methylenediamine linkages of secondary nitrogens show a strong tendency to become tertiary upon cyclization (*4–10*). However, the secondary nitrogens of methylenediamine linkages can be stabilized when coordinated to the metal ion, and therefore ligands containing methylenediamine linkages with secondary nitrogens are stable as long as they exist as part of metal complexes.

Free ligands containing methylenediamine linkages have not been isolated because such ligands decompose when the metal ion is taken out of the complex.

a. Square-Planar Nickel(II) Complexes with Monocyclic Ligand. Hexaaza macrocyclic ligand complexes **1**, **2** and those with various alkyl groups at the uncoordinated bridgehead nitrogen atoms have been synthesized by template condensation of ethylenediamine, formaldehyde, and primary alkylamine in the presence of $NiCl_2$ in MeOH, followed by addition of the salt containing appropriate anion as summarized in Eq. (1). The Ni(II) complexes form square-planar geometry without coordination of the tertiary nitrogens at the bridgehead position (*7, 11*). Similarly, the Ni(II) complexes of pentaaza macrocyclic ligand **3a** and their analogues have been synthesized by employing 3,7-

diazanonane-1,9-diamine (2,3,2-tet), formaldehyde, and primary amine as described in Eq. (2) (*12*).

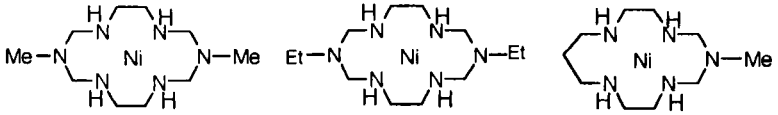

1 **2** **3a**

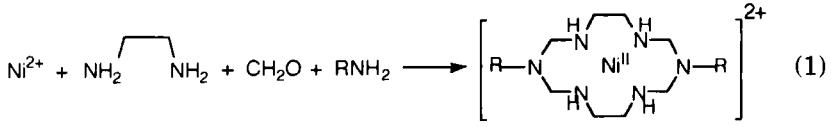

1: R = Me, 2: R = Et

(1)

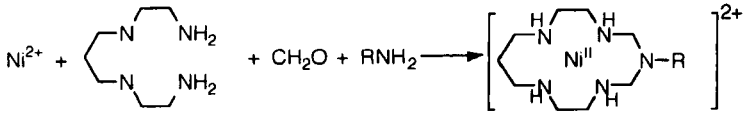

(2)

The functional groups can be attached to the macrocyclic ligands by using methods similar to Eqs. (1) and (2). The Ni(II) complexes of pentaaza macrocyclic ligands, **3b–3g**, in which functional groups are appended at the bridgehead nitrogen atom, are prepared by the template reaction of $[Ni(2,3,2\text{-tet})]^{2+}$ and formaldehyde with carboxamide or sulfonamide in the presence of base. The complexes **3b** and **3c** are

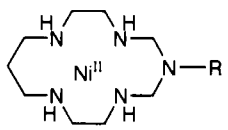

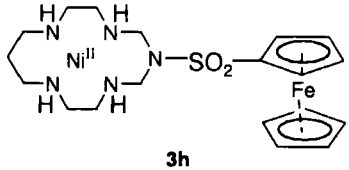

3h

3b: R = CO-(2-pyridyl)

3c: R = CO-(4-pyridyl)

3d: R = CO-CH_3

3e: R = CO-(X-phenyl) (X = H, *o*- or *p*-NO_2)

3f: R = SO_2-R' (R' = CH_3, $C_{16}H_{33}$, C_6H_5)

3g: R = SO_2-(X-phenyl) (X = CH_3, Cl, NO_2)

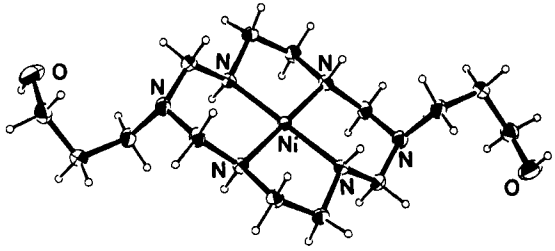

FIG. 1. Structure of $[Ni^{II}(\mathbf{5})](ClO_4)_2$. [Reprinted with permission from (*16*). Copyright 1994, American Chemical Society.]

obtained as $[Ni(L)](ClO_4)_2 \cdot HClO_4$, in which the pendent pyridine subunit becomes protonated. The pyridine pendants react with $[Pt^{II}Cl_4]^{2-}$ and *cis*-$[Ru^{II}(bipy)_2Cl_2]$ in a 2:1 ratio to give supercomplexes *cis*-$[(Ni^{II}L)_2Pt^{II}Cl_2](PtCl_4)(ClO_4)_2$ and *cis*-$[(Ni^{II}L)_2Ru^{II}(bipy)_2](ClO_4)_6$, respectively (*13, 14*). The Ni(II) complex, **3h**, in which a ferrocene subunit is covalently linked to the azacyclam ligand also has been synthesized by a similar reaction, using 2,3,2-tet, formaldehyde, and ferrocenesulfonamide in the presence of Ni(II) ion (*15*).

The nickel(II) complexes **4–7**, which incorporate functional groups –OH and –CN into the pendent arms attached to the uncoordinated bridgehead nitrogen atoms, are synthesized by the template condensation reactions of ethylenediamine, formaldehyde, and primary amines with appropriate functional groups (*16*). The complexes **4–7** are square-planar in solutions. The pendent hydroxyl groups in $[\mathbf{4}]^{2+}$ and $[\mathbf{5}]^{2+}$ do not coordinate Ni(II) ion in water at pH $\leq$ 13.0 and ionic strength 1.0 *M* ($NaClO_4$). In the solid state, the complexes **4**, **5**, and **7** form square-planar complexes as the functional groups do not coordinate metal ions (Fig. 1). However, $[\mathbf{6}](BF_4)_2$, the complex containing a $-CH_2CH_2$—CN functional group, is a coordination polymer with an octahedral geometry around the metal (Fig. 2). The coordination polymer is formed by the coordination of both nitrile pendants of the ligand to the intermolecular Ni(II) ions.

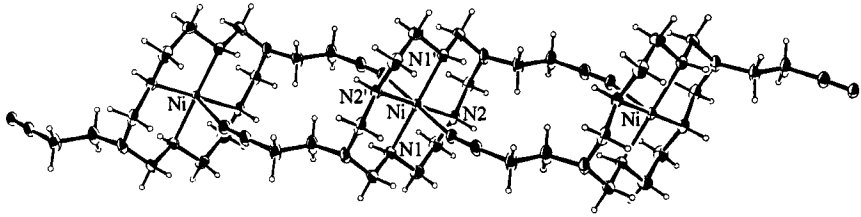

FIG. 2. Structure of $[Ni^{II}(\mathbf{6})]_n(BF_4)_{2n}$. [Reprinted with permission from (*16*). Copyright 1994, American Chemical Society.]

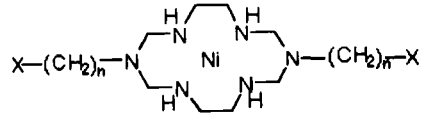

4: X = OH, n = 2 **5**: X = OH, n = 3
6: X = CN, n = 2 **7**: X = CN, n = 5

Nitroethane also has been utilized in place of primary amine or amide as a locking fragment in the template condensation reaction of amines and formaldehyde for the synthesis of macrocyclic complexes. For example, the square-planar Ni(II) complex of L_1 was prepared by the reaction of $Ni(en)_3^{2+}$, formaldehyde, and nitroethane (*17*).

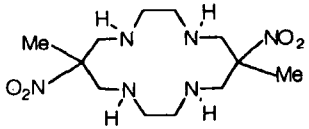

L_1

b. Square-Planar Nickel(II) Complexes with Macropolycyclic Ligands. The Ni(II) complexes of various polyaza polycyclic ligands, **8–14**, have been synthesized by heating formaldehyde and appropriate amines at reflux in the presence of $NiCl_2$ in methanol solutions for 4–12 hr, and then precipitating with $LiClO_4$ or CF_3SO_3Li as summarized in Eqs. (3)–(9) (*6, 8, 10, 18*). The yields were generally high (50–90%). All ligands in **8–14** contain methylenediamine linkages in which nitro-

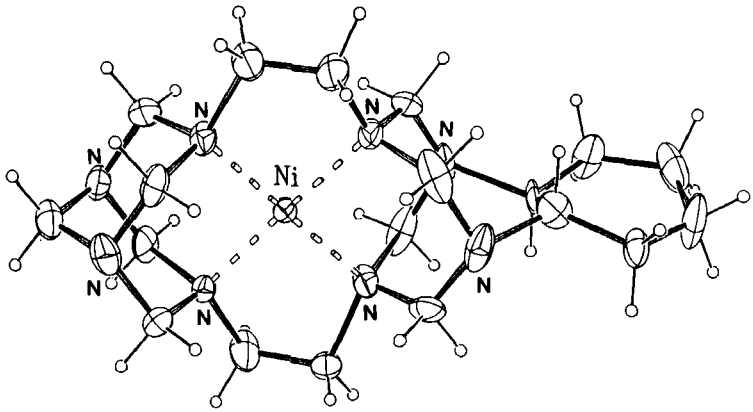

FIG. 3. Structure of $[Ni^{II}(\mathbf{10})](PF_6)_2$. [Reprinted with permission from (*18*). Copyright 1994, The Royal Society of Chemistry.]

gen atoms are either tertiary or coordinated secondary groups. The complexes **8–10** contained football-shaped tetraazabicyclononane moieties (Fig. 3). The complexes **11–14** contained uncommon 1,3-diazacyclopentane and 1,3-diazacyclohexane sub-ring moieties in the hexaaza macrocyclic framework. Although the ligands in **8–14** contained more than four nitrogen atoms, they acted as a tetradentate to form the square-planar complexes.

The Ni(II) macrocyclic complexes, **9–14**, are extremely stable and become only slightly decomposed even in highly acidic media.

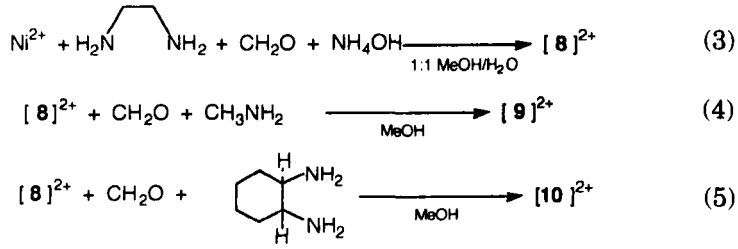

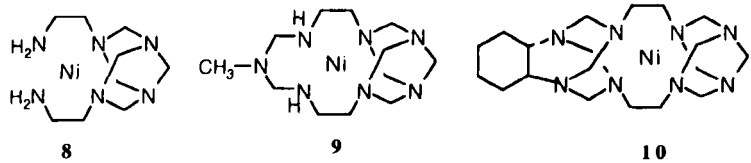

8 **9** **10**

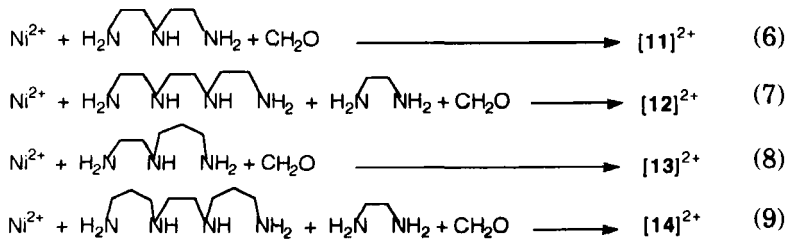

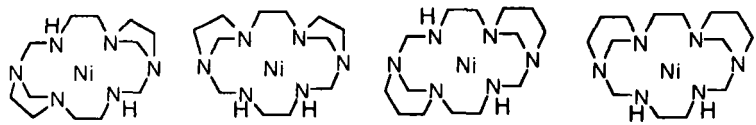

11 **12** **13** **14**

In cases where nitroethane is used instead of methylamine as shown in Eq. (4), the Ni(II) complex of hexaaza macrotricyclic ligand, L_2, can be prepared (*19*).

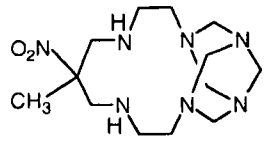

L_2

c. Octahedral Nickel(II) Complexes with Macrobicyclic Ligands. The Ni(II) complex of **15** was synthesized by a reaction similar to that used in the synthesis of complex **12**, but with a different mole ratio of reactants (*9*). The hexaaza macrocyclic ligand in **15** serves as a pentadentate, and the Ni(II) complex forms a distorted octahedral structure having an extra axial Cl^- ligand. The complex includes an uncommon four-membered chelate ring and the methoxy methyl pendent chain.

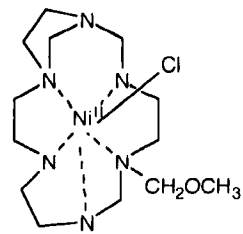

15

The octahedral Ni(II) complex of **16** was obtained from the reaction of $[Ni(en)_3]^{2+}$, formaldehyde, and ammonia, similarly to Eq. (3). The yield was low (ca. 1%), probably because the Ni(II) ion is a labile metal ion (*4*). The complex was extraordinarily stable against ligand substitution with donors such as NCS^-, Me_2SO, H_2O, or MeCN. The electronic spectrum of the complex was similar to that of $[Ni(en)_3]^{2+}$, but the ligand field strength of the complex was slightly stronger than that of $[Ni(en)_3]^{2+}$ because of capping with tris(methylene)amino moieties.

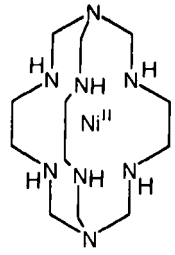

16

d. Bismacrocyclic Nickel(II) Complexes. The macrocycles that can provide dinuclear complexes of a well-defined structure are important for mimicking of metallobiosites (*20*), to activate simple molecules (*21, 22*), and to investigate the mutual effect of two metal centers on their physicochemical properties (*23, 24*).

The dinickel(II) complexes of bis-heptaazamacrocyclic ligands, **17–19**, have been prepared by the template condensation reactions of the nickel(II) complex of 3,7-bis(2-aminoethyl)-1,3,5,7-tetraazabicyclo-[3.3.1]nonane (**8**) with formaldehyde and the appropriate primary diamines such as ethylenediamine, 1,4-butanediamine, and *p*-xylenediamine. The electrochemical data indicated that each Ni(II) ion was independent, without interaction between the two Ni(II) metal centers (*25*).

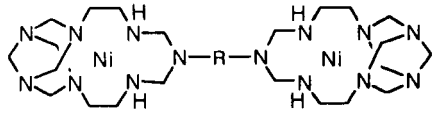

17: R = $-(CH_2)_2-$
18: R = $-(CH_2)_4-$
19: R = $-p-CH_2-C_6H_4-CH_2-$

Similarly, the dinuclear Ni(II) complexes of bis-monocyclic ligands, **20**, were prepared by using $[Ni(2,3,2\text{-tet})](ClO_4)_2$, formaldehyde, and $NH_2—(CH_2)_n—NH_2$(n = 2,3,4). No interactions between the metal centers were observed in these dinickel complexes, either (*26, 27*).

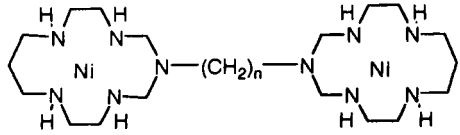

20 (n = 2,3,4)

2. Other Template Reactions

The square-planar Ni(II) complex of an anionic macrocyclic ligand, **21**, was prepared from the template reaction of 3,3′-(ethylenebis(iminomethylidene)bis(2,4-pentanedionato)nickel(II) with 1,3-diamino-2-propanol [Eq. (10)]. The uncoordinated –OH group reacted smoothly with acylating agents, resulting in –COPh and $-COCH_3$ (*28*).

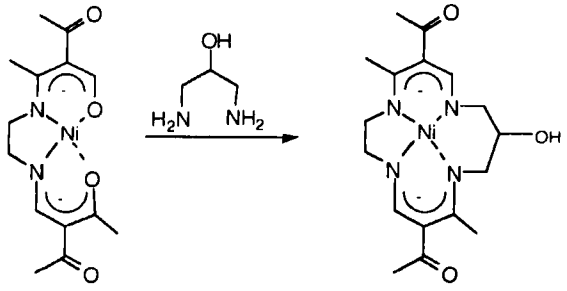

(10)

21

The Ni(II) complex of a 16-membered macrocycle, 2,7-dimethyl-3,6-(1,1′-(2,2′-biimidazole)-1,3,6,8,11,14-hexaazacyclohexadeca-1,7-diene, **22**, was synthesized by Schiff base condensation of the Ni(II)-triethylenetetramine complex and 1,1′-diacetyl-2,2′-bisimidazole (*29*). The Ni(II) complex formed square-planar geometry with iodide or perchlorate anions and an octahedral structure with chloro or bromo ligands.

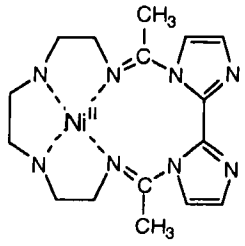

22

The heterodinuclear Ni(II)M(II) (M = Pb, Mn, Fe, Co, Ni, Cu, Zn) complexes, **23**, have been prepared from the template reaction of Ni(II) complex of *N,N′*-ethylenebis(3-formyl-5-methylsalicylideneiminato), diethylenetriamine, and $Pb(ClO_4)_2 \cdot 3H_2O$ salt, followed by the transmetallation of Pb(II) ion with M(II). In the complexes, where Ni(II) ion is found located at the 4-coordination site, the M(II) ion is observed located at the 5-coordination site of the macrocycle (*30*).

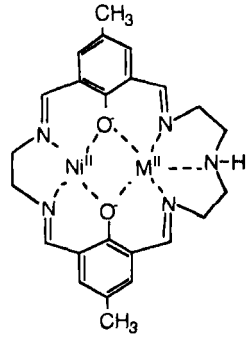

23

3. *Synthesis of Macrocyclic Complexes from Free Ligands*

Macrocyclic Ni(II) complexes with a series of elegantly designed macrocyclic ligands were prepared by inserting the metal ions into the presynthesized free ligands. In particular, various complexes containing pendent functional groups were prepared by this method. The functional groups often affected the properties of the macrocyclic complexes through the coordination of metal ion. The most common ligands synthesized were cyclam derivatives.

Various functional groups, such as amine, hydroxyl, amide, carboxylic, and nitrile functional groups, have been attached to the side chains of the coordinated nitrogen donors (*31–34*). Some of these donors bound to metal ions intramolecularly at the axial position and dramatically altered the properties of the complexes. For example, the cyclam derivative with tetranitrile pendent chains, L_3, was prepared by heating cyclam directly in acrylonitrile (*34*). The Ni(II) complex of L_3 formed a square-planar geometry without coordination of any of its nitrile groups to the metal ion. However, the ligand with an amide functional derivative yielded an octahedral and a five-coordinate complex in which two and one of the pendent amide groups, respectively, became bonded to the Ni(II) ion.

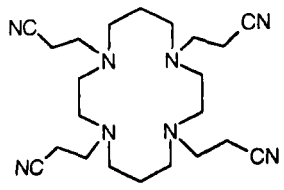

L_3

N-(Aminoethyl)cyclam was prepared from the reaction between tritosylated cyclam and tosylaziridine. In the Ni(II) complexes of the ligand, the amine group of the side chain displayed acidity-dependent coordination behavior. At pH > 2.8 the side arm apically bound to Ni(II) ion to form a blue high-spin complex $[Ni(\mathbf{L}_4)]^{2+}$, but at pH < 2.8 the amine of the side chain became protonated and formed $[Ni^{II}(\mathbf{L}_4H)]^{3+}$ as a mixture of a blue high-spin form and a yellow low-spin form (*35*).

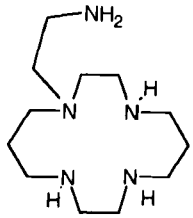

$\mathbf{L}_4$

In addition, Ni(II) complexes with macrocyclic ligands containing pyridine in the macrocyclic framework with a single pyrrolidinyl pendent arm, $\mathbf{L}_5$-**1** and $\mathbf{L}_5$-**2**, have been prepared (*36*). Such complex formed octahedral $[Ni(\mathbf{L}_5\text{-}\mathbf{2})(OClO_3)][ClO_4]$ by coordinating four nitrogens of the macrocycle, the pendent pyridine, and a ClO_4^- ion. In the complex, the macrocyclic ligand coordinated close the corners of a square pyramid with the pendent group at the apical position.

The 12-membered tetraaza-macrocyclic ligand with four pendant pyrazole groups, $\mathbf{L}_6$, was synthesized by the reaction of 1-(hydroxymethyl)pyrazole with 1,4,7,10-tetraazacyclododecane in MeCN. The Ni(II) complex $[Ni\mathbf{L}_6]I_2$ formed a distorted octahedral structure with

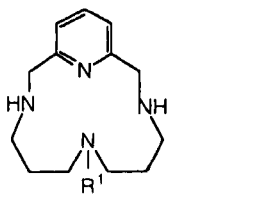

$\mathbf{L}_5$-**1**: R^1 = 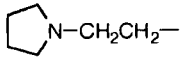

$\mathbf{L}_5$-**2**: R^1 = 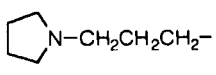

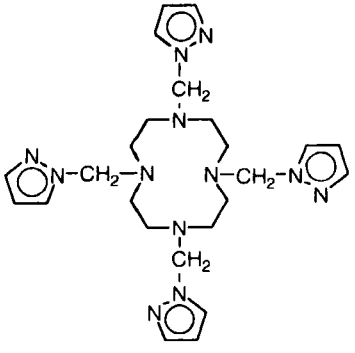

$\mathbf{L}_6$

two pendent arms of the ligand being coordinated. In this complex, the four amine nitrogens span two contiguous faces of the distorted octahedron about the nickel atom, with the pyrazole nitrogens occupying the remaining pair of cis positions (*37*).

The pendent-arm macrocycles L_7-**1** and L_7-**2** have been synthesized by the reaction of L_7-**3** and L_7-**4**, respectively: They were prepared by the reaction of $[Ni(DMSO)_n](ClO_4)_2$ and the free ligand in EtOH, with aqueous NaOH followed by the addition of 2-chloromethylpyridine and 1-(hydroxymethyl)pyrazole under nitrogen. The Ni(II) complexes of L_7-**1** and L_7-**2** are six-coordinate, and the X-ray crystal structure of $[Ni(L_7\text{-}1)](ClO_4)_2$ shows that the macrocycle has a folded conformation with the two pendent 2-pyridylmethyl arms occupying *cis*-coordination sites (*38*).

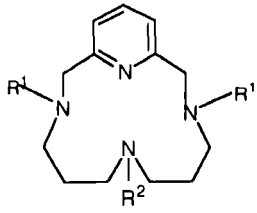

L_7-**1** : $R^1 = X$, $R^2 = H$
L_7-**2** : $R^1 = Y$, $R^2 = Me$
L_7-**3** : $R^1 = R^2 = H$
L_7-**4** : $R^1 = H$, $R^2 = Me$

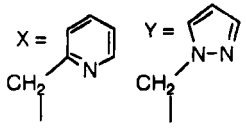

Some functional groups such as phenol, pyridyl, catechol, imidazole, and amine, which are attached to the carbon atoms of macrocyclic framework, also affect the coordination geometry of the metal ions (*39–44*).

The 12-membered macrocyclic triamine bearing a phenol pendant, L_8, was synthesized by one-pot annealation from coumarin and 1,7-

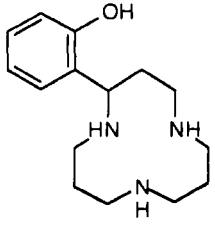

L_8

diamino-4-azaheptane. The pendent phenol readily dissociated its proton at acidic pH upon coordination of metal ions such as Ni(II), Zn(II), and Cu(II) and became a strong fourth donor (*45*).

The cyclam with an amine pendent donor attached at the bridgehead carbon atom was synthesized from diethylaminomalonate and 1,9-diamino-3,7-diazanonane in refluxing MeOH, followed by BH_3-thf reduction (*41*). The ligand coordinated Ni(II) ion in pH 8.5 as a pentadentate and formed a six-coordinate complex with a water molecule binding at the axial site. The X-ray crystal structure of the complex indicated that the pendent NH_2 coordinated at the axial site and the cyclam moiety took a *trans*-I configuration.

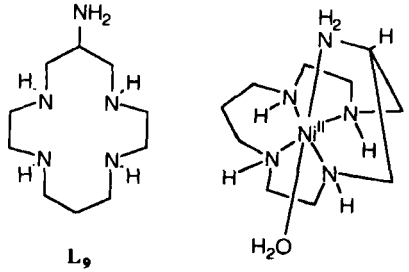

L_9

The encapsulating ligand with N_4S_2 donors (L_{10}) was prepared, and it coordinated to Ni(II) to give an octahedral complex (*46*).

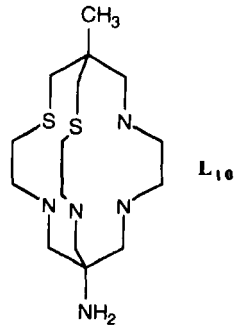

L_{10}

4. Synthesis of New Nickel(II) Complexes by Using Presynthesized Nickel(II) Macrocyclic Unit

a. Synthesis of N-Alkylated Nickel(II) Complexes. *N*-Methylated macrocyclic Ni(II) complexes were prepared, in general, by the deprotonation of secondary amines of Ni(II) macrocyclic complexes with pulverized KOH in Me_2SO or MeCN media, followed by alkylation with CH_3I.

It is also possible to prepare the complexes from presynthesized *N*-alkylated macrocycles.

Bis-*N*-alkylated complexes of Me_2-**9** and Me_2-**11**, as well as the tetramethylated Ni(II)cyclam (**Ni^{II}TMC**) derivatives, have been synthesized by the deprotonation of secondary amines followed by alkylation (*34, 47, 48*). When EtI or other alkyl halide with β-hydrogen was added to the deprotonated Ni(II) complex of cyclam or **11**, HX elimination occurred instead of S_N2 reaction. Therefore, ethylene gas was produced instead of *N*-ethylated complex formation when EtI was added to the deprotonated complex of cyclam or **11**. However, in the case of **8**, bis-*N*-ethylated Ni(II) complex was isolated. This may be because HX elimination is slower than S_N2 reaction. The bis-*N*-alkylated Ni(II) complexes of **9** (**Me_2-9** and **Et_2-9**) and **Me_2-11** were stable against ligand dissociation in acidic aqueous solutions. The *N*-alkylated complexes were dealkylated when the complexes were heated in aqueous solutions (*34, 47*).

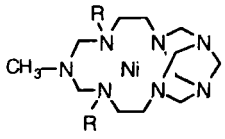

Me_2-9: R = Me

Et_2-9: R = Et

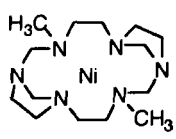

Me_2-11

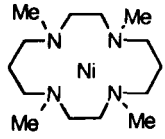

Ni-TMC

b. Synthesis of Dinucleating Ligand Complexes. The dinuclear bis-macrocyclic complex **24** has been prepared from the reaction of **25** and *o*-xylyl chloride followed by reduction with $NaBH_4$ in H_2O (pH 5–6). The two cyclam rings in **24** were arranged in a face-to-face manner. The complex coordinated the bridging ligand such as Cl^-, Br^-, or CO_3^{2-}. The chloro-bridged dinickel(II) complex had a pseudo-one-dimensional Ni–Cl alternate linear chain structure in the solid state. The

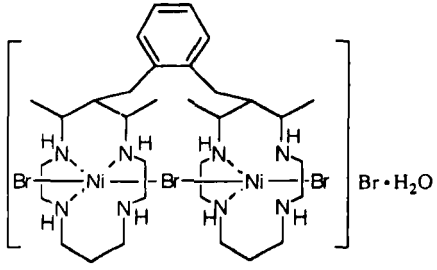

24

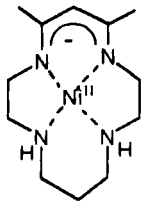

25

complex exhibited an antiferromagnetic interaction between the two Ni(II) ions (*49*).

The reaction of the Ni(II) complex, **25**, with isophthaloyl dichloride resulted in the dinuclear Ni(II) complex, **26**. The two coordination planes were nearly coplanar with the metal ions being 12.8 Å apart (*50*).

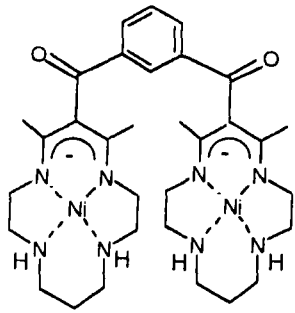

26

B. Electronic Absorption Spectra

The UV-vis spectrophotometric properties of Ni(II) macrocyclic complexes are affected by the substituents, the degree of unsaturation, the cavity size, and the chelate ring sequences of the macrocyclic ring (*13, 51, 52*). In addition, the presence of tertiary amine donors and the size of the sub-ring moieties fused to the macrocyclic framework may alter such properties. In general, introduction of tertiary amine donors in the Ni(II) macrocyclic complexes results in a decrease in the ligand field strength, thus causing the maximum absorption to shift to longer wavelengths. For the macrotricyclic complexes with fused sub-ring moieties such as **11–14**, the ligand field strength is shown to decrease as the size of the sub-ring increases.

1. Effect of Uncoordinated Tertiary Nitrogens and Type of Pendent Chain

Square-planar Ni(II) macrocyclic complexes are typically yellow, red, or brown in color and absorb around 400–500 nm, depending on the ligand structure. The octahedral Ni(II) complexes absorb at 500–600 nm.

Spectrophotometric data on some Ni(II) macrocyclic complexes are summarized in Table I. The maximum absorption of the square-planar Ni(II) complex with neutral azamacrocyclic ligand shifts to a longer

TABLE I

ELECTRONIC ABSORPTION SPECTRA AND ELECTROCHEMICAL DATA FOR NICKEL(II) MACROCYCLIC COMPLEXES

Complex	λ_{max}/nm (ε, $M^{-1}cm^{-1}$)	E_{ox}[a,b] Ni(II)/Ni(III)	E_{red}[a,b] Ni(II)/Ni(I)	Ref.
	Square-planar complexes			
1	449 (56)[c]	+0.93	−1.55	*7*
2	449 (64)[c]	+0.90	−1.47	*7*
3a	450[d]			*12*
4	448 (82),[c] 446 (56)[d]	+0.94(q)	−1.47(qr)	*16*
5	449 (77),[c] 445 (56)[d]			*16*
6	445 (27),[d] 451 (39)[f]			*16*
7	449 (63),[c] 445 (57)[d]			*16*
cyclam	445[d]	+0.91	−1.46	*58*
Me_6[14]aneN$_4$[g]		+1.11	−1.33	*58*
Me_2[13]aneN$_4$[g]	428 (145)			*62*
8	435 (83)[c]			*6*
9	438 (83),[c] 442 (80)[e]	+1.32	−1.39	*6*
10	425 (209)[d]	>+1.53	−1.38 (r)	*18*
11	447 (80),[c] 449 (78)[e]	+1.50 (i)	−1.28	*8, 10*
12	456 (89),[c] 459 (80)[e]	+1.43 (i)	−1.25	*10*
13	465 (95),[c] 471 (41)[e]	+1.34	−1.20 (qr)	*8, 10*
***R,R,S,S*-14**	471 (90),[c] 480 (28)[e]	+1.25	−1.14	*10*
***R,S,R,S*-14**	489 (116),[c] 496 (106)[e]	+1.39	−1.01	*56a*
17	440	+1.31 (qr)	−1.42 (r)	*25*
18	434 (71),[c] 440 (152)[e]	+1.48 (i)	−1.37 (qr)	*25*
19	442 (161)[e]	>+1.90	−1.33 (r)	*25*
	Octahedral complexes			
15	554 (15), 363 (23)[f]			*9*
	534 (8), 350 (13)[d]			
16	510 (8), 316 (11)[e]			*4*
$Ni(en)_3^{2+}$	540 (7), 333 (9)[e]			

[a] Measured in acetonitrile solutions, 0.1 *M* $(n\text{-Bu})_4NClO_4$, volts vs SCE.
[b] i = irreversible; qr = quasi-reversible.
[c] Measured in $MeNO_2$.
[d] Measured in H_2O.
[e] Measured in MeCN.
[f] Measured in Me_2SO.
[g] Abbreviations: Me_6[14]aneN$_4$ = 5,5,7,12,12,14-hexamethyl-1,4,8,11-tetraazacyclotetradecane, Me_2[13]aneN$_4$ = 8,10-dimethyl-1,4,7,11-tetraazacyclotridecane.

wavelength in the visible region (λ_{max}) as the ligand field strength decreases. Extinction coefficients of the square-planar Ni(II) complexes without double-bond conjugation in the macrocycle are in the range of 30–100 nm, depending on the solvent. The electronic spectra of Ni(II)

complexes of monocyclic ligands **1–7** are similar to those of Ni(II) complexes of cyclam, indicating that the presence of two extra uncoordinated tertiary nitrogens at the bridgehead position does not affect the ligand field strength of the complexes. In addition, a variation of alkyl groups and the types of the pendent functional groups at the bridgehead nitrogen atoms slightly affect the spectra of the complexes (*7, 11, 13, 16*).

2. Effect of Fused Sub-ring Moieties of Macrocycle

The Ni(II) complexes **8–10**, which contain a football-shaped moiety fused to the ligands, absorb at significantly shorter wavelengths than the complexes of the 14-membered tetraaza monocycle and exhibit unusually strong ligand field strength. This is attributed to the short N--N bite distances of the six-membered chelate ring involving the tetraazabicyclononane ("football") moieties (*7, 18*). The N--N bite distances involving the tetraazabicyclononane moieties are similar to the values for five-membered chelate ring. Therefore, the macrocycles in **9** and **10** are rather similar to a [13]aneN$_4$ and a [12]aneN$_4$, respectively.

For the macrotricyclic complexes **11–14**, which retain the same 14-membered macrocyclic framework, the size of the sub-ring moieties affects the spectroscopic properties of the complexes. The complexes of **11** and **12** contain uncommon 1,3-diazacyclopentane, and **13** and **14** contain 1,3-diazacyclohexane sub-ring moieties in the hexaaza macrocyclic framework. The Ni(II) complexes **13** and **14** exhibit λ_{max} values that are ca. 20 nm longer than those of **11** and **12**, indicating the weaker ligand field strength of **13** and **14**. The weaker interaction between the Ni(II) ion and the macrocyclic ligand with 1,3-diazacyclohexane sub-ring moieties is related to the Ni—N bond distances in **13** and **14**, which are longer by 0.03 Å than those in **11** and **12** (*8, 10*). There is a qualitative relationship between Ni—N bond distances and λ_{max} values. As the Ni—N bond distance increases, the λ_{max} value increases.

3. Effect of Bridging Chains in Bismacrocycles

The spectra and redox potentials of the binuclear bismacrocyclic Ni(II) complexes, **17–19** and **20**, are similar to those of the corresponding mononuclear complexes of **9** and **3a**, respectively. That is, the ligand field strength of the complexes is only slightly affected by the type or the length of bridging chain that links the two macrocyclic units.

4. Effect of Tertiary Amine Donors

The introduction of *N*-alkyl substituents to the secondary nitrogens of **9** and **11**, as well as cyclam, results in the shift of λ_{max} values to

TABLE II

PROPERTIES OF SQUARE-PLANAR NICKEL(II) COMPLEXES OF *N*-ALKYLATED MACROTRICYCLIC LIGANDS

Ligand	λ_{max}[a,b] nm (ε, $M^{-1}cm^{-1}$)	E_{ox}[c,d] Ni(II)/Ni(III)	E_{red}[c,d] Ni(II)/Ni(I)	Ref.
Cyclam	445	+0.91	−1.46	*55a*
N-Me-cyclam	454 (85)[a]	+1.01	−1.40	*55a*
N-Me_4-cyclam	511 (71),[a] 492[b]			*55b, 59*
9	438 (83)[b]	+1.32	−1.39	*6, 47*
***N*-Me_2-9**	447 (75),[a] 447 (103)[b]	+1.60 (i)	−1.07	*6, 47*
***N*-Et_2-9**	455 (118),[a] 457 (119)[b]	+1.41	−1.12	*47*
11	447 (80)[b]	+1.50 (i)	−1.28	*47*
***N*-Me_2-11**	455 (92),[a] 466 (102)[b]	+1.64 (i)	−0.94 (qr)	*47*

[a] Measured in H_2O at 20°C.
[b] Measured in $MeNO_2$ at 20°C.
[c] Measured in acetonitrile solutions; 0.1 *M* $(n\text{-Bu})_4NClO_4$; volts vs SCE.
[d] i = irreversible, qr = quasi-reversible.

10–20 nm longer wavelengths (Table II), indicating a decrease in the ligand field strength upon *N*-alkylation (*47, 53–55b*). The weaker ligand field strength of the *N*-alkylated complexes is explained by the longer Ni—N bond distances of the complexes. For example, the square-planar Ni(II) TMC complex has an average Ni—N distance ca. 0.04 Å longer than that of Ni(II) cyclam and shows a λ_{max} value that is 65 nm red-shifted compared to that of Ni(II) cyclam (*54*). The spectra of the Ni(II) complexes of *N*-alkylated ligands of **9** indicate that *N*-ethyl substituents weaken the ligand field strength better than *N*-methyl substituents (*47*). Nitrogen donors with bulky substituents would tend to form sp^2 hybridization rather than sp^3, thus causing further elongation in the Ni—N bonds.

The spectrum of the octahedral Ni(II) complex with hexaaza macrobicyclic ligand, **16**, is similar to that of $[Ni(en)_3]^{2+}$, but the ligand field strength of the complex is increased slightly by the capping of the $[Ni(en)_3]^{2+}$ moiety with two tris(methylene)amino groups (*4*).

5. *Effect of Configuration of Macrocyclic Ligand*

The configuration of the macrocyclic ligand affects the λ_{max} and the extinction coefficient of Ni(II) complex (Table I) (*56a, 56b*). For example, the maximum absorption band of (*R,S,R,S*)-[Ni(**14**)]$^{2+}$ appears at ~20 nm longer wavelengths than that of the *R,R,S,S* isomer. In addition, the value of the extinction coefficient for the *R,S,R,S* complex is greater than that for the *R,R,S,S* isomer, in the visible region. Similar observa-

tions are also made with other macrocyclic complexes (*56b, 56c*). In the square-planar *R,S,R,S* complex, the metal ion locates out of the coordination plane and the five-membered chelate rings display an asymmetric gauche conformation. Therefore, the *R,S,R,S* complex has steric strain of the macrocycle that causes poor overlap between the Ni(II) ion and the nitrogen orbitals and provides weaker ligand field strength.

C. Electrochemical Properties

Electrochemical properties of the Ni(II) macrocyclic complexes are related to the cavity size, the unsaturation, the degree of functionalization, and the sub-ring moieties fused to the macrocycles (*10, 47, 51, 57*).

1. Monocyclic Ligand Complexes vs Polycyclic Ligand Complexes

Cyclic voltammetry data for the Ni(II) complexes of monocyclic ligands **1–7** and of polycyclic ligands **9–14** are summarized in Table 1. For the monocyclic complexes **1–7**, oxidation to Ni(III) occurs at +0.90–+0.93 V and reduction to Ni(I) at −1.46–−1.55 V vs SCE. However, in the macropolycyclic ligand complexes **9–14**, oxidation and reduction occur at +1.25–+1.60 V and at −0.94–−1.40 V vs SCE, respectively. That is, electrochemical oxidation of Ni(II) complex to Ni(III) species is easier for the monocyclic complexes, whereas electrochemical reduction to Ni(I) is easier for the macropolycyclic complexes. The anodic shifts in both oxidation and reduction potentials for Ni(II) macropolycyclic complexes in part may be attributed to the tertiary nitrogen donors of the ligands.

2. Effect of Uncoordinated Tertiary Amines and Pendent Groups

The redox properties of the hexaaza monocyclic complexes **1–7** are similar to those of the cyclam. This indicates that the electrochemical properties of the complexes are only slightly affected by the presence of uncoordinated tertiary nitrogen atoms, the length of the pendent chain, and the type of the functional group appended at the bridgehead nitrogen (*16, 58*).

However, the redox potentials of the Ni(II) complexes of the azacyclam (**3b–3g**) containing carboxamide or sulfonamide functional groups are reported to be influenced by the nature of the functional group. In particular, the amide fragment controls the reduction potential for the Ni^{III}/Ni^{II} and Ni^{II}/Ni^{I} redox couples, which may be attributed to the π interaction between the nickel ion and the amido group (*14*).

3. *Effect of Tertiary Amine Donors*

The introduction of *N*-alkyl substituents to the secondary amine donors of the macrocycle results in anodic shifts in both oxidation and reduction potentials of the complexes relative to the parent ligand systems (Table II). The extent of anodic shifts depends on the number of alkyl groups introduced to the ligand (*47, 55a*). That is, *N*-alkylation makes the attainment of the Ni(I) state easier and the Ni(III) state more difficult. The stabilization of Ni(I) species by *N*-alkylation is ascribed to solvation and stereochemical effects (*55b, 60*). *N*-Ethyl groups have greater inductive effects than *N*-methyl groups and yield less anodic shift in both oxidation and reduction potentials (*47*). This anodic shift of redox potentials may be attributed to weaker Ni–N interactions in the *N*-alkylated complexes. The weaker Ni–N interaction for the tertiary amine results in the stabilization of antibonding σ-orbitals of the Ni(II) complex, which makes it more favorable to add an electron, but less favorable to remove an electron.

4. *Effect of Configuration of Macrocyclic Ligand*

The configuration of the macrocyclic ligand affects the electrochemical properties of Ni(II) complexes (Table I) (*56a, 54*). For example, the oxidation and reduction potentials of (*R,S,R,S*)-[Ni(**14**)]$^{2+}$ are shifted by +0.14 and +0.13 V, respectively, compared with those of the *R,R,S,S* isomer. Similar trends are also observed for a series of *R,S,R,S* and *R,R,S,S* isomers of *N*-methylated cyclam derivatives (*61a, 61b*). The anodic shift of the redox potentials for the *R,S,R,S*-Ni(II) complex indicates that the complex is more difficult to oxidize to Ni(III) but easier to reduce to Ni(I), compared with the *R,R,S,S* complex. This may be related to the reduced ligand field strength of the *R,S,R,S* complex, which stabilizes the antibonding σ-orbitals and thus makes addition of an electron more favorable while removal of an electron is less favorable.

D. X-Ray Structures

The Ni—N bond distances, N–N bite distances, and N–M–N bite angles of Ni(II) macrocyclic complexes depend on the coordination number of the metal ion and the type of macrocycle. These structural parameters influence the electronic spectra and the electrochemical data. In general, Ni—N bond distances of square-planar complexes are shorter than those of the octahedral complexes because of the absence of electrons in $d_{x^2-y^2}$. Furthermore, as the Ni—N bond distance in-

creases, the value of λ_{max} for the square-planar Ni(II) complex shifts to the longer wavelength. In addition, Ni(II) → Ni(I) electrochemical reduction of the complexes becomes easier and Ni(II) → Ni(III) electrochemical oxidation becomes more difficult as the Ni—N bond distances increase.

The structural parameters of various Ni(II) macrocyclic complexes are summarized in Table III. Square-planar Ni(II) complexes with saturated macrocyclic ligands have Ni—N bond distances ranging from 1.90 to 1.95 Å, depending on the type of ligand. The Ni—N bond distances increase when square-planar Ni(II) complexes bind axial ligands to form octahedral species. For example, the square-planar Ni(II) complex **[5]**$(ClO_4)_2$ has an average Ni—N bond distance of 1.929(2) Å, while the Ni(II) coordination polymer $[\mathbf{6}]_n(BF_4)_{2n}$, where the Ni(II) ion is in an octahedral geometry by coordinating two nitrile groups of the neighboring macrocycles, has an average Ni—N(macrocycle) bond distance of 2.056(3) Å (*16*).

Square-planar Ni(II) complexes of the 14-membered tetraazamacrocycle have several possible ligand configurations. The most stable configuration of the ligand is the *R,R,S,S*-(*trans*-III) configuration, in which the hydrogen atoms on the nitrogens of six-membered chelate rings are positioned at the same side of the macrocycle while the hydrogen atoms trans to them are at the opposite side of the plane (*62*). Most of the Ni(II) complexes including **1–14** have the *trans*-III configuration, although some complexes having the *trans*-I configuration are also

TABLE III

DIMENSIONS FOR SOME SQUARE-PLANAR NICKEL(II) COMPLEXES

Complex	Ni[a]	Ni–L[b]	Chelate rings		Ref.
			Bite distances[c] (Å)	Bite angles[d] (deg)	
[3]$(ClO_4)_2$	0.018	1.932		86.4, 93.5	*12*
[5]$(ClO_4)_2$	0	1.929(2)	2.647(3), 2.807(3)	86.6(1), 93.4(1)	*16*
$[\mathbf{6}]_n(BF_4)_{2n}$	0	2.056(3)	2.797(6), 3.013(7)	85.7(2), 94.3(2)	*16*
[9]$(ClO_4)_2$	0.034	1.918(3)	2.65, 2,66, 2.84, 2.69	87.7, 89.1, 95.4	*6*
[10]$(PF_6)_2$	0.057	1.904(7)	2.70(1), 2.68(1)	90.4(2), 89.5(2)	*18*
[11]Cl_2		1.920	2.627(9), 2.801(9)	86.3(3), 93.7(3)	*8*
[12]ClO_4	0.020	1.923(4)	2.65, 2.79	87.2, 93.0	*10*
[14]$(ClO_4)_2$	0.025	1.951(2)	2.67, 2.84	86.5, 93.5	*10*

[a] Displacement of Ni atom from NiN_4 plane (Å).
[b] Average Ni—N bond distance (Å).
[c] N–N bite distances (Å).
[d] Bite (NMN) angles.

isolated. In the Ni(II) complexes of macropolycyclic ligands **11–14**, the macrocycles adopt the most stable *trans*-III configurations, and thus two small sub-ring moieties are located at opposite sides and almost perpendicularly with respect to the square-coordination plane (*8, 10*).

For the macropolycyclic Ni(II) complexes containing two sub-ring moieties, **11–14**, the Ni—N bond distances depend on the size of the sub-ring. For example, the complex $[\mathbf{14}](ClO_4)_2 \cdot \frac{1}{2}H_2O$, which contains two six-membered sub-rings, has an average Ni—N bond distance of 1.95 Å, whereas the complexes $[\mathbf{11}]Cl_2 \cdot 2H_2O$ and $[\mathbf{12}](ClO_4)_2$, which contain five-membered sub-rings, have average Ni—N bond distances of 1.92 Å. The weaker ligand field strength of the complexes **13** and **14** with six-membered sub-rings is attributed to the longer Ni—N bond distances (*10*).

In Ni(II) macrocyclic complexes containing uncoordinated tertiary nitrogen atoms, **1–14**, shortening of bonds and flattening of bond angles involving the tertiary nitrogen atoms have been observed, which indicates the partial contribution of sp^2 hybridization of the tertiary nitrogen atoms (*5, 6, 8, 10, 12, 13*). For instance, the average N—C bond distance involving bridgehead tertiary nitrogen atom in $[\mathbf{5}](ClO)_4)_2$ is 1.44 Å, which is shorter than the normal C—N single-bond distance, and the C–N–C angles are 114–116°, which is larger than the angles of sp^3 hybridization (*16*).

The octahedral Ni(II) complex **16** of encapsulating macrocyclic ligand also shows short C—N bond distances, 1.41(2) and 1.44(2) Å, and large C—N—C bond angles, 117(1)° and 118(1)°, involving tertiary amines at the apices of the caps, which indicates sp^2 hybridization (*4*).

The bite distances and angles are a measure of the macrocyclic hole size. In general, the bite distances of the five-membered and six-membered chelate rings are ca. 2.6–2.7 Å and ca. 2.8–2.9 Å, respectively, while the bite angles of five-membered and six-membered chelate rings are 84–88° and 92–96°, respectively (*64*). Table III presents the bite distances and bite angles of some Ni(II) macrocyclic complexes. Complexes that contain strained moieties show unusual behaviors. For example, in $[\mathbf{9}](ClO_4)_2$ the bite distances and N–Ni–N bite angles involving the tetraazabicyclononane ring are 2.691(6) Å and 89.1(2)°, respectively, although the ring consists of six-membered chelate rings. In addition, the octaazamacrocyclic complex $[\mathbf{10}](PF_6)_2$ shows bite distances of 2.706(6) Å and 2.698(6) Å and bite angles of 90.4(2)° and 90.3(2)° for five-membered chelate rings, and bite distances of 2.703(6) Å and 2.665(7) Å and bite angles of 90.3(2)° and 88.8(2)° for six-membered chelate rings involving cage ring moieties (*18*). These results indicate that the N–N bite distances involving the cage ring moieties

are similar to those of the five-membered chelate rings, although each cage ring consists of two six-membered chelate rings. Therefore, the complexes **9** and **10** are more like the complexes of a [13]aneN$_4$ and a [12]aneN$_4$, respectively, rather than that of a [14]aneN$_4$. Consequently, the Ni—N bond distance (1.904 Å) of [**10**](PF$_6$)$_2$, which is 0.015 Å shorter than that of [**9**](ClO$_4$)$_2$, results in the unusually strong ligand field strength for [**10**]$^{2+}$.

E. Equilibrium Between Square-Planar And Octahedral Species in Coordinating Solvent

Some macrocyclic Ni(II) complexes exist as equilibrium mixtures of the yellow, diamagnetic, square-planar [Ni(L)]$^{2+}$ and blue (or violet), paramagnetic, octahedral [Ni(L)(S)$_2$]$^{2+}$ species in coordinating solvents (S) such as water, acetonitrile, or Me$_2$SO (*7, 10, 12–14, 16, 65, 66*). Interconversion between these two forms depends on the ligand structure and reflects a balance between endothermic solvent coordination and exothermic Ni—N bond lengthening in octahedral species.

In water, the equilibrium constant K of Eq. (11) is reduced when either the concentration of supporting electrolyte (e.g., NaClO$_4$) or the temperature is increased. Existence of the equilibrium is indicated by the absorption coefficients at λ_{max} measured in water for [Ni(L)]$^{2+}$, which are smaller than those measured in a noncoordinating solvent such as nitromethane or acetone.

$$[Ni(L)]^{2+} + 2H_2O \overset{K}{\rightleftharpoons} [Ni(L)(H_2O)_2]^{2+} \qquad (11)$$

The Ni(II) complexes **1–3g** with hexaaza and pentaaza macrocyclic ligands as well as the Ni(II) cyclam complex display a low-spin square-planar and high-spin octahedral complex interconversion in aqueous solution (*7, 12–14*). However, complexes **1–3a** favor formation of the high-spin form upon addition of acid, which is in contrast to the cyclam complex. The protonation of tertiary nitrogen atoms at the bridgehead position facilitates the axial coordination of anion or water because of hydrogen-bonding between them (*12, 14a*).

The thermodynamic data of Eq. (11) for the various Ni(II) macrocyclic complexes are summarized in Table IV. Since the octahedral species should have longer Ni—N bond distances than the square-planar species, the complexes with flexible macrocyclic ligands have larger K values. For example, the formation constants of octahedral species for [**13**]$^{2+}$ and [**14**]$^{2+}$ are ca. 10 times greater than those for [**11**]$^{2+}$ and

TABLE IV

EQUILIBRIUM THERMODYNAMIC DATA[a]

L	K, 25°C	$-\Delta H°$ kJ mol^{-1}	$-\Delta S°$ kJ mol^{-1}	Ref.
1	0.17[d]	36[d]	136[d]	
	0.44[b]	17[b]	64[b]	*7*
2	0.23[d]	19[d]	75[d]	
	0.36[b]	10[b]	43[b]	*7*
11	0.0511	24.5	106	*10*
	0.0538[b]	21.4[b]	96.2[b]	
12	0.0398	31.57	132	*10*
	0.0707[b]	12.9[b]	65.4[b]	
13				*10*
	0.772[b]	20.9[b]	72.4[b]	
14	0.297	34.1	124	*10*
	0.646[b]	24.6[b]	86.1[b]	
[**12**]dioxoaneN$_4$	0.15	−36.4	−138	*68*
[**13**]dioxoaneN$_4$	2.0	−17.5	−53.5	*68*
Me$_2$[**14**]aneN$_4$	2.5			*69*

$$[Ni(\mathbf{L})]^{2+} + 2H_2O \overset{K}{\rightleftharpoons} [Ni(\mathbf{L})(H_2O)_2)]^{2+}$$

[a] I = 0.07 M $NaClO_4$ and T = 25°C unless otherwise specified.
[b] Measured in pure water.
[c] Data cannot be measured in I = 0.07 M $NaClO_4$ because of insolubility of the complex.
[d] I = 0.1 M $NaClO_4$.

[**12**]$^{2+}$ at room temperature and comparable to those of the complexes of monocyclic ligands Me$_2$[14]aneN$_6$ and Et$_2$[14]aneN$_6$ (*10*). The complexes **13** and **14**, which have larger macrocyclic holes than **11** and **12**, accommodate larger octahedral Ni(II) ions better.

It has been reported that interconversion of square-planar to octahedral species for the Ni(II) complexes of the lipophilic macrocycle **L-a**

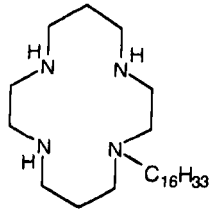

L-a

occurs in noncoordinating solvents that contain background electrolyte. The interconversion depends on the coordinating ability of the X ions of electrolyte $(n - Bu)_4NX$ in CH_2Cl_2 solution and can be monitored by measuring the Ni(III)/Ni(II) reduction potential (*67*).

F. Reactions

1. Oxidative Dehydrogenation with H_2O_2

Oxidation of Ni(II) cyclam complex with hydrogen peroxide in acidic perchlorate media results in the formation of a dimeric bismacrocyclic complex $[Ni_2(\mathbf{L_{12}})][(ClO_4)_4$. This complex contains five double bonds in the two macrocyclic ligands linked together through the bridgehead position. The complex forms square-planar geometry and there exists planarity across the carbon bridging framework (*70*). A similar oxidation reaction occurs with the Fe(II) cyclam complex [Fe(cyclam) $(MeCN)_2]^{2+}$ to produce $[Fe_2(\mathbf{L_{12}})(MeCN)_2](ClO_4)_4$, which is the dinuclear bismacrocyclic Fe(II) complex having an octahedral geometry (*71*).

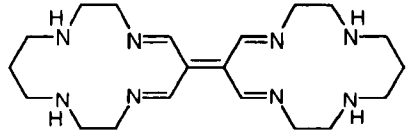

$\mathbf{L_{12}}$

2. Reactions with Molecular Oxygen

Although most of the square-planar Ni(II) macrocyclic complexes are not air-sensitive, some Ni(II) macrocyclic complexes, especially those with negatively charged ligands, are air-sensitive and react with molecular oxygen.

Pentadentate macrocyclic ligands $\mathbf{L_{13}}$–$\mathbf{L_{15}}$ accommodate Ni(II) ion with simultaneous dissociation of the two amide protons to form the square-pyramidal high-spin complex of $[NiH_{-2}L]^0$, **27**. These complexes are air-sensitive and show a very low Ni(II)/Ni(III) oxidation potential of +0.24 V vs SCE (*72, 73*). They form 1 : 1 dioxygen adducts, **27-O_2**, at room temperature in aqueous solution, which are formulated as Ni^{III}–O_2^- based on the EPR spectral data. The magnetic moment of the 1 : 1 O_2 adduct is 2.83 BM, which is interpreted in terms of weak interactions of Ni(III) with the superoxide where the spin coupling is weak. The oxygen uptake reaction is first-order with respect to both $[O_2]$ and $[NiH_{-2}L]^0$ in aqueous solutions and yields a second-order rate constant

of 1.7×10^2 $M^{-1}s^{-1}$ at 35°C. The O_2 complexation constant K is 1.9×10^4 M^{-1} at 35°C (*73*, *74*). The dioxygen adducts react with added substrates such as benzene, toluene, and anisole to produce hydroxylated products of organic substrates, except with nitrobenzene. This suggests that the activated O_2 species has an electrophilic character (*73*). The dioxygen adducts of Ni(II) complexes are proposed as the models of mono-oxygenase because the complexes are able to activate the dioxygen.

The dioxygen complexes also undergo facile irreversible degradation in aqueous solutions and result in the hydroxylated derivatives of the corresponding ligands being formed in a good yield (85 ± 5%)(*72*, *75*).

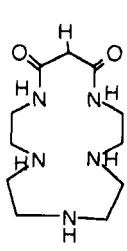

L_{13}

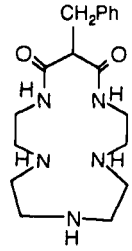

L_{14}

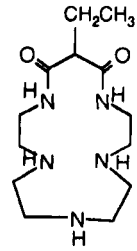

L_{15}

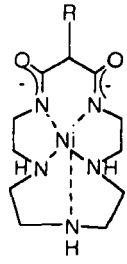

27

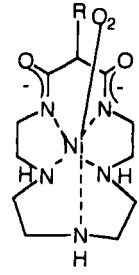

27-O_2

G. CATALYSIS

1. Electrocatalytic Reduction of Alkyl Halides

The square-planar Ni(II) complexes of L_{16} and L_{17} catalyze the cathodic reduction of several alkyl halides in aprotic solvents (*76*). In the presence of activated olefins such as CH_2=CHCN or CH_2=CH $COOC_2H_5$, the reduction of alkyl bromide leads to mixtures of products that are compatible with those formed by radical addition to the double

bond. The Ni(II) complex of cyclam also catalyzes the electrochemical reduction of alkyl halides. It has been proposed that the electrochemically generated Ni(I) species mediates the reduction of alkyl halides (*77, 78*).

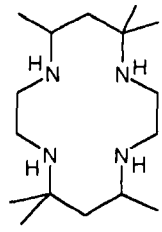

L_{16}

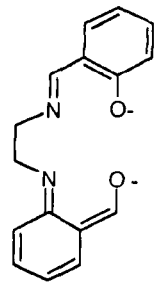

L_{17}

2. *Electrocatalytic Reduction of CO_2*

Some Ni(II) complexes show catalytic activity for the electrocatalytic reduction of CO_2 in water, where an intermediate formation of Ni(I) species has been proposed. To obtain a useful electrocatalyst in the electroreduction of CO_2, the selectivity of the process is highly important. As many electrochemical systems available for reducing CO_2 require the presence of water, the reduction of molecular hydrogen is always a competing reaction that needs to be avoided.

The Ni(II) complexes of 14-membered tetraaza macrocyclic ligands, cyclam, L_{16}, L_{18}, and L_{19} show catalytic activity in H_2O or aqueous MeCN. The total mole-for-mole yields of CO and H_2 are ca. 1 in most cases. The $[Ni(cyclam)]^{2+}$ complex is a very effective and selective catalyst for the electrochemical reduction of CO_2 to CO relative to the reduction of water to H_2 in aqueous solution when it is adsorbed onto mercury. The CO/H_2 product ratio is >100 for $[Ni(cyclam)]Cl_2$ (*79*). It is suggested that the greater selectivity for the electroreduction of CO_2 compared with water is related to the size of the macrocyclic ligand

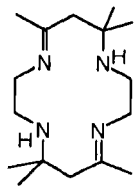

L_{18}

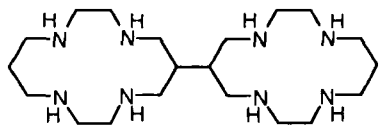

L_{19}

and the presence of N—H groups in $[Ni(cyclam)]Cl_2$. The complexes $[Ni(cyclam)]^{2+}$ and $[Ni_2(\mathbf{L_{19}})]^{4+}$ display analogous properties with respect to CO_2, leading to CO formation in water but $HCOO^-$ in addition to CO in low-water-content DMF (*79–84*).

The Ni(II) complex of $\mathbf{L_9}$, with protonated amine pendant with *trans*-III configuration, also catalyzes the electrochemical reduction of CO_2 to CO efficiently (*41*).

The Ni(II) complex of the hexaaza macrocyclic ligand **1** is reported to show a high activity for the electrocatalytic reduction of CO_2 to CO when a rotating copper disc electrode is used (*85*). In addition, water-soluble Ni^{II}–azacyclam complexes, **3a–3g**, where R = carboxamide or sulfonamide, either aliphatic or aromatic, are found to be active in the electrocatalytic reduction of CO_2 at a mercury cathode. The efficiency is comparable to that of $[Ni(cyclam)]^{2+}$ (*14*).

The complexes *R,R,S,S*-$[Ni(HTIM)](ClO_4)_2$ and $[Ni(DMC)](ClO_4)_2$ have been shown to be better catalysts than $[Ni(cyclam)]^{2+}$ in terms of larger catalytic currents and more positive potentials in aqueous solution using a hanging mercury electrode. However, *R,S,S,R*-$[Ni^{II}HTIM]^{2+}$ does not show good catalytic activity, and this indicates that structural differences may be an important factor. The axial methyl group of the *R,S,S,R*-$[Ni(HTIM)]^{2+}$ may sterically hinder effective adsorption of the complex onto Hg, and may also hinder CO_2 binding to the complex (*86*).

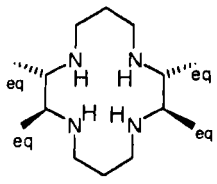

C-RRSS-**HTIM**

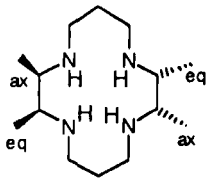

C-RSSR-**HTIM**

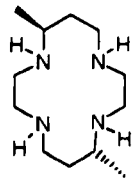

C-meso-**DMC**

3. *Photoreduction of CO_2*

Some Ni(II) macrocyclic complexes mediate electron transfer and produce CO during the photochemical reduction of CO_2. However, photochemical reduction of CO_2 using a photosensitizer, a sacrificial electron donor, and $[Ni(cyclam)]^{2+}$ as the catalyst has been only moderately successful compared to the electrochemical reduction of CO_2 using $[Ni(cyclam)]^{2+}$.

The Ru^{II}–Ni^{II} heteronuclear complexes, **28–30**, in which the photosensitizer $[Ru(bpy)_3]^{2+}$ or $[Ru(phen)_3]^{2+}$ is covalently attached to the Ni^{II}–cyclam complex, have been synthesized in order to improve the efficiency of electron transfer from the photoexcited photosensitizer to the catalytic site (*87–89*). However, the complex **28** did not perform well, because it has an unusual *trans*-I configuration of the Ni(II)–cyclam subunit, and the resulting steric hindrance then impeded CO_2 access to the Ni(II)–cyclam catalytic site. The distortion in the coordination environment of the $[Ru(bpy)_3]^{2+}$ subunit and the resulting short lifetime of the excited state of the $[Ru(bpy)_3]^{2+}$ moiety are also important. The complex **29** has the normal *trans*-III configuration and there is no distortion around the Ru(II) center of the $[Ru(phen)_3]^{2+}$ subunit. However, the emission lifetime of $[Ru(phen)_3]^{2+}$ is not sufficiently long to permit effective reductive quenching of the excited state of the $[Ru(phen)_3]^{2+}$ subunit by a reductant. The Ni(II)–cyclam complexes (**30** and **31**) containing a pendent pyridinium group show improved catalytic efficiency for CO_2 photoreduction, although they show photocleavage of the complex that is induced during the process.

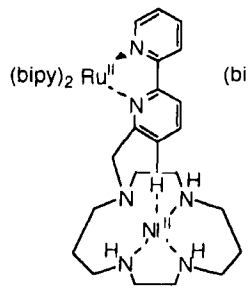

28

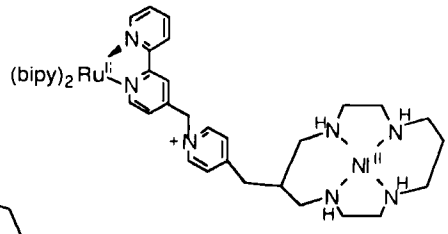

29

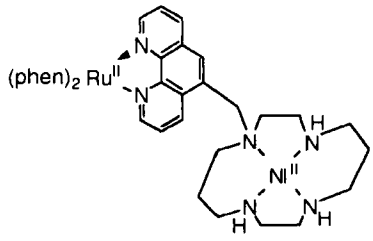

30

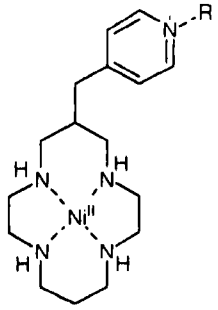

31

4. Alkene Epoxidation

Many transition-metal complexes have been widely studied in their application as catalysts in alkene epoxidation. Nickel is unique in the respect that its simple soluble salts such as $Ni(NO_3)_2 \cdot 6H_2O$ are completely ineffective in the catalytic epoxidation of alkenes, whereas soluble manganese, iron, cobalt, or copper salts in acetonitrile catalyze the epoxidation of stilbene or substituted alkenes with iodosylbenzene as oxidant. However, the Ni(II) complexes of tetraaza macrocycles as well as other chelating ligands dramatically enhance the reactivity of epoxidation of olefins (*90, 91*).

Ni(II) complexes of cyclam and oxocyclam derivatives catalyze the epoxidation of cyclohexene and various aryl-substituted alkenes with PhIO and NaOCl as oxidants, respectively. In the epoxidation catalyzed by the Ni(II) cyclam complex using PhIO as a terminal oxidant, the high-valent nickel–oxo complexes (e.g., $LNi^{III}–O^{\cdot}$, $LNi^{IV}=O$, $LNi^{III}–O–I–Ph$, or $LNi^{III}–O–Ni^{III}L$) have been proposed as the active oxidant (*92*). In the reaction, E olefins are more reactive than the corresponding Z isomers, and a strong correlation was observed between the electron-donating effect of the para substituents in styrene and the initial reaction rate (*91*). Isotope labeling studies have shown that the epoxide oxygen is derived from PhIO.

Introduction of optically active functionalized pendants to cyclam to give **32** and **33** was tried in order to examine their effects on reactivity and enantioselectivity. However, the overall result was not much different from that for simple cyclam, and no enantiomeric excess was observed (*93*).

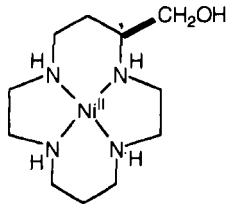

32

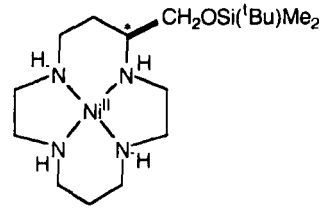

33

In an effort to introduce C_2 symmetry into nickel complexes for their application in catalysis of asymmetric epoxidation, a series of oxocyclam analogues derived from amino acids **34** were synthesized. They did not react in the presence of PhIO as oxidant. However, they showed enhanced reactivity with NaOCl as the terminal oxidant under phase-

transfer conditions. Asymmetric induction was not observed in this case, either, and their reactivity showed rough correlation with their relative solubilities in organic phase (*94, 95*). The high-valent radical species $LNi^{III}–O^{\cdot}$ was proposed as an intermediate for this system.

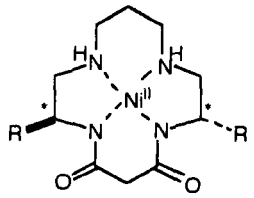

R=CH_2Ph
$CH_2CH(CH_3)_2$
$CH(CH_3)_2$
H

34

The Ni(II) complex of salen **35** was found to be a highly efficient epoxidation catalyst when used in conjunction with NaOCl. Enhanced selectivity and high turnover rate were observed (*96*). By adjusting pH of the aqueous phase, significant increase in turnover rate as high as >600 min^{-1} for *trans*-β-methylstyrene can be achieved, which is comparable to that of the Mn(III) tetraarylporphyrin (*97*). From the pH dependence of the rate constants, it was proposed that transfer of HOCl to the organic phase was required to become an efficient catalyst, and its reaction with the Ni(II) salen complex led to formation of the active species $LNi^{III}–O^{\cdot}$.

The Ni(II) complexes of salen analogues with bipyridine units **36** showed higher catalytic activity than Ni(II)(salen) in the epoxidation of an electron-deficient olefin, allyl chloride. Their enhanced reactivity was ascribed partially to their higher stability relative to the salen complex (*98*).

Recently, the Ni(II) complexes of cyclam, **1**, **4**, **11**, **12**, and **14**, have been adopted in the epoxidation of *trans*-β-methylstyrene using PhIO as a terminal oxidant in order to assess the structural effect of the macrocyclic ligand and the relative importance of each step in the oxygen transfer mechanism (*99*). In general, monocyclic ligand complexes are better catalysts than polycyclic complexes with respect to the epoxide yield. The presence of the pendent chain at the bridgehead nitrogen reduces epoxide yield. The oxygen transfer process from PhIO to the Ni(II) complex is the most important step in the epoxidation reaction, and it is greatly influenced by steric factors around the metal center to allow the easy axial approach of the terminal oxidant, PhIO. The process is also affected by the oxidation potential of Ni(II) to Ni(III).

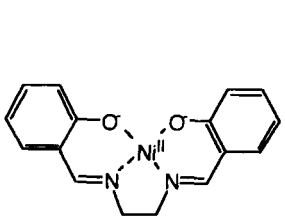

35

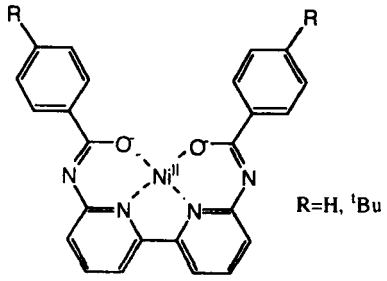

36

5. DNA Modification

Various Ni(II) complexes promote oxidative modification of DNA in the presence of peracid oxidants and effect strand scission subsequent to alkaline treatment. Especially, complexes with neutral tetraaza-macrocyclic cyclam and cyclam-like ligands are known to enhance the reactivity of Ni(II) in promoting DNA oxidation using $KHSO_5$. These reactions depend strongly on the nature of the metal complex, and several features have been found to be important for efficient DNA oxidation: (i) square-planar rather than octahedral coordination, (ii) positively charged complexes with neutral rather than anionic ligands, and (iii) relatively high $E_{1/2}$ values for Ni(II)/Ni(III) oxidation. The 14-membered macrocycles with nitrogens present as pyridine or imine groups are more efficient complexes for such a reaction. A high degree of unsaturation in the ring leads to conformational rigidity, which may be detrimental to the formation of key intermediates bound to DNA. Accordingly the complex **37** was found to be one of the most effective catalysts for the DNA oxidation, while analogous Cu(II) complexes are unreactive. A mechanism in which the square-planar Ni(II) complex is oxidized to a square-pyramidal or octahedral Ni(III) complex possessing labile axial sites to bind to N7 of guanine has been proposed (*100a, 100b*).

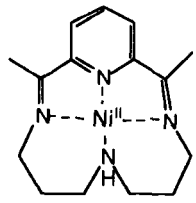

37

H. Configurational Isomerization of Macrocycles

A 14-membered tetraaza macrocyclic complex may exist in one of five possible configurations I–V based on the stereochemistry of the donor nitrogens. Most of the known square-planar complexes of aza-macrocyclic ligand have the *R,R,S,S* configuration, which is thermodynamically the most stable. In the case of the *R,S,R,S* complex, the asymmetric gauche conformation in the five-membered chelate rings exerts significant strain on the ligand structure and leads to isomerization to the more stable *R,R,S,S* configuration. For example, in H_2O–MeCN media, (*R,S,R,S*)-[Ni(**14**)]$^{2+}$ isomerizes to (*R,R,S,S*)-[Ni(**14**)]$^{2+}$ via axial coordination of water followed by Ni—N(tert) bond cleavage assisted by water acting as a general acid (*56a*).

The reverse isomerization from the *R,R,S,S* to the *R,S,R,S* configuration is also possible. In this process, a strongly coordinating solvent (*100c*) or pendent donor group induces the configurational change of the macrocycle (*41*).

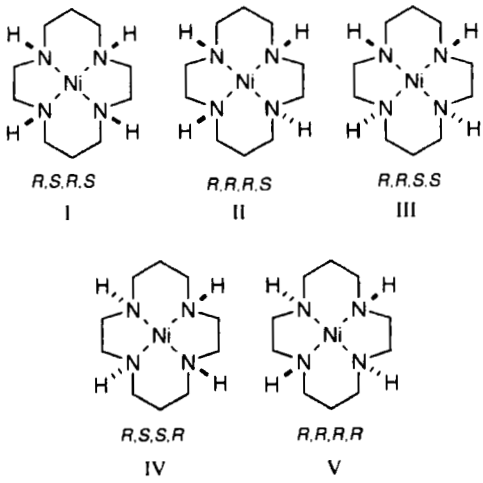

III. Nickel(III) Complexes

The Ni(III) oxidation state is biologically significant (*101,102*). Moreover, high-valent nickel species may be intermediates in some catalytic oxidations (*97*) and in the nickel-mediated sequence-specific oxidative cleavage of DNA by designed metalloproteins (*103*) as discussed in Section I,G. The chemistry of Ni(III) macrocyclic complexes has been

extensively reviewed elsewhere (*104*), and therefore only more recent results are reviewed in this article.

A. Synthesis and Properties

Complexes of Ni(III) are synthesized by the oxidation of Ni(II) analogues in aqueous or nonaqueous media. Electrochemical oxidation (*51, 105, 106*), chemical oxidation using $(NH_4)_2S_2O_8$, conc. HNO_3, $NOBF_4$, or $Co(H_2O)_6^{3+}$, and pulse radiolysis (*107–110*) are the most commonly used methods. Ni(III) complexes can be prepared from Ni(II) complexes when the Ni(II)/Ni(III) oxidation potentials are less than +1.1 V vs SCE. For instance, the Ni(III) species can be prepared from [Ni(cyclam)]$^{2+}$ and **1–3a**, but cannot be obtained from the polycyclic complexes (**9–14**), which have Ni(II)/Ni(III) oxidation potentials in the range +1.25–+1.50 V vs SCE.

In general, the Ni(III) complexes of tetraaza macrocyclic ligands are isolated as distorted octahedral species in which high-valent metal ion is electronically neutralized by extra axial ligands. Square-planar Ni(III) macrocyclic complexes are extremely rare, and most examples have a negatively charged macrocyclic ligand (*111, 112*). The color of octahedral Ni(III) macrocyclic complexes ranges from green to brown depending on the ligand structure. The square-planar Ni(III) complex of **38** is, by contrast, a deep purple.

The latter complex containing the elegantly designed macrocyclic ligand (L_{20}) was synthesized by oxidation of the Ni(II) form with benzoyl peroxide (*112*). In the salt-prepared $[Et_4N][Ni(L^{-4})]$, **38**, all amine protons are deprotonated, and in solution it has a low affinity for axial ligands at 20°C. The complex shows an axial epr spectrum with $g_\perp > g_\parallel$ in noncoordinating solvent glasses. The Ni(III)/Ni(II) couple occurs at −0.58 V vs Fc^+/Fc in CH_2Cl_2, 0.1 M $(n\text{-}Bu)_4NClO_4$, or at +0.13 V vs NHE. The average Ni(III)–N distance is 1.84 Å, which is considerably shorter (ca. 0.1 Å) than other Ni(III)–N distances (*113–116*).

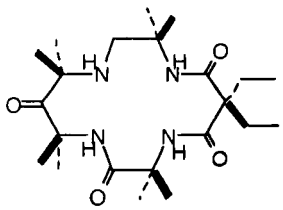

L_{20}

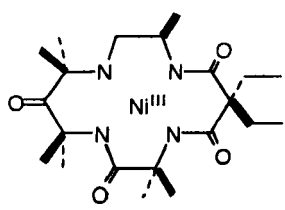

38

It has been reported that the trans-dichloro Ni(III) complex, $[Ni^{III}(H_2L_{21})Cl_2](Cl)(ClO_4)_2 \cdot 2H_2O$, was isolated during the crystallization of the Ni(II) complex of $H_2L_{21}^{2+}$ in acidic perchlorate media containing chloride (*117*). The Ni(III) species shows an axial epr spectrum with $g_\perp = 2.17$ and $g_\parallel = 2.02$, and $A = 30$ G. This complex has a pseudooctahedral geometry with an average Ni(III)—N bond distance of 1.893(14) Å and Ni—Cl bond distance of 2.415(60) Å.

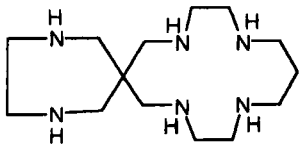

L_{21}

The Ni(III) cyclam species is fairly stable in solution. In the case of aqueous media, persistence is affected by the solution acidity. At higher acidity, the complex is found to be more persistent. The bright, deep green color of $[Ni^{III}cyclam]^{3+}$ lasts indefinitely in aqueous 1 *M* H_2SO_4 at room temperature. However, if the solution is made alkaline, the color changes to yellow-orange, which is characteristic of the Ni(II) species. When it is added to a solution buffered at pH = 7 ± 1, a violet transient is observed, which is ascribed to Ni(III)-ion-promoted deprotonation of an amine group of cyclam: the pK_a value of the amine is 7.1 ± 0.2 (*118*).

Some other Ni(III) complexes containing saturated macrocyclic ligands are reported to decompose to Ni(II) complexes of oxidized macrocycles in alkaline solution of $9.0 < pH < 11.0$. The reaction involves the Ni(III) complex of the deprotonated ligand (*119*).

Ni(III) complexes often exhibit equilibrium with Ni(II) ligand radical species. For example, the Ni(III) complex of lacunar cyclidene is octahedral $[Ni^{III}L(CH_3CN)_2]^{3+}$ at low temperature, but at high temperature it transforms into the Ni(II) complex with an oxidized ligand radical $[Ni^{II}L^+]^{3+}$, identifiable by the absorption at 590 nm. The Ni(III) complexes and Ni(II) species with an oxidized ligand radical exhibit a thermal equilibrium (Eq. 12) (*105*).

$$[Ni^{III}(L)B]^{3+} \underset{\text{heat}}{\rightleftharpoons} [Ni^{II}(L^+)]^{3+} + B \qquad (12)$$

B. Spectra

UV-vis spectra of some Ni(III) macrocyclic complexes are summarized in Table V. The spectra depend on the type of macrocyclic ligand

TABLE V

ELECTRONIC SPECTRAL DATA FOR SOME NICKEL(III) MACROCYCLIC COMPLEXES

Complex	λ_{max}, nm (ε, $M^{-1}cm^{-1}$)	Solvent	Ref.
(Et_4N)[**36**]	380 (5480), 532 (3620) 650 (2330), 808 (4180)	CH_2Cl_2	*112*
$[Ni(L_{14}H_{-2})H_2O]ClO_4 \cdot 2H_2O$	270 (8150)	H_2O	
$[Ni(L_{20}H_2)Cl_2](ClO_4)_2 \cdot Cl \cdot 2H_2O$	219 (8000), 303 (6700) 358 (sh. 3200)	0.1 *M* $HClO_4$	*117*
$[Ni(L_{16})X_2](ClO_4)$			
X = H_2O	325 (sh, 3300), 395 (4300)	acidic H_2O	*51, 114*
Cl^-	315 (9400), 400 (sh, 5000)		
$H_2PO_4^-$	280 (8000), 385 (7500), 730 (50)		
SO_4^{2-}	310 (11000), 410 (7000), 710 (60)		
$[Ni(L_{21})X_2](ClO_4)$			
X = Cl^-	318 (11700), 775 (26)	MeCN	*110*
Br^-	305 (5120), 360 (sh. 3540) 769 (39)		
NCO^-	303 (1880), 6730 (16)		
NO_3^-	321 (11100), 714 (42)		

as well as the axial ligand type. There is no general understanding of the UV-vis spectra, because the Ni(III) complexes tend to be dominated by low-energy charge-transfer bands that obscure the *d-d* structure.

The epr spectra of Ni(III) complexes of various macrocyclic ligands are well documented (*104*). In general, frozen solutions of octahedral Ni(III) complexes with the formula $[Ni(L)B_2]^{x+}$ (B = MeCN, Cl^-, Br^-, NCO^-, or NO_3^-; x = 1–3), which have elongated tetragonal geometry, show anisotropic axial spectra with $g_\perp$ values being greater than $g_\parallel$ values. The square-planar Ni(III) complex **38**, $(Et_4N)[Ni(LH_{-4})]$, gives a rhombic spectrum with g_1 = 2.366, g_2 = 2.303, g_3 = 1.994 in frozen toluene/CH_2Cl_2.

C. STRUCTURE

The Ni(III) complexes can be isolated as solids, and some of their X-ray crystal structures have been determined (*113, 120, 120a*). The Ni(III) complexes are usually found to have an octahedral geometry with axially elongated bonds, and the square-planar complex is extremely rare. The X-ray structural parameters for some Ni(III) complexes are summarized in Table VI. The average Ni—N bond distances of octahedral Ni(III) complexes are ca. 0.1 Å longer than those of the

TABLE VI

STRUCTURAL DATA FOR NICKEL(III) MACROCYCLIC COMPLEXES

Complex	Av. Ni^{III}–N_{mac}, Å	Av. Ni^{III}–axial ligand	Ref.
(Et_4N)[**36**]	1.84		*112*
[Ni(**$L_{20}H_2$**)Cl_2]$Cl(ClO_4)_2 2H_2O$	1.983(14)	Ni–Cl: 2.415(6)	*117*
[Ni(**cyclam**)Cl_2](ClO_4)	1.970(4)	Ni–Cl: 2.452(4)	*113*
[Ni(**cyclam**)$(NCS)_2$](ClO_4)	1.972(7)	Ni–NCS: 2.081(3)	*120*
[Ni(**$L_{14}H_{-2}$**)(H_2O)]$(ClO_4)2H_2O$	Ni–N(amine): 1.963(5) Ni–N(amide): 1.890(4)	Ni–N(axial): 2.067(4) Ni–O: 2.340(4)	*121*
[Ni(**L_{16}**)$(H_2PO_4)_2$](ClO_4)	1.993(4) 2.013(3)	Ni–O: 2.061(3)	
[Ni(**L_{22}**)]	Ni–N: 1.93 Ni–O: 1.91		

square-planar Ni(II) complexes. The bond distances of Ni-axial ligands are longer than in-plane Ni—N bond distances.

D. REACTIONS

Ni(III) complexes oxidize some substrates. For example, [Ni(cyclam)]$^{3+}$ oxidizes hydroquinone and catechol in aqueous perchlorate media. The kinetics of the reactions have been studied (*122*).

The Ni(III) complex of L_{16} oxidizes the cyclohexanone in MeCN containing CF_3CO_2H (*123*).

IV. Nickel(I) Complexes

Currently, Ni(I) macrocyclic complexes have attracted much attention. This is because Ni(II) tetraaza macrocyclic complexes catalyze the electrochemical reduction of CO_2 and alkyl halides, and it is proposed that the Ni(I) species are involved in such reactions (*1, 2, 76–79, 82, 124–126*). Furthermore, F430, a Ni(II) hydrocorphinoid complex, is a prosthetic group of methyl coenzyme M reductase that catalyzes the reductive cleavage of *S*-methyl coenzyme M to methane in the final stage of CO_2 reduction to methane (*127–130*). An EPR signal detected in whole cells of *Methanobacterium thermoautotrophicum* has been attributed to an Ni(I) form of F430 in intact active enzyme (*131, 132*).

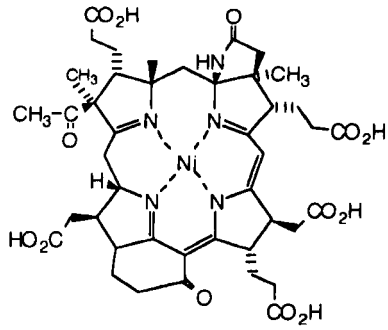

F430

Macrocyclic ligands often stabilize metal ions in uncommon oxidation states, and a number of Ni(I) species have been detected in solutions mainly by epr spectroscopy. However, the Ni(I) species are usually unstable, and only a few Ni(I) macrocyclic complexes have been isolated in the solid state thus far. Their electronic absorption spectra, epr spectra, and X-ray crystal structures have been measured.

A. Synthesis

Complexes of Ni(I) are prepared by the reduction of Ni(II) macrocycles by electrochemical or photochemical methods (*55b, 133*), or by using chemical reducing agents (*18, 25, 27, 57, 133–135*). It is difficult to obtain Ni(I) complexes in high purity by the electrochemical method, because the reduction should be carried out to only ~50% completion to avoid oxygen contamination (*133*), and the added electrolyte should be removed after the reduction step. The photochemical reduction is based on the strong reducing properties of the $(CH_3)_2CO^-\cdot$ radical that is produced by the irradiation of acetone (*133*). Pulse radiolysis involving e^-_{aq} and CO_2^- or $\cdot CH_2C(CH_3)_2OH$ radical has also been applied (*55b*). The chemical reagent that is most commonly used in the reduction of Ni(II) macrocyclic complexes is Na(Hg) (*18, 25, 57, 134, 135*). When Ni(II) perchlorate salts are reduced with Na(Hg) in acetonitrile, a mixture of $NaClO_4$ and Ni(I) perchlorate complex precipitates, from which the Ni(I) complex is isolated by recrystallization (*57*). Metallic nickel may be formed if Ni(II) complexes are treated with Na(Hg) for a prolonged period of time (*57*).

The reduction of various square-planar Ni(II) complexes of saturated macrocyclic ligands in acetonitrile leads to the formation of square-planar Ni(I) complexes (*57, 135*). In the case of Ni(II) complexes that

contain conjugated double bonds in the macrocyclic ligands, the reduction yields the nickel-stabilized ligand radicals, Ni^{II} (mac^-), instead of Ni(I) species (*135*).

The Ni^{II} (mac^-) turns to the five-coordinate Ni(I)–CO species on reaction with CO. Introduction of CO gas into the solution of square-planar Ni(I) species also produces five-coordinate Ni(I)–CO complexes, although they unusually contain 19 valence electrons (*66*, *135*).

The five-coordinate Ni(I) macrocyclic complex [Ni(**14**)(NHC(OH)CH_3)]ClO_4, in which Ni(I) ion is coordinated by the nitrogen atom of acetamide in the iminol form, has been prepared (*136*). The complex is obtained by the reduction of square-planar Ni(II) complex [Ni(**14**)]$(ClO_4)_2 \cdot \frac{1}{2}H_2O$ with Na(Hg) in MeCN under a nitrogen atmosphere or by the addition of acetamide to the square-planar Ni(I) complex of **14**. Although the starting Ni(II) and Ni(I) complexes have the *R,R,S,S* configuration, the resulting five-coordinate complex has the *R,S,R,S* configuration. In the formation of the complex, the solvent MeCN is hydrated to acetamide by OH^- ion, which is produced by the reaction between Na(Hg) and the lattice water contained in the starting Ni(II) complex. The five-coordinate (*R,S,R,S*)-[Ni(**14**)(NHC(OH)CH_3)]$^+$ equilibrates with four-coordinate (*R,R,S,S*)-[Ni(**L**)]$^+$ species in MeCN.

The Ni(II) complexes that are reduced to Ni(I) species show the Ni(II)/Ni(I) electroreduction potential of less than -1.45 V vs SCE.

B. Spectroscopic Properties

1. Electronic Absorption Spectra

Spectral data for selected square-planar Ni(I) macrocyclic complexes are summarized in Table VII. The reduced nickel species are deeply colored, and their electronic absorption spectra consist of intense charge-transfer bands. Ni(I) complexes with saturated aza-type macrocyclic ligands are red, purple, blue, or green, depending on the type of macrocycle. All Ni(II) complexes with ligand radicals are green and exhibit qualitatively similar spectral patterns to those of the Ni(I) complexes. The *d–d* transition of the square-planar Ni(I) complexes occurs at 540–600 nm, which is ca. 100 nm red-shifted compared to the corresponding square-planar Ni(II) complexes. This indicates that the ligand-field strength decreases upon reduction of the metal. In the case of Ni(I) polycyclic ligand complexes, the absorption coefficients of the Ni(I) complexes are several hundreds to thousands of $M^{-1}cm^{-1}$, which are ca. 5–10 times greater than those of the corresponding Ni(II) complexes (*18*, *25*, *57*, *134*). This is due to the distortion of the coordina-

TABLE VII

ELECTRONIC ABSORPTION AND EPR SPECTRAL DATA FOR FOUR-COORDINATE NICKEL(I) MACROCYCLIC COMPLEXES

Compound[a]	λ_{max},[b] nm(ε, $M^{-1}cm^{-1}$)	Epr data[c]	Ref.
$[Ni^{I}(\mathbf{9})]ClO_4$	538 (600), 330 (2020), 234 (2670)	$g_{\parallel} = 2.240, g_{\perp} = 2.062$	*57*
$[Ni^{I}(\mathbf{11})]ClO_4$	560 (330), 338 (1180), 246 (3110)	$g_1 = 2.197, g_2 = 2.122, g_3 = 2.065$	*57*
$[Ni^{I}(\mathbf{12})]ClO_4$	559 (450), 340 (1840), 240 (1990)	$g_{\parallel} = 2.253, g_{\perp} = 2.071$	*57*
$[Ni^{I}(\mathbf{13})]ClO_4$	596 (250), 354 (810), 252 (2530)	$g_{\parallel} = 2.272, g_{\perp} = 2.075$	*57*
$[Ni^{I}(\mathbf{Me_2 9})]ClO_4$	572[c]		*57*
$[Ni^{I}(\mathbf{Me_2 11})]ClO_4$	564, 338[c]		*57*
$[Ni^{I}(\mathbf{10})]PF_6$	549 (170), 323 (1800)	$g_{\parallel} = 2.200, g_{\perp} = 2.050$	*134*
$[Ni^{I}(\mathbf{18})](ClO_4)_2$	535 (690), 328 (2400)	$g_{\parallel} = 2.239, g_{\perp} = 2.061$	*25*
$[Ni^{I}(\mathbf{19})](PF_6)_2 \cdot 2CH_3CN$	536 (1300), 332 (4600)	$g_{\parallel} = 2.238, g_{\perp} = 2.059$	*25*
C-*RSRS*-$[Ni^{I}(\mathbf{TMC})]^{+}$	684 (130), 348 (3370), 250 (3890)		*66*
$[Ni^{I}(\mathbf{dieneN_4})]^{+}$	600 sh (1270), 468 (4120), 340 sh (2300), 305 (2930)		*137*
C-RRSS-$[Ni^{I}(\mathbf{HTIM})]^{+}$	564 (40), 388 (4340), 270 (3610)		*66*
$[Ni^{I}(\mathbf{DMC})]^{+}$	570 (36), 384 (4010), 268 (3440)		*66*
$[Ni^{I}(\mathbf{cyclam})]^{+}$	560 (80), 384 (4400), 267 (4300)		*66*

[a] Structures of the macrocyclic ligands are shown in Sections I,A and IV,B.
[b] Measured in MeCN.
[c] The spectra were measured with powder samples at room temperature.

tion core, which lowers the symmetry of the complexes, as discussed in Section IV,C. However, the Ni(I) complexes with the monocyclic ligands such as cyclam, DMC, and C-*RRSS*-$[NiHTIM]^{+}$ show visible bands with low absorption coefficients ranging from 30 to 80 $M^{-1}cm^{-1}$. The charge transfer bands of the Ni(I) complexes appear at 330–390 and 230–270 nm depending on the type of macrocycle (*57, 66, 137*). The dinickel(II) complexes of bismacrocyclic ligands can also be reduced with Na(Hg) in MeCN, leading to the dinickel(I) complexes, which have similar spectra to the mononuclear Ni(I) complexes (*25*).

The spectral data of the five-coordinate complexes of Ni^{I}–CO and Ni^{I}–NH—$C(OH)CH_3$ are summarized in Table VIII. The visible band of the five-coordinate Ni^{I}–CO complex of the macrocycle that does not

TABLE VIII

ELECTRONIC ABSORPTION SPECTRAL DATA FOR FIVE-COORDINATE NICKEL(I) COMPLEXES WITH MACROCYCLIC LIGANDS

Compound	λ_{max},[a] nm(ε, $M^{-1}cm^{-1}$)	Ref.
$[Ni^{I}$(**cyclam**)CO$]^{+}$	620 (100), 400 sh (940), 348 (1540)	*66*
C-RRSS-$[Ni^{I}$(**HTIM**)CO$]^{+}$	635 sh (27), 470 (790), 296 (2450), 246 (7710)	*66*
$[Ni^{I}$(**dieneN$_4$**)CO$]^{+}$	620 (40), 410 sh (1500), 345 sh (3600), 301 (3300), 238 (8100)	*137*
$[Ni^{I}$(**DMC**)CO$]^{+}$	632 (59), 410 sh (960), 352 (1430), 240 (7580)	*66*
C-RSRS-$[Ni^{I}$(**TMC**)CO$]^{+}$	706 (<100), 450 (680), 350 sh (960)	*66*
$[Ni^{I}$(**TIM**)CO$]^{+}$[b]	680 sh (3020), 546 (6000), 480 sh (4710), 400 sh (4100), 378 (4420)	*137*
$[Ni^{I}$(**14**)-(NHC(OH)CH$_3$)$]^{+}$	645 (53), 401 (120)	*136*

[a] In MeCN at 25°C unless otherwise specified.
[b] In C_3H_7CN at −120°C.

contain conjugated double bonds appears around 620–635 nm with relatively low absorption coefficients of less than 100 $cm^{-1}M^{-1}$ (*66, 137*). The five-coordinate Ni(I)–acetamide complex, (*R,S,R,S*)-[Ni(**14**)(NHC(OH)CH$_3$)]ClO_4 shows color and UV-vis spectra similar to those of the five-coordinate Ni(I)–CO complexes (Table VIII) (*136*). The electronic spectrum of (*R,S,R,S*)-[Ni(**14**)(NHC(OH)CH$_3$)]$^{+}$ depends on the amount of added acetamide as well as the temperature because of the axial acetamide dissociation in MeCN. The maximum absorption peaks of the complex appear at 628 nm (ε = 76 $cm^{-1}M^{-1}$) and 389 nm (ε = 140 $cm^{-1}M^{-1}$) in MeCN, and they further shift to longer wavelength, 645 nm (ε = 53 $cm^{-1}M^{-1}$), 401 nm (ε = 120 $cm^{-1}M^{-1}$), upon addition of excess acetamide.

2. Epr Spectra

The four-coordinate Ni(I) complexes with saturated ligands exhibit anisotropic axial spectra with $g_{\parallel}$ values being greater than $g_{\perp}$ values. The Ni(II) species of ligand-stabilized radical, which is produced from the reduction of the four-coordinate Ni(II) macrocyclic complexes with conjugated double bonds, exhibit isotropic spectra. The isotropic spectra of Ni^{II} (mac^{-}) turn to anisotropic axial spectra as the complexes coordinate CO to form five-coordinate Ni(I)–CO adducts (*135, 137*). The anisotropic axial epr spectra of four-coordinate Ni(I) complexes become rhombic as the complexes coordinate extra axial ligand such as CO or acetamide to form five-coordinate Ni(I) species (*135, 136*). The epr spectral data of some Ni(I) complexes are summarized in Table VII.

C. X-Ray Crystal Structure

Few X-ray structures have been reported for the square-planar Ni(I) macrocyclic complexes (*57, 66, 134, 137*), and only one has been reported thus far for the five-coordinate Ni(I) macrocyclic complexes (*136*). In general, Ni—N bond distances in Ni(I) complexes are anticipated to be much longer than in Ni(II) complexes, since the Ni(I) ion should be larger than the Ni(II) ion in the square-planar geometry, and UV-vis spectra indicate that ligand field strengths of Ni(I) complexes must be significantly weaker than those of Ni(II) complexes. However, X-ray structures of Ni(I) macrocyclic complexes are often inconsistent with such expectations.

The X-ray crystal structures of four-coordinate Ni(I) complexes that were prepared from Ni(II) complexes of macropolycyclic ligands, **9**, **12**, and **14**, and those of **HTIM** and $\mathbf{L_{18}}$ ($\mathbf{dieneN_4}$) have been reported (*16, 57, 66, 137*). For all four-coordinate Ni(I) complexes, the macrocyclic ligands adopt the *R,R,S,S* (*trans*-III) configuration, which is thermodynamically the most stable structure. The most interesting structural observation in Ni(I) macrocyclic complexes relates to the Ni—N bond distances. Two different sets of Ni—N bond distances have been observed in all square-planar Ni(I) complexes reported thus far (*57, 66, 134, 137*). In the Ni(I) complexes obtained from the Ni(II) complexes of **9**, **12**, and **14**, a separation into shorter and longer Ni—N bond distances was observed without an increase in average Ni—N bond distances compared to the structures of Ni(II) analogues (*57, 134*). The Ni(I) complexes of **9**, **12**, and **14** contain secondary and tertiary nitrogen donors, but each set is not differentiated by the secondary and the tertiary nitrogen donors. For the Ni(I) complexes of **9** and **12**, each set is formed by two *cis*-Ni—N bonds involving the six-membered chelate rings (Fig. 4). In the case of the Ni(I) complex of **14**, however, a set is formed by three long bonds consisting of two Ni—N(tert) and one Ni—N(sec) bonds, and the other set by a short Ni—N(sec) bond (Fig. 5) (*134*).

For the Ni(I) complexes of HTIM and dien$\mathbf{eN_4}$($\mathbf{L_{18}}$) ligands, Ni—N bond distances increase by about 0.11 and 0.13 Å, respectively, upon reduction of the Ni(II) complexes to Ni(I). In addition, there are two sets of Ni—N bond distances, although the differences between the two sets are not large (*66, 137*). In the case of the Ni(I) complex of dien$\mathbf{eN_4}$($\mathbf{L_{18}}$), Ni—N bond distances involving amine nitrogens are longer than those involving imine nitrogens (*137*). However, similar observations were also made for Ni(II) complexes, although the difference between Ni—N_{amine} and Ni—N_{imine} bond distances is greater in case of Ni(I) complexes.

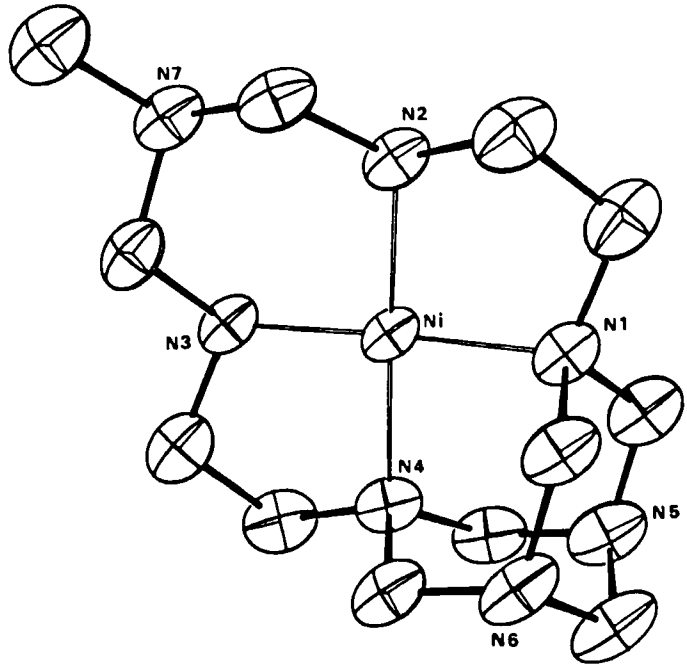

FIG. 4. Structure of $[Ni^{I}(\mathbf{9})]ClO_4$. [Reprinted with permission from (*57*). Copyright 1992, American Chemical Society.]

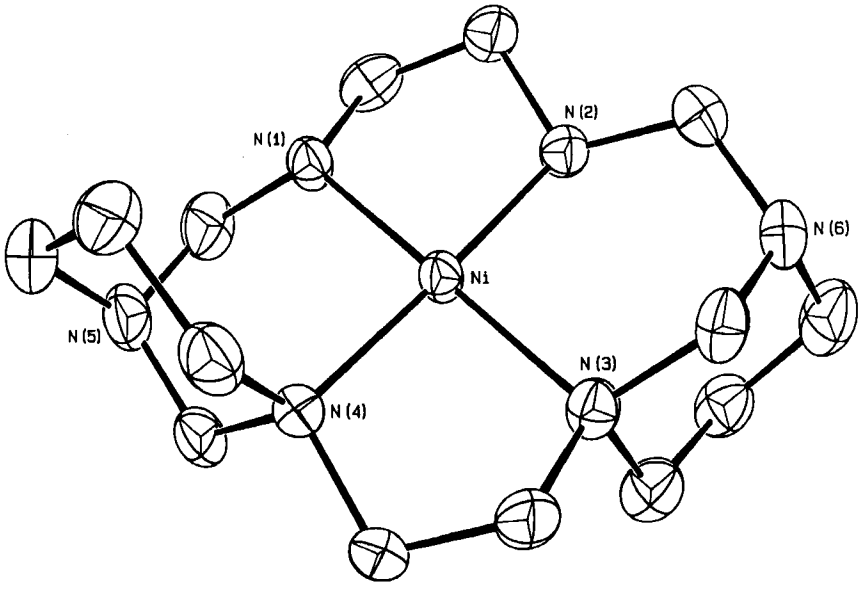

FIG. 5. Structure of $[Ni^{I}(\mathbf{14})]ClO_4$. (Reprinted with permission from *Inorg. Chem. 31*, 3620–3625. Copyright 1992 American Chemical Society.)

In short, Ni(I) complexes with flexible symmetric ligands such as HTIM and dieneN$_4$ show expansion of the core, while those of rigid ligands in **9**, **12**, and **14** exhibit distortion of the core without an expansion of the hole. The structural characteristics of Ni(I) complexes are summarized in Tables IX and X and compared with those of Ni(II) complexes.

Reports on EXAFS data analyses for the Ni(I) F430 (*138a*), Ni(I) iBC (*138b*), and Ni(I) OEiBC complexes (*139*) also suggest two sets of Ni—N bond distances rather than a simple expansion of the macrocyclic core. Therefore, the occurrence of two sets of Ni—N bond distances is common in all square-planar Ni(I) species reported thus far. Although it is unclear whether this distortion is electronic in nature or a consequence of the ligands examined, comparison of the structural features of isoelectronic Ni^{I} and Cu^{II}–(OEiBC) complexes suggested that the two distinct sets of Ni—N distances observed for Ni(I)(OEiBC) was not an electronic configuration effect. It might be the reflection of a balance

TABLE IX

COMPARISON OF STRUCTURES BETWEEN NICKEL(I) AND NICKEL(II) PERCHLORATE COMPLEXES OF MACROCYCLIC LIGANDS

Complex	Av. Ni—N (Å)	Distortion[a] (Å)		Five-membered rings		Six-membered rings		Ref.
		Ni	N	N—N (Å)	N—Ni—N (°)	N—N (Å)	N—Ni—N (°)	
$[Ni^{I}(\mathbf{9})]^{+}$	1.893(2)	0.04	±0.01	2.67(1)	88.4(1)	2.76(1)	93.6(1)	*57*
	1.936(2)			2.68(1)	88.9(1)	2.72(1)	89.0(1)	
$[Ni^{II}(\mathbf{9})]^{2+}$	1.918(3)	0.03	±0.01	2.66(1)	87.7(2)	2.84(1)	95.4(2)	*6, 57*
				2.65(1)	87.7(2)	2.69(1)	89.1(2)	
$[Ni^{I}(\mathbf{12})]^{+}$	1.859(7)	0.03	±0.09	2.69(2)	88.1(5)	2.74(2)	94.0(5)	*57*
	1.974(7)			2.60(2)	85.5(5)	2.86(2)	92.9(5)	
$[Ni^{II}(\mathbf{12})]^{2+}$	1.923(2)	0.02	±0.08	2.66(1)	87.4(2)	2.75(1)	91.3(2)	*10, 57*
				2.64(1)	86.9(2)	2.83(1)	94.7(2)	
$[Ni^{I}(\mathbf{14})]^{+}$	1.878(4)	0.006	±0.026	2.62(1)	86.4(2)	2.80(1)	92.7(2)	*134*
	1.978(3)			2.74(1)	87.2(2)	2.88(1)	93.7(2)	
$[Ni^{II}(\mathbf{14})]^{2+}$	1.942(1)	0.025	±0.020	2.63(1)	85.2(1)	2.86(1)	93.2(1)	*134*
	1.961(1)			2.72(1)	87.9(1)	2.83(1)	93.8(1)	
$[Ni^{I}(dieneN_4)]^{+}$	1.979(7)							*137*
	2.068(6)							
$[Ni^{II}(dieneN_4)]^{2+}$	1.907(2)							*137*
	1.938(2)							
$[Ni^{I}(C\text{-}RSSR\text{-}HTIM)]^{+}$	2.053(3)				84.6		95.4	*66*
	2.083(3)							
$[Ni^{II}(C\text{-}RSSR\text{-}HTIM)]^{2+}$	1.969(1)				85.7		94.3	*66*
	1.948(2)							

[a] The shift from the least squares plane made by four nitrogen donors.

TABLE X

DIFFERENCES IN TWO Ni–N BOND DISTANCES (Å) IN FOUR-COORDINATE NICKEL(I) COMPLEXES OF VARIOUS MACROCYCLIC LIGANDS[a]

Ligand	Ni(I) complex			Ni(II) complex	Ref.
	Short	Long	Δd^b		
9	1.893(2)	1.936(2)	0.043	1.918(3)	*57*
12	1.859(7)	1.974(7)	0.115	1.923(4)	*57*
14	1.878(4)	1.978(3)	0.100	1.951(2)	*134*
HTIM	2.053(3)	2.083(3)	0.030	1.948(2), 1.969(1)	*66*
dieneN$_4$	1.988(7)	2.063(6)	0.075	1.907(2), 1.938(2)	*137*
	1.979(7)	2.068(6)	0.089		
F430[c]	1.88(3)	2.03(3)	0.15	1.90(2)	*138b*
iBC[c]	1.85(5)	2.00(3)	0.15	1.93(2)	*138a*
OEiBC[c]	1.91(2)	2.07(2)	0.16	1.94(2)	*139*

[a] X-ray crystal structure data unless otherwise specified.
[b] Differences between long and short Ni—N bonds.
[c] EXAFS data.

between metal–nitrogen interaction energies and the macrocycle's conformation energy (*139*).

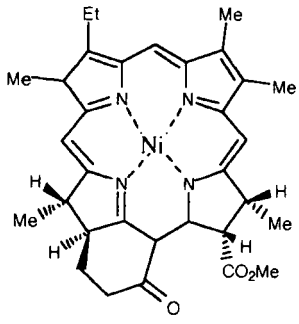

Ni-iBC

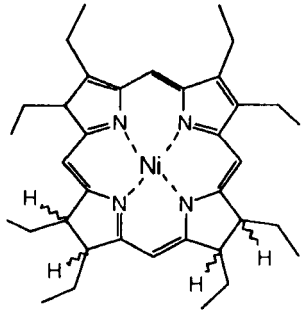

Ni-OEiBC

In the five-coordinate Ni(I) complex (*R,S,R,S*)-[Ni(**14**)(NHC(OH)CH_3)]ClO_4 (*136*), the Ni(I) ion displays a square-pyramidal geometry with an *R,S,R,S* (*trans*-I) configuration of the macrocycle. The complex also shows two sets of Ni—N(macrocycle) bond distances (Fig. 6). They are 2.09 and 2.14 Å, ca. 0.1–0.2 Å longer than those of the square-planar Ni(I) complex (*R,R,S,S*)-[Ni(**14**)]ClO_4. The axial Ni—N(iminol) bond distance (1.97 Å) is much shorter than the equatorial Ni—N(mac) bond distances, although it is significantly longer than the Ni(I)—CO

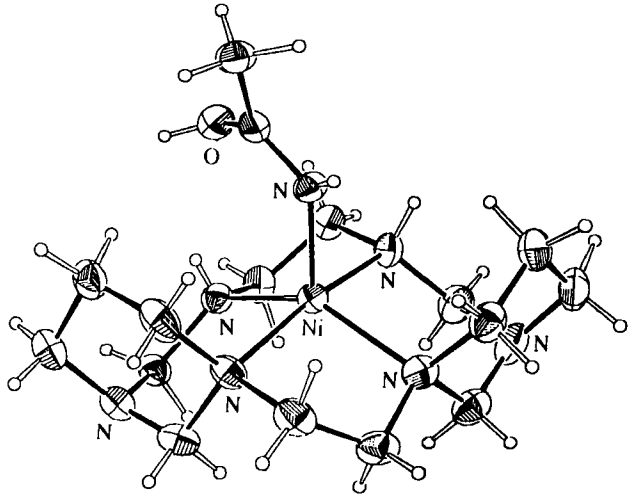

FIG. 6. Structure of $[Ni^{I}(\mathbf{14})(NHC(OH)CH_3)]ClO_4$. [Reprinted with permission from (*136*). Copyright 1996, American Chemical Society.]

bond distance (1.80 Å) of $[Ni(\mathbf{dieneN_4})(CO)]ClO_4$ determined by EXAFS analysis (*137*). The short Ni—N or Ni—CO axial bond must be attributed to the π back-bonding between Ni(I) ion and the axial ligand such as acetamide in the iminol form and CO.

D. Reactions of Square-Planar Complexes

1. Reactions with Carbon Monoxide

The square-planar Ni(I) complexes form five-coordinate Ni(I) carbonyl complexes when CO gas is introduced into solutions of the complexes, because they contain electron-rich Ni(I) ions capable of π back-donation (*66, 135*). The CO binding constants and carbonyl vibrational frequencies are summarized in Table XI. Because of the back-bonding interaction between the Ni(I) atom and the CO ligand, CO stretching frequencies for the Ni(I) carbonyl complexes decrease as NiL^+ becomes a more powerful reductant, which is represented by the $E_{1/2}$ values (*66*).

2. Reactions with Alkyl Halide

The Ni(I) complex of tetramethylated cyclam, $[Ni(TMC)]^+$, generated from the corresponding Ni(II) complex by electrochemical or photochemical methods, reacts with alkyl halides (RX) (*133, 140–143*). It is a radical reaction, generating R$^\cdot$ transients and/or Ni–alkyls, which then decay to form alkanes, alkenes, and dimeric or cyclic organics.

TABLE XI

CARBONYL VIBRATIONAL FREQUENCIES AND CARBON MONOXIDE BINDING CONSTANTS FOR NICKEL(I) CARBONYL COMPLEXES OF MACROCYCLIC LIGANDS

Compound	ν_{CO},[a] cm^{-1}	K_{CO},[a] M^{-1}	Ref.
C-*RRSS*-$[Ni^{I}$(**HTIM**)$]^{+}$	1939	$(9.0 \pm 2.0) \times 10^{4}$	*66*
$[Ni^{I}$(**cyclam**)$]^{+}$	1955	$(2.8 \pm 0.6) \times 10^{5}$	*137*
$[Ni^{I}$(**DMC**)$]^{+}$	1956	$(1.8 \pm 0.4) \times 10^{5}$	*137*
C-*RSRS*-$[Ni^{I}$(**TMC**)$]^{+}$	1967	$(1.2 \pm 0.4) \times 10^{5}$	*137*
$[Ni^{I}$(**dieneN$_4$**)$]^{+}$	1962	$(5.6 \pm 1.5) \times 10^{4}$	*66*
$[Ni^{I}$(**TIM**)$]^{+}$ [b]	2012	$(1.3 \pm 0.3) \times 10^{2}$	*66*

[a] In MeCN at 25°C.

[b] For C-*RSRS*-[Ni(TIM)]$^{+}$, K_{CO} is defined by the equation

$$[Ni^{II}(\mathbf{TIM}\cdot)]^{+} + CO \rightleftharpoons [Ni^{I}(TIM)CO]^{+}$$

The identity and distribution of the products varies with organic substrates and with the ratio of substrate : nickel complex employed.

Organonickel(II) species are believed to be formed during the reaction between $[Ni(TMC)]^{+}$ and primary alkyl halides, and subsequently undergo hydrolysis with cleavage of the Ni—C bond. Kinetic data measured in the presence of excess alkyl halide indicate a rate law $-d[Ni^{I}(TMC)^{+}]/dt = k[Ni^{I}(TMC)^{+}][RX]$. The rate constants increase for R and X in the order methyl < primary < secondary < allyl < benzyl halides and Cl < Br < I (*133, 140*). This suggests that the rate-determining step is electron transfer from the Ni(I) complex to R—X via an inner-sphere atom-transfer mechanism (*143*).

The complex $[Ni(TMC)]^{+}$ also reacts with disubstituted alkanes, $X(CH_2)_nY$ (X, Y, = Cl, Br, I, OH, OTs) (n = 2–6) in aqueous solutions (*144–146*). With vicinal disubstituted alkanes (n = 2, 3), alkenes are formed quantitatively and the transient organonickel species is not detected. The reaction of $[Ni(TMC)]^{+}$ with $Br(CH_2)_3OH$ yields 1-propanol, but reactions with 1,3-disubstituted propanes (X, Y = Br, Cl, OTs) form cyclopropane exclusively. The reaction of 1,5-dibromopentane with excess Ni(I) complex results in cyclopentane.

In contrast to the $[Ni(TMC)]^{+}$ complex, $[Ni^{I}(OEiBC)]^{+}$ shows reactivity patterns for R and X of methyl > primary > secondary > tertiary and I > Br > Cl. This is consistent with the rate-determining step being S_N2-type nucleophilic attack at R—X by $[Ni^{I}(OEiBC)]^{+}$ to generate Ni^{III}–alkyl species (*147, 148*).

The reaction between the Ni(I) complex of **12** and CH_3I also has an S_N2-type mechanism. The Ni(I) complex of **12** reacts with CH_3I in a 2 : 1 stoichiometry in MeCN to yield the corresponding Ni(II) complexes, I^-, CH_4, and C_2H_6. The rate law measured in MeCN is $-d[Ni^I]/dt = k[Ni^I][CH_3I]$. The second-order rate constants increase in the order methyl > ethyl > propyl. The rate-determining step proposed is an S_N2-type nucleophilic attack at R—X by Ni(I) complex to generate Ni^{III}–alkyl transients (*149, 150*).

3. *Reaction with Carbon Dioxide*

Some Ni(I) complexes bind CO_2. The CO_2-binding properties have been investigated in Me_2SO by electrochemical methods. The Ni(I) complex of cyclam binds CO_2 irreversibly, whereas the Ni(I) complex of Me_6[14]ane (L_{16}) shows no observable reaction. The Ni(II) and Ni(I) complexes of dieneN_4(L_{18}) show a very low affinity for CO_2 binding (*151*). The Ni(I) complexes of **9**, **11**, and **12** have been observed to react with CO_2 to form Ni(II) complexes, although the reduction products of CO_2 are not easily identifiable (*63*).

4. *Reaction with Amide*

The square-planar Ni(I) complex *R,R,S,S*-$[Ni(14)]^+$ reacts with acetamide in MeCN to form the amide adduct *R,R,S,S*-$[Ni(14)(NHC(OH)CH_3)]^+$ (*136*). In the acetamide complex, the Ni(I) ion binds acetamide in the iminol form through the nitrogen atom. The coordination chemistry of the metal–amide linkage is important in the context of metal ion–peptide chemistry (*152–154*). In general, 2+ or 3+ metal ions coordinate amide via the carbonyl oxygen (*155–160*) or the anionic nitrogen (*160–165*), and the acetamide coordination in the iminol form is quite uncommon (*166, 167*). It is apparent that the soft and electron-rich Ni(I) ion binds acetamide in the iminol form via the nitrogen atom, which is a softer and weaker σ-donor than oxygen, and there must be the $d\pi$–$\pi*$ interaction between the Ni(I) ion and nitrogen of iminol.

ACKNOWLEDGMENTS

Financial support from the Korean Science Foundation and the Ministry of Education, Republic of Korea, is gratefully acknowledged.

REFERENCES

1. Jaun, B.; Pfaltz, A. *J. Chem. Soc., Chem. Commun.* **1986,** 1327.
2. Jaun, B.; Pfaltz, A. *J. Chem. Soc., Chem. Commun.* **1988,** 293.

3. Barton, O.; Ollis, W. D. "Comprehensive Organic Chemistry"; Pergamon Press: Oxford, U.K., 1979; Vol. 2, p. 83.
4. Suh, M. P.; Shin, W.; Kim, D.; Kim, S. *Inorg. Chem.* **1984,** *23*, 618.
5. Suh, M. P.; Kim, D. *Inorg. Chem.* **1985,** *24*, 3712.
6. Suh, M. P.; Shin, W.; Kim, H.; Koo, C. H. *Inorg. Chem.* **1987,** *26*, 1846.
7. Suh, M. P.; Kang, S. *Inorg. Chem.* **1988,** *27*, 2544.
8. Suh, M. P.; Shin, W.; Kang, S.-G.; Lah, M. S.; Chung, T. M. *Inorg. Chem.* **1989,** *28*, 1602.
9. Suh, M. P.; Choi, J. W.; Kang, S. G.; Shin, W. C. *Inorg. Chem.* **1989,** *28*, 1763.
10. Suh, M. P.; Kang, S.-G.; Goedken, V. L.; Park, S. H. *Inorg. Chem.* **1991,** *30*, 365.
11. Jung, S.; Kang, S.; Suh, M. P. *Bull. Kor. Chem. Soc.* **1989,** *10*, 362.
12. Fabbrizzi, L.; Lanfredi, A. M. M.; Pallavicini, P.; Perotti, A.; Taglietti, A.; Ugozzoli, F. *J. Chem. Soc., Dalton Trans.* **1991,** 3263.
13. Blas, A. D.; Santis, G. D.; Fabbrizzi, L.; Licchelli, M.; Lanfredi, A. M.; Pallavicini, P.; Poggi, A.; Ugozzoli, A. *Inorg. Chem.* **1993,** *32*, 106.
14. Abba, F.; Santis, G. D.; Fabbrizzi, L.; Licchelli, M.; Lanfredi, A. M. M.; Pallavicini, P.; Poggi, A.; Ugozzoli, F. *Inorg. Chem.* **1994,** *33*, 1366.
14a. Suh, M. P.; Kang, S. G. *Bull. Kor. Chem. Soc.* **1995,** *16*, 217.
15. Santis, G. D.; Fabbrizzi, L.; Liccelli, M.; Pogi, A. *Inorg. Chem.* **1993,** *32*, 854.
16. Suh, M. P.; Shim, B. Y.; Yoon, T. S. *Inorg. Chem.* **1994,** *33*, 5509.
17. Boucher, H. A.; Lawrance, G. A.; Lay, P. A.; Sargeson, A. M.; Bond, A. M.; Sangster, D. F.; Sullivan, J. C. *J. Am. Chem. Soc.* **1983,** *105*, 4652.
18. Suh, M. P.; Kim, I. S.; Cho, S.-J.; Shin, W. *J. Chem. Soc., Dalton Trans.* **1994,** 2765.
19. Bernhardt, P. V.; Curtis, N. F.; Lawrance, G. A.; Skelton, B. W.; White, A. H. *Aust. J. Chem.* **1989,** *42*, 1.
20. Fenton, D. A. *Adv. Inorg. Bioinorg. Mech.* **1983,** *2*, 187.
21. Vigato, P. A.; Tamburini, S.; Fenton, D. E. *Coord. Chem. Rev.* **1990,** *106*, 25.
22. Aratake, Y.; Okawa, H.; Asato, E.; Sakiyama, H.; Kodera, M.; Kida, S.; Sakmoto, M. *J. Chem. Soc., Dalton Trans.* **1990,** 2941.
23. Kahn, O. *Struct. Bonding (Berlin)* **1987,** *68*, 89.
24. Zanello, P.; Tamburini, S.; Vigato, P. A.; Mazzocchin, G. A. *Coord. Chem. Rev.* **1987,** *77*, 165.
25. Suh, M. P.; Kim, S. K. *Inorg. Chem.* **1993,** *32*, 3563.
26. Rosokha, S. V.; Lampeka, Y. *J. Chem. Soc., Chem. Commun.* **1991,** 1077.
27. Rosokha, S. V.; Lampeka, Y.; Maloshtan, I. M. *J. Chem. Soc., Dalton Trans.* **1993,** 631.
28. Stephenson, N.; Tweedy, H. E.; Busch, D. H. *Inorg. Chem.* **1989,** *28*, 4376.
29. Kandil, S. S.; Collier, H. L. *Inorg. Chem.* **1988,** *27*, 4542.
30. Nishio, J.; Okawa, H.; Ohtsuka, S.; Tomono, M. *Inorg. Chim. Acta* **1994,** *218*, 27.
31. Hay, R. W.; Pujari, M. P.; Thomas Moodie, W.; Craig, S.; Richens, D. T.; Perotti, A.; Ungaretti, L. *J. Chem. Soc., Dalton Trans.* **1987,** 2605.
32. Barefield, E. K.; Foster, K. A.; Freeman, G. M.; Hodges, K. D. *Inorg. Chem.* **1986,** *25*, 4663.
33. Tschudin, D.; Basak, A.; Kaden, T. A. *Helv. Chim. Acta* **1988,** *71*, 100.
34. Freeman, G. M.; Barefield, E. K.; Van Derveer, D. G. *Inorg. Chem.* **1984,** *23*, 3092.
35. Pallavicini, P. S.; Perotti, A.; Poggi, A.; Seghi, B.; Fabbrizzi, L. *J. Am. Chem. Soc.* **1987,** *109*, 5139.
36. Alcock, N. W.; Balakrishnan, K. P.; Moore, P.; Omar, H. A. A. *J. Chem. Soc., Dalton Trans.* **1987,** 545.
37. Norante, G. M.; Vaira, M. D.; Mani, F.; Mazzi, S.; Stoppioni, P. *Inorg. Chem.* **1990,** *29*, 2822.

38. Balakrishnan, K. P.; Omar, H. A.; Moore, P.; Alcock, N. W.; Pike, G. A. *J. Chem. Soc. Dalton Trans.* **1990,** 2965.
39. Kimura, E. *Tetrahedron,* **1992,** *48,* 6175.
40. Kimura, E. In "Crown Ethers and Analogous Compounds"; Kiraoka, M., Ed.; Elsevier: Amsterdam, **1992,** p. 381.
41. Kimura, E.; Haruta, M.; Koike, T.; Shionoya, M.; Takenouchi, K.; Iitaka, Y. *Inorg. Chem.* **1993,** *32,* 2779.
42. Bernhardt, P. V.; Lawrance, G. A. *Coord. Chem. Rev.* **1990,** *104,* 297.
43. Kaden, T. A. *Comments Inorg. Chem.* **1990,** *10,* 25.
44. Lawrance, G. A.; Martinez, M.; Skelton, B. W.; White, A. H. *J. Chem. Soc., Dalton Trans.* **1992,** 823.
45. Kimura, E.; Yamaoka, M.; Morioka, M.; Koike, T. *Inorg. Chem.* **1986,** *25,* 3883.
46. Donlevy, T. M.; Gahan, L. R.; Stranger, R.; Kennedy, S. E.; Byriel, K. A.; Kennard, C. H. *Inorg. Chem.* **1993,** *32,* 6023.
47. Suh, M. P.; Kim, M. J.; Kim, H. K.; Oh, K. Y. *Bull. Kor. Chem. Soc.* **1992,** *13,* 80.
48. Wagner, F.; Barefield, E. K. *Inorg. Chem.* **1976,** *15,* 408.
49. Kajiwara, T.; Yamaguchi, T.; Kido, S.; Kawabata, S.; Kuroda, R.; Ito, T. *Inorg. Chem.* **1993,** *32,* 4990.
50. Matsumoto, N.; Koikawa, M.; Baba, N.; Okawa, H. *Bull. Chem. Soc. Jpn.* **1992,** *65,* 258.
51. Lovecchio, F. V.; Gore, E. S.; Busch, D. H. *J. Am. Chem. Soc.* **1974,** *96,* 3109.
52. Jubran, N.; Cohen, H.; Meyerstein, D. *Isr. J. Chem.* **1985,** *25,* 118.
53. Sabatini, L.; Fabbrizzi, L. *Inorg. Chem.* **1979,** *18,* 438.
54. Barefield, E. K.; Freeman, G. M.; Van Derveer, D. G. *Inorg. Chem.* **1986,** *25,* 552.
55a. Ciampolini, M.; Fabbrizzi, L.; Liccelli, M.; Perotti, A.; Pezzini, F.; Poggi, A. *Inorg. Chem.* **1986,** *25,* 4131.
55b. Jubran, N.; Ginzburg, G. G.; Cohen, H.; Koresh, Y.; Meyerstein, D. *Inorg. Chem.* **1985,** *24,* 251.
56a. Lee, D.; Suh, M. P.; Lee, J. W.; Shin, W. Submitted for publication.
56b. Hancock, R. D.; Ngwenya, M. P.; Wade, P. W.; Boeyens, J. A.; Dobson, S. M. *Inorg. Chim. Acta* **1989,** *164,* 73.
56c. Iwamoto, E.; Yokoyama, T.; Yamasaki, S.; Yabe, T.; Kumamaru, T.; Yamamoto, Y. *J. Chem. Soc., Dalton Trans.* **1988,** 1935.
57. Suh, M. P.; Kim, H. K.; Kim, M. J.; Oh, K. Y. *Inorg. Chem.* **1992,** *31,* 3620.
58. Pezzini, F.; Poggi, A. *Inorg. Chem.* **1986,** *25,* 4131.
59. Barefield, E. K.; Wagner, F. *Inorg. Chem.* **1973,** *12,* 2435.
60. Golub, G.; Cohen, H.; Meyerstein, D. *J. Chem. Soc. Chem., Commun.* **1992,** 397.
61a. Crick, I. S.; Gable, R. W.; Hoskins, B. F.; Tregloan, P. A. *Inorg. Chim. Acta* **1986,** *111,* 35.
61b. Hambley, T. W. *J. Chem. Soc., Dalton Trans.* **1986,** 565.
62. Holtmann, M. S.; Cummings, S. C. *Inorg. Chem.* **1976,** *15,* 660.
63. Suh, M. P. Unpublished results.
64. Melson, G. A., Ed. "Coordination Chemistry of Macrocyclic Compounds"; Plenum Press: New York, 1979.
65. Bernhardt, P. V.; Harrowfield, J. M.; Hockless, D. C. R.; Sargeson, A. M. *Inorg. Chem.* **1994,** *33,* 5659.
66. Szalda, D. J.; Fujita, E.; Sanzenbacher, R.; Paulus, H.; Elias, H. *Inorg. Chem.* **1994,** *33,* 5855.
67. Casa, M. D.; Fabbrizzi, L.; Mariani, M.; Seghi, B. *J. Chem. Soc., Dalton Trans.* **1990,** 55.

68. Hay, R. W.; Bembi, R.; Sommerville, W. *Inorg. Chim. Acta* **1982,** *59*, 157.
69. Fairbank, M. G.; McAuley, A. *Inorg. Chem.* **1987,** *26*, 2844.
70. McAuley, A.; Xu, C. *Inorg. Chem.* **1992,** *31*, 5549.
71. Suh, M. P.; Kong, G.-H.; Kim, I. S. *Bull. Kor. Chem. Soc.* **1993,** *14*, 439.
72. Chen, D.; Martell, A. E. *J. Am. Chem. Soc.* **1990,** *112*, 9411.
73. Kimura, E.; Machida, R. *J. Chem. Soc., Chem. Commun.* **1984,** 499.
74. Kimura, E. *J. Am. Chem. Soc.* **1984,** *106*, 5497.
75. Chen, D.; Motekaitis, R. J.; Martell, A. E. *Inorg. Chem.* **1991,** *30*, 1396.
76. Gosden, C.; Pletcher, D. *J. Organomet. Chem.* **1980,** *186*, 401.
77. Gosden, C.; Healy, K. P.; Pletcher, D.; Rosas, R. *J. Chem. Soc., Dalton Trans.* **1978,** 972.
78. Gosden, C.; Kerr, J. B.; Pletcher, D.; Rosas, R. *J. Electroanal. Chem.* **1981,** *117*, 101.
79. Beley, M.; Collin, J. P.; Ruppert, R.; Sauvage, J.-P. *J. Am. Chem. Soc.* **1986,** *108*, 7461.
80. Fischer, B.; Eisenberg, R. *J. Am. Chem. Soc.* **1980,** *102*, 7361.
81. Beley, M.; Collin, J.-P.; Ruppert, R.; Sauvage, J.-P. *Chem. Commun.* **1984,** 1315.
82. Collin, J. P.; Jouaiti, A.; Sauvage, J. P. *Inorg. Chem.* **1988,** *27*, 1986.
83. Fujihira, H.; Hirata, Y.; Suga, K. *J. Electroanal. Chem.* **1990,** *292*, 199.
84. Taniguchi, I. In "Modern Aspects of Modern Electrochemistry"; Bockris, J. O'M., White, R. E., and Conway, B. E., Eds.; Plenum Press: New York, **1989,** Vol. 20, p. 327.
85. Smith, C. I.; Crayston, J. A.; Hay, R. W. *J. Chem. Soc., Dalton Trans.* **1993,** 3267.
86. Fujita, E.; Haff, J.; Sanzenbacher, R.; Elias, H. *Inorg. Chem.* **1994,** *33*, 4627.
87. Kimura, E.; Shionoya, M.; Wada, S.; Maruyama, S. *Inorg. Chem.* **1992,** *31*, 4542.
88. Kimura, E.; Mitsuhiko, S.; Okazaki, Y. *Inorg. Chem.* **1994,** *33*, 770.
89. Fujita, E.; Brunswig, B. S.; Ogata, T.; Yanagida, S. *Coord. Chem. Rev.* **1994,** *132*, 195.
90. VanAtta, R. B.; Franklin, C. C.; Valentine, J. S. *Inorg. Chem.* **1984,** *23*, 4123.
91. Kinneary, J. F.; Albert, J. S.; Burrows, C. J. *J. Am. Chem. Soc.* **1988,** *110*, 6124.
92. Koola, J. D.; Kochi, J. K. *Inorg. Chem.* **1987,** *26*, 908.
93. Kinneary, J. F.; Wagler, T. R.; Burrows, C. J. *Tetrahedron Lett.* **1988,** *29*(8), 877.
94. Wagler, T. R.; Burrows, C. J. *Tetrahedron* **1988,** *29*, 5091.
95. Wagler, T. R.; Fang, Y.; Burrows, C. J. *J. Org. Chem.* **1989,** *54*, 1584.
96. Yoon, H.; Burrows, C. J. *J. Am. Chem. Soc.* **1988,** *110*, 4087.
97. Yoon, H.; Wagler, K. J.; O'Conner, K. J.; Burrows, C. J. *J. Am. Chem. Soc.* **1990,** *112*, 4568.
98. Yamada, M.; Ochi, S.; Suzuki, H.; Hisazumi, A.; Kuroda, S.; Shimao, I.; Araki, K. *J. Mol. Cat.* **1994,** *87*, 195.
99. Lee, D.; Suh, M. P. *Inorg. Chem.*, submitted for publication.
100a. Chen, X.; Rokita, S. E.; Burrows, C. J. *J. Am. Chem. Soc.* **1991,** *113*, 5884.
100b. Muller, J. G.; Chen, X.; Dadis, A. C.; Rokita, S. E.; Burrows, C. J. *J. Am. Chem. Soc.* **1992,** *114*, 6407.
100c. Moore, P.; Sachinidis, J.; Willey, G. R. *J. Chem. Soc., Chem. Commun.* **1983,** 522.
101. Cammack, R. *Adv. Inorg. Chem.* **1988,** *32*, 297.
102. Lancaster, J. R., Jr., Ed. "Bioinorganic Chemistry of Nickel"; VCH: New York, 1988.
103. Mack, D. P.; Dervan, P. B. *J. Am. Chem. Soc.* **1990,** *112*, 4604.
104. Lappin, A. G.; McAuley, A. *Adv. Inorg. Chem.* **1988,** *32*, 241.
105. Chavan, M. Y.; Meade, T. J.; Busch, D. H.; Kuwana, T. *Inorg. Chem.* **1986,** *25*, 314.
106. Buttafava, A.; Fabbrizzi, L.; Perotti, A.; Poggi, A.; Doli, G.; Seghi, B. *Inorg. Chem.* **1986,** *25*, 1456.
107. Fairbank, M. G.; McAuley, A. *Inorg. Chem.* **1986,** *25*, 1233.
108. McAuley, A.; Norman, P. R.; Olubuyide, O. *Inorg. Chem.* **1984,** *23*, 1938.

109. Bencini, A.; Fabbrizzi, L.; Poggi, A. *Inorg. Chem.* **1981,** *20*, 2544.
110. Gore, E. S.; Busch, D. H. *Inorg. Chem.* **1973,** *12*, 1.
111. Kimura, E.; Koike, T.; Machida, R.; Nagai, R.; Kodama, M. *Inorg. Chem.* **1984,** *23*, 4181.
112. Collins, T. J.; Nichols, T. R.; Uffelman, E. S. *J. Am. Chem. Soc.* **1991,** *113*, 4708.
113. Ito, T.; Sugimoto, M.; Toriumi, K.; Ito, H. *Chem. Lett.* **1981,** 1477.
114. Zeigerson, E.; Bar, I.; Bernstein, J.; Kirschenbaum, L. J.; Meyerstein, D. *Inorg. Chem.* **1982,** *21*, 736.
115. van der Merwe, M. J.; Boeyens, J. C. A.; Hancock, R. D. *Inorg. Chem.* **1983,** *22*, 3489.
116. Grove, D. M.; van Koten, G.; Zoet, R. *J. Am. Chem. Soc.* **1983,** *105*, 1379.
117. McAuley, A.; Subramanian, S. *Inorg. Chem.* **1991,** *30*, 371.
118. Santis, G. D.; Fabbrizzi, L.; Poggi, A.; Taglietti, A. *Inorg. Chem.* **1994,** *33*, 134.
119. Zeigerson, E.; Ginzburg, G.; Bedker, J. Y.; Kirschenbaum, L. J.; Cohen, H.; Meyerstein, D. *Inorg. Chem.* **1981,** *20*, 3988.
120. Yamashita, M.; Toriumi, K.; Ito, T. *Acta. Cryst.* **1985,** *C41*, 1607.
120a. Yamashita, M.; Miyamae, H. *Inorg. Chim. Acta* **1989,** *156*, 71.
121. Machida, R.; Kimura, E.; Kushi, Y. *Inorg. Chem.* **1986,** *25*, 3461.
122. Brodovitch, J. C.; McAuley, A.; Oswald, T. *Inorg. Chem.* **1982,** *21*, 3442.
123. Welsh, W. A.; Otutakowski, J.; Henry, P. M. *Can. J. Chem.* **1981,** *59*, 697.
124. Beley, M.; Collins, J. P.; Ruppert, R.; Sauvage, J. P. *J. Chem. Soc., Chem. Commun.* **1984,** 1315.
125. Becker, J. K.; Kerr, J. B.; Pletcher, D.; Rosas, R. J. *J. Electroanal. Chem. Interfacial Electrochem.* **1981,** *117*, 87.
126. Healy, K. P.; Pletcher, D. *J. Organomet. Chem.* **1978,** *161*, 109.
127. Gunsalus, R. P.; Wolfe, R. S. *FEMS Microbiol. Lett.* **1978,** *3*, 191.
128. Pfalts, A.; Juan, B.; Fassler, A.; Eshenmoser, A.; Jaenchen, R.; Gilles, H. H.; Diekert, G.; Thauer, R. R. *Helv. Chim. Acta* **1982,** *65*, 828.
129. Pfaltz, A.; Livingston, D. A.; Jaun B.; Diekert, G.; Thauer, R.; Eshenmoser, A. *Helv. Chim. Acta* **1985,** *68*, 1338.
130. Livingston, D. A.; Pfaltz, A.; Schreiber, J.; Eshenmoser, A.; Ankel-Fusch, D.; Moll, J.; Jaenchen, R.; Thauer, R. K. *Helv. Chim. Acta* **1984,** *67*, 334.
131. Albracht, S. P. J.; Ankel-Fusch, D.; Van der Zwaan, J. W.; Fontijn, R. D.; Thauer, R. K. *Biochim. Biophys. Acta* **1986,** *870*, 57.
132. Albracht, S. P. J.; Ankel-Fusch, D.; Boecher, R.; Ellerman, J.; Moll, J.; Van der Zwaan, J. W.; Thauer, J. K. *Biochim. Biophys. Acta* **1988,** *955*, 86.
133. Bakac, A.; Espenson, J. H. *J. Am. Chem. Soc.* **1986,** *108*, 713.
134. Suh, M. P.; Lee, Y. J.; Jeong, J. W. *J. Chem. Soc., Dalton Trans.* **1995,** 1557.
135. Gagne, R. R.; Ingle, D. M. *Inorg. Chem.* **1981,** *20*, 420.
136. Suh, M. P.; Oh, K. Y.; Lee, J. W.; Bae, Y. Y. *J. Am. Chem. Soc.* **1996,** *118*, 777.
137. Furenlid, L. R.; Renner, M. W.; Szalda, D. J.; Fujita, E. *J. Am. Chem. Soc.* **1991,** *113*, 883.
138a. Furenlid, L. R.; Renner, M. W.; Smith, K. M.; Fajer, J. *J. Am. Chem. Soc.* **1990,** *112*, 1634.
138b. Furenlid, L. R.; Renner, M. W.; Fajer, J. *J. Am. Chem. Soc.* **1990,** *112*, 8987.
139. Renner, M. W.; Furenlid, L. R.; Stolzenberg, A. M. *J. Am. Chem. Soc.* **1995,** *117*, 293.
140. Ram, M. S.; Bakac, A.; Espenson, J. H. *Inorg. Chem.* **1986,** *25*, 3267.
141. Bakac, A.; Espenson, J. H. *J. Am. Chem. Soc.* **1986,** *108*, 5353.
142. Ram, M. S.; Espenson, J. H.; Bakac, A. *Inorg. Chem.* **1986,** *25*, 4115.
143. Sadler, N.; Scott, S. L.; Bakac, A.; Espenson, J. H.; Ram, M. S. *Inorg. Chem.* **1989,** *28*, 3951.

144. Ram, M. S.; Bakac, A.; Espenson, J. H. *Inorg. Chem.* **1988,** *27*, 2011.
145. Ram, M. S.; Bakac, A.; Espenson, J. H. *Inorg. Chem.* **1988,** *27*, 4231.
146. Espenson, J. H.; Ram, M. S.; Bakac, A. *J. Am. Chem. Soc.* **1987,** *109*, 6892.
147. Stolzenberg, A. M.; Stershic, M. T. *J. Am. Chem. Soc.* **1988,** *110*, 5397.
148. Lahiri,G. K.; Schussel, L. J.; Stolzenberg, A. M. *Inorg. Chem.* **1992,** *31*, 4991.
149. Suh, M. P. *Proc. Korea–U.S. Inorg. Chem. Conf.* (Seoul, Korea) **1993,** 73.
150. Suh, M. P.; Bea, Y. Y.; Lee, D. W. Submitted for publication.
151. Schmidt, M. H.; Miskelly, G. M.; Lewis, N. S. *J. Am. Chem. Soc.* **1990,** *112*, 3420.
152. Chin, J. *Acc. Chem. Res.* **1991,** *24*, 145.
153. Sigel, H.; Martin, R. B. *Chem. Rev.* **1982,** *82*, 385.
154. Corradi, A. B. *Coord. Chem. Rev.* **1992,** *117*, 45.
155. Stone, M. E.; Johnson, K. E. *Can. J. Chem.* **1973,** *51*, 1260.
156. Dixon, N. E.; Fairlie, D. P.; Jackson, W. G.; Sargeson, A. M. *Inorg. Chem.* **1983,** *22*, 4038.
157. Curtis, N. J.; Sargeson, A. M. *J. Am. Chem. Soc.* **1984,** *106*, 625.
158. Wilkinson, G.; Gillard, R. D.; McCleverty, J. A. "Comprehensive Coordination Chemistry"; Pergamon Press: Oxford, 1987; Vol. 2, pp. 490–494.
159. Angus, P. M.; Fairlie, D. P.; Jackson, W. G. *Inorg. Chem.* **1993,** *32*, 450.
160. Fairlie, D. P.; Angus, P. M.; Fenn, D.; Jackson, W. G. *Inorg. Chem.* **1991,** *30*, 1564.
161. Fairlie, D. P.; Jackson, W. G.; McLaughlin, G. M. *Inorg. Chem.* **1989,** *28*, 1983.
162. Buckingham, D. A.; Kneene, F. R.; Sargeson, A. M. *Inorg. Chem.* **1983,** *22*, 4038.
163. Curtis, N. J.; Sargeson, A. M. *J. Am. Chem. Soc.* **1984,** *106*, 625.
164. Jensen, C. M.; Trogler, W. C. *J. Am. Chem. Soc.* **1986,** *108*, 723.
165. Chou, M. H.; Szalda, D. J.; Creutz, C.; Sutin, M. *Inorg. Chem.* **1994,** *33*, 1674.
166. Woon, T. C.; Fairlie, D. P. *Inorg. Chem.* **1992,** *31*, 4069.
167. Cini, R.; Fanizzi, F. P.; Intini, F. P.; Maresca, L.; Natile, G. *J. Am. Chem. Soc.* **1993,** *115*, 5123.

ADVANCES IN INORGANIC CHEMISTRY, VOL. 44

ARSENIC AND MARINE ORGANISMS

KEVIN A. FRANCESCONI* and JOHN S. EDMONDS

Western Australian Marine Research Laboratories, North Beach W. A. 6020, Australia

I. Introduction

At the next dinner party, as your host proudly serves the lobster thermidor, you may wish to momentarily stray from the conventions of a polite but conservative guest, the archetypal chemist, by casually inquiring about the arsenic content of the meal. Given arsenic's reputation as a potent poison, your host may be affronted or bemused, but he or she is sure to be interested.

* New address for correspondence: Institute of Biology, Odense University, DK-5230 Odense M, Denmark

The following review could provide you with at least some of the answers to the probable ensuing questions about arsenic and marine organisms. It is intended to inform the reader of the rich and varied chemistry shown by arsenic in marine systems, and to stimulate some interest and debate in chemical circles regarding the origin and possible role of these compounds. The review begins with a brief overview of marine arsenic research and a summary of arsenic concentrations in the various marine compartments. General chemical and analytical characteristics of the arsenic compounds of significance in marine arsenic studies are then considered, followed by an outline of their occurrence, distribution, and biotransformation in marine samples. Finally, questions concerning the origin of arsenobetaine in marine animals are discussed.

Workers in the area have applied different scientific disciplines to advance various aspects of the problem over the years. For example, progress in biological and biochemical studies of the uptake of arsenic by algae was made following chemical studies identifying the natural arsenic constituents of algae. Subsequent chemical synthesis of the arsenic compounds enabled toxicological assessment and further biotransformation studies to be carried out. What follows is a welding together of results from these different disciplines, with an emphasis on chemical aspects.

II. Arsenic Concentrations in Marine Samples

Although there had been earlier reports (*1–3*) of the presence of arsenic in marine samples, the first comprehensive study was presented by Jones (*4*) in 1922. He examined marine algae collected from British coastal waters, reporting concentrations of arsenic and information on its extraction with water and ethanol. He referred to the arsenic as organic arsenic and, perhaps somewhat mischievously, remarked that the reputed medicinal properties of some algae may be due to their organic arsenic content.

In work related to the human toxicology of arsenic, Cox (*5*) noted that within 24 hours after a person eats fish, arsenic can be measured in the urine at levels normally indicative of chronic arsenic poisoning. The subsequent study of Chapman (*6*) in 1926 established the occurrence of high levels of arsenic in a wide range of marine organisms. Arsenic concentrations in seawater were also reported at this time (*7*). Over the ensuing years there followed only infrequent reports (e.g., *8*) on arsenic in marine samples until the late 1960s. Renewed interest

TABLE I

ARSENIC CONCENTRATIONS IN SEDIMENTS

Type	Location	Arsenic concentration (mg/kg dry wt.)	Ref.
Coastal/estuary	Bellingham Bay	10–15	*11*
Coastal/estuary	Central Puget Sound	4–35	*11*
Coastal/estuary	Thames	4–16	*12*
Coastal/estuary	Humber	18–94	*12*
Coastal/estuary	Severn and Bristol Channel	7–12	*12*
Coastal/estuary	Southampton Water	5–28	*12*
Deep-sea	West Pacific Ocean	14–20	*13*
Deep-sea	Sea of Japan	6–14	*13*
Deep-sea	North Atlantic Ocean	11–26	*14*
Deep-sea	Indian Ocean	4–86	*14*
Deep-sea	Equatorial Pacific Ocean	23–455	*14*
Deep-sea	South Pacific Ocean	3–32	*14*

TABLE II

ARSENIC CONCENTRATIONS IN MARINE ALGAE

Type	Location (no. of species)	Arsenic concentration (mg/kg dry wt.)		Ref.
		Range	Mean	
Brown	India (8)	8–68	30	*15*
	Norway (7)	15–109	44	*16*
	USA (24)	1–32	10	*17*
	Australia (14)	21–179	62	*18*
	Japan (13)	2–72	21	*19*
Red	India (5)	0–5	1.5	*15*
	Norway (2)	10–13	12	*16*
	USA (15)	0.4–3.2	1.4	*17*
	Australia (10)	12–31	19	*18*
	Japan (25)	6–45	17	*19*
Green	India (5)	0.1–6.3	2.2	*15*
	USA (16)	0.2–23	1.5	*17*
	Australia (9)	6–16	11	*18*
	Japan (5)	12–19	16	*19*
Phytoplankton	Australia (mixed samples)	—	9	*20*

was based on human toxicological issues related to arsenic in seafoods, and a large body of data on arsenic levels in marine samples resulted.

Tables I to III provide a summary of some representative data for total arsenic concentrations in sediments, marine algae, and marine animals. There can be considerable variation in the arsenic levels in these samples, in contrast to the levels in seawater, which are reasonably uniform in the world's oceans at about 0.5–2 μg/liter (*9, 10*). For sediments, there is perhaps a tendency for arsenic concentrations to be lower in samples from coastal regions and estuaries compared with deep-sea sediments. Industrial discharges of arsenic-enriched effluents can, however, result in arsenic contamination of near-shore sediments (*11, 12*). Arsenic concentrations in marine algae are generally considerably higher in brown algae than in either red or green algae. Reasons

TABLE III

ARSENIC CONCENTRATIONS IN MARINE ANIMALS

Type	Location (no. of species)	Arsenic concentration (mg/kg wet or dry wt. as shown) Range	Mean		Ref.
Finfish	Australia (9)	0.8–14	6.5	dry	*21*
	Northern Europe (14)	1.3–37	7.7	wet	*22*
	Greenland (5)	8–307	60	dry	*23*
	Norway (8)	0.6–8	2.7	wet	*24*
	USA (many)	Range of means from 1 to 7		wet	*25*
	Arabian Gulf (13)	0.3–32	4.9	wet	*26*
Crustaceans	Australia (5)	7–91	27	dry	*21*
	Arabian Gulf (3)	6–16	12	wet	*26*
	Scotland (3)	3–38	12	wet	*27*
	USA (16)	Range of means from 3 to 50		wet	*25*
Bivalve molluscs	Japan (5)	1–10	3.6	wet	*18*
	U.K. (5)	2.6–15	7.8	dry	*29*
	USA (12)	Range of means from 2 to 20		wet	*25*
	Goa (4)	2.3–11	5.0	dry	*30*
Gastropod molluscs	Japan (10)	1.6–107	26	wet	*28*
	U.K. (6)	8.1–38	16	dry	*29*
	USA (2)	3.0–27	14	wet	*25*

for this are not known at present. The trend in arsenic concentrations between groups of marine animals is less clear, although crustaceans are generally higher than other animals. Certainly, there is no indication that arsenic accumulates along food chains.

III. Key Arsenic Compounds: Chemical and Analytical Considerations

In chemical combination, arsenic can exist in oxidation state III or V and can have a coordination number of 3, 4, 5, or 6. In marine samples, arsenic is mainly found in the V oxidation state, although, usually as a consequence of biological factors, arsenic (III) compounds can also occur and may at times be predominant. The properties and analysis of the various arsenic-containing compounds of significance in marine arsenic research are briefly discussed, and information is provided on their synthesis. For ease of reference, the arsenic compounds frequently mentioned by name (or abbreviation/acronym) are listed in Table IV together with their structure numbers.

A. Inorganic Arsenic

In normal seawater, the major As(V) species is calculated to be $HAsO_4^{2-}$ (**1**) (98% of total) with trace amounts of $H_2AsO_4^-$ and AsO_4^{3-} (*31*). Similar calculations for As(III) indicate that in seawater the major species would be the neutral H_3AsO_3 (**2**), although hydrolysis may

TABLE IV

Names, Abbreviations, and Structures of Some Marine Arsenic-Containing Compounds

Compound	Abbreviation	Structure no.
Arsenate	As (V)	**1**
Arsenite	As (III)	**2**
Monomethylarsonic acid	MMA	**3**
Dimethylarsinic acid	DMA	**4**
Trimethylarsine oxide	TMAO	**5**
Tetramethylarsonium ion	TeMA	**6**
Arsenobetaine	—	**7**
Arsenocholine	—	**8**
Dimethylarsinoylribosides	Arsenosugars	e.g., **17**
Trimethylarsonioribosides	Arsenosugars	e.g., **33**
Dimethylarsinoylethanol	DMAE	**39**
Glycerophospho(arsenocholine)	GPAC	**44**

result in up to 13% of H_4AsO_4. As noted by Cullen and Reimer (*32*) in their comprehensive discussion of aqueous complexes of arsenic, most researchers in the field do not distinguish between the different levels of protonation of the inorganic arsenic species, referring to them collectively as either arsenite or arsenate for the As(III) or As(V) forms, respectively. That convention is also used here. The two inorganic forms of arsenic are readily interconverted in solution by simple oxidizing or reducing agents, and changes in arsenic speciation have been reported on storage of seawater samples (*33*). Consequently, care must be taken when preparing marine samples for As(III)/As(V) speciation analysis to ensure that the sample chemistry remains unchanged from the time of collection to analysis.

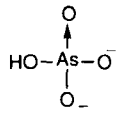

(1)

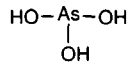

(2)

The most useful chemical species in the analysis of arsenic is the volatile hydride, namely arsine (AsH_3, bp −55°C). Analytical methods based on the formation of volatile arsines are generally referred to as hydride, or arsine, generation techniques. Arsenite is readily reduced to arsine, which is easily separated from complex sample matrices before its detection, usually by atomic absorption spectrometry (*33*). A solution of sodium borohydride is the most commonly used reductant. Because arsenate does not form a hydride directly, arsenite can be analyzed selectively in its presence (*34*). Specific analysis of As(III) in the presence of As(V) can also be effected by selective extraction methods (*35*).

Anion-exchange chromatography can also be used to separate As(III) and As(V) where the difference in pK_a's (9.3 vs 2.3) allows good resolution (*36*). High-performance liquid chromatography (HPLC) coupled to element-specific detectors is being increasingly used to separate and analyze chemical forms of arsenic found in marine samples (*33*). The detection systems used include atomic absorption spectrometry (AAS), inductively coupled plasma–atomic emission spectrometry (ICP-AES), and inductively coupled plasma–mass spectrometry (ICP-MS). Although these HPLC methods are suitable for separating and determining the inorganic arsenic species (*37*), the less sophisticated methods, such as hydride generation, are still the most commonly used.

B. Simple Methylated Arsenic Compounds

Arsenic compounds with one to four methyl groups attached to the arsenic atom are common constituents of marine samples. The relevant species are monomethylarsonic acid (MMA) (**3**), dimethylarsinic acid (DMA) (**4**), trimethylarsine oxide (TMAO) (**5**), and tetramethylarsonium ion (TeMA) (**6**). Of these, MMA and DMA are readily separated

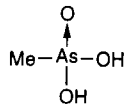

(3)

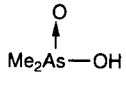

(4)

(5)

(6)

from each other and from arsenite and arsenate on ion-exchange media (*38*). At pH < 3.5, DMA can protonate (*39*), giving the charged species $Me_2As^+(OH)_2$, which may be retained on cation-exchange media. The acronyms MMA and DMA are used to refer to the species regardless of whether they are present as the anions, free acids, or cations. Trimethylarsine oxide can also protonate, giving the cationic species Me_3As^+OH, which is retained on cation-exchange columns and eluted by dilute ammonia. Tetramethylarsonium ion, however, is tightly bound to cation-exchange media, requiring 6 M HCl for its elution (*40*). Because of the large differences in their anionic/cationic properties, these four methylated arsenicals are easily separated by chromatography, and techniques such as HPLC/ICP-MS are most suitable for their determination.

The compounds MMA, DMA, and TMAO are reduced in acidic aqueous media by borohydride solutions to methylarsine ($MeAsH_2$, bp 2°C), dimethylarsine (Me_2AsH, bp 35°C), and trimethylarsine (Me_3As, bp 55°C), respectively. These products are useful derivatives for speciation analysis of arsenic because they are readily separated from complex sample matrices and may be further separated from each other by distillation (*41*) or by gas chromatography (*42*) prior to their determination by element-specific detectors. Consequently, arsine generation techniques are the most commonly used methods for determining MMA, DMA, and TMAO in marine samples.

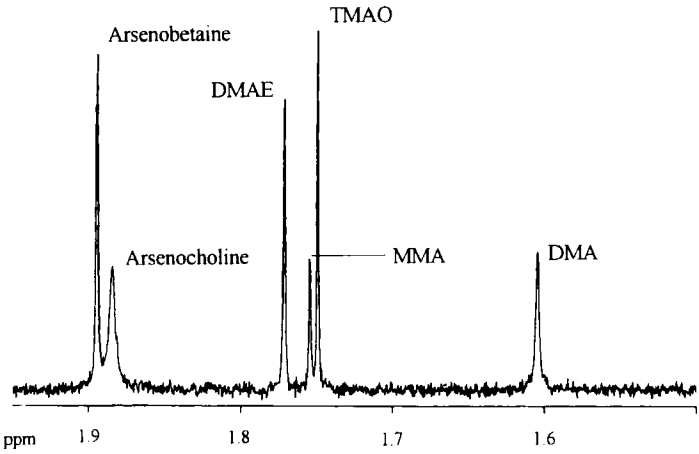

FIG. 1. NMR spectrum (^{1}H, 500 MHz) of a synthetic mixture of six marine arsenic compounds in seawater. Each compound was present at a concentration of 10 μg As/mL. (Spectrum courtesy of Dr. L. Byrne.)

The chemical shifts in the NMR for the methyl groups on arsenic can vary depending on pH. They are, however, sufficiently different from each other and from other marine arsenic compounds that they are readily distinguishable even in seawater solutions (Fig. 1). Thus, the possibility exists for examining marine arsenic transformations in solutions or cells by NMR spectroscopy. Little work has been done in this area.

C. ARSENOBETAINE AND ARSENOCHOLINE

Arsenobetaine (**7**) and arsenocholine (**8**) are both resistant to attack from acids, and this property, in regard to arsenobetaine, probably

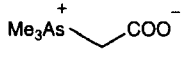

(7)

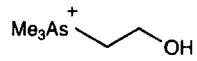

(8)

accounts for the problems of low recovery often associated with the analysis of arsenic in marine samples (*43*). Wet digestion techniques employing nitric acid are not sufficiently robust to decompose arsenobetaine to a form (arsenate) that it is possible to analyze (*44, 45*). Arsenobetaine and arsenocholine, however, differ markedly in their stability toward NaOH. Treatment with hot 2 *M* NaOH results in complete decomposition of arsenobetaine, whereas arsenocholine remains intact

(*46*). Attempts have been made to use this difference in reactivity to distinguish between the two arsenic-containing compounds in marine samples. Although some success was achieved on synthetic materials, the results from marine samples (*47*) have been misleading and have been questioned (*32*).

Arsenobetaine is zwitterionic in solution, displaying cationic properties at pH <3.5 (*39*). The first reported isolation of arsenobetaine was greatly facilitated by its retention on a cation-exchange resin and subsequent elution with dilute aqueous ammonia (*48*). Arsenocholine, however, remains cationic at high pH and requires forceful conditions (e.g., 6 *M* HCl) to displace it from cation-exchange resins—a property it shares with TeMA.

Importantly, neither arsenobetaine nor arsenocholine forms an arsine on treatment with borohydride solutions. Consequently, arsenobetaine and arsenocholine may remain undetected in samples, seawater for example, when arsines are generated and determined in an arsenic speciation analysis. The technique HPLC/ICP-MS is most suitable for the analysis of these (non-arsine-forming) compounds (*49*). Use of the highly sensitive ICP-MS detector allows application of small quantities of material to the chromatography column, thereby obviating possible sample matrix effects previously observed for arsenobetaine (*50*).

Arsenobetaine can be prepared by treatment of trimethylarsine with ethyl bromoacetate followed by basic hydrolysis (*51*). Because the material so obtained is deliquescent and difficult to handle, preparation of the bromide salt beginning with bromoacetic acid, though lower-yielding, may be preferable (*52*). Arsenocholine bromide is synthesized by prolonged heating of trimethylarsine with 2-bromoethanol (*53*); it is readily changed to the nonhygroscopic iodide salt by treatment with NaI in acetonitrile (*53*) or by passage through an anion-exchange column (*54*). Both arsenobetaine and arsenocholine display the characteristic singlet (Me_3As) at about δ 2.0 in the ^1H NMR, although this can vary depending on pH and concentration (see Fig. 1). The methylene protons in arsenobetaine exchange slowly ($t_{1/2} \approx 24$ h) in D_2O at room temperature.

D. Arsenic-Containing Ribosides (Arsenosugars)

A number of arsenic-containing ribosides, also referred to here simply as arsenosugars, occur in marine samples. Most of the arsenosugars are dimethylarsinoylribosides (Fig. 2, compounds **9** to **25**). This group of compounds was unknown prior to 1981, when **9** and **12** were isolated from a brown alga (*55*). Structures for the two compounds were origi-

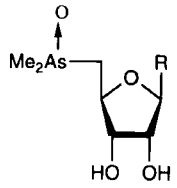

R

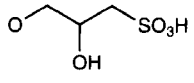

(9)

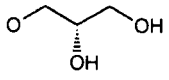

(14)

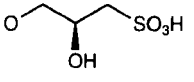

(10)

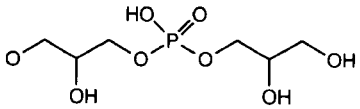

(15)

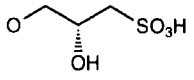

(11)

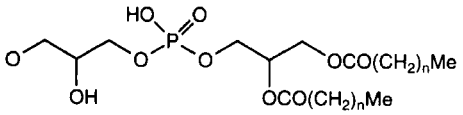

(16)

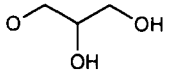

(12)

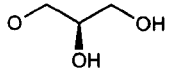

(13)

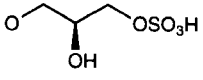

(17)

FIG. 2. Structures of dimethylarsinoylribosides. With the exception of **14**, all the compounds have been isolated from marine sources.

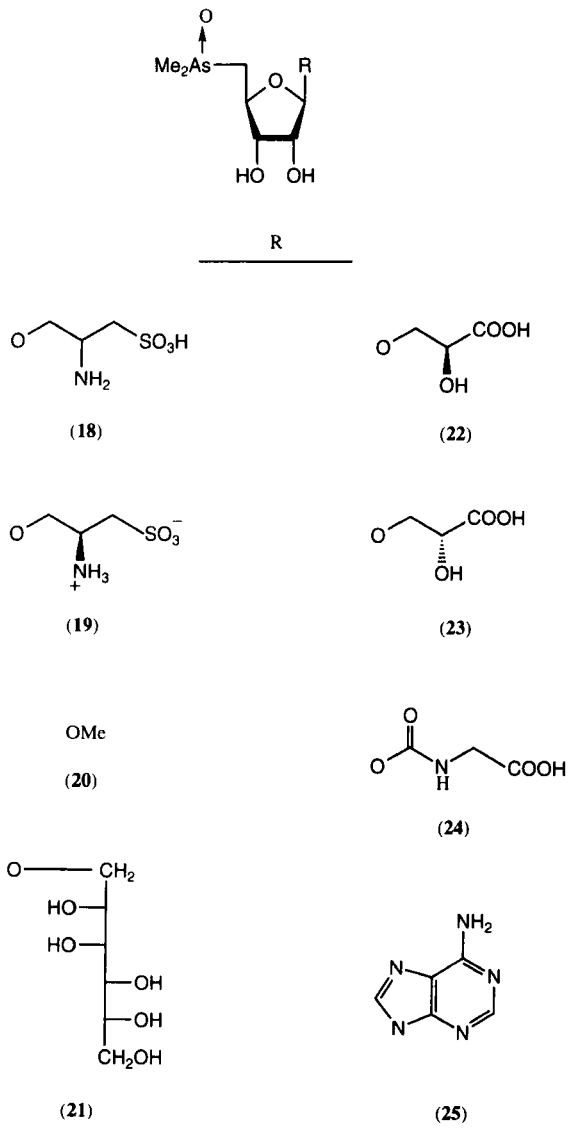

FIG. 2. *Continued.*

nally assigned chiefly from NMR data. Subsequent synthetic studies (*56, 57*) provided confirmation of the proposed structures and allowed assignment of the configuration at C-2 in the aglycone as represented by **10** and **13**. X-ray crystallographic analysis of the related compound **17** had previously confirmed the β-D-ribo ring structure for the dimethyl-

arsinoylribosides (*58*). The bond lengths and angles for **17** were as expected for this type of compound, the As-O bond length being 0.173 nm—comparable with that for arsono compounds (*59*). With the exception of **14**, which was obtained by chemical synthesis, all compounds shown in Fig. 2 have been isolated from marine samples.

Although dimethylarsinoylribosides form arsines on treatment with borohydride solutions, these derivatives have not proved useful for arsenic speciation analysis. In this instance the arsines are too involatile to be readily removed from the sample matrix, and too polar to allow their extraction from the aqueous phase. The dimethylarsinoylribosides display acidic or basic properties depending on the aglycone. In compounds containing a neutral aglycone (e.g., compound **13**), the arsine oxide moiety may be protonated at low pH, imparting cationic characteristics to the molecule. Consequently, HPLC/ICP-MS techniques employing ion-exchange or ion-pairing conditions have been successfully applied to the analysis of these compounds (Fig. 3) (*60, 61*).

Compound **13** was the first arsenosugar to be synthesized (Fig. 4) (*56*). The orthoester **26** was transesterified with the alcohol **27** to give an intermediate orthoester, which rearranged on treatment with mercury(II) bromide to the riboside **28**. Removal of the ester protecting groups yielded the triol **29**, which was converted to the isopropylidene derivative and then the chloride **30**. The key intermediate **31** was then prepared by treating the chloride **30** with dimethylarsinosodium after the method of Feltham *et al.* (*62*). Attempts to purify this arsine proved difficult. Instead, it was oxidized without purification, giving **32**, which

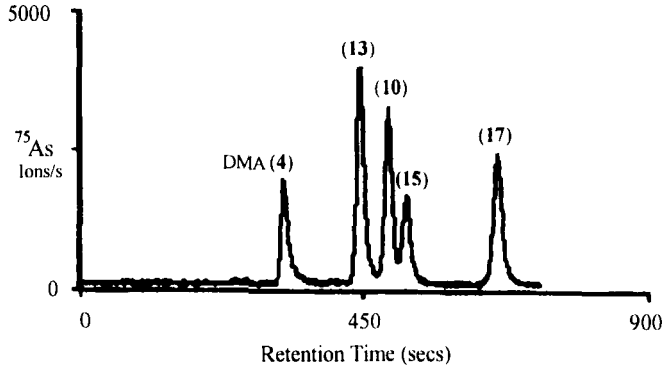

FIG. 3. Typical separation of four arsenosugars and DMA by HPLC/ICP-MS using an ODS reversed-phase column at pH 3.2 under conditions described in Ref. *60*. The sensitivity and specificity of the detector allows the determination of arsenosugars and other arsenic compounds to be conducted on dilute aqueous extracts of the marine samples.

then yielded the desired compound **13** on brief exposure to aqueous acid. The related carboxylic acid **22** was prepared by selective deprotection of the diisopropylidene derivative **32**, followed by oxidation of the resultant diol and hydrolysis (*63*).

Beginning with the enantiomer of **27**, the reaction sequence outlined in Fig. 4 was repeated, leading to compound **14** (*63*). Selective oxidation of **14** afforded the carboxylic acid **23** (*63*). The arsenic-containing nucleoside **25** was obtained by treating 5′-chloro-5′-deoxyadenosine with excess dimethylarsinosodium and oxidation of the resultant arsine (*63*).

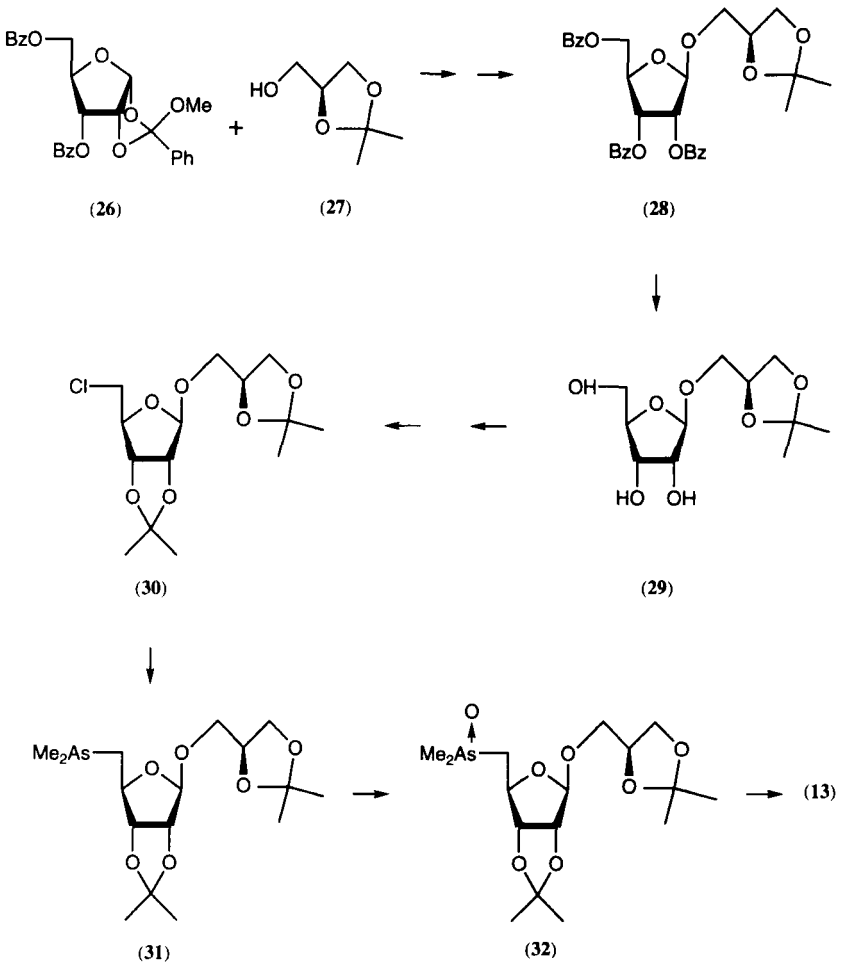

(26) (27) (28) (30) (29) (31) (32)

FIG. 4. Reaction sequence for the synthesis of the arsenosugar **13**.

Trimethylarsonioribosides have also been synthesized (Fig. 5). Compound **33** was first isolated from a brown alga and was subsequently prepared by addition of methyl iodide to the arsine obtained on reduction of the natural product **17** with borohydride solution (*64*). Compound **33** has also been prepared by using 2,3-dimercaptopropanol as the reductant, and this procedure was similarly used for the synthesis of compounds **34** to **37** from the respective dimethylated compounds (*65*).

Two unusual trialkylarsonioriboside diastereoisomers were also isolated as a mixture from a brown alga (*57*). Although the exact nature of the diastereoisomerism could not be established, it seems probable that the compounds differed only in the configuration at the methine attached to the carboxy group, as shown in structure **38**. The diastereoisomers have recently been separated by HPLC.

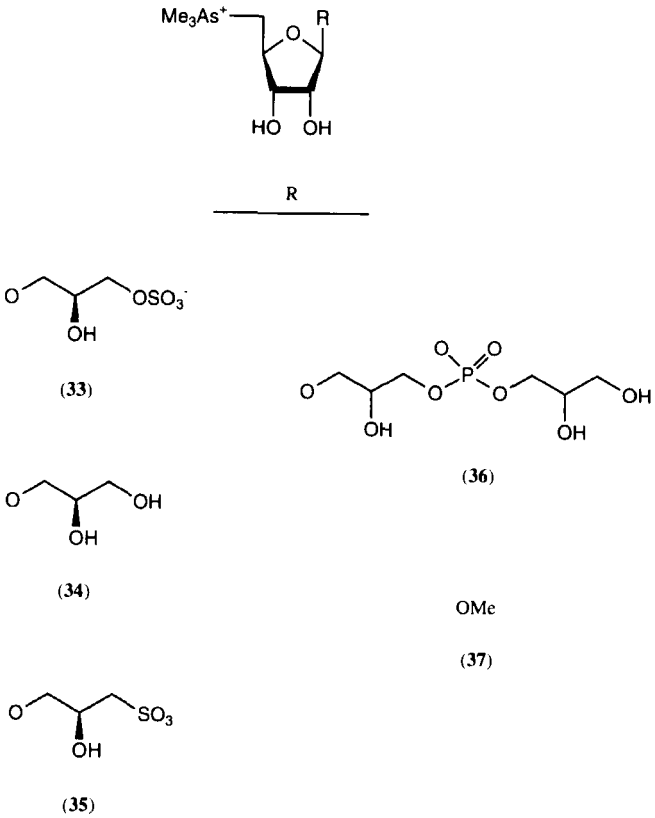

FIG. 5. Structures of trimethylarsonioribosides. Compound **33** is, thus far, the only trimethylarsonioriboside identified as a marine natural product.

The NMR signals for the groups attached to arsenic are distinctive for the di- and trimethylated arsenosugars. The methyl groups in the dimethylarsinoylribosides give two characteristic singlets at about δ 1.86 and δ 1.89, the one exception being the nucleoside **25** with signals at δ 1.69 and δ 1.70 (*63*). The methyl groups in the trimethylarsonio compounds, however, give a sharp singlet at δ 1.99–2.01 (*65*). Thus, NMR spectroscopy may be suitable for studying biotransformations of arsenosugars, particularly those processes involving methylation.

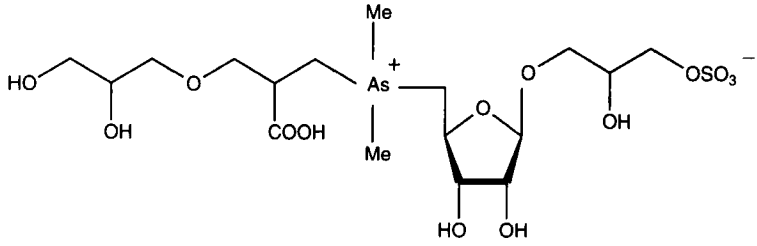

(38)

E. Other Arsenic-Containing Compounds

Several other arsenic compounds with possible significance in marine arsenic chemistry have been synthesized. Dimethylarsinoylethanol (DMAE) **39** was prepared by treating bis(dimethylarsenic) oxide, generated from iododimethylarsine, with 2-bromoethanol (*66*). Dimethylarsinoylacetic acid **40** was similarly prepared, but in low yield, from bis(dimethylarsenic) oxide and sodium chloroacetate (*66*). In solution, **40** exists as the zwitterion $Me_2As^+(OH)CH_2COO^-$, as shown by the ^1H NMR spectrum, which registered the singlet for the methyl groups at δ 2.21, well downfield compared with the equivalent groups in other arsine oxides (*54*). For the ammonium salt of **40**, the methyl groups resonate at δ 1.87. Similar effects resulting from the protonation of the arsine oxide moiety in the arsenosugar **13** have also been observed (*56*). Dimethylarsinothioylethanol **41** was formed by bubbling H_2S through an aqueous solution of the oxide **39** (*67*).

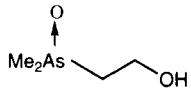

(39)

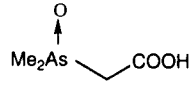

(40)

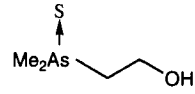

(41)

The betaines trimethylarsoniopropionate **42** and trimethylarsoniobutyrate **43** have been prepared by heating trimethylarsine in a sealed tube with 3-bromoproprionic acid or 4-bromobutyric acid, respectively (*68*). Glycerophospho(arsenocholine) (GPAC) **44** was prepared by treating phenylphosphoryl dichloride with 1,2-*O*-isopropylideneglycerol, followed by arsenocholine, and removal of the protecting groups (*69*). The compound GPAC has also been obtained from marine samples following basic hydrolysis of the lipids, presumably from deacylation of phosphatidylarsenocholine **45** (*70*). Finally, the naturally occurring taurine derivative **46** was synthesized by treating 4-dimethylarsinoylbutanoic acid, prepared from ethyl-4-bromobutanoate and dimethylarsinosodium, with taurine in the presence of ethyl chloroformate (*63*).

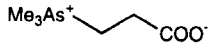

(42)

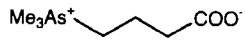

(43)

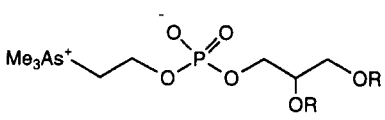

(44) R=H

(45) R=$CO(CH_2)_nMe$

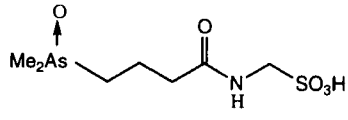

(46)

IV. Occurrence and Distribution of Arsenic Compounds in Marine Samples

A. Seawater and Sediments/Porewater

Thermodynamic considerations suggest that in oxygenated seawater, arsenic should exist almost entirely as arsenate (*71*). It was apparent from the early work on arsenic in seawater, however, that arsenite was also present in significant concentrations and could at times predominate over arsenate (*7, 8, 72, 73*). Marine bacteria (*74*) and marine phytoplankton (*75*) were shown to reduce arsenate to arsenite, thereby providing an explanation for the observed As(III)/As(V) ratio in seawater. The compounds MMA and DMA also occur in seawater, generally as minor constituents (*9, 34, 71, 76*). The concentrations of As(III), MMA, and DMA are positively correlated with primary productivity,

indicating that algae are important in the transformation of As(V) in seawater (*9, 71*). Andreae (*71*) proposed that phytoplankton were involved in the uptake of arsenate and its release to seawater as As(III), MMA, and DMA; a sharp rise in the concentration of arsenate at the base of the photic zone suggested rapid regeneration of this species by demethylation and oxidation.

Further work in this area has shown large changes in arsenic speciation depending on season and biological activity in the water column (*10, 77–79*). Although As(III), As(V), MMA, and DMA are the only species to be identified in seawater to date, additional arsenic, unaccounted for by those species, has also been reported (*80*). The analytical method for determining arsenic species in seawater involves the generation of volatile arsines, and is thus restricted to analysis of those species forming suitable analytes. Arsenic compounds such as TeMA, arsenobetaine, arsenocholine, and arsenosugars would not be detected by such analytical systems. These compounds and others are, however, decomposed to As(V) by UV irradiation (*81*). When coastal seawater was analyzed before and after UV irradiation, there was an average 25% increase in the amount of arsenic detected as arsines (*80*). This so-called "hidden" arsenic was believed to be derived from compounds related to arsenosugars, although no firm evidence was provided to support that view. Arsenic other than that accounted for by arsine-forming species constituted about 20% of the total arsenic in the waters of the lower Tagus estuary (*82, 83*). On that occasion some of the arsenic remained refractory after treatment with NaOH; arsenosugars and arsenobetaine (but not arsenocholine and TeMA) would be decomposed by such treatment.

Only limited information has so far been obtained from examination of the arsenic-containing compounds in sediments, primarily because the arsenic is bound in such a way that the reagents commonly used for sediment extraction are likely to change the form of arsenic originally present (*33*). Milder extracting agents are required, but little work has been done in this area. Rather, work has focused on the arsenic compounds in the porewaters (interstitial waters) of the sediments. Both As(III) and As(V) occurred in the porewaters of sediments from the northeast Pacific, but methylated arsenic compounds were not detected (*71*). However, MMA and DMA constituted 1–4% of the total arsenic in porewaters of the Tamar estuary (*84*). These two methylated species in addition to TMAO were detected in all samples from 10 stations off British Columbia (*41*). Again, the methylated forms were minor constituents, representing <10% of the total dissolved arsenic. There was a strong positive correlation between the methylated arsenicals

and total dissolved arsenic, suggesting that microbial methylation may be taking place *in situ*. The possibility remains, however, that the methylated arsenic compounds represent degradation products from biological material in the sediments.

The total dissolved arsenic concentrations for the stations off British Columbia were 3–52 μg/liter (*41*), consistent with results for fjord porewaters (*42*) and estuarine porewaters (*84*). These results, however, rely on analytical techniques that would not detect the "hidden" or refractory arsenic levels reported earlier as occurring in seawater, and the true values may be slightly higher than those reported. The identity of the hidden and refractory arsenic remains unknown; possible candidates include arsenosugars, TeMA, arsenobetaine, and arsenocholine.

Clearly there is much to be learned from further examination of arsenic levels in seawater and porewaters. However, low concentrations and analytical difficulties presented by the salt matrix continue to complicate these analyses (*33*, *85*). Techniques such as HPLC/ICP-MS suffer from interference by the molecular ion $^{40}Ar^{35}Cl^{+}$, formed by combination of the plasma gas and chloride ion, with the monoisotopic $^{75}As^{+}$. Techniques to separate the arsenic compounds from the salt matrix before HPLC/ICP-MS have not been fully investigated because they may result in fractionation of the compounds and loss of speciation information. Nevertheless, methods to establish the presence or otherwise in seawater of some of the arsenic-containing compounds important in other marine compartments is worth pursuing.

B. Marine Algae

Although Jones (*4*) first reported that marine algae contained appreciable levels of organoarsenic in 1922, the structures of the compounds were not established until 1981, when the two novel arsenosugars **10** and **13** were isolated and identified from the brown macroalga *Ecklonia radiata* (*55*). A repeat extraction of *E. radiata* produced the related compound **15** (*87*). Expansion of the work to other species of brown algae and other algal families has revealed a total of 15 arsenosugars (*88*). With only two exceptions (compounds **33** and **38**), the compounds are all dimethylarsinoylribosides differing only in the aglycone. The various aglycones represent common metabolites present in algae, although the relative abundance of the arsenosugars does not appear to reflect the abundance of the alcohol able to form the glycosidic bond. Mannitol, for example, is a common major constituent of marine algae (*89*), but the corresponding arsenic compound **21** is a trace constituent only (*57*).

The early work adopted a natural products approach and focused on the brown algae (Phaeophyta) primarily because of their high arsenic

concentrations. The brown alga *Sargassum lacerifolium* provides an example of this type of work, producing the most complex pattern of arsenic compounds so far with the isolation of eight arsenosugars and some DMA (*57*). Most of the arsenic compounds in *Sargassum* were present as minor or trace constituents, and 40 kg of fresh alga was extracted to ensure that adequate quantities of pure compounds were obtained for NMR spectroscopic analysis, or, in the case of the crystalline compound **19**, X-ray molecular structure determination. The availability of naturally occurring or synthetic arsenosugars for use as reference compounds, together with the application of HPLC with element-specific detectors, has led to the examination of many other algal species, particularly the red algae (Rhodophyta) and green algae (Chlorophyta). Table V provides information on all the arsenic com-

TABLE V

ARSENIC-CONTAINING COMPOUNDS FROM MARINE ALGAE

Type	Species	Arsenic concentration (mg/kg wet or dry wt. as shown)	% Water-soluble	Arsenic compounds[a]			Ref.
				Significant	Minor	Trace	
Brown	*Ecklonia radiata*	10 wet	>80	**10, 13, 15**	—	—	*55, 87*
	Hizikia fusiforme	10 wet	>80	**1, 17**	**10**	**15, 19**	*90*
	Laminaria japonica	4 wet	>80	**10, 11**	**13, 15**	—	*91*
	Sphaerotrichia divaricata	2 wet	75	**13**	**15, 10, 19**	—	*92*
	Undaria pinnatifida	2.8 wet	71	**16**[b]	—	—	*19, 93*
	Sargassum thunbergii	4 wet	51	**17**	—	**33**	*19, 64*
	Sargassum lacerifolium	40 wet	>80	**17**	**15, 10, 11, 13**	**19, 4, 20, 21, 38**	*57*
	Spathoglossum pacificum	16.3 dry	69	**10**	**13, 15**	—	*19*
	Pachydictyon coriaceum	16.7 dry	72	**10**	**13, 15**	—	*19*
Green	*Codium fragile*	0.6 wet	67	**13**	**15, 4**	—	*19, 94*
	Ulva pertusa	17.1 dry	40	**13**	**15**	u	*19*
	Bryopsis maxima	19.4 dry	20	**15**	**13**	u	*19*
	Caulerpa brachypus	11.6 dry	32	u	—	—	*19*
Red	*Corallina pilulifera*	21.6 dry	15	**15**	**13, u**	—	*19*
	Cyrtymenia sparsa	44.8 dry	69	**15**	**13**	—	*19*
	Ahnfeltia paradoxa	11.7 dry	58	**15, u**	**13, 17**	—	*19*
	Coeloseira pacifica	23.1 dry	35	**15, u**	**13**	—	*19*
	Laurencia okamurai	19.2 dry	47	**13, 17**	**15, u**	—	*19*

[a] Significant, ≥20% of total water-soluble arsenic; minor, 1–19% of total water-soluble arsenic; trace, <1% of total water-soluble arsenic; u, unknown.

[b] Lipid arsenic.

pounds isolated from algae in addition to presenting a selection of the large body of data where identification has been achieved with HPLC and comparison with reference compounds (*19*).

Some general trends in the data are apparent. For Rhodophyta and Chlorophyta, the arsenosugars with the glycerol (**13**) and phosphoric acid diester (**15**) aglycones predominate, while the sulfonic acid **10** and the sulfuric acid ester **17** are generally minor constituents. In Phaeophyta, however, arsenosugars **10** or **17** are the major arsenic compounds. There also appear to be differences between orders of Phaeophyta: the sulfonic acid **10** is the major compound in the three species of the order Laminariales so far examined, whereas the sulfuric acid ester **17** predominates in the three representatives of the order Fucales (*95*). Thus, arsenosugars may have chemotaxonomic significance. In this regard, and perhaps more important, these compounds may prove to be useful as highly specific food chain tracers in marine biological studies.

The precise chemical structures of the arsenic constituents of unicellular algae have been less well studied. A natural products approach was not feasible when dealing with unicellular algae because of the difficulties in getting sufficient quantities of material. Instead, radiolabeling experiments were carried out to determine the identity of the arsenic compounds (*39, 96*). Progress in this area was hindered when early work assigned incorrect structures to the major arsenic compounds in *Chaetoceros concavicornis*. Those early results have been reinterpreted, and it is now accepted that unicellular algae contain the same arsenosugars as found in macroalgae (*97*). Later work has confirmed the arsenosugar **17** as the major arsenical in the unicellular alga *Chaetoceros concavicornis* when grown in culture (*98*). Although it appears probable that arsenosugars are widespread in unicellular algae, it should be noted that the unicellular alga *Polyphysa peniculus* does not produce detectable quantities of arsenosugars in culture experiments (*99*).

Lipid-soluble arsenic also occurs in algae, often as a major constituent. Early studies showed that the lipid-soluble and water-soluble arsenic compounds are related (see Section VI,B). Identification of the glycerophospho compound **15** in algae (*87*) suggested that the lipid-soluble arsenicals might be phospholipids, and this was subsequently shown to be the case when compound **16** was isolated and identified from the brown alga *Undaria pinnatifida* (*93*). It seems likely that other lipid arsenic compounds found in marine algae are also acylated, perhaps monoacylated (*39*), derivatives of arsenosugar **15**, although derivatives of **38** are also possible.

Although inorganic arsenic is usually a minor component of algae, two species of brown algae, *Sargassum muticum* and *Hizikia fusiforme*, have been found to contain appreciable quantities of inorganic arsenic, representing 38 to 61% of the total (*100–102*). Extraction of arsenic compounds from algae is usually carried out with water, methanol, chloroform, or mixtures of these solvents. Only a small proportion of the total arsenic remains in the insoluble residue following extraction with these solvents.

The arsenic constituents of marine algae have been the subject of several detailed studies over the past 15 years. It is of interest that arsenobetaine, arsenocholine, TMAO, and TeMA are yet to be detected in marine algae.

C. Marine Animals

Arsenobetaine was the first arsenic compound identified in a marine animal when it was isolated in 1977 in a crystalline form from the tail muscle of the western rock lobster *Panulirus cygnus* (*48*). The large body of work that followed established that arsenobetaine was by far the predominant form of arsenic in marine animals (Table VI). It occurs at all trophic levels, although there is a tendency for it to be present at higher concentrations (or at least constitute the greater percentage

TABLE VI

Arsenobetaine in Marine Animals[a]

Animal (no. of species)	Arsenic concentration[b] (mg/kg, wet wt.)	Arsenobetaine content[b] (% of total arsenic)
Fish		
Elasmobranchs (7)	3.1–44.3	≥94
Teleosts (17)	0.1–166	48 to >95
Crustaceans		
Lobsters (4)	4.7–26	77 to >95
Prawns (5)	5.5–20.8	55 to >95
Crabs (6)	3.5–8.6	79 to >95
Molluscs		
Bivalves (4)	0.7–2.8	44–88
Gastropods (6)	3.1–116.5	58 to >95
Cephalopods (3)	49	72 to >95

[a] Ref. *88*.

[b] Values refer to muscle tissue only.

of total arsenic) in the higher-trophic-level animals. The ubiquity of arsenobetaine in the marine animal kingdom has been highlighted by recent work identifying arsenobetaine in shrimp and mussels from hydrothermal vent communities living at depths of more than 3000 m in the region of the Mid-Atlantic Ridge (*103*).

The initial studies determining the chemical forms of arsenic in marine animals were carried out on crustaceans and fish; they failed to detect any arsenic compounds other than arsenobetaine. Examination of other marine animals, however, revealed the presence of considerable quantities of unidentified arsenic in addition to arsenobetaine (*28*) and led to the identification of TeMA in the clam *Meretrix lusoria* (*104*). The distribution of TeMA varied considerably among the various tissues of *M. lusoria*. The gill contained the highest concentrations, suggesting that it was an important site for arsenic metabolism involving TeMA. TeMA was subsequently shown to be widespread among marine animals (*40, 105–108*), particularly in bivalve molluscs where it can replace arsenobetaine as the major arsenic compound (*108*).

Arsenosugars also occur in some marine animals where they are probably derived from ingested algal metabolites (*58, 63, 70, 106*). They have also been recently reported in mussels from a hydrothermal vent community where algal metabolites are unlikely to be significant (*103*). The presence of these compounds in high concentrations in the kidney of the clam *Tridacna maxima* resulted from the accumulation of arsenic compounds elaborated by unicellular algae growing in the mantle of the clam (*58, 63*).

Inorganic arsenic is a minor component in marine animals, generally constituting less than 2% of the total arsenic (*109*).

The application of high-sensitivity ICP-MS detectors coupled to HPLC has enabled the detection of trace arsenic compounds present in marine animals. Thus, arsenocholine has been reported as a trace constituent (<0.1% of the total arsenic) in fish, molluscs, and crustaceans (*37*) and was found to be present in appreciable quantities (up to 15%) in some tissues of a marine turtle (*110*). Earlier reports (*46, 47*) of appreciable concentrations of arsenocholine in some marine animals appear to have been in error (*32*). Phosphatidylarsenocholine **45** was identified as a trace constituent of lobster digestive gland following hydrolysis of the lipids and detection of GPAC in the hydrolysate by HPLC/ICP-MS analysis (*70*). It might result from the substitution of choline with arsenocholine in enzyme systems for the biogenesis of phosphatidylcholine (*111*).

TMAO has been detected in fish (*37, 112, 113*), molluscs (*37, 108*), and crustaceans (*37*). It may occur from microbial decomposition of

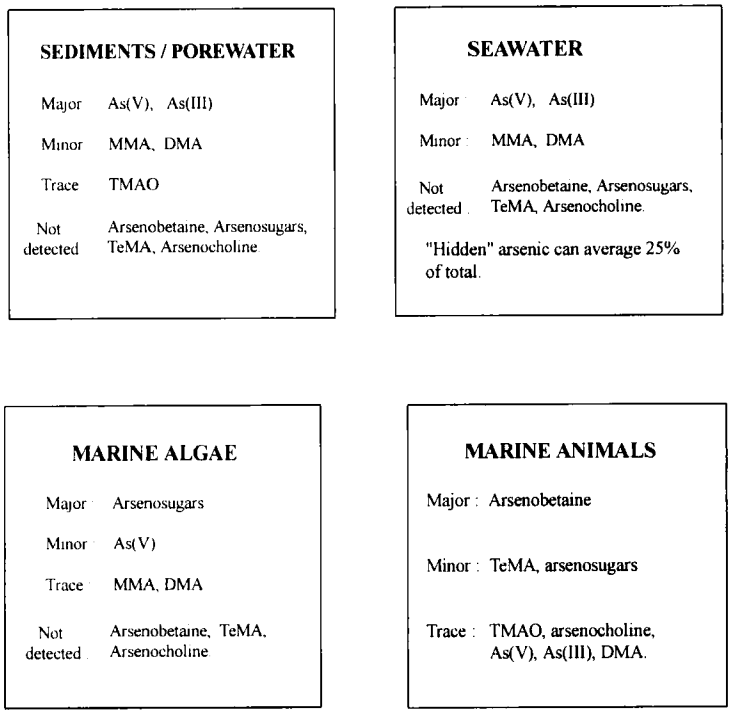

FIG. 6. Arsenicals in the various marine compartments.

arsenobetaine (*113*, *114*) or from microbial methylation of arsenate by the gut flora of the animals (*112*). Traces of trimethylarsine have been reported in six species of prawns and two species of lobster (*115*), where it was thought to arise from microbial methylation of arsenate within the animals' digestive glands.

The distribution of the chemical forms of arsenic in the various marine compartments is summarized in Fig. 6.

V. Toxicological Considerations

Toxicological issues fall into two quite distinct areas: first, human health concerns resulting from consumption of arsenic compounds in seafood, and second, ecological concerns arising from the effects of these compounds on marine organisms.

Since the early work in the 1920s (*4–6*), it had been accepted that arsenic in marine organisms was organic and nontoxic. This appeared

to be a reasonable assumption in the absence of any data whatsoever that ingestion of marine arsenic was detrimental to human health. Animal studies had long established that so-called shrimp arsenic was nontoxic to rats and rapidly excreted in the urine (*116*). The confidence placed in these early studies was shaken in the late 1960s when it was discovered that naturally acquired mercury in fish was present in an organic form as the potentially toxic methylmercury species. The view that arsenic in marine animals was of no toxicological concern because it was natural and organic clearly required reassessment.

Consequently, there was renewed interest in marine arsenic research, and several groups worked in this area during the 1970s. Not surprisingly, they were from countries such as Japan and Australia and those in Scandinavia, where seafood is either widely consumed or is an important export commodity. The research activity resulted in the identification of arsenobetaine and the range of other arsenic compounds reported in Section IV.

Synthesis of arsenobetaine allowed detailed toxicological assessment, which rigorously established the nontoxic nature of this common seafood constituent (*117–119*). Toxicological studies of other arsenic compounds have yet to be conducted. In particular, TeMA requires assessment; it is widespread in marine animals and its nitrogen analogue, tetramine, is a known toxin (*120*). The toxicology of the arsenosugars currently available by synthesis also needs to be determined. In some countries, many of those in east Asia, for example, algae are common components of the human diet.

Although the intake of inorganic arsenic from seafood is low, it may also require reassessment in the face of growing evidence that it acts as a carcinogen with no threshold value (*121*). In that regard, the old literature on the arsenic eaters of Styria provides interesting reading with claims of bright complexion and general healthy and strong appearance among individuals consuming arsenous oxide on a regular basis (*122, 123*).

Aquatic toxicological studies of inorganic arsenic have been reported for fish, crustaceans, molluscs, echinoderms, and algae (*124*). Generally, the data indicate low to moderate toxicity, with marine animals, including larval stages, not acutely affected by arsenic levels below 200 μg/liter. The results for algae are more variable, with some species growing well in seawater containing arsenic at up to 10,000 μg/liter (*125*)—testimony to an efficient detoxification mechanism. Relatively low levels of arsenate (1 to 10× ambient concentration), however, can inhibit some phytoplankton species in mixed natural assemblages, leading to marked changes in species composition (*126*). Ecotoxicologi-

cal effects of arsenic at different trophic levels have been little studied. Presumably, the assimilative capacity of marine waters receiving arsenic contamination would depend largely on the presence of suitable algal species able to transform the arsenic to less toxic forms.

VI. Biotransformation of Marine Arsenic Compounds

A. Microbiological Transformations

The classic studies by Challenger (*127–129*) on microbial methylation of arsenic still provide the basis of our understanding of these processes. Although Challenger's work focused on mycological methylations (he mistakenly believed that bacteria did not methylate arsenic), the scheme he proposed is applicable to other biological systems as well. It is briefly discussed here, together with the confirmatory studies of Cullen and co-workers.

According to Challenger (*127*), arsenate is transformed to trimethylarsine by the mold *Scopulariopsis brevicaulis*, by sequential reduction and oxidative methylation of the arsenic species (Fig. 7). The proposed intermediates in the pathway were MMA, DMA, and TMAO. Although Challenger could not detect these compounds, when they were added to a culture of *S. brevicaulis* trimethylarsine was formed. Challenger (*129*) considered that the likely source of methyl groups was *S*-adenosylmethionine (AdoMet), which had previously been identified as an

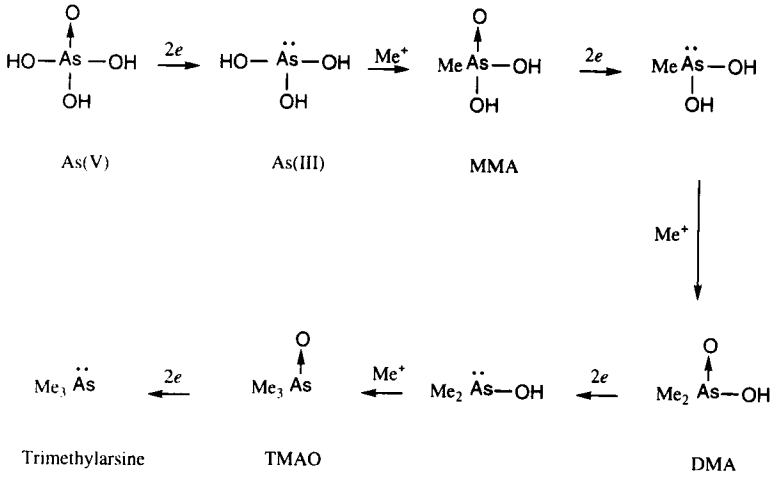

FIG. 7. Challenger's pathway for the methylation of arsenic by microorganisms.

active methyl donor in enzymatic systems (*130, 131*). The proposal that AdoMet is the source of Me^+ in mycological methylation of arsenic was strongly supported by the later work of Cullen and co-workers (*132*).

The source of the electrons in the reduction of arsenic outlined in Fig. 7 is not known, but a sound model involving reduction by thiols has been proposed (*133*). A reexamination of Challenger's proposed methylation pathway looked at the effects of adding low levels of As(III), As(V), MMA, and DMA to cultures of two microorganisms including *S. brevicaulis* (*134*). By the use of sensitive analytical methodology involving arsine generation, the arsenic intermediates proposed in Fig. 7 were identified in the growth medium. A significant result was the detection of TMAO, rather than trimethylarsine, as the major methylation product. The low concentrations of arsenic employed in these experiments resulted in TMAO being present at less than toxic concentrations, and further detoxification by reducing TMAO to the arsine was considered unnecessary. Whether or not TeMA was produced in these experiments is not known; its presence was not reported, but it would not have been detected by the analytical technique used.

Bacterial methylation of arsenate by a methanogen was first reported by McBride and Wolfe (*135*) in 1971, and reports of nonmethanogenic bacterial methylation followed. These transformations are now known to be effected by a range of bacteria, and the mechanisms are likely to be similar to those proposed for fungi (*32*).

Transformations of arsenic by marine microorganisms have been shown to occur, but have not been the subject of detailed mechanistic studies. Bacteria in seawater can reduce arsenate to arsenite (*74*). This process of reduction might provide energy for microbial growth; a microorganism isolated from freshwater sediments was recently reported to derive energy for growth by reducing arsenate to arsenite (*136*). When exposed to arsenate, bacteria can produce MMA in addition to As(III), while a marine yeast was shown to produce As(III), MMA, and DMA (*137*). Microorganisms also mediate demethylation and oxidation of methylated arsenic compounds in seawater (*138, 139*), and the marine pseudomonad readily reduces TMAO to trimethylarsine (*140*). Thus, in marine systems microbial activity effects interconversions of arsenic among As(III), As(V), and the simple methylated forms.

Hanaoka and co-workers (*141*) have reported several experiments describing the microbial degradation of arsenobetaine. Unspecified microorganisms derived from sediments, algae, mollusc intestine, or suspended sediments were incubated with arsenobetaine under various conditions. Arsenobetaine was degraded to TMAO and DMA in all cases and, for sediments and suspended sediments, further degradation

to As(V) was observed. A similar degradation to TMAO was observed in seawater during arsenobetaine uptake experiments with mussels of the species *Mytilus edulis* (*85*). Microorganisms in the seawater were thought to be involved, although this was not proved. TeMA appeared to be unaffected by these conditions.

Cullen and Nelson (*142*) reported an interesting study on microbial transformations in seawater by employing mussels as arsenic bioaccumulators. Thus, *M. edulis* were maintained for four days in seawater containing [^{3}H]MMA or [^{3}H]DMA. The arsenic compounds in the seawater and mussels were then examined by HPLC and measurements of the ^{3}H activity in the fractions. Chromatograms were compared with those for arsenic standards detected by atomic absorption spectrometry. The ^{3}H-labeled arsenobetaine was found in mussels kept in either [^{3}H]MMA or [^{3}H]DMA, with the latter being more readily transformed. The [^{3}H]arsenobetaine was also detected in the seawater, and the quantities *increased* in the absence of the mussels, indicating that arsenobetaine was being biosynthesized by microorganisms in the seawater and bioaccumulated by the mussels. A similar study with *M. californianus* and [^{3}H]MMA produced essentially the same result, although on that occasion two unkown compounds were also detected (*143*). These studies would seem to provide the answer to the origin of arsenobetaine in marine animals. It would be relevant to know, however, if TMAO was produced by the microorganisms, as it might be thought a more likely product of this system than arsenobetaine. No mention is made of TMAO, yet the chromatographic properties used to identify the major product as arsenobetaine also appear to fit TMAO.

Microbial transformations occuring in sediments have been studied under laboratory conditions designed to mimic natural marine systems. When the brown alga *Ecklonia radiata* was incubated under anaerobic conditions with seawater and sediment, its naturally occurring dimethylarsinoylribosides were transformed to DMAE in virtually quantitative yield (*66*). Similar experiments with pure dimethylarsinoylriboside **10** produced identical results (*144*). This conversion was thought to occur by cleavage of the C3—C4 bond of the sugar residue as shown in Fig. 8a. A modification of this experiment recorded the transformation of DMAE as it moved through anaerobic sediments into oxygenated seawater (*54*). DMAE was partly converted to the sulfide **41** in the sediments, presumably chemically by H_2S formed *in situ* by the action of sulfate-reducing bacteria on the porewater sulfate. In the water column, both DMAE and the sulfide **41** were transformed to arsenate. The kinetics of this transformation indicated that it was microbially mediated with a change in the microbial population with time; DMAE

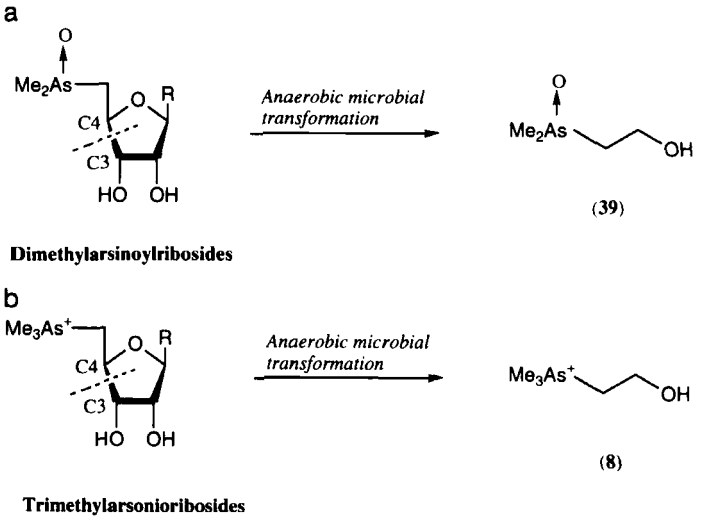

FIG. 8. Microbial transformation of (a) dimethylarsinoylribosides and (b) trimethylarsonioribosides.

and the sulfide **41** remained unchanged until day 14 of the experiment, after which time the compounds were rapidly transformed to arsenate.

When subjected to anaerobic microbial conditions, the trimethyarsonioriboside **33** was transformed quantitatively into arsenocholine, suggesting that cleavage of the C3—C4 bond of the sugar ring had occurred in an analogous manner to that observed for the dimethylarsinoylribosides (Fig. 8b) (*145*).

B. TRANSFORMATION BY ALGAE

As mentioned in Section II, arsenate is present in seawater at a fairly uniform concentration (about 0.5–2 μg As/liter), and in nutrient-deficient waters its concentrations may exceed that of the essential phosphate (*146*). In oxygenated seawater, the species exist predominantly as $H_2PO_4^-$ and $H_2AsO_4^-$, and algae may absorb arsenate because it is similar to the phosphate anion (*147*). In terrestrial plants and other organisms, arsenic is taken up by the phosphate transport mechanism (*148*), but the situation with algae is less clear, with several apparently conflicting reports in the literature. For example, although arsenate and phosphate were shown to compete for uptake by unicellular algae (*149*), a related study with two species of brown macroalgae could provide no evidence for a common uptake mechanism (*150*). In one study with unicellular algae at low phosphate levels, arsenate uptake

increased with increasing phosphate concentrations, presumably as a consequence of increased algal metabolism (*151*). In a study of several natural algal populations in Southampton water, arsenate was readily assimilated by the algae even though phosphate concentrations remained high, indicating that arsenate uptake was not contingent upon phosphate depletion (*152*). Although additional detailed work is required, it seems likely that more than one mechanism is involved in arsenic uptake by algae (*151*).

On being assimilated by the alga, by whatever mechanism, arsenate can produce toxic effects including inhibition of growth and phosphorus metabolism, and changes in algal cell morphology (*153, 154*). Possibly, algae biotransform the arsenate to which they are exposed, and have inadvertently absorbed, as a process of detoxification. The transformations or detoxification processes taking place when algae are exposed to arsenic in seawater have been the subject of several radiolabeling studies using ^{74}As arsenate (*39, 96, 125, 155, 156*). The studies were conducted with varying degrees of complexity, but produced essentially the same results; one of them, the study of Klumpp and Peterson (*156*), is discussed here in more detail.

The brown macroalga *Fucus spiralis* was exposed to ^{74}As arsenate and the bioaccumulation and transformation of arsenic was monitored over time with electrophoretic and chromatographic techniques. After exposure for 5 min, arsenate predominated in the alga; two major water-soluble organoarsenic compounds (W1 and W2) were also present, along with a small amount of lipid arsenic. Over time the arsenate concentrations decreased, with concomitant increases in the levels of W1, W2, and lipid arsenic. The lipid arsenic continued to increase during the experiment and had stabilized at 60% of the total label after 16 hr. Chemical treatment (methanolic KOH) of the lipid arsenic or W2 produced W1. Although the chemical structures of the arsenic compounds were not identified (the study was essentially biological), it was clear that arsenic was being taken up by the alga as arsenate and transformed into water-soluble organoarsenic compounds, which were then further transformed into a lipid-soluble organoarsenic compound. From the subsequent large number of chemical studies on algae (see Section IV,B), it would appear that W1, W2, and the lipid arsenic are well accommodated by the arsenosugars **13, 15,** and **16,** respectively.

The later observation of Morita and Shibata (*19*) is relevant here. They examined the distribution of the various arsenic compounds in *Hizikia fusiforme* (this alga is unusual in that it contains about 50% of its total arsenic as arsenate). The total arsenic concentrations were higher at the surface layers than in the center of the alga. Arsenate

was located only at the surface of the alga, whereas the arsenosugars were distributed evenly throughout. A process of transformation following adventitious uptake of arsenate is accommodated by these results.

Although it is apparent that algae transform their assimilated arsenate into arsenosugars, the precise mechanisms involved remain to be elucidated. A pathway for the biogenesis of arsenosugars has been proposed, however, based on Challenger's pathway for mycological methylation of arsenate. Whereas in Challenger's pathway, *S*-adenosylmethionine provides the methyl groups to arsenic leading to trimethylarsine, in algae, AdoMet is proposed as the donor of the methyl groups *and* the ribosyl moiety (Fig. 9). Thus, following the addition of two methyl groups to arsenic, AdoMet transfers its adenosyl group, forming the proposed intermediate **25**, which on glycosidation with one or other of the common algal metabolites produces the range of arsenosugars observed in algae.

The key intermediate in this proposed pathway is the arsenic-containing nucleoside **25**. The isolation of **25** from *Tridacna* kidney (the

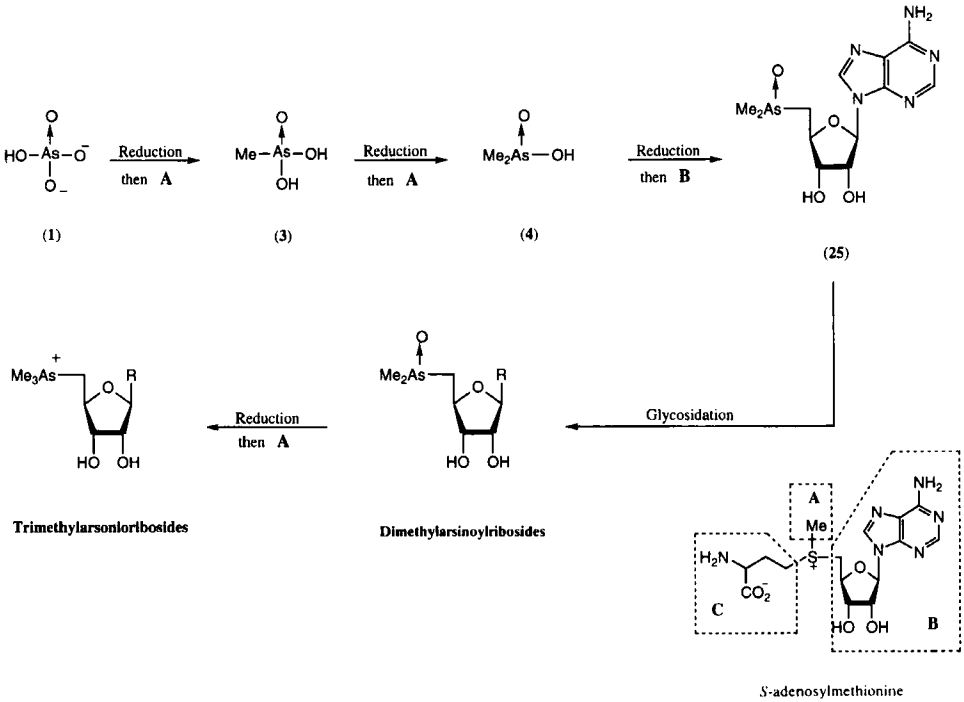

FIG. 9. Proposed pathway for the biogenesis of arsenosugars from arsenate (**1**). All proposed intermediates are marine natural products.

kidney accumulates products from *Tridacna*'s symbiotic alga growing in the mantle) has provided considerable support for the pathway (*63*). The C—S bonds for the three alkyl groups in AdoMet (groups A, B, and C in Fig. 9) are chemically equivalent, and the transfer of the other alkyl groups from AdoMet to a suitable receptor had been predicted by Cantoni (*157*). The transfer of the four-carbon group (group C, the 3-amino-3-carboxypropyl moiety) of AdoMet to a nucleophilic nitrogen species has also been observed (*158*). Possibly, the biogenesis of the taurine derivative **46** also involves donation of the four-carbon alkyl group of AdoMet (*63*).

Although the order of methylation and adenosylation proposed in Fig. 9 appears reasonable, the adenosylation step may precede the methylation step(s). Compounds with structures consistent with that order of alkylation have not been identified, whereas both MMA and DMA occur in algae. Other compounds resulting from methylation only, namely TMAO and TeMA, have not been identified in algae, but they may be present at low, currently undetectable, levels. TeMA is a significant, often major, form of arsenic in algal-feeding bivalve molluscs (*108*). An expansion of the early radiolabeling studies on arsenic transformations by algae carried out in the light of current knowledge of the precise chemical structures involved would be most informative.

The major compounds in marine algae are the dimethylarsinoylribosides (trialkylarsine oxides); the trimethylarsonioribosides (tetraalkyl compounds) are trace constituents (<1%). Hence, the process of alkylation of arsenic by algae essentially stops at the trialkyl stage. Chemically, the addition of the fourth alkyl group is a facile process; tertiary arsines generated from dimethylarsinoylribosides by reduction with a thiol are readily methylated by methyl iodide to give the tetraalkyl compounds (see Section III,D). It is interesting to speculate that the arsenosugars may serve a biochemical function in algae that depends on their being trialkylarsine oxides. These compounds are readily reduced to their respective arsines and can be regenerated under mild oxidizing conditions. Such conversions may take place within algal cells, allowing dimethylarsinoylribosides to participate in cellular redox reactions.

Tetraalkylated arsenic compounds have not been observed as metabolites of arsenate detoxification in the many experimental studies conducted with organisms including fungi, bacteria, fish, and mammals (*112, 127, 159*). Although, for some of the studies at least, the methods of detection may not have been suitable for determining such metabolites, their apparent universal absence in experimental systems suggests a fundamental difficulty in adding the final alkyl group by purely biological processes.

C. Transformations within Marine Animals

In metabolic studies with animals it is often difficult to distinguish between processes carried out by the animal and those performed by resident microorganisms, such as the gut microflora. In the following, the transformations refer to those taking place within the marine animal, whether microbially mediated or otherwise. Metabolic studies with marine animals are faced with further complications because water can be an important uptake route. A chemical, in this instance arsenic in its various forms, may undergo microbial conversions in the water, and the resultant metabolites may be accumulated by the marine animal. Thus, careful experimentation may be required to determine what is occurring inside rather than outside the animal.

1. Uptake from Water

Most of the studies on the uptake and transformation of arsenic in water have dealt with arsenate: it is the predominant arsenic component in seawater, and radiolabeling experiments are most easily carried out with this chemical species. Generally, the results have shown that uptake of arsenate from water is a slow process and is unlikely to be significant in natural environments (*160–163*).

The study of Klumpp and Peterson (*156*), however, remains of interest. When two species of gastropod were exposed to ^{74}As-labeled arsenate, they accumulated a single cationic organoarsenic product. The arsenic compound was not identified, but comparison with available standards established that it was not arsenobetaine or arsenocholine. Although TeMA was not used as a standard in that study, the reported properties of the unknown are at least consistent with that assignment. The mussel *Mytilus edulis*, however, did not accumulate arsenic when maintained in seawater containing elevated levels of arsenate or arsenite (*85*). Unlike the studies employing ^{74}As, however, transformations of trace amounts of arsenate would not have been detected in this study.

Uptake experiments have also been conducted with other forms of arsenic. *M. edulis* exposed separately to a number of organoarsenic compounds in seawater were found to be selective in their arsenic uptake (*85*). They did not accumulate arsenic when it was present as MMA, DMA, TMAO, or DMAE. When exposed to the three quaternary arsonium compounds (arsenobetaine, arsenocholine, and TeMA), however, the mussels accumulated substantial quantities of arsenic, with arsenobetaine being the most efficiently accumulated (Table VII). The chemical form of the accumulated arsenic was also examined. Mussels

TABLE VII

UPTAKE OF ARSENIC COMPOUNDS BY MUSSELS

As compound	Bioaccumulation efficiency[a]
C-2 betaine (**7**) (arsenobetaine)	100
C-3 betaine (**42**)	65
Arsenocholine (**8**)	30
TeMA (**6**)	8
C-4 betaine (**43**)	6
Arsenate (**1**)	<2
Arsenite (**2**)	<2
MMA (**3**)	<2
DMA (**4**)	<2
TMAO (**5**)	<2
DMAE (**39**)	<2

[a] As a percentage relative to C-2 betaine (arsenobetaine).

exposed to arsenobetaine or TeMA accumulated the arsenic unchanged, whereas those exposed to arsenocholine accumulated most of the arsenic as arsenobetaine with about 5% present as GPAC. It could not be established that the conversion of arsenocholine to arsenobetaine was actually taking place within the animal, because arsenobetaine was also being formed in the water, presumably by microbial oxidation of arsenocholine. The presence of GPAC in the mussels, however, suggests that at least some arsenocholine was taken up and metabolized by the mussels. GPAC was not detected in the water.

It is of interest that arsenobetaine is accumulated so much more readily than other similar arsenic species. The cationic nature of the compounds may be significant; those compounds not bioaccumulated by the mussel are all anionic or neutral at seawater pH, whereas those accumulated all contain a positive charge. The zwitterionic nature of arsenobetaine may also be a factor, and recent experiments with C-3 and C-4 arsenic containing betaines (compounds **42** and **43**) support this view. Preliminary results (*164*) show that mussels bioaccumulate these compounds readily; the relative bioaccumulation efficiency was C-2 betaine (arsenobetaine) 100, C-3 betaine 65, and C-4 betaine 6 (Table VII). These results also suggest that the distance between the charges in the molecules may be an additional factor. Expansion of studies on arsenic uptake from water may elucidate the actual processes of absorption of arsenobetaine, which may involve a specific ion channel.

2. Uptake from Food

When arsenate is administered orally to fish, a small percentage of it is transformed into organoarsenic compounds. Penrose (*165*) showed that radiolabeled arsenate was converted to two unidentified organoarsenic products following oral administration to brown trout. In a similar experiment with rainbow trout, MMA and two unidentified arsenic compounds were formed (*166*). Experiments with catfish and whiting showed that ingested arsenate was methylated to TMAO and small quantities (<1% of administered dose) were accumulated in that form in the muscle tissue of the fish (*112*). The conversions were probably mediated by the microflora in the gut of these fish (*112, 166*). Arsenobetaine, the common native arsenical in fish, could not be detected in these experiments, indicating that it was not formed *de novo* from ingested arsenate.

Uptake of ingested organoarsenicals has also been investigated (*67*). Separate groups of yelloweye mullet were administered one of five organoarsenic compounds (**7**, **8**, **39**, **40**, **41**). Analysis of the arsenic concentrations in the fish and comparison with a control group showed that the three dimethylated compounds DMAE (**39**), **40**, and **41** were not accumulated by the fish (an accumulation of >0.1% would have been detected), whereas both arsenobetaine and arsenocholine were readily accumulated. Importantly, arsenocholine was rapidly transformed to arsenobetaine within the fish; minor metabolites were GPAC and phosphatidylarsenocholine **45**.

Transformations of organoarsenic compounds in short food chains have been studied using radiolabeling experiments. The assumptions made when interpreting the results of such biological studies, performed before the chemical structures of the arsenic compounds in algae were elucidated, have been previously discussed (*97*). In the study of Cooney and Benson (*167*), the unicellular alga *Dunaliella tertiolecta* was cultured in seawater containing ^{74}As-arsenate, and subsequently processed and fed to juvenile lobsters (*Homarus americanus*). The radiolabeled organoarsenic compounds, predominantly arsenosugars, contained in the alga were not substantially changed within the lobsters (some conversion from lipid-soluble to water-soluble forms was observed). Importantly, ^{74}As-arsenobetaine was not detected in the lobsters, even though all the naturally occurring arsenic in *H. americanus* is present as arsenobetaine (*168*). Thus, a direct link between arsenosugars occurring in algae and arsenobetaine occurring in animals could not be established.

A related study (*156*) beginning with ^{74}As-arsenate in seawater and employing similar techniques examined the short food chain

macroalga ⟶ herbivorous gastropod ⟶ carnivorous gastropod

In these experiments, ^{74}As-arsenobetaine was similarly not detected, again showing that conversion of arsenosugars to arsenobetaine was not taking place within the animals. Unlike the study with *Homarus*, however, a single unknown transformation product was observed in the gastropods.

Preliminary experiments in which HPLC/ICP-MS techniques have been used to monitor arsenic transformations within planktonic crustaceans feeding on a cultured unicellular alga containing arsenosugars at high concentrations have also been unable to demonstrate the production of arsenobetaine (*98*). Clearly there is much scope for work in this area.

3. *Uptake from Sediments*

Possible uptake of arsenic from sediments has been little studied. TMAO in estuary catfish is presumed to result from methylation within the fish of arsenate contained in surface sediments ingested as a consequence of the fish's foraging behavior (*112*). Benthic-feeding organisms generally contain high levels of arsenic, which might suggest that uptake from sediments is significant. A benthic organism, the polychaete *Tharyx marioni*, contained >2000 mg As/kg dry weight—the highest natural level of arsenic reported for a marine organism (*169*). Radiolabeling experiments suggested that the sediments were the source of arsenic for *T. marioni*. The chemical form of this arsenic remains unknown. The possibility exists that arsenobetaine or its precursors might be formed by microbial transformations occurring in sediments and accumulated by the benthic feeders.

VII. Origin of Arsenobetaine

It is now almost 20 years since arsenobetaine was first isolated and identified in a marine animal, and its presence has been recorded in the whole spectrum of marine animals including planktonic crustaceans, large ocean-roaming carnivorous sharks, and hydrothermal vent organisms occupying a tiny ecological niche thousands of meters below the sea surface. There has been, however, no substantiated pathway proposed for the formation and accumulation of arsenobetaine by marine animals. The role, if any, of this compound is also to be demonstrated, although its nitrogen analogue glycine betaine is widespread in marine organisms, where it is believed to protect cytoplasmic constit-

uents from water stress associated with a high-salt environment (*89*). Possibly, arsenobetaine behaves similarly and serves merely as an adventitiously acquired osmolyte.

Before considering possible biogenetic pathways for arsenobetaine, it may be worth offering some explanation for the apparent absence of arsenobetaine in marine algae, sediments, and seawater. A similar paradox initially faced those workers examining the origin of methylmercury in fish. In marine systems, mercury exists essentially in two chemical forms, namely inorganic mercury (Hg^{2+}) and methylmercury ($MeHg^{+}$). Methylmercury exists at trace levels only in sediments (usually <1% of total) and seawater (≪1% of total), and yet constitutes >90% of the total mercury in fish (*170, 171*). Other organisms can have intermediate percentages of methylmercury (*172*). Laboratory experimentation (e.g., *173*) with marine animals showed that methylmercury was more readily accumulated than inorganic mercury from water and food, and thus selective bioaccumulation offered an explanation for the observed mercury distribution in natural systems. A similar process may also apply for arsenic. For marine animals, however, the selectivity favoring accumulation of arsenobetaine over inorganic arsenic is much greater than that observed for methylmercury/inorganic mercury. Consequently, arsenobetaine may need to be present in seawater and sediments at only trace levels in order to account for its ubiquity and predominance in marine animals.

The structural similarity between arsenobetaine and glycine betaine suggested that arsenic may substitute for nitrogen in pathways of phospholipid biosynthesis and was the basis for a proposed biogenetic pathway for arsenobetaine (*174*). The proposed pathway begins with arsenic present as either arsenoethanolamine or arsenocholine. However, the origin of these two compounds is not discussed, and there has been no experimental evidence to support the hypothesis.

A possible pathway for the biogenesis of arsenobetaine became apparent following work showing that dimethylarsinoylribosides were the major arsenic compounds in algae. Although experimentation had shown that the arsenic compounds in algae (arsenosugars) were not transformed into arsenobetaine within marine animals (Section VI,C), later studies demonstrated that dimethylarsinoylribosides were readily degraded to DMAE (**39**) (Section VI,A) and offered an explanation for the origin of the two-carbon side chain in arsenobetaine. Further necessary steps involve methylation of arsenic and oxidation of the alcohol function, both of which were envisaged to occur readily in marine systems (Fig. 10). However, laboratory and related studies have been unable to substantiate the proposed role of DMAE in the formation

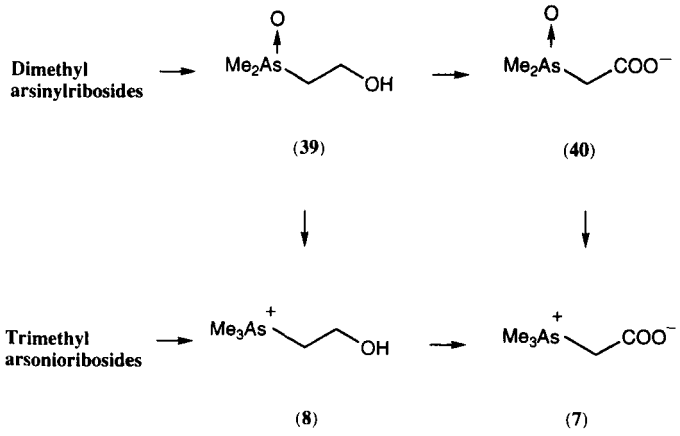

FIG. 10. Possible pathways for the biogenesis of arsenobetaine (**7**) from arsenosugars.

of arsenobetaine. In particular, DMAE is yet to be identified as a naturally occurring compound, and attempts to further methylate it in laboratory experiments designed to simulate marine systems have proved unsuccessful (*54, 67*). Mention should be made, however, of a recent report of the presence of trace amounts of dimethylarsinoylacetic acid (**40**), together with arsenosugars, in a mussel sample (*61*). If substantiated, this result would offer support for the involvement of DMAE, and hence dimethylarsinoylribosides, in the formation of arsenobetaine.

The identification of small quantities of the trimethylarsonioriboside **33** in algae (*64*) suggested a possible simpler route to arsenobetaine (Fig. 10). The pathway requires only cleavage of the C3—C4 bond in the riboside and oxidation of the resultant alcohol, arsenocholine. Both these processes have been demonstrated to occur, in virtually quantitative yield, in laboratory experiments under biological conditions expected to exist in natural marine systems (*67, 145*). The pathway from trimethylarsonioribosides does not depend on an additional, presently unknown, methylation process; all the carbons required for arsenobetaine have come from the trimethylarsonioriboside produced by the algae. So facile is the transformation of trimethylarsonioriboside **33** to arsenobetaine in the laboratory that it seems likely that trimethylated arsenosugars in algae are at least contributing to the levels of arsenobetaine found in marine animals. Estimates of how significant this contribution might be would need to consider that trimethylated arsenosugars are present as only trace constituents of algae (probably $<1\%$ of the total arsenic), but should also take into account the huge biomass of marine algae relative to that of marine animals.

It should be mentioned that although transformation of the arsenosugars has, so far, only been reported to occur in sediments under laboratory conditions, such processes might also take place in seawater. Transformations of mercury first observed in sediments were subsequently shown to occur in seawater as well (*171*), and the estimated production of methylmercury from these two compartments is comparable (*175*).

The work of Cullen and co-workers (*142, 143*) supports the earlier studies (*156, 167*) indicating that arsenosugars are not directly involved in the biogenesis of arsenobetaine. They showed that both MMA and DMA can serve as precursors to arsenobetaine, with the transformations carried out in the water column by microorganisms. The source of the carboxymethyl group in arsenobetaine was not specified, but the inference was that it did not originate from arsenosugars because algae were absent from the system. The arsenosugars might, however, still be the source of methylated arsenic, if not in the reported experiments, then at least in natural seawater where MMA and DMA are associated with algal productivity and may represent breakdown products of arsenosugars.

An assumption made in much of the foregoing is that arsenosugars are synthesized exclusively by algae. Recent work has shown that mussels from a deep-sea hydrothermal vent, an environment where primary productivity by algae plays no significant part, contain both arsenosugars and arsenobetaine (*103*). The observation suggests that arsenosugars may be synthesized by other organisms in addition to algae—for example, by chemolithoautotrophic bacteria in the hydrothermal vent environment. This is perhaps not unexpected when one considers the similarities in the pathways (and the methylating agent) proposed for arsenic methylation by fungi, bacteria, and algae. The presence of both arsenobetaine and arsenosugars in the one organism, particularly one from such an isolated and self-contained environment, might be taken as support for the view that arsenosugars are serving as precursors to arsenobetaine. Alternatively, arsenobetaine in these hydrothermal vent mussels and in marine animals from other environments may arise from a pathway independent of the presence of arsenosugars. In this regard, a report of the occurrence of arsenobetaine in mushrooms is highly significant (*176*). This is the first report of arsenobetaine occurring in a terrestrial organism, and there is no suggestion of the involvement of arsenosugars in this instance. Further work on terrestrial organisms may well provide answers to problems previously thought to be confined to the marine environment.

Clearly, much work is still required to elucidate the processes resulting in the accumulation of arsenobetaine in marine animals. The studies so far have focused on biological transformations, and abiotic processes have been little investigated. As mentioned previously, biological systems readily methylate arsenic to the trialkyl stage, but further alkylation affording tetraalkylarsonium species is rare. Possibly, the final alkylation step leading to arsenobetaine occurs abiotically in the water column or in sediments. Future studies should explore this possibility, but would first need to address analytical difficulties associated with determining low, but possibly significant, yields of arsenobetaine produced in a complex sample matrix.

REFERENCES

1. Bertrand, G. *C. R. Hebd. Seances Acad. Sci.* **1902,** *134,* 1434.
2. Gautier, A. *C. R. Hebd. Seances Acad. Sci.* **1903,** *137,* 232.
3. Tassilly, E.; Leroide, J. *Bull. Soc. Chim. France* **1911,** *9,* 63.
4. Jones, A. J. In "Year Book of Pharmacy, Transactions of the British Pharmaceutical Conference, July 24–28, 1992"; Hampshire, C. H., Ed.; J. and A. Churchill: London, 1922, p. 388.
5. Cox, H. E. *Analyst* **1925,** *50,* 3.
6. Chapman, A. C. *Analyst* **1926,** *51,* 548.
7. Atkins, W. R. G.; Wilson, E. G. *J. Mar. Biol. Assoc. U.K.* **1926,** *14,* 609.
8. Gorgy, S.; Rakestraw, N. W.; Fox, D. L. *J. Mar. Res.* **1948,** *7,* 22.
9. Andreae, M. O. *Deep-Sea Res.* **1978,** *25,* 391.
10. Santosa, S. J.; Wada., S.; Tanaka, S. *Appl. Organomet. Chem.* **1994,** *8,* 273.
11. Crecelius, E. A.; Bothner, M. H.; Carpenter, R. *Environ. Sci. Tech.* **1975,** *9,* 323.
12. Langston, W. J. *J. Mar. Biol. Assoc. U.K.* **1980,** *60,* 869.
13. Onishi, H.; Sandell, B. *Geochim. Cosmochim. Acta.* **1955,** *7,* 1.
14. Boström, K.; Valdes, S. *Lithos* **1969,** *2,* 351.
15. Dhandhukia, M. M.; Seshadri, K. *Phykos* **1969,** *8,* 108.
16. Lunde, G. *J. Sci. Food Agric.* **1970,** *21,* 416.
17. Sanders, J. G. *Chemosphere* **1979,** *3,* 135.
18. Maher, W. A.; Clarke, S. M. *Mar. Pollut. Bull.* **1984,** *15,* 111.
19. Morita, M.; Shibata, Y. *Appl. Organomet. Chem.* **1990,** *4,* 181.
20. Benson, A. A.; Summons, R. E. *Science* **1981,** *211,* 482.
21. Maher, W. A. *Mar. Pollut. Bull.* **1983,** *14,* 308.
22. Ballin, U.; Kruse, R.; Rüssel, H.-A. *Fresenius J. Analyt. Chem.* **1994,** *350,* 54.
23. Bohn, A. *Mar. Pollut. Bull.* **1975,** *6,* 87.
24. Egaas, E.; Brækkan, O. R. *Fiskeridir. skrf. Serie Ernær.* **1977,** *1,* 93.
25. Hall, R. A.; Zook, E. G.; Meaburn, G. M. *NOAA Tech. Rep.* NMFS SSRF-721; 313 pages, 1978.
26. Attar, K. M.; El-Faer, M. Z.; Rawdah, T. N.; Tawabini, B. S. *Mar. Pollut. Bull.* **1992,** *24,* 94.
27. Falconer, C. R.; Shepherd, R. J.; Pirie, J. M.; Topping, G. *J. Exp. Mar. Biol. Ecol.* **1983,** *71,* 193.

28. Shiomi, K.; Shinagawa, A.; Igarashi, T.; Hirota, K.; Yamanaka, H.; Kikuchi, T. *Bull. Jap. Soc. Sci. Fish.* **1984,** *50,* 293.
29. Leatherland, T. M.; Burton, J. D. *J. Mar. Biol. Assoc. U.K.* **1974,** *54,* 457.
30. Zingde, M. D.; Singbal, S. Y. S.; Moraes, C. F.; Reddy, C. V. G. *Ind. J. Mar. Sci.* **1976,** *5,* 212.
31. Turner, D. R.; Whitfield, M.; Dickson, A. G. *Geochim. Cosmochim. Acta* **1981,** *45,* 855.
32. Cullen, W. R.; Reimer, K. J. *Chem. Rev.* **1989,** *89,* 713.
33. Francesconi, K. A.; Edmonds, J. S.; Morita, M. In "Arsenic in the Environment, Part I: Cycling and Characterization"; Nriagu, J. O., Ed.; John Wiley & Sons; New York, 1994; p. 189.
34. Braman, R. S.; Foreback, C. C. *Science* **1973,** *182,* 1247.
35. Chakraborti, D.; Adams, F.; Irgolic, K. J. *Analyt. Chem.* **1986,** *323,* 340.
36. Agget, J.; Kadwani, R. *Analyst* **1983,** *108,* 1495.
37. Larsen, E. H.; Pritzl, G.; Hansen, S. H. *J. Analyt. Atom. Spectrom.* **1993,** *8,* 1075.
38. Grabinski, A. A. *Analyt. Chem.* **1981,** *53,* 966.
39. Cooney, R. V.; Mumma, R. O.; Benson, A. A. *Proc. Nat. Acad. Sci. USA* **1978,** *75,* 4262.
40. Francesconi, K. A.; Edmonds, J. S.; Hatcher, B. G. *Comp. Biochem Physiol. C* **1988,** *90,* 313.
41. Reimer, K. J.; Thompson, J. A. J. *Biogeochemistry* **1988,** *6,* 211.
42. Talmi, Y.; Bostick, D. T. *Analyt. Chem.* **1975,** *47,* 2145.
43. Phillips, D. J. H. In "Arsenic in the Environment, Part I: Cycling and Characterization"; Nriagu, J. O., Ed.; John Wiley & Sons: New York, 1994; p. 263.
44. Welz, B.; Melcher, M. *Analyt. Chem.* **1985,** *57,* 427.
45. Jin, K.; Ogawa, H.; Taga, M. *Bunseki Kagaku* **1983,** *32,* E 171.
46. Norin, H.; Christakopoulos, A. *Chemosphere* **1982,** *11,* 287.
47. Norin; H.; Ryhage, R.; Christakopoulos, A.; Sandström, M. *Chemosphere* **1983,** *12,* 299.
48. Edmonds, J. S.; Francesconi, K. A.; Cannon, J. R.; Raston, C. L.; Skelton, B. W.; White, A. H. *Tetrahedron Lett.* **1977,** *18,* 1543.
49. Beauchemin, D.; Bednas, M. E.; Berman, S. S.; McLaren, J. W.; Siu, K. W. A.; Sturgeon, R. E. *Analyt. Chem.* **1988,** *60,* 2209.
50. Francesconi, K. A.; Micks, P.; Stockton, R. A.; Irgolic, K. J. *Chemosphere* **1985,** *14,* 1443.
51. Cannon, J. R.; Edmonds, J. S.; Francesconi, K. A.; Raston, C. L.; Saunders, J. B.; Skelton, B. W.; White, A. H. *Aust. J. Chem.* **1981,** *34,* 787.
52. McShane, W. J. Ph.D. thesis, Texas A&M University, 1982.
53. Irgolic, K. J.; Junk, T.; Kos, C.; McShane, W. S.; Pappalardo, G. C. *Appl. Organomet. Chem.* **1987,** *1,* 403.
54. Francesconi, K. A. Ph.D. thesis, The University of Western Australia, 1991.
55. Edmonds, J. S.; Francesconi, K. A. *Nature* **1981,** *289,* 602.
56. McAdam, D. P.; Perera, A. M. A.; Stick, R. V. *Aust. J. Chem.* **1987,** *40,* 1901.
57. Francesconi, K. A.; Edmonds, J. S.; Stick, R. V.; Skelton, B. W.; White, A. H. *J. Chem. Soc. Perkin Trans. 1* **1991,** 2707.
58. Edmonds, J. S.; Francesconi, K. A.; Healy, P. C.; White, A. H. *J. Chem. Soc. Perkin Trans. 1* **1982,** 2989.
59. Dixon, H. B. F. *Adv. Inorg. Chem.* **1996,** *44,* 191.
60. Shibata, Y.; Morita, M. *Analyt. Sci.* **1989,** *5,* 107.
61. Larsen, E. H. *Fresenius J. Analyt. Chem.* **1995,** *352,* 582.

62. Feltham, R. D.; Kasenally, A.; Nyholm, R. S. *J. Organomet. Chem.* **1967,** *7,* 285.
63. Francesconi, K. A.; Edmonds, J. S.; Stick, R. V. *J. Chem. Soc. Perkin Trans. 1* **1992,** 1349.
64. Shibata, Y.; Morita M. *Agric. Biol. Chem.* **1988,** *52,* 1087.
65. Francesconi, K. A.; Edmonds, J. S.; Stick, R. V. *Appl. Organomet. Chem.* **1994,** *8,* 517.
66. Edmonds, J. S.; Francesconi, K. A.; Hansen, J. A. *Experientia* **1982,** *38,* 643.
67. Francesconi, K. A.; Edmonds, J. S.; Stick, R. V. *Sci. Total Environ.* **1989,** *79,* 59.
68. Gailer, J. Unpublished results.
69. Francesconi, K. A.; Stick, R. V.; Edmonds J. S. *Experientia* **1990,** *46,* 464.
70. Edmonds, J. S.; Shibata, Y.; Francesconi, K. A.; Yoshinaga, J.; Morita, M. *Sci. Total Environ.* **1992,** *122,* 321.
71. Andreae, M. O. *Limnol. Oceanography* **1979,** *24,* 440.
72. Gohda, S. *J. Oceanogr. Soc. Jpn.* **1974,** *30,* 163.
73. Sugawara, K.; Kanamori, S. *Bull. Chem. Soc. Jpn.* **1964,** *37,* 1358.
74. Johnson, D. L. *Nature* **1972,** *240,* 44.
75. Johnson, D. L.; Burke, R. M. *Chemosphere* **1978,** *7,* 645.
76. Andreae, M. O. *Analyt. Chem.* **1977,** *49,* 820.
77. Howard, A. G.; Arbab-Zavar, M. H.; Apte, S. *Mar. Chem.* **1982,** *11,* 493.
78. Howard, A. G.; Apte, S. C. *Appl. Organomet. Chem.* **1989,** *3,* 499.
79. Millward, G. E.; Ebdon, L.; Walton, A. P. *Appl. Organomet. Chem.* **1993,** *7,* 499.
80. Howard, A. G.; Comber, S. D. W. *Appl. Organomet. Chem.* **1989,** *3,* 509.
81. Cullen, W. R.; Dodd, M. *Appl. Organomet. Chem.* **1988,** *2,* 1.
82. de Bettencourt, A. M. M.; Andreae, M. O. *Appl. Organomet. Chem.* **1991,** *5,* 111.
83. de Bettencourt, A. M. M.; Florêncio, M. H.; Duarte, M. F. N.; Gomes, M. L. R.; Vilas Boas, L. F. C. *Appl. Organomet. Chem.* **1994,** *8,* 43.
84. Ebdon, L.; Walton, A. P.; Millward, G. E.; Whitfield, M. *Appl. Organomet. Chem.* **1987,** *1,* 427.
85. Gailer, J.; Francesconi, K. A.; Edmonds, J. S.; Irgolic, K. J. *Appl. Organomet. Chem.* **1995,** *9,* 341.
86. Peterson, M. L.; Carpenter, R. *Geochim. Cosmochim. Acta* **1986,** *50,* 353.
87. Edmonds, J. S.; Francesconi, K. A. *J. Chem. Soc. Perkin Trans. 1* **1983,** 2375.
88. Francesconi, K. A.; Edmonds, J. S. In "Oceanography and Marine Biology: An Annual Review"; Ansell, A. D., Gibson, R. N., and Barnes, M., Eds.; UCL Press: London 1993; Vol. 31, p. 111.
89. Yancey, P. H.; Clark, M. E.; Hand, S. C.; Bowlus, R. D.; Somero, G. N. *Science* **1982,** *217,* 1214.
90. Edmonds, J. S.; Morita, M.; Shibata, Y. *J. Chem. Soc. Perkin Trans. 1* **1987,** 577.
91. Shibata, Y.; Morita, M.; Edmonds, J. S. *Agric. Biol. Chem.* **1987,** *51,* 391.
92. Jin, K.; Shibata, Y.; Morita, M. *Agric. Biol. Chem.* **1988,** *52,* 1965.
93. Morita, M.; Shibata, Y. *Chemosphere* **1988,** *17,* 1147.
94. Jin, K.; Hayashi, T.; Shibata, Y.; Morita, M. *Appl. Organomet. Chem.* **1988,** *2,* 365.
95. Edmonds, J. S.; Francesconi, K. A.; Stick, R. V. *Nat. Prods. Reports* **1993,** *10,* 421.
96. Lunde, G. *Acta Chem. Scand.* **1973,** *27,* 1586.
97. Francesconi, K. A.; Edmonds, J. S. In "Arsenic in the Environment, Part I: Cycling and Characterization"; Nriagu, J. O., Ed.; John Wiley & Sons; New York, 1994; p. 221.
98. Edmonds, J. S.; Francesconi, K. A.; Shibata, Y.; Morita, M. *Appl. Organomet. Chem.* in press.
99. Cullen, W. R.; Harrison, L. G.; Li, H.; Hewitt, G. *Appl. Organomet. Chem.* **1994,** *8,* 313.

100. Whyte, J. N. C.; Englar, J. R. *Bot. Mar.* **1983,** *26,* 159.
101. Yasui, A.; Tsutsumi, C.; Toda, S. *Agric. Biol. Chem.* **1978,** *42,* 2139.
102. Shinagawa, A.; Shiomi, K.; Yamanaka, H.; Kikuchi, T. *Bull. Jpn. Soc. Sci. Fish.* **1983,** *49,* 75.
103. Larsen, E. H.; Donard, O. F. X. submitted.
104. Shiomi, K.; Kakehashi, Y.; Yamanaka, H.; Kikuchi, T. *Appl. Organomet. Chem.* **1987,** *1,* 177.
105. Shiomi, K.; Aoyama, M.; Yamanaka, H.; Kikuchi, T. *Comp. Biochem. Physiol. C* **1988,** *90,* 361.
106. Morita, M.; Shibata, Y. *Analyt. Sci.* **1987,** *3,* 575.
107. Shiomi, K.; Sakamoto, Y.; Yamanaka, H.; Kikuchi, T. *Nippon Suisan Gakkaishi* **1988,** *54,* 539.
108. Cullen, W. R.; Dodd, M. *Appl. Organomet. Chem.* **1989,** *3,* 79.
109. Edmonds, J. S.; Francesconi, K. A. *Mar. Pollut. Bull.* **1993,** *26,* 665.
110. Edmonds, J. S.; Shibata, Y.; Prince, R. I. T.; Francesconi, K. A.; Morita, M. *J. Mar. Biol. Assoc. U.K.* **1994,** *74,* 463.
111. Marafante, E.; Vahter, M.; Dencker, L. *Sci. Total Environ.* **1984,** *34,* 223.
112. Edmonds, J. S.; Francesconi, K. A. *Sci. Total Environ.* **1987,** *64,* 317.
113. Norin, H.; Christakopoulos, A.; Sandström, M.; Ryhage, R. *Chemosphere* **1985,** *14,* 313.
114. Kaise, T.; Hanaoka, K.; Tagawa, S. *Chemosphere* **1987,** *16,* 2551.
115. Whitfield, F. B.; Freeman, D. J.; Shaw, K. J. *Chem. Ind.* **1983,** *20,* 786.
116. Coulson, E. A.; Remington, R. E.; Lynch, K. M. *J. Nutr.* **1935,** *10,* 255.
117. Vahter, M.; Marafante, E.; Dencker, L. *Sci. Total Environ.* **1983,** *30,* 197.
118. Jongen, W. M. F.; Cardinaals, J. M.; Bos, P. M. J.; Hagel, P. *Food Chem. Toxicol.* **1985,** *23,* 669.
119. Sabbioni, E.; Fischbach, M.; Pozzi, G.; Pietra, R.; Gallorini, M.; Piette, J. L. *Carcinogenesis* **1991,** *12,* 1287.
120. Asano, M.; Itoh, M. *Ann. N. Y. Acad. Sci.* **1960,** *90,* 674.
121. Hopenhayn-Rich, C.; Smith, A. H.; Goeden, H. M. *Environ. Res.* **1993,** *60,* 161.
122. Roscoe, H. E. *Mem. Lit. Phil. Soc. Manchester, 3rd series* **1862,** *1,* 208.
123. MacLagen, C. *Edinburgh Medical Journal* **1875,** *21,* 526.
124. GESAMP (IMO/FAO/UNESCO/WMO/WHO/IAEA/UN/UNEP Joint group of experts on the scientific aspects of marine pollution). "Reports and Studies No. 28," 172 pages; World Health Organization: Geneva, 1986.
125. Irgolic, K. J.; Woolson, E. A.; Stockton, R. A.; Newman, R. D.; Bottino, N. R.; Zingaro, R. A.; Kearney, P. C.; Pyles, R. A.; Maeda, S.; McShane, W. J.; Cox, E. R. *Environ. Health Perspectives* **1977,** *19,* 61.
126. Sanders, J. G.; Cibik, S. J. *Mar. Ecol. Prog. Ser.* **1985,** *22,* 199.
127. Challenger, F. *Chem. Rev.* **1945,** *36,* 315.
128. Challenger, F. *Adv. Enzymology* **1951,** *12,* 429.
129. Challenger, F.; Lisle, D. B.; Dransfield, P. B. *J. Chem. Soc.* **1954,** 1760.
130. Cantoni, G. L. *J. Am. Chem. Soc.* **1952,** *74,* 2942.
131. Cantoni, G. L. *J. Biol. Chem.* **1953,** *204,* 403.
132. Cullen, W. R.; Froese, C. L.; Lui, A.; McBride, B. C.; Patmore, D. J.; Reimer, M. *J. Organomet. Chem.* **1977,** *139,* 61.
133. Cullen, W. R.; McBride, B. C.; Reglinski, J. *J. Inorg. Biochem.* **1984,** *21,* 45.
134. Cullen, W. R.; Li, H.; Hewitt, G.; Reimer, K. J.; Zalunardo, N. *Appl. Organomet. Chem.* **1994,** *8,* 303.
135. McBride, B. C.; Wolfe, R. S. *Biochemistry* **1971,** *10,* 4312.

136. Ahmann, D.; Roberts, A. L.; Krumholz, L. R.; Morel, F. M. M. *Nature* **1994,** *371,* 750.
137. Vidal, F. V.; Vidal, V. M. V. *Mar. Biol.* **1980,** *60,* 1.
138. Sanders, J. G. *Chemosphere* **1979,** *3,* 135.
139. Scudlark, J. R.; Johnson, D. L. *Estuar. Coast. Shelf Sci.* **1982,** *14,* 693.
140. Pickett, A. W.; McBride, B. C.; Cullen, W. R. *Appl. Organomet. Chem.* **1988,** *2,*479.
141. Hanaoka, A. G.; Tagawa, S.; Kaise, T. *Appl. Organomet. Chem.* **1992,** *6,* 139.
142. Cullen, W. R.; Nelson, J. *Appl. Organomet. Chem.* **1993,** *7,* 319.
143. Cullen, W. R.; Pergantis, S. A. *Appl. Organomet. Chem.* **1993,** *7,* 329.
144. Edmonds, J. S.; Francesconi, K. A. Unpublished results.
145. Francesconi, K. A.; Edmonds, J. S.; Stick, R. V. *Appl. Organomet. Chem.* **1992,** *6,* 247.
146. Johnson, D. L.; Pilson, M. E. Q. *J. Mar. Res.* **1972,** *30,* 140.
147. Maugh, T. H. *Science* **1979,** *203,* 637.
148. Meharg, A. A.; Macnair, M. R. *J. Exp. Bot.* **1992,** *43,* 519.
149. Sanders, J. G.; Windom, H. L. *Estuar. Coast. Mar. Sci.* **1980,** *10,* 555.
150. Klumpp, D. *Mar. Biol.* **1980,** *58,* 257.
151. Andreae, M. O.; Klumpp, D. *Environ. Sci. Tech.* **1979,** *13,* 738.
152. Howard, A. G.; Comber, S. D. W.; Kifle, D.; Antai, E. E.; Purdie, D. A. *Estuar. Coast. Shelf Sci.* **1995,** *40,* 435.
153. Planas, D.; Healey, F. P. *J. Phycol.* **1978,** *14,* 337.
154. Bottino, N. R.; Cox, E. R.; Irgolic, K. J.; Maeda, S.; McShane, W. J.; Stockton, R. A.; Zingaro, R. A. *ACS Symp. Ser.* **1978,** *82,* 116.
155. Wrench, J. J.; Addison, R. F. *Can. J. Fish. Aquat. Sci.* **1981,** *38,* 518.
156. Klumpp, D. W.; Peterson, P. J. *Mar. Biol.* **1981,** *62,* 297.
157. Cantoni, G. L. In "The Biochemistry of Adenosylmethionine"; Salvatore, F., Borek, E., Zappia, V., Williams-Ashman, H. G., and Schlank, F., Eds.; Columbia University Press: New York, 1977; p. 557.
158. Nishimura, S.; Taya, Y.; Kuchino, Y.; Ohashi, Z. *Biochem. Biophys. Res. Commun.* **1974,** *57,* 702.
159. Vahter, M. *Appl. Organomet. Chem.* **1994,** *8,* 175.
160. Lunde, G. *Fisk. skrifter Serie Teknologiske Undersokelser* **1972,** *5,* 1.
161. Pentreath, R. J. *International Council for the Exploration of the Sea* **1977,** CM 1977/E:17.
162. Fowler, S. W.; Ünlü, M. Y. *Chemosphere* **1978,** *7,* 711.
163. Anderson, J. L.; Depledge, M. H. *Mar. Biol.* **1994,** *118,* 285.
164. Francesconi, K. A.; Edmonds, J. S.; Gailer, J.; Irgolic, K. J. Unpublished results.
165. Penrose, W. R. *J. Fish. Res. Board Can.* **1975,** *32,* 2385.
166. Oladimeji, A. A.; Qadri, S. U.; Tam, G. K. H.; De Freitas, A. S. W. *Ecotoxicol. Environ. Saf.* **1979,** *3,* 394.
167. Cooney, R. V.; Benson, A. A. *Chemosphere* **1980,** *9,* 335.
168. Edmonds, J. S.; Francesconi, K. A. *Chemosphere* **1981,** *10,* 1041.
169. Gibbs, P. E.; Langston, W. J.; Burt, G. R.; Pascoe, P. L. *J. Mar. Biol. Assoc. U.K.* **1983,** *63,* 313.
170. Bartlett, P. D.; Craig, P. J.; Morton, S. F. *Nature* **1977,** *267,* 606.
171. Davies, I. M.; Graham, W. C.; Pirie, J. M. *Mar. Chem.* **1979,** *7,* 111.
172. Francesconi, K. A.; Lenanton, R. C. J. *Mar. Environ. Res.* **1992,** *33,* 189.
173. Riisgård, H. U.; Famme, P. *Mar. Pollut. Bull.* **1986,** *17,* 255.
174. Phillips, D. J. H.; Depledge, M. H. *Mar. Environ. Res.* **1985,** *17,* 1.
175. Topping, G.; Davies, I. M. *Nature* **1981,** *290,* 243.
176. Byrne, A. R.; Slejkovec, Z.; Stijve, T.; Fay, L.; Gössler, W.; Gailer, J.; Irgolic, K. J. *Appl. Organomet. Chem.* **1995,** *9,* 305.

This Page Intentionally Left Blank

ADVANCES IN INORGANIC CHEMISTRY, VOL. 44

THE BIOCHEMICAL ACTION OF ARSONIC ACIDS ESPECIALLY AS PHOSPHATE ANALOGUES

HENRY B. F. DIXON

Department of Biochemistry, University of Cambridge, Cambridge, CB2 1QW, United Kingdom

I. Scope of Review

Every time a fish dies, its bones fall to the bottom of the sea. This can leave the shallower waters, where light intensity is enough for growth of phytoplankton, short of the phosphate they require, and this applies particularly in equatorial waters where the temperature and density differences between deep and shallow levels minimize mixing (Atkins, *1–5*). This puts a high selective pressure on organisms to be

able to concentrate phosphate from very low environmental concentrations. The chemical similarity of phosphate and arsenate means that they cannot avoid concentrating arsenate, too. As described in Sections II,A and B, arsenate is harmful to organisms, and hence there is selective pressure toward rendering it nontoxic. This gives rise to the amazing pathways of arsenic metabolism in marine organisms, which have long been studied and are the subject of the review by Francesconi and Edmonds (*6*) in this volume. The present review deals with a more artificial situation, where experimenters have deliberately added arsenic compounds to living organisms or systems derived from them. It is largely restricted to arsonic acids, R—AsO_3H_2, which contain As(V), and particularly those that possess the arsonomethyl group, –CH_2—AsO_3H_2, because of their similarity to phosphates containing the phosphono-oxy group, –O—PO_3H_2. Ni Dhubhghaill and Sadler (*7*) have discussed arsenic chemistry more widely in relation to biological activity.

As shown later (Section IV), a compound R—CH_2—AsO_3H_2 is often a substrate for an enzyme that normally acts on the corresponding R—O—PO_3H_2. The consequences of this enzymic action may be unusual. If the action of the enzyme is to alkylate, acylate, or phosphorylate the phospho group of R—O—PO_3H_2, then a new futile cycle can be established (Section IV,B,2,a), because the product may be spontaneously hydrolyzed to release the original R—CH_2—AsO_3H_2. Applications are obvious if this property can give selective toxicity to the compounds concerned. Even an enzyme-catalyzed reaction of the R group of R—CH_2—AsO_3H_2 can have different consequences from such a reaction of R—O—PO_3H_2, as described in Section IV,B,2,c, where the highly toxic arsenite ion is released. Of course, an arsonomethyl compound may bind to an enzyme that naturally binds a phosphate or even a carboxylate, and, if not a substrate, or only a poor one, it will inhibit the enzyme. Before discussion of these properties of arsonic acids as substrate analogues, some background is given on the biochemical actions of arsenate (Section II) and arsenite (Section III).

II. The Biochemistry of Arsenate

A. Comparison of Arsenate with Phosphate

Arsenic and phosphorus are adjacent members of the same group of the periodic table, Group 15 in the IUPAC numbering that avoids the earlier confusion of contradictory systems that gave it both designations

VA and VB (*8*). It is therefore not surprising that arsenate and phosphate are very similar, and that enzymes consequently hardly distinguish between them. The first obvious difference is that the arsenic atom is larger; As—O bonds are typically about 10% longer than P—O bonds. In the dianion of arsonomethylphosphonic acid, $H_2O_3As—CH_2—PO_3H_2$, for example, the As—O bond lengths range from 0.168 to 0.171 nm, and the P—O lengths from 0.153 to 0.154 nm by X-ray crystallography (*9*). It is probably this that is responsible for the main difference in behavior between phosphates and arsenates. Whereas monoesters and diesters of phosphoric acid are very stable (without this, DNA could not be the genetic material, since its phosphate groups link adjoining nucleosides as diesters), the monoesters, i.e., R—O—AsO_3H_2, of arsenic acid, H_3AsO_4, are labile in water. This is presumably because water can more readily enter the coordination shell of a four-coordinate arsenic atom, and one of the original four ligands can leave. Typically, monoesters of arsenate have half-lives in water at neutral pH of about 30 min (*10–12*); if the arsenate is acylated or phosphorylated instead of being alkylated, i.e., if the arsenic atom bears a better leaving group, the half-life falls to seconds or less (*13–15*). This explains the long-known biochemical actions of arsenate: enzymes accept it in place of phosphate to incorporate into other compounds such as ATP, but the analogues formed hydrolyze immediately. Thus, arsenate uncouples oxidative metabolism from ATP biosynthesis.

B. Arsenate as a Substrate of Enzymes That Use Phosphate

The idea that enzymes whose normal substrate is orthophosphate can use arsenate in its place, and that the esters of arsenate formed are rapidly hydrolyzed, was given by Braunstein (*16*) in 1931, to explain the effects of arsenate on glycolysis. This idea was formulated more precisely for glyceraldehyde–phosphate dehydrogenase in 1939. This enzyme, E—SH, normally oxidizes its aldehyde substrate with phosphate uptake to give an acyl phosphate, as follows:

$$E—SH + R—CH=O \longrightarrow E—S—CHOH—R \qquad \text{hemithioacetal formation}$$

$$E—S—CHOH—R \longrightarrow E—S—CO—R + 2H\,(\text{to NAD}^+) \qquad \text{oxidation}$$

$$E—S—CO—R + {}^-O—PO_3H_2 \longrightarrow E—SH + R—CO—O—PO_3H^- \qquad \text{acylation}$$

but forms the carboxylic acid if arsenate is present. Warburg and Christian (*17*) realized that this was because arsenate replaces phosphate so that an acyl arsenate is produced, which rapidly decomposes to

regenerate arsenate and form the carboxylic acid. The acyl arsenate formed has a detectable half-life in water (*18*), although probably less than 2.5 s (*19*). Arsenate is often used in the assay of this enzyme, since the overall reaction in its presence has a favorable equilibrium for aldehyde oxidation, not achieved when an acyl phosphate is the product. It is interesting that whereas thiols with small molecules rapidly react with arsenate (*20–22*) to reduce it according to the equation

$$H_3AsO_4 + 5\ R{-}SH \longrightarrow As({-}S{-}R)_3 + R{-}S{-}S{-}R + 4\ H_2O$$

the enzyme does not react with arsenate in this way, although it is very sensitive to most reagents for mercapto groups. This is presumably because this reaction of –SH groups requires that more than one of them should reach the same arsenate ion.

Arsenate similarly replaces phosphate in ATP synthesis, and the ATP analogue formed, a phosphorylated arsenate, has a similarly short lifetime, possibly up to a few seconds (*13–15*). $R{-}COO^-$ might be expected to be a better leaving group than $R{-}PO_3^{2-}$, since it is a weaker base. The arsenic compound analogue is capable of being trapped by hexokinase, since the glucose 6-arsenate formed is much more stable (*12*).

Arsenate similarly replaces phosphate in various phosphorolysis reactions, so that sucrose phosphorylase catalyzes the hydrolysis of sucrose in its presence (*23*), potato phosphorylase can hydrolyze amylose and amylopectin (*24*), nucleoside phosphorylase can hydrolyze inosine (*25*), and an acetyltransferase can hydrolyze acetyl phosphate (*26*). Fitting and Doudoroff (*27*) made use of this to confirm the difference between the mechanisms of sucrose phosphorylase and maltose phosphorylase. The former transfers the glucosyl group via a group on the enzyme, so that both sucrose and glucose 1-phosphate are hydrolyzed by it in the presence of arsenate, whereas maltose phosphorylase, which transfers the glucosyl group directly from glucose onto phosphate, will hydrolyze maltose in the presence of arsenate, but does not hydrolyze glucose 1-phosphate (unless glucose is also present to receive the glucosyl group.)

C. Spontaneous Formation of Esters of Arsenate

The lability of esters of arsenate is of course mirrored in their ease of formation. Hence, merely mixing an alcohol with arsenate leads to

their condensation. Appreciable concentrations of esters can be made in this way, although the equilibrium is unfavorable in water, since the dissociation constant is about 500 *M*, as Lagunas *et al.* (*11*) showed for adenosine 5′-arsenate.

More interesting is the fact that enzymes that act on phosphorylated substrates, R—O—PO_3H_2, often bind both R—OH and either phosphate or arsenate. When R—OH and arsenate are bound in proximity, the ester R—O—AsO_3H_2 forms and acts as a substrate for the enzyme, as shown for many enzymes by Lagunas and co-workers (*10, 28, 29*). Hence, enzymes that act on R—O—PO_3H_2 also act on R—OH if arsenate is present. So these studies, like that of Long and Ray (*12*) with its elegant method of measuring glucose 6-arsenate concentrations, include determining the substrate properties of R—O—AsO_3H_2 as an analogue of R—O—PO_3H_2; it usually proves to be a good substrate. This phenomenon can be used in chemical synthesis when it is desired to convert R—OH into R′—OH and an enzyme is available that converts R—O—PO_3H_2 into R′—O—PO_3H_2; the enzyme will perform the desired step in the presence of arsenate, since this temporarily esterifies the hydroxy group (*30*). The rates of reactions that involve formation of this analogue from R—OH and arsenate at the active site of the enzyme are low, presumably because this esterification is slow. The same effect can therefore be seen better when R—O—PO_3H_2 is a coenzyme rather than a substrate, because then one esterification can lead to many turnovers of the enzyme. Indeed, a stable and active aspartate aminotransferase, presumably containing pyridoxal arsenate, forms from the apoenzyme, i.e., the protein freed from pyridoxal phosphate, when free pyridoxal and arsenate are added (Ali and Dixon, *31*).

III. The Biochemistry of Arsenite

A. Interaction with Thiols

Arsenic(III) oxide is the main arsenic-based poison. The As_4O_6 molecule easily interconverts with arsenious acid, $As(OH)_3$, and its salts, the arsenites. Other compounds of the general structure R—AsX_2, where X is a displaceable ligand, are also highly toxic. Many, often with aromatic R groups, are used chemotherapeutically, and there is a large literature on this (e.g., *7*); some have been used in chemical warfare. Their toxicity is due to their high affinity with the dihydrolipoyl groups of pyruvate dehydrogenase, 2-oxoglutarate dehydroge-

nase, and 3-methyl-2-oxobutyrate dehydrogenase. Some of the early evidence for this was the effectiveness of dithiols, especially 2,3-dimercaptopropanol, in reversing the toxic effects of these 3-valent arsenic compounds (*32*). Both 1,2- and 1,3-dithiols have high affinity for the arsenic atom in such compounds, forming five- and six-membered rings.

The relative affinities of various hydroxylic dithiols for arsenite were measured by Zahler and Cleland (*33*), but proved hard to understand (since seven-membered rings seemed to give the most stable complexes) until Cruse and James (*34*) showed that an oxygen atom of such a compound acted as a third ligand for arsenic, so that bicyclic complexes were formed.

Some compounds of this type may have a high affinity for proteins that is not due to their binding to two thiol groups (*35*). In particular, arsenite also reacts with the molybdenum-pterin cofactor of many enzymes (*35a–d*). This usually inhibits the enzyme, but in particular cases (*35e*) the arsenite may be oxidized; indeed the enzyme arsenite oxidase contains such a center (*35f*).

B. The Place of Arsenite in the Detoxification of Arsenate

As stated in Section I, arsenate and phosphate are very similar. Hence, organisms have difficulty in assimilating phosphate without taking up arsenate, and this will uncouple their metabolism (Section II). They make use of an important difference between arsenate and phosphate to avoid this, i.e., the vastly greater ease of reduction of arsenate to arsenite than of phosphate to phosphite. By itself such a reduction would be no help, since arsenite is intensely toxic, but further processes can follow, such as alkylation to produce organoarsenic compounds (*6*), or extrusion of arsenite from the organism (e.g., *36, 37*), driven by hydrolysis of ATP (*38*). Extruded arsenite may then be rendered less toxic by oxidation to arsenate by the arsenite oxidase mentioned in section III,A.

An analogous mechanism is seen in the utilization of arsonoacetate by a bacterium as its sole source of energy and carbon (*39*). Arsenate is the product, and since the bacteria can oxidize arsenite, the original degradation of the arsonoacetate may be reductive and form arsenite, which is then oxidized to the less toxic arsenate.

Hence, for some organisms it is advantageous to oxidize arsenite to arsenate, whereas the reverse process may be beneficial to others, particularly if the arsenite is further metabolized.

IV. Arsonates as Analogues of Natural Phosphates or Phosphonates

A. Phosphonates as Analogues of Natural Phosphates

There is a large literature on the use of phosphonates in place of natural phosphates as enzyme substrates. If the natural substrate is $R—O—PO_3H_2$, then $R—CH_2—PO_3H_2$ is frequently a good substrate; occasionally, $R—PO_3H_2$ is, too. The subject has been well reviewed by Engel (*40*); other phosphonates that are good substrates for enzymes include the phosphonomethyl analogue of fructose 6-phosphate (*41*) and amino acyl AMP (*42*). The pK values of $R—O—PO_3H_2$ are close to the lower two of phosphoric acid, about 2 and 7 (or a little below), and $R—CH_2—PO_3H_2$ has slightly raised values, so that the higher is about 7.5.

Enzymes frequently bind their phospho substrates in the doubly ionized form. Evidence of this can be obtained by comparison between $R—O—PO_3H_2$ and $R—CH_2—PO_3H_2$ as substrates. Since the latter has a higher pK, it becomes a better substrate relative to the former as the pH is raised, at least up to a value where the $R—CH_2—PO_3^{2-}$ form predominates (*43*). Although the substrate is in the dianionic form, its binding to a positively charged site in the enzyme molecule may make it resemble the $-PO_3H_2$ form in its effects on the rest of the substrate; thus, in inositol biosynthesis, the grouping $-CO—CH_2—O—PO_3^{2-}$ of the enzyme-bound, 5-dehydrogenated glucose 6-phosphate contains an active methylene, capable of loss of H^+, and hence able to react with the aldehydic atom C-1 to form a cyclohexane ring (*44, 45*).

Blackburn and colleagues (*46, 47*) have emphasized the advantage of using $R—CHF—PO_3H_2$ or $R—CF_2—PO_3H_2$ rather than $R—CH_2—PO_3H_2$ as a substrate for an enzyme that normally acts on $R—O—PO_3H_2$. They are often better substrates. Part of this effect can be due to their lower pK, so that there will be more of the form $-PO_3^{2-}$ compared with $-PO_3H^-$. But this can only be a small effect: the upper pK of $R—CH_2—PO_3H_2$ is about 7.5, so the concentration of the $-PO_3^{2-}$ will form about one quarter of the total at pH 7, and therefore cannot be raised by more than about fourfold when the group becomes a stronger acid. The hydrogen-bonding ability and other electronic properties therefore seem responsible for the better substrate properties of the fluorinated compounds.

If the action of the enzyme is to transfer the phospho group, e.g., to water in a hydrolysis, or intramolecularly, e.g., in converting 3-phosphoglycerate into 2-phosphoglycerate (*48*), it cannot transform the phosphonomethyl analogue. This is because $R—CH_2^-$ is an incompara-

bly worse leaving group than R—O^-. The enzyme may still bind the analogue strongly, and hence be inhibited by it (*48*). When, however, its action is entirely within the R group, the phosphonomethyl analogue is usually a good substrate, showing a limiting velocity of 1/20 or more that of the natural substrate, and a Michaelis constant only slightly raised. There are certainly exceptions; the action of triose-phosphate isomerase on the phosphonomethyl analogue of glyceraldehyde 3-phosphate is low (*49*) and is not even detectable in the reverse reaction (*50*). Further, fructose-bisphosphatase did not hydrolyze the 1-phosphate from the 6-phosphonomethyl analogue of fructose 1,6-bisphosphate (although there was some binding), so this was done chemically (*41*), and later with alkaline phosphatase (unpublished).

One of the uses of phosphonate analogues may be appreciated from Fig. 1. If a phosphate is naturally converted into a diester, as in linking the residues of a nucleic acid, this may diagrammatically be represented by Equation 1 in the figure. In fact, of course, the biosynthetic reaction is not a direct alkylation and goes through several steps, with diphosphate as the leaving group X^-, but the principles are shown in the equation. If the phosphonate is a substrate for this conversion, Equation 2 results. We note that the ester produced, an analogue of a diester, will be incapable of hydrolysis by any enzyme that hydrolyzes the actual diester of Equation 1 into R—OH and R′—O—PO_3H_2. Such

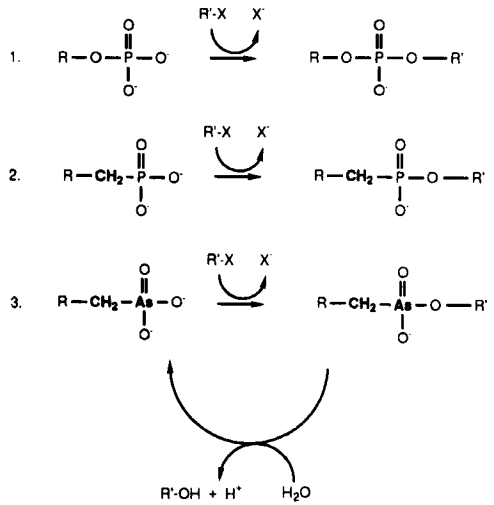

FIG. 1. A conceivable pathway for converting a monoester of phosphoric acid into a diester. It is shown with (1) the original ester, (2) its phosphonomethyl analogue, and (3) its arsonomethyl analogue.

unhydrolyzable analogues may be useful in X-ray crystallographic study of the binding of the substrate, as shown by Richards *et al.* (*51*), who used such an analogue of a dinucleotide in studying ribonuclease A. Webster *et al.* (*41*) showed that enzymes could be used to convert synthetic $H_2O_3P—\mathbf{CH_2}—CH_2—CHOH—COOH$, the analogue of 3-phosphoglycerate, into the corresponding phosphonomethyl analogue of fructose 6-phosphate (Fig. 2), which they isolated. They obtained evidence for the enzymic conversion of this into the analogue of glucose 6-phosphate [these two analogues were later separated (*52*)], and on into the analogues of 6-phosphogluconate (see *53*) and ribulose 5-phosphate. It is therefore possible that enzymes would produce such analogues of nucleotides, which could be used to insert unhydrolyzable bonds into nucleic acids, at least bonds not hydrolyzed by those nucleases that form 3′-phosphates.

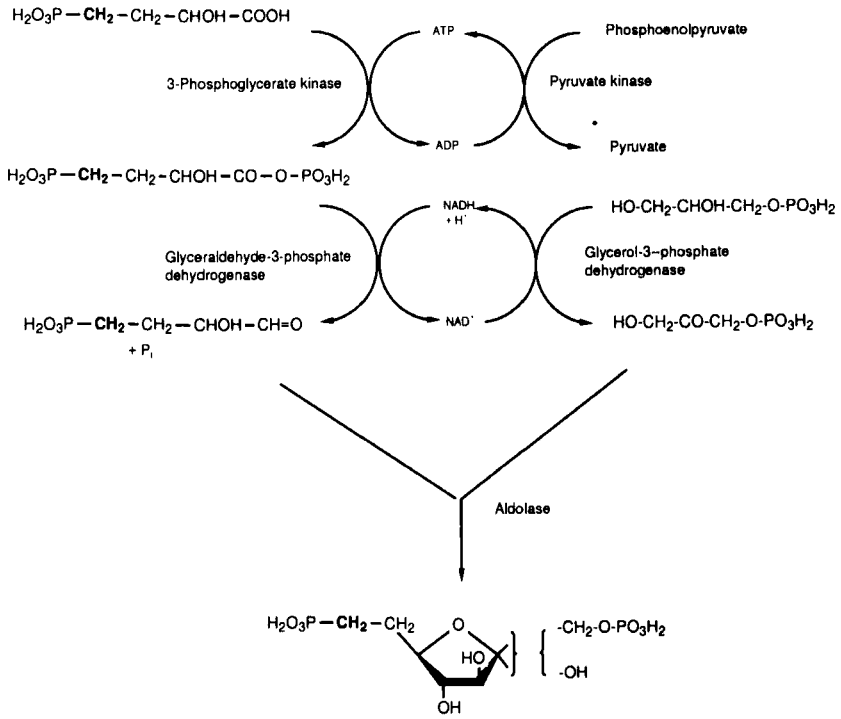

FIG. 2. Enzymic synthesis of an analogue of fructose 6-phosphate. The specificity of synthesis of the chiral centers, including selection of the correct enantiomer of the starting compound, was achieved with the enzymes shown. The product could be hydrolyzed to give the phosphonomethyl analogue of fructose 6-phosphate (*41*).

B. Comparison of Arsonates with Phosphonates

1. Acid Strength

Although arsenic and phosphoric acids, $(HO)_3X{=}O$, have almost identical pK values of about 2, 7, and 12, the effect of replacing their hydroxy groups by other substituents is very different. R—O—PO_3H_2, as noted earlier, typically still has values of about 2 and 7 (or a little below), and R—CH_2—PO_3H_2 slightly higher. When this substitution of an alkyl group for a hydroxy group is made in arsenic acid, to give an arsonic acid R—CH_2—AsO_3H_2, the pK values are raised much more, to about 4 and 9; indeed, repetition of this substitution raises the value by a further two units, so that cacodylic acid, $Me_2As(O)$—OH, has a pK of 6.

2. Interactions of Arsonates with Enzymes

a. Enzymes That Can Catalyze Reactions of the Arsono Group: New Futile Cycles. Figure 1, Equation 3, shows what is possible if an enzyme that normally makes a diester acts on an arsonate rather than the natural phosphate. A new futile cycle can be made, since the ease of access of water to the arsenic atom allows hydrolysis of the ester of an arsonic acid that can be formed.

To check that this approach was feasible, my colleagues and I first made the arsonomethyl analogue of ADP (*54*). It proved disappointing, in that it was either not a substrate, or a very poor substrate, for the ADP-using enzymes that were checked. This is not very surprising, since the phosphonomethyl analogue of ADP is also a poor substrate for many such enzymes (*55*, Table III). Conceivably the replacement of H_2O_3**P—O**– by H_2O_3**P—CH$_2$**– or H_2O_3**As—CH$_2$**– matters more in a diphosphate, H_2O_3P—O—P(O)(OH)—R, than in an alkyl phosphate, since the enzymic site for binding the compound is likely to bind several of the oxygen atoms of the diphosphate group; there may be no room for slight readjustment of the molecule between the different parts that are bound since these are so close to each other. Of course, the bridging oxygen atom may itself be bound.

It seemed desirable to check whether arsonomethyl analogues of natural phosphates would act as substrates for the enzymes that acted on the corresponding phosphates even when these enzymes did not act on the phospho group. Adams *et al.* (*56*) therefore checked whether H_2O_3**As—CH$_2$**—CH_2—CHOH—COOH would be acted on as the analogue of 3-phosphoglycerate, H_2O_3**P—O**—CH_2—CHOH—COOH. It proved to be a substrate for phosphoglycerate kinase, although not a good one. Its Michaelis constant was only slightly higher than that

for the natural substrate, but its catalytic constant was 1300 times less. The corresponding phosphonomethyl analogue, $H_2O_3P—CH_2—CH_2—CHOH—COOH$, however, has a catalytic constant diminished less than twofold from that of the natural substrate (*43*). It remains to be seen if the arsonomethyl analogue is a good enough substrate to allow its enzymic conversion into the arsonomethyl analogue of fructose 6-phosphate, by the pathway used for the phosphonomethyl analogue (Fig. 2).

Adams *et al.* then (*57*) synthesized the arsonomethyl analogue of AMP. The method used appears to be a fairly general one for converting an alcohol, R—OH, into the arsonomethyl analogue of its phosphate, $R—CH_2—CH_2—AsO_3H_2$ (see Section VII,A,1). It gave a futile cycle of the type hoped for (Fig. 3). Transfer of the phospho group of ATP by adenylate kinase, which accepted the analogue as AMP, evidently gave an ADP analogue, which was hydrolyzed to give the observed product, orthophosphate. In effect, the presence of this analogue endowed adenylate kinase with ATPase activity. Again, however, the arsonomethyl analogue was not a good substrate; the enzyme's limiting velocity with it was only 1/17 that with AMP, and the Michaelis constant was raised 70-fold to about 10 m*M*; hence, the specificity constant was lowered about 1200-fold.

Although, as noted earlier, enzymes that act on diphosphates are usually specific for diphosphate in comparison with methylenebis(phosphoric acid), $H_2O_3P—CH_2—PO_3H_2$, an exception is RNA polymerase, which accepts many analogues of diphosphate in the reverse reaction. This reaction occurs with the formation of nucleoside triphosphates when the newly formed RNA, still attached to the template DNA and the polymerase, is deprived of nucleoside triphosphates and supplied with inorganic diphosphate. Some of these analogues of diphosphate, including phosphonoacetic acid, $H_2O_3P—CH_2—COOH$, gave analogues of nucleoside triphosphates that hydrolyze spontaneously un-

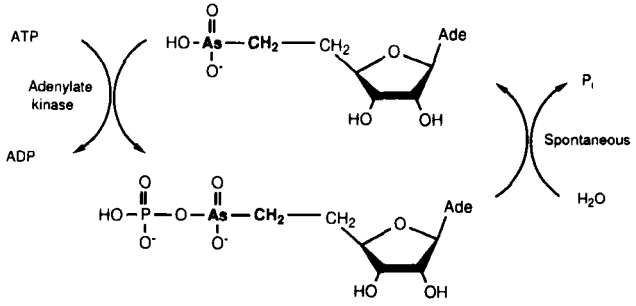

FIG. 3. The action of adenylate kinase on the arsonomethyl analogue of AMP (*57*).

der the conditions of the reaction (*58*). It is not surprising that arsonomethylphosphonic acid, $H_2O_3As—CH_2—PO_3H_2$, and methylenebis(arsonic acid), $H_2O_3As—CH_2AsO_3H_2$, are two of these (*59*), as shown in Fig. 4. The relative rates with the different analogues have not been measured, but the molecular dimensions of the arsonomethylphosphonic acid have been found by X-ray crystallography (*9*).

A somewhat different kind of futile cycle was obtained by Visedo-Gonzalez and Dixon (*60*). This arose from the fact that the incorporation of ethanolamine (i.e., 2-aminoethanol) into phospholipids starts with the reaction of its phosphate with CTP (Fig. 5). This forms the compound

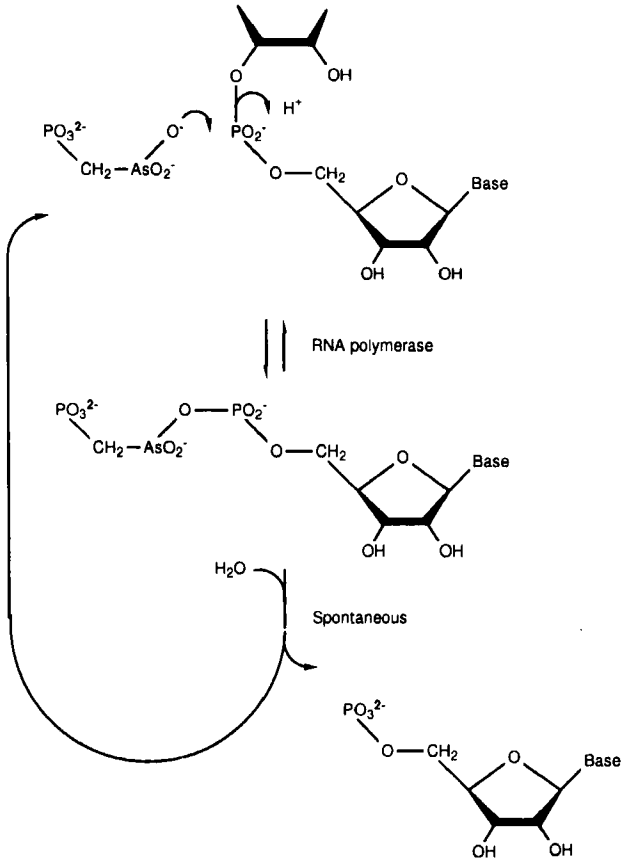

FIG. 4. The use of arsonomethyl phosphonate as an analogue of diphosphate by RNA polymerase. The enzyme accepts the analogue in the reverse of polymerase action. Since the product hydrolyzes, the overall effect is that of an exonuclease, producing nucleoside 5′-phosphates (*59*).

known as CDP-ethanolamine, by transfer of the cytidylyl group (i.e., cytidylic acid, CMP, lacking an –OH) from diphosphate onto phosphoethanolamine. In this way the phosphonoethanolamine is provided with a good leaving group, to form a donor of the $H_3N^+—CH_2—CH_2—O—PO_2^-$– group. Some protozoa and coelenterates synthesize the C—P bond and replace the ester phosphoethanolamine (2-aminoethyl phosphate, $H_3N^+—CH_2—CH_2—O—PO_3H^-$) in their phospholipids with 2-aminoethyl phosphonate, $H_3N^+—CH_2—CH_2—PO_3H^-$. Not only do they use the same type of mechanism for incorporating this into phospholipids that other animals, including mammals, use with the ester, but the mammalian enzyme transfers the cytidylyl group onto the phosphonate as well as onto the phosphate (*62*).

This use by an enzyme of $R—PO_3H_2$ in place of $R—O—PO_3H_2$ is fairly unusual; it is normally only $R—CH_2—PO_3H_2$ (see Section IV,A) that will be transformed. It was therefore not surprising that $R—AsO_3H_2$ proved to be a substrate (*60*). At least, we presume that it was, but the expected product (Fig. 5, Reaction 2) would be a phosphorylated

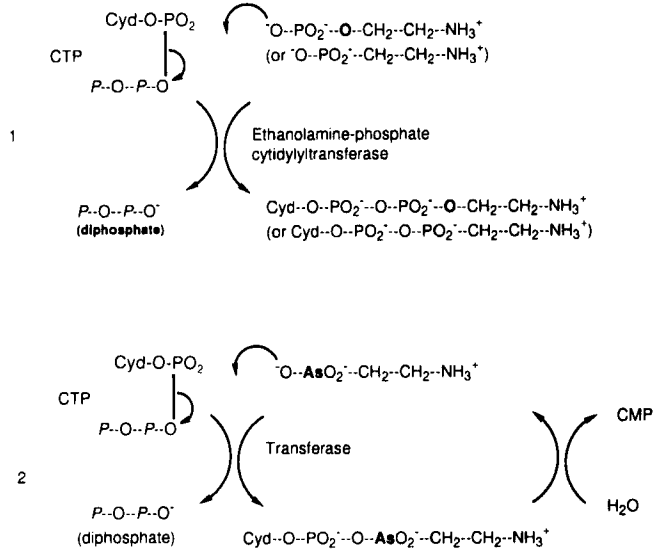

FIG. 5. The reaction of ethanolamine-phosphate cytidylytransferase with substrates and analogues. Reaction 1 shows the normal reaction of the enzyme with ethanolamine phosphate (2-aminoethyl phosphate), which is part of the route of phospholipid synthesis. The alternative reaction with 2-aminoethylphosphonate, in parentheses, is used by some marine organisms to insert a C—P bond into their phospholipids. Reaction 2 shows the futile cycle obtained with 2-aminoethylarsonate (*59*). The symbol –*P* signifies $-PO_3H_2$ and its ionized forms, and –*P*– signifies –P(O)(OH)– and its ionized form (*61*).

arsonic acid,and so would be expected (Section II,A) to be instantly hydrolyzed. Certainly the observed products were CMP and diphosphate. It is likely that the same result would be obtained with 3-aminopropylarsonic acid, NH_2—$[CH_2]_3$—AsO_3H_2, since it is a closer analogue of phosphoethanolamine than the 2-aminoethylarsonic acid, NH_2—$[CH_2]_2$—AsO_3H_2, but although this proved in 1992 to be readily made (*63*) by modifying a method of 1928, we had not done so by the time of our studies (*60*) in 1989.

Each futile cycle provides a new way of damaging living organisms, by using the donor of the group transferred. This may prove useful for achieving selective toxicity, but no studies have been made on the entry into cells of the arsonates used. Conceivably some arsonates may penetrate more easily than phosphates, because with a lower p*K* of 4, about one-thousandth of each will be in the un-ionized form at neutral pH, and this form may be capable of penetrating a membrane. Nevertheless, the arsono group is highly polar even in its hydronated form, and the arsonates used possess other polar groups, so entry into cells by mere diffusion is likely to be very slow. This may, however, be helpful in achieving a toxicity that could be selective, since it is only cells that possess a transport system for the compound concerned that will be affected.

A remarkable reaction of the phospho group is its transfer onto carbon in the biosynthesis of the C—P bond (Fig. 6). Incidentally, this leads to a difficulty with nomenclature, because the group $-PO_3H_2$, which is known to chemists as "phosphono," is called "phospho" only when on a heteroatom (*64*), so the transfer changes its name! Despite much ealier guessing from labeling patterns that phosphoenolpyruvate was the source of the C—P bond, it was only in 1988 (*65, 66*) that the enzyme responsible was isolated. The difficulty proved to be that the equilibrium favors phosphoenolpyruvate by about 2000-fold (*67*), so that assays only detected the enzyme in the direction contrary to biosynthesis; evidently the biosynthesis takes place because subsequent reac-

FIG. 6. Interconversion of phosphoenolpyruvate and 3-phosphonopyruvate. 1. Biosynthetic direction, in which the C—P bond is made. 2. Direction greatly favored at equilibrium.

tions, such as decarboxylation, efficiently remove the phosphonopyruvate. We decided to try arsonopyruvate as a substrate for the enzyme, after we had made this compound (see Section VII,D,2) in four steps from glycine (*68*); the enzyme proved to transform it, with a Michaelis constant of 20 μM, similar to that for phosphonopyruvate, and similar to its K_i as an inhibitor of the reaction of phosphonopyruvate, but with a catalytic constant 6000 times lower. The products were pyruvate and arsenate; any $H_2O_3As—O—C(=CH_2)—COOH$ formed would be expected to hydrolyze rapidly.

The enzyme that hydrolyzes phosphonoacetaldehyde (Fig. 7) is bacterial and provides a pathway for breaking the C—P bond. It has a mechanism like that of aldolase (*69–71*) in that an imine forms between the carbonyl group of substrate and an amino group of the enzyme; since this imine is hydronated at neutral pH, the electron attraction is increased, and this facilitates the breakage of the C—P bond. When arsonoacetaldehyde was tried in this reaction (*63*), it proved not to be a substrate, and it did not inhibit the enzyme appreciably.

b. Enzymes That Can Catalyze Reactions of Arsonates Outside the Arsono Group. As mentioned in the previous section, 4-arsono-2-hydroxybutyrate, $H_2O_3\mathbf{As}—\mathbf{CH_2}—CH_2—CHOH—COOH$, is a substrate for 3-phosphoglycerate kinase. A few other cases are known where this substitution is tolerated.

Enolase also proved (*72*) to use as a substrate the arsonomethyl analogue of its substrate 2-phosphoglyceric acid, i.e., 3-arsono-2-(hydroxymethyl)propionic acid, $H_2O_3\mathbf{As}—\mathbf{CH_2}—CH(—CH_2—OH)—$

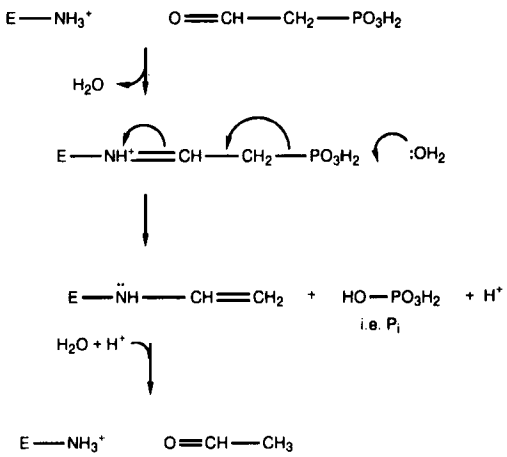

FIG. 7. The mechanism of action of phosphonoacetaldehyde hydrolase.

COOH. The Michaelis constant was 6.5 m*M*, about 80 times that for the phosphate (or 40 times if one of the enantiomers was inert), and the catalytic constant was 230 times lower than for the phosphate. Similarly, phospholipase A_2 cleaves the acyl group from O-2 of 2,3-dihydroxypropylarsonic acid that is acylated on O-2 and O-3 (M. K. Jain, personal communication, 1995).

Arsonates can also be substrates for enzymes that naturally act on phosphonates as well as for those that act on phosphates. 2-Aminoethyl phosphonate (ciliatine) occurs widely in protozoa and marine organisms and is broken down by bacteria (as shown in Fig. 8) (*73, 74*). The transaminase that catalyzes the first reaction has an interesting specificity, since it causes transamination between $NH_2—CH_2—CH_2—PO_3H_2$ and $O{=}CH—CH_2—PO_3H_2$, but not their corresponding carboxylic acids, and between alanine and pyruvate, but not their corresponding phosphonic acids. Lacoste *et al.* (*63*) showed that it accepted aminoethylarsonic acid in place of aminoethylphosphonic acid, as a good substrate with a Michaelis constant close to that of the phosphonate. As already mentioned, the arsonoacetaldehyde formed is not a substrate for the second enzyme of Fig. 8.

Mutenda *et al.* (*75*) found that racemic 3,4-dihydroxybutylarsonic acid, $HO—CH_2—CHOH—CH_2—\mathbf{CH_2}—\mathbf{AsO_3H_2}$, the arsonomethyl analogue of *sn*-glycerol 3-phosphate, was a good substrate for glycerol-3-phosphate dehydrogenase. The K_m obtained was 0.55 m*M* and under the same conditions; *sn*-glycerol 3-phosphate gave a K_m of 0.29 m*M*. Hence, they were identical if one enantiomer was inert. The limiting velocity with the analogue was about 75% that with the natural substrate. 2,3-Dihydroxypropylarsonic acid, a nonisosteric analogue, $HO—CH_2—CHOH—CH_2—AsO_3H_2$, did not show substrate activity.

c. Consequences of One Enzymic Reaction Outside the Arsono Group. The reaction just described gained added interest when its consequences were appreciated. As we found (*75*), after frustrating attempts first to isolate and then to synthesize the expected product,

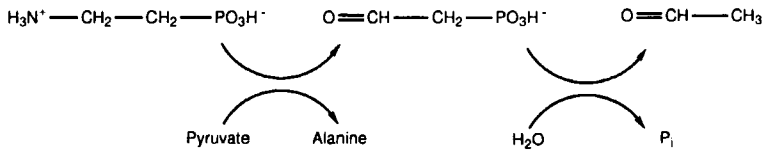

FIG. 8. The pathway of breakdown of 2-aminoethyl phosphonate in bacteria.

4-hydroxy-3-oxobutylarsonic acid (Fig. 9, Reaction 1), this compound is unstable and eliminates arsenite. The presumed mechanism is via enolization, as shown in the further reactions of Fig. 9.

This mechanism is supported by the fact that every 3-oxoalkylarsonic acid studied also eliminated arsenite. First, 3-hyroxypropylarsonic acid proved to be a substrate for alcohol dehydrogenase from yeast, and similarly eliminated arsenite. Further, the oxidation by periodate of the $HO—CH_2—CHOH—CH_2—CH_2—AsO_3H_2$, expected to produce $O{=}CH—CH_2—CH_2—AsO_3H_2$ (another 3-oxoalkylarsonic acid), also yielded arsenite, and conditions that normally transaminate amino acids, when applied to the glutamate analogue $HOOC—CH(—NH_2)—CH_2—CH_2—AsO_3H_2$, and so expected to form $HOOC—CO—CH_2—CH_2—AsO_3H_2$, did so, too.

In the two enzyme-catalyzed oxidations, there was a considerable lag in arsenite release behind NADH production, and indeed this re-

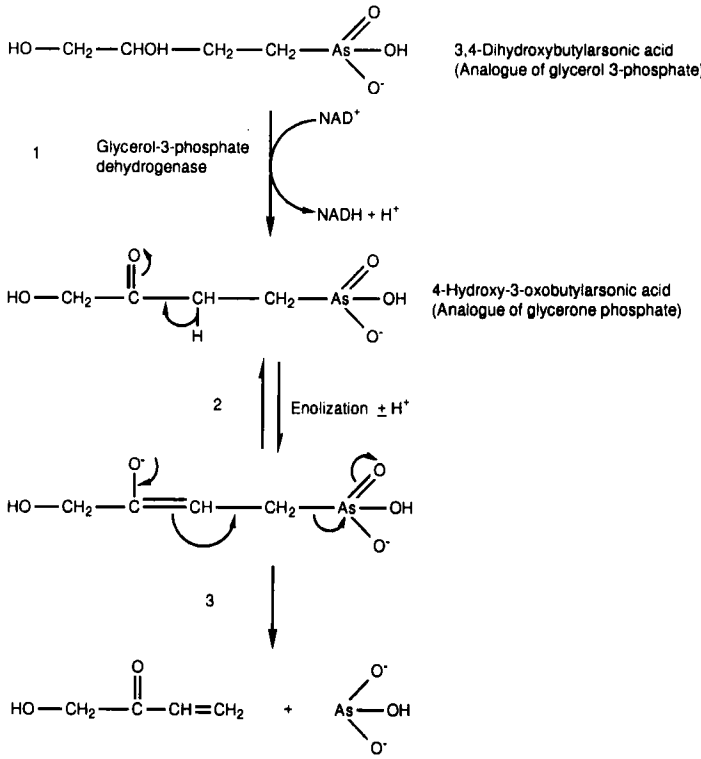

FIG. 9. The action of glycerol-3-phosphate dehydrogenase on 3,4-dihydroxybutylarsonic acid.

lease was not quantitative. It seems likely that the intermediate 3-oxoalkylarsonic acid undergoes competing reactions, since arsenite elimination is slow; indeed, this was shown for the periodate oxidation (*75*). The complete elimination in the attempted transamination may be explained by the fact that this reaction should go through an intermediate of the type $HOOC—C(=NH^+—R)—CH_2—CH_2—AsO_3H_2$ (actually a metal ion replacing the hydrogen on nitrogen), so that the electron withdrawal that facilitates enolization may be much higher in it than in an aldehyde or ketone.

A consequence of this arsenite release is that a compound such as 3,4-dihydroxybutylarsonic acid may be selectively toxic to cells that can take it up. The compound itself is fairly harmless. Delivery of such compounds into cells and their subsequent oxidation inside the cell will result in release of arsenite. The arsenite may then kill the cell by inactivating enzymes that contain dihydrolipoyl groups (Section III,A). The other product formed when arsenite is released, a vinyl ketone, is a strong electrophile, and hence may also be toxic.

3. Other Arsenic Analogues of Natural Phosphates

As part of an impressive series of papers on arsenic chemistry, Ioannou and colleagues have developed methods for making arsenic analogues of natural phospholipids. They first made racemic 2,3-dihydroxypropylarsonic acid, the nonisosteric analogue of glycerol 3-phosphate (*76*), and acylated it to obtain analogues of phosphatidic acids (*77*). They then made the two enantiomers separately and also acylated these (*78*). They developed (*79*) a better acylation of these by temporarily converting the arsono group into $-As(—S—Ph)_2$. Interactions with enzymes have been studied, e.g., with phospholipase A_2 (Section IV,B,2,b); further, the (*S*)-enantiomers (i.e., those differing from natural phosphatidate) of 2,3-diacyloxypropylarsonic acid inhibit carbonic anhydrase (*79a*). They and we have jointly made (*80*) the isosteric analogue 3,4-dihydroxybutylarsonic acid, reported (*75*) in Sections IV,A,2,b and c.

Although the isosteric analogue $R—CH_2—PO_3H_2$ is usually accepted by enzymes as an analogue of $R—O—PO_3H_2$ much better than the nonisosteric analogue $R—PO_3H_2$, this last may bind well enough at least to inhibit an enzyme. The same applies to arsonates. Thus, Vas (*81*) has found marked competitive inhibition of phosphoglycerate kinase by both $H_2O_3P—CH_2—CHOH—COOH$ and $H_2O_3As—CH_2—CHOH—COOH$.

V. Arsonates as Analogues of Nonphosphate Metabolites

Phosphonates have been widely used as analogues of carboxylic acids. They have been particularly effective as analogues of tetrahedral transition states that occur in the course of enzyme-catalyzed reactions such as hydrolysis of the amide (peptide) bond. As such, they may be used as inhibitors of enzymes (e.g., *82, 83*) or as haptens for producing antibodies that are catalytic (e.g., *84*). A notable example is H_2O_3P—CH_2—CH_2—CH(—NH_2)—COOH, which has effects that are likely to be due to its interference with glutamate as a neurotransmitter (*85*).

The malate, oxaloacetate, and fumarate analogues 3-arsonolactate (*86*), 3-arsonopyruvate (*68*), and (*E*)-3-arsonoacrylate (*87, 88*) have been made; Ali and Dixon (*88*) found that the fumarate and malate analogues were not substrates for fumarate hydratase, but competitive inhibitors, arsonoacrylate, H_2O_3As—CH=CH—COOH, with fumarate (K_i/K_m 1.8) and arsonolactate, H_2O_3As—CH_2—CHOH—COOH, with malate (K_i/K_m 1.6). Incidentally, although phosphonopyruvate is a poor substrate for malate dehydrogenase (*89, 90*), 3-(hydroxyphosphinoyl)pyruvate, HO—P(H)(O)—CH_2—CO—COOH, is much better (*89*). It proved impossible to show the reverse reaction with arsonolactate (*89, 91*).

The racemic arsenic compound and glutamate analogue H_2O_3As—CH_2—CH_2—CH(—NH_2)—COOH was made as an intermediate in the synthesis of the phosphoglycerate analogue H_2O_3As—CH_2—CH_2—CHOH—COOH (*56*). It proved not to be a substrate for cattle glutamate dehydrogenase, but a competitive inhibitor with a K_i of 7.3 m*M*, which may be compared with the K_m for L-glutamate of 1.7 m*M* (*92*). Treatment with pyridoxal phosphate and borohydride converted it into the *N*-phosphopyridoxyl derivative, which bound to the active site of the apoenzyme of aspartate aminotransferase and was used in X-ray crystallographic studies (*93*).

The racemic aspartate analogue, H_2O_3As—CH_2—CH(—NH_2)—COOH, has also been made. It inhibited aspartate-ammonia lyase, competitively with L-aspartate (K_i/K_m 0.23) (*88*), almost the same valueas found with the phosphonate analogue (*94*). In attempted nonenzymic transamination, as mentioned in Section IV,B,2,c, the glutamate analogue loses arsenite, presumably because of the instability of 3-oxoalkylarsonic acids (*75*). The aspartate analogue 3-arsonoalanine also eliminates arsenite (*88*), but 3-phosphoalanine can break down differently (Fig. 10). The arsonate eliminates arsenite at an early stage in the reaction pathway that would otherwise lead to transamination, presumably because of the greater stability of the reduced form for arsenite/arsenate than for phosphite/phosphate, and because of the

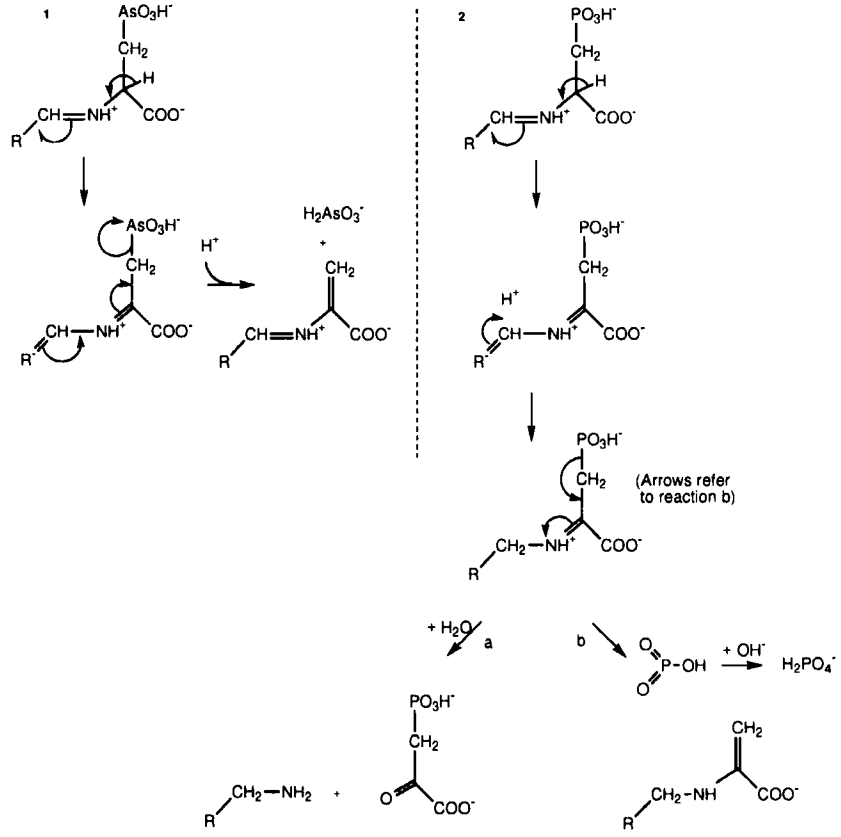

FIG. 10. Attempted nonenzymic transaminations of arsonoalanine and phosphonoalanine. Pathway 1 shows the arsenite elimination by arsonoalanine. Pathway 2 shows (a) the successful transamination to phosphonopyruvate under some conditions, and (b) the production of phosphate under others (*88*).

weakness of the C—As bond. In contrast, the phosphonate loses monomeric metaphosphate (although it is not clear that this is free, i.e., whether O—P bond formation lags behind C—P bond scission) at a later stage; under slightly different conditions phosphonoalanine is successfully transaminated to phosphonopyruvate.

Arsonoalanine was not a substrate or inhibitor of aspartate aminotransferase under the conditions tested (*88*), but it inactivated it progressively. Many alanine derivatives in which there is a good leaving group on C-3 do this (*95–97*), both to this enzyme and other pyridoxal enzymes (*96*), with some interesting results, e.g., the difference in reac-

tion outcome when glutamate decarboxylase reacts with two enantiomers of serine 3-*O*-sulfate (*98*), which is a glutamate analogue.

Sukhareva and colleagues (*99*) studied the action of both the glutamate and aspartate analogues on glutamate decarboxylase, which is responsible for the biosynthesis of the neurotransmitter 4-aminobutyrate (GABA). This decarboxylation is accompanied by a side reaction in which the enzyme is inactivated by transamination of its pyridoxal phosphate to form pyridoxamine phosphate. The glutamate analogue was a very poor substrate, and the aspartate analogue even worse, but with both, small amounts of decarboxylation could be shown. Both inactivated the enzyme; with the glutamate analogue, this inactivation was reversed with pyridoxal phosphate, and so probably due to a higher transamination : decarboxylation ratio, but with the aspartate analogue, this reaction was only partial, so some other inactivation occurred, as might be expected from a compound with a good leaving group on C-3.

It is obvious that phosphates and arsonates may bind badly to sites in enzymes and other receptors that fit the carboxylate group, because they are tetrahedral, whereas carboxylate is planar. Kluger and colleagues (*100*) noted a more subtle cause for poor fitting, when an enzyme would not accept the phosphono group $-PO_3H_2$ in place of a carboxy, $-COOH$, but would accept a different tetrahedral group, namely sulfo, $-SO_3H$. Thus, they found that acetonesulfonic acid, $CH_3—CO—CH_2—SO_3H$, was a substrate for 3-hydroxybutyrate dehydrogenase, whereas 2-oxopropylphosphonic acid, $CH_3—CO—CH_2—PO_3H_2$, was not. They attributed this to the fact that the anion-binding site holds a monoanion, so binding may force the phosphono group to adopt its $-PO_3H^-$ form. This form, unlike $-CO_2^-$ and $-SO_3^-$, does not have its charge symmetrically distributed with respect to the bond that joins the acidic group to the rest of the molecule, so that the electrostatic vector is along this bond for $-CO_2^-$ and $-SO_3^-$, but at an angle to it for $-PO_3H^-$. Hence, binding to a positive charge in the site may misorient the phosphonate molecule with respect to the catalytic site. Such an argument would equally apply to arsonates. But the next section shows that dipole direction does not easily explain all such observations.

VI. Other Biological Actions of Arsonates

A. Transport of Arsonates

Few studies have been made of arsonate transport. Lacoste *et al.* (*63*), after finding that *Pseudomonas aeruginosa* would take up both

2-aminoethyl- and 3-aminopropyl arsonic acids, analogues of aminoethylphosphonate and of phosphoethanolamine, respectively, also showed that they inhibited the uptake of labeled aminoethylphosphonate competitively with a K_i of 18 μM for each; the K_m for the aminoethylphosphonate was 6 μM.

Nicklin *et al.* (*101*) studied uptake of aspartate and glutamate by human intestinal cells, a system with K_m values of 56 and 65 μM for these amino acids. The K_i values for (racemic) 3-arsonoalanine and 3-phosphonoalanine were 1.1 and 3.3 mM, so they bound much less tightly (and the corresponding glutamate analogues hardly inhibited). What is surprising is that cysteate, in which $-AsO_3H_2$ and $-PO_3H_2$ are replaced by $-SO_3H$, binds strongly (K_i 65 μM), as does the compound in which they are replaced by $-PO_2H_2$. As these are binding studies, the system is different from that of Kluger's group (*100*), and distortion by dipole direction will not explain the difference. The difference between the values for the phosphonate and arsonate is small enough that the difference in their fractions in the monoanionic form (see their pK values, Section IV,B,1) could explain it.

B. Arsonoacetate as a Nutrient

Quinn and McMullan (*102*) have found a bacterium with the ability to live on arsonoacetate as its sole source of carbon and energy. It excreted the arsenic as arsenate, which did not harm it up to a concentration of 30 mM. Since it was also able to oxidize arsenite to arsenate, the breakage of the C—As bond may be reductive (Fig. 11). This organism was also able to convert racemic arsonochloroacetate, H_2O_3As—CHCl—COOH, quantitatively into arsenate (so it must convert both enantiomers), although it could not use it as its energy source. It could not use chloroacetate as its energy source, either, and this is the most likely product of the C—As bond cleavage.

VII. Aspects of the Chemistry of Arsonates

A. C—As Bond Formation in the Synthesis of Arsonic Acids

1. The Meyer Reaction: Nucleophilic Attack on Carbon

The best-known route for making aliphatic arsonic acids is the Meyer (*103*) reaction, in which an alkyl halide reacts with alkaline arsenite by simple nucleophilic displacement:

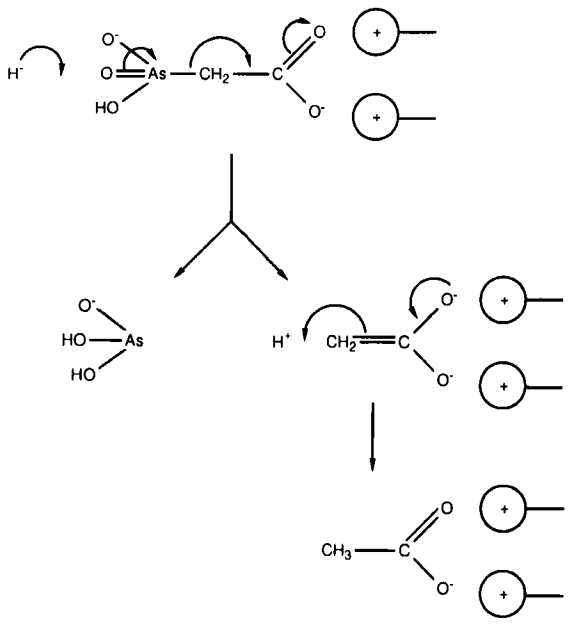

FIG. 11. A conceivable reductive cleavage of arsonoacetate.

$$R{-}X + As(-O^-)_3 \longrightarrow R{-}As(=O)(-O^-)_2 + X^-$$

Even in the strong alkali that favors this reaction, very little of the arsenite will be as the trianion; nevertheless, there is evidence that it is this form that is responsible for the reaction (*104*). The insolubility of many alkyl halides in the necessarily aqueous solution of strong alkali is a limitation on this, so ways around must be found. Further, the R group of R—X should not carry a nucleophilic atom on C-4 or C-5, or else it will attack C-1 with expulsion of halide and cyclization. This includes a hydroxy group, since it will be in the nucleophilic $-O^-$ form in the alkaline conditions.

The Meyer reaction is intrinsically reversible. As the pH rises and arsenite becomes progressively dehydronated, it becomes an increasingly good nucleophile, whereas it becomes an increasingly good leaving group as the pH falls and the C—As bond can break (see *75*, p. 987).

In our synthesis (*57*) of the arsonomethyl analogue of AMP, we developed a method (Fig. 12) for converting an alcohol, $R{-}CH_2{-}OH$, into the arsonomethyl analogue, $R{-}CH_2{-}CH_2{-}AsO_3H_2$, of its phosphate, $R{-}CH_2{-}O{-}PO_3H_2$. In this pathway the Meyer reaction is used on a 2-halocarboxylic acid, so that the reactant will be soluble in aqueous

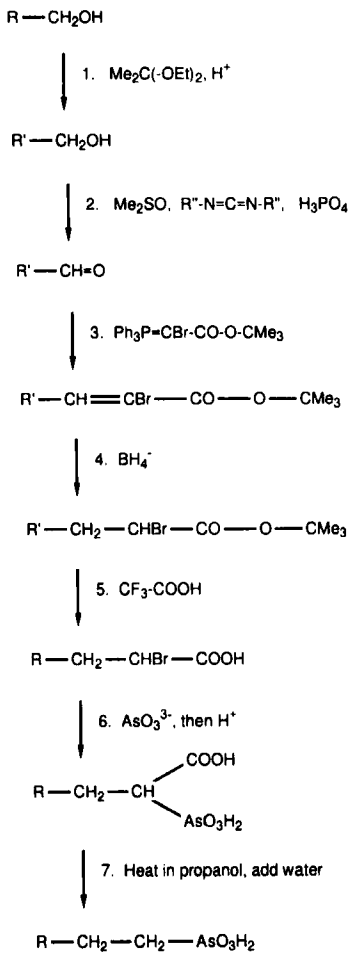

FIG. 12. A method for converting an alcohol, R—CH_2OH, into the arsonomethyl analogue of its phosphate. This was used to make the arsonomethyl analogue of AMP. R—CH_2OH represents adenosine, and R'—CH_2OH its 2',3'-isopropylidene derivative.

alkali, and the halide activated for displacement. This can be done because we had found a simple way of decarboxylating arsonoacetic acids (step 7). To convert an arsonic acid into its diester, one has merely to dissolve it in an alcohol. To be sure of complete esterification, one must remove the water formed in the reaction

$$R—AsO_3H_2 + 2\ R'—OH = R—As(O)(—OR')_2 + 2\ H_2O$$

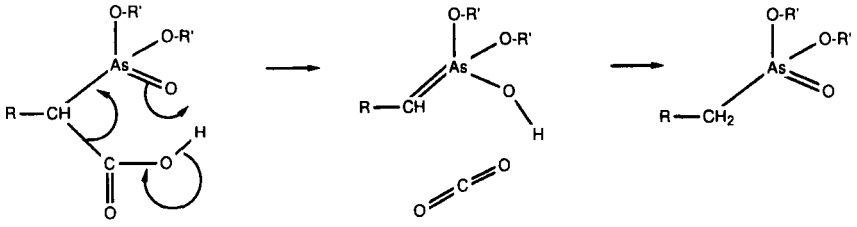

FIG. 13. Conceivable mechanism for the decarboxylation of arsonoacetic acids. When an arsonoacetic acid is boiled in propan-1-ol, and the propanol–water azeotrope is distilled off, the acid will be esterified completely on the arsono group but not on the carboxy group. Decarboxylation is observed.

This is easily done if R′ is propyl, because the azeotrope of water and propan-1-ol boils at a temperature well below the boiling point of the propanol, so one can distill off this azeotrope up a fractionating column until the temperature of the vapor reaches the boiling point of propanol. When this is done with an arsonoacetic acid, decarboxylation results. It may be that that hydron is involved, as shown in Fig. 13, since the reaction does not proceed if one starts with a monoanion of the arsonoacetic acid.

So step 1 is protection of other hydroxy groups, step 2 is a normal Moffatt–Pfitzner oxidation, and step 3 is a Wittig reaction. The tertiary butyl ester is used to provide steric hindrance in step 4 to any approach of borohydride to the carbonyl group; when an ethyl ester was used, some reduction of the ester grouping was found.

This method does not seem to be applicable if R is aromatic, as would be necessary to make the arsonomethyl analogue of pyridoxal phosphate. Despite protection of groups capable of interference, the reaction proved impossible, and evidence of elimination of HBr with formation of R—CH=CH—COOH from R—CH_2—CHBr—COOH in attempting step 6 was obtained (*105*).

A related synthesis of the C—As bond was used (*106*) in the synthesis of the natural compound (see *6*) trimethylarsonioacetate, Me_3As^+—CH_2—COO^-, by treating ethyl bromoacetate with trimethylarsine. Although this reaction has not been used to make arsonic acids, it could conceivably be adapted for this by replacing the methyl groups with more labile alkyl groups.

2. *Nucleophilic Attack on Arsenic*

Another synthesis of the carbon—arsenic bond is also most useful in making arsonomethyl compounds. The problems mentioned earlier

with the Meyer reaction are faced in the synthesis of 3,4-dihydroxybutylarsonic acid, the arsonomethyl analogue of glycerol phosphate considered in Sections IV,B,2,b and c. If a Meyer reaction is attempted with 4-bromobutane-1,2-diol or an ester, yields are low because of cyclization in the alkaline arsenite solution as $-O^-$ expels bromide (*80*, route C). If the Meyer reaction is attempted with 4-bromobut-1-ene, the insolubility of this in alkaline arsenite lowers the yield (*80*, route A). For this reason, the method of McBrearty *et al.* (*107*) was also used (*80*, route B). This consists of allowing a carbanion to displace chloride from $Cl—As(—NEt_2)_2$, but since this is rather unreactive, a reagent as powerful as a Grignard compound, R—MgCl, must be used. The product $R—As(—NEt_2)_2$ does not need to be isolated, and oxidative workup gives $R—AsO_3H_2$. In an earlier method from the same laboratory (*108*), two molecules of Grignard reagent reacted with $Cl_2As–NEt_2$ to give $R_2As(O)—OH$ on oxidative workup. Even with this valuable alternative method (*107*) for making arsonic acids, our overall yield for this route, i.e., making $CH_2=CH—CH_2—CH_2—AsO_3H_2$ and later hydroxylating it (*80*, route B), was not very good.

In view of the ease with which water attacks an ester of arsenate in water, we wondered if carbon nucleophiles would similarly attack a trialkyl arsenate to form a C—As bond. We (Sparkes and Dixon, unpublished work) therefore treated the sodium salt of diethyl malonate with tripropyl arsenate, and hydrolyzed during workup. Some arsonoacetic acid was formed, but we have not found conditions that give a useful yield.

The earliest synthesis of a carbon—arsenic bond was published in 1760 by Cadet (*109*). Modern versions of this reaction are the methods of making methylenebis(arsonic acid), $H_2O_3As—CH_2—AsO_3H_2$, by Popp (*110*), in which As_4O_6 is treated with acetyl chloride, and by Titov and Levin (*111*), in which it is treated with acetic anhydride. The first of these leads to a somewhat easier isolation by distilling the $Cl_2As—CH_2—AsCl_2$ formed. Evidently, the carbanion formed attacks As, and decarboxylation follows. The $H_2O_3As—CH_2—AsO_3H_2$ formed by oxidizing the first product is an analogue of diphosphate and is accepted by RNA polymerase (Section IV,B,2,a).

B. "Nonexistent" Arsonic Acids

No reports have appeared of compounds of the formula $R—CH(—NH_2)—AsO_3H_2$, and they might have considerable interest in view of the large literature on 1-aminoalkylphosphonic acids, $R—CH(—NH_2)—PO_3H_2$, as well as reports (e.g., *112–114*) of 1-aminoal-

kylphosphinic acids, R—CH(—NH_2)—PO_2H_2. These last contain the hydroxyphosphinoyl group, with a phosphorus-bound hydrogen, H—P(=O)(—OH)—. Although this group is tetrahedral, the small size of the hydrogen on the phosphorus atom makes it fit better into sites for carboxylate.

The postulated 1-aminoalkylarsonic acids have something in common with 1-hydroxyalkanesulfonic acids, R—CHOH—SO_3^-. These are not usually known as such, but as bisulfite addition compounds of aldehydes. They are not usually isolable, because of the ease of the reaction shown in Fig. 14. In just the same way we might expect R—CH(—NH_3^+)—AsO_3H^- to lose arsenite as $H_2AsO_3^-$ and H^+, i.e., $H_2AsO_3^-$ overall, leaving the imine R—CH=NH_2^+, which would equilibrate with R—CH=O and NH_4^+. So this would explain why 1-aminoalkylarsonic acids may not exist as stable compounds.

That, however, does not mean that they cannot exist in solution. They may be formed, possibly only in small concentrations, in solutions of aldehydes and ammonium arsenite, so that a binding site for an amino acid might pull the equilibrium over to give bound R—CH(—NH_3^+)—AsO_3H^-, in much the same way that the apoenzyme of aspartate aminotransferase binds pyridoxal arsenate, even though the concentration of free pyridoxal arsenate in the solution of pyridoxal and arsenate is minute (*30*; see also Section II,C). Much the same applies to R—CHOH—AsO_3H_2 as to R—CH(—NH_2)—AsO_3H_2, although it might form more easily because it requires only the two reactants of the aldehyde and arsenite.

Since acylphosphonic acids have interesting properties, e.g., acetylphosphonic acid is a poor substrate for lactate dehydrogenase (*115*), and acylphosphinic acids can be powerful inhibitors of enzymes that act on 2-oxo acids, e.g., acetylphosphinic acid on pyruvate dehydrogenase (*116*, *117*, *114*), the possibility of the existence of acylarsonic acids (i.e., 1-oxoalkylarsonic acids) arises. Such existence seems improbable, however, because arsenite is a good leaving group, and carboxylates are poor electrophiles. Raising the pH to make arsenite a better nucleophile makes a carboxylic acid a worse electrophile.

FIG. 14. The breakdown of 1-hydroxyalkanesulfonic acids.

C. Behavior of Oxoalkylarsonic Acids

3-Oxoalkylarsonic acids lose arsenite by elimination, presumably after enolization, as described earlier (Section IV,B,2,c, and Fig. 9). In contrast, 3-oxoalkylphosphonic acids are stable; e.g., the phosphonomethyl analogue of glycerone phosphate is a substrate for aldolase (*118*). The elimination of arsenite from 3-oxoalkylarsonic acids, but not of phosphite from 3-oxoalkylphosphonic acids, may reflect the fact that arsenite is relatively stable compared with arsenate, whereas phosphite is unstable compared with phosphate.

2-Oxoalkylarsonic acids, exemplified by arsonoacetaldehyde and 3-arsonopyruvate, are only moderately stable; they release arsenate by hydrolysis, rather than arsenite by elimination. They are presumably hydrolyzed by the mechanism of Fig. 7, but they do not need the added electron attraction of forming the imine $E—NH^+=CR—CH_2—AsO_3H_2$; $O=CR—CH_2—AsO_3H_2$ is fairly easily attacked by water. 2-Oxoalkylphosphonic acids can be hydrolyzed in this way (*119*), as in the enzyme-catalyzed hydrolysis of phosphonoacetaldehyde (*73, 69–71*), but with much more difficulty. The lability of 2-oxoalkylarsonic acids presumably reflects the ease with which water can more easily enter the coordination shell of arsenic than that of phosphorus, because of the larger size of the atom, i.e., the same feature expressed in the lability of esters and anhydrides of arsenate.

D. Handling of Arsonic Acids During Syntheses

1. Reduction

It is often necessary to handle arsenic compounds during syntheses in the reduced form, e.g., in converting 2-hydroxyethylarsonic acid, $HO—CH_2—CH_2—AsO_3H_2$, into 2-chloroethylarsonic acid, $Cl—CH_2—CH_2—AsO_3H_2$. This is because the reagents used for the conversion of the hydroxymethyl group would be oxidized by the arsono group in such an acid medium. The classical method (*120–122*) is to saturate a solution of the acid in aqueous HCl with SO_2. Catalytic quantities of iodide or iodine are added, so the real reducing agent is HI. We found (*56*) that the isolation of the product, $HO—CH_2—CH_2—AsCl_2$, needed changing, but that the reduction worked well. We have since found (Sparkes and Dixon, unpublished work) a more convenient and possibly milder method, which is to boil the arsonic acid, still with catalytic amounts of iodine, in 50% aqueous formic acid. This avoids the need to get rid of the sulfuric acid produced from the SO_2, since the formic acid is merely oxidized to carbon dioxide.

Just as arsenate itself reacts with thiols (Section II,B), arsonic acids are also reduced by them, with formation of dialkyl alkyldithioarsonites (*123*, *124*), as follows:

$$R{-}AsO_3H_2 + 4R'{-}SH \longrightarrow R'{-}S{-}S{-}R' + R{-}As({-}S{-}R')_2$$

2. *Formation of 2-Oxoalkylarsonic Acids*

As described in Section VII,C, these are easily hydrolyzed to arsenate and the corresponding aldehyde or ketone. Our first attempts to make arsonoacetaldehyde failed, because it is so easily broken down, and indeed we were not convinced that it was stable enough to exist until

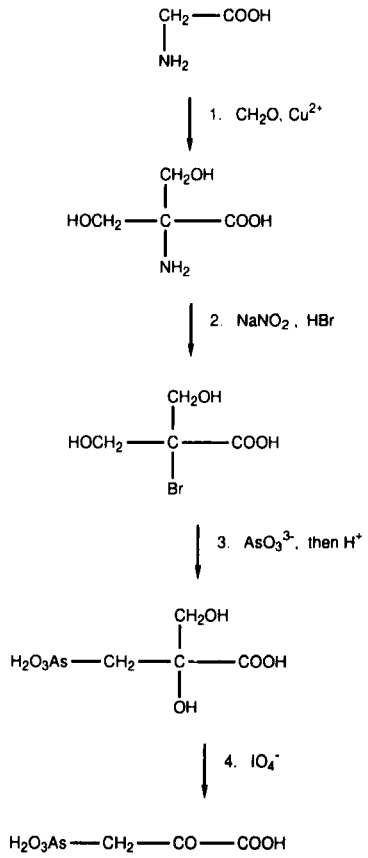

FIG. 15. The synthesis of 3-arsonopyruvic acid. Step 3 is explained by the temporary cyclization to an epoxide in the alkali of the reagent.

our colleagues in Bordeaux showed (*63*) that the transaminase that acted on 2-aminoethylphosphonate also acted on 2-aminoethylarsonate (as shown by conversion of pyruvate into alanine) without producing acetaldehyde. We then succeeded in making it, by the periodate oxidation of 2,3-dihydroxypropylarsonic acid, $HO—CH_2—CHOH—CH_2—AsO_3H_2$, and this time were careful to add only the required amount of periodate (*63*). In this way the labile structure was only formed at the last step. Even so, the product has not been isolated from solution, as it breaks down when this is attempted; its solution is used in preparing arsonoalanine by the Strecker synthesis (*88*), though milder hydrolysis than we reported gives a better yield; this is presumably because of the reversal of the Meyer reaction under acid conditions (Section VII,A,1).

When we required 3-arsonopyruvate, it was similarly necessary to make the labile $-CO—CH_2—AsO_3H_2$ structure only at the last stage, and again we used periodate for this (*68*), as shown in Fig. 15. The pathway makes use of the recently emphasized (*76*) fact that when the Meyer reaction (Section VII,A,1) is performed with a 2-haloalcohol, the halide is not directly displaced by arsenite, but the alkali first causes formation of an epoxide, which is then opened by arsenite at its less hindered carbon. As with the arsonoacetaldehyde, the compound was not isolated from solution.

3. *Formation of Aminoalkylarsonic Acids*

As described in Section VII,B, 1-aminoalkylarsonic acids are probably too unstable to exist, except as minor components of an equilibrium. We needed 2-aminoethylarsonic acid as an analogue (*60*) of the natural 2-aminoethylphosphonic acid (see Section IV,B,2,a). Gough and King (*120*) specifically mention failing to make it. We therefore used the mild synthesis of primary amines shown in Fig. 16. Ammonia is an unreactive nucleophile, and its volatility prevents easy compensation for this by raising the temperature. Hence, we used aminoethanol (ethanolamine) and released the amino compound from hydroxyethylamino compound with periodate (*125*). We find that a 50% (v/v) aqueous solution of aminoethanol is the most generally useful reagent. Even compounds labile to periodate can be made in this way, if the correct quantity of periodate is used, in view of the fact that periodate cleaves 2-aminoalcohols about a thousand times faster than 1,2-diols (and also much faster than 1,2-diamines) (*126*, *127*); thus, we obtained the 2-aminoethylarsonic acid. In fact, the same approach proved useful (*63*) in making 3-aminopropylarsonic acid, even though this can be made with ammonia (*120*).

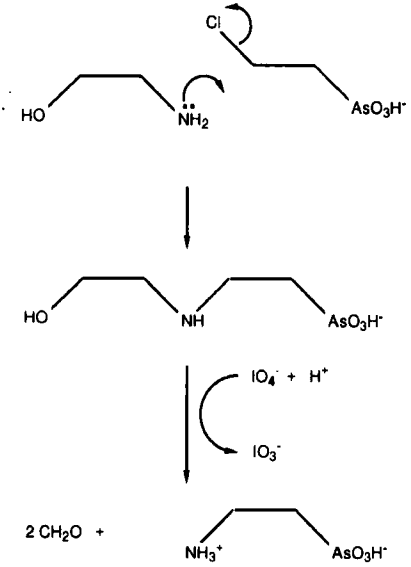

FIG. 16. The synthesis of 2-aminoethylarsonic acid using a mild synthesis of primary amines.

4. *The Inertness of 1-Haloalkylarsonic Acids*

When Schwarzenbach *et al.* used chloromethylphosphonic acid to phosphonomethylate amines, they noted (*128*, p. 1185) how slowly it reacts. The slowness is presumably due to the staggered conformation of the chloromethyl and phosphono groups, so that one of the oxygen atoms must be in the Cl—C—C plane and must hinder the approach of any nucleophile that could displace the chloride. They overcame this with long reaction times and high temperatures. In view of the lability of C—As bonds, this approach is not available with 1-haloalkylarsonic acids. Indeed, arsonochloroacetic, chloromethylarsonic, and dibromomethylarsonic acids (*129*) proved inert to substitution.

5. *Miscellaneous Techniques for Handling Arsonic Acids*

The toxic forms of arsenic are mainly (Section III,A) compounds of the type R—AsX_2, where X is a ligand that is easily displaced by thiols. Many such compounds are volatile, and this increases their hazard. As mentioned in Section VII,A,2, one such compound, Cl_2As—CH_2—$AsCl_2$, is a convenient intermediate in the synthesis of the diphosphate analogue H_2O_3As—CH_2—AsO_3H_2. Obviously, its distillation and that of any similar compound should be performed in a fume

cupboard with good ventilation. Soaking all the glassware after such a distillation in alkaline peroxide will convert the $-AsCl_2$ groups into arsono groups, and so render the compounds involatile and much less toxic.

Arsonic acids are easily detected on paper electrophoresis and chromatography by the fact that they bind Fe^{3+} tightly. Hence, they show up in the test of Wade and Morgan (*130*) for phosphates, in which the paper is sprayed with a solution of $FeCl_3$ (1%) and sulfosalicylic acid (1%). Phosphonates and arsonates show up like phosphates as white spots on a purple background, because they remove the Fe^{3+} from its purple complex with the acid. For following column effluent, a test with a similar principle may be used. The sample is mixed with a buffered, acidic solution of Fe^{3+} and azide, and the absorbance at 450 nm is diminished by phosphates and phosphonates (*52*); we have since used this method successfully with arsonates.

If there is doubt whether a spot on paper after electrophoresis is an arsonic acid, e.g., because it contains other groups that bind iron, addition of mercaptoethanol before the run to one of two spots of the substance will show the change of mobility as $-AsO_3H_2$ is reduced to $-As(—S—CH_2—OH)_2$ (compare *123*, *124*).

Many arsonic acids can be isolated by adsorption onto the acetate of a strongly basic ion-exchange resin, and elution with steps of increasing strength of acetic and formic acids. Of course, this is not good chromatography, since much sharper separations could be obtained by chromatography on these resins in a buffer of constant composition and high concentration of competing ion, but it is rapid, and often all that is needed.

VIII. Summary

Biochemical effects of arsenate and arsenite are considered in this review. Enzymes that normally act on substrates of structure $R—O—PO_3H_2$ (i.e., of oxidation state V) often act on the analogues $R—CH_2—PO_3H_2$ and $R—O—AsO_3H_2$. The further arsonic acid analogue $R—CH_2—AsO_3H_2$, which may have unusual effects, is considered.

If the action of the enzyme is to produce $R—CH_2—As(O)(OH)—OR'$ (Section IV,B,2,a), the product will spontaneously hydrolyze, because water can approach the arsenic atom as a fifth ligand in a way it cannot do with the corresponding phosphorus compound. If R'OH is a carboxylic or phosphoric acid rather than an alcohol, the hydrolysis is rapid, with a half-life of seconds or less, rather than of about half an

hour. This hydrolysis generates a new futile cycle, with regeneration of the original $R—CH_2—AsO_3H_2$, using up the donor of the R′ group, so that new ways of poisoning organisms arise.

Even if the action of the enzyme is on the R group, unusual consequences may follow, such as the release of highly toxic arsenite by an elimination reaction (Section IV,B,2,c).

Some relevant chemistry of arsonic acids is given.

ACKNOWLEDGMENTS

I thank many colleagues for helpful discussions and joint work, most especially Mr. M. J. Sparkes, and also Dr. S. R. Adams, Dr. B. R. S. Ali, Dr. M. Barrett, Miss S. Chawla, Dr. S. Freeman, Dr. K. F. Geoghegan, Dr. J. S. Edmonds, Professor P. V. Ioannou, Dr. J. J. R. Kamal, Dr. E. K. Mutenda, Dr. J. P. Quinn, Miss E. Visedo-Gonzalez, Dr. D. Webster, and many others.

REFERENCES

1. Atkins, W. R. G. *J. Marine Biol. Assoc. U.K.* **1923,** *13,* 119–150.
2. Atkins, W. R. G. *J. Marine Biol. Assoc. U.K.* **1924,** *13,* 319–324.
3. Atkins, W. R. G. *J. Marine Biol. Assoc. U.K.* **1924,** *13,* 693–699.
4. Atkins, W. R. G. *J. Marine Biol. Assoc. U.K.* **1924,** *13,* 700–720.
5. Atkins, W. R. G. *J. Marine Biol. Assoc. U.K.* **1924,** *14,* 447–467.
6. Francesconi, K. A.; Edmonds, J. S. *Adv. Inorg. Chem.*, present volume.
7. Ni Dhubhghaill, O. M.; Sadler, P. J. *Structure and Bonding* **1991,** *78,* 129–190.
8. Fleck, E. *Pure Appl. Chem.* **1988,** *60,* 431–436.
9. Falvello, L.; Jones, P. G.; Kennard, O.; Sheldrick, G. M. *Acta Cryst.* **1977,** *B33,* 3207–3209.
10. Lagunas, R. *Arch. Biochem. Biophys.* **1980,** *205,* 67–75.
11. Lagunas, R.; Pestaña, D.; Diez-Masa, J. C. *Biochemistry* **1984,** *23,* 955–960.
12. Long, J. W.; Ray, W. J. *Biochemistry* **1973,** *12,* 3932–3937.
13. Moore, S. A.; Moennich, D. M. C.; Gresser, M. J. *J. Biol. Chem.* **1983,** *258,* 6266–6271.
14. Slooten, L.; Nuyten, A. *Biochim. Biophys. Acta* **1983,** *725,* 49–59.
15. Slooten, L.; Nuyten, A. *Biochim. Biophys. Acta* **1984,** *766,* 88–97.
16. Braunstein, A. E. *Biochem. Z.* **1931,** *240,* 68–93.
17. Warburg, O.; Christian, W. *Biochem. Z.* **1939,** *303,* 40–68.
18. Teipel, J.; Koshland, D. E. *Biochim. Biophys. Acta* **1970,** *198,* 183–191.
19. Byers, L. D.; She, H. S.; Alayoff, A. *Biochemistry* **1979,** *18,* 2471–2480.
20. Scott, N.; Hatelid, K. M.; MacKenzie, N. E.; Carter, D. E. *Chem. Res. Toxicol.* **1993,** *6,* 102–106.
21. Delnomdedieu, M.; Basti, M. M.; Otvos, J. D.; Thomas, D. J. *Chemico-Biological Interactions* **1994,** *90,* 139–155.
22. Serves, S. V.; Charalambidis, Y. C.; Sotiropoulos, D. N.; Ioannou, P. V. *Phosphorus, Sulfur, and Silicon* **1995,** *105,* 109–116.
23. Doudoroff, M.; Barker, H. A.; Hassid, W. Z. *J. Biol. Chem.* **1947,** *170,* 147–150.

24. Katz, J.; Hassid, W. Z. *Arch. Biochem.* **1951,** *30,* 272–281.
25. Kline, P. C.; Schramm, V. L. *Biochemistry* **1993,** *32,* 13212–13219.
26. Stadtman, E. R.; Barker, H. A. *J. Biol. Chem.* **1950,** *184,* 769–793.
27. Fitting, C.; Doudoroff, M. *J. Biol. Chem.* **1952,** *199,* 153–163.
28. Lagunas, R.; Sols, A. *FEBS. Lett.* **1970,** *1,* 32–34.
29. Lagunas, R. *Biochim. Biophys. Acta* **1970,** *220,* 108–115.
30. Drueckhammer, D. G.; Durrwachter, J. R.; Pederson, R. L.; Crans, D. C.; Daniels, L.; Wong, C.-H. *J. Org. Chem.* **1989,** *54,* 70–77.
31. Ali, B. R. S.; Dixon, H. B. F. *Biochem. J.* **1992,** *84,* 349–352.
32. Peters, R. A.; Stocken, L. A.; Thompson, R. H. S. *Nature,* **1945,** *156,* 616–619.
33. Zahler, W. L.; Cleland, W. W. *J. Biol. Chem.* **1968,** *243,* 716–719.
34. Cruse, W. B. T.; James, M. N. G. *Acta Crystallogr.* **1972,** *B28,* 1325–1331.
35. Lin, J.; Pickart, C. M. *Biochemistry* **1995,** *34,* 15829–15837.
35a. George, G. N.; Bray, R. C. *Biochemistry* **1983,** *22,* 1013–1021.
35b. Hille, R.; Stewart, R. C.; Fee, J. A.; Massey, V. *J. Biol. Chem.* **1983,** *258,* 4849–4856.
35c. Stewart, R. C.; Hille, R.; Massey, V. *J. Biol. Chem.* **1984,** *259,* 14426–14436.
35d. Lehmann, M.; Tshisuaka, B.; Fetzner, S.; Roger, P.; Lingens, F. *J. Biol. Chem.* **1994,** *269,* 11254–11260.
35e. Gardlik, S.; Rajagopalan, K. V. *J. Biol. Chem.* **1991,** *266,* 16627–16632.
35f. Anderson, G. L.; Williams, J.; Hille, R. *J. Biol. Chem.* **1992,** *267,* 4849–4856.
36. Gladysheva, T. B.; Oden, K. L.; Rosen, B. P. *Biochemistry* **1994,** *33,* 7288–7293.
37. Ji, G. Y.; Garber, E. A. E.; Armes, L. G.; Chen, C. M.; Fuchs, J. A.; Silver, S. *Biochemistry* **1994,** *33,* 7294–7299.
38. Dey, S.; Dou, D. X.; Rosen, B. P. *J. Biol. Chem.* **1994,** *269,* 25442–25446.
39. Quinn, J. P.; McMullan, G. *Microbiology* **1995,** *141,* 721–727.
40. Engel, R. *Chem. Rev.* **1977,** *77,* 349–367.
41. Webster, D.; Jondorf, W. R.; Dixon, H. B. F. *Biochem. J.* **1976,** *155,* 433–441.
42. Southgate, C. C. B.; Dixon, H. B. F. *Biochem. J.* **1978,** *175,* 461–465.
43. Orr, G. A.; Knowles, J. R. *Biochem. J.* **1974,** *141,* 721–723.
44. Barnett, J. E. G.; Corina, D. L. *Biochem. J.* **1968,** *108,* 125–129.
45. Barnett, J. E. G.; Rasheed, A.; Corina, D. L. *Biochem. J.* **1973,** *131,* 21–30.
46. Blackburn, G. M. *Chem. Ind. (London)* **1981,** 134.
47. Blackburn, G. M.; Jakeman, D. L.; Ivory, A. J.; Williamson, M. P. *Med. Chem. Lett.* **1994,** *4,* 2573–2578.
48. McAleese, S. M.; Fothergill-Gilmore, L. A.; Dixon, H. B. F. *Biochem. J.* **1985,** *230,* 535–542.
49. Belasco, J. G.; Herlihy, J. M.; Knowles, J. R. *Biochemistry* **1978,** *17,* 2971–2978.
50. Dixon, H. B. F.; Sparkes, M. J. *Biochem. J.* **1974,** *141,* 715–719.
51. Richards, F. M.; Wyckoff, H. W.; Carlson, W. D.; Allewell, N. M.; Lee, B.; Mitsui, Y. *Cold Spring Harbor Symp. Quant. Biol.* **1971,** *36,* 35–43.
52. Ben-Yoseph, O.; Sparkes, M. J.; Dixon, H. B. F. *Analyt. Biochem.* **1993,** *210,* 195–198.
53. Roach, D. J. W.; Harrison, R. *Biochem. J.* **1981,** *197,* 731–737.
54. Webster, D.; Sparkes, M. J.; Dixon, H. B. F. *Biochem. J.* **1977,** *169,* 239–244.
55. Yount, R. G. *Advanc. Enzymol.* **1975,** *43,* 1–56.
56. Adams, S. R.; Sparkes, M. J.; Dixon, H. B. F. *Biochem. J.* **1983,** *213,* 211–215.
57. Adams, S. R.; Sparkes, M. J.; Dixon, H. B. F. *Biochem. J.* **1984,** *221,* 829–836.
58. Rozovskaya, T. A.; Chenchik, A. A.; Tarusova, N. B.; Bibilashvili, R. Sh.; Khomutov, R. M. *Mol. Biol.* **1981,** *15,* 1205–1223 (*Engl. Transl. 15,* 931–944).
59. Rozovskaya, T. A.; Rechinsky, V. O.; Bibilashvili, R. Sh.; Karpeisky, M. Ya.; Tarusova, N. B.; Khomutov, R. M.; Dixon, H. B. F. *Biochem. J.* **1984,** *224,* 645–650.

60. Visedo-Gonzalez, E.; Dixon, H. B. F. *Biochem. J.* **1989,** *260,* 299–301.
61. IUPAC-IUB Commission on Biochemical Nomenclature. *Biochem. J.* **1978,** *171,* 1–19; *Eur. J. Biochem.* **1977,** *79,* 1–9; *Hoppe-Seyler's Z. Physiol. Chem.* **1977,** *358,* 519–616; *Proc. Natl. Acad. Sci. USA* **1977,** *74,* 2222–2230; also in "Biochemical Nomenclature and Related Documents"; Portland Press: London, 1992; 2nd Ed., pp. 256–265.
62. Tamari, M.; Maget-Dana, R.; Marmouyet, J.; Douste-Blazy, L. *Biochimie* **1973,** *55,* 1311–1312.
63. Lacoste, A.-M.; Dumora, C.; Ali, B. R. S.; Neuzil, E.; Dixon, H. B. F. *J. Gen. Microbiol.* **1992,** *138,* 1283–1287.
64. IUPAC. "Nomenclature of Organic Chemistry"; Pergamon: Oxford, 1979; D-5.52, 396.
65. Seidel, H. M.; Freeman, S.; Seto, H.; Knowles, J. R. *Nature* **1988,** *335,* 457–458.
66. Bowman, E.; McQueney, M.; Barry, R. J.; Dunaway-Mariano, D. *J. Am. Chem. Soc.* **1988,** *110,* 5575–5576.
67. Seidel, H. M.; Knowles, J. R. *Biochemistry* **1994,** *33,* 5641–5646.
68. Chawla, S.; Mutenda, E. K.; Dixon, H. B. F.; Freeman, S.; Smith, A. W. *Biochem. J.* **1995,** *308,* 931–935.
69. La Nauze, J. M.; Coggins, J. R.; Dixon, H. B. F. *Biochem. J.* **1977,** *165,* 409–411.
70. Olsen, D. B.; Hepburn, T. W.; Moos, M.; Mariano, P. S.; Dunaway-Mariano, D. *Biochemistry,* **1988,** *27,* 2229–2234.
71. Olsen, D. B.; Hepburn, T. W.; Lee, S.-l.; Martin, B. M.; Mariano, P. S.; Dunaway-Mariano, D. *Arch. Biochem. Biophys.* **1992,** *296,* 144–151.
72. Chawla, S.; Dixon, H. B. F. *J. Enzym. Inhib.* **1995,** *8,* 255–259.
73. La Nauze, J. M.; Rosenberg, H. *Biochim. Biophys. Acta* **1968,** *165,* 438–447.
74. La Nauze, J. M.; Rosenberg, H.; Shaw, D. C. *Biochim. Biophys. Acta* **1970,** *212,* 332–350.
75. Mutenda, E. K.; Sparkes, M. J.; Dixon, H. B. F. *Biochem. J.* **1995,** *310,* 983–988.
76. Tsivgoulis, G. M.; Sotiropoulos, D. N.; Ioannou, P. V. *Phosphorus, Sulfur, and Silicon* **1991,** *57,* 189–193.
77. Tsivgoulis, G. M.; Sotiropoulos, D. N.; Ioannou, P. V. *Phosphorus, Sulfur, and Silicon* **1991,** *63,* 329–334.
78. Serves, S. V.; Tsivgoulis, G. M.; Sotiropoulos, D. N.; Ioannou, P. V. *Phosphorus, Sulfur, and Silicon* **1992,** *71,* 99–105.
79. Serves, S. V.; Sotiropoulos, D. N.; Ioannou, P. V.; Jain, M. K. *Phosphorus, Sulfur, and Silicon* **1993,** *81,* 181–190.
79a. Supuran, C. T.; Serves, S. V.; Ioannou, P. V. *J. Inorg. Biochem.* **1996,** *62,* 207–212.
80. Serves, S. V.; Sotiropoulos, D. N.; Ioannou, P. V.; Mutenda, E. K.; Sparkes, M. J.; Dixon, H. B. F. *Phosphorus, Sulfur, and Silicon* **1995,** *101,* 75–82.
81. Vas, M. *Eur. J. Biochem.* **1990,** *194,* 639–645.
82. Biryukov, A. I.; Ishmuratov, B. Kh.; Khomutov, R. M. *FEBS Lett.* **1978,** *19,* 249–252.
83. Jacobsen, N. E.; Bartlett, P. A. *J. Am. Chem. Soc.* **1981,** *103,* 654–657.
84. Suzuli, H. *J. Biochem.* **1994,** *115,* 623–628.
85. Cull-Candy, S. G.; Donnellan, J. F.; James, R. W.; Lunt, G. G. *Nature* **1976,** *262,* 408–409.
86. Sparkes, M. J.; Kamal, J. J. R.; Nayeem, N.; Dixon, H. B. F. *Eur. J. Biochem.* **1990,** *194,* 376.
87. Adams, S. R. Ph.D. thesis, 1985, University of Cambridge.
88. Ali, B. R. S.; Dixon, H. B. F. *Eur. J. Biochem.* **1993,** *215,* 161–166.

89. Dasgupta, M.; Dive, C.; Sansom, C. E.; Schwalbe, C. H.; Freeman, S.; Dixon, H. B. F. *J. Pharm. Pharmacol.* **1990,** *42,* 175P.
90. Freeman, S.; Pollack, S. J.; Knowles, J. R. *J. Am. Chem. Soc.* **1992,** *114,* 377–378.
91. Nayeem, N. Unpublished observations.
92. Couée, I.; Dixon, H. B. F.; Tipton, K. F. *J. Enzym. Inhib.* **1991,** *4,* 365–368.
93. Borisov, V. V.; Borisova, S. N.; Sosfenov, N. I.; Dixon, H. B. F. *Mol. Biol.* **1983,** *17,* 705–713.
94. Falzone, C. J.; Karsten, W. E.; Conley, J. D.; Viola, R. E. *Biochemistry* **1988,** *27,* 9089–9093.
95. John, R.; Fasella, P. *Biochemistry* **1969,** *8,* 4477–4482.
96. Ueno, H.; Likos, J. J.; Metzler, D. E. *Biochemistry* **1982,** *21,* 4387–4393.
97. Likos, J. J.; Ueno, H.; Feldhaus, R. W.; Metzler, D. E. *Biochemistry* **1982,** *21,* 4377–4386.
98. Rose, J. E.; Leeson, P. D.; Gani, D. *J. Chem. Soc. Perkin Trans. 1* **1994,** 3089–3094.
99. Khristoforov, R. R.; Sukhareva, B. S.; Dixon, H. B. F.; Sparkes, M. J.; Krasnov, V. P.; Bukrina, I. M. *Biochem. Mol. Biol. Int.* **1995,** *36,* 77–85.
100. Kluger, R.; Nakaoka, K.; Tsui, W.-C. *J. Am. Chem. Soc.* **1978,** *100,* 7388–7392.
101. Nicklin, P. L.; Irwin, W. J.; Hassan, I. F.; Mackay, M.; Dixon, H. B. F. *Biochim. Biophys. Acta* **1995,** *1269,* 176–186.
102. Quinn, J. P.; McMullan, G. *Microbiology* **1995,** *141,* 721–727.
103. Meyer, G. *Ber. Dtsch. Chem. Ges.* **1883,** *16,* 1439–1443.
104. Serves, S. V.; Sotiropoulos, D. N.; Ioannou, P. V.; Dixon, H. B. F. *Phosphorus, Sulfur, and Silicon* **1994,** *90,* 103–109.
105. Adams, S. R. Ph.D. thesis, Cambridge University, 1985, pp. 124–144.
106. Cannon, J. R.; Edmonds, J. S.; Francesconi, K. A.; Taston, C. L.; Saunders, J. B.; Skelton, B. W.; White, A. H. *Aust. J. Chem.* **1981,** *34,* 787–798.
107. McBrearty, C. F.; Irgolic, K.; Zingaro, R. A. *J. Organometal. Chem.* **1968,** *12,* 377–387.
108. Irgolic, K.; Zingaro, R. A.; Smith, M. R. *J. Organometal. Chem.* **1966,** *6,* 17–24.
109. Cadet, L. C. *Mémoires de Mathematique et de Physique Présentés à l'Académie Royale des Sciences* **1760,** *3,* 623–637.
110. Popp, F. *Chem. Ber.* **1949,** *82,* 152–156.
111. Titov, A. I.; Levin, B. B. *Sb. Statei Obshch. Khim.* **1953,** *2,* 1469–1472 (*Chem. Abstr. 49,* 4503).
112. Khomutov, R. M.; Osipova, T. I. *Izv. Akad. Nauk SSSR, Ser. Khim.* **1978,** 1951 (*Chem. Abstr. 89,* 197655).
113. Baylis, E. K.; Campbell, C. D.; Dingwall, J. G.; Pickles, W. *ACS Symp Ser.* **1981,** *171,* 183–186.
114. Laber, B.; Amrhein, N. *Biochem. J.* **1987,** *248,* 351–358.
115. Dixon, H. B. F.; Giddens, R. A.; Harrison, R. A.; Henderson, C. E.; Norris, W. E.; Parker, D. M.; Perham, R. N.; Slater, P.; Sparkes, M. J. *J. Enzym. Inhib.* **1991,** *5,* 111–117.
116. Baillie, A. C.; Wright, B. J.; Wright, K. Eur. Patent Appl. 1980, 9348.
117. Baillie, A. C.; Wright, B. J.; Wright, K.; Earnshaw, C. G. *Pesticide Biochem. Physiol.* **1988,** *30,* 103–112.
118. Stribling, D. *Biochem. J.* **1974,** *141,* 725–728.
119. Clark, V. M.; Hutchinson, D. W.; Kirby, A. J.; Warren, S. G. *Angew. Chem. Int. Ed. Eng.* **1964,** *3,* 678–685.
120. Gough, G. A. C.; King, H. *J. Chem. Soc.* **1928,** 2426–2447.
121. Nekrassow, W. W.; Nekrassow, A. S. *Ber. Dtsch. Chem. Ges.* **1928,** *61,* 1816–1821.

122. Scherlin, S. M.; Epstein, G. *Ber. Dtsch. Chem. Ges.* **1928,** *61,* 1821–1825.
123. Barber, H. J. *J. Chem. Soc.* **1929,** 1020–1024.
124. Barber, H. J. *J. Chem. Soc.* **1929,** 1024–1026.
125. Geoghegan, K. F.; Dixon, H. B. F. *Biochem. J.* **1989,** *260,* 295–297.
126. Barlow, C. B.; Guthrie, R. D.; Prior, A. M. *J. Chem. Soc. Chem. Commun.* **1966,** 268.
127. Fields, R.; Dixon, H. B. F. *Biochem. J.* **1968,** *108,* 883–887.
128. Schwarzenbach, G.; Ackermann, H.; Ruckstuhl, P. *Helv. Chim. Acta* **1949,** *32,* 1175–1186.
129. Sparkes, M. J.; Dixon, H. B. F. *Microbiology* **1995,** *141,* 726–727.
130. Wade, H. E.; Morgan, D. M. *Nature* **1953,** *171,* 529–530.

This Page Intentionally Left Blank

ADVANCES IN INORGANIC CHEMISTRY, VOL. 44

INTRINSIC PROPERTIES OF ZINC(II) ION PERTINENT TO ZINC ENZYMES

EIICHI KIMURA and TOHRU KOIKE

Department of Medical Chemistry, School of Medicine, Hiroshima University, Hiroshima 734, Japan

I. Introduction

Zinc(II) ion is a biologically essential element. Knowledge of its importance is increasing, as more and more enzymes are shown to contain zinc(II) ion at the active center. Carbonic anhydrase, carboxypeptidase A, thermolysin, angiotensin coverting enzyme, aminopeptidase, superoxide dismutase, yeast aldolase, β-lactamase II, alcohol dehydrogenase, nucleic acid polymerase, alkaline phosphatase, phospholipase C, and P1 nuclease may be classified as classic zinc enzymes (*1*). More recently added are phosphotriesterase (or "organophosphorus hydrolase," which has a binuclear active center and hydrolyzes pesticides and nerve gases) (*2*); the *hedgehog* family of secreted signaling proteins (*3*); collagenase (a member of the matrix metalloproteinase family) (*4*); and so on. There are now more than 300 known zinc enzymes (*1d*). The X-ray crystallographic structures of a considerable number of zinc enzymes have now been established. Many of the zinc(II) ions in those enzyme active sites are coordinated by three amino acid residues (His, Glu, Cys) and sometimes H_2O (see Fig. 1) (*5*). The Zn^{II}-bound H_2O may be activated by deprotonation (or polarization) for nucleophilic attack toward the substrates, or poised for displacement with another strong

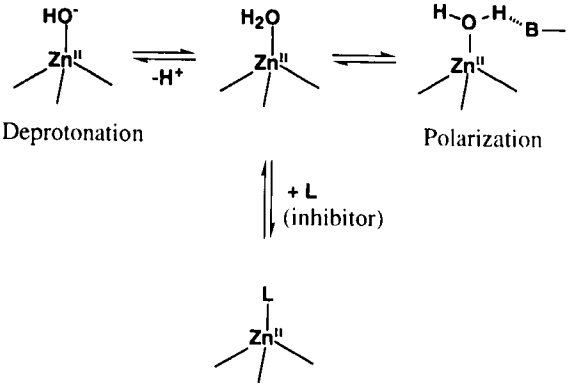

FIG. 1. Activation of zinc(II)-bound water and inhibitor binding to zinc(II) in zinc enzyme.

ligand, inhibitors: e.g., sulfonamide, alcohol, thiol, phosphate, or phenol.

Earlier, we have reviewed the most fundamental properties about zinc(II)'s nucleophilicity and the basicity of $L—Zn^{II}—OH^-$ (L = model ligands such as macrocyclic polyamines or tris(pyrazolyl)borate) (*6*). More recent model studies by us and other groups have been trying to answer further questions: (i) Why (or how) is serine needed in alkaline phosphatase? More indirectly, what are the points of the serine OH group intervening as acyl- or phosphoryl-transfer agents? (ii) Why is a bimetallic system favorable for phosphate hydrolysis? (iii) Why does nature adopt zinc(II) as a Lewis acid in zinc enzymes or imidazole as a Lewis base (in the serine–imidazole–carboxylate triad) in serine enzymes? (iv) Why are four zinc(II)-bound cysteines used for demethylation (repair) of methyl-DNA phosphotriester, damaged DNA? In this review, we want to present the latest results related to these puzzles.

II. Why Zinc(II) and Serine in Alkaline Phosphatase?

Alkaline phosphatase (AP) is a $(Zn^{II})_2$-containing phosphomonoesterase that hydrolyzes phosphomonoesters ($RO—PO_3^{2-}$) at alkaline pH (*7*). Ser_{102} under the influence of one of the zinc(II) ions at the active center **1** (Fig. 2) is directly involved in phosphate hydrolysis (*8*). On the basis of X-ray structure and NMR studies (*9*), the mechanism now accepted is that the phosphate substrate, initially recognized by cooperative

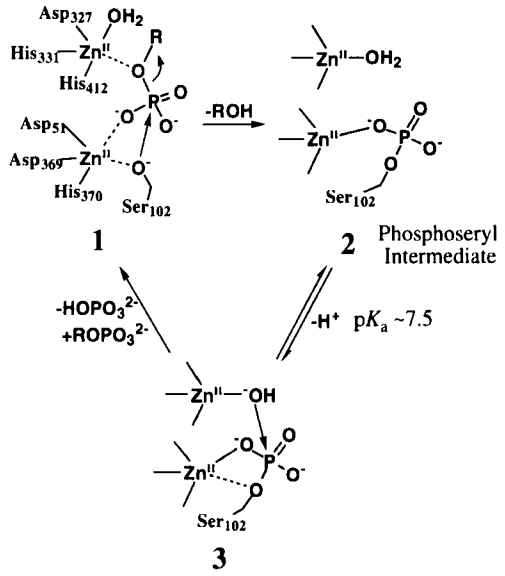

FIG. 2. Phosphomonoester hydrolysis at active center of alkaline phosphatase.

action of the two zinc(II) ions, is attacked by the Zn^{II}-activated Ser_{102} to yield a transient phosphoseryl intermediate **2**, which intramolecularly reacts with the adjacent Zn^{II}-activated water (see **3**) to complete the hydrolysis and regenerate the free form of Ser_{102}, thus completing the catalytic cycle. Several interesting chemical questions would be raised concerning this mechanism: (i) Why are two zinc(II) essential? (ii) How does the Ser_{102} hydroxyl group become a nucleophile upon association with the zinc(II) ion? (iii) What is the special chemical advantage of forming the phosphoseryl intermediate **2** by such an indirect hydrolysis? In most of the past metalloenzyme models, e.g., for carbonic anhydrase (*10–13*), β-lactamase II (*14*), and carboxypeptidase A (*15*), the nucleophiles were metal hydroxide species ($M—OH^-$).

As early as 1972, Sigman and Jorgensen used a ternary zinc(II) complex of *N*-(2-hydroxyethyl)ethylenediamine **4** and 4-nitrophenyl picolinate **5** as a model for Zn^{II}-alkoxide-promoted transesterification (see Scheme 1) (*16*). Although the Zn^{II}-bound alkoxide (its pK_a kinetically determined to be 8.4) was shown to be a possible reactive species to give **6**, the subsequent hydrolysis for completion of the ester hydrolysis as well as the catalytic cycle failed.

In 1994, we built a 12-membered macrocyclic triamine ([12]aneN_3)

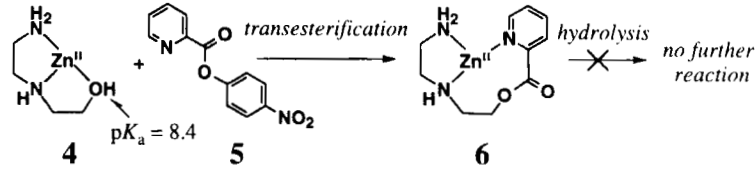

SCHEME 1.

appended with a hydroxyethyl group **7** and its zinc(II) complex **8** as a serine-containing zinc enzyme model (*17*). Earlier, a zinc(II) complex with [12]aneN$_3$ **9** was shown to yield a Zn^{II}-OH^- nucleophile as shown in hydrolytic zinc enzymes such as carbonic anhydrase (*12a*) and phosphatase (*18*). The Zn^{II}-bound OH^- species **9b** is generated at physiological pH with a pK_a value of 7.3 and acts as a good nucleophile toward the electrophilic center of the substrates (e.g., carboxy esters; see Scheme 2). Likewise, **7** yielded a 1:1 zinc(II) complex **8**, where the alcoholic OH deprotonated with a pK_a value of 7.4 (for **8a** $\rightleftarrows$ **8b** + H^+). The Zn^{II}-bound alkoxide complex **8b** was isolated as a dimeric form, which dissociates into monomeric species in aqueous solution to make a very reactive nucleophile and catalyzes hydrolysis of 4-nitrophenyl acetate (NA) (see Scheme 3). Through a kinetic study of NA hydrolysis with **8b** in 10% (v/v) CH_3CN at 25°C and pH 9.3 (20 m*M* CHES buffer) with I = 0.10 ($NaNO_3$), a second-order rate constant of 0.14 $M^{-1}sec^{-1}$, which is four times greater than the corresponding value of 3.6 × 10^{-2} by the Zn^{II}–[12]aneN$_3$ complex **9b** under the same conditions, was established.

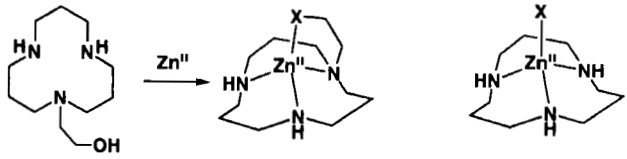

A comparison of NA hydrolysis by **8** and **9** shows for the first time that Zn^{II}-bound alkoxides may lead to better nucleophiles than Zn^{II}-bound hydroxides in an aqueous environment. Unless the alkoxide anion is bound to zinc(II) ion, it may rather work as a general base to yield hydroxide, which then yields the active nucleophile. Hence, zinc(II) ion may be viewed as an alkoxide-protecting agent. It is of

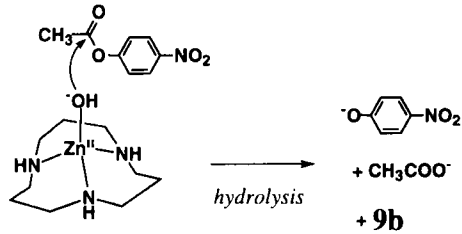

9b
good nucleophile

SCHEME 2.

interest to point out that the basicity of the alkoxide in **8b** (pK_a = 7.4) is almost the same as that of the hydroxide in **9b** (pK_a = 7.3 for **9a** $\rightleftarrows$ **9b** + H^+). Zinc(II) ion thus plays a dual role. Moreover, with **8b**, the initial reaction was an acetyl-transfer from the substrate, 4-nitrophenyl acetate (NA), to the pendent alkoxide, yielding a transient *O*-acetylated intermediate **10**, which was unambiguously identified by independent synthesis of **10** from **8b** and acetic anhydride. **10** was then very rapidly hydrolyzed in aqueous solution. It is of biological interest to refer to a recent kinetic study of the NA hydrolysis by Ser_{102}-mutated alkaline phosphatase (*8*). The displacement of Ser_{102} by leucine or alanine opens up a ligand site for water. Thus, a Zn^{II}-activated water (i.e., Zn^{II}—OH^-) may well be positioned for a direct attack at the electrophilic P atom. These mutant enzymes still catalyze the hydrolysis of phosphate monoester with similar Michaelis–Menten and inhibition constants, although the catalytic efficiency is 1/1000–1/500 that of the wild-type enzymes. This fact implies weaker nucleophilicity of Zn^{II}—OH^- with respect to Zn^{II}–serine.

For reaction between **8b** and NA, the activation energy E_a was 51

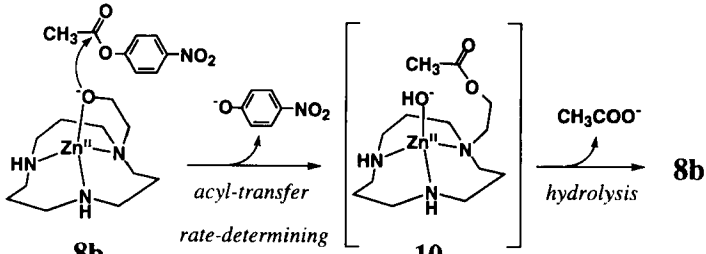

8b
better nucleophile

10
acyl-intermediate

SCHEME 3.

kJ mol^{-1} and the frequency factor (A) 1.2×10^8 $M^{-1}sec^{-1}$, whereas for the **9b** reaction, E_a was estimated to be 49 kJ mol^{-1} and A to be 1.4×10^7 $M^{-1}sec^{-1}$ (*17*). In both reactions, almost no isotope effect was observed in D_2O solution, which implies that the Zn^{II}-bound alkoxide (**8b**) and hydroxide (**9b**) both directly and efficiently attack NA. Besides, if the alkoxide in **8b** *indirectly* (via H_2O) attacks at the substrate, the product should not be **10**, but acetate anion, which was not the case. Since O^- anion nucleophilic attack is the rate-determining step, the faster rate with **8b** may be accounted for by the Zn^{II}—^-OR site being *more naked* (i.e., less solvated because of steric hindrance from the lipophilic ethylene group attached to the O^- anion), whereas the Zn^{II}—OH^- in **9b** is more efficiently solvated and better shielded. This interpretation also agrees with the larger frequency factor (i.e., collision frequency) for **8b** over **9b**. In support of this rationalization, an X-ray study showed that **9b** readily precipitates from aqueous solution as a trimer **11** with three intermolecular hydrogen bonds (*12a*).

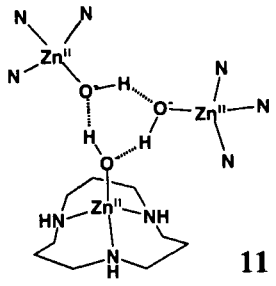

11

The labile character of the Zn^{II}—^-OR species **8b** (although isolable as crystals, **8b** is stable only at a limited alkaline pH region in aqueous solution) and the vulnerability of the acyl intermediate **10** in aqueous solution prevented more extensive, quantitative studies about the nature of Zn^{II}-bound alkoxide.

It had been discovered that the Zn^{II}–cyclen complex **12** also provided a Zn^{II}—OH^- species **12b**, with pK_a value of 7.9 (25°C and I = 0.1), which is also a good nucleophile to catalyze NA hydrolysis (*18*). An advantage of cyclen for **12** over [12]aneN_3 for **9** as a ligand is that zinc(II) ion is more firmly held in the macrocyclic cavity of **12**, i.e., a 1 : 1 ZnL complex is much more stable with cyclen (K(ZnL) = [ZnL]/[Zn^{II}][L] = $10^{15.3}$) than in that of [12]aneN_3(K(ZnL) = $10^{8.4}$). As a consequence, we could study the reactivity of ZnL in a wider range of pH without observing any degradation of the zinc(II) complex. Accordingly,

an alcohol-pendent cyclen zinc(II) complex **13** was synthesized as a more stable model (*19*).

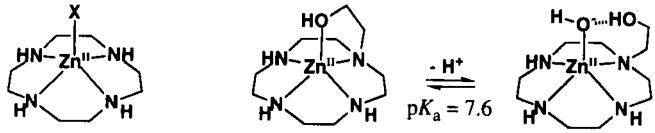

12a: X = H_2O **13** **14**
b: X = HO^-

The potentiometric pH titration disclosed monodeprotonation with a pK_a value of 7.6 at 25°C. On the basis of NMR spectroscopic and anion-binding studies of **13**, the monodeprotonated species was assigned to the OH^--bound ZnL complex **14**, rather than the pendent alkoxide complex as seen with [12]aneN_3 **8b**. Nevertheless, among all past zinc(II) complexes, **14** seems to be the most active catalyst for NA hydrolysis. From kinetic studies in 10% (v/v) CH_3CN at 25°C and pH 6.4–9.5 with I = 0.1, where the zinc(II) complex remains stable either as **13** or **14**, the rate–pH profile gave a sigmoidal relationship with an inflection point (i.e., kinetic pK_a) at pH 7.7, which almost corresponds to the pK_a value for the **13** ⇄ **14** equilibrium (see Fig. 3). The second-order (first-order each in [**14**] and [NA]) rate constant of 0.46 $M^{-1}sec^{-1}$ is ca. 10 times greater than the corresponding value of 4.7×10^{-2} M^{-1} sec^{-1} for a reference *N*-methylcyclen–Zn^{II}—OH^- **15b** (pK_a for **15a** ⇄ **15b** is 7.6 at 25°C with I = 0.1) (*19*). Furthermore, NA is hydrolyzed

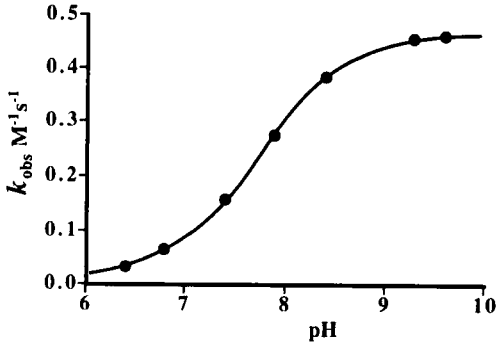

FIG. 3. Rate–pH profile for the second-order rate constants (k_{obs}) of 4-nitrophenyl acetate hydrolysis with alcohol–pendent cyclen zinc(II) complex at 25°C and [**13**] + [**14**] = 1 mM in 10% (v/v) CH_3CN.

through a double displacement of the acetyl group (see Fig. 4), as found with the triamine case **8b** (Scheme 1). In the initial rate-determining reaction, the pendent alcoholic OH "activated" by the adjacent base (i.e., Zn^{II}—OH^-) attacks NA to yield an "acyl intermediate" **16**. This intermediate **16a** was independently synthesized by the reaction of **13** with acetic anhydride in CH_3CN. In the subsequent reaction, **16** is subject to extremely fast hydrolysis ($t_{1/2}$ = 6 sec at 25°C and pH 9.3). A plot of the observed first-order rate constant against pH (= 6.1–9.3) for the second reaction gave a sigmoidal relationship with its inflection point at pH 7.7, which is similar to the pK_a of the Zn^{II}–cyclen complex **13**. Accordingly, it was concluded that the *very fast* nucleophilic attack of the Zn^{II}—OH^- **16b** occurred at the intramolecular acetyl group. Thus, the overall NA hydrolysis by **14** is catalytic. This study demonstrated that the Zn^{II}-bound OH^- plays a dual role: (i) as a general base in the first acyl-transfer reaction to activate the remote alcoholic OH, and (ii) as a nucleophile to attack the proximate electrophilic carbonyl group in the second hydrolysis step. This, along with an earlier result with the [12]aneN_3 complex **8**, led to the conclusion that alcoholic OH can be a better nucleophile than water when it is activated either directly (**8b**) or indirectly (**14**) by zinc(II) ion. The alcoholic OH group

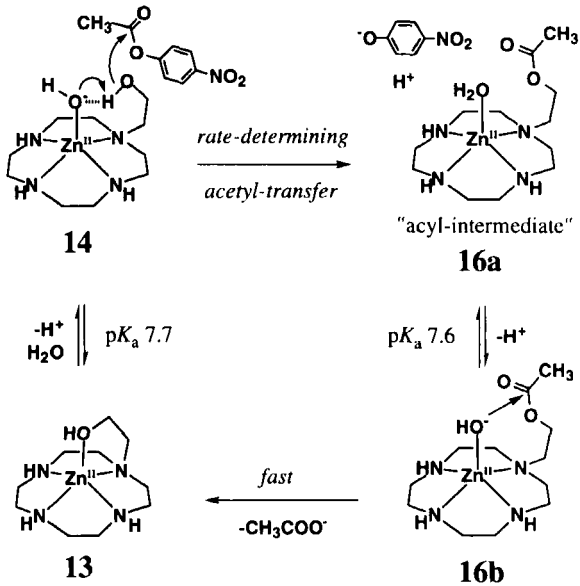

FIG. 4. An overall reaction mechanism for 4-nitrophenyl acetate hydrolysis catalyzed by alcohol–pendent cyclen zinc(II) complex 14.

(serine, threonine) in zinc enzymes, which lies in the outer zinc(II) coordination sphere, may thus be activated by the Zn^{II}—OH^- general base.

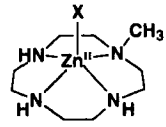

15a: X = H_2O
b: X = HO^-

The reaction of **14** may remind one of the well-established reaction mechanism for chymotrypsin (Fig. 5) (*20*). By comparing the acyl-transfer reaction of complex **14** with that of chymotrypsin **17**, we find that the alcoholic nucleophiles in **14** and **17** are activated by Zn^{II}—OH^- and imidazole (in a triad), respectively. Several common features should be pointed out: (i) Both reactions proceed via "two-step reaction" (i.e., double displacement). (ii) The basicity of Zn^{II}—OH^- (pK_a = 7.7) is somewhat similar to that of imidazole (pK_a = ca. 7). (iii) The initial acyl-transfer reactions to alcoholic OH groups are rate determining. (iv) In NA hydrolysis with chymotrypsin, the pH dependence of both the acylation (**17** → **18**) and the deacylation (**19** → **17**) steps point to the involvement of a general base or nucleophile with a kinetically revealed pK_a value of ca. 7. A major difference here is that while the

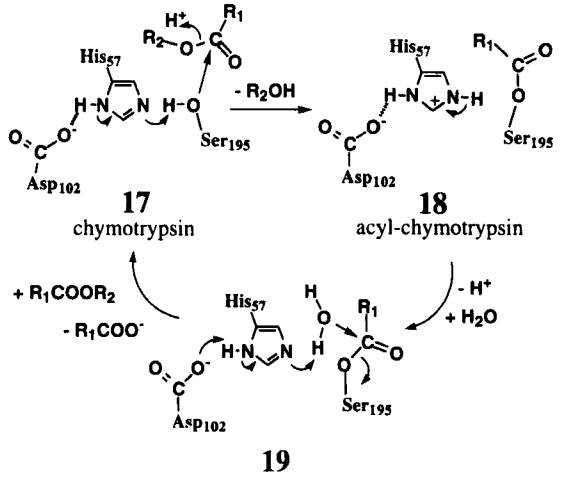

FIG. 5. Reaction mechanism for carboxyl ester hydrolysis by chymotrypsin.

active center of chymotrypsin involves three components, a catalytic triad Asp–His–Ser, the zinc(II) macrocyclic complex models are made of two components, zinc(II)–alcohol. Remembering an earlier report that 4-hydroxymethyl imidazole **20** is ca. four times less reactive than imidazole itself toward NA (*21*), we were brought to a basic question: What is the difference between imidazole and Zn^{II}—OH^-? Table I summarizes the second-order rate constants for cleavage of various ester bonds with imidazole and Zn^{II}—OH^- species. Inspection reveals that imidazole is a better catalyst than Zn^{II}—OH^- species for NA hydrolysis. In the reaction of imidazole, a major pathway may be the direct nucleophilic attack of imidazole at the carbonyl in the rate-determining step, followed by fast hydrolysis of the acyl intermediate **21** (see Fig. 6) (*22*). As expected for such a mechanism, the catalytic rate constant for imidazole is the same in D_2O as in H_2O. On the other hand, for hydrolysis of methyl acetate and bis(4-nitrophenyl)phosphate (BNP^-), the Zn^{II}—OH^- species are better nucleophiles than imidazole (see Table I). It may thus be concluded that imidazole is a superior nucleophile to neutral carboxyesters with good leaving alcohols (i.e., less basic alkoxides), whereas the Zn^{II}—OH^- species are better nucleophiles toward neutral carboxyesters with poor leaving alcohols (i.e., more basic alkoxides) and toward anionic substrates such as phosphodiester anions. An advantage of Zn^{II}—OH^- as a nucleophile attacking methyl acetate is that its real active species is OH^-, and accordingly it reacts like a strong base OH^-. This means that the strong base methoxide anion can be displaced and be permitted to leave from methyl acetate upon hydrolysis. Another advantage of the Zn^{II}—OH^- nucleophile in anionic phosphodiester hydrolysis is that zinc(II) as a cation facilitates the access of OH^- to the anionic substrate and stabilizes the reaction's anionic intermediate.

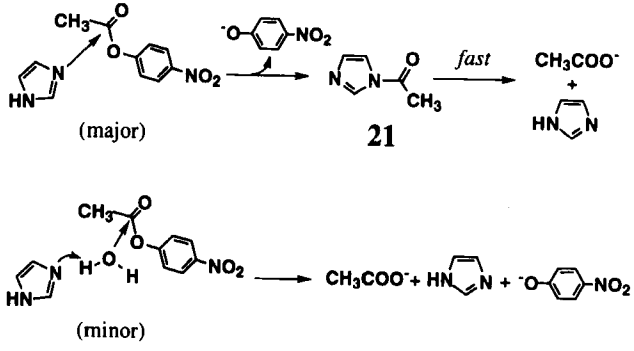

FIG. 6. Reaction mechanism for 4-nitrophenyl acetate hydrolysis by imidazole.

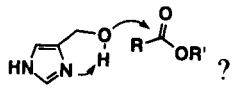

20

A zinc(II) complex **22a** with an alcohol-pendent polyamine has been synthesized (*23*). The alcoholic OH deprotonates with pK_a of 8.6 (determined by pH-metric titration), yielding **22b**. Reaction of **22** (2 mM) with a phosphotriester diethyl(4-nitrophenyl) phosphate (0.1 mM) in 10 mM TAPS buffer (pH 8.6) at 25°C seemed to promote phosphoryl-transfer reactions to **23**, just like acyltransferred intermediates **10** and **16a** in the reactions between Zn^{II}–macrocyclic complexes with an alcohol pendent and NA (see Scheme 4). The pH dependence of the first-order rate constants gave a sigmoidal curve with an inflection point around the pK_a value of 8.6. The hydrolysis of the substrate phosphotriester to the phosphodiester product diethyl phosphate thus seemed to

TABLE I

COMPARISON OF SECOND-ORDER RATE CONSTANTS ($M^{-1}sec^{-1}$) IN HYDROLYSIS (OR ACETYL AND PHOSPHORYL TRANSFER) OF 4-NITROPHENYL ACETATE, METHYL ACETATE AND BIS(4-NITROPHENYL) PHOSPHATE

	Substrates		
Nucleophile	4-Nitrophenyl acetate[a] k(NA)	Methyl acetate[b] k(MA)	Bis(4-nitrophenyl) phosphate k(BNP^-)
Zn^{II}–[12]aneN_3–OH^- **9b**	0.04	3.6×10^{-4}	8.5×10^{-5}[c]
Zn^{II}–cyclen–OH^- **12b**	0.10	3.6×10^{-4}	2.1×10^{-5}[c]
OH^-_{aq}	8.1		2.4×10^{-5}[c]
Imidazole	0.38	$<10^{-5}$	No reaction[d]
14b	0.46[e]		5.0×10^{-4}[d,f]
15b	0.05		5.2×10^{-6}[d]
24b	0.31[e]		6.5×10^{-4}[d,f]
	(1.1×10^2)[g]		(1.1)[h]

[a] In 10% (v/v) CH_3CN at 25°C with I = 0.10 ($NaNO_3$).
[b] In aqueous solution at 25°C with I = 0.10 ($NaNO_3$).
[c] In aqueous solution at 35°C with I = 0.20 ($NaClO_4$).
[d] In aqueous solution at 35°C with I = 0.10 ($NaNO_3$).
[e] Acetyl transfer rate, which is equivalent to hydrolysis rate constant.
[f] Phosphoryl transfer rate constant.
[g] In DMF at 35°C. Acetyl transfer rate constant.
[h] In DMF at 35°C. Phosphoryl transfer rate constant.

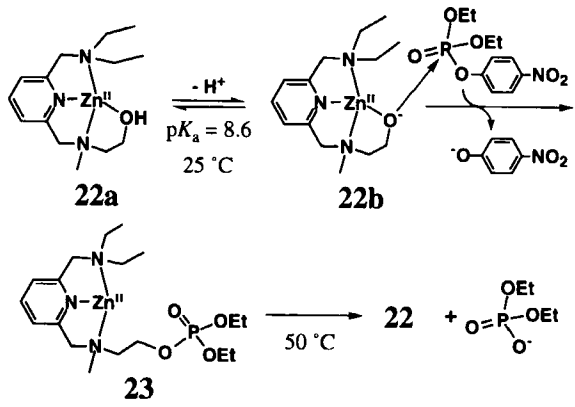

SCHEME 4.

occur via a phosphoryl-transfer step. The mechanism of the subsequent hydrolysis step (**23** → **22**) was not clarified. However, those presented for **10** and **16** hydrolysis would be applicable.

Unequivocal evidence for intermediation of phosphoryl transfer and a more detailed picture for the hydrolysis of phosphate esters by the Zn^{II}-activated alcohols was recently provided by another model reaction between **24** and bis(4-nitrophenyl)phosphate (BNP^-) (see Fig. 7) (*24*). The pK_a value of the pendent alcohol (**24a** ⇄ **24b**) was determined by potentiometric pH titration to be 7.30 at 35°C. Both the acidic (**24a**) and basic forms (**24b**) were isolated as crystals. The X-ray crystal structure of **24b** shows the alkoxide being closely coordinated (Zn—O^- bond length of 1.91 Å) at the fifth coordination site. *Again, the Zn^{II}-bound alkoxide anion in **24b** was proven to be a more reactive nucleophile than a reference (N-methylcyclen)Zn^{II}—OH^- species **15b**.* In the kinetic study with **24** in aqueous solution (pH 6.0–10.3) at 35°C with I = 0.10, the rate–pH profile for the phosphoryl-transfer reaction from BNP^- (to **25**) gave a sigmoidal curve with an inflection point at pH 7.4, corresponding to the pK_a value for **24a** ⇄ **24b**. *The second-order rate constant k(BNP^-) of 6.5 × 10^{-4} $M^{-1}sec^{-1}$ is 125 times greater than the corresponding value of 5.2 × 10^{-6} $M^{-1}sec^{-1}$ for the BNP^- hydrolysis (to 4-nitrophenyl phosphate) by **15b**.* The rate constants of the BNP^- ester bond cleavage with various nucleophiles are compared in Table I. The Zn^{II}–alkoxide complex **24b** is the strongest nucleophile. The product of the nucleophilic attack by **24b** is the alcohol-phosphorylated species **25**, which was unequivocally determined by independent isolation of

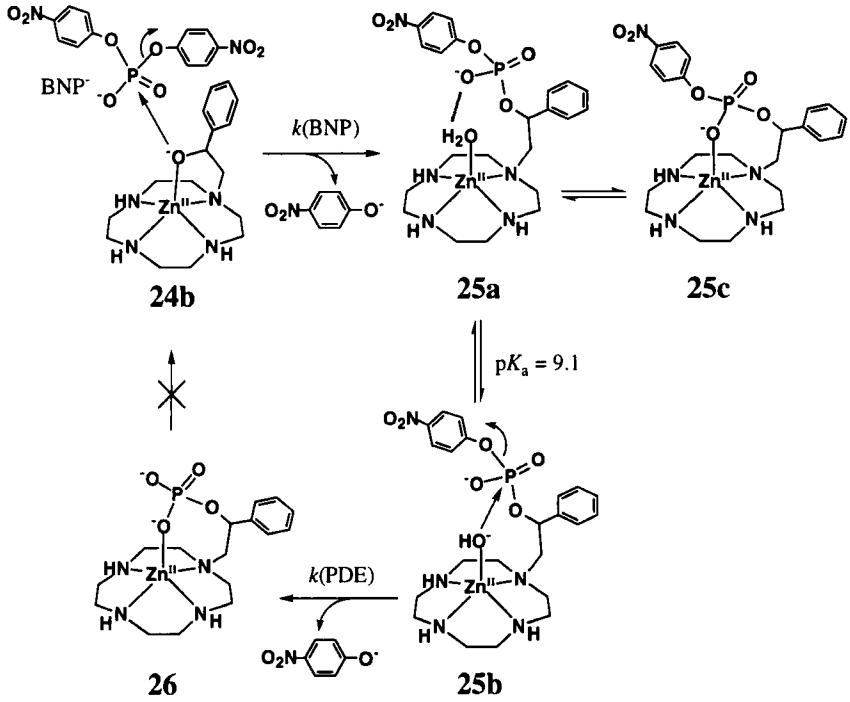

FIG. 7. Reaction mechanism for P—O ester bond cleavage of bis(4-nitrophenyl) phosphate by alkoxide–pendent cyclen zinc(II) complex.

crystalline **25a** · ClO_4 by reacting **24b** with BNP^- in dimethylformamide (DMF).

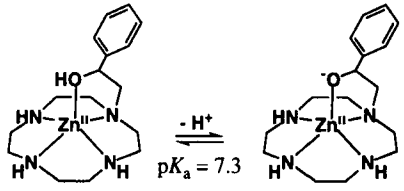

Kinetics of the reaction between BNP^- and **24b** · ClO_4 in dry DMF at 35°C was studied (*24*). The second-order rate constant $k(BNP^-)$ of 1.1 $M^{-1}sec^{-1}$ with respect to $[BNP^-]$ and [**24b**] was obtained. Comparison of the rate constants $k(BNP^-)$ in DMF and aqueous solution showed that the Zn^{II}-bound alkoxide nucleophile acts 1700 times more effectively in this aprotic solvent than in water, which is accounted for by a

lower solvation in DMF than in H_2O. The observation with this model suggests that the phosphoryl-transfer reactions at the enzyme active center might occur quite effectively in hydrophobic environments. It should also be pointed out that a second-order rate constant of 1.1×10^2 $M^{-1}sec^{-1}$ for the reaction of NA with **24b** in DMF (yielding acetyl-transferred intermediate **25**) is also 350 times greater than that of 0.31 $M^{-1}sec^{-1}$ in aqueous solution at 25°C (yielding the hydrolyzed product).

The potentiometric pH titration of **25a** at 35°C with $I = 0.10$ using 0.10 M aqueous NaOH (done quickly before the subsequent hydrolysis could occur to any extent) showed the monodeprotonation with a pK_a value of 9.1, which was assigned to the **25a** $\rightleftarrows$ **25b** equilibrium. The pK_a value was higher than that of 7.3 for **24a** under the same conditions, which is ascribable to the proximate phosphate anion interaction with zinc(II) (like **25c**). The pendent phosphodiester in **25b** underwent spontaneous hydrolysis in alkaline buffer to yield a phosphomonoester-pendent zinc(II) complex **26**. Plots of the first-order rate constants vs pH (= 7.5–10.5) gave a sigmoidal curve with an inflection point at pH 9.0, which is almost the same as the pK_a value for **25a**. Hence, it is concluded that the pendent phosphodiester underwent an intramolecular nucleophilic attack by the Zn^{II}-bound OH^- in **25b**. The first-order rate constant k(PDE) for **25b** $\rightarrow$ **26** is 3.5×10^{-5} sec^{-1} at 35°C with $I = 0.10$. As a reference to this intramolecular hydrolysis, ethyl (4-nitrophenyl) phosphate (NEP^-) was intermolecularly hydrolyzed by **15b**. In this case, the second-order rate constant $k(NEP^-)$ was 7.9×10^{-7} $M^{-1}sec^{-1}$ at 35°C with $I = 0.10$. Thus, the intramolecular hydrolysis is 45,000 times faster than the intermolecular NEP^- hydrolysis with 1 mM **15b**. That is to say, the effective molarity is 45 M ($=k$(PDE)/$k(NEP^-)$) in favor of the intramolecular phosphate of **25b**. The final phosphomonoester product **26** was completely inert and was not hydrolyzed even at high pH (up to ca. 12). Therefore, one could not use the Zn^{II}–alkoxide in **24** as a catalyst for phosphate hydrolysis, as was the case for carboxyester hydrolysis. The Zn^{II}–cyclen complex **12** was shown to strongly bind to dianionic phosphomonoesters (e.g., $K = 10^{3.3}$ M^- for 1:1 NPP^{2-}–Zn^{II}–cyclen). It is highly probable that the pendent phosphomonoester in **26** itself is too strong a competitive inhibitor, by occupying the Zn^{II} catalytic site, to generate Zn^{II}—OH^- species.

The two-step mechanism of phosphate ester hydrolysis by the $(Zn^{II})_2$-containing alkaline phosphatase (AP) (*7*) is thus somewhat mimicked by **24**. The phosphoryl intermediate **25** is generated by nucleophilic attack of the alkoxide moiety in **24b** at BNP^- and is hydrolyzed by the intramolecular Zn^{II}—OH^- species in **25b**. Thus, the attack at the BNP^-

substrate and subsequent hydrolysis of the intermediate both require zinc(II). In AP, these two functions of zinc(II) are performed separately by two proximate zinc(II) ions. One is involved in the activation of Ser_{102} to yield a phosphoryl-serine intermediate **2**, while the other is involved in the activation of water to attack the intermediate (see Fig. 2). The intramolecular arrangement of these two zinc(II) ions in AP is more advantageous than the single-zinc(II) system to exercise the dual zinc(II) role. In the single zinc(II) system, the pK_a value of 9.1 for the **25a** $\rightleftarrows$ **25b** equilibrium is higher than the reported pK_a value of 7.5 (**2** $\rightleftarrows$ **3**) for the phosphoryl-serine intermediate. The dinuclear zinc(II) system is also essential in the initial interaction with phosphomonoester; see Section IV.

The principle found for zinc(II) was applied to copper(II) complex models by Young *et al.* (*25*). The hydroxyl function of copper complex **27a** deprotonates with a pK_a value of 8.8 to yield **27b**, which cleaves phosphodiester bis(2,4-dinitrophenyl) phosphate (BDP^-) by transesterification to produce **28** ($k(BDP^-) = 7.2 \times 10^{-1}\ M^{-1}sec^{-1}$ at 25°C; see Scheme 5). The analogous complex with a hydroxyethyl pendent cleaves the diester predominantly by hydrolysis, which suggests that the reactive species is not Cu^{II}–alkoxide, but Cu^{II}—OH^-. The rate $k(BDP^-)$ of $9.5 \times 10^{-3}\ M^{-1}sec^{-1}$ is about two orders of magnitude smaller than the phosphoryl-transfer reaction. This copper model study shows that metal-alkoxide species may be more effective nucleophiles, as has been seen with zinc(II)–model complex **24**. Thus, future models may be designed that are composed of a metal–alkoxide function and a proximate metal–hydroxide function.

Another phosphomonoesterase family, the purple acid phosphatases, have been attracting interest, since they contain a mixed-valence binuclear iron(II/III) center (*26*). Although the exact roles of iron(II) and iron(III) have not been clarified yet, it has recently been reported that the direct nucleophilic attack of Fe^{III}—OH^- at the phosphate P atom is the most likely mechanism (*27*).

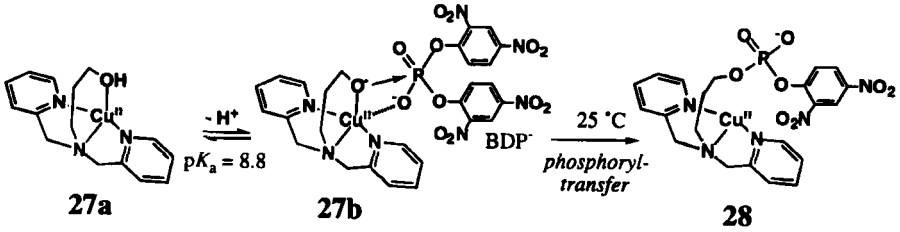

SCHEME 5.

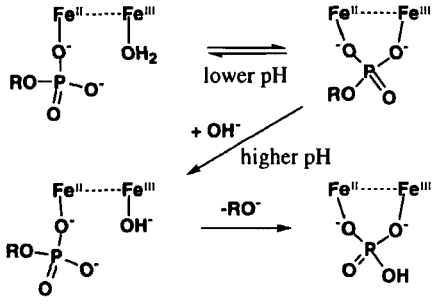

SCHEME 6.

The iron(II)–iron(III) form of purple acid phosphatase (from porcine uteri) was kinetically studied by Aquino *et al.* (*28*). From the hydrolysis of α-naphthyl phosphate (with the maximum rate at pH 4.9) and phosphate binding studies, a mechanism was proposed as shown in Scheme 6. At lower pH (ca. 3), iron(III)-bound water is displaced for bridging phosphate dianion, but little or no hydrolysis occurs. At higher pH, the iron(III)-bound OH^- substitutes into the phosphorus coordination sphere with displacement of naphthoxide anion (i.e., phosphate hydrolysis). The competing affinity of a phosphomonoester anion and hydroxide to iron(III) in purple acid phosphatase reminds us of a similar competing anion affinity to zinc(II) ion in carbonic anhydrase (*12a, 12b*).

In a model study using $[Fe_2O(TPA)_2(H_2O)(ClO_4)]^{3+}$ **29** (TPA = tris(2-pyridiylmethyl)amine), Wilkinson *et al.* showed that the Fe^{III}-OH^- indeed can act as a nucleophile, promoting hydration of acetonitrile to acetamide, yielding **30** (see Scheme 7) (*29*).

The first crystal structure (with a resolution of 2.9 Å) of purple acid phosphatase (kidney bean, composed of 432 amino acid residues) containing a dinuclear Fe^{III}–Zn^{II} active site **31** has been reported (*30*).

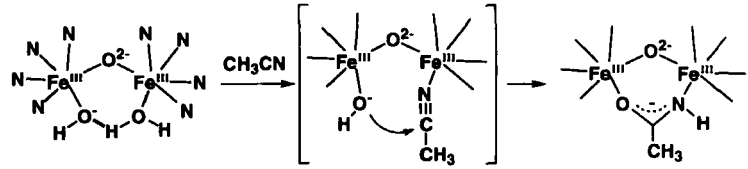

29 **30**

SCHEME 7.

The two metal ions are 3.1 Å apart and bridged monodentately by Asp_{164}. A postulated reaction mechanism is that the phosphate group of the substrate interacts with the zinc(II) ion, thereby displacing H_2O ligand, followed by an S_N2-type nucleophilic attack at the phosphate P atom from the back side by an Fe^{III}—OH^-. The active site of the Fe^{III}–Zn^{II} phosphatase seems to be similar to that of a mammalian Fe^{III}–Fe^{II} purple acid phosphatase. For instance, exchange of Zn^{II} for Fe^{II} resulted in nearly identical spectroscopic and kinetic behaviors. Although the hydrolysis by alkaline phosphatase proceeds differently, via a phosphoseryl intermediate with retention of the overall configuration at the P atom, the functional role of both metals appears similar to that of the metals in purple acid phosphatase. The weaker Lewis acidity of zinc(II) compared to iron(III) may be responsible for the shift of the alkaline phosphatase reaction to the more alkaline side.

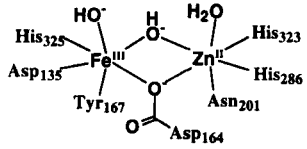

31 *Kidney Bean Purple Acid Phosphatase Active Site*

III. Reactivity of Zinc(II)-Bound Thiolate

Escherichia coli employs the Ada protein both to repair DNA alkylation products and to regulate the transcription of genes (*31*). The primary lesions repaired by Ada are O^6-methylguanosine, O^4-methylthymine, and the S_p diastereomer of methylphosphotriesters. Ada removes the offending methyl groups by direct, stoichiometric, and irreversible transfer to specific cysteine residues in the protein. Cys_{321} is responsible for repair of the base adducts, and Cys_{69} repairs the methyl phosphotriesters. Cys_{69} is one of four cysteines tightly bound to zinc(II) and essential for protein activity.

Wilker and Lippard (*32*) mimicked the $[Zn^{II}(^-S$—cysteine$)_4]^{2-}$ site with $[Zn^{II}(^-SC_6H_5)_4]^{2-}$ **32**, which, in DMSO-d_6, was reacted with $(CH_3O)_3PO$ (see Scheme 8), a model of the DNA methylphosphotriester lesion, and the reaction was followed by ^1H NMR spectroscopy. The 1:1 reaction yielded quantitatively $(CH_3O)_2PO_2^-$ and $CH_3SC_6H_5$. This reaction is a model for the DNA methyl phosphotriester repair by Ada.

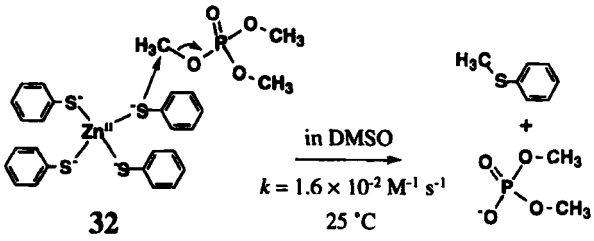

32

SCHEME 8.

It is of interest that the Zn^{II}-bound thiophenolate attacks at a methyl carbon atom as electrophilic site, while the Zn^{II}-bound alkoxides, as described in Section II, attack at the P atom. In **32**, zinc(II) assembles and protects (from oxidation) the four strong nucleophiles $C_6H_5S^-$. While alcohols and water (pK_a both ca. 15) need zinc(II) to be activated at physiological pH, thiophenol (pK_a ca. 7) may not require zinc(II) for activation.

$[Zn^{II}(^-SC_6H_5)_3(MeIm)]^-$ **33** and $[Zn^{II}(^-SC_6H_5)_2(MeIm)_2]^0$ **34** were synthesized to compare the reactivity of Zn^{II}-$^-SC_6H_5$ in different ligand-field environments (*32*). Both reacted with $(CH_3O)_3PO$ to yield $(CH_3O)_2PO_2^-$ and $CH_3SC_6H_5$, although the rate constants (1.1×10^{-3} and $\leq 10^{-5}$ $M^{-1}sec^{-1}$ with **33** and **34**, respectively) are much smaller than that of **32**. Certainly, labilization of $C_6H_5S^-$ (from zinc(II) complex) is highest with **32**. The extremely slow demethylation reaction with **34** suggests that the $[Zn^{II}(^-S—cysteine)_2(N—histidine)_2]^0$ site in the prototypical zinc finger motif is a poor general nucleophile. The reactivity of $[Zn^{II}(^-SC_6H_5)_4]^{2-}$ **32** is almost comparable to that of $(CH_3)_4N^+(^-SC_6H_5)$ ($k = 2 \times 10^{-2}$ M^-sec^{-1}) in DMSO, which yields the same product. However, C_6H_5SH does not react with $(CH_3O)_3PO$ at all. These results imply that the coordination of Cys_{69} to zinc(II) ion in Ada may be required for the deprotonation of the cysteine SH group ($pK_a \approx 8$) and for sustaining nucleophilicity of Cys_{69} under anhydrous conditions. It might be interesting to check whether or not $Zn^{II}(^-SR)_4$ complexes are formed with thioalcohols and then react with $(CH_3O)_3PO$ similarly at physiological pH in aqueous solution. Earlier, it was reported that captopril (a Zn^{II}-containing angiotensin-converting enzyme inhibitor, an antihypertensive drug) very strongly binds as a thiolate anion to Zn^{II}–cyclen (**35**, $K = 10^{7.0}$ M^{-1} at 25°C) in neutral pH aqueous solution (*14*). Apparently, this Zn^{II}-bound thiolate anion is kinetically inert and shows no activity at all in NA hydrolysis.

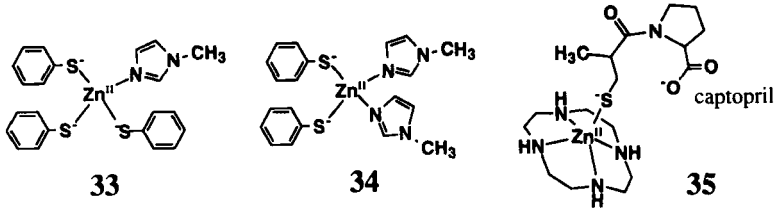

33 34 35

IV. Dinuclear Metal Systems for Group Transferases and Their Models

Recently, investigation of multinuclear metal complex systems in metalloenzymes has begun to attract attention (*5, 33*). A few examples are shown in Table II. The metal-ion centers in these proteins have carboxylate anions that provide effective binding sites for a variety of cationic metals, but would lower the effective charge on the complexes, making formation of metal-hydroxide nucleophiles at physiological pH less feasible by metals alone. Meanwhile, the carboxylate anions play the most important role in linking two metals. In contrast, carbonic anhydrase consists of one zinc(II) surrounded by three neutral histidine donors, which facilitates generation of a nucleophilic Zn^{II}—OH^- by

TABLE II

PEPTIDASE AND PHOSPHATASE ENZYMES WITH MULTINUCLEAR METAL COMPLEX ACTIVE SITES

Metal active site	*Enzyme and function*
Zinc	
2 Zn	Leucine aminopeptidase
2 Zn, 1 Mg (or 3 Zn)	Alkaline phosphatase
3 Zn	P1 nuclease
3 Zn	Phospholipase C
Iron	
2 Fe (or Fe, Zn)	Purple acid phosphatase
Cobalt	
2 Co	*E. coli* methionine aminopeptidase
Manganese	
2 Mn	Arginase (arginine → ornithine + urea)
2 Mn (Mg)	Enolase
2 Mn, 2 M^{II}	Ribonuclease H domain of HIV-1 (phosphodiesterase)
3 Mn	*Saccharomyces cerevisiae* inorganic pyrophosphatase
Nickel	
2 Ni	Urease (urea → carbonic acid + ammonia)
Other	
2 Mg, 2 Mn, or 2 Zn	*E. coli* DNA polymerase I

zinc(II) alone (*34*). The catalytic power in these multinuclear metalloenzymes may be provided by the presence of proximate substrate and metal-bound water, with a cooperative activation through hydrogen-bonding interactions by protein (basic) residues.

The "two-metal" mechanisms have been known for most phosphotransferases: e.g., alkaline phosphatase (*7*), inositol monophosphatase (*35*), serine/threonine phosphatase-1 (*36*), and purple acid phosphatase (*30*). The catalytic function of the metals in these multinuclear metalloenzymes may be rather electrostatic and seems insensitive to the nature of the metal ions.

Hydrolyses of single-stranded ribo- and deoxyribonucleotides and of phospholipids are catalyzed by P1 nuclease from *Penicillium citronum* (*37*) and phospholipase C from *Bacillus cereus* (*38*), respectively. Both proteins contain three zinc(II) atoms close to each other in their active sites, two of which (the most essential) are bridged by an aspartate residue and water with a distance of 3.2–3.3 Å. The crystal structure of the phospholipase C active site showed the tri-zinc(II) system **36**. Prominent features include His and Asp or Glu ligation, pentacoordinate zinc(II), and a bridging carboxylate and H_2O (or hydroxide) for the dinuclear pair, Zn(1) and Zn(3). The latter are 3.3 Å apart, while the third zinc(II) ion, Zn(2), is close enough that the inorganic phosphate PO_4^{3-} can simultaneously bridge all zinc(II) ions. This active-site structure is similar to that found in alkaline phosphatase (*9*) and P1 nuclease (*37*).

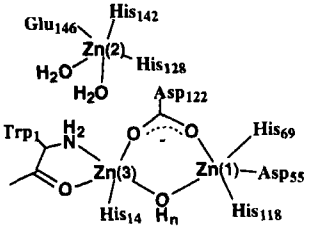

36 *Phospholipase C Active Site*

The X-ray crystal structure of the inorganic phosphate (an inhibitor) complex of alkaline phosphatase from *E. coli* (*9*) showed that the active center consists of a Zn_2Mg(or Zn) assembly, where the two zinc(II) atoms are 3.94 Å apart and bridged by the bidentate phosphate (which suggests a phosphomonoester substrate potentially interacting with two zinc(II), as depicted in Fig. 2), and the Mg (or the third Zn) is linked to one atom of the zinc pair by an aspartate residue at a distance

of 4.18 Å. DNA polymerase I from *E. coli* contains a dizinc active site bridged by an aspartate residue, which can house a monodentate bridging dinucleotide with a Zn–Zn separation of 3.9 Å (*39*). It has been proposed that during phosphate ester hydrolysis, the dinuclear metal center binds, orients, and activates the substrate, while stabilizing a pentacoordinate phosphorous transition state.

Phosphotriesterase from *Pseudomonas dimenuta* is a dizinc metalloenzyme (*40*) that catalyses the hydrolysis of a broad spectrum of organophosphotriesters, including the pesticides paraoxon and related acetylcholinesterase inhibitors. Site-directed mutagenesis experiments have indicated that six of the seven histidine residues in the native phosphotriesterase are at or near the active site (*41*). The X-ray crystal structure of the phosphotriesterase has recently been determined, disclosing existence of two bridging ligands to the two metals, Lys_{169} and a water molecule (*42, 43*). The other ligands are His_{55}, His_{57}, His_{201}, and Asp_{301}. CO_2 is required for the activation, which reacts with the ε-amino residue of Lys_{169} to form a carbamate **37**, being a bridging ligand between two zinc(II) ions (*43*). The same metal-binding mode has recently been disclosed for urease containing two nickel(II) (*44*), as described later. The metal ions stabilize the carbamate, which in turn binds to and holds the metals in the active site. When the bridging Lys_{169} is mutated to either methionine or alanine, the catalytic activity is drastically reduced. However, a significant fraction of the wild-type activity can be restored upon addition of carboxylic anions such as CH_3COO^- and propionate, which substitute the carbamate bridge (see **38**).

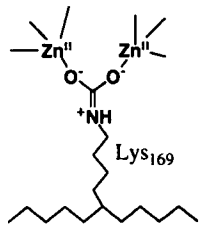

37

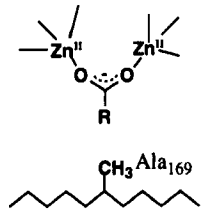

38

Although the detailed catalytic mechanisms of these phosphatases have not been elucidated, an accepted general mechanism is that the two metal ions are cooperatively working by interacting directly with the scissible phosphate and stabilizing the pentacovalent intermediate (*33, 45*). Moreover, one zinc(II) ion generates the attacking OH^- ion.

X-ray structures of a ternary complex of rat DNA polymerase β (pol

β) (containing two Mg^{II}), a DNA template-primer, and dideoxycytidine triphosphate (ddCTP) were recently determined (*46*). The pol β active site is shown in Fig. 8. Again, a two-metal-ion mechanism was described for the nucleotidyl transfer reaction, as for other polymerases such as *E. coli* DNA polymerase I, HIV-1 reverse transcriptase, and bacteriophage T7 RNA polymerase. ddCTP is a nucleotide analogue that targets the reverse transcriptase of HIV and is at present used to treat AIDS. The nucleotidyl transfer reaction is generally depicted as follows: Template-primer$_n$ + ddCTP $\rightarrow$ template-primer–ddCMP$_{n+1}$ + pp$_i$. The crystal is a pseudo-Michaelis–Menten ternary complex in which both "substrates" are present, namely, a nonreactive template-primer and a nucleoside triphosphate. At the phosphoryl transfer, a Mg^{II} ion, acting as a Lewis acid, activates the 3′-OH of the primer terminus, while one of its ligands, Asp_{256}, acts as the proton acceptor. The pentacoordinated transition state is stabilized by another Mg^{II}. This evidence leads to a proposal that hydrolysis involving self-splicing ribozymes proceeds through a similar two-metal ion mechanism.

The crystal structure of urease form *Klebsiella aerogenes* has recently been determined (*47*). The two nickel(II) ions in the active site are 3.5 Å apart. One nickel(II) ion, Ni(1), is coordinated by three ligands,

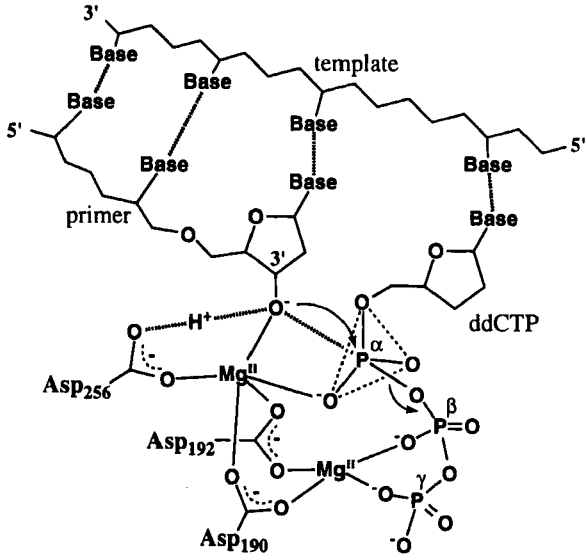

FIG. 8. Transition state of the pentacoordinate α phosphate of ddCTP in pol β active site.

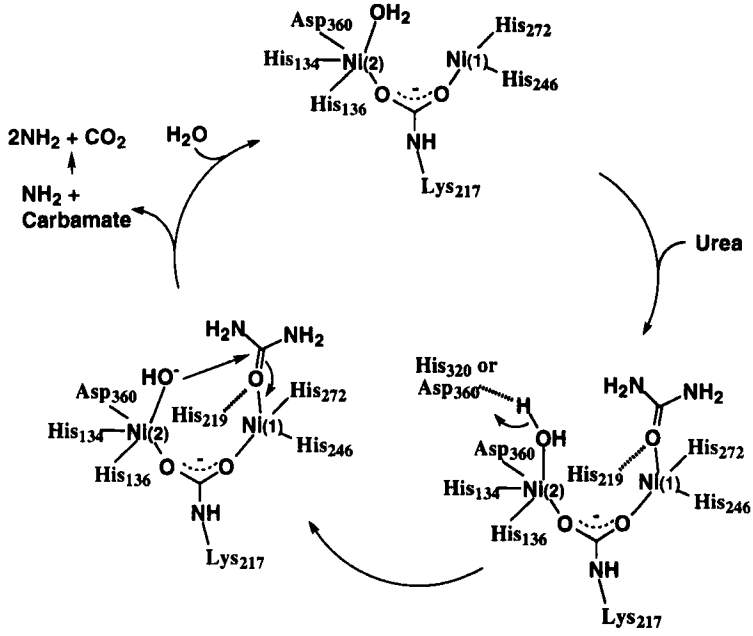

FIG. 9. A possible mechanism for urea hydrolysis at the catalytic site of urease.

and the second, Ni(2), by five ligands. A carbamylated lysine provides an oxygen ligand to each nickel(II) ion, explaining why CO_2 is required for the activation of urease apoenzyme. The structure is compatible with a catalytic mechanism whereby urea ligates to Ni(1) to complete its tetrahedral coordination and a hydroxide ligand of Ni(2) attacks the carbonyl C atom (see Fig. 9).

The structure of the urease active center is similar to that of adenosine deaminase, an enzyme containing one zinc(II) per active site (though see *48*). This enzyme catalyzes the deamination of adenosine to inosine and NH_3 (see Scheme 9), a reaction mechanistically related

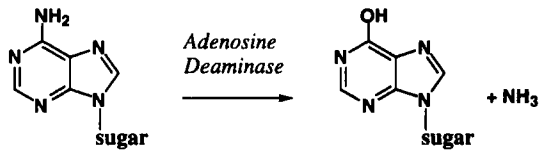

Adenosine Inosine

SCHEME 9.

to that of urease. Both mechanisms involve the attack of metal–OH^- on the electrophilic amido carbon.

While there have been a considerable number of structural models for these multinuclear zinc enzymes (*49*), there have only been a few functional models until now. Czarnik *et al.* have reported phosphate hydrolysis with bis(Co^{III}–cyclen) complexes **39** (*50*) and **40** (*51*). The flexible binuclear cobalt(III) complex **39** (1 mM) hydrolyzed bis(4-nitrophenyl)phosphate (BNP^-) (0.05 mM) at pH 7 and 25°C with a rate 3.2 times faster than the parent Co^{III}–cyclen (2 mM). The more rigid complex **40** was designed to accommodate inorganic phosphate in the internuclear pocket and to prevent formation of an intramolecular μ-oxo dinuclear complex. The dinuclear cobalt(III) complex **40** (1 mM) indeed hydrolyzed 4-nitrophenyl phosphate (NP^{2-}) (0.025 mM) 10 times faster than Co^{III}–cyclen (2 mM) at pH 7 and 25°C (see Scheme 10). The final product was postulated to be **41** on the basis of ^{31}P NMR analysis. In **40**, one cobalt(III) ion probably provides a nucleophilic water molecule, while the second cobalt(III) binds the phosphoryl group in the form of a four-membered ring (see **42**). The reaction of the phosphomonoester NP^{2-} can therefore profit from the special placement of the two metal ions. As expected from the weaker interaction of BNP^- with cobalt(III), **40** did not show enhanced reactivity toward BNP^-. However, in the absence of more quantitative data, a detailed reaction mechanism cannot be drawn.

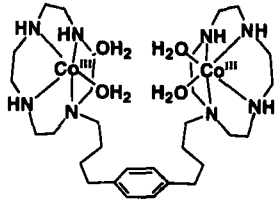

39

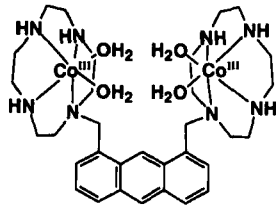

40

Wall *et al.* built a binuclear copper(II) complex **43** in order to see acceleration of phosphodiester cleavage (*52*). With the substrate (50 μM) shown, the reaction might be considered as a model for the first step of the hydrolysis of RNA, in which the alcohol function of the side chain intramolecularly attacks the Cu^{II}-activated phosphate as a nucleophile for a ring closure reaction. Compared to an analogous mononuclear complex **44** (at 1 mM), a rate constant ca. 50 times larger for **43** (at 1 mM) was observed at 25°C and pH 7, implying that the two metal ions probably cooperate. An analogous zinc(II) complex **45** was reported only as a structural model for the active site of phospholi-

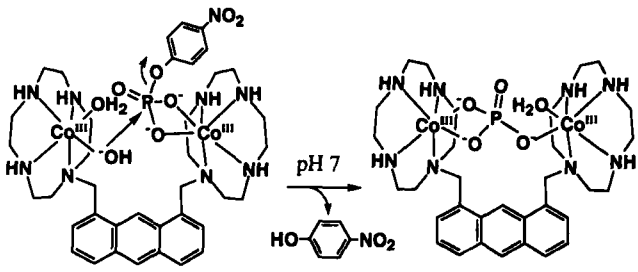

41 42

SCHEME 10.

pase C (*53*). The Zn—Zn bond distance is 3.44 Å, which is comparable to that of 3.3 Å for the carboxylate-bridged Zn—Zn in phospholipase C.

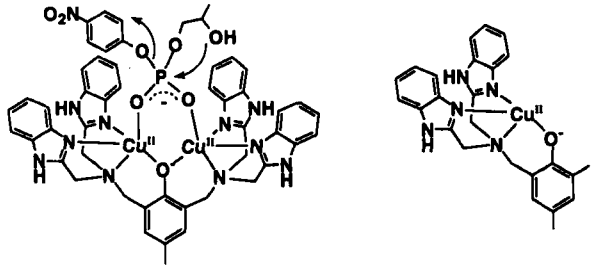

43 44

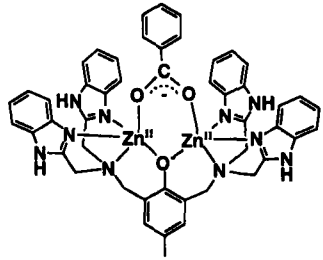

45

Tsubouchi and Bruice demonstrated remarkable rate enhancement (ca. 10^{13}) in phosphonate ester hydrolysis catalyzed by two La^{III} ions using a phosphonate attached with two 8-hydroxyquinoline moieties (*54*). The complex with two La^{III} **46** showed double metal ion cooperativity: (i) facile formation of metal ligated hydroxide (pK_a = 7.2 at 30°C) as an intramolecular nucleophile, (ii) stabilization of the transition

state of the hydrolysis by neutralization of the phosphonate negative charge, and (iii) interaction with the incipient oxyanion of the leaving alcohol. The first-order rate constant for the hydrolysis of **46** was determined as 1.36×10^{-3} sec^{-1} at 30°C, which is much larger than the pseudo-first-order rate constant (5×10^{-17} sec^{-1} at 30°C and pH 8) for hydrolysis of the ligand phosphonate itself. However, a 1 : 1 complex **47** is hydrolytically inert, but subject to catalysis by external nucleophiles such as aqueous La^{III}—OH^- ion.

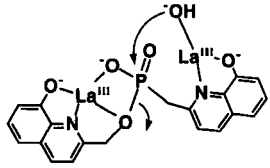

46

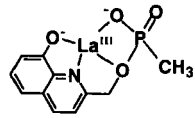

47

Chapman and Breslow synthesized zinc(II) complexes of monomer and dimers derived from 1,4,7-triazacyclododecane with phenyl **48** and 4,4′-biphenyl linkers **49** (*55*). They were examined as catalysts for the hydrolysis of 4-nitrophenyl phosphate (NP^{2-}) and bis(4-nitrophenyl) phosphate (BNP^-) in 20% (v/v) DMSO at 55°C. On the basis of the comparison of the pseudo-first-order rate constants, the dinuclear zinc(II) complexes **48** with 1,3-phenyl and 1,4-phenyl linkers are ca. 5 times more efficient than monomer or **49** in the hydrolysis of NP^{2-}, leading to the conclusion that the two zinc(II) ions are simultaneously involved in the hydrolysis, as in the enzyme alkaline phosphatase. For the hydrolysis of BNP^-, a longer dimer **49** is ca. six times more effective than 1,3-phenyl-linked dimer **48** and monomers.

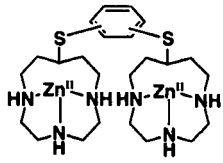

48

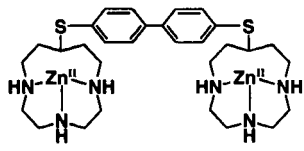

49

A bell-shaped pH vs rate profile with a maximum rate at pH 7.8 was seen in NP^{2-}-hydrolysis by 1,3-phenyl-linked dimer **48**. The phosphomonoester NP^{2-} prefers the two zinc(II) ions to be close, and hence two alternative mechanisms as shown in Scheme 11 (a or b) are proposed for the hydrolysis. The loss of catalytic activity at pH > 12 may be accounted for by the formation of a double OH^--bridged zinc(II)

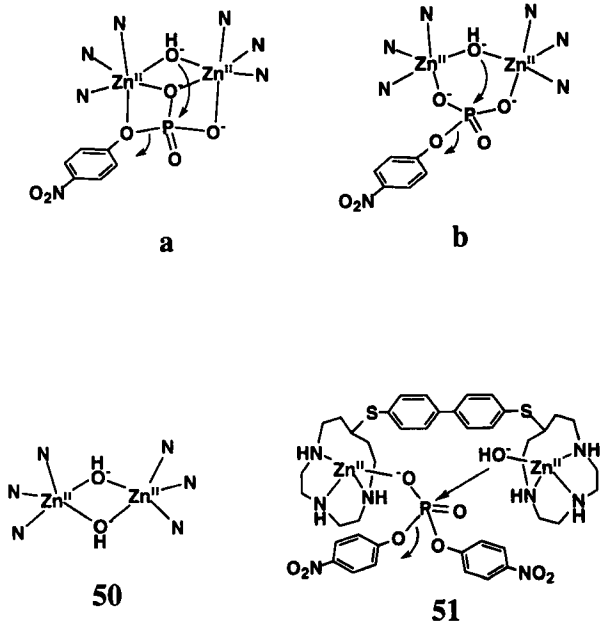

SCHEME 11.

species **50**. For BNP^- hydrolysis, a greater Zn–Zn separation is preferred. A bell-shaped pH vs rate profile was found, with the ascending leg corresponding to a pK_a value of 8 and the descending leg to a pK_a value of 12. As a result, a similar mechanism **51** to that for **41** and **46** was proposed. However, conclusions in this paper might be inaccurate for lack of quantitative titration data or possibly too high concentrations of catalyst (e.g., 227 mM).

Yun *et al.* have reported a carboxylate- and a phosphodiester-bridged dinuclear magnesium(II) complex with dicarboxylate ligand **52** (*56*). The reaction of **52** with 2 equivalents of $Mg(NO_3)_2$ in MeOH gave a carboxylate-bridged complex **53** (see Scheme 12). The Mg–Mg distance

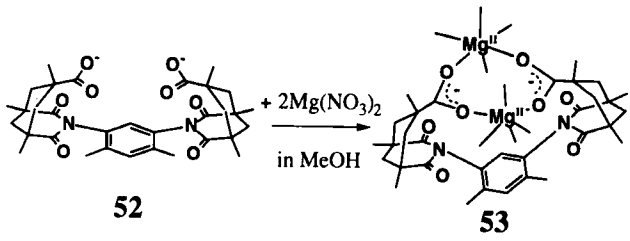

SCHEME 12.

is 4.78 Å, and the retained octahedral coordination spheres of the two Mg^{II} ions are filled by labile solvent and nitrate ligands. The dicarboxylate ligand thus offers the first assembly for a discrete dimagnesium (II) center.

Further reaction of **53** with diphenyl phosphate afforded a phosphodiester-bridged dinuclear magnesium(II) complex **54**. The Mg–Mg distance of 4.11 Å is comparable to similar distances in the Klenow fragment of *E. coli* DNA polymerase I (3.9 Å) (*39*), rat DNA polymerase β (4 Å) (*46*), and inositol monophosphatase (3.8 Å) (*35*). The flexibility of the bridging carboxylates in **52** is manifested by the ca. 0.75-Å range of Mg–Mg distances in these complexes, which can readily adjust the metal coordination environment.

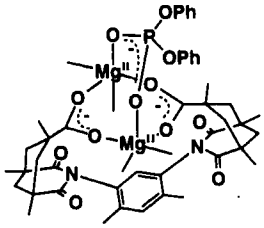

54

A variable-temperature ^{31}P NMR study of **54** in d_4-MeOH disclosed a free energy of 60 kJmol^{-1} for the activation of the bridging phosphodiester exchange with free diphenyl phosphate. This value is comparable to that obtained by a similar method for an analogous dinuclear zinc(II) complex with **52**, 45 kJ mol^{-1} (*57*). The phosphodiester exchange rate of the dimagnesium(II) complex (1.9×10^2 sec^{-1} at 25°C) is ca. 400 times slower than that of the dizinc(II) analogue, which is similar to the difference in H_2O exchange rates of hydrated Mg^{II} (10^5 sec^{-1}) and Zn^{II} (3×10^7 sec^{-1}). The observed differences in phosphate exchange rates may be useful information to explain the metal ion preferences of phosphatases that employ a carboxylate-bridged dimetallic center.

The crystal structure of serine/threonine phosphatase-1 (*36*) revealed that it contains two metal ions M(1) and M(2) (unidentified as yet) close to each other (see Fig. 10). Each of the metal ions is coordinated by five ligands. The distance between the two metal ions is 3.3 Å, which is facilitated by Asp_{92} and a water molecule (or OH^- ion); each bridges the two ions. Both metal ions and two arginine residues together create the active site. The metal ions, by stabilizing negative charges, can make a phosphomonoester more susceptible to nucleophilic attack,

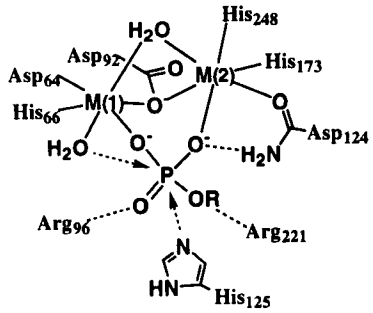

FIG. 10. A possible mechanism for phosphomonoester hydrolysis at the catalytic site of serine/threonine phosphatase-1 active site.

probably by the metal-bound H_2O. The requirement for a general acid catalysis for the leaving group serine (or threonine) of the substrate may be met by His_{125}. Alternatively, the reaction might proceed via a covalent phosphoryl-histidine intermediate with His_{125}. So far, however, there is direct evidence for the reaction mechanism.

More recently, a new cryptand **55** has been synthesized, which at pH > 4 formed a dizinc(II) complex of an alkoxide-bridged octaazacryptand **56**. The novel cryptate **56** disclosed more detailed intrinsic properties of dinuclear zinc(II) system useful for catalytic activities (*58*). The X-ray crystal structure of **56** showed the two zinc(II) ions being equivalent in a distorted trigonal–bipyramidal environment involving two NH groups (with an average Zn–N distance of 2.07 Å) and an alkoxide O^- anion (Zn–O^- distance 1.93 Å) as equatorial donors, while the tertiary amine and an NH (with an average Zn–N distance of 2.23 Å) are in apical positions. Although these two zinc(II) in the cryptate appeared to be coordinatively saturated and hence were assumed unreactive, they were shown to work cooperatively, selectively recognized a phosphomonoester, 4-nitrophenyl phosphate dianion (NP^{2-}), and promote the cleavage of its P—O ester bond by the nucleophilic attack of one of the apically coordinated NHs at pH 4.9–9.5 in aqueous solution (see **57** in Scheme 13). The Zn–Zn bond distance of 3.42 Å in **56** is appropriate to allow interaction with the phosphomonoester substrate. The reaction product was isolated from aqueous solution as a novel phosphoramide derivative **58** and identified by X-ray crystal structure analysis. The structure of **58** featured the two phosphoryl oxygens bound to each zinc(II) ion (an average Zn–OP distance 2.02 Å) in place of the original two apical NHs. The Zn–Zn distance is a little widened, to 3.65 Å. A mechanism for the phosphate P—O bond cleavage is that as a substrate NP^{2-} approaches to bridge both zinc(II), the apical NHs

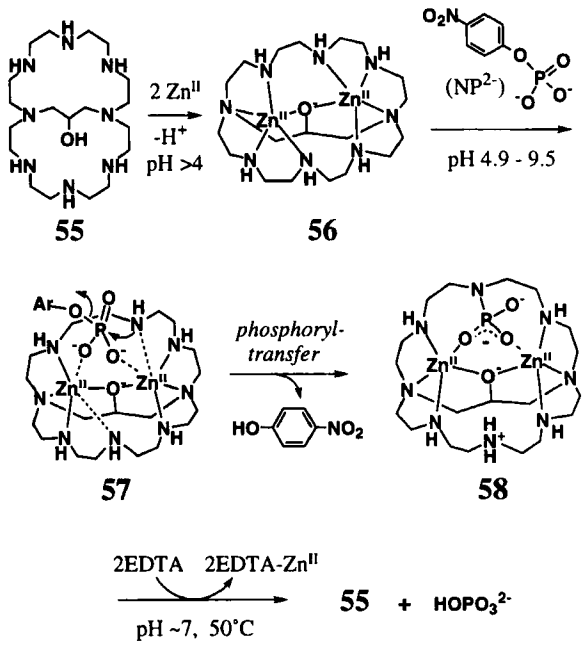

SCHEME 13.

dissociate, and one of them becomes an intramolecular nucleophile to attack at the incoming phosphorus atom to perform a phosphoryl transfer reaction. The phosphoryl transfer by **56** stops at the **58** stage, which is extremely stable in presence of two zinc(II) ions, and hence **56** by itself does not catalyze for phosphomonoester hydrolysis. However, when the zinc(II) ions were removed with ethylenediaminetetraacetic acid (EDTA) at pH 7 in aqueous solution at ca. 60°C, the P—N bond was hydrolyzed to yield the starting cryptand **55** and inorganic phosphate. The phosphoamide group in **58** is stabilized by the two zinc(II), just as the carbamates in **37** (*43*) and urease (*47*) are stabilized by two metal ions.

V. Concluding Remarks

An increasing number of crystal structures of metalloenzymes have been reported, with more molecular structures of the metal active centers. We believe, however, that this is only the beginning of a new bioinorganic chemistry. The structural data provide more questions

than answers, especially in terms of chemical reaction mechanisms. Design of useful models is therefore a great help in elucidating the role of metals, functions of amino acid residues, and principles of multimetal functions. Now that the principle of the mononuclear system seems to be well investigated, the major concern seems to be shifting to more practical applications such as development of artificial nuclease and phosphatase. However, investigation of multinuclear or multifunctional systems composed of metals and amino acid residues has just begun. We are convinced that bioinorganic chemists are capable of designing more and more sophisticated models for those goals.

REFERENCES

1. (a) Bertini, I.; Luchinat, C.; Maret, W.; Zeppezauer, M., Eds. "Zinc Enzymes"; Brikhäuser: Boston, 1986; (b) Coleman, J. E. *Annu. Rev. Biochem.* **1992,** *61,* 897; (c) Ochiai, E. *J. Chem. Educ.* **1988,** *65,* 943; (d) Vallee, B. L.; Auld, D. S. *Biochemistry* **1990,** *24,* 5647.
2. Benning, M. M.; Kuo, J. M.; Raushel, F. M. *Biochemistry* **1994,** *33,* 15001.
3. Tanaka Hall, T. M.; Porter, J. A.; Beachy, P. A.; Leahy, D. J. *Nature* **1995,** *378,* 212.
4. Lovejoy, B.; Cleasby, A.; Hassell, A. M.; Longley, K.; Luther, M. A.; Weigl, D.; McGeehan, G.; McElroy, A. B.; Drewry, D.; Lambert, M. H.; Jordan, S. R. *Science* **1994,** *263,* 375.
5. Vallee, B. L.; Auld, D. S. *Proc. Natl. Acad. Sci. USA* **1990,** *87,* 220.
6. (a) Kimura, E.; Koike, T. In "Comprehensive Supramolecular Chemistry"; Elsevier Science: Oxford; in press; (b) Kimura, E. In "Progress in Inorganic Chemistry"; Karkin, K. D., Ed.; John Wiley & Sons: New York, 1994; Vol. 41, p. 443; (c) Kimura, E.; Shionoya, M. In "Transition Metals in Supramolecular Chemistry"; Fabbrizzi, L.; Poggi, A., Eds.; Kluwer Academic Publishers, 1994; p. 245; (d) Kimura, E.; Koike, T. *Comments Inorg. Chem.* **1991,** *11,* 285.
7. Coleman, J. E. *Annu. Rev. Biophys. Biomol. Struct.* **1992,** *21,* 441.
8. Butler-Ransohoff, J. E.; Rokita, S. E.; Kendall, D. A.; Banzon, J. A.; Carano, K. S.; Kaiser, E. T.; Matlin, A. R. *J. Org. Chem.* **1992,** *57,* 142.
9. Kim, E. E.; Wyckoff, H. W. *J. Mol. Biol.* **1991,** *218,* 449.
10. Woolley, P. *Nature* **1975,** *258,* 677.
11. Slebocka-Tilk, Cocho, J. L.; Frakman, Z.; Brown, R. S. *J. Am. Chem. Soc.* **1984,** *106,* 2421.
12. (a) Kimura, E.; Shiota, T.; Koike, T.; Shiro, M.; Kodama, M. *J. Am. Chem. Soc.* **1990,** *112,* 5805; (b) Koike, T.; Kimura, E.; Nakamura, I.; Hashimoto, Y.; Shiro, M. *J. Am. Chem. Soc.* **1992,** *114,* 7338; (c) Zhang, X.; von Eldic, R.; Koike, T.; Kimura, E. *Inorg. Chem.* **1993,** *32,* 5749; (d) Kimura, E.; Koike, T.; Shiota, T.; Iitaka, Y. *Inorg. Chem.* **1990,** *29,* 4621; (e) Kimura, E.; Koike, T.; Shionoya, M.; Shiro, M. *Chem. Lett.* **1992,** 787.
13. Kitajima, N.; Hikichi, S., Tanaka, M.; Moro-oka, Y. *J. Am. Chem. Soc.* **1993,** *115,* 5496.
14. Koike, T.; Takamura, M.; Kimura, E. *J. Am. Chem. Soc.* **1994,** *116,* 8443.
15. Groves, J. T.; Barton, L. A. *J. Am. Chem. Soc.* **1989,** *111,* 5442.

16. Sigman, D. S.; Jorgensen, C. T. *J. Am. Chem. Soc.* **1972,** *94,* 1724.
17. Kimura, E.; Nakamura, I.; Koike, T.; Shionoya, M.; Kodama, Y.; Ikeda, T.; Shiro, M. *J. Am. Chem. Soc.* **1994,** *116,* 4764.
18. Koike, T.; Kimura, E. *J. Am. Chem. Soc.* **1991,** *113,* 8935.
19. Koike, T.; Kajitani, S.; Nakamura, I.; Kimura, E.; Shiro, M. *J. Am. Chem. Soc.* **1995,** *117,* 1210.
20. (a) Blow, D. M.; Birktoft, J. J.; Hartley, B. S. *Nature* **1969,** *221,* 337; (b) Dugas, H. "Bioorganic Chemistry"; Springer-Verlag: New York, 1989; p. 196.
21. Bruice, T.; Schmir, G. L. *J. Am. Chem. Soc.* **1958,** *80,* 148.
22. Kirsch, J. F.; Jencks, W. P. *J. Am. Chem. Soc.* **1964,** *86,* 837.
23. Kady, I. O.; Tan, B.; Ho, Z.; Scarborough, T. *J. Chem. Soc., Chem. Commun.* **1995,** 1137.
24. Kimura, E.; Kodama, Y.; Koike, T.; Shiro, M. *J. Am. Chem. Soc.* **1995,** *117,* 8304.
25. Young, M. J.; Wahnon, D.; Hynes, R. C.; Chin, J. *J. Am. Chem. Soc.* **1995,** *117,* 9441.
26. (a) Vincent, J. B.; Crowder, M. W.; Averill, B. A. *J. Biol. Chem.* **1991,** *266,* 17737; (b) David, S. S.; Que, L., Jr. *J. Am. Chem. Soc.* **1990,** *112,* 6455.
27. Mueller, E. G.; Crowder, M. W.; Averill, B. A.; Knowles, J. R. *J. Am. Chem. Soc.* **1993,** *115,* 2974.
28. Aquino, M. A. S.; Lim, J.; Sykes, A. G. *J. Chem. Soc. Dalton Trans.* **1994,** 429.
29. Wilkinson, E. C.; Dong, Y.; Que, L., Jr. *J. Am. Chem. Soc.* **1994,** *116,* 8394.
30. Sträter, N.; Klabunde, T.; Tucker, P.; Witzel, H.; Krebs, B. *Science* **1995,** *268,* 1489.
31. Sedgwick, B.; Robins, P.; Totty, N.; Lindahl, T. *J. Biol. Chem.* **1988,** *263,* 4430.
32. Wilker, J. J.; Lippard, S. *J. Am. Chem. Soc.* **1995,** *117,* 8682.
33. Karlin, K. D. *Science* **1993,** *261,* 701.
34. Eriksson, A. E.; Jones, T. A.; Lilijas, A. *Proteins* **1988,** *4,* 274.
35. Bone, R.; Frank, L.; Springer, J. P.; Atack, J. R. *Biochemistry* **1994,** *33,* 9468.
36. Goldgerg, J.; Huang, H.; Kwon, Y.; Greengard, P.; Nairn, A. C.; Kuriyan, J. *Nature* **1995,** *376,* 745.
37. Volbeda, A.; Lahm, A.; Sakiyama, F.; Suck, D. *EMBO J.* **1991,** *10,* 1607.
38. Hough, E.; Hansen, L. K.; Brinkes, B.; Jynge, K.; Hansen, S.; Hordvik, A.; Little, C.; Dodson, E.; Derewenda, Z. *Nature* **1989,** *338,* 357.
39. Beese, L. S.; Steitz, T. A. *EMBO J.* **1991,** *10,* 25.
40. (a) Dumas, D. P.; Raushel, F. M. *J. Biol. Chem.* **1990,** *265,* 21498; (b) Omburo, G. A.; Kuo, J. M.; Mullins, L. S.; Raushel, F. M. *J. Biol. Chem.* **1992,** *267,* 13278.
41. Lai, K.; Dave, K. I.; Wild, J. R. *J. Biol. Chem.* **1994,** *269,* 16579.
42. Benning, M. M.; Kuo, J. M.; Raushel, F. M.; Holden, H. M. *Biochemistry* **1994,** *33,* 15001.
43. Hong, S.; Kuo, J. M.; Mullins, L. S.; Raushel, F. M. *J. Am. Chem. Soc.* **1995,** *117,* 7580.
44. Blakeley, R.; Zerner, B. *J. Mol. Catalysis* **1984,** *23,* 263.
45. Gani, D.; Wilkie, J. *Chem. Soc. Rev.* **1995,** 55.
46. Pelletier, H.; Sawaya, M. R.; Kumar, A.; Wilson, S. H.; Kuraut, J. *Science* **1994,** *264,* 1891.
47. Jabri E.; Carr, M. B.; Hausinger, R. P.; Karplus, P. A. *Science* **1995,** *268,* 998.
48. Wilson, D. K.; Rudolph, F. B.; Quiocho, F. A. *Science* **1991,** *252,* 1278.
49. Fenton, D. E.; Okawa, H. *J. Chem. Soc., Dalton Trans.* **1993,** 1349.
50. Chung, Y.; Akkaya, E. U.; Venkatachalam, T. K.; Czarnik A. W. *Tetrahedron Lett.* **1990,** *31,* 5413.
51. Vance, D. H.; Czarnik A. W. *J. Am. Chem. Soc.* **1993,** *115,* 12165.
52. Wall, M.; Hynes, R. C.; Chin, J. *Angew. Chem., Int. Ed. Eng.* **1993,** *32,* 1633.
53. Uhlenbrock, S.; Krebs, B. *Angew. Chem., Int. Ed. Eng.* **1992,** *31,* 1647.

54. Tsubouchi, A.; Bruice, T. C. *J. Am. Chem. Soc.* **1995,** *117,* 7399.
55. Chapman, W. H., Jr.; Breslow, R. *J. Am. Chem. Soc.* **1995,** *117,* 5462.
56. Yun, J. W.; Tanase, T.; Pence, L. E.; Lippard, S. J. *J. Am. Chem. Soc.* **1995,** *117,* 4407.
57. Tanase, T.; Yun, J. W.; Lippard, S. J. *Inorg. Chem.* **1995,** *34,* 4220.
58. Koike, T.; Inoue, M.; Kimura, E.; Shiro, M. *J. Am. Chem. Soc.* **1996,** *118,* 3091.

This Page Intentionally Left Blank

ADVANCES IN INORGANIC CHEMISTRY, VOL. 44

ACTIVATION OF DIOXYGEN BY COBALT GROUP METAL COMPLEXES

CLAUDIO BIANCHINI and ROBERT W. ZOELLNER*

Istituto per lo Studio della Stereochimica ed Energetica dei Composti di Coordinazione, Consiglio Nazionale delle Ricerche, 50132 Firenze, Italy

* Permanent address: Northern Arizona University, Department of Chemistry, P.O. Box 5698, Flagstaff, Arizona 86011-5698, U.S.A.

I. Introduction

The activation of dioxygen by transition metal complexes may appear at first to be both oxymoronic and redundant: Common sense describes dioxygen as a powerful oxidant and a reactive species. Thermodynamically this is certainly true, but kinetically dioxygen is fairly inert. Dioxygen is a paramagnetic molecule in a triplet ($^3\Sigma_g^-$) ground state with two unpaired electrons in degenerate antibonding orbitals; its reactivity must follow rules governing the conservation of spin in a reaction. Therefore, dioxygen must either react with another radical or form products with a triplet ground state (*1a*). Such processes are rare, leading to the kinetic inertness of dioxygen.

Dioxygen could overcome the kinetic barrier of its unpaired electrons and triplet ground state by excitation to its first excited state ($^1\Delta_g$), in which all electrons are paired. Unfortunately, this species, referred to as singlet oxygen, is generally too reactive and too short-lived for most situations (*1b*, *1c*). However, dioxygen complexation to a transition metal can also result in activation and create stable complexes that can be studied, modified, and used in further reactions in a controlled manner (*2*). This latter type of activation is the subject of this chapter.

A. Scope

The activation of dioxygen by transition metals is already a topic far too broad to be covered in a review of this kind. We have therefore chosen to focus only on the cobalt subgroup metals (cobalt, rhodium, and iridium), and even within this limited range, attention will be confined to novel aspects and only the most recent developments. Chromium, molybdenum, and tungsten peroxo and superoxo complexes have recently been reviewed (*3a*), as have similar complexes of vanadium (*3b*), manganese (*3c*), and copper (*3d*). Theoretical calculations of metal–dioxygen complexes have also been the subject of a recent review (*3e*). Our focus forces us to ignore many of the biochemical aspects of dioxygen activation (involving iron and copper), but some of these topics have also been the subject of recent reviews (*4*). In addition to primary literature sources, we also refer to relevant reviews.

B. Bonding Modes of Dioxygen as a Ligand

In Fig. 1 some of the most common metal–dioxygen binding modes found for mononuclear and dinuclear transition metal complexes are diagrammed. Note that the terms "superoxo" and "peroxo" ultimately

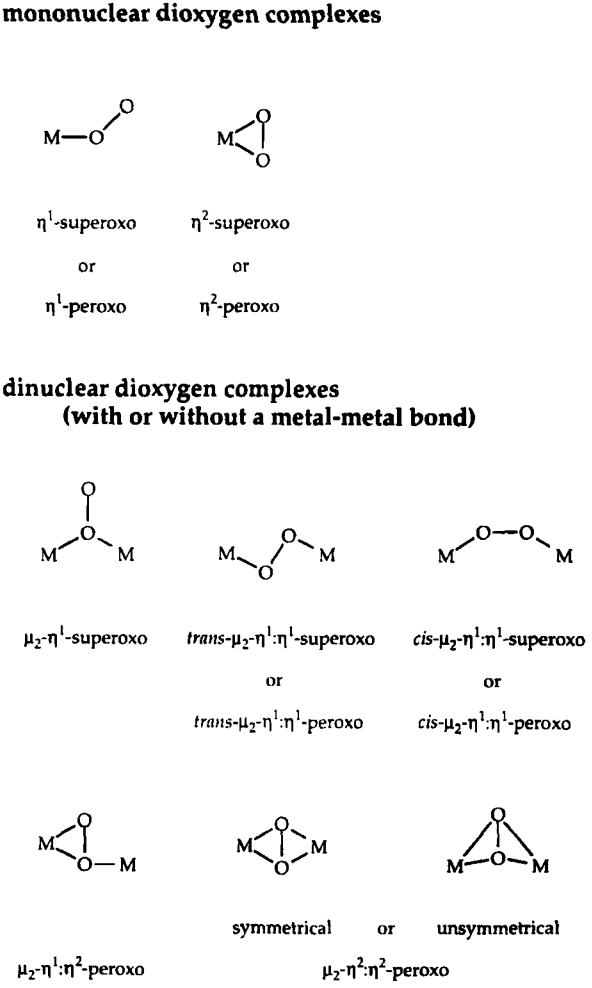

FIG. 1. The common binding modes of dioxygen as a ligand in mononuclear and dinuclear metal complexes.

refer back to the classical inorganic species "superoxide" [O_2^-] and "peroxide" [O_2^{2-}], but these designations are often quite relative and depend strongly on the formal oxidation state assigned to the central metal (*5a*), most often based on spectroscopic observations (*5b*). Some of these binding modes are more rare than others, and not all complexes fit neatly into the classification given. However, a knowledge of these generic structures will aid in an understanding of the discussions that follow.

As research in the area of dioxygen transition-metal complexes progresses, the relative novelty of each structure may change. The structures that seem common now may be overtaken by newer structures. Thus, Fig. 1 should be used as an outline rather than as the definitive word on possible structures for metal–dioxygen complexes.

II. Nitrogen Donor Ligands

Although a wide variety of nitrogen donor ligands exist in transition-metal complexes, relatively few general types have been employed in those complexes that have been found to activate dioxygen. Generally, the ligands are at least bidentate, and often are multidentate.

A. Amines

Both acyclic and cyclic amines, as well as ammonia, can act as ligands, primarily in cobalt(II) and cobalt(III) complexes, so as to produce systems that react with and/or activate dioxygen. With some inevitable overlap, we have separated these topics into distinct sections to aid in the clarity of presentation.

1. Ammonia (Ammine) Complexes

Both μ-peroxo and μ-superoxo complexes of cobalt-containing ammine ligands are well known. A fair number of examples of μ-peroxodicobalt complexes with the general formula $[L_5Co(\mu\text{-}O_2)CoL_5]^{4+}$ can be cited (*6–9*). Among these complexes are those with $L_5 = (NH_3)_5$ (*6*), $L_5 = (NH_3)_2$(deta), (NH_3)(pda)$_2$, (NH_3)(dap)$_2$, or (NH_3)(bda)$_2$ (*7*), $L_5 = (NH_3)$(eda)$_2$ (*8a, 8b*), and $L_5 = (NH_3)$(teta) (*9*). In addition, the di-bridged μ-hydroxo-μ-peroxo complex $[(NH_3)_4Co(\mu\text{-}O_2)(\mu\text{-}OH)Co(NH_3)_4]^{3+}$ (*8c*) is well known. [The ligand abbreviations we have used refer to the following: deta, diethylenetriamine, $(H_2NCH_2CH_2)_2NH$; pda, propylenediamine, $H_2N(CH_2)_3NH_2$; dap, 1,2-diaminopropane, $H_2NCH_2CH(NH_2)CH_3$; bda, butylenediamine, $H_2N(CH_2)_4NH_2$; eda, ethylenedia-

mine, $H_2N(CH_2)_2NH_2$; and taea, tris(aminoethyl)amine, $(H_2NCH_2CH_2)_3N$.] These complexes, and their superoxo relatives, can be characterized by their Raman spectra (*10*).

A rare (*11*) example of an alkylcobalt(III) compound containing solely saturated ligands, $[CH_3Co(NH_3)_5]^{2+}$, has been synthesized and spectroscopically characterized (*12*). The synthesis of this complex utilized dioxygen as the oxidizing agent (*13*) for cobalt(II) nitrate hexahydrate in water, followed by reaction with methylhydrazine. Although at first glance such a reaction does not appear to fit the definition of dioxygen activation, it has been shown (*14*) that this general class of reactions involves intermediate cobalt(III)-containing superoxy radical species, as shown in Eq. (1), in which salen is an abbreviation for the ligand *N,N'-ethylenebis*(salicylideneaminato):

$$LCo^{II}(salen) + O_2 \rightarrow LCo^{III}(salen)OO\cdot \qquad (1)$$

These radical species may (slowly) combine to form the μ-peroxodicobalt species or, as in the preparation of $[CH_3Co(NH_3)_5]^{2+}$, react (more rapidly) with the alkyl hydrazine to form the alkylated cobalt(III) species and dinitrogen. Schiff base complexes such as these are discussed in more detail later in this article.

Marcus theory (*15*) has been applied to the study of the reductions of the μ_2-superoxo complexes $[Co_2(NH_3)_8(\mu_2\text{-}O_2)(\mu_2\text{-}NH_2)]^{4+}$ and $[Co_2(NH_3)_{10}(\mu_2\text{-}O_2)]^{5+}$ with the well-characterized outer-sphere reagents $[Co(bipy)_3]^{2+}$, $[Co(phen)_3]^{2+}$, and $[Co(terpy)_2]^{2+}$, where bipy = 2,2'-bipyridine, phen = 1,10-phenanthroline, and terpy = 2,2':6',2''-terpyridine (*16a*). The kinetics of these reactions could be adequately described using a simple outer-sphere pathway, as predicted by Marcus theory. However, the differences in reactivity between the mono-bridged and di-bridged systems do not appear to be explicable in purely structural terms. Rather, the reactivity differences appear to be caused by charge-dependent effects during the formation of the precursor complex. Some of the values for reduction potentials reported earlier for these species (*16a*) have been revised and corrected by later work (*16b*).

2. *Acyclic Amines*

The length of the "arms" of tripodal donor ligands can have significant effects on the properties of the complexes in which they are a part. The symmetrical tetradentate ligands taea (*vide supra*) and tapa [tris(aminopropyl)amine, $(H_2NCH_2CH_2CH_2)_3N$], as well as the novel (*17*) asymmetric ligand abap [aminoethylbis(aminopropyl)amine,

$H_2NCH_2CH_2N(CH_2CH_2CH_2NH_2)_2]$, have been used to prepare complexes of cobalt(III) via the air oxidation of the analogous cobalt(II) complexes. With the last ligand, abap, the peroxo-bridged dimer $[(abap)(NO_2)Co(\mu\text{-}O_2)Co(NO_2)(abap)]^{2+}$ could be isolated and characterized. When the ligand taea was used (*18*), however, a stronger oxidant, PbO_2, was necessary to effect to oxidation.

The novel pentadentate ligand $(H_2NCH_2CH_2NHCH_2)_2C(NH_2)CH_3$, tamdn (1,5,9-triamino-5-methyl-3,7-diazanonane), could be shown to coordinate to cobalt(III), and the brown dicobalt peroxo- and green dicobalt superoxo-bridged dimers $[(tamdn)Co(\mu\text{-}O_2)Co(tamdn)]^{4+/5+}$ could be prepared (*19*). An X-ray crystal structure of the superoxo species (redrawn in Fig. 2) showed the expected structure. In addition, spectroscopic studies supported an analogous structure for the peroxo species.

Earlier studies of acyclic polyamine complexes have focused on the electronic structures of the complexes (*20*) and on detailed electrochemical investigations of the systems (*21a*). The cobalt(II) complexes of polyamine ligands cover a fairly wide range of oxygen affinities, and small changes in the ligand can impart significant changes to the spectral and redox properties of the systems. In a report of electrochemical investigations (*21a*), a linear relationship was found between the peak potentials for the cobalt(II) complexes and the $\log(K_{eq})$ for the formation of the $(\mu\text{-}O_2)Co^{II}$ species. This report parallels earlier studies (*21b*) that demonstrated a linear free energy relationship between the $\log(K_{stab})$ and the sum of the pK_as of the coordinated ligands. A related study of the reduction of the peroxo-bridge in dicobalt complexes containing multidentate amine donors, in contrast to the earlier (*21a*)

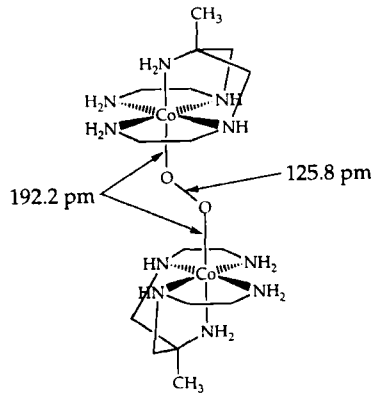

FIG. 2. The structure of the green μ_2-superoxo–dicobalt(III) cationic complex of tamdn, redrawn with selected bond distances included.

work, demonstrated that the complexes were less reactive than the reaction of hydrogen peroxide with ferrous ion as the reductant (*22*).

3. *Cyclic Amines*

The macrocyclic polyamine ligands discussed here are saturated, generally neutral, amine donors (unlike the Schiff bases, which are generally unsaturated and may carry a charge, or the porphyrins and their analogues, which carry a dinegative charge; *vide infra*). The common nomenclature of these systems is somewhat ambiguous and historically full of nonstandard abbreviations. For example, 1,4,8,11-tetraazacyclotetradecane is referred to both as "cyclam" and as [14]aneN$_4$, neither of which is as descriptive or unambiguous as the "longer" systematic terminology. When appropriate, and as dictated by the original authors, we shall use either the "ane" nomenclature (*23*) or common shortened names, but shall attempt to define the ligands unambiguously and/or give our chosen abbreviations as well to limit confusion.

Electrochemical (*24*) and chemical (*25, 26*) techniques have been utilized to investigate the kinetics and the mechanisms of the addition of dioxygen to a metal center, and to follow its subsequent reduction to hydrogen peroxide when catalyzed by cobalt(III) complexes of macrocyclic amine ligands. Such complexes have also been involved in the general investigation of dioxygen addition to cobalt complexes (*27, 28*).

The well-characterized (*29*) cobalt(II) complex of [14]aneN$_4$, which is highly reactive toward dioxygen (*26c, 30*), was used as a catalyst in the two-electron reduction of dioxygen to hydrogen peroxide at a rotating ring-disk electrode (*24b*). Two different mechanisms were identified, depending on whether the cobalt(III) complex and its cobalt(II) derivative (the actual catalyst in the reaction, see Scheme 1), or dioxygen (Scheme 2), was present in excess.

Whether in the presence of excess cobalt(III) complex [Co([14]aneN$_4$)(OH$_2$)$_2$]$^{3+}$ (**1**) or in the presence of excess dioxygen, the first step in either mechanism is the electrochemical reduction event of the cobalt(III) complex to the cobalt(II) complex [Co([14]aneN$_4$)(OH$_2$)$_2$]$^{2+}$ (**2**), followed by the rapid addition of dioxygen to form the dioxygen adduct [Co([14]aneN$_4$)(OH$_2$)$_2$O$_2$]$^{2+}$ (**3**). At this point, the two mechanisms diverge. When excess complex (and, thus, catalyst) is present, **3** dimerizes with **2** to form [{Co([14]aneN$_4$)(OH$_2$)}$_2$O$_2$]$^{4+}$ (**4**), which, after the addition of two protons and two electrons, eliminates hydrogen peroxide to reform **2**. Some of the intermediates in this mechanism have been identified independently and have been found to be stable at room temperature (*28*).

In the presence of excess dioxygen, rather than undergo dimerization,

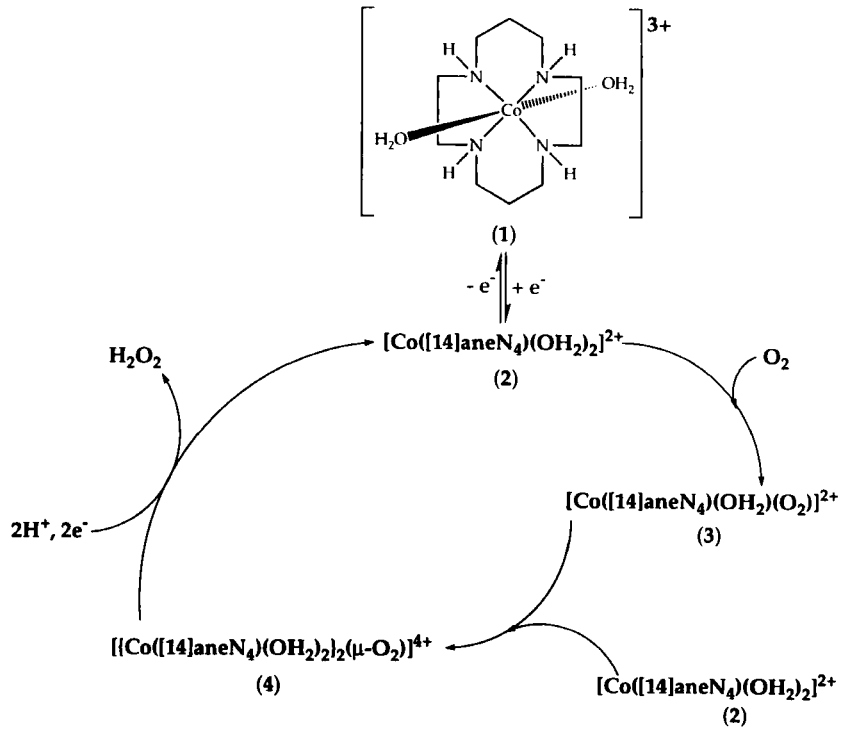

SCHEME 1. The proposed mechanism for the reduction of dioxygen to hydrogen peroxide in the presence of excess $[Co([14]aneN_4)(OH_2)_2]^{3+}$ (**1**).

3 adds a proton and an electron, forming the hydroperoxo intermediate **5**, which then adds another proton and another electron, eliminates hydrogen peroxide, and reforms **2**. The hydroperoxo species has been tentatively formulated as an "end-on" bonded species (*24b*).

The cobalt(III) complex of $Me_6[14]aneN_4$ (hmc or C-*meso*-5,7,7,12,14,14-hexamethyl-1,4,8,11-tetraazacyclotetradecane) has also been used to investigate the reduction of dioxygen to (in this case) hydroperoxide (*24a*). The hmc ligand has been shown (*25e*) to prevent the formation of a μ_2-peroxo dinuclear complex because of the significant steric crowding of the six methyl groups, thus simplifying the interpretation of the electrochemical data. The electrochemical behavior of the $(hmc)Co^{3+/2+}$ system closely resembled the previously described (*24b*) $([14]aneN_4)Co^{3+/2+}$ system. However, the predicted inability of the hmc complex to dimerize was experimentally realized, and the $(hmc)Co^{3+/2+}$ system was found to be only a modestly active catalyst for the reduction of dioxygen to hydrogen peroxide.

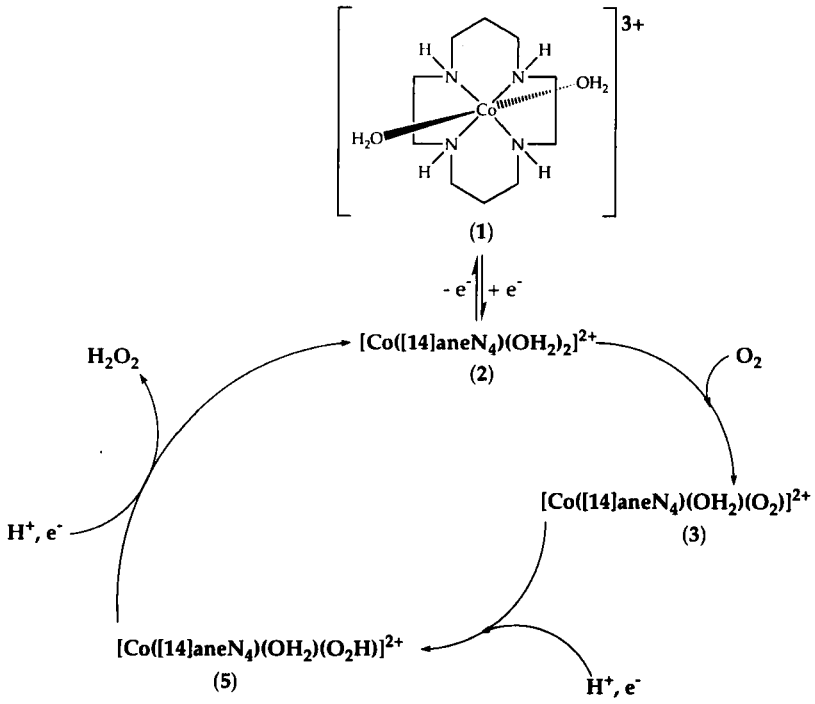

SCHEME 2. The proposed mechanism for the reduction of dioxygen to hydrogen peroxide in the presence of excess dioxygen.

The formation of dioxygen adducts of $[Co(hmc)(OH_2)_n]^{2+}$ (**6**) has been intensively studied (*25*). The rate constants for dioxygen binding to and its subsequent release from $[Co(hmc)(OH_2)_n(O_2)]^{2+}$ have been experimentally determined to be 5.0×10^6 $M^{-1}s^{-1}$ and 1.66×10^4 s^{-1}, respectively (*25e*). The effect of such coordinating anions (*25d*) as Cl^- and SCN^- has also been investigated. [Generally, the counter anion for the cobalt complex is $CF_3SO_3^-$ (*25e*).] While the rate of binding of dioxygen is little affected by these anions, the rate of autoxidation is enhanced, especially for those cases in which the thiocyanate anion is present.

The effect of pH on the formation of dioxygen adducts of **6** (*25c*), as well as the establishment of volume profiles for the reaction (*25b*) have been reported. In aqueous solution, dioxygen adducts of **6** form at pH > 7, with the kinetics of the reaction remaining approximately constant with those measured at pH < 7. However, at high pH values, the rate drops off by a factor of about five, corresponding to the point at which complex **6** is deprotonated (pK_a = 11.68). When the rate

constants for dioxygen adduct formation were investigated with respect to pressure (*25b*), the results indicated that an interchange mechanism for the substitution at the cobalt(II) center was occurring.

The synthesis of an exceptionally large decadentate macrocycle, 1,4,7,10,13,16,19,22,25,28-decaazacyclotriacontane (**7**), [30]aneN_{10}, and its ability to bind to cobalt(II) under anaerobic conditions to form both mononuclear and dinuclear species have been reported (*31*). In the presence of dioxygen (*27*), both mononuclear and dinuclear bridging peroxo systems can be prepared, depending on the ratios of the concentrations of the ligand **7** to the cobalt(II) complexes. Unlike the dimeric cobalt systems described earlier, these systems are *internal* dimers: one molecule of [30]aneN_{10} can form a complex with either one or two metal centers, and, with two metals, the bound dioxygen bridges the centers intramolecularly.

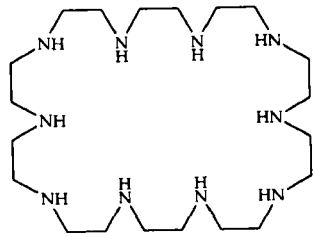

(7)

4. Pyridines and Related Ligands

It has long been known that, when bound to cobalt(II), the pyridine-based chelate ligands 2,2′-bipyridine (bipy), 1,10-phenanthroline (phen), and 2,2′:6′,2″-terpyridine (terpy) form complexes that react with dioxygen in aqueous solution (*32–34*). The mixed-ligand complexes $[Co(terpy)(bipy)]^{2+}$ and $[Co(terpy)(phen)]^{2+}$ can act as oxygen carriers in aqueous solutions at pH values as low as 3.0 (*34b*), and the superoxo species thus formed are apparently dinuclear. In addition, the dinuclear bipyridine complex $[(bipy)_2Co^{III}(\mu_2\text{-}OH)(\mu_2\text{-}O_2)Co^{III}(bipy)_2]^{3+}$ has been shown to catalyze the oxidation of 2,6-di-*tert*-butylphenol to the *tert*-butyl-substituted diphenoquinone and quinone (*35*).

The $[Co^{II}(bipy)_2]^{2+}$ species has also been reported to activate hydrogen peroxide and *tert*-butyl hydroperoxide for the selective ketonization of methylenic carbons, the oxidation of alcohols and aldehydes, and the dioxygenation of aryl olefins and acetylenes (*36*). Later reports (*37*), however, while confirming that the cobalt complexes did indeed cata-

lyze these reactions, indicated that other metal centers such as copper(II) were better catalysts.

The reaction of a 1,10-phenanthroline complex of iridium, $[Ir(cod)(phen)]^+$, with dioxygen in methanol solution has been studied (*38*). When the anion for this cationic complex is chloride, no anion–cation interaction occurs, and the iridium system remains four-coordinate. However, when either iodide or thiocyanate is present due to the addition of their sodium salts (or in the presence of added triphenylphosphine when the anion is chloride), the iridium system becomes five-coordinate because of the interaction between I^-, SCN^-, or PPh_3 and the iridium center. These five-coordinate systems react more rapidly with dioxygen than did the four-coordinate system at both normal and elevated pressures. An "end-on" oxidative addition of the dioxygen moiety, with displacement of the I^-, SCN^-, or PPh_3 ligands, was postulated.

5. *Interactions with Zeolites*

The attachment and encapsulation of metals and metal complexes in the cavities of zeolites is an active area of research and provides a versatile method for the modification of these "molecular sieves" (*39*). Because of the enforced dispersion of the metal complexes in the zeolite, systems not readily observable in solution can be investigated in zeolites. For example, the mononuclear superoxo adduct of the cobalt(III)–ammine system, $[Co(NH_3)_5(OO\cdot)]^{2+}$, which would be expected to dimerize in solution, could be observed entrapped in zeolite Y (*40*).

The interactions of acyclic and cyclic polyamine ligands with NaY zeolites exchanged with transition metal ions have been reported (*41*). In addition to zeolites containing nickel(II), manganese(II), or chromium(III), an NaY zeolitic system containing cobalt(II) was prepared through the cation exchange of the sodium ions with cobalt(II) acetate, followed by drying. The dry zeolite was then allowed to react with the dry solid polyamine ligand under nitrogen at 100°C.

The $[NaY : Co^{II}(cyclam)]$ and $[NaY : Co^{II}(tepa)]$ systems (*41*) both react with dioxygen to form mononuclear superoxo adducts. The former system is much more easily reversible than the latter, which may be due to the ability of the tepa ligand to increase the electron density at the metal center to a much greater degree than can the cyclam ligand (*42*).

B. Pyrazoles

The pyrazole structural entity is a nitrogen-donor ligand that (at least within the limitations of this review) can be formally negatively

charged as a pyrazolate or can be viewed as the neutral donor portion of an overall negatively charged hydridotris(pyrazolyl)borate. Thus, we consider pyrazoles to be significantly different from other nitrogen donors, and to merit a separate section for discussion.

1. Hydridotris(pyrazolyl)borates

The hydridotris(pyrazolyl)borate (Tp) ligand has become well known and well established as a formal analogue of the cyclopentadienyl (Cp) ligand (*43*). Unlike Cp, however, when appropriately substituted, Tp can become what has been described (*44, 45*) as a *tetrahedral enforcer* ligand, producing complexes that are constrained to be tetrahedral even when other factors might allow octahedral coordination.

In addition to the enforcement of tetrahedral structures, Tp derivatives also confer unusual and novel reactivities upon their complexes. For example (*46*), Tp' [hydridotris(3-*tert*-butyl-5-methylpyrazolyl)borate] reacts with CoX_2 to produce Tp'CoX complexes that can be reduced in the presence of N_2, yielding the dinitrogen complex Tp'Co(N_2). Excess dioxygen converts this dinitrogen complex into an unusual side-on bound superoxo complex (**8**). Further, **8** reacts, via hydrogen abstraction (with the hydrogen apparently arising from the *tert*-butyl portion of the pyrazolyl substituent), to form the hydroxo complex (**9**). (The residual radical presumed to be formed on the *tert*-butyl group is then thought to abstract hydrogen from the solvent to regenerate the *tert*-butyl group.)

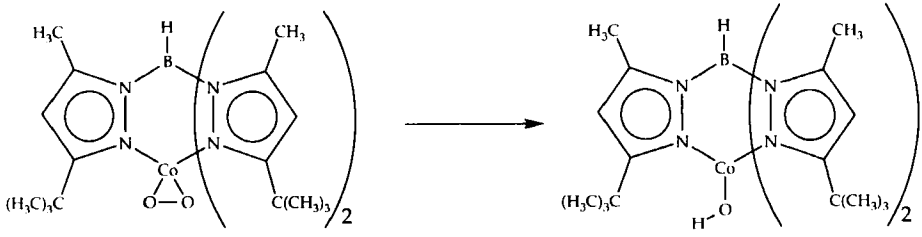

(**8**) (**9**)

Although variations in the substituent groups on Tp are expected to result in differing reactivities, synthetic problems arise when attempts to vary the substituents are made. With less sterically demanding ligands than *tert*-butyl, the pyrazolyl group can bind to the boron center in two different fashions, yielding a difficult-to-separate mixture of isomers. For example (*45*), the reaction of 3-*iso*-propyl-5-methylpyra-

zole with KBH_4 yields a mixture of three[1] almost inseparable regioisomers. One regioisomer, Tp″, however, was separated from the other regioisomers by an unusual method (*47*) termed *inverse recrystallization*. This method involved allowing the regioisomeric mixture of hydridotris(pyrazolyl)borates to react with CoI_2, forming a corresponding regioisomeric mixture of iodocobalt[hydridotris(3/5-*iso*-propyl-5/3-methylpyrazolyl)borate] complexes. This mixture of regioisomeric cobalt complexes is insoluble in acetonitrile. However, an acetonitrile suspension of the mixture, when cooled to −30°C, changes from a blue suspension to a greenish-yellow solution. Upon warming to room temperature, a blue solid crystallized, and this blue solid was found to be enriched in one regioisomer. Two repetitions of this procedure resulted in the isolation of pure **10**. The cause of this unusual separation is reported to be an equilibrium that exists between **10** (and its regioisomers) and **11** (and its regioisomers).

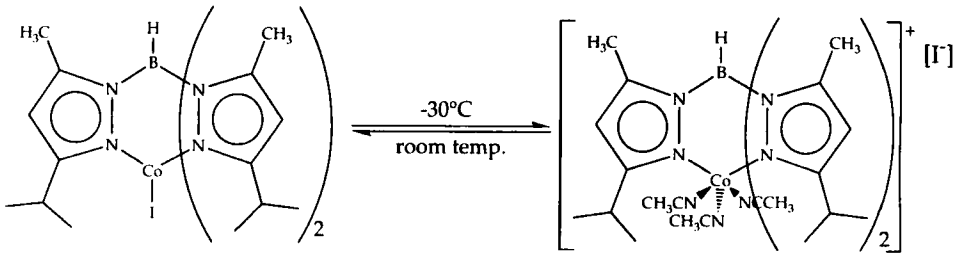

(10) **(11)**

Apparently, inverse recrystallization is possible in this case because of the sterically based differences in the affinity of the regioisomers of **10** for acetonitrile. Fortuitously, the most sterically demanding isomer, **10**, is least prone to add acetonitrile ligands and become an octahedral complex, and most prone to revert to the insoluble tetrahedral form. This allows the enrichment to occur upon warming.

Following the preparation of pure **10**, the dimeric dinitrogen complex (**12**) was prepared via magnesium reduction of **10** under a dinitrogen atmosphere. Following this reduction under dinitrogen, the reactions in Scheme 3 were directly investigated to develop an understanding of the activation of dioxygen by the system of Tp″Co complexes.

[1] In this reaction, *four* isomers should have been produced. However, the hydridotris(3-methyl-5-*iso*-propylpyrazolyl)borate isomer either was not produced in the reaction, or was formed in amounts too small to be detected. This isomer would be expected to be the most sterically hindered, at boron, of the four possibilities.

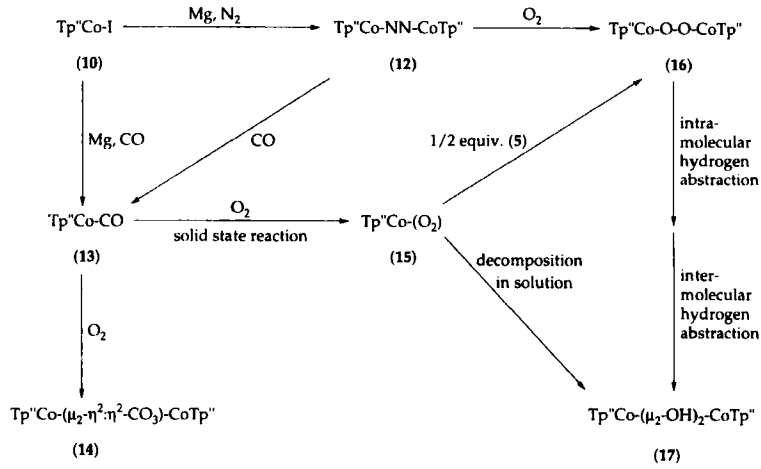

SCHEME 3. Some of the reactions of Tp″Co complexes.

The (μ-O_2) complex, **16**, which is similar to Kitajima's dimeric (μ-O_2)hydridotris(3,5-di-*iso*-propylpyrazolyl)borate complex of copper (*48*), was determined to abstract a hydrogen atom from the *iso*-propyl group of the Tp″ ligand, forming the (μ-OH)$_2$ complex (**17**). Evidence implicating *hydrogen tunnelling* in this hydrogen-atom abstraction step was found. This evidence included a large kinetic isotope effect, k_H/k_D(281 K), of 22(1), a difference in the apparent activation enthalpies, $\Delta(\Delta H^{\ddagger})$, of 2.8 kcal/mol, and a difference in the preexponential factors resulting from an Arrhenius analysis, A_H/A_D, of 0.13. No significant curvature in the Eyring plot was observed, however, because the experimentally accessible temperature range was not large enough to establish nonlinearity.

Based on the analysis of the reactions in Scheme 3 and on previous studies (*46*, *47*), a mechanism for the reaction was proposed in which the μ-peroxo complex, **16**, may simultaneously abstract two hydrogen atoms from *iso*-propyl groups on the pyrazolyl ligands. Alternatively, because of the weak O—O bond, **16** may homolytically dissociate to form two Tp″Co(O·) oxo-radical moieties, and these species would then abstract hydrogen from the *iso*-propyl groups. In either case, the resulting carbon-centered radical can either react with solvent, as was observed for the Tp′ complex (*46*), or with another carbon-centered radical so as to regenerate the Tp″Co(OH) complex and produce a derivative of the Tp″ complex with an *iso*-propenyl substituent, **18**. Ultimately, either route would produce the (μ-OH)$_2$ complex, **17**.

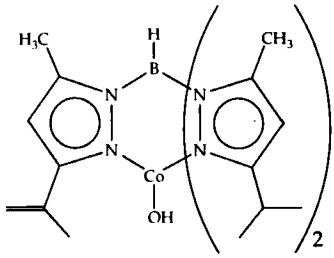

(18)

Infrared spectroscopy can be used to classify metal–dioxygen complexes as either superoxo species (ν(O–O) from 1200 to 1070 cm^{-1}) or as peroxo species (ν(O–O) from 930 to 740 cm^{-1}) (*49*). However, this system fails to accurately define the type of dioxygen species present in **8** and **15**, as these complexes exhibit ν(O–O) absorptions at 961 and 941 cm^{-1}, respectively. Preparation of the complexes with ^{18}O-enriched dioxygen confirmed that the dioxygen was bound "side-on" (η^2) in these complexes: Complex **8** exhibited isotopically shifted vibrations indicative of a side-on bound dioxygen ($\nu(^{16}O–^{16}O)$ absorption at 961 cm^{-1}, $\nu(^{16}O–^{18}O)$ at 937 cm^{-1}, and $\nu(^{18}O–^{18}O)$ at 908 cm^{-1}), as did complex (**15**) ($\nu(^{16}O–^{16}O)$ absorption at 941 cm^{-1} and $\nu(^{18}O–^{18}O)$ at 890 cm^{-1}).

While the approximation might be advanced that the values are close enough to the peroxo range to allow such a classification, an X-ray crystallographic analysis of **8** was undertaken so as to confirm the matter (*46*). The structure (redrawn in Fig. 3) was confirmed as containing a side-on bound dioxygen ligand, with d(O–O) of 1.262(8) Å d(Co–O) of 1.816(5) and 1.799(6) Å, and an ∠O–Co–O of 40.9(3)°. Thus,

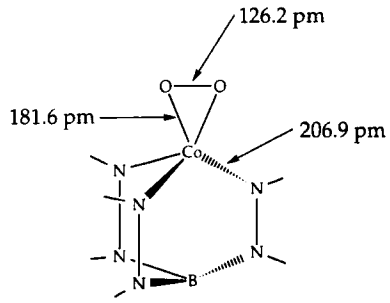

(8)

FIG. 3. The central portion of the crystal structure of **8**, redrawn to show selected bond distances.

since the O–O distance is reasonable for a superoxo ligand, the complex is best described as a cobalt(II)–superoxo complex, and, by comparison, **15** is also an example of such a side-on bound superoxo species.

The Tp″ complex of cobalt, [Tp″Co(CO)], continues to yield its secrets (*50*). As illustrated earlier (Scheme 3), when this complex, as the solid, is exposed to dioxygen, the [Tp″Co(O_2)] complex is formed. In solution, however (CH_2Cl_2 or CH_3CN), the complex forms a dimer that could be isolated and characterized crystallographically. The dimer [Tp″Co(μ_2-O_2)$_2$CoTp″] is linked by two dioxygen bridges such that the resulting six-membered ring composed of the dioxygen bridges and the cobalt centers is arranged in a "chair" conformation. The dimer is less stable thermally than is the monomer, even in the solid state. However, the dimer holds promise in the continuing study of the activation of dioxygen, which, in this system, depends on the simultaneous binding of one dioxygen molecule to two metals in the presence of excess dioxygen.

2. *Pyrazolates*

A dirhodium complex containing μ_2-pyrazolate ligands, **21**, has been shown (*51*), after reaction with HBF_4, to activate dioxygen in the transformation of a μ_2-vinylidene group into an η^1-acyl ligand (see Scheme 4). These final steps are part of an overall series of reactions, beginning with the dirhodium complex (**19**), in the degradation and oxidation of 1,1,1-trichloroethane. This process may find applications in the search for catalytic (*52*) or stoichiometric (*53*) reactions useful in the removal of organochloro pollutants from the environment.

C. Schiff Bases and Related Ligands

A Schiff base is the common name for the (usually acyclic) imine product of the reaction of a primary aryl amine with an aldehyde or ketone. These imines are stable if there is at least one aryl group on the imino nitrogen or on the imino carbon (*54*). A cyclidene is generically a cyclic, multidentate imine.

1. *Schiff Bases*

A cobalt(II) Schiff base complex has been reported to have been assembled *in situ* in zeolite Y (*55*). The zeolite was ion-exchanged with cobalt(II), followed by treatment with an excess of the Schiff base ligand salen (**22**). This synthetic methodology was employed because the preformed cobalt(II)–salen complex was expected to be too large to diffuse into the pores of zeolite Y. Since the acyclic salen ligand is flexible, the ligand was reported to be able to gain access to the cobalt-exchanged

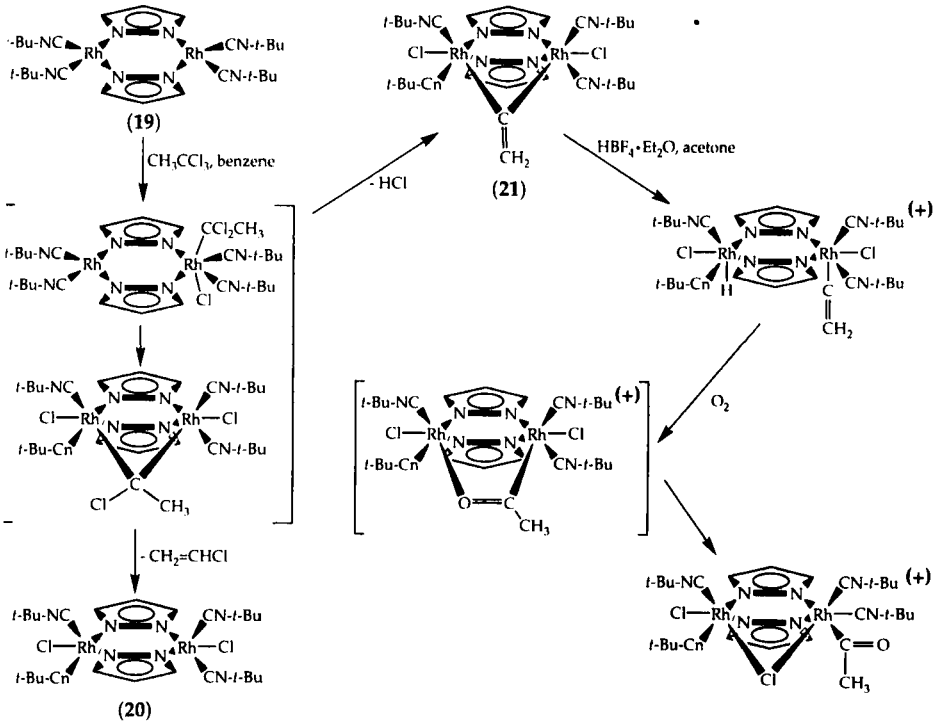

SCHEME 4. The reaction of **19** with 1,1,1-trichloroethane. Intermediates presumed to be present in these reactions, but not actually detected or isolated, are enclosed in square brackets.

sites in the zeolite, but, once a complex was formed with the cobalt(II) ion, the inflexible complex (**23**) could not be extracted from the zeolite matrix.

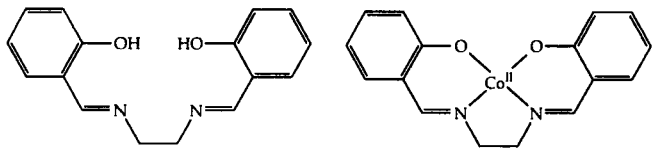

(**22**) (**23**)

Exposure of the zeolite-bound **23** to dioxygen at low temperatures indicated (as evidenced by a very weak axial electron spin resonance, ESR, signal) that a weakly bound oxygen adduct formed that was similar to the solution-phase adducts observed in noncoordinating sol-

vents (*56*). However, after treatment with pyridine (and removal of excess base under vacuum), the oxygen binding behavior improved dramatically and also was observed at room temperature. Further, the ESR parameters reported resembled the ESR parameters of the same complex, in solution, containing an axial pyridine ligand (*57*).

Later reports (*58*) have questioned whether the earlier report (*55*) was correct in concluding that the *planar* cobalt(II) complex of salen was formed in zeolite Y. The characteristics of the supposedly zeolite-entrapped [Co^{II}(salen)] are apparently not as similar to the same species in solution as previously reported. For example, *planar* [Co^{II}(salen)] and its adducts with axially disposed bases are generally ESR-detectable low-spin complexes (*59*), and cyclic voltammetry of the entrapped complex revealed a Co^{3+}/Co^{2+} redox transition that is absent in solution (*60*). These data, and more recent work (*58*), indicate that, in the zeolite Y environment, [Co^{II}(salen)] is probably *not* a planar system. Further, the role of pyridine in the observed reactivity with dioxygen is unclear, since, once the pyridine ligand is bound to the cobalt center, it is doubtful that the complex could actually even fit in the zeolite Y cage. The lack of planarity may account for the differences in properties between [Co^{II}(salen)] entrapped in zeolite Y and its properties in solution.

The cobalt(II)–pentadentate Schiff base complex **24** has also been investigated in a communication (*58a*) to determine its properties when entrapped in a zeolitic structure. The additional nitrogen amine donor site on the ligand obviates the necessity of adding an external axial donor ligand. Because of the difficulty in fitting **24** into a zeolite Y cage (as estimated using molecular graphics and modeling simulations), the faujasite hexagonal polymorph EMT was used in place of zeolite Y. After preparation of the faujasite-entrapped **24**, the complex did, in fact, appear (from ESR evidence) to bind dioxygen in a superoxo fashion.

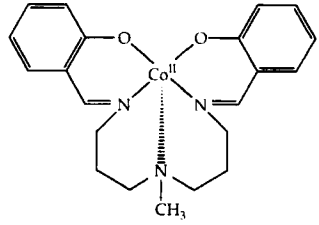

(**24**)

A more complete article (*58b*) further details the properties of faujasite EMT-entrapped cobalt(II)–Schiff base complexes as compared to the same complexes entrapped in zeolite Y. The Schiff bases used to

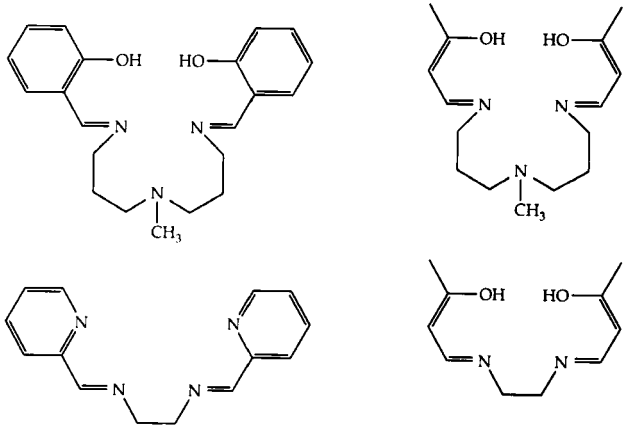

FIG. 4. Schiff bases used, in addition to salen (**22**), to complex Co^{II} in faujasites.

complex cobalt(II) are detailed in Fig. 4. The formation of a dioxygen adduct was detected to a much greater extent when a pentadentate ligand, rather than a tetradentate ligand, was utilized.

The copper-containing enzyme quercetinase, isolated from *Aspergillus flavus,* catalyzes the total insertion of oxygen into quercetin (**25**) and other related 3-hydroxyflavones. The products of the reaction are carbon monoxide and molecules resulting from cleavage of the heterocyclic ring (*61*). This catalytic reaction has been modeled using [Co^{II}(salen)] as the oxygenation catalyst (*62a*). The mechanism of this reaction, shown in Scheme 5 (*62b*), indicates that with dimethylformamide (DMF) as solvent, the initially catalytically active species is not a dioxygen adduct of the [Co^{II}(salen)] complex, but rather is an adduct containing both DMF and hydroxide, i.e., the complex [Co^{II}-(salen)(OH)(DMF)]. This species reacts with the hydroxyflavone and complexes with it. Ultimately, dioxygen incorporation occurs in a nonradical bimolecular manner under the influence of the cobalt(III) species.

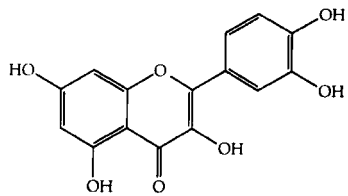

(**25**)

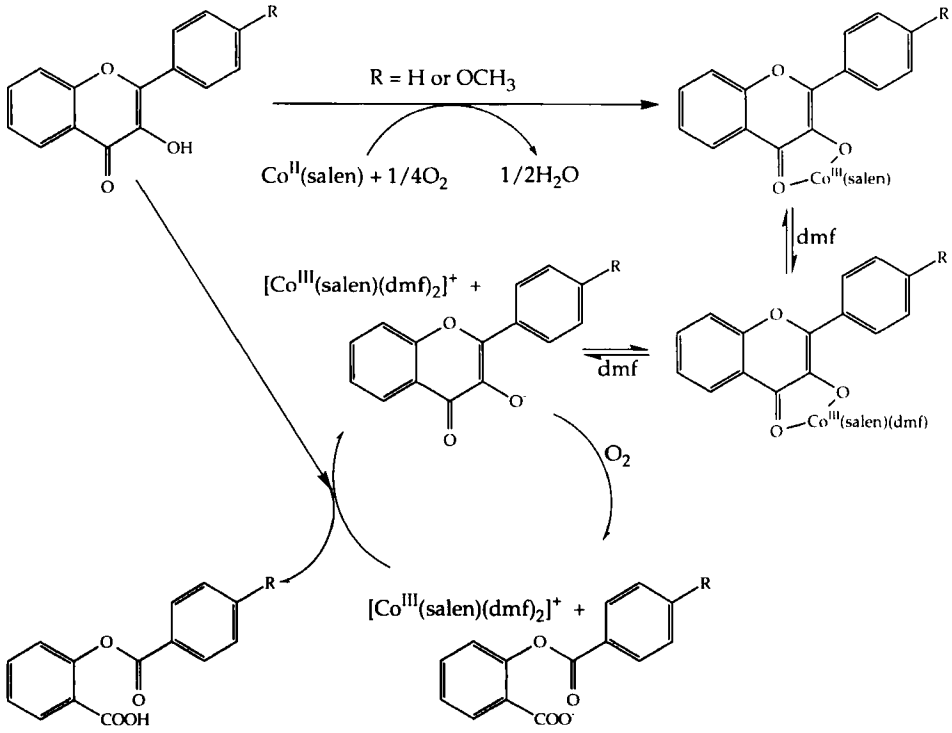

SCHEME 5. The proposed mechanism for the insertion of dioxygen into quercetin and other related 3-hydroxyflavones.

The effect of substituting a chloro, methyl, or *tert*-butyl group for the *para*-hydrogens of the phenyl rings of Schiff base **26** has been studied with regard to their catalytic activities in the oxygenation of 2,6-di-*tert*-butylphenol (*63*). In the presence of an appropriate axial ligand (i.e., pyridine, 4-(dimethylamino)pyridine, or dimethyl sulfoxide), each of the cobalt(II) complexes of these Schiff base ligands formed dioxygen complexes, and each was more active than [Co^{II}(salen)] in the oxidation of 2,6-di-*tert*-butylphenol and produced much smaller by-product-to-quinone ratios than [Co^{II}(salen)]. Electron-donating substituents appeared to give higher concentrations of the dioxygen adducts.

2. *Cyclidenes*

As mentioned earlier, cyclidenes are cyclic multidentate imino-donor ligands. The *lacunar* cyclidenes developed by Busch and co-workers

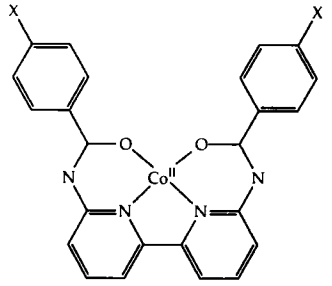

X = H, Cl, CH_3, $C(CH_3)_3$

(26)

(*64–66*) comprise a family of these ligands in which the ends of the cyclidene system are tied together with an alkyl chain, as shown schematically here as their cobalt complexes (the view on the left is a normal two-dimensional rendering, while that on the right attempts to illustrate the three-dimensional shape of the complex). Such lacunar systems, as their cobalt complexes, exhibit favorable characteristics as dioxygen carriers, including (i) significant dioxygen affinities at ambient temperatures, (ii) the ability to function in a variety of polar (water) and nonpolar (organic) solvents, and (iii) the ability to control and manipulate dioxygen affinity through the use of substituents and the sizes of the cyclidene and alkyl chain rings (*67*).

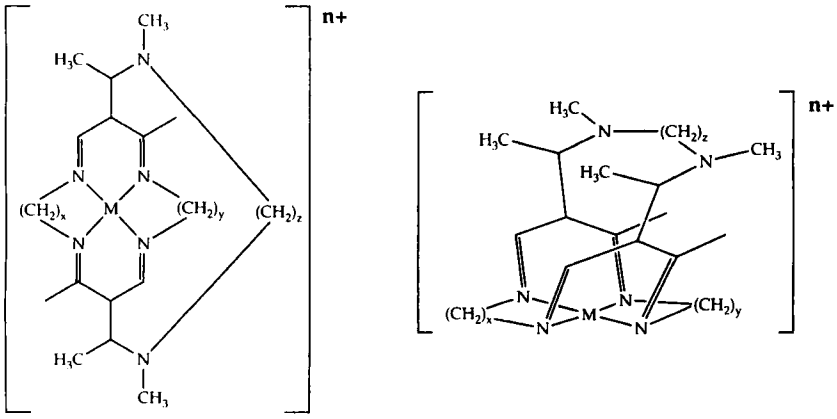

x = y = 2: [14]cyclidene
x = 2, y = 3: [15]cyclidene } z = 4, 5, 6, ..., 12
x = y = 3: [16]cyclidene

Although cyclidenes with 16-membered rings are most commonly used (*68*), cyclidenes with even smaller ring systems (down to 14-membered ring (*67*) cyclidenes) have been synthesized, and their affinity toward dioxygen examined. The three-dimensional structure of the ligand forms an intrinsic cavity within which the dioxygen molecule can bind, with a superstructure (the alkyl bridge) that pulls up the "sides" of the cyclidene to bridge the cavity (*69*). For otherwise similar cyclidenes, as the bridge length increases from $-(CH_2)_4-$ to $-(CH_2)_8-$, the dioxygen binding affinity of cobalt(II) complexes systematically increases over four orders of magnitude and can be correlated with the width of the cyclidene cavity (*65b*, *70*).

When the bridging alkyl chain is longer than $-(CH_2)_8-$, the ability of the cobalt(II) complexes to reversibly bind dioxygen is reduced. By the time chain lengths of up to $-(CH_2)_{12}-$ have been reached, the affinity for dioxygen has dropped to about one-fifth of the value for the $-(CH_2)_9-$ system. The rates of autoxidation of the cyclidenes with longer chain bridges are also increased (*68b*). When the ring size of the donor portion of the molecule is reduced to a 14-membered ring, the dioxygen affinity of the cobalt(II) complex is also reduced, and this reduction in affinity has been ascribed to the cavity shape (*67*). In addition to a reduced dioxygen affinity, the autoxidation of the system is also faster than that of the 16-membered ring.

Polymer-bound cobalt(II)-complexed cyclidenes have been reported (*71*), and these cyclidene systems apparently exhibit substantially longer dioxygen adduct lifetimes than the corresponding complexes in the solution phase. Other modifications (*72*) of the basic lacunar cyclidene structure include changing the bridging alkyl chain so as to include an –NR group (R = H, CH_3, *para*-vinylbenzoyl, and *para*-chlorobenzoyl) at the center of the chain, making the cyclidene system potentially pentadentate. (A previous report (*66d*) indicated that even without this –NR group in the bridging alkyl chain, the exocyclic nitrogen atoms can reorient themselves to a "lid-on"/"lid-off" conformation, bringing the bridging alkyl chain directly over or to the side of the cyclidene cavity, respectively.) The –NR group does, in fact, complex to the cobalt(II) center, and this pentadentate complex binds dioxygen reversibly and exhibits reasonable autoxidation stability (*72*).

D. Porphyrins and Related Ligands

Porphyrins are cyclic tetrapyrrole-containing systems; phthalocyanines are related systems containing benzene rings fused to the external bond of the pyrrole units (see Fig. 5).

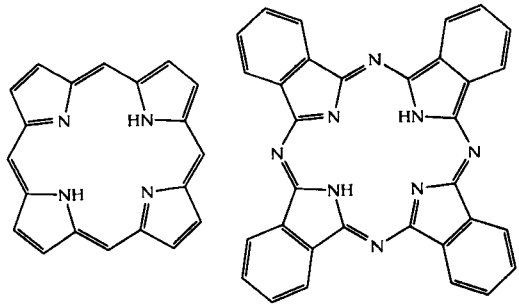

FIG. 5. The porphyrin nucleus (left) and the phthalocyanine nucleus (right).

1. Porphyrins

The discussion of porphyrin complexes in the activation of dioxygen in solution can be readily subdivided into discussions of monomeric systems and dimeric systems. The dimeric systems (cofacial metallodiporphyrins) have recently been reviewed by Collman, Wagenknecht, and Hutchison (*73*). That review highlights the significant amount of research stimulated by the initial discovery by Collman and co-workers (*74*), confirmed later by Chang and co-workers (*75*), that dicobalt cofacial diporphyrins can promote the direct four-electron reduction of dioxygen to water.

Cofacial diporphyrins can be bridged by one, two, three, or four links. In each case, the relative arrangement of the two bound metal atoms (one per porphyrin) can be described by the interplanar distance (P–P), the metal-center-to-metal-center distance (Ct–Ct), and the lateral shift (LS) of the metal centers with respect to each other (*76*), as shown in Fig. 6. Variations in these structural parameters should markedly affect the reactivity of the dimetallodiporphyrin.

The electrochemical and structural properties of a variety of bridged diporphyrins containing a substituted nitrogen atom in the center of

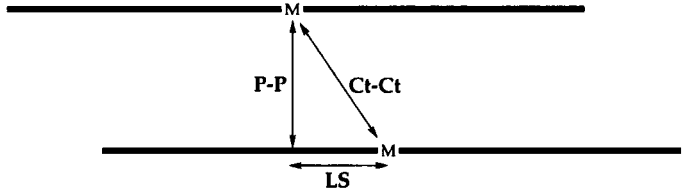

FIG. 6. The structural parameters describing the relative arrangement of the two bound metal atoms in a cofacial diporphyrin. The heavy horizontal lines indicate a view of the porphyrin "edge-on," in the plane of the porphyrins.

the bridging chain have been studied (*77*). The Ct–Ct distances were shown to decrease with increasing steric demand of the substituent on the nitrogen atom of the bridging groups, but this change did not significantly alter the catalytic efficiency of the systems. However, if the substituent on the nitrogen center is positively charged, the catalyst activity increases with respect to the electrochemical reduction of dioxygen.

An electron-deficient derivative of the cofacial diporphyrin **27**, formed from **27** under strictly anhydrous conditions through a two-electron oxidation to produce ($\mathbf{27}^{2+}$), has been shown to reversibly bind dioxygen (*78*). Neutral **27** does not bind dioxygen, but its one-electron oxidized analogue $\mathbf{27}^{2+}$, did form a remarkably strong complex with dioxygen (*79*). The binding of dioxygen to such an electron-deficient system as $\mathbf{27}^{2+}$ is unprecedented.

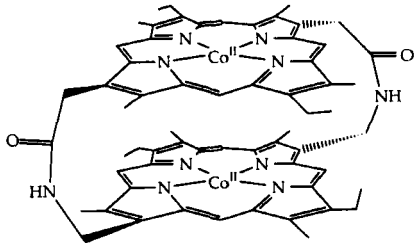

(27)

Although the cofacial diporphyrins represent a vibrant and innovative direction in dioxygen activation, simple porphyrins and their derivatives also remain an important research area. The dichlorophenyl-substituted porphyrin tdcpp [5,10,15,20-tetrakis(2,6-dichlorophenyl)-porphyrin] forms a complex with cobalt(II), [Co(tdcpp)], and catalyzes the oxidation of conjugated olefins to (after experimental workup) ketones in the presence of dioxygen and triethylsilane (*80*); a hydroperoxide intermediate has been isolated from these reactions (*81*).

A number of iridium–porphyrin systems, including mononuclear and cofacial diporphyrins, have been adsorbed on pyrolytic edge-plane graphite electrodes and tested for their ability to reduce dioxygen to water (*82*). The original system investigated, [Ir(oep)H], where oep = 2,3,7,8,12,13,17,18-octaethylprophyrinato, was unique in that, while monomeric, the complex was still active in acidic solutions at potentials of +0.72 V vs NHE at pH 1 (*82a*). The [Ir(oep)H] did become inactive at potentials less than +0.2 V vs NHE, unlike the cofacial dicobalt diporphyrin systems. In the more recent report of these systems (*82b*),

a large number of porphyrin systems were examined; based on the electrochemical results for these systems, the active species in the four-electron reduction of dioxygen to water is proposed to be an iridium(II) center.

With respect to mononuclear porphyrins, two derivatives deserve at least a special brief mention here: the so-called "C-clamp" and "picnic-basket" porphyrins. The former, C-clamp variety contain a substituent group (such as naphthoic acid in **28**, or **29** in which Kemp's acid has been incorporated) on the planar porphyrin ring that, through hydrogen bonding, can act as a "clamp" to assist in the binding of dioxygen to the metal center. Systems such as **29** and its anthranoic acid analogue **30** have been synthesized (*83*) and, as the cobalt(II) complexes, successfully bind dioxygen more strongly than the naphthoic acid–containing system **28**. (In the drawings of **28**, **29**, and **30**, the "clamp-assist" hydrogen bonding site has been indicated by a broken line.)

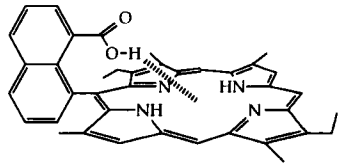

(28)

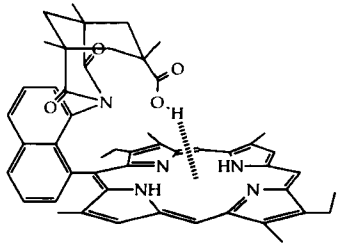

(29)

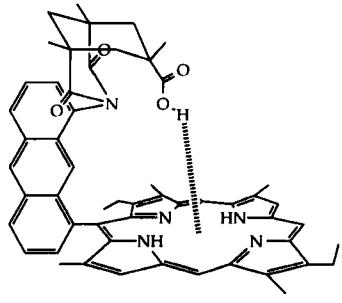

(30)

A picnic-basket porphyrin is reminiscent of the lacunar cyclidenes mentioned earlier, in which an alkyl chain tied the ends of the cyclidene together and formed a pocket for the complexation of dioxygen. Cobalt complexes of the picnic-basket porphyrins **31** bind dioxygen reversibly at room temperature with high oxygen affinities (*84*). The oxygen affinity increases as the basket size decreases (as determined by the length

of the basket "handle"), indicating that dipole–dipole interactions between the amide protons and the bound dioxygen may play a role in the stability of these complexes.

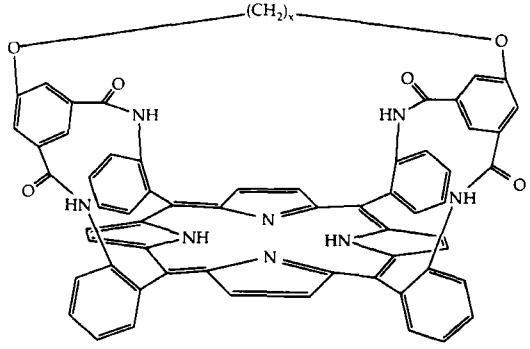

x = 2, 4, 6, or 8

picnic-basket porphyrin nucleus (31)

The coordination of up to four pentaammineruthenium(II) moieties to a porphyrin nucleus has been accomplished through the substitution of pyridine groups at the 5,10,15,20-positions on the porphyrin (*85*). The mono- and diruthenated complexes catalyze the two-electron reduction of dioxygen to hydrogen peroxide, while the tri- and tetraruthenated complexes catalyze the four-electron reduction of dioxygen to water, on electrode surfaces. However, the tetraruthenated species only catalyze a two-electron reduction in solution, and the rates of intramolecular electron transfer from the ruthenium moieties on the periphery of the molecule to the coordinated dioxygen molecule are quite slow.

It has been known since 1930 (*86*) that iron(II) porphyrins, when treated with dioxygen in the presence of a reducing agent, produce a deep green solution containing a diamagnetic iron complex called *verdoheme* (see Scheme 6). The presence of an oxaporphyrin in verdoheme is now well established (*87*). Cobalt(II)-containing porphyrins analogous to the iron(II) system in Scheme 6 also have been shown to react with dioxygen in the presence of ascorbic acid (the reducing agent) to produce the cobalt analogues of verdoheme, and the cobalt(II)–oxaporphyrin complex thus formed has been crystallographically characterized (*88*).

2. *The Use of Porphyrins in the Physical Separation of Air Components*

The separation of dioxygen from air has been carried out using a cobalt porphyrin complex tethered to the surface of a Vycor glass mem-

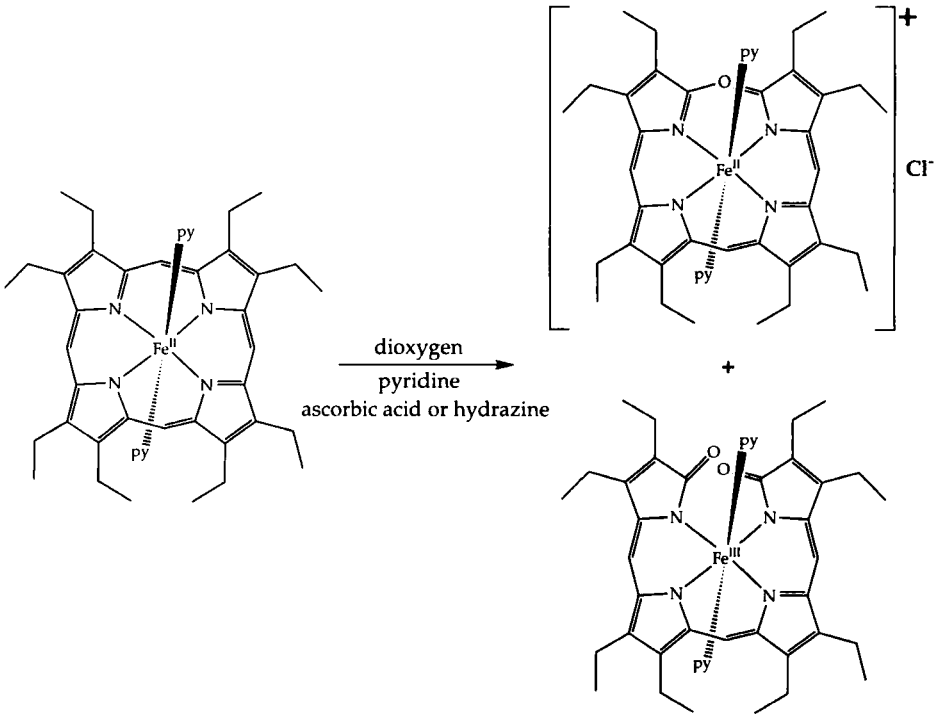

SCHEME 6. The reaction of iron(II) porphyrins with dioxygen in the presence of a reducing agent to produce *verdoheme* (top right) and a biliverdin-type complex (bottom right).

brane (*89*). In this process, in order to covalently bond an imidazolyl group to the Vycor surface, (3-chloropropyl)dimethoxymethylsilane was allowed to react with the surface of the Vycor, followed by reaction with imidazole. The known (*90*) oxygen carrier [$\alpha,\alpha,\alpha,\alpha$-tetrakis-(*ortho*-pivalamidophenyl)porphyrinato]cobalt was then attached to the surface through the complexation of the cobalt center to the imidazolyl group tethered to the surface through the propyl arm of the silane.

Dioxygen adduct formation with the bound cobalt-porphyrin complex was verified by infrared absorption studies (ν(O–O) at 1150 cm^{-1}), and the oxygen-binding equilibrium constant was measured (K = 1.8 torr^{-1}) on the basis of the Langmuir oxygen-binding isotherm. The bound cobalt–porphyrin complex acts as a chemically specific oxygen-binding site and is an effective carrier for the passage of dioxygen.

Incorporation of (*meso*-tetraphenylporphyrinato)cobalt(II), [Co(tpp)], into plasma polymer thin films for the possible use as dioxygen-selective permeable membranes has also been reported (*91*). Comparisons to

thin films prepared by sublimation of the [Co(tpp)] onto NaCl windows were made. These thin films, after exposure to 1-methylimidazole, reacted reversibly (reversed on exposure to a dinitrogen stream) with dioxygen, as indicated by infrared frequencies consistent with a dioxygen moiety bound to the cobalt center of the complex. When the [Co(tpp)] was incorporated into the *trans*-2-butene plasma polymer films, after exposure to 1-methylimidazole, the films again exhibited evidence for reversible (upon heating, but not after exposure to a dinitrogen stream) reactivity with dioxygen. However, where the sublimed films exhibit multiple ν(O–O) absorptions, the plasma polymer film exhibits only a single ν(O–O) absorption. This suggests that the plasma polymer has only *one* type of environment in which the [Co(tpp)] resides, while the sublimed films have *multiple,* slightly different environments. Further, the plasma polymer-incorporated [Co(tpp)] apparently has a higher affinity for dioxygen than does the sublimed film, since heat is required to reverse the binding. This is consistent with a report that [Co(tpp)] coordinated to polystyrene-bound 1-methylimidazole has a higher affinity for dioxygen than does the complex in solution (*92*).

3. *Phthalocyanines*

It has long been known (*93*) that cobalt(II) complexes of phthalocyanines interact with molecular oxygen. The water-soluble tetrasulfonato derivative of the parent phthalocyanine selectively and catalytically oxidizes 2,6-di-*tert*-butylphenol to the benzoquinone and the diphenoquinone in both homogeneous solution (*94*) and when polymer-supported (*95*). The active intermediate in the catalytic cycle is proposed to be the (as expected) mononuclear dioxygen complex of the cobalt–tetrasulfonatophthalocyanine system (*92*). It has been proposed that the formation of a peroxo-bridged dinuclear complex is responsible for the deactivation of the cobalt(II)-tetrasulfonatophthalocyanine system, since such a dinuclear system would be unable to further bind and activate dioxygen (*96*). Such deactivation results, ultimately, in loss of the catalyst and low turnover ratios.

Recently, the cobalt(II)–tetrasulfonatophthalocyanine system was reinvestigated for its catalytic activity while intercalated into a $Mg_5Al_{2.5}$-layered double hydroxide. The intercalate exhibited catalytic properties in the activation of atmospheric dioxygen for the oxidation of a thiolate to a disulfide (*97a*) and for the oxidation of 2,6-di-*tert*-butylbenzene to (nearly exclusively) the 2,6,2′,6′-tetra-*tert*-butyldiphenoquinone (*97b*). In marked contrast to the results reported for the homogeneous catalyst, this intercalated catalyst remained active for

more than 3200 turnovers and could be recovered by filtration without deactivation.

E. Miscellaneous Nitrogen Donors

Ligands with nitrogen donor sites not otherwise readily classifiable are discussed in this section. Mixed nitrogen–oxygen-containing donors (other than the Schiff bases discussed earlier) are discussed in Section II,F.

1. Nitriles

The catalysis of the selective oxidation of alkanes is a commercially important process that utilizes cobalt carboxylate catalysts at elevated (165°C, 10 atm air) temperatures and pressures (*98*). Recently, it has been demonstrated that $[Co(NCCH_3)_4][(PF_6)_2]$, prepared *in situ* from $CoCl_2$ and $AgPF_6$ in acetonitrile, was active in the selective oxidation of alkanes (adamantane and cyclohexane) under somewhat milder conditions (75°C, 3 atm air) (*99*). Further, under these milder conditions, the commercial catalyst system exhibited no measurable activity. Experiments were reported that indicated that the mechanism of the reaction involves a free radical chain mechanism in which the cobalt complex acts both as a chain initiator and as a hydroperoxide decomposition catalyst.

2. Hemerythrin and Hemocyanin

While hemoglobin and related molecules are most often considered as the prime examples of biological oxygen-carrying proteins, nonporphyrin-based iron centers are also quite important (*100*). One such protein is hemerythrin, a dioxygen-carrying nonporphyrin-di-iron protein found in some marine invertebrates (*101*). At the di-iron-containing site of each of the protein subunits (hemerythrins are often octameric), one molecule of dioxygen can be reversibly bound (*102*). The structure here is unusual, with the peroxo HO_2^- ligand bound end-on to only one of the iron atoms.

In order to study the relationship between protein folding and the dimetal site assembly process, as well as the potential for the analogue to bind dioxygen, the dicobalt analogue of hemerythrin was prepared (*103a*) from the apo-hemerythrin [originally isolated from *Phascolopsis gouldii,* followed by removal (*103b*) of the iron centers to produce the apoprotein]. The cobalt-substituted hemerythrin so formed closely resembled the native iron-containing protein in structure. In the cobalt-containing hemerythrin, EXAFS studies confirmed that the dicobalt site contained cobalt atoms ligated by histidine residues, as is the case

for the di-iron site in the native protein. Unfortunately, the dicobalt analogue of hemerythrin was completely unaffected by variations in pH or by the presence of azide, dioxygen, or hydrogen peroxide, all of which cause changes in the spectrum of the native di-iron-containing protein.

Like hemerythrin, hemocyanin is an oxygen transport non-heme-containing protein found in some arthropods and molluscs (*104*, *105*). In the O_2-bound form, hemocyanin contains an antiferromagnetically coupled binuclear copper(II) system (*106*) ligated by histidine residues, with a sideways μ_2-η^2 : η^2 peroxo group bound to both Cu^{II} centers (*104*), which superseded the previous model (*107*).

In order to provide additional insight into the active-site geometry and chemistry of hemocyanin, and to clarify earlier reports (*48a*, *108*) with regard to details of preparation, chemistry, and spectroscopy, the preparation of the cobalt(II)-substituted hemocyanin from the apoprotein (originally isolated from *Limulus polyphemus*) has been reported (*109*). This cobalt(II)-substituted protein exhibited spectroscopic properties consistent with each cobalt center being bound to three imidazole residues, and the protein reversibly bound dioxygen. The hypothesis that the bridging ligand in the native hemocyanin is endogenous hydroxide was also supported.

F. Mixed Nitrogen–Oxygen Donor Ligands

Studies of donor molecules with both nitrogen and oxygen donor sites allows the relative interactive effect of these donors to be investigated. In some cases the oxygen donor is merely a secondary perturbation in the ligand (as with OBISDIEN), while in other systems, the oxygen atom imparts an important donor site along with the nitrogen sites. (Schiff bases, formally a part of this section, were discussed earlier, as we believe that these ligands are more closely related to the cyclidenes.)

1. OBISDIEN and OBISTREN

The potentially binucleating macrocyclic ligand OBISDIEN (**32**), 1,13-dioxa-4,7,10,16,19,22-hexaazacyclotetracosane, is composed of two diethylenetriamine moieties separated by diethyl ether linkages (*110*). Under most experimental conditions, only three of the six nitrogen atoms in this macrocycle coordinate to a single metal ion; the coordination of two metal ions, each by three of the nitrogen centers, is thus possible. The two oxygen atoms are normally *not* coordinated to either of the metal ions, but the presence of these two oxygen atoms alters the overall reactivity of the coordination sphere within the macrocycle,

making the discussion of the complexes of OBISDIEN appropriate for this section.

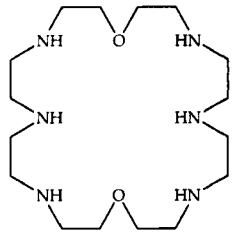

(32)

The OBISDIEN macrocycle forms both mono- and dinuclear complexes with cobalt(II), and the dinuclear system reacts with dioxygen to form a complex containing a bridging peroxo moiety as well as a bridging hydroxide group (*111*). The dioxygen complex of the dinuclear OBISDIEN–dicobalt(II) system has been employed to study the intramolecular oxidation of a number of species, including oxalate (*112*), ketomalonate (*113*), phosphite (*114*), catechol (*115*), and disodium 1,2-dihydroxybenzene-3,5-disulfonate (TIRON) (*115*). The peroxo complex is thought to be a good oxidant primarily because of the ligand-enforced proximity of the peroxo oxidant group to the substrate to be oxidized.

A system related to OBISDIEN is the cryptate ligand OBISTREN (**33**), 7,19,30-trioxa-4,10,16,22,27,33-hexa-azabicyclo[11.11.11]pentatricontane (*110a*, *116*). This molecule also strongly binds two cobalt(II) cations, and the complex has been shown to bind dioxygen as well. However, compared to the cobalt complexes of OBISDIEN, the binding of dioxygen in cobalt complexes of OBISTREN is significantly weaker (*117*). Spectrophotometric studies indicate that the dicobalt complex of the OBISTREN cryptate ligand has the potential to act as a reagent for the chemical separation of oxygen from gaseous mixtures (*118*).

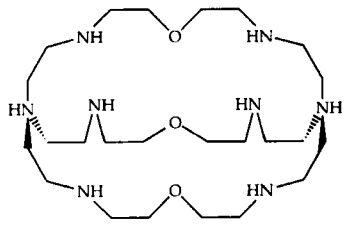

(33)

2. *Modified Amino Acids*

The two isomeric amino acid derivatives *N*,*N*-bis(2-aminoethyl)glycine (**34**) and diethylenetriamine-*N*-acetic acid (**35**) were found to react with cobalt(II) to form monomeric complexes (*119*). Upon exposure to dioxygen, these complexes reacted to form a dimeric oxygen adduct wherein the dioxygen bridges the two cobalt centers (along with a bridging hydroxide group). This reaction was easily reversed by either purging the system with nitrogen gas or adding acid.

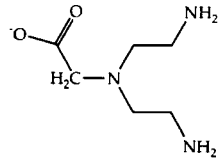

(34)

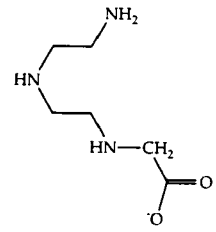

(35)

Complexes of other amino acids or their derivatives with cobalt(II) that have been investigated include dipeptides (*120*); these complexes have long been known to absorb dioxygen. For example, the mononuclear cobalt(II) complex of *N*,*N*,*N*‴,*N*‴-diglycylethylenediaminetetraacetic acid (*121*) absorbs one mole of dioxygen per two moles of complex. This system has been proposed as a simple, convenient model system for the study of dioxygen complexes of cobalt(II) peptides in solution because of its relatively slow conversion to the irreversibly formed cobalt(III) dioxygen complex.

III. Phosphorus Donor Ligands

Like carbon monoxide as a stabilizing ligand in organometallic chemistry, phosphine ligands are common ligands for the stabilization of the complexes reviewed in this article. Accordingly, phosphorus-containing ligands can also be found in complexes formally assigned to other sections of this review. In this section, however, only those complexes in which the phosphorus donor plays a significant role (rather than simply being a member of the "supporting cast" of ligands) have been included. The discussion in this section begins with heterodonor (P,N) systems, and continues with mono- and polydentate phosphorus-donor systems.

A. Mixed Phosphorus–Nitrogen Donor Ligands

The coordination of dioxygen to rhodium(I) centers so as to form either peroxo or superoxo adducts is well known: the ability of these complexes to transfer oxygen atoms to a variety of inorganic and organic substrates has been demonstrated (*122*). Recently, the synthesis, characterization, and reactivity of square-planar rhodium(I) complexes with the bidentate iminophosphine donor ligand *ortho*-$Ph_2PC_6H_4CH{=}NR$, where R = ethyl, *n*-propyl, *iso*-propyl, or *tert*-butyl, have been reported (*123*). This ligand is a bidentate, P,N-donor that, because of the nature of the substituent on the nitrogen atom, can exhibit variable steric requirements when bound to the rhodium center.

The complexes [Rh(*ortho*-$Ph_2PC_6H_4CH{=}NR)_2$][BPh_4], when R = ethyl, *n*-propyl, or *iso*-propyl (but not *tert*-butyl), react rapidly with pure dioxygen (or more slowly with atmospheric dioxygen) to form the pseudo-octahedral peroxo complexes [Rh(*ortho*-$Ph_2PC_6H_4CH{=}NR)_2(O_2)$][$BPh_4$]; the crystal structure of the *iso*-propyl derivative confirmed the peroxo designation with an O–O distance of 1.436(9) Å (*124*). Upon reaction with SO_2, the *iso*-propyl derivative reacts to form an isolatable bidentate sulfate complex, indicating that the bound dioxygen ligand is reactive. However, no similar reactivity of the bound dioxygen moiety with carbon dioxide or carbon monoxide was observed; the *tert*-butyl substituent was apparently too sterically demanding to allow the reaction with dioxygen to occur.

More recently, the iridium analogues of the aforementioned rhodium(I) complexes have been reported (*125*). Again, the bis(iminophosphine) complexes were square planar, and the steric hindrance of the alkyl substituent was the limiting factor in dioxygen uptake; all derivatives except the *tert*-butyl formed peroxo complexes. During the study of the electrochemistry of these iridium(I) bis(iminophosphine) complexes, it was found that the addition of an electron (reduction of an Ir^I to an Ir^0 species) was always a reversible process for each derivative, but that the removal of an electron (oxidation of an Ir^I to an Ir^{II} species) was only reversible for the *tert*-butyl derivative. Unlike the rhodium(I) complexes, these iridium(I) dioxygen complexes do not behave as oxygen carriers: the dioxygen molecule is irreversibly coordinated to the iridium center and cannot be removed even at elevated temperatures.

B. Monodentate Phosphorus Ligands

The addition reaction of normal, triplet dioxygen to Vaska's complex, *trans*-$Ir(CO)Cl(PPh_3)_2$, has been well studied (*126*, *127*). The kinetics

of the reaction of singlet dioxygen ($^1O_2$) with Vaska's complex has been studied (*128*), and the result has been compared to the rate of the triplet dioxygen reaction. Singlet dioxygen was found to be approximately 10^9 times more reactive than ground-state triplet dioxygen: if the excitation energy of singlet dioxygen is also taken into account, the relative rate of the reaction of singlet dioxygen compared to the ground state triplet reaction rate with Vaska's complex would be an astonishing (but not experimentally meaningful) 10^{16}! In addition to the reaction of singlet dioxygen with Vaska's complex, the physical quenching of the excited-state singlet by Vaska's complex was also noted and was found to dominate the peroxo formation reaction by approximately an order of magnitude.

Unlike Vaska's complex, the rhodium analogue *trans*-$Rh(CO)Cl(PPh_3)_2$ does not react with triplet dioxygen, and thus the corresponding rhodium–dioxygen complex is unknown (*129*). (The reaction of dioxygen with the related complex $RhCl(PPh_3)_3$ does result in the formation of two crystalline products after long reaction times (*130a*): the monomeric $RhCl(PPh_3)_3(O_2)$ (*130b*) and the dimeric system $(PPh_3)ClRh(O_2)_2RhCl(PPh_3)$ (*130c*). The monomeric system forms more rapidly.) However, at low temperatures (−40°C) in the presence of a sensitizer (methylene blue or C_{60}), singlet dioxygen *will* react with the rhodium analogue of Vaska's complex to form the peroxo complex $Rh(CO)Cl(PPh_3)_2(O_2)$ (*131*). Although only stable at low temperatures (warming causes the distinctive infrared peroxo absorption stretches to disappear), the complex exhibits a peroxo stretch at 901 cm^{-1} and a carbonyl stretch at 2044 cm^{-1}, both of which compare well to the iridium analogue's properties. The preparation of this hitherto unknown dioxygen complex may presage the preparation of other novel energetic and/or transient metal–oxygen complexes with interesting and perhaps unprecedented reactivities.

The chemistry of Vaska's complex and its derivatives with respect to the kinetics of the oxidative addition of methyl iodide and dihydrogen, and the association and dissociation of dioxygen, have been reinvestigated (*132*). The experimental results for these reactions were analyzed in terms of three stereoelectronic parameters. These three parameters were χ, an electronic parameter derived from previously reported infrared data for $Ni(CO)_3L$ (L = substituted phosphine) complexes; θ, the calculated cone angle of the phosphine ligands; and E_{ar}, an electronic parameter dependent on the number of aryl groups attached to the phosphine ligand. The dissociation of dioxygen from $Ir(CO)Cl(L_2)(O_2)$ was found to be relatively insensitive to both the χ and θ parameters, but the dissociation did exhibit a significant dependence on E_{ar}.

Square-planar iridium complexes containing the strongly electron-donating ligand tris(cyclohexyl)phosphine (PCy_3) have been investigated (*133a*) for their reactivity with small gaseous molecules. The complexes investigated were *trans*-$Ir(CO)(X)(PCy_3)_2$, where X = Cl and OH. The presence of the PCy_3 ligand inhibited reactions with dihydrogen or dioxygen, but had little effect on reactions with dichlorine or sulfur dioxide. Earlier studies (*133b*, *133c*) with similar iridium complexes containing a variety of phosphine ligands indicated that heightened electron density at the iridium center was the factor that enhanced the binding of dioxygen to the iridium center.

C. Polydentate Phosphorus Ligands

In general, the oxidation of primary alcohols to carboxylic acids using η^2-dioxygen metal complexes is rare. To our knowledge, only one report (*134*) communicates such a process.

Following the preparation of the yellow, air-stable peroxo complex [(triphos)$IrCl(\eta^2\text{-}O_2)$], where triphos = $CH_3C(CH_2PPh_2)_3$, from the ethylene complex [(triphos)$IrCl(\eta^2\text{-}C_2H_2)$], reactions of the peroxo complex with primary alcohols were studied. When the peroxo complex is dissolved in methanol, ethanol, or benzyl alcohol, the carboxylate complexes [(triphos)$IrH(O_2CR)$][BPh_4], R = H, CH_3, or Ph, can be isolated in high yield upon the addition of $NaBPh_4$.

The reaction mechanism shown in Scheme 7 illustrates the reactions involved, supported by the following information: (i) Water is a side product of the reaction; based on deuterium labeling experiments, both of the protons of the water molecule come from the alcohol, and no IrD species, which, if present, would indicate deuterium exchange between the deuterated alcohol and water, are seen. (ii) The reaction also occurs in CH_2Cl_2 when an equimolar amount of the alcohol is present. (iii) Acetaldehyde does not undergo reaction unless a protic acid such as triflic acid is present, and under such conditions, the acetate derivative, R = CH_3, is formed. (iv) When the peroxo complex is allowed to react with equimolar C_2H_5OD and excess aldehyde (R'CHO, R' = *n*-propyl, *n*-butyl, or Ph), the carboxylate hydride thus formed contains the aldehyde R' group, and both acetaldehyde and HOD are co-products. (v) By NMR spectrometry, evidence for an intermediate species such as that labeled "**A**" in the scheme, with three different ligands trans to the triphos ligand, was observed over the temperature range −60 to +20°C.

An unusual peroxo-bridged binuclear iridium complex containing an Ir—Ir bond has been reported (*135a, 135b*). The reaction of the electron-

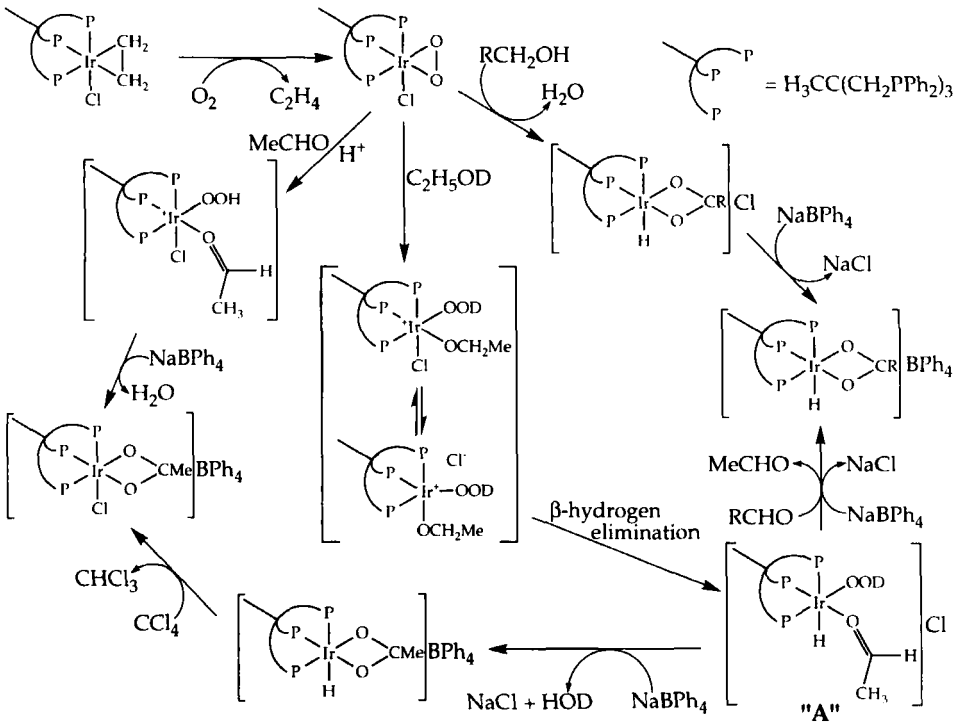

SCHEME 7. The steps in the oxidation of primary alcohols to carboxylic acids mediated by the peroxo complex [(triphos)IrCl(η^2-O_2)]. Although not isolated, experimental evidence indicates that an intermediate with the proposed structure indicated by "**A**" in the scheme is present.

rich di-iridium complex $[Ir_2I_2(CO)(\mu\text{-}CO)(dppm)_2]$ (*135c*) with air after several hours, or more rapidly on exposure to pure dioxygen, resulted in the formation of the binuclear Ir^{II}/Ir^{II} species $[Ir_2I_2(CO)_2(\mu_2\text{-}O_2)(dppm)_2]$ (**36**). X-ray crystallography confirmed both the structure and the presence of the bridging peroxo ligand. The presence of an Ir—Ir bond was indicated by the short Ir—Ir separation [2.705(1) Å].

The reactivity of **36** with small molecules was also reported. When SO_2 was passed through a CH_2Cl_2 or benzene suspension of **36**, a μ_2-SO_4 complex (**37**) was formed; the same complex could be formed through the reaction of **36** with H_2SO_4 (liberating hydrogen peroxide), or upon reaction with $CuSO_4$. Reaction of **36** with NO_2 yields the nitrate-bridged cation as the nitrate salt, or, on addition of $NaBF_4$, as the tetrafluoroborate salt $[Ir_2I_2(CO)_2(\mu_2\text{-}NO_3)(dppm)_2][BF_4]$ (**38**). Note that in **38**, the arrangement of the iodo and carbonyl ligands is different

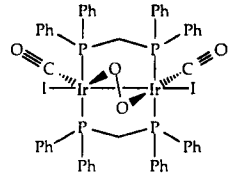

(36)

from that in **36** and **37**. Such a difference in ligand arrangement is not unusual for these complexes (*135c*).

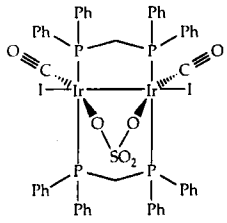

(37)

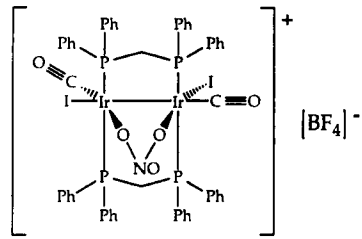

(38)

The reaction of **36** with carbon monoxide results in the formation of the neutral $[Ir_2I_2(CO)_2(\mu_2\text{-}CO)(\mu_2\text{-}O_2)(dppm)_2]$ **39**, which, according to an X-ray crystallographic analysis, no longer contains an Ir—Ir bond [the M–M separation is 3.388(2) Å]. This compound may be the first example of a compound that contains a five-membered metallocycle in which the $-O_2-$ unit and the carbonyl unit are both bridging.

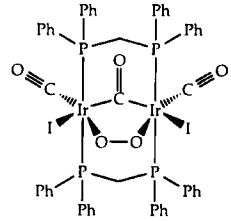

(39)

IV. Oxygen and Sulfur Donor Ligands

A "hard" oxygen donor ligand is fairly common in complexes containing a dioxygen ligand, especially when chelation is possible. Such systems include the β-diketonates and catechols and catecholates, and those Schiff base complexes described earlier. However, donation by a "soft" sulfur-containing ligand to dioxygen-containing complexes is rarer.

A. Carboxylates and β-Diketonates

The well-known rhodium (*136*) and iridium (*137*) peroxo complexes $(Ph_3P)_3RhCl(O_2)$ (**40**), $[(Ph_3P)_2RhCl(O_2)]_2$ (**41**), and $(Ph_3P)_2(CO)IrCl(O_2)$ (**42**) have been investigated for their reactivity with acetylacetone, acacH (*138*). Only the former complex, **40**, exhibited any reactivity (in the presence of two equivalents of triphenylphosphine), yielding the hydroperoxo complex (**43**), (see Scheme 8). Complex **43** reacts with PPh_3 to form triphenylphosphine oxide, but does not react with any active methylene compounds (methyl acetoacetate, diethyl malonate, or acetone) save for cyclopentadiene. In the last instance, a poorly characterized, unstable system tentatively formulated as **44** may have been formed. In refluxing benzene, **43** did react with excess acacH to form the bis(acac) complex **45**.

The investigation of phosphine complexes of rhodium(I) as catalysts (or catalyst precursors) for the hydroformylation reaction continues both to better elucidate the reaction mechanism and to improve catalyst activity. The presence of dioxygen often decreases the catalytic activity (*139*), but can also, surprisingly, *re*activate hydroformylation catalysts

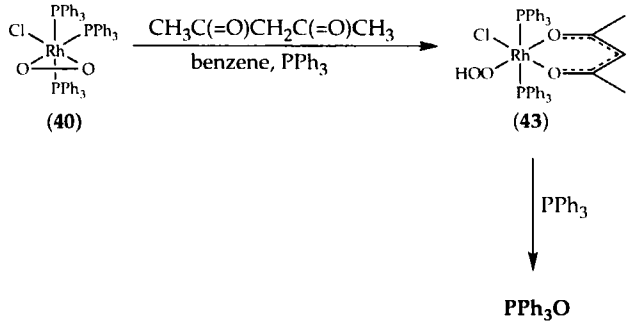

Scheme 8. The synthesis of an acetylacetonate complex of rhodium from the peroxo complex.

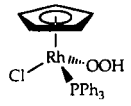

(44)

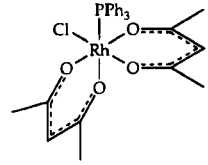

(45)

after prolonged use (*140*). Such previous reports, and the report (*141*) of the formation of a salicylate complex as one of the products of the reaction of (acac)Rh(CO)(PPh_3) (**46**) with salicylic acid, led to the detailed investigation (*142*) of the reactivity of **46**, as shown in Scheme 9. Crystal structures of the mono- and bis-salicylate complexes **47** and **48** were reported, as well as detailed spectroscopic information concerning other complexes identified in Scheme 9.

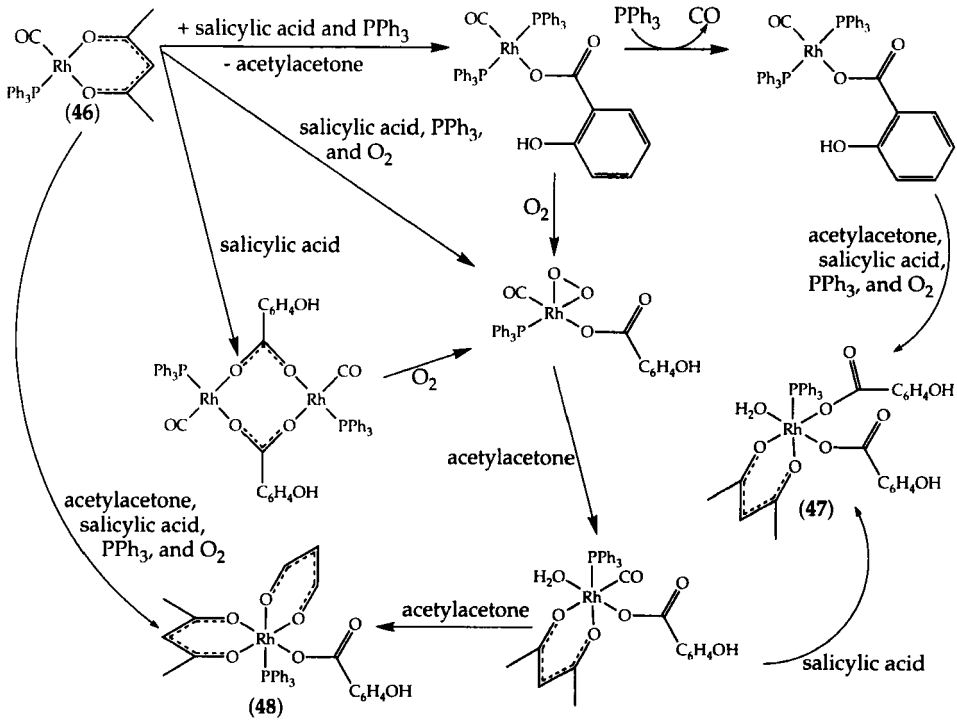

SCHEME 9. Reactions of acetylacetonato and salicylato complexes of rhodium.

B. Catechols and Catecholates

Many of the enzymes crucial to the life of aerobic organisms are those which catalyze the reaction of dioxygen with organic substrates. These enzymes are often classified as being either oxygenases (which catalyze the insertion of oxygen into the substrate) or oxidases (which catalyze electron transfer from substrate to molecular oxygen) (*143*). Further, the oxygenases may be simple *mono*oxygenases (which catalyze the insertion of only one oxygen atom into the substrate) or more complex *di*oxygenases (in which both atoms of dioxygen are inserted into the substrate). A subset of the latter category contains the catechol dioxygenases, which are widespread in nature. An understanding of the mechanism of action of these catechol dioxygenases is an important stated goal of many chemists and biologists. Catechol dioxygenases can catalyze intradiol insertions (i.e., catechol 1,2-dioxygenase) and extradiol insertions (i.e., catechol 2,3-dioxygenase) (*144*). Tyrosinase is an example of an enzyme that is both a monooxygenase and an oxidase (*145*).

It has been suggested that the use of high-valent transition metal complexes with *noninnocent* ligands may provide a method for the activation and transport of molecular oxygen (*146*). Studies were undertaken in order to shed some light on the interaction between metal catecholate complexes and dioxygen and also on the mechanism of activity of catechol dioxygenases. A large number of $[(triphos)M(cat)]^+$ complexes [cat = substituted catecholate ligand, including those illustrated in Fig. 7, triphos = $CH_3C(CH_2PPh_2)_3$, and M = Co, Rh, or Ir] were synthesized. The nature of both the metal and the catecholate ligand could be systematically varied in these complexes. The tripodal ligand triphos was chosen because such tripodal tri- and tetradentate ligands have been shown to provide metal complexes with a remarkable kinetic inertness, thus allowing reaction mechanisms to be more easily studied (*147*).

All of the compounds studied were shown to undergo electron transfer reactions encompassing the metal-centered M^{III}, M^{II}, and M^{I} formal oxidation states, and the catecholate(2^-), semiquinone(1^-), and quinone(0) ligand-centered oxidation states (*148*). With very few exceptions, all of the compounds react reversibly with dioxygen to give adducts in which the metal is octahedrally coordinated by the three phosphorus atoms of the triphos ligand and by three oxygen atoms, one from dioxygen and two from the catecholate ligand, which has now attained a semiquinoid character. The X-ray crystal structure (*146a*) of the complex cation $[(triphos)Ir(O—O)(phensq)]^+$, redrawn in Fig. 8

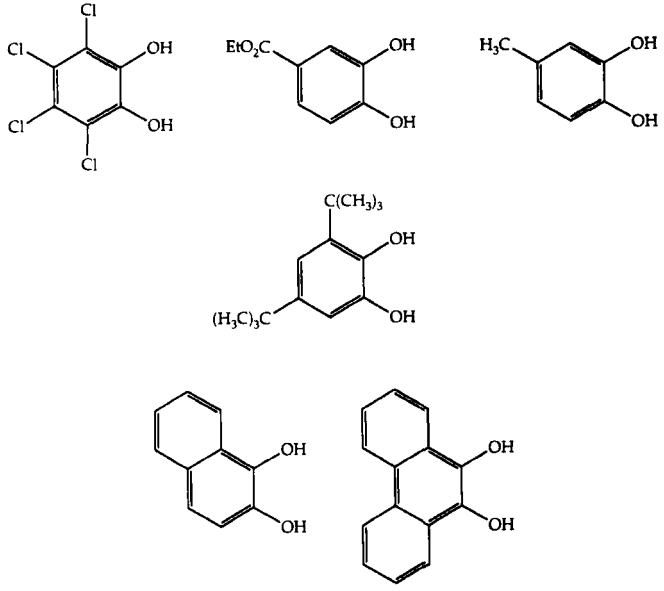

FIG. 7. The catechols used to prepare the [(triphos)Ir(cat)]$^+$ complexes.

(phensq = 9,10-phenanthrenesemiquinonate, with the tetraphenylborate counterion), illustrates the bonding in this system.

Several factors were found to affect dioxygen uptake by the metal catecholates. Of particular importance were (i) the coordination number of the metal, (ii) the relative basicity of both the catecholate ligand and the metal, (iii) the temperature, and (iv) the pressure of dioxygen. Under some circumstances, both the product containing reacted dioxygen and the unreacted starting catecholate complex existed in equilib-

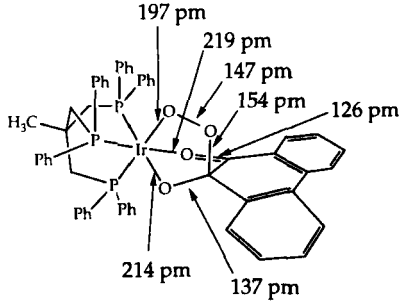

FIG. 8. The structure of [(triphos)Ir(O—O)(phensq)]$^+$, redrawn to show bond distances about the oxygen atoms.

rium, and, in these cases, the system could be shifted toward either the reactant or the product system by varying the reaction conditions (*148*). The electrochemical behavior of the dioxygen adducts has also been studied and reported. Depending on the $E^{\circ\prime}$ values relative to the $M^{III}(sq)/M^{III}(cat)$ couples of the parent metal catecholates, the dioxygen adducts undergo either a one-electron oxidation to give *ortho*-quinone (qu) complexes $[(triphos)M(qu)]^{3+}$ and the superoxide ion (O_2^-), or a two-electron oxidation to give $[(triphos)M(qu)]^{3+}$ and dioxygen.

Based upon experimental data and molecular orbital (MO) considerations, a mechanistic interpretation of the formation of the $[(triphos)M(O—O)(sq)]^+$ complexes was proposed (*146c, 148*). The proposed mechanism contained the features of a concerted closure of the five-membered metallacycle M—O—C—O—O, in which the metal complex appears to activate dioxygen because the dioxygen has, in close proximity to it, both an acidic metal center and an electron rich (basic) ligand. In simple MO terms, this is equivalent to the unusual coexistence of a ligand-centered HOMO (highest occupied molecular orbital) with a metal-centered LUMO (lowest unoccupied molecular orbital). It is the *bifunctionality* of the metal catecholate complexes that appears to be necessary for the reaction with dioxygen to occur, probably via the polarization of the dioxygen molecule itself.

Each of the $[(triphos)M(dtbc)]^+$ complexes [M = Rh (**49**) or Ir (**50**), and dtbc = di-*tert*-butylcatecholate] proved to be effective catalysts for both the oxidation and oxygenation of catechols under mild conditions (*146b, 149*). The selective oxidation of 3,5-di-*tert*-butylcatechol ($dtbcH_2$) to 3,5-di-*tert*-butyl-*o*-benzoquinone (dtbq) by molecular oxygen is catalyzed by **50** through its dioxygen semiquinone adduct. The rates of reaction of the substrate as well as the formation of products were shown to be first-order with respect to [catalyst] and [substrate], and zeroth-order with respect to pO_2 in the range 15 psi $\leq$ P $\leq$ 725 psi. On the basis of kinetic, spectroscopic, and chemical data, a catalytic cycle, as shown in Scheme 10, was proposed. At $pO_2 > 725$ psi, the oxygenation of $dtbcH_2$ to 3,5-di-*tert*-butyl-1-oxacyclohepta-3,5-diene-2,7-dione competes with dtbq formation.

The catalytic reaction of complex **49** with $dtbcH_2$ and dioxygen is less selective than that of **50**. In addition to the formation of dtbq and 3,5-di-*tert*-butyl-1-oxa-cyclohepta-3,5-diene-2,7-dione, some muconic acid anhydride and 2-pyrone derivatives are also produced as a result of both intra- and extradiol insertion of one of the oxygen atoms from dioxygen. Such products are consistent with the mechanism in Scheme 10, with the proviso that both the rhodium and iridium systems share the same mechanism, at least in the initial stages of the reaction.

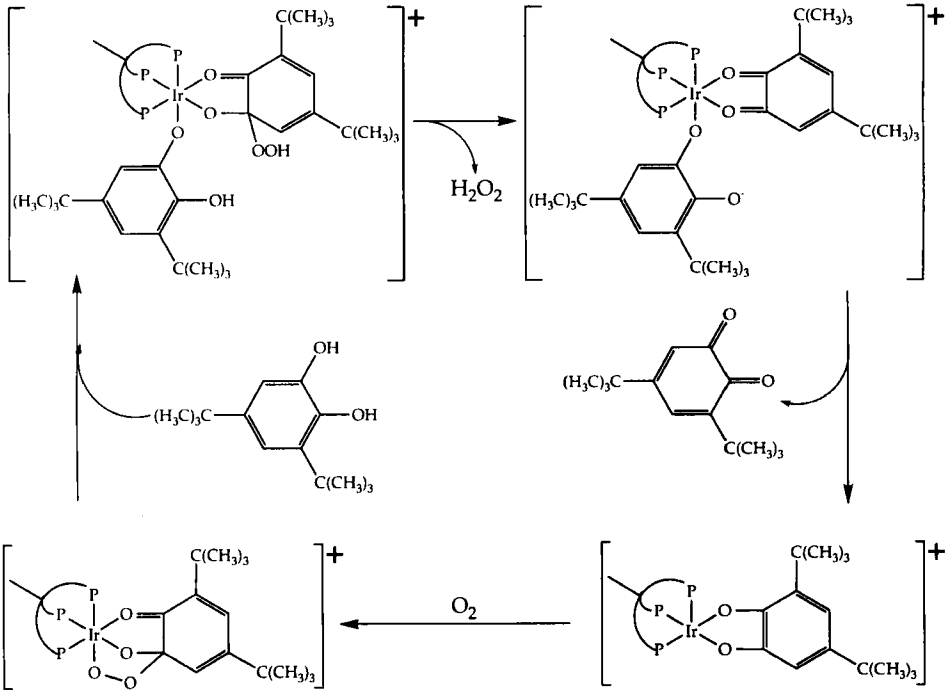

SCHEME 10. The proposed catalytic cycle for the selective oxidation of 3,5-di-*tert*-butylcatechol to 3,5-di-*tert*-butyl-*o*-benzoquinone.

These studies are part of a rare family of examples of the chemoselective oxidation of catechols (*150*). The identification of the catalyst and the interception of the catalyst–dioxygen adduct are of particular relevance when the chemistry of catechol dioxygenase and tyrosinase enzymes is concerned.

C. SULFUR DONORS

The anionic ligand (*151*) 7,8-dicarba-*nido*-undecaborate(1^-), substituted at the carbon-7 and -8 positions with sulfur-containing groups (see Fig. 9), has been shown to coordinate to the $[Ir(PPh_3)_2]$ moiety. Although the differences in ligands **51** through **54** appear to be quite subtle, their reactions with dioxygen in acetone solution are diverse (*152*). Only the iridium complex with **51** reacted with dioxygen to form the iridium(III) side-on bound peroxo complex **55**; the analogous complexes with **53** and **54** failed to react at all, while the iridium complex of **52** decomposed to produce borates.

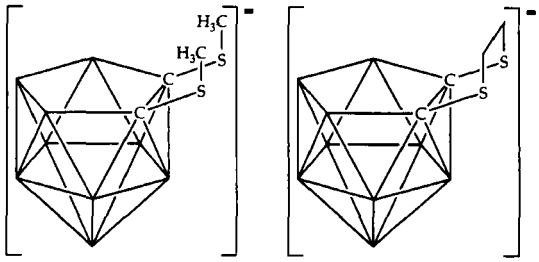

(51) (52)

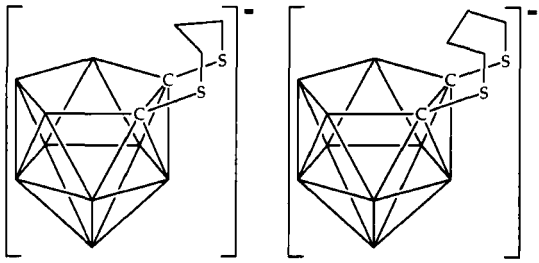

(53) (54)

FIG. 9. The sulfur-substituted anionic 7,8-dicarba-*nido*-undecaborate(1^-) ligands.

An X-ray crystal structure of **55**, redrawn as Fig. 10, supported the formulation of the complex as that of a peroxo system. Further, the structure demonstrated that no interactions between the $[O_2^{2-}]$ ligand and the borate moiety were possible because of the relative arrangement of the $[O_2^{2-}]$ and borate ligands about the iridium center. Such interactions *were* implicated in the oxygen-initiated decomposition of the iridium complex of **52**, while the lack of reactivity of the iridium complexes of **53** and **54** was attributed to steric factors arising from the alkyl chains connecting the sulfur atoms.

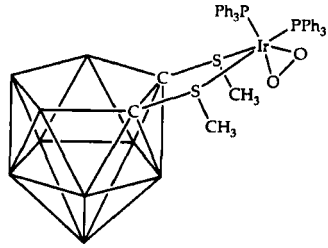

(55)

FIG. 10. The dioxygen adduct of the $Ir(PPh_3)_2$ complex of **51**.

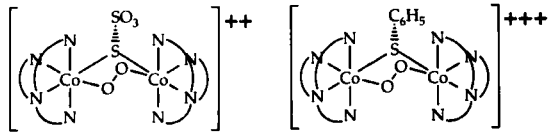

(56) (57)

FIG. 11. Dinuclear cobalt(III) complexes bridged by a peroxo linkage and either thiosulfate(2^-) (**56**) or benzenethiolate(1^-) (**57**).

Recently, the improved syntheses and structures (*153*) of a number of doubly bridged dinuclear cobalt(III) peroxo complexes containing bridging sulfur-donor ligands has been reported. These complexes, $[(taea)Co(\mu\text{-}O_2)(\mu\text{-}SR)Co(taea)]^{n+}$ [SR = S_2O_3 or $SCH_2CH_2SO_3$, n = 2; SR = SCH_2CH_2OH, SC_6H_5, or $SCH_2CH_2N(C_2H_5)_2$, n = 3] are sulfur analogues of the well-known (*154*) similar complexes with a hydroxy group in place of the bridging sulfur donor. The X-ray structures of the (μ-S_2O_3) analogue as the iodide salt, **56**, and the (μ-SC_6H_5) analogue as the perchlorate salt, **57**, redrawn as Fig. 11, exhibit comparatively long Co· · ·Co distances (>3.55 Å) and, subsequently, corresponding Co–O–O–Co torsion angles that are unprecedentedly large (>70°).

The benzenethiolato ligand has been coordinated to a rhodium center in the complex $Rh(SPh)[P(CH_3)_3]_3$. This complex, prepared from sodium thiophenolate and $Rh(Cl)[P(CH_3)_3]_3$, reacts smoothly with air either in the solid state or in solution (*155*) to form the yellow dioxygen complex $Rh(O_2)(SPh)[P(CH_3)_3]_3$. In a similar fashion, a mixture of $\{Rh[P(CH_3)_3]_4\}\{Cl\}$ and the thiophenolate ion reacts with air in solution to form the dioxygen complex: The analogous complex with *para*-methoxythiophenolate can also be formed in this manner. Although the mechanism of formation of the dioxygen complexes directly from the thiophenolate anion and $\{Rh[P(CH_3)_3]_4\}\{Cl\}$ is not fully understood, the initial formation of a rhodium(I)–thiophenolato complex such as $Rh(SR)[P(CH_3)_3]_n$, n = 3 or 4, is possible; the extreme sensitivity of the intermediate thiophenolato complex prevented its isolation.

An unusual sulfur–nitrogen donor, benzothiazole-2-thiolate (**58**), has been reacted with Vaska's complex to produce **59** in high yield; no bidentate adducts of **58** are produced even in refluxing solvent (*156*). Upon reaction with dioxygen, the extremely sensitive and reactive complex **60** is produced. Addition of water to **60** caused rearrangement to the carboxylate complex **61**, while the addition of sulfur dioxide to **60** produces **62** (see Scheme 11). A proposed mechanism for the reaction of water with **60**, based on labeling experiments, was outlined and can be found in Scheme 12.

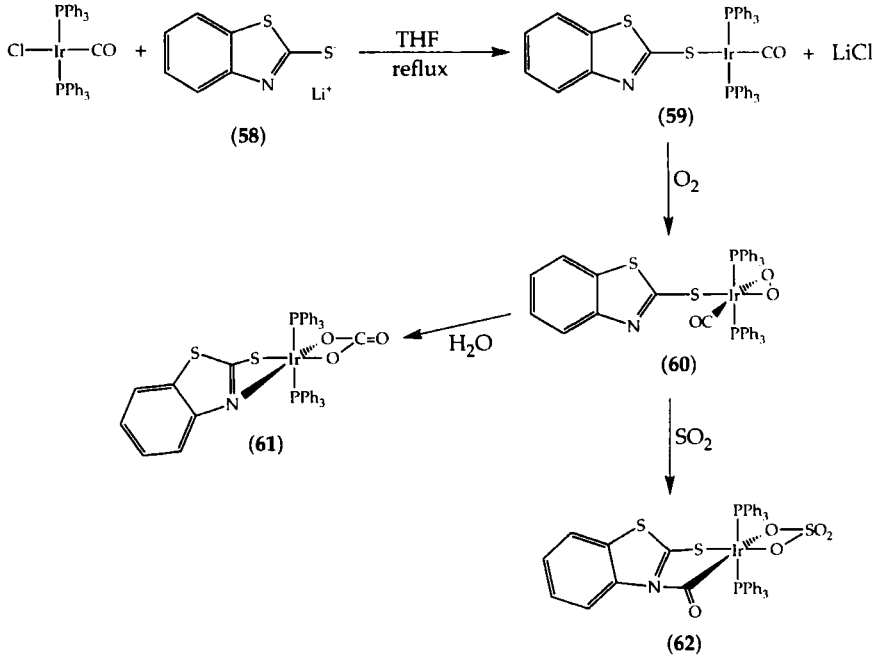

SCHEME 11. Selected reactions of [(*S*-benzothiazole-2-thiolato)Ir(PPh_3)$_2$(CO)] (**59**).

V. Carbon Donor Ligands

The cyclopentadienyl group, or its substituted derivatives, might be expected to stabilize dioxygen complexes or to ultimately react with dioxygen under the influence of transition metal centers. In rare cases, other (uncharged) dienes can also be found to stabilize dioxygen complexes of rhodium. Also discussed here are some reports of metallabenzene systems and their reactions with dioxygen.

A. Cyclopentadienyl and Diene Ligands

Reactions of the 19-valence-electron cobaltocene system are discussed first, followed by a brief discussion of an application to phase-transfer catalysis. Diene complexes are also considered.

1. Ligand Reactivity

As early as 1962, it was reported (*157*) that one mole of dioxygen would react with four moles of cobaltocene at 0°C, but no oxygenated products could be successfully isolated and characterized from this

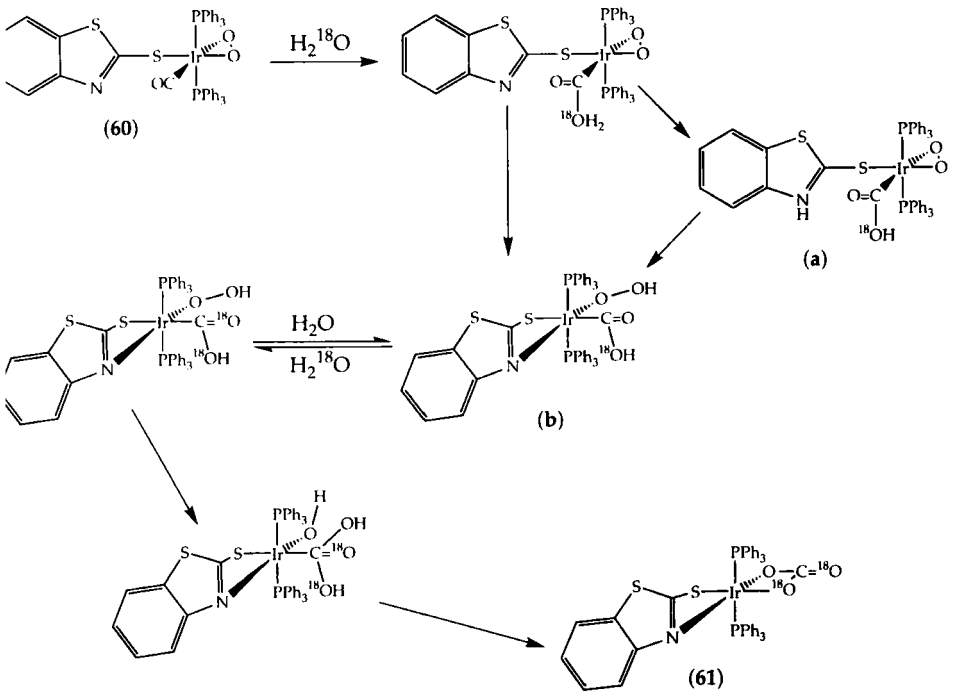

SCHEME 12. The proposed mechanism for the reaction of water with **60**. Alternative pathways, involving either initial protonation at nitrogen followed by proton transfer to oxygen, or direct protonation at oxygen, are illustrated in the upper right section of the scheme.

reaction. Later, it was found (*158*) that, under an oxygen atmosphere, organic compounds containing an active hydrogen atom (i.e., chloroform, acetonitrile, propionitrile, phenylacetylene, or acetone) would react with cobaltocene to produce (η^5-cyclopentadienyl)(2,3,4,5-η^4-1-*exo*-alkylcyclopentadiene)cobalt(I) complexes in high yield, as shown in Fig. 12. (The alkyl group in these compounds can be, respectively, trichloromethyl, cyanomethyl, 1-cyanoeth-1-yl, or phenylacetylenyl; the reaction with acetone produced a dinuclear complex in which the two cyclopentadiene ligands are bridged by a $-CH_2C(O)CH_2-$ group in an exo linkage arrangement.)

Further experiments (*159*), including gas titrations, reactivity studies, and spectroscopic evidence, led to the formulation of the intermediate, earlier postulated (*158*) to be an oxygenated cobaltocene adduct, as the organic peroxide structure **63**, in which the dioxygen bridge once again links the cyclopentadiene ligands in an exo fashion. This complex

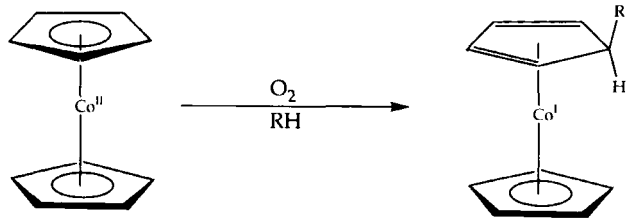

R = $-CCl_3$, $-CH_2CN$, $-CH(CH_3)CN$, $-CCC_6H_5$, or $-CH_2C(O)CH_3$

FIG. 12. Reactions of cobaltocene with organic compounds containing active hydrogen atoms in the presence of dioxygen.

was also found to react with α-diketones, oxidatively cleaving them to yield cobaltocinium carboxylates (*160*).

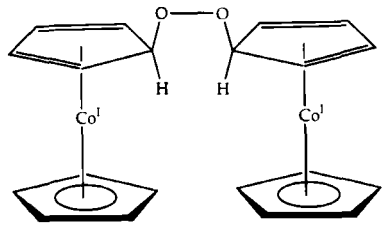

(63)

Similar reactions have been reported (*161*) for cobaltocene with nitric oxide (NO). (See Scheme 13.) In this case, however, rather than producing the peroxide-bridged structure **63**, the more stable ether-linked species **64** was produced. Complex **64** was crystallographically characterized, its reactions were studied, and a mechanism for its formation was proposed.

2. *Phase-Transfer Catalytic Reactions*

The rhodium complex [CpRh(bipy)Cl_2] is reported (*162*) to act as one-half of a redox couple that, in concert with a manganese porphyrin system, catalyzes the epoxidation of olefins by dioxygen. In this two-phase system, the aqueous phase contains sodium formate, and the organic phase is a trichloroethane solution of $[Mn^{III}(tpp)]^{1+}$ and the rhodium complex (tpp = *meso*-tetraphenylporphyrin). Apparently, the rhodium complex catalyzes the reduction of $[Mn^{III}(tpp)]^{1+}$ by formate, and the manganese(II) species thus formed binds dioxygen and reacts with the substrate olefin to form the epoxide. However, the intermedi-

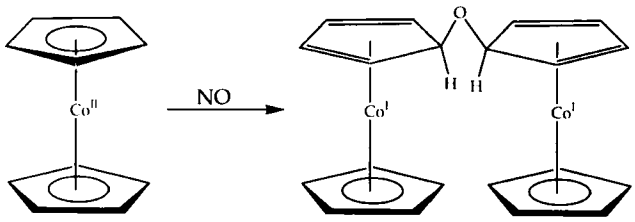

(64)

SCHEME 13. The reaction of cobaltocene with nitrous oxide to produce **64**, an ether-linked system (compare to **63**, a peroxo-linked system).

acy of a rhodium superoxo species (*163*) may also be indicated, as the $[Mn^{III}(tpp)]^{1+/0}$ complex is ultimately degraded during the reaction. The authors speculated that such a rhodium superoxo species might catalyze the manganese–porphyrin complex degradation.

3. *Diene Complexes*

A single brief communication some years ago (*164*) reported the preparation of a series of dirhodium complexes containing a labile peroxo bridge. These complexes, prepared by the action of solid potassium peroxide on $LRh(\mu_2\text{-}Cl)_2RhL$, where L = cyclooctadiene, dicyclopentadiene, or norbornadiene, contained no other ligands save the neutral dienes. The complexes were shown to oxidize Ph_3P to Ph_3PO, as well as to react with water and alcohols to give the corresponding μ_2-hydroxy or -alkoxy complexes, as well as H_2O_2, lending support to the assignment of the $\mu_2\text{-}O_2$ system as a peroxo moiety.

B. METALLABENZENES

In general, stable metallabenzenes can certainly be considered rare systems, as only the osmabenzene of Roper and co-workers (*165*) and the molybdabenzene of Ernst and co-workers (*166*) had been reported prior to the synthetic report of Bleeke and co-workers (*167*) of the iridiabenzene **65**. In addition to reactions (*168*) with dihydrogen, which yields the known (*169*) complex **66**, and with diiodine (see Scheme 14), **65** reacts with dioxygen to give **67**, an unusual dioxygen-bridged species. (In related chemistry, the synthesis (*170*) of an iridiaoxacyclohexadiene or "iridiapyran" species has been reported.) Complex **65**, whose structural and spectroscopic properties clearly indicate the presence of an aromatic system, also reacts with (η^6-*para*-xylene)$Mo(CO)_3$.

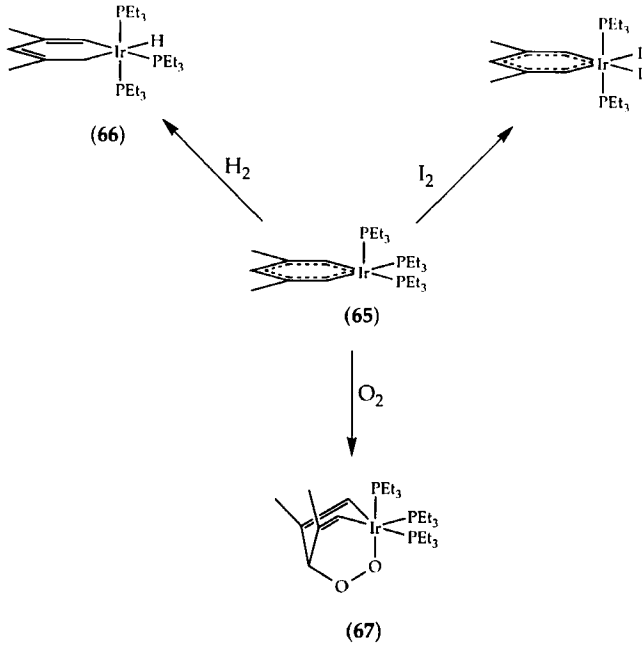

SCHEME 14. Some reactions of the iridiabenzene complex (**65**).

In this latter reaction, the iridiabenzene complex cleanly displaces the *para*-xylene ligand so as to form complex **68**, in which the iridiabenzene acts as if it were a normal η^6-ligand coordinated to the molybdenum tricarbonyl moiety.

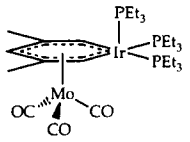

(68)

VI. Special Applications

A. Aqueous Studies

Because of the interest in the potential biological applications of complexes containing coordinated dioxygen, and the importance of superoxides as a by-product of aerobic metabolic processes, aqueous stud-

ies of dioxygen-containing complexes are gaining increasing importance. In addition, some aqueous species of rhodium, known for many years as "rhodiates" but never fully characterized, have recently been reinvestigated and classified as complexes containing bound dioxygen.

1. *Cobalt*

The reduction of dinuclear complexes of μ-peroxo- and μ-superoxo–cobalt(III) species have been investigated using both mononuclear (*171*) and dinuclear (*172*) metal-centered reductants for many years. Definitive methods for the preparation of these complexes have been reported (*173*).

Somewhat more recently, the reduction of the superoxo-containing species $[(eda)_2Co(\mu\text{-}NH_2)(\mu\text{-}O_2)Co(eda)_2]^{4+}$ and its peroxo-containing counterpart $[(eda)_2Co(\mu\text{-}NH_2)(\mu\text{-}O_2)Co(eda)_2]^{3+}$ with sulfite, nitrite, and arsenite have been reported (*174*). When sulfite or nitrite are used as the reductants, the ultimate product formed contains bridging sulfate or nitrate, respectively, in place of the μ-O_2 group. In the case of arsenite, however, the arsenite is oxidized to arsenate (AsO_4^{3-}), and a complex with a μ-OH group in place of the μ-O_2 group results.

The superoxo-containing species $[(NC)_5Co(\mu\text{-}O_2)Co(CN_5)]^{5-}$ can be reduced with thiols such as 2-aminoethanethiol or L-cysteine (*175*), and the reduction reaction is catalyzed by copper(II) ions in aqueous solution. When copper(II) is present, the role of the thiol is to reduce copper(II) to copper(I), which then reacts with the superoxo species through an inner-sphere mechanism. Conversely, when the superoxo complex $[(H_3N)_5Co(\mu\text{-}O_2)Co(NH_3)_5]^{5+}$ is reduced with thiol (*176*), the reaction follows an outer-sphere mechanism, as would be expected. Ascorbic acid also reduces both complexes (*177*), but only the reduction of the cyano-containing complex exhibits copper(II) catalysis.

2. *Rhodium*

The violet-blue solutions prepared by chlorination of an initially alkaline aqueous solution of $RhCl_3$ and the related deep blue solids (readily precipitated from the solutions on the addition of aqueous $Ba(OH)_2$ to the chlorinated but still alkaline rhodium-containing solutions) have been given the generic name *Claus' blues,* named after the author of the original report (*178*) of their preparation. Originally, the Claus' blue solutions were formulated as containing rhodium(VI) species, probably in the form of RhO_4^{2-}. This conclusion was made primarily by analogy to the insolubility of $BaSO_4$ and $BaCrO_4$ salts then thought to be similar.

A report (*179*) demonstrated that the presumed oxidation of rho-

dium(III) in aqueous solutions by Cl_2, by OCl^-, or by other methods did *not* produce oxidized rhodium species such as rhodium(IV), rhodium(V), or rhodium(VI). Rather, the $[Rh^{III}(\mu\text{-}O_2)Rh^{III}]^{5+}$ fragment was generated in these systems, thereby allowing large quantities of superoxo–dirhodium complexes to be made quickly and easily. Thus, the idea that Claus' blues are rhodium(VI) species became doubtful.

A spectroscopic study of Claus' blue, with comparisons to the much better characterized (*180*) ion $[Rh_2(OH)_2(H_2O)_n(\mu\text{-}O_2)]^{3+}$, was thus undertaken (*181*). By the use of UV-vis, ESR, and IR/Raman spectroscopies, as well as magnetic susceptibility measurements and voltammetric studies, it was determined that Claus' blue solutions actually contain superoxo–dirhodium complexes, and not RhO_4^{2-} ions. The superoxo bridge does *not,* however, derive from dioxygen, but from oxidation of coordinated hydroxide. Finally, Claus' blue solutions were demonstrated to be good starting materials for the preparation of superoxo-dirhodium carboxylate complexes, which could be isolated and characterized.

The rhodium complexes *cis-* and *trans*-$[Rh(eda)_2(NO_2)X]^+$, where $X = NO_2^-$, Cl^- or ONO^-, photoreact (*182*) with dioxygen in aqueous solution to form monomeric $[Rh(eda)_2(H_2O)(O_2)]^{2+}$ and dimeric complexes. These complexes act as one-electron oxidizing agents, oxidizing I^- to I_2 and Fe^{II} to Fe^{III}.

In an analogous fashion to that described for the similar cobalt species (*vide supra*), the redox reactions of $[Rh_2^{III}(OH)_2(H_2O)_8(\mu\text{-}O_2)]^{3+}$ have been investigated (*183*). This species can be reduced to the peroxo species with a variety of metal ions or by using either ascorbic acid or hydroquinone. The reduction process appears to follow an outer-sphere mechanism for vanadium(II), but with iron(II) the reduction occurs through an inner-sphere mechanism. The attempted reductions with Sn^{II}, U^{IV}, or $(Mo^{IV})_2$ were anomalous: none of these reducing agents produced the peroxo species, nor did they produce a species from which the superoxo species could be regenerated.

B. Oxidative Reactions with Noncoordinated Molecules

Coordinated dioxygen has been shown to react with noncoordinated molecules in a few instances: Generally the product results from the oxidation of the reactant, noncoordinated molecule, which may or may not itself then be coordinated to the original metal center.

1. Sulfur Dioxide

Because of both its environmental impact and its chemical usefulness, sulfur dioxide continues to play an important role in chemical

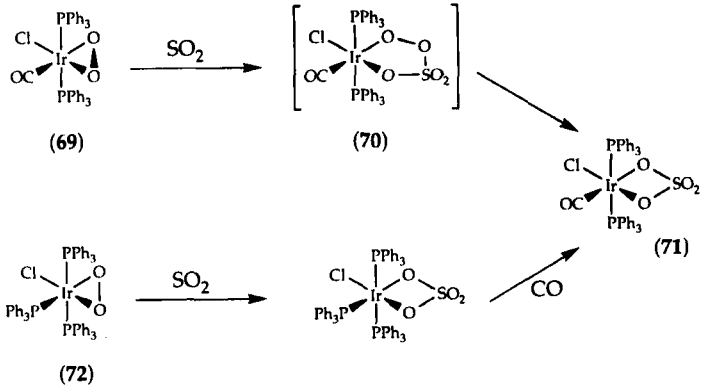

(69) (70) (71) (72)

SCHEME 15. The reactions of sulfur dioxide with dioxygen complexes of iridium.

research. The effect of SO_2 in the phenomenon known as *acid rain*, caused in part by the combustion of fossil fuels containing sulfur, is an environmental problem worldwide (*184*). On the other hand, it has been stated that SO_2 may be the most versatile complexing agent/ligand known (*185*). Even when SO_2 does not displace or react with ligands bound to a metal complex, recent work demonstrates that SO_2 will form charge transfer complexes with iridium and rhodium half-sandwich complexes (*186*).

It has long been known that the dioxygen–iridium(III) complex **69** (see Scheme 15), derived from Vaska's complex, will react smoothly with SO_2 to form sulfato complexes (*187*). Through ^{18}O-labeling experiments (*188*), the intermediate in this reaction was determined to be most probably the peroxysulfito complex **70**. The isolated product, **71**, could also be prepared (*187*) from the oxygen adduct of $IrCl(PPh_3)_3$, **72**, because of the ease with which the phosphine trans to the sulfato group could be replaced by CO.

Generally, while SO_2 reacts with dioxygen complexes of iridium, the reverse reaction, in which dioxygen reacts with SO_2–Ir complexes, is rare (*187*). However, when the chelating triphos ligand, $H_3CC(CH_2PPh_2)_3$, is used, as in **73**, such a reaction can be observed (*189*) for both iridium and rhodium.

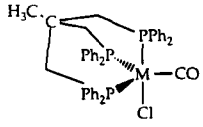

M = Rh, Ir

(73)

Competitive reactions of *trans*-Ir(CO)X[P(*ortho*-tolyl)$_3$]$_2$, where X = Cl or CH_3, with SO_2/O_2 mixtures (*190*) demonstrated that sulfur dioxide *kinetically* binds to the iridium center more rapidly than does dioxygen, but that the *thermodynamic* order of binding is $H_2 \approx O_2 > SO_2 > CO > CO_2 \approx H_2O$. When X = Cl, the reaction with SO_2/O_2 mixtures resulted in the formation of the sulfato complex overnight, while when X = CH_3, only about 15% of the dioxygen complex was converted to the sulfato complex, Ir(CO)X(SO_4)[P(*ortho*-tolyl)$_3$]$_2$, after 24 h (*190*). The reaction was faster with the tris(*para*-tolyl)phosphine complex (*191*). When X = OCH_3 or OH and the phosphorus ligand is PPh_3, the reaction to form the sulfato complex is rapid, demonstrating the steric effect of the phosphine ligands (*192*). The crystal structure of Ir(OCH_3)(CO)(SO_4)(PPh_3)$_2$ has been reported (*193*).

The reactivity of cobalt(II) complexes with SO_2 under both aerobic and anaerobic conditions has been reported (*194*). When the complexes Co($OPPh_3$)X_2 or Co($OAsPh_3$)X_2, with X = Cl or Br, were allowed to react with air in SO_2-saturated toluene solutions, the starting cobalt complexes could be recovered unchanged even after more than 28 days. However, when X = I or NCS, slow (approximately 7 days) reactions occurred. For X = I, the products isolated were solid $CoSO_4 \cdot H_2O$, I_2, and crystalline (Ph_3PO)(Ph_3POH)(HSO_4); the triphenylarsine oxide complex also formed the additional product Ph_3AsI_4. When X = NCS, similar reactivity patterns were observed. However, in this latter reaction, thiocyanogen $(NCS)_n$, the product analogous to I_2 which might be expected to form, was not isolated. Under the reaction conditions, this polymer is known (*195*) to degrade to yield hitherto uncharacterized products. None of these compounds appear to react with air except in the presence of sulfur dioxide.

2. *Sulfite*

The reaction of a dicobalt complex bridged by a peroxo ligand with the sulfite ion has been reported. In this reaction, a dicobalt complex containing a bridging sulfato ligand is formed, along with free sulfate (*196*).

3. *Carbon Dioxide and Carbon Monoxide*

In the course of studying the reactions of carbon dioxide, carbon disulfide, and other small molecules with peroxobis(triphenylphosphine)platinum(II) (*197*), the reactions of Ir(CO)Cl(PPh_3)$_2$(O_2) and RhCl(PPh_3)$_3$(O_2) with CO_2, CS_2, aldehydes, and ketones were also attempted. In every case the metal-containing reactant was recovered unchanged. Somewhat later (*198*), it was demonstrated that Ir(CO)X(PPh_3)$_2$(O_2),

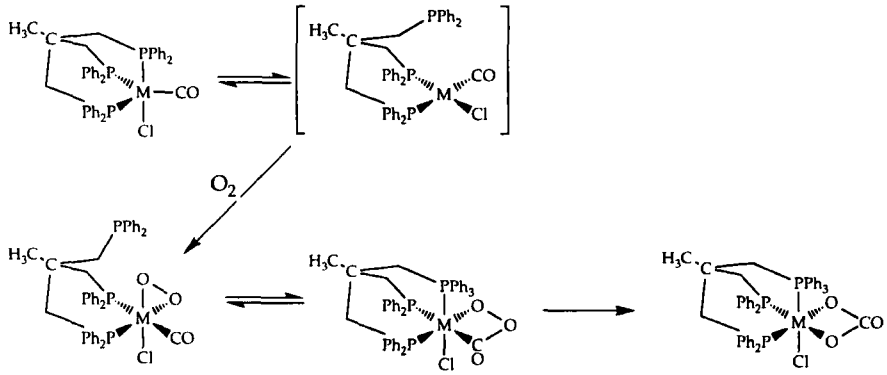

SCHEME 16. Reaction of coordinated carbon monoxide with bound dioxygen at an iridium center.

with X = CH_3 or Ph, would, in fact, react with *liquid* CO_2 to form the peroxycarbonate complex **74**. The evidence supported a mechanism that involved an external attack by the CO_2 molecule, rather than requiring a precoordination step.

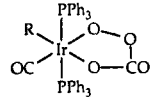

(**74**), R = CH_3 or C_6H_5

The reaction of CO_2 with $Ir(CH_3)CO(O_2)[P(p\text{-tolyl})_3]_2$ also results in the formation of a peroxycarbonate complex (*191*) via external attack by carbon dioxide. In this case, however, only gaseous carbon dioxide is required, rather than the more strenuous conditions of liquid CO_2. This same complex reacts with gaseous carbon monoxide to form the carbonate complex. Labeling experiments demonstrate that the *coordinated* CO does not participate in the reaction: External attack by the added CO is responsible for the reaction (*191*). Coordinated CO *has* been shown to react with bound dioxygen, as is seen in Scheme 16. In this case, the chelating triphos ligand obviously has a significant effect on the reactivity (*189*).

4. Ketones

The activated, electron-deficient ketone hexafluoroacetone, hfa, reacts with the iridium complex $IrX(CO)L_2(O_2)$ (in which X = Cl, Br, or I and L = PPh_3, or in which X = Cl and L = $AsPh_3$, $PMePh_2$, P(*para*-tolyl)$_3$, or P(*para*-anisyl)$_3$) by an apparently direct electrophilic attack

on the coordinated dioxygen to form the ozonide (**75**) via an ionic transition state (*199*). The reaction is second-order (first-order in each reactant), and the rate of the reaction depends on the substituents on iridium and upon the solvent, as follows:

Reaction rate (substituents): $Cl > Br > I$
$PMePh_3 > AsPh_3 > PPh_3$
Reaction rate (solvent): 3-pentanone > $CH_3CN > C_6H_6$

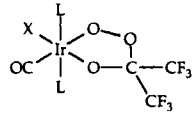

(**75**), X = Cl, Br, or I when L = PPh_3
X = Cl when L = $AsPh_3$, $PMePh_2$, $P(para\text{-}MeC_6H_4)_3$, or $P(para\text{-}MeOC_6H_4)_3$

5. *Phosphines*

The methyl iridium dioxygen complex $Ir(CH_3)CO(O_2)[P(p\text{-tolyl})_3]_2$ reacts with added triphenylphosphine to produce triphenylphosphine oxide (*191*). That this is a bimolecular reaction was demonstrated both by the complete absence of any oxidation of the tris(*para*-tolyl)-phosphine and by the lack of any substitution of the bound tris(*para*-tolyl)phosphine by triphenylphosphine.

C. Studies with Cubanes

As part of an attempt to model the tetramanganese center presumed to be responsible for the oxidation of water in photosynthetic green plants and the cyanobacteria, cobalt(III) systems were investigated (*200*). It was hoped that structurally similar systems that would exhibit enhanced stability under experimental conditions could be produced in this fashion. (The Mn_4 species present in the actual photosynthetic system has been difficult to study because of its instability when removed from the environment of the plant cell.)

Following the treatment of a 1:1 mixture of $Co(OAc)_2 \cdot 4H_2O$ and bipyridine (bipy) in 3:1 methanol:water with H_2O_2, heating, and the addition of THF and $LiClO_4$, red crystals of the dicobalt system **76** could be isolated (see Scheme 17). Under similar conditions (1.5:1 $Co(OAc)_2 \cdot 4H_2O$:bipy in 6:1 ethanol:water), greenish-black crystals

of the tricobalt semicubane system **77** were isolated. Finally, treatment of **76** with 5 equivalents of Li_2O_2 yielded brown crystals of **78**, a tetracobalt cubane system. Both **76** and **77** were characterized by X-ray crystallography; **78** was a weak diffractor of X-rays and was converted from the acetate derivative to the *para*-toluic acid derivative **79** for structural analysis.

Although these cobalt species do not in themselves activate dioxygen, they do exhibit similarities to the proposed structures of manganese complexes that may be involved in photosynthetic water oxidation (*201*). Such important studies may be relevant to the activation of dioxygen by other transition-metal complexes and to the investigation of the mechanism of the evolution of dioxygen by photosynthetic manganese–oxo complexes.

Because of the common presence of cubane and pseudocubane structures in the active sites of many different types of enzymes and cofactors (*202*), the synthesis of heterocubane systems containing sulfur, sele-

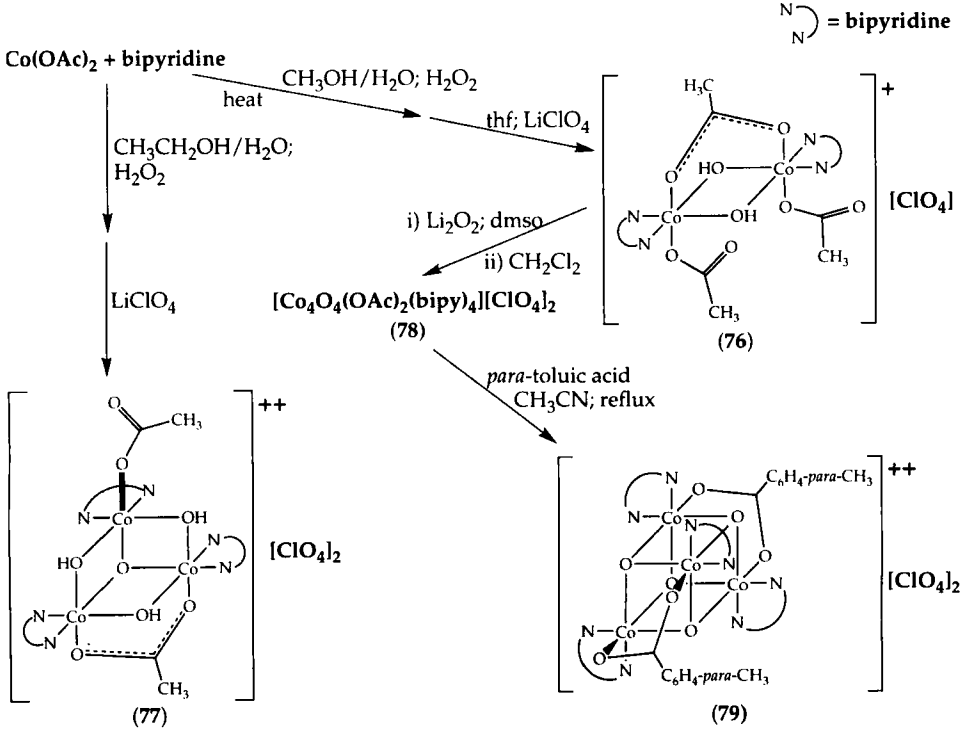

SCHEME 17. Cobalt–oxo semicubane and cubane preparations and structures.

nium, and even tellurium has been attempted. For some leading references to this area, see Ref. *203*.

D. Studies Related to DNA and RNA

Oxygen activation has been shown to be important both in the presumed mechanism of attack on DNA by metal complexes of antibiotics, and in the synthesis of dexoyribonucleotides from the corresponding ribonucleotides. Although primarily centered on iron complexes, and thus outside of the scope of this review, some cobalt analogue complexes have been discussed.

1. Bleomycin

The antitumor antibiotic bleomycin (BLM) is believed to cause cytotoxicity through its ability, in the combined presence of dioxygen and a metal ion cofactor (*204*), to bind to and degrade DNA (*205*). Iron complexes of BLM have aroused special attention, as such complexes are the "first" (*vide supra* concerning the discussion of hemerythrin and hemocyanin) non-heme-iron complexes with a significant capacity for dioxygen activation (*206*).

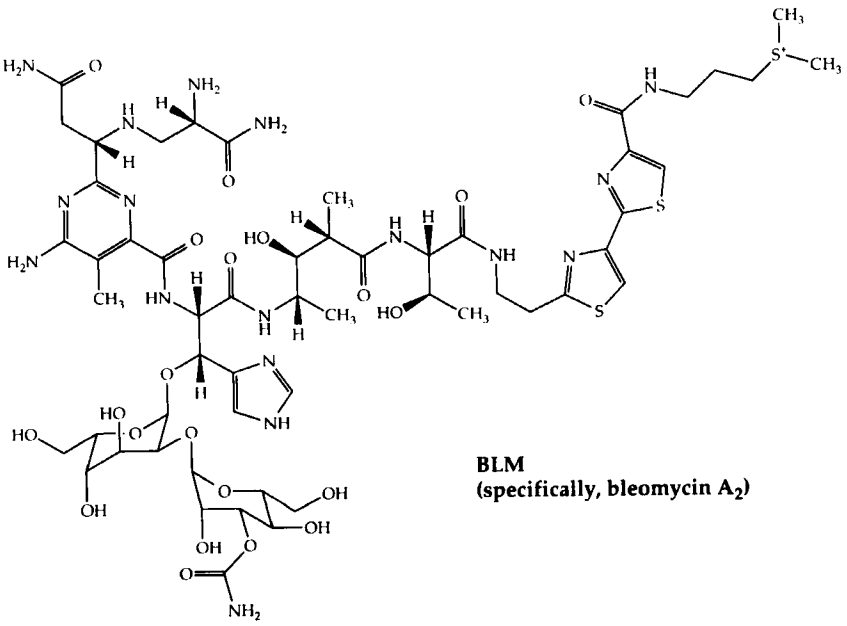

BLM
(specifically, bleomycin A_2)

The hydroperoxide form of the cobalt(III)–bleomycin congener is known to cleave DNA only in the presence of light (*207*), and its structure in solution has been solved by NMR methods (*208*). In reactions with a carefully defined decameric oligonucleotide analogue of DNA [$d(C^1C^2A^3G^4G^5C^6C^7T^8G^9G^{10})_2$], the Co–BLM complex forms a 1 : 1 intercalated complex, and experimental evidence supports the conclusion that the metal binding domain on the oligonucleotide is in the C^6C^7/$G^{15}G^{14}$ region of the decanucleotide (*209*).

It has been established that it is the bithiazole moiety of bleomycin that participates in DNA binding (*210*). In order to investigate the reactivity and binding ability of this bithiazole section of bleomycin, a modified version of the bithiazole moiety, containing a 2-(1,3-diaminopropyl) substituent rather than bleomycin's 2-(2-aminoethyl) substituent, was prepared (*211*) (see the drawing of these bithiazole moieties). In the presence of cobalt(II), the modified bithiazole does in fact mediate the production of alkali-labile lesions on double-stranded DNA. These lesions, following treatment with alkali, exhibited guanosine-specific DNA strand scission. However, this degradation did not require molecular oxygen, even though the degradation did require light.

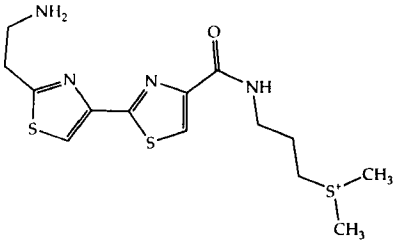

bithiazole from native bleomycin A_2

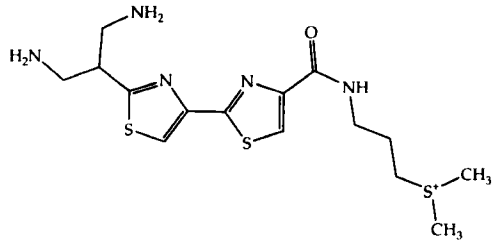

modified bithiazole

Finally, in the presence of oxygen, a complex containing the modified bithiazole, a cobalt(II) center, and dioxygen could be inferred from absorption spectroscopic studies, which suggested that this oxygenated complex in some way mediated the oxidative alteration of the guanine base, making the site susceptible to reaction to the hot alkali treatment. This reactivity was apparently due to the preferentially enhanced reactivity at the guanosine sites of DNA, rather than a site binding selectivity response of the bithiazole complex.

2. *Ribonucleotide Reductase*

The enzymatic conversion of all four ribonucleotides to their corresponding deoxyribonucleotides is mediated by the enzyme ribonucleo-

tide reductase, RNR (*212*). In its active state, RNR contains binuclear iron(III) centers, and, in the inactive iron(II) form, is able to react with dioxygen to regenerate the all-important tyrosine radical (*213*). The data suggests that unlike the iron(III) atoms neither of the iron(II) centers is six-coordinate: one iron atom is five-coordinate, while the other is either four- or five-coordinate, thus facilitating O_2 binding (*214*).

In order to better understand the structure of the di-iron active sites of RNR, the iron centers can be removed (*215*) and the apoprotein then can be reconstituted with iron(II) in the presence of ascorbate (*216*), or with manganese(II) (*217*). In the former case, the resulting reconstituted protein retains all of the activity of the original protein, while in the latter case, the structure of the active site in the manganese-containing protein is apparently similar to that presumed to exist for the native iron-containing analogue. The apoprotein form of RNR was reported to be reconstituted using cobalt(II) (*218*). This substituted RNR was spectroscopically characterized and interpreted as being consistent with a five-coordinate high-spin cobalt(II) center ligated by nitrogen- and oxygen-donor ligands. However, the cobalt-substituted enzyme did not exhibit the oxygen reactivity of the diferrous form of RNR. Only after exposure to dioxygen for several days did spectral features change in such a way as to indicate that some partial oxidation to cobalt(III) had occurred.

E. Gas-Phase Studies with Metal–Oxo Systems

Under thermal, non-excited-state conditions, the reaction of the gas-phase Co^+ ion with dioxygen, Eq. (2), is endothermic (*219*), while that with N_2O, Eq. (3), although exothermic by about 40 kcal/mol, has a relatively high kinetic barrier (*220*); neither reaction produces CoO^+ in appreciable amounts.

$$Co^+ + O_2 \rightarrow CoO^+ + O \tag{2}$$

$$Co^+ + N_2O \rightarrow CoO^+ + N_2 \tag{3}$$

The attempt to react thermalized $[Co(C_2H_4)]^+$ in the gas phase with dioxygen was also unsuccessful (*221*).

Thus, since ground-state Co^+ does not react with dioxygen or N_2O, in order to produce appreciable amounts of CoO^+, N_2O can be allowed to react with translationally (produced through radio-frequency excitation) or electronically (produced via laser desorption) excited $Co^{+}*$, leading to a conversion of $Co^{+}*$ to $CoO^{+}*$ of about 20% (*222*). The

excited-state CoO^{+*} so produced can then be thermalized in an argon buffer gas.

Guided-ion-beam mass spectrometry (GIBMS) was used to study the reaction of CoO^+ with CH_4 and with D_2 (*223*). The exothermic reaction with methane, Eq. (4), was found to have an activation barrier of 0.56 ± 0.08 eV, while Eq. (5), also exothermic, had an activation energy of 0.75 ± 0.04 eV.

$$CoO^+ + CH_4 \rightarrow Co^+ + CH_3OH \quad (4)$$

$$CoO^+ + D_2 \rightarrow Co^+ + D_2O \quad (5)$$

A study (*222*) of the reactions of a number of substrates with CoO^+ in the gas phase, using Fourier-transform ion cyclotron resonance mass spectrometry (FTICRMS), did not find an activation barrier in reaction (4), such as was reported for the GIBMS study, although a barrier to the reaction of CoO^+ with H_2 was noted (*221*). Schemes 18, 19, 20, and

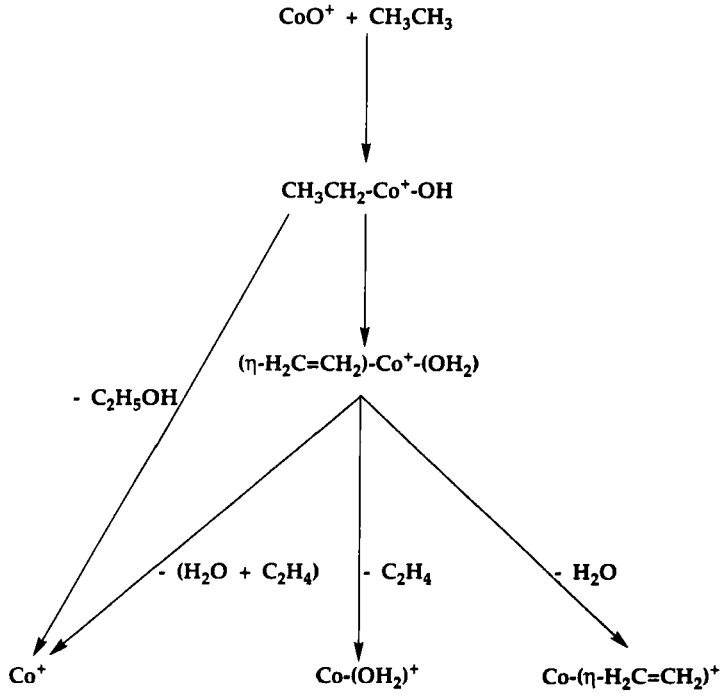

SCHEME 18. The gas-phase reactions of CoO^+ with ethane.

TABLE I

PRODUCT DISTRIBUTIONS (REPORTED AS BRANCHING RATIOS) FOR THE NEUTRAL PRODUCTS OF THE REACTIONS OF CoO^+ WITH ALKANES

Substrate	Neutral product	Branching ratio
Methane	CH_3OH	1.00
Ethane	H_2O	0.67
	C_2H_5OH	0.21
	C_2H_4	0.12
Propane	H_2O	0.73
	C_3H_7OH	0.16
	CH_3OH	0.06
	C_3H_6	0.05
n-Butane	H_2O; H_2	0.67
	C_2H_4; H_2O	0.20
	CoOH	0.09
	C_4H_8	0.04
iso-Butane	CoOH	0.30
[2-methylpropane]	C_4H_9OH	0.20
	H_2O; H_2	0.18
	CH_3OH	0.16
	H_2O	0.16
n-Pentane	C_2H_5OH	0.43
	CH_4; H_2O	0.20
	CoOH	0.14
	C_3H_8O	0.12
	H_2O	0.17
	C_5H_{10}	0.04
iso-Pentane	C_2H_5OH	0.40
[2-methylbutane]	CH_4; H_2O	0.30
	CoOH	0.30
neo-Pentane	$CoCH_3O$	0.64
[2,2-dimethylpropane]	"CH_5O"	0.10
	CH_3OH	0.10
	CH_4; H_2O	0.04
	CoOH	0.04
	CoC_2H_5O	0.04
	C_3H_8O	0.02
	H_2O; H_2	0.02

21 depict the reaction pathways (*222*) in the reactions of CoO^+ with ethane, propane, *n*-butane, and 2-methylpropane (*iso*-butane).

Table I lists the neutral products and the branching ratios for the reactions of CoO^+ with both linear (methane, ethane, propane, *n*-bu-

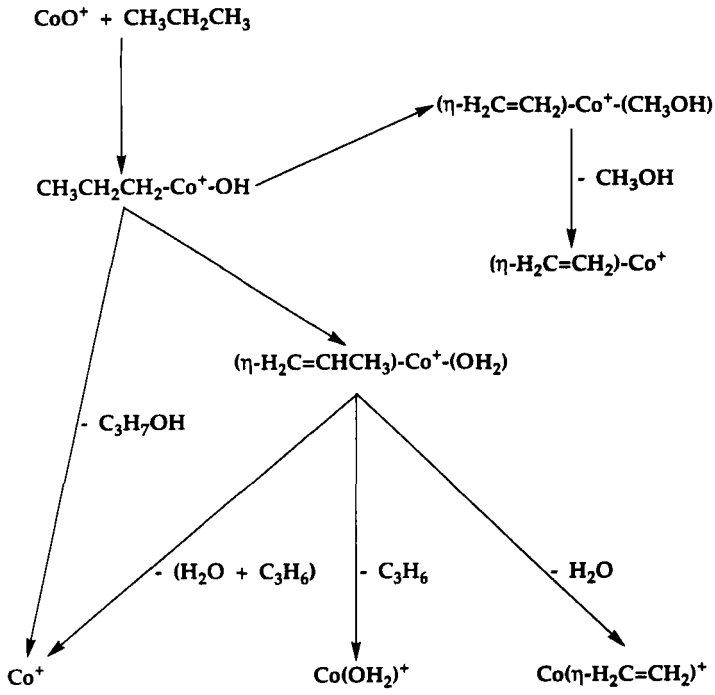

SCHEME 19. The gas-phase reactions of CoO^+ with propane.

tane, and *n*-pentane) and branched (2-methylpropane, 2-methylbutane, and 2,2-dimethylpropane) alkanes. Although the activation of methane to form methanol is a very inefficient, albeit exothermic, process, the higher alkanes are much more reactive with CoO^+. The production of neutral CoOH occurs only for alkanes larger than propane, and generally more complicated reaction schemes are seen for these systems. Unlike, for example, "CH_6O," which can be readily identified as being composed of CH_4 and H_2O, the product "CH_5O" in the reaction of *neo*-pentane with CoO^+ (Table I) is not readily identifiable with specific neutral products and was reported as a simple empirical formula.

Finally, the electronic structures of the first-row, late transition-metal monoxide cations, including CoO^+, having been calculated (*224*) using approximate density functional theory (DFT) (*225, 226*) augmented with complete active space second-order perturbational theory (CASPT2D) (*227*). Unlike a previous report (*228*) in which the ground state of CoO^+ was assigned as the $^3\Sigma^-$ configuration ($1\sigma^2 2\sigma^2 1\pi^4 1\delta^4 2\pi^2 3\sigma^0$), the current calculations indicate that the ground state is the $^5\Delta$ configuration ($1\sigma^2 2\sigma^2 1\pi^4 1\delta^3 2\pi^2 3\sigma^1$). The similarity of the

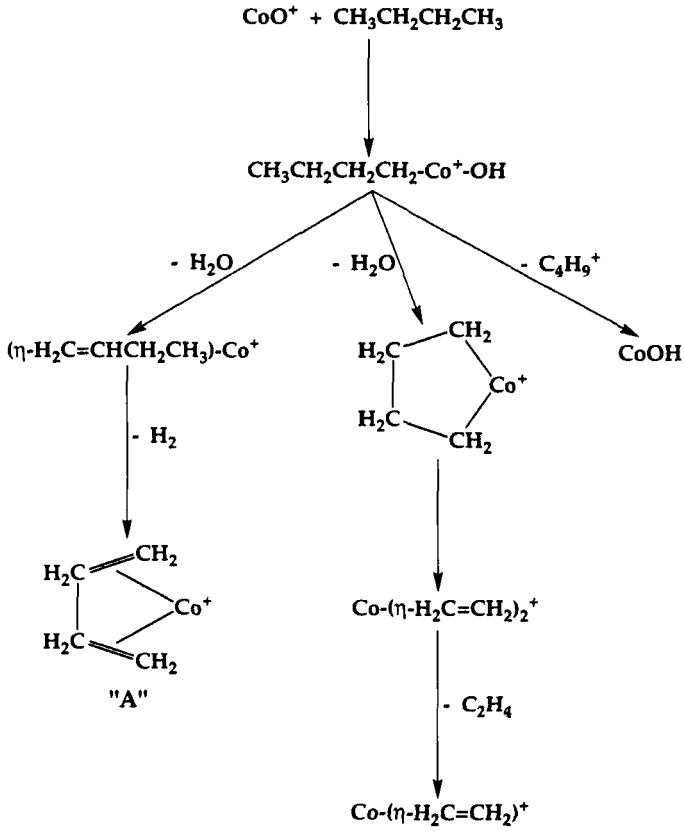

SCHEME 20. The gas-phase reactions of CoO^+ with *n*-butane. Note that the compound labeled "**A**" is a butadiene complex of Co^+.

electronic structures of FeO^+, CoO^+, and NiO^+ to that of the triplet ground state of dioxygen, discussed earlier (*228*), is also noted in the more recent report (*224*).

F. SOLID-STATE OXIDATIONS

Although the vast majority of this review has been concerned with homogeneous systems, supported catalyst and single-crystal studies of rhodium are important topics that have also been considered by some researchers. This topic extends and dovetails nicely with the discussion of the interactions of acyclic and cyclic polyamine ligands and Schiff

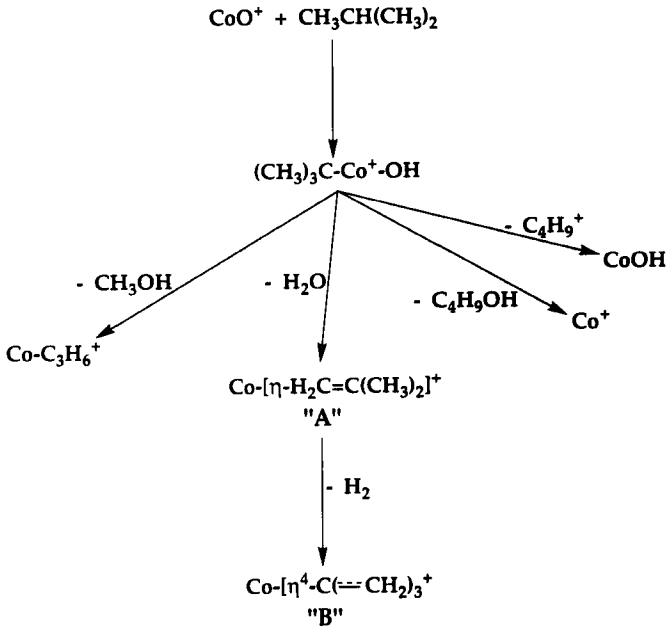

SCHEME 21. The gas-phrase reactions of CoO^+ with 2-methylpropane (*iso*-butane). Note that the compound labeled "**A**" is a 2-methyl-1-propene (*iso*-butylene) complex of Co^+, while the compound labeled "**B**" is a trimethylenemethane complex of Co^+.

bases with zeolite-supported cobalt(II) species, presented earlier in the section dealing with nitrogen-donor ligands (*vide supra*).

1. Alumina-Supported Rhodium

The $[(CO)_2Rh]$ moiety can be supported on alumina through the reaction (*229*) of $[(\eta^3\text{-allyl})Rh(CO)_2]$ in octane with alumina. In addition, the same moiety can be supported on alumina through the reaction of $[(\eta^3\text{-allyl})_2Rh]$ in toluene, followed by a carbonylation step. This supported $[(CO)_2Rh]$ species, symbolized $(Al_2O_3)\cdot Rh(CO)_2$, will react reversibly with dioxygen to form a species described as $(Al_2O_3)\cdot Rh(O_2)$ (**80**) based upon X-ray photoelectron spectra (XPS). In a similar fashion, reaction of $(Al_2O_3)\cdot Rh(CO)_2$ with dry ozone produced a supported ozone complex, $(Al_2O_3)\cdot Rh(O_3)$ (**81**), and this latter complex could be shown to react with carbon monoxide to produce carbon dioxide and to regenerate the dioxygen complex **80**.

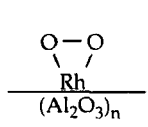

(80)

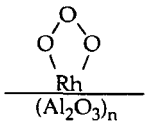

(81)

More recently, it was demonstrated that **80** is a catalyst for the partial oxidation of olefins using dioxygen (*230*). For example, dry propene was oxidized to acetone; when water vapor was present in the catalyst stream, some propanal could also be detected. Other reactions reported included the conversion of styrene to acetophenone and phenylacetaldehyde in an 80 : 20 product ratio, and 2-norbornene to 2-norbornanone and cyclohexene-4-carboxyaldehyde in a 70 : 30 product ratio.

2. *Single-Crystal Rhodium*

Using ultrahigh-vacuum techniques, clean Rh(111) surfaces could be exposed to dioxygen to form a surface covered with atomic oxygen, which was characterized as an Rh(111)-p(2×1)-O surface from low-energy electron diffraction (LEED) patterns (*231*). This surface could partially oxidize styrene to acetophenone (*231c*), propene to acetone (*231b*), and norbornene to norbornanone (*231a*). In the last instance, no skeletal rearrangement product (which would be 3-cyclohexene-1-carboxaldehyde) was observed.

The extent of oxygen coverage on a Rh(111) surface changes the selectivity of the oxidation reaction of 2-propanethiolate (*232*). When either 2-propanethiol or di-*iso*-propyl disulfide reacts with an oxygen-covered Rh(111) surface, acetone, propene, and propane are formed. The oxygen (i) inhibits the nonselective C—H bond cleavage on the surface, (ii) removes hydrogen from the surface through the formation of water, (iii) slows C—S bond cleavage, and (iv) adds directly to the 2-propyl group to form 2-propoxide on the rhodium surface. The last reaction only occurs at high oxygen coverages of the rhodium surface, however.

G. Molten Salts

As an appropriate concluding section in this wide-ranging review of oxygen activation by cobalt-, rhodium-, and iridium-containing systems, it has been reported (*233*) that molten sodium *meta*-phosphate ($NaPO_3$), at 850°C, reacts with dioxygen to produce the superoxide

anion. The ESR spectrum of this mixture exhibited an absorption with a g-value of 2.000 with a width of 38 G. In melts containing CoO, this species could also be recognized. However, in the presence of CoO in the $NaPO_3$ melt, the superoxide species could not be completely removed from the melt by bubbling helium through the system, as was the case when CoO was not present. This inability to "reverse" the reaction was ascribed to an interaction between the superoxide and the CoO species in the melt, which may have been due to a cobalt(II)–superoxide complex (*234*).

VII. Concluding Remarks

The activation of dioxygen encompasses a broad spectrum of research fields, from biology/biochemistry to chemistry, and hence to catalysis, industrial processes, and theoretical analyses. The studies outlined in this review are indicative of the range of ongoing research in the area, and of the challenges and opportunities presented. While we have attempted to address many of the accomplishments we feel are important and interesting, this is one of the broader and more complex fields of chemistry, and one that is expected to develop and change rapidly.

ACKNOWLEDGMENTS

The support of Northern Arizona University in the form of a sabbatical leave appointment for the 1994–95 academic year (to R. W. Z.) is gratefully acknowledged, as is the international assistance of Dr. Maurizio Peruzzini.

REFERENCES

1. (a) Conry, R. R.; Karlin, K. D. In "The Encyclopedia of Inorganic Chemistry" King, R. B., Ed.; John Wiley and Sons: Chichester, U.K., 1994; Vol. 2, p. 1036; (b) Sawyer, D. T. "Oxygen Chemistry"; Oxford University Press: New York, 1991; (c) Ingrahim, L. L.; Meyer, D. L. "Biochemistry of Dioxygen"; Plenum Press: New York, 1985.
2. (a) Hill, H. A. O.; Tew, D. G. In "Comprehensive Coordination Chemistry"; Wilkinson, G.; Gillard, R. D.; McCleverty, J. A., Eds.; Pergamon Press, New York, 1987; Vol. 2, p. 315; (b) Summerville, D. A.; Jones, R. D.; Hoffman, B. M.; Basolo, F. *J. Chem. Ed.* **1979,** *56,* 157; (c) Jones, R. D.; Summerville, D. A.; Basolo, F. *Chem. Rev.* **1979,** *79,* 139; (d) Lever, A. B. P.; Gray, H. G. *Acc. Chem. Res.* **1978,** *11,* 348.
3. (a) Dickman, M. H.; Pope, M. T. *Chem. Rev.* **1994,** *94,* 569; (b) Butler, A.; Clague, M. J.; Meister, G. E. *Chem. Rev.* **1994,** *94,* 625; (c) Pecoraro, V. L.; Baldwin, M. J.;

Gelasco, A. *Chem. Rev.* **1994,** *94,* 807; (d) Kitajima, N.; Moro-oka, Y. *Chem. Rev.* **1994,** *94,* 737; (e) Bytheway, I.; Hall, M. B. *Chem. Rev.* **1994,** *94,* 639.

4. (a) Springer, B. A.; Sligar, S. G.; Olson, J. S.; Phillips, G. N., Jr. *Chem. Rev.* **1994,** *94,* 699; (b) Momenteau, M.; Reed, C. A. *Chem. Rev.* **1994,** *94,* 659.
5. (a) Drago, R. S. *Inorg. Chem.* **1979,** *18,* 1408; (b) Solomon, E. I.; Tuczek, F.; Root, D. E.; Brown, C. A. *Chem. Rev.* **1994,** *94,* 827.
6. (a) Fronczek, F. R.; Schaefer, W. P.; Marsh, R. E. *Acta Crystallogr., Sect. B* **1974,** *30,* 117; (b) Davies, R.; Mori, M.; Sykes, G. G.; Weil, J. A. *Inorg. Synth.* **1970,** *12,* 197; (c) Schaefer, W. P. *Inorg. Chem.* **1968,** *7,* 725.
7. Lawrance, G. A.; Lay, P. A. *J. Inorg. Nucl. Chem.* **1979,** *41,* 301.
8. (a) Duffy, D. L.; House, D. A.; Weil, J. A. *J. Inorg. Nucl. Chem.* **1969,** *31,* 2053; (b) Mori, M.; Weil, J. A. *J. Am. Chem. Soc.* **1967,** *89,* 3732; (c) Mori, M.; Weil, J. A.; Ishiguro, M. *J. Am. Chem. Soc.* **1968,** *90,* 615.
9. Sasaki, Y.; Fujita, J.; Saito, K. *Bull. Chem. Soc. Japan* **1971,** *44,* 3373.
10. (a) Barraclough, C.; Lawrance, G. A.; Lay, P. A. *Inorg. Chem.* **1978,** *17,* 3317; (b) Strekas, T. C.; Spiro, T. G. *Inorg. Chem.* **1975,** *14,* 1421; (c) Freedman, T. B.; Yoshida, C. M.; Loehr, T. M. *J. Chem. Soc., Chem. Commun.* **1974,** 1016.
11. (a) Lee, S.; Espenson, J. H.; Bakac, A. *Inorg. Chem.* **1990,** *29,* 3442; (b) Bakac, A.; Espenson, J. H. *Inorg. Chem.* **1987,** *26,* 4353; (c) Mok, C. H.; Endicott, J. F. *J. Am. Chem. Soc.* **1978,** *100,* 123; (d) Roche, T. S.; Endicott, J. F. *Inorg. Chem.* **1974,** *13,* 1575; (e) Roche, T. S.; Endicott, J. F. *J. Am. Chem. Soc.* **1972,** *94,* 8622.
12. Kofod, P. *Inorg. Chem.* **1995,** *34,* 2768.
13. (a) Goedken, V. L.; Peng, S.-M.; *J. Chem. Soc., Chem. Commun.* **1975,** 258; (b) Goedkin, V. L.; Peng, S.-M. *J. Am. Chem. Soc.* **1974,** *96,* 7826; (c) Goedkin, V. L.; Peng, S.-M.; Park, Y. *J. Am. Chem. Soc.* **1974,** *96,* 284.
14. Samsel, E. G.; Kochi, J. K. *Inorg. Chem.* **1986,** *25,* 2450.
15. (a) Hush, N. S. *Trans. Faraday Soc.* **1961,** *57,* 557; (b) Marcus, R. A. *J. Phys. Chem.* **1968,** *72,* 891; (c) Wherland, S.; Gray, H. *Biol. Aspects Inorg. Chem. Symp.* **1978,** 323.
16. (a) McLendon, G.; Mooney, W. F. *Inorg. Chem.* **1980,** *19,* 12; (b) Richens, D. T.; Sykes, A. G. *J. Chem. Soc., Dalton Trans.* **1982,** 1621.
17. Fanshawe, R. L.; Blackman, A. G. *Inorg. Chem.* **1995,** *34,* 421.
18. (a) Banaszczyk, M.; Lee, J. J.; Menger, F. M. *Inorg. Chem.* **1991,** *30,* 1972; (b) Massoud, S. S.; Milburn, R. M. *Inorg. Chim. Acta* **1988,** *154,* 115.
19. Bernhardt, P. V.; Lawrance, G. A.; Hambley, T. W. *J. Chem. Soc., Dalton Trans.* **1990,** 235.
20. Pickens, S. R.; Martell, A. E. *Inorg. Chem.* **1980,** *19,* 15.
21. (a) Harris, W. R.; McLendon, G. L.; Martell, A. E.; Bess, R. C.; Mason, M. *Inorg. Chem.* **1980,** *19,* 21; (b) McLendon, G.; Martell, A. E. *J. Chem. Soc., Chem. Commun.* **1975,** 223.
22. Al-Shatti, N.; Ferrer, M.; Sykes, A. G. *J. Chem. Soc., Dalton Trans.* **1980,** 2533.
23. Melson, G. A. In "Chemistry of Macrocyclic Compounds"; Melson, G. A., Ed.; Plenum Press: New York, 1979; p. 1.
24. (a) Anson, F. C.; Kang, C. *Inorg. Chem.* **1995,** *34,* 2771; (b) Anson, F. C.; Geiger, T. *J. Am. Chem. Soc.* **1981,** *103,* 7489.
25. (a) Wang, W.-D.; Bakac, A.; Espenson, J. H. *Inorg. Chem.* **1995,** *34,* 4049; (b) Zhang, M.; van Eldik, R.; Espenson, J. H.; Bakac, A. *Inorg. Chem.* **1994,** *33,* 130; (c) Marchaj, A.; Bakac, A.; Espenson, J. H. *Inorg. Chem.* **1992,** *31,* 4164; (d) Bakac, A.; Espenson, J. H. *Inorg. Chem.* **1990,** *29,* 2062; (e) Bakac, A.; Espenson, J. H. *J. Am. Chem. Soc.* **1990,** *112,* 2273.
26. (a) Endicott, J. F.; Kumar, K. *Inorg. Chem.* **1984,** *23,* 2447; (b) Endicott, J. F.; Wong,

C.-L. *Inorg. Chem.* **1981,** *20,* 2233; (c) Wong, C.-L.; Switzer, J. A.; Balakrishnan, K. P.; Endicott, J. F. *J. Am. Chem. Soc.* **1980,** *102,* 5511; (d) Endicott, J. F.; Liteplo, M. P. *Inorg. Chem.* **1971,** *10,* 1420.

27. Bencini, A.; Bianchi, A.; Cabani, S.; Ceccanti, N.; Paoletti, P.; Tinè, M. R. *J. Chem. Soc., Dalton Trans.* **1993,** 695.
28. Shinohara, N.; Ishii, K.; Hirose, M. *J. Chem. Soc., Chem. Commun.* **1990,** 700.
29. Bosnich, B.; Poon, C. K.; Tobe, M. L. *Inorg. Chem.* **1965,** *4,* 1102.
30. McLendon, G.; Mason, M. *Inorg. Chem.* **1978,** *17,* 362.
31. Bencini, A.; Bianchi, A.; Garçia-España, E.; Micheloni, M.; Paoletti, P. *Inorg. Chem.* **1989,** *28,* 2480.
32. Sasaki, Y.; Fujita, K. *Bull. Chem. Soc. Jpn.* **1964,** *42,* 2089.
33. Davies, K. M.; Sykes, A. G. *J. Chem. Soc. A* **1971,** 1418.
34. (a) Nakon, R.; Martell, A. E. *J. Am. Chem. Soc.* **1972,** *94,* 3026; (b) Huchital, D. H.; Martell, A. E. *Inorg. Chem.* **1974,** *13,* 2966; (c) Bogucki, R. F.; McLendon, G.; Martell, A. E. *J. Am. Chem. Soc.* **1976,** *98,* 3202.
35. Bedell, S. A.; Martell, A. E. *Inorg. Chem.* **1983,** *22,* 364.
36. Tung, H.-C.; Sawyer, D. T. *J. Am. Chem. Soc.* **1990,** *112,* 8214.
37. (a) Tung, H.-C.; Kang, C.; Sawyer, D. T. *J. Am. Chem. Soc.* **1992,** *114,* 3445; (b) Sobkowiak, A.; Qui, A.; Liu, X.; Llobet, A.; Sawyer, D. T. *J. Am. Chem. Soc.* **1993,** *113,* 609.
38. de Waal, D. J. A.; Gerber, T. I. A.; Louw, W. J.; van Eldik, R. *Inorg. Chem.* **1982,** *21,* 2002.
39. (a) Corbin, D. R.; Herron, N. *J. Mol. Catal.* **1994,** *86,* 343; (b) De Vos, D. E.; Thibault-Starzyk, F.; Knops-Gerrits, P.-P.; Parton, R. F.; Jacobs, P. A. *Makromol. Chem., Macromol. Symp.* **1994,** *80,* 157; (c) Ozin, G. A.; Gil, C. *Chem. Rev.* **1989,** *89,* 1749.
40. Vansant, E. F.; Lunsford, J. H. *Adv. Chem. Ser.* **1973,** *100,* 441.
41. De Vos, D. E.; Vanoppen, D. L.; Li, X.-Y.; Libbrecht, S.; Bruynseraede, Y.; Knops-Gerrits, P.-P.; Jacobs, P. A. *Chem. Eur. J.* **1995,** *1,* 144.
42. Niederhoffer, E. C.; Timmons, J. H.; Martell, A. E. *Chem. Rev.* **1984,** *84,* 137.
43. (a) Trofimenko, S. *Chem. Rev.* **1972,** *72,* 497; (b) McCleverty, J. A. *Chem. Soc. Rev.* **1982,** *12,* 331; (c) Trofimenko, S. *Prog. Inorg. Chem.* **1986,** *34,* 115.
44. Trofimenko, S.; Calabrese, J. C.; Thompson, J. S. *Inorg. Chem.* **1987,** *26,* 3522.
45. Cano, M.; Heras, J. V.; Trofimenko, S.; Monge, A.; Gutierrez, E.; Jones, C. J.; McCleverty, J. A. *J. Chem. Soc., Dalton Trans.* **1990,** 3577.
46. Egan, J. W., Jr.; Haggerty, B. S.; Rheingold, A. L.; Sendlinger, S. C.; Theopold, K. H. *J. Am. Chem. Soc.* **1990,** *112,* 2445.
47. Reinaud, O. M.; Rheingold, A. L.; Theopold, K. H. *Inorg. Chem.* **1994,** *33,* 2306.
48. (a) Kitajima, N.; Fujisawa, K.; Moro-oka, Y.; Toriumi, K. *J. Am. Chem. Soc.* **1989,** *111,* 8975; (b) Baldwin, M. J.; Root, D. E.; Pate, J. E.; Fujisawa, K.; Kitajima, N.; Solomon, E. I. *J. Am. Chem. Soc.* **1992,** *114,* 10421.
49. Suzuki, M.; Ishiguro, T.; Kozuka, M.; Nakamoto, K. *Inorg. Chem.* **1981,** *20,* 1993.
50. Reinaud, O. M.; Yap, G. P. A.; Rheingold, A. L.; Theopold, K. H. *Angew. Chem., Int. Ed. Engl.* **1995,** *34,* 2051; *Angew. Chem.* **1995,** *107,* 2171.
51. Tejel, C.; Ciriano, M. A.; Oro, L. A.; Tiripicchio, A.; Ugozzoli, F. *Organometallics* **1994,** *13,* 4153.
52. (a) Ferrughelli, D. T.; Horváth, I. T. *J. Chem. Soc., Chem. Commun.* **1992,** 806; (b) Grushin, V. V.; Alper, H. *Organometallics* **1991,** *10,* 1620; (c) Labat, G.; Seris, J. L.; Meunier, B. *Angew. Chem., Int. Ed. Engl.* **1990,** *29,* 1471.
53. Rondon, D.; He, X.; Chaudret, B. *J. Organomet. Chem.* **1992,** *433,* C18.
54. Budavari, S., Ed. "The Merck Index, Eleventh Edition"; Merck and Company: Rahway, NJ, 1989; p. 1331.

55. Herron, N. *Inorg. Chem.* **1986,** *25,* 4714.
56. Jones, R. D.; Summerville, D. A.; Basolo, F. *Chem. Rev.* **1979,** *79,* 139.
57. Able, E. W.; Pratt, J. N.; Whelan, R. *Inorg. Nucl. Chem. Lett.* **1971,** *7,* 901.
58. (a) De Vos, D. E.; Thibault-Starzyk, F.; Jacobs, P. A. *Angew. Chem., Int. Ed. Engl.* **1994,** *33,* 431; *Angew. Chem.* **1994,** *106,* 447; (b) De Vos, D. E.; Feijen, E. J. P.; Schoonheydt, R. A.; Jacobs, P. A. *J. Am. Chem. Soc.* **1994,** *116,* 4746.
59. (a) Earnshaw, A.; Hewlett, P. C.; King, E. A.; Larkworthy, L. F. *J. Chem. Soc. A* **1968,** 241; (b) Von Zelewsky, A.; Fierz, H. *Helv. Chim. Acta* **1973,** *56,* 977; (c) Ochiai, E. *J. Chem. Soc., Chem. Commun.* **1972,** 489; (d) Busetto, C.; Cariati, F.; Fantucci, P.; Galizzioli, D.; Marazzoni, F. *J. Chem. Soc., Dalton Trans.* **1973,** 1712.
60. Bedioui, F.; De Boysson, E.; Devynck, J.; Balkus, K. J. *J. Chem. Soc., Faraday Trans.* **1991,** *87,* 3831.
61. (a) Oka, T.; Simpson, F. J.; Krishnamurty, H. G. *Can. J. Microbiol.* **1972,** *18,* 493; (b) Sakamoto, H. *Seikagaku* (*J. Jpn. Biochem. Soc.*) **1963,** *35,* 633; (c) Hattori, S.; Noguchi, I. *Nature* (*London*) **1959,** *184,* 1145.
62. (a) Nishinaga, A.; Tojo, T.; Matsuura, T. *J. Chem. Soc., Chem. Commun.* **1974,** 896; (b) Nishinaga, A.; Kuwashige, T.; Tsutsui, T.; Mashino, T.; Maruyama, K. *J. Chem. Soc., Dalton Trans.* **1994,** 805.
63. Araki, K.; Kuboki, T.; Otohata, M.; Kishimoto, N.; Yamada, M.; Shirashi, S. *J. Chem. Soc., Dalton Trans.* **1993,** 3647.
64. Busch, D. H.; Alcock, N. W. *Chem. Rev.* **1994,** *94,* 585.
65. (a) Stevens, J. C.; Jackson, P. J.; Schammel, W. P.; Christoph, G. G.; Busch, D. H. *J. Am. Chem. Soc.* **1980,** *102,* 3283; (b) Stevens, J. C.; Busch, D. H. *J. Am. Chem. Soc.* **1980,** *102,* 3285.
66. (a) Schammel, W. P.; Mertes, K. S. B.; Christoph, G. G.; Busch, D. H.; *J. Am. Chem. Soc.* **1979,** *101,* 1622; (b) Herron, N.; Busch, D. H. *J. Am. Chem. Soc.* **1981,** *103,* 1236. (c) Busch, D. H.; Olszanski, D. J.; Stevens, J. C.; Schammel, W. P.; Kojima, M.; Jerron, N.; Zimmer, L. L.; Holter, K. S.; Mocak, K. *J. Am. Chem. Soc.* **1981,** *103,* 1472; (d) Busch, D. H.; Jackels, S. C.; Callahan, R. C.; Grzybowski, J. J.; Zimmer, L. L.; Kojima, M.; Olszanski, D. J.; Schammel, W. P.; Stevens, J. C.; Holter, K. S.; Mocak, K. *Inorg. Chem.* **1981,** *20,* 2834; (e) Herron, N.; Cameron, J. H.; Neer, G. L.; Busch, D. H. *J. Am. Chem. Soc.* **1983,** *105,* 298; (f) Herron, N.; Zimmer, L. L.; Grzybowski, J. J.; Olszanski, D. J.; Jackels, S. C.; Callahan, R. C.; Cameron, J. H.; Christoph, G. G.; Busch, D. H. *J. Am. Chem. Soc.* **1983,** *105,* 6585.
67. Chen, J.; Ye, N.; Alcock, N. W.; Busch, D. H. *Inorg. Chem.* **1993,** *32,* 904.
68. (a) Busch, D. H.; Jackson, P. J.; Kojima, M.; Chmielewski, P.; Matsumoto, N.; Stevens, J. C.; Wu, W.; Nosco, D.; Herron, N.; Ye, N.; Warburton, P. R.; Masarwa, M.; Stephenson, N. A.; Christoph, G.; Alcock, N. W. *Inorg. Chem.* **1994,** *33,* 910; (b) Chia, P. S. K.; Masarwa, M.; Warburton, P. R.; Wu, W.; Kojima, M.; Nosco, D.; Alcock, N. W.; Busch, D. H. *Inorg. Chem.* **1993,** *32,* 2736.
69. Busch, D. H. *Transfus. del Sangue* **1988,** *33,* 57.
70. (a) Goldsby, K. A.; Meade, T. J.; Kojima, M.; Busch, D. H. *Inorg. Chem.* **1985,** *24,* 2588; (b) Alcock, N. W.; Padolik, P. A.; Pike, G. A.; Busch, D. H. *Inorg. Chem.* **1990,** *29,* 2599; (c) Busch, D. H.; Stephenson, N. A. *J. Inclusion Phenom. Mol. Recognit. Chem.* **1989,** *7,* 137; (d) Alcock, N. W.; Lin, W.-K.; Cairns, C.; Pike, G. A.; Busch, D. H. *J. Am. Chem. Soc.* **1989,** *111,* 6630.
71. Cameron, J. H.; Graham, S. *J. Chem. Soc., Dalton Trans.* **1989,** 1599.
72. Cameron, J. H.; Scott, E. L. *J. Chem. Soc., Dalton Trans.* **1993,** 397.
73. Collman, J. P.; Wagenknecht, P. S.; Hutchison, J. E. *Angew. Chem., Int. Ed. Engl.* **1994,** *33,* 1537; *Angew. Chem.* **1994,** *106,* 1620.

74. (a) Collman, J. P.; Marrocco, M.; Denisevich, P.; Koval, C.; Anson, F. C. *J. Electroanal. Chem. Interfacial Electrochem.* **1979,** *101,* 117; (b) Collman, J. P.; Denisevich, P.; Konai, Y.; Marrocco, M.; Koval, C.; Anson, F. C. *J. Am. Chem. Soc.* **1980,** *102,* 6027.
75. (a) Liu, H. Y.; Weaver, M. J.; Wang, C. B.; Chang, C. K. *J. Electroanal. Chem. Interfacial Electrochem.* **1983,** *145,* 439; (b) Chang, C. K.; Liu, H. Y.; Abdalmuhdi, I. *J. Am. Chem. Soc.* **1984,** *106,* 2725.
76. (a) Collman, J. P.; Hendricks, N. H.; Leider, C. R.; Ngameni, E.; L'Her, M. *Inorg. Chem.* **1988,** *27,* 387; (b) Chang, C. K. *J. Heterocyclic Chem.* **1988,** *12,* 1287; (c) Sawaguchi, T.; Matsue, T.; Itaya, K.; Uchida, I. *Electrochim. Acta* **1991,** *36,* 703; (d) Karaman, R.; Almarsson, Ö.; Bruice, T. C. *J. Org. Chem.* **1992,** *57,* 1555.
77. Jeon, S.; Almarsson, Ö.; Karaman, R.; Blaskó, A.; Bruice, T. C. *Inorg. Chem.* **1993,** *32,* 2562.
78. Le Mest, Y.; L'Her, M. *J. Chem. Soc., Chem. Commun.* **1995,** 1441.
79. (a) Le Mest, Y.; L'Her, M.; Courtot-Coupez, J.; Collman, J. P.; Evitt, E. R.; Benzosme, C. S. *J. Chem. Soc., Chem. Commun.* **1983,** 1286; (b) Le Mest, Y.; L'Her, M.; Collman, J. P.; Hendricks, N. H.; McElwee-White, L. *J. Am. Chem. Soc.* **1986,** *108,* 533.
80. (a) Matsushita, Y.; Matsui, T.; Sugamoto, K. *Chem. Lett.* **1992,** 1381; (b) Matsushita, Y.; Sugamoto, K.; Matsui, T. *Chem. Lett.* **1992,** 2165; (c) Matsushita, Y.; Sugamoto, K.; Matsui, T. *Chem. Lett.* **1994,** 1083.
81. Matsushita, Y.; Sugamoto, K.; Nakama, T.; Matsui, T. *J. Chem. Soc., Chem. Commun.* **1995,** 567.
82. (a) Collman, J. P.; Kim, K. *J. Am. Chem. Soc.* **1986,** *108,* 7847; (b) Collman, J. P.; Chng, L. L.; Tyvoll, D. A. *Inorg. Chem.* **1995,** *34,* 1311.
83. Chang, C. K.; Liang, Y.; Avilés, G.; Peng, S.-M. *J. Am. Chem. Soc.* **1995,** *117,* 4191.
84. Collman, J. P.; Zhang, X.; Wong, K.; Brauman, J. I. *J. Am. Chem. Soc.* **1994,** *116,* 6245.
85. (a) Shi, C.; Anson, F. C. *J. Am. Chem. Soc.* **1991,** *113,* 9564; (b) Shi, C.; Anson, F. C. *Inorg. Chem.* **1992,** *31,* 5078; (c) Steiger, B.; Shi, C.; Anson, F. C. *Inorg. Chem.* **1993,** *32,* 2107; (d) Shi, C.; Anson, F. C. *Inorg. Chim. Acta* **1994,** *225,* 215; (e) Steiger, B.; Anson, F. C. *Inorg. Chem.* **1994,** *33,* 5767; (f) Steiger, B.; Anson, F. C. *Inorg. Chem.* **1995,** *34,* 3355; (g) Shi, C.; Anson, F. C. *Inorg. Chem.* **1995,** *34,* 4554.
86. Warburg, O.; Negelein, E. *Chem. Ber.* **1930,** *63,* 1816.
87. Balch, A. L.; Latos-Grazynski, L.; Noll, B. C.; Olmstead, M. M.; Szterenberg, L.; Safari, N. *J. Am. Chem. Soc.* **1993,** *115,* 1422.
88. Balch, A. L.; Mazzanti, M.; St. Claire, T. N.; Olmstead, M. M. *Inorg. Chem.* **1995,** *34,* 2194.
89. Nishide, H.; Suzuki, T.; Nakagawa, R.; Tsuchida, E. *J. Am. Chem. Soc.* **1994,** *116,* 4503.
90. (a) Tsuchida, E.; Nishide, H. *Top. Curr. Chem.* **1986,** *132,* 63; (b) Collman, J. P. *Acc. Chem. Res.* **1977,** *10,* 265.
91. Skelly, J. M.; Morosoff, N. C.; Stannett, V. T.; Crumbliss, A. L. *Inorg. Chem.* **1993,** *32,* 1306.
92. Collman, J. P.; Gagne, R. R.; Kouba, J.; Ljusberg-Wahren, H. *J. Am. Chem. Soc.* **1974,** *96,* 6800.
93. (a) Busetto, C.; Cariati, F.; Galizzioli, D.; Morazzoni, F. *Gazz. Chim. Ital.* **1974,** *104,* 161; (b) Abel, E. W.; Pratt, J. M.; Whelan, P. *J. Chem. Soc., Chem. Commun.* **1971,** 449.
94. Kothari, V. M.; Tazuma, J. J. *J. Catal.* **1976,** *41,* 180.

95. Ford, W. T.; Chandran, R.; Turk, H. *Pure Appl. Chem.* **1988,** *60,* 395.
96. Schutten, J. H.; Piet, P.; German, A. L. *Makromol. Chem.* **1979,** *180,* 2341.
97. (a) Perez-Bernal, M. E.; Ruano-Casero, R.; Pinnavaia, T. J. *Catal. Lett.* **1991,** *11,* 55; (b) Chibwe, M.; Pinnavaia, T. J. *J. Chem. Soc., Chem. Commun.* **1993,** 278.
98. (a) Mimoun, H. In "Comprehensive Coordination Chemistry"; Wilkinson, G.; Gillard, R. D.; McCleverty, J. A., Eds. Pergamon Press: New York, 1987; Vol. 6, p. 317; (b) Parshall, G. "Homogeneous Catalysis"; John Wiley and Sons: New York, 1980; (c) Tolman, C.; Druliner, J. D.; Nappa, M. J.; Herron, N. In "Activation and Functionalization of Alkanes"; Hill, C., Ed.; John Wiley and Sons: New York, 1989.
99. Goldstein, A. S.; Drago, R. S. *Inorg. Chem.* **1991,** *30,* 4506.
100. Feig, A. L.; Lippard, S. J. *Chem. Rev.* **1994,** *94,* 718.
101. (a) Holmes, M. A.; Le Trong, I.; Turley, S.; Sieker, L. C.; Stenkamp, R. E. *J. Mol. Biol.* **1991,** *218,* 583; (b) Stenkamp, R. E. *Chem. Rev.* **1994,** *94,* 718.
102. (a) Wilkins, R. G.; Harrington, P. C. *Adv. Inorg. Biochem.* **1983,** *5,* 51; (b) Kurtz, D. M., Jr.; Klotz, I. M. *Acc. Chem. Res.* **1984,** *16,* 17; (c) Sanders-Loehr, J. In "Iron Carriers and Iron Proteins"; Loehr, T. M., Ed.; VCH Publishers: New York, 1989; p. 373.
103. (a) Zhang, J.-H.; Kurtz, D. M., Jr.; Maroney, M. J.; Whitehead, J. P. *Inorg. Chem.* **1992,** *31,* 1359; (b) Zhang, J.-H.; Kurtz, D. M., Jr.; Xia, Y.-M.; Debrunner, P. G. *Biochemistry* **1991,** *30,* 583.
104. Magnus, K. A.; Ton-That, H.; Carpenter, J. E. *Chem. Rev.* **1994,** *94,* 727.
105. (a) Solomon, E. I. In "Copper Proteins"; Spiro, T. G., Ed.; John Wiley and Sons: New York, 1981; p. 41; (b) Solomon, E. I.; Penfield, K. W.; Wilcox, D. E. *Struct. Bonding* **1983,** *53,* 1.
106. (a) Himmelwright, R. S.; Eickman, N. C.; Solomon, E. I. *J. Am. Chem. Soc.* **1979,** *101,* 1576; (b) Himmelwright, R. S.; Eickman, N. C.; LuBien, C. D.; Solomon, E. I. *J. Am. Chem. Soc.* **1980,** *102,* 5378; (c) Woolery, G. L.; Winkler, M.; Solomon, E. I. *J. Am. Chem. Soc.* **1984,** *106,* 86; (d) Pavlosky, M. A.; Larrabee, J. A. *J. Am. Chem. Soc.* **1988,** *110,* 5349.
107. Wilcox, D. E.; Long, J. R.; Solomon, E. I. *J. Am. Chem. Soc.* **1984,** *106,* 2186.
108. (a) Suzuki, S.; Kino, J.; Nakahara, A. *Bull. Chem. Soc. Jpn.* **1982,** *55,* 212; (b) Lorosch, J.; Haase, W. *Biochemistry* **1986,** *25,* 5850; (c) Salvato, B.; Beltramini, M.; Piazzesi, A.; Alviggi, M.; Ricchelli, F.; Magliozzo, R. S.; Peisach, J. *Inorg. Chim. Acta* **1986,** *125,* 55; (d) Suzuki, S.; Kino, J.; Kimura, M.; Mori, W.; Nakahara, A. *Inorg. Chim. Acta* **1982,** *66,* 41.
109. Dutton, T. J.; Baumann, T. F.; Larrabee, J. A. *Inorg. Chem.* **1990,** *29,* 2272.
110. (a) Lehn, J.-M.; Pine, S. H.; Watanabe, E.; Willard, A. K. *J. Am. Chem. Soc.* **1977,** *99,* 6766; (b) Comarmond, J.; Plumeré, P.; Lehn, J. M.; Agnus, Y.; Louis, R.; Weiss, R.; Kahn, O.; Morgenstern-Badarau, I. *J. Am. Chem. Soc.* **1982,** *104,* 6330.
111. Motekaitis, R. J.; Martell, A. E.; Lecomte, J.-P.; Lehn, J.-M. *Inorg. Chem.* **1983,** *22,* 609.
112. (a) Martell, A. E.; Motekaitis, R. J. *J. Chem. Soc., Chem. Commun.* **1988,** 915; (b) Martell, A. E.; Motekaitis, R. J. *J. Am. Chem. Soc.* **1988,** *110,* 8059; (c) Martell, A. E. *J. Inclusion Phenom.* **1989,** *7,* 99.
113. Motekaitis, R. J.; Martell, A. E. *Inorg. Chem.* **1991,** *30,* 694.
114. Motekaitis, R. J.; Martell, A. E. *Inorg. Chem.* **1994,** *33,* 1032.
115. Szpoganicz, B.; Motekaitis, R. J.; Martell, A. E. *Inorg. Chem.* **1990,** *29,* 1467.
116. Lehn, J.-M. *Pure Appl. Chem.* **1980,** *52,* 2441.
117. Motekaitis, R. J.; Martell, A. E.; Lehn, J.-M.; Watanabe, E.-I. *Inorg. Chem.* **1982,** *21,* 4253.

118. Motekaitis, R. J.; Martell, A. E. *J. Chem. Soc., Chem. Commun.* **1988,** 1020.
119. McLendon, G.; MacMillan, D. T.; Hariharan, M.; Martell, A. E. *Inorg. Chem.* **1975,** *14,* 2322.
120. (a) Gilbert, J. B.; Otey, M. C.; Price, J. E. *J. Biol. Chem.* **1951,** *190,* 377; (b) Tanford, C.; Kirk, D. C.; Chantooni, M. K., Jr. *J. Am. Chem. Soc.* **1954,** *76,* 5325; (c) Michailidis, M. S.; Martin, R. B. *J. Am. Chem. Soc.* **1969,** *91,* 4683; (d) Crook, E. M.; Rabin, R. B. *Biochem. J.* **1958,** *68,* 177.
121. Nakon, R.; Martell, A. E. *Inorg. Chem.* **1972,** *11,* 1002.
122. (a) Bianchini, C.; Mealli, C.; Meli, A.; Proserpio, D. M.; Peruzzini, M.; Vizza, F.; Frediani, P. *J. Organomet. Chem.* **1989,** *369,* C6; (b) Bianchini, C.; Frediani, P.; Laschi, F.; Vizza, F.; Zanello, P. *Inorg. Chem.* **1990,** *29,* 3402.
123. Ghilardi, C. A.; Midollini, S.; Moneti, S.; Orlandini, A.; Scapacci, G. *J. Chem. Soc., Dalton Trans.* **1992,** 3371.
124. (a) Laing, M.; Nolte, M. J.; Singleton, E. *J. Chem. Soc., Chem. Commun.* **1975,** 660; (b) Gubelmann, M. H.; Williams, A. F. *Struct. Bonding (Berlin)* **1983,** *55,* 1.
125. Barbaro, P.; Bianchini, C.; Laschi, F.; Midollini, S.; Moneti, S.; Scapacci, G.; Zanello, P. *Inorg. Chem.* **1994,** *33,* 1622.
126. (a) Vaska, L. *Science (Washington, D.C.)* **1963,** *140,* 840; (b) Vaska, L.; Bath, S. S. *J. Am. Chem. Soc.* **1966,** *88,* 1333; (c) Vaska, L.; Chen, L. S. *Chem. Commun.* **1971,** 1080.
127. Chock, P. B.; Halpern, J. *J. Am. Chem. Soc.* **1966,** *88,* 3511.
128. Selke, M.; Foote, C. S. *J. Am. Chem. Soc.* **1993,** *115,* 1166.
129. Some tetrameric dioxygen complexes having the general formula $Rh_4Cl_4(CO)_4(O_2)_2(PR_3)_2$, with $PR_3 = PPh_3$, PPh_2(O-*i*-butyl), $PPhEt_2$, or PEt_3, have been prepared from *trans*-Rh(CO)Cl(PR_3) after prolonged reflux in benzene under a dioxygen atmosphere: Cullen, W. R.; James, B. R.; Strukul, G. *Inorg. Chem.* **1978,** *17,* 484.
130. (a) Bennett, M. J.; Donaldson, P. B. *J. Am. Chem. Soc.* **1971,** *93,* 3307; (b) Bennett, M. J.; Donaldson, P. B. *Inorg. Chem.* **1977,** *16,* 1581; (c) Bennett, M. J.; Donaldson, P. B. *Inorg. Chem.* **1977,** *16,* 1585.
131. Selke, M.; Foote, C. S.; Karney, W. L. *Inorg. Chem.* **1993,** *32,* 5425.
132. Wilson, M. R.; Liu, H.; Prock, A.; Giering, W. P. *Organometallics* **1993,** *12,* 2044.
133. (a) Miller, C. A.; Lake, C. H.; Churchill, M. R.; Atwood, J. D. *Organometallics* **1995,** *14,* 5442; (b) Miller, C. A.; Janik, T. S.; Lake, C. H.; Toomey, L. M.; Churchill, M. R.; Atwood, J. D. *Organometallics* **1994,** *13,* 5080; (c) Lawson, H. J.; Atwood, J. D. *J. Am. Chem. Soc.* **1989,** *111,* 6223.
134. Bianchini, C.; Meli, A.; Peruzzini, M.; Vizza, F. *J. Am. Chem. Soc.* **1990,** *112,* 6726.
135. (a) Vaartstra, B. A.; Xiao, J.; Cowie, M. *J. Am. Chem. Soc.* **1990,** *112,* 9425; (b) Xiao, J.; Santarsiero, B. D.; Vaartstra, B. A.; Cowie, M. *J. Am. Chem. Soc.* **1993,** *115,* 3212; (c) Vaartstra, B. A.; Xiao, J.; Cowie, M. *Organometallics* **1990,** *112,* 9425.
136. (a) Bennett, M. J.; Donaldson, P. B. *Inorg. Chem.* **1977,** *16,* 1581; (b) Bonati, F.; Wilkinson, G. *J. Chem. Soc.* **1946,** 3156.
137. Vaska, L. *Science (Washington, D.C.)* **1963,** *140,* 809.
138. Suzuki, H.; Matsuura, S.; Moro-oka, Y.; Ikawa, T. *J. Organomet. Chem.* **1985,** *286,* 247.
139. Matsumoto, M.; Tamura, T. *J. Mol. Catal.* **1982,** *16,* 209.
140. Mieczynska, E.; Trzeciak, A. M.; Ziółkowski, J. J. *J. Mol. Catal.* **1992,** *73,* 1.
141. Mieczynska, E.; Trzeciak, A. M.; Ziółkowski, J. J. *J. Mol. Catal.* **1993,** *80,* 189.
142. Mieczynska, E.; Trzeciak, A. M.; Ziółkowski, J. J.; Lis, T. *J. Chem. Soc., Dalton Trans.* **1995,** 105.
143. (a) Bertini, I.; Drago, R. S.; Luchinat, C.; Eds.; "The Coordination Chemistry of

Metalloenzymes"; Reidel Publishing: Dordrecht, The Netherlands, 1983; (b) Dixon, M.; Webb, E. C. "Enzymes"; Longman: New York, 1981; (c) Ochiai, E. "Bioinorganic Chemistry"; Allyn and Bacon: Boston, 1977.

144. (a) Que, L., Jr. *Adv. Inorg. Biochem.* **1983,** *5,* 167; (b) Que, L., Jr. *Struct. Bonding (Berlin)* **1980,** *40,* 139; (c) Wood, J. T. In "Metal Ion Activation of Dioxygen"; Spiro, T. G., Ed.; John Wiley and Sons: New York, **1980;** Chapter 4.
145. (a) Makino, N.; McMahill, P.; Mason, H. S. *J. Biol. Chem.* **1974,** *249,* 6062; (b) Malmström, B. G.; Ryden, L. In "Biological Oxidations"; Singer, T., Ed.; Wiley Interscience: New York, **1968;** p. 415; (c) Bouchilloux, S.; McMahill, P.; Mason, H. S. *J. Biol. Chem.* **1963,** *238,* 1699.
146. (a) Barbaro, P.; Bianchini, C.; Mealli, C.; Meli, A. *J. Am. Chem. Soc.* **1991,** *113,* 3181; (b) Bianchini, C.; Frediani, P.; Laschi, F.; Meli, A.; Vizza, F.; Zanello, P.; *Inorg. Chem.* **1990,** *29,* 3402; (c) Bianchini, C.; Masi, D.; Mealli, C.; Meli, A.; Martini, G.; Laschi, F.; Zanello, P. *Inorg. Chem.* **1987,** *26,* 3683.
147. (a) Bianchini, C.; Peruzzini, M.; Zanobini, F.; Frediani, F.; Albinati, A. *J. Am. Chem. Soc.* **1991,** *113,* 5453; (b) Bianchini, C.; Caulton, K. G.; Chardon, C.; Eisenstein, O.; Folting, K.; Johnson, T. J.; Meli, A.; Peruzzini, M.; Rauscher, D. J.; Streib, W. F.; Vizza, F. *J. Am. Chem. Soc.* **1991,** *113,* 5127; (c) Barbaro, P.; Bianchini, C.; Meli, A.; Peruzzini, M.; Vacca, A.; Vizza, F. *Organometallics* **1991,** *10,* 2227; (d) Bianchini, C. *Pure Appl. Chem.* **1991,** *63,* 829; (e) Bianchini, C.; Meli, A.; Peruzzini, M.; Vizza, F.; Frediani, P. *Organometallics* **1990,** *9,* 226; (f) Cox, D. D.; Que, L., Jr. *J. Am. Chem. Soc.* **1988,** *110,* 8085.
148. Barbaro, P.; Bianchini, C.; Linn, K.; Mealli, C.; Meli, A.; Vizza, F.; Laschi, F.; Zanello, P. *Inorg. Chim. Acta* **1991,** *113,* 5127.
149. Barbaro, P.; Bianchini, C.; Frediani, P.; Meli, A.; Vizza, F. *Inorg. Chem.* **1992,** *31,* 1523.
150. (a) Tsuruya, S.; Yanai, S.; Masai, M. *Inorg. Chem.* **1986,** *25,* 141; (b) Tyson, C. A.; Martell, A. E. *J. Am. Chem. Soc.* **1972,** *94,* 939.
151. Teixidor, F.; Rudolph, R. W. *J. Organomet. Chem.* **1983,** *241,* 301.
152. Teixidor, F.; Ayllón, J. A.; Viñas, C.; Sillanpää, R.; Kivekäs, R.; Casabó, J. *Inorg. Chem.* **1994,** *33,* 4815.
153. (a) Yamanari, K.; Mori, M.; Dogi, S.; Fuyuhiro, A. *Inorg. Chem.* **1994,** *33,* 4807; (b) Yamanari, K.; Mori, M.; Dogi, S.; Fuyuhiro, A. *Chem. Lett.* **1993,** 1855.
154. (a) Fallab, S.; Zender, M.; Thewalt, U. *Helv. Chem. Acta* **1980,** *63,* 1491; (b) Macke, H.; Zender, M.; Thewalt, U.; Fallab, S. *Helv. Chim. Acta* **1979,** *62,* 1804; (c) Zender, M.; Thewalt, U.; Fallab, S. *Helv. Chim. Acta* **1976,** *59,* 2290; (d) Thewalt, U.; Struckmeier, G. *Z. Anorg. Allg. Chem.* **1976,** *419,* 163; (e) Fallab, S.; Mitchell, P. R. *Adv. Inorg. Bioinorg. Mech.* **1984,** *3,* 311.
155. Osakada, K.; Hataya, K.; Yamamoto, T. *Inorg. Chem.* **1993,** *32,* 2360.
156. (a) Ciriano, M. A.; Lanfranchi, M.; Oro, L. A.; Pérez-Torrente, J. J.; Tiripicchio, A.; Tiripicchio-Camellini, M. *J. Organomet. Chem.* **1994,** *468,* C31; (b) Ciriano, M. A.; López, J. A.; Oro, L. A.; Pérez-Torrente, J. J.; Lanfranchi, M.; Tiripicchio, A.; Tiripicchio-Camellini, M. *Organometallics* **1995,** *14,* 4764.
157. Weiher, J. F.; Katz, S.; Voight, A. F. *Inorg. Chem.* **1962,** *1,* 504.
158. Kojima, H.; Takahashi, S.; Yamazaki, H.; Hagihara, N. *Bull. Chem. Soc. Jpn.* **1970,** *43,* 2272.
159. Kojima, H.; Takahashi, S.; Hagihara, N. *J. Chem. Soc., Chem. Commun.* **1973,** 230.
160. Kojima, H.; Takahashi, S.; Hagihara, N. *Tetrahedron Lett.* **1973,** *22,* 1991.
161. Hay-Motherwell, R. S.; Wilkinson, G.; Sweet, T. K. N.; Hursthouse, M. B. *J. Chem. Soc., Dalton Trans.* **1994,** 2223.

162. Gosling, P. A.; van Esch, J. H.; Hoffmann, M. A. M.; Nolte, R. J. M. *J. Chem. Soc., Chem. Commun.* **1993,** 472.
163. Addison, A. W.; Gillard, R. D. *J. Chem. Soc. A* **1970,** 2523.
164. Sakurai, F.; Suzuki, H.; Moro-oka, Y.; Ikawa, T. *J. Am. Chem. Soc.* **1980,** *102,* 1749.
165. Elliott, G. P.; Roper, W. R.; Waters, J. M. *J. Chem. Soc., Chem. Commun.* **1982,** 811.
166. Kralik, M. S.; Rheingold, A. L.; Ernst, R. D. *Organometallics* **1987,** *6,* 2612.
167. (a) Bleeke, J. R.; Peng, W.-J.; Xie, Y.-F.; Chiang, M. Y. *Organometallics,* **1990,** *9,* 1113; (b) Bleeke, J. R.; Xie, Y.-F.; Peng, W.-J.; Chiang, M. *J. Am. Chem. Soc.* **1989,** *111,* 4118.
168. Bleeke, J. R.; Xie, Y-F.; Bass, L.; Chiang, M. Y. *J. Am. Chem. Soc.* **1991,** *113,* 4703.
169. Bleeke, J. R.; Peng, W.-J. *Organometallics* **1987,** *6,* 1576.
170. Bleeke, J. R.; Haile, T.; Chiang, M. Y. *Organometallics* **1991,** *10,* 19.
171. (a) McLendon, G.; Mooney, W. F. *Inorg. Chem.* **1980,** *19,* 12; (b) Davies, R.; Sykes, G. G. *J. Chem. Soc. A* **1968,** 2831; (c) Hoffman, A. B.; Taube, H. *Inorg. Chem.* **1968,** *7,* 1971; (d) Sykes, A. G. *Trans. Faraday Soc.* **1963,** *59,* 1325.
172. Sasaki, Y. *Bull. Chem. Soc. Jpn.* **1977,** *50,* 1939.
173. Davies, R.; Mori, M.; Sykes, A. G.; Weil, J. A. *Inorg. Synth.* **1970,** *12,* 197.
174. Edwards, J. D.; Yang, C. H.; Sykes, A. G. *J. Chem. Soc., Dalton Trans.* **1974,** 1561.
175. Ghosh, S. K.; Saha, S. K.; Ghosh, M. C.; Bose, R. N.; Reed, J. W.; Gould, E. S. *Inorg. Chem.* **1992,** *31,* 3358.
176. Ghosh, S. P.; Saha, S. K.; Bose, R. N.; Reed, J. W.; Ghosh, M. C.; Gould, E. S. *Inorg. Chem.* **1993,** *32,* 2261.
177. Saha, S. K.; Ghosh, M. C.; Gould, E. S. *Inorg. Chem.* **1991,** *31,* 5439.
178. Claus, C. *Petersb. Akad. Bull.* **1860,** *2,* 177.
179. Ellison, I. J.; Gillard, R. D. *J. Chem. Soc., Chem. Commun.* **1992,** 851.
180. Meszner, M.; Ziolkowski, J. J. *Inorg. Chim. Acta* **1988,** *145,* 299.
181. Ellison, I. J.; Gillard, R. D.; Moszner, M.; Wilgocki, M.; Ziolkowski, J. J. *J. Chem. Soc., Dalton Trans.* **1994,** 2531.
182. (a) Gillard, R. D.; Pedrosa de Jesus, J. D. *J. Chem. Soc., Dalton Trans.* **1984,** 1895; (b) Raynor, J. B.; Gillard, R. D.; Pedrosa de Jesus, J. D. *J. Chem. Soc., Dalton Trans.* **1982,** 1165; (c) Gillard, R. D.; Pedrosa de Jesus, J.; Tipping, L. R. H. *J. Chem. Soc., Chem. Commun.* **1977,** 58.
183. Ghosh, S. P.; Gelerinter, E.; Pyrka, G.; Gould, E. S. *Inorg. Chem.* **1993,** *32,* 4780.
184. Woollins, J. D. In "Encyclopedia of Inorganic Chemistry"; King, R. B., Ed.; John Wiley and Sons: New York, **1994;** Volume VII, Rho-S, pp. 3954–3988.
185. Kubas, G. J. *Acc. Chem. Res.* **1994,** *27,* 183.
186. Hall, C.; Harris, J. L.; Killey, A.; Maddox, T. P.; Palmer, S.; Perutz, R. N.; Rooney, A. D.; Goff, S. E. J.; Kazarian, S. G.; Poliakoff, M. *J. Chem. Soc., Dalton Trans.* **1994,** 3516.
187. Valentine, J.; Valentine, D., Jr.; Collman, J. P. *Inorg. Chem.* **1971,** *10,* 219.
188. Horn, R. W.; Weissberger, E.; Collman, J. P. *Inorg. Chem.* **1970,** *9,* 2367.
189. Siegl, W. O.; Lapporte, S. J.; Collman, J. P. *Inorg. Chem.* **1971,** *10,* 2158.
190. Randall, S. L.; Miller, C. A.; Jamik, T. S.; Churchill, M. R.; Atwood, J. D. *Organometallics* **1994,** *13,* 141.
191. (a) Lawson, H. J.; Atwood, J. D. *J. Am. Chem. Soc.* **1989,** *111,* 6223; (b) Lawson, H. J.; Atwood, J. D. *J. Am. Chem. Soc.* **1988,** *110,* 3680.
192. Randall, S. L.; Thompson, J. S.; Buttrey, L. A.; Ziller, J. W.; Churchill, M. R.; Atwood, J. D. *Organometallics* **1991,** *10,* 683.
193. Fettinger, J. C.; Churchill, M. R.; Bernard, K. A.; Atwood, J. D. *J. Organomet. Chem.* **1988,** *340,* 377.

194. Godfrey, S. M.; Kelly, D. G.; McAuliffe, C. A.; Pritchard, R. G. *J. Chem. Soc., Dalton Trans.* **1995,** 1095.
195. Newmann, A. A., Ed. "The Chemistry and Biochemistry of Thiocyanic Acid and Its Derivatives"; Academic Press: New York, **1975.**
196. Sykes, A. G.; Mast, R. D. *J. Chem. Soc. A* **1967,** 784.
197. Hayward, P. J.; Blake, D. M.; Wilkinson, G.; Nyman, C. J. *J. Am. Chem. Soc.* **1970,** *92,* 5873.
198. Mason, M. G.; Ibers, J. A. *J. Am. Chem. Soc.* **1982,** *104,* 5153.
199. Beaulieu, W. B.; Mercer, G. D.; Roundhill, D. M. *J. Am. Chem. Soc.* **1978,** *100,* 1147.
200. Dimitrou, K.; Folting, K.; Streib, W. E.; Christou, G. *J. Am. Chem. Soc.* **1993,** *115,* 6432.
201. (a) Brudvig, G. W.; Thorp, H. H.; Crabtree, R. H. *Acc. Chem. Res.* **1991,** *24,* 311; (b) Thorp, H. H.; Brudvig, G. W. *New J. Chem.* **1991,** *15,* 479, (c) Christou, G. *Acc. Chem. Res.* **1989,** *22,* 328; (d) Christou, G.; Vincent, J. B. *Biochim. Biophys. Acta* **1987,** *895,* 259; (e) Brudvig, G. W.; Crabtree, R. H. *Proc. Natl. Acad. Sci. USA* **1986,** *83,* 4586.
202. (a) Stack, T. D. P.; Holm, R. A. *J. Am. Chem. Soc.* **1988,** *110,* 2484; (b) Palermo, R. E.; Singh, R.; Bashkin, J. K.; Holm, R. A. *J. Am. Chem. Soc.* **1984,** *106,* 2600; (c) Berg, J. M.; Holm, R. A. "Metal Ions in Biology"; Interscience: New York, 1982; Vol. 4; (d) Ibers, J. A.; Holm, R. A. *Science (Washington, DC)* **1980,** *209,* 223.
203. (a) Schulz, S.; Andruh, M.; Pape, T.; Heinze, T.; Roesky, H. W.; Häming, L.; Kuhn, A.; Herbst-Irmer, R. *Organometallics* **1994,** *13,* 4004; (b) Dobbs, D. A.; Bergman, R. G. *J. Am. Chem. Soc.* **1992,** *114,* 6908.
204. (a) Sausville, E. A.; Peisach, J.; Horwitz, S. B. *Biochemistry* **1978,** *17,* 2740; (b) Sausville, E. A.; Peisach, J.; Horwitz, S. B. *Biochem. Biophys. Res. Commun.* **1976,** *73,* 814.
205. (a) Petering, D. H.; Byrnes, R. W.; Antholine, W. E. *Chem.-Biol. Interact.* **1990,** *73,* 133; (b) Stubbe, J.; Kozarich, J. W. *Chem. Rev.* **1987,** *87,* 1107; (c) Hecht, S. M. *Acc. Chem. Res.* **1986,** *19,* 83; (d) Murugesan, N.; Hecht, S. M. *J. Am. Chem. Soc.* **1985,** *107,* 493.
206. Guajardo, R. J.; Chavez, F.; Farinas, E. T.; Mascharak, P. K. *J. Am. Chem. Soc.* **1995,** *117,* 3883.
207. Chang, C. H.; Meares, C. F. *Biochemistry* **1982,** *21,* 6332.
208. Xu, R. X.; Nettesheim, D.; Otvos, J. D.; Petering, D. H. *Biochemistry* **1994,** *33,* 907.
209. Wu, W.; Vanderwall, D. E.; Stubbe, J.; Kozarich, J. W.; Turner, C. J. *J. Am. Chem. Soc.* **1994,** *116,* 10843.
210. (a) Chien, M.; Grollman, A. P.; Horwitz, S. B. *Biochemistry* **1977,** *16,* 3641; (b) Povirk, L. F.; Hogan, M.; Dattagupta, N. *Biochemistry* **1979,** *18,* 96; (c) Kross, J.; Henner, W. D.; Haseltine, W. A.; Rodriguez, L.; Levin, M. D.; Hecht, S. M. *Biochemistry* **1982,** *21,* 3711; (d) Kilkuskie, R. E.; Suguna, H.; Yellin, B.; Murugesan, N.; Hecht, S. M. *J. Am. Chem. Soc.* **1985,** *107,* 260; (e) Fisher, L. M.; Kuroda, R.; Sakai, T. T. *Biochemistry* **1985,** *24,* 3199.
211. Kane, S. A.; Sasaki, H.; Hecht, S. M. *J. Am. Chem. Soc.* **1995,** *117,* 9107.
212. (a) Stubbe, J. *J. Biol. Chem.* **1990,** *265,* 5329; (b) Sjöberg, B.-M.; Gräslund, A. *Adv. Inorg. Biochem.* **1983,** *5,* 87; (c) Reichard, P.; Ehrenberg, A. *Science (Washington, DC)* **1983,** *221,* 514.
213. Petersson, L.; Gräslund, A.; Ehrenberg, A.; Sjöberg, B.-M.; Reichard, P. *J. Biol. Chem.* **1980,** *255,* 6706.
214. McCormick, J. M.; Reem, R. C.; Foroughi, J.; Bollinger, J. M.; Jensen, G. M.; Stephens, P. J.; Stubbe, J.; Solomon, E. I. *New J. Chem.* **1991,** *15,* 439.

215. Atkin, C.; Thelander, L.; Reichard, P.; Land, G. *J. Biol. Chem.* **1973,** *248,* 7464.
216. Brown, N. C.; Eliasson, R.; Reichard, P.; Thelander, L. *Eur. J. Biochem.* **1969,** *9,* 512.
217. Atta, M.; Nordlund, P.; Åberg, A.; Eklund, H.; Fontecave, M. *J. Biol. Chem.* **1992,** *267,* 2682.
218. Elgren, T. E.; Ming, L.-J.; Que, L., Jr. *Inorg. Chem.* **1994,** *33,* 891.
219. Kappes, M. M.; Staley, R. H. *J. Phys. Chem.* **1981,** *85,* 9421.
220. (a) Armentrout, P. B.; Halle, L. F.; Beauchamp, J. L. *J. Chem. Phys.* **1982,** *76,* 2449; (b) Fisher, E. R.; Elkind, J. L.; Clemmer, D. E.; Georgiadis, R.; Loh, S. K.; Aristov, N.; Sunderlin, L. S.; Armentrout, P. B. *J. Chem. Phys.* **1990,** *93,* 2676.
221. Schröder, D.; Schwarz, H. *Angew. Chem.* **1993,** *105,* 1493; *Angew. Chem., Int. Ed. Engl.* **1993,** *32,* 1420.
222. Ryan, M. F.; Fiedler, A.; Schröder, D.; Schwarz, H. *Organometallics* **1994,** *13,* 4072.
223. Chen, Y.-M.; Clemmer, D. E.; Armentrout, P. B. *J. Am. Chem. Soc.* **1994,** *116,* 7815.
224. Fiedler, A.; Schröder, D.; Shaik, S.; Schwarz, H. *J. Am. Chem. Soc.* **1994,** *116,* 10734.
225. (a) Broclawik, E.; Salahub, D. R. *J. Mol. Catal.* **1993,** *82,* 117; (b) Ziegler, T. *Chem. Rev.* **1991,** *91,* 651.
226. (a) Becke, A. D. *Phys. Rev.* **1988,** *A38,* 2398; (b) Perdew, J. P. *Phys. Rev.* **1986,** *B33,* 8822; *Phys. Rev.* **1986,** *B34,* 7406; (c) Vosko, S. J.; Wilk, L.; Nusair, M. *Can. J. Chem.* **1980,** *58,* 1200.
227. Andersson, K.; Malmquist, P.-A.; Roos, B. O.; Sadlej, A. L.; Wolinski, K. *J. Phys. Chem.* **1990,** *94,* 5483.
228. Carter, E. A.; Goddard, W. A. III *J. Phys. Chem.* **1988,** *92,* 2109.
229. Fischer, H. E.; Schwartz, J. *J. Am. Chem. Soc.* **1989,** *111,* 7644.
230. McMillan, J. W.; Fischer, H. E.; Schwartz, J. *J. Am. Chem. Soc.* **1991,** *113,* 4014.
231. (a) Xu, X.; Friend, C. M. *J. Am. Chem. Soc.* **1991,** *113,* 8572; (b) Xu, X.; Friend, C. M.; *J. Am. Chem. Soc.* **1991,** *113,* 6779; (c) Xu, X.; Friend, C. M. *J. Am. Chem. Soc.* **1990,** *112,* 4571.
232. Bol, C. W. J.; Friend, C. M. *J. Am. Chem. Soc.* **1995,** *117,* 5351.
233. Volkov, S. V.; Bandur, V. A.; Buryak, N. I. *Polyhedron* **1995,** *14,* 3515.
234. Buryak, N. I.; Bandur, V. A.; Volkov, S. V. *Zh. Neorg. Khim.* **1987,** *32,* 2634.

This Page Intentionally Left Blank

ADVANCES IN INORGANIC CHEMISTRY, VOL. 44

RECENT DEVELOPMENTS IN CHROMIUM CHEMISTRY

DONALD A. HOUSE

Chemistry Department, University of Canterbury, Christchurch, New Zealand

I. Introduction and Scope

This article summarizes areas of chromium chemistry that are often neglected in modern textbooks of inorganic chemistry, and yet are topics of considerable research importance.

It has become customary to classify transition-metal compounds in terms of oxidation state, and then discuss various types of ligand arrangements within that state. Much of the single element chemistry in "Comprehensive Coordination Chemistry" (*1*) follows this pattern (e.g., Re), but one or two elements (e.g., Co), are discussed in terms of ligand type. Using the latter approach, patterns of reactivity can be specified by considering changes in oxidation state.

Reviews and texts including substantial coverage of chromium chemistry (*2, 3*) and mechanistic studies (*4, 5*) have appeared. In what follows, reference is made to the developing chemistry of the Cr(IV)

and Cr(V) states, as well as to the more familiar Cr(II), Cr(III), and Cr(VI). Extensive use is made of UV-vis spectrophotometry in the characterization of species in solution. *Peak positions* λ/nm $(\varepsilon/M^{-1}\ cm^{-1})$ *refer to the absorbance of the molecular species (monomer, dimer, trimer, etc.) present.*

II. Oxo and Peroxo Ligands

The chemistry in this area (*6–8*) has been approached from two different directions: reduction of Cr(VI) or oxidation of Cr(II); it is only recently that an overall, self-consistent picture has emerged (*7, 9*). The key experiment is the observation that the reaction between Cr(VI) and alcohols in acid solution under an O_2 atmosphere yields $[(H_2O)_5Cr^{III}O_2]^{2+}$, a Cr(III) superoxo complex,[1] according to the sequence (1).

$$HCr^{VI}O_4^- \xrightarrow{-2e} [(H_2O)_5Cr^{IV}O]^{2+} \xrightarrow{-2e} [Cr^{II}(OH_2)_6]^{2+} \underset{K}{\overset{O_2}{\rightleftharpoons}} [(H_2O)_5Cr^{III}O_2]^{2+} \qquad (1)$$

This (reversible) reaction scheme allows much of the redox chemistry of chromium to be rationalized.

A. Chromium(II) plus Dioxygen (Aqueous)

The reaction between O_2 and $[Cr(OH_2)_6]^{2+}$ in acidic solution has been well studied (*7, 10, 11*), and the final products are $[HCrO_4]^-$ (2–20%), $[Cr(OH_2)_6]^{3+}$ (45–67%), and $[(H_2O)_4Cr(OH)_2Cr(OH_2)_4]^{4+}$ (0–51%). No $[(H_2O)_5CrO_2Cr(OH_2)_5]^{4+}$ (a Cr(III) μ-peroxo species, Section II,B) was detected (*10*) although it has been proposed as an intermediate (*11*).

With O_2 in excess, the first product is $[(H_2O)_5CrO_2]^{2+}$, UV-vis absorption maxima 290(3100), 245(7000), and magnetic and spectroscopic data are consistent with a $Cr(III)O_2$ (superoxo) formulation. Rate constants for the forward and reverse steps (*6*) are $1.6 \times 10^8\ M^{-1}\ sec^{-1}$ and $2.5 \times 10^{-4}\ sec^{-1}$ ($t_{1/2} \approx 50$ min) giving $K = 6.4 \times 10^{11}$ at 25°C (pH = 0–2).

The superoxo complex, $[(H_2O)_5CrO_2]^{2+}$, reacts further ($k \approx 2 \times 10^8\ M^{-1}\ sec^{-1}$, 25°C, pH = 0–2) with $[Cr(OH_2)_6]^{2+}$ to give $[(H_2O)_5Cr^{IV}O]^{2+}$,

[1] In a number of formulas the degree of hydration is presumed.

(3). Thus, both O_2 and $[(H_2O)_5CrO_2]^{2+}$ are competing for $[Cr(OH_2)_6]^{2+}$, and this limits the concentration of the superoxo complex to ca. 10^{-4} M. Addition of an alcohol (0.1 M MeOH) results in the Cr(IV) species being reduced to $[Cr(OH_2)_6]^{2+}$ (6), which, in the presence of O_2, gives the superoxo complex (2), and concentrations up to 10^{-3} M can be obtained.

Decomposition of the superoxo complex occurs by two pathways in the reaction sequence, (2)–(5), which account for the production of $[HCrO_4]^-$ and $[(H_2O)_2Cr(OH)_2Cr(OH_2)_4]^{4+}$ but not for $[Cr(OH_2)_6]^{3+}$. Aquation of the dimer is not sufficiently rapid to allow for any significant formation of $[Cr(OH_2)_6]^{3+}$, but this is produced by decomposition of $[(H_2O)_5CrO_2H]^{2+}$ as in (7) or (12).

$$O_2 + [Cr^{II}(OH_2)_6]^{2+} \underset{k_1}{\overset{k_{-1}}{\rightleftharpoons}} [(H_2O)_5Cr^{III}O_2]^{2+} \tag{2}$$

$$[(H_2O)_5Cr^{III}O_2]^{2+} + [Cr^{II}(OH_2)_6]^{2+} \longrightarrow 2[(H_2O)_5Cr^{IV}O]^{2+} \tag{3}$$

$$[(H_2O)_5Cr^{IV}O]^{2+} + [Cr^{II}(OH_2)_6]^{2+} \longrightarrow [(H_2O)_4Cr(OH)_2Cr(H_2O)_4]^{4+} \tag{4}$$

$$2[(H_2O)_5CrO_2]^{2+} \longrightarrow 2[HCr^{VI}O_4]^- + 6H_3O^+ \tag{5}$$

$$[(H_2O)_5Cr^{IV}O]^{2+} + RCH_2OH \longrightarrow RCHO + [Cr(OH_2)_6]^{2+} \tag{6}$$

Reduction of the superoxo form with $[Ru(NH_3)_6]^{2+}$ (7) or electrochemically (*12*) produces first the Cr(III) hydroperoxo complex $[(H_2O)_5CrO_2H]^{2+}$ absorption maxima, ~450, ~630 nm (*13*). This spontaneously decomposes (7) to $[Cr(OH_2)_6]^{3+}$ with a half-life of ca. 10 min at room temperature, $[H^+] = 0.1$ M (*12, 14*).

$$[(H_2O)_5CrO_2H]^{2+} + H+ \longrightarrow [Cr(OH_2)_6]^{3+} + H_2O_2 \tag{7}$$

The hexaaqua ion, $[Cr(OH_2)_6]^{3+}$, is also the final product in the reduction process (*7, 12*). The complete process using Fe(II) as a reducing agent is shown in the reaction sequence (8)–(11), where a Fenton-type (*15*) mechanism is proposed (*7, 16*), with $[(H_2O)_5Cr^{IV}O]^{2+}$ behaving as the chromium equivalent of the ·OH radical (*16*).

$$[(H_2O)_5Cr^{III}O_2]^{2+} + [Fe(OH_2)_6]^{2+} \longrightarrow [(H_2O)_5CrO_2Fe(OH_2)_5]^{4+} \tag{8}$$

$$\longrightarrow [(H_2O)_5CrO_2H]^{2+} + [Fe(OH_2)_6]^{3+} \tag{9}$$

$$[(H_2O)_5Cr^{III}O_2H]^{2+} + [Fe(OH_2)_6]^{2+} \longrightarrow [(H_2O)_5Cr^{IV}O]^{2+} + [Fe(OH_2)_6]^{3+} \tag{10}$$

$$[(H_2O)_5Cr^{IV}O]^{2+} + [Fe(OH_2)_6]^{2+} \longrightarrow [Cr(OH_2)_6]^{3+} + [Fe(OH_2)_6]^{3+} \tag{11}$$

If $[Cr(OH_2)_6]^{2+}$ is added to an air-saturated solution of the hydroperoxo product formed in (9), *oxidation* takes place to give the superoxo product. This is because reactions (2) and (3) generate $[(H_2O)_5Cr^{IV}O]^{2+}$, which reacts with the hydroperoxo form (12).

$$[(H_2O)_5Cr^{III}O_2H]^{2+} + [(H_2O)_5Cr^{IV}O]^{2+} \longrightarrow [Cr(OH_2)_6]^{3+} + [(H_2O)_5Cr^{III}O_2]^{2+} \quad (12)$$

For comparison, the reaction between $[Cr(OH_2)_6]^{2+}$ and H_2O_2 proceeds via a modified Fenton reaction as in Eqs. (13) and (14) (*17–19*).

$$[Cr(OH_2)_6]^{2+} + H_2O_2 + H+ \longrightarrow [Cr(OH_2)_6]^{3+} + \cdot OH + H_2O \quad (13)$$

$$[Cr(OH_2)_6]^{2+} + \cdot OH + H^+ \longrightarrow [Cr(OH_2)_6]^{3+} + H_2O \quad (14)$$

The $[Cr(OH_2)_6]^{2+}/H_2O_2$ reaction is important in the synthesis of air-stable cationic organochromium(III) complexes (see Section III,B), as the initially produced ·OH radicals react rapidly with added organic substrates to form alkyl radicals, which, in turn, react with $[Cr(OH_2)_6]^{2+}$ (15), (16).

$$HCR_3 + \cdot OH \longrightarrow \cdot CR_3 + H_2O \quad (15)$$

$$[Cr(OH_2)_6]^{2+} + \cdot CR_3 \longrightarrow [(H_2O)_5CrCR_3]^{2+} \quad (16)$$

The observation that reaction (13) is the slowest step, and that the organochromium complexes are highly colored with peak maxima at 300 (2500) and ~400 (~300), provides a means of determining rate constants for (13) (*18*).

Further oxidation of the superoxo intermediate (17) can be achieved with $[Ru^{III}(bpy)_3]^{3+}$ (*19*).

$$[(H_2O)_5CrO_2]^{2+} + [Ru(bpy)_3]^{3+} \longrightarrow [Cr(OH_2)_6]^{3+} + [Ru(bpy)_3]^{2+} + O_2 \quad (17)$$

All this chemistry shows that H_2O_2 and $[(H_2O)_5CrO_2H]^{2+}$ have very similar redox properties in terms of kinetics, but $[(H_2O)_5CrO_2H]^{2+}$ is a more powerful one-electron oxidant than H_2O_2 by more than one volt (Fig. 1) (*14*).

The other important product from the Cr(II) + O_2 reaction is $[(H_2O)_5CrO]^{2+}$, absorbance maxima at 260 (5000) and ~300 sh (*20*). Stopped-flow mixing of 3×10^{-3} M $[Cr(OH_2)_6]^{2+}$ and 2.6×10^{-3} M O_2 (aq) in 1 M $HClO_4$ produces ca. 4.5×10^{-4} M $[(H_2O)_5CrO]^{2+}$ with a half-life of ca. 30 sec at 25°C. This species is a powerful, mainly two-electron oxidant (18), and many kinetic studies have been made (7).

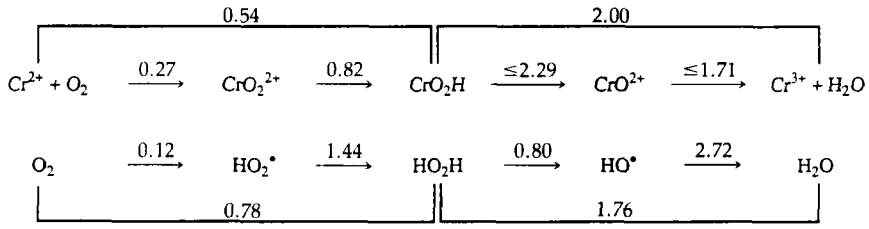

FIG. 1. Estimated Latimer diagrams for the reduction of aqueous dioxygen calculated on the thermodynamic assumption of $[O_2] = 1$ M at pH = 0, 25°C. The overall four-electron process has the same potential (1.27 V) for both the chromium free and chromium mediated processes (*14*).

$$[(H_2O)_5Cr^{IV}O]^{2+} + RH_2 \longrightarrow [Cr^{II}(OH_2)_6]^{2+} + R + H_2O \qquad (18)$$

The complex is normally described as the oxochromium(IV) $[(H_2O)_5Cr{=}O]^{2+}$ or chromyl cation, by analogy with the vanadyl cation $[(H_2O)_5V^{IV}O]^{2+}$. It can also be regarded as a chromium(III) substituted hydroxyl radical (Fig. 1) and its H-atom abstracting properties are parallel to those of ·OH (15).

The chromyl cation reacts with H_2O_2 to give the chromium(III) superoxo. In this case, the oxidant acts via a one-electron hydride abstraction process and $[Cr(OH_2)_6]^{2+}$ is not involved (19).

$$[(H_2O)_5Cr^{IV}O]^{2+} + H_2O_2 \longrightarrow [(H_2O)_5Cr^{III}O_2]^{2+} + H_2O \qquad (19)$$

As an oxidant, $[(H_2O)_5Cr^{IV}O]^{2+}$ is kinetically more reactive than $HCr^{VI}O_4^-$. The half-life for the oxidation of excess MeOH (5×10^{-4} M, 0.1 M $HClO_4$, $I = 1.0$ M, 25°C) with the chromyl cation is about 12 sec, whereas under the same conditions the corresponding reaction with $HCrO_4^-$ takes several hours to complete.

Although the preceding refers to chromyl or aquachromium(IV) chemistry, an extensive chemistry of chelated chromium(IV) complexes is now developing (*21*). The treatment of the Krumpole complex (*22*) $Na[Cr^V(2\text{-ethyl-2-hydroxybutanoate})_2O] \cdot 1.5H_2O$ (Fig. 2) (*23*) with one-

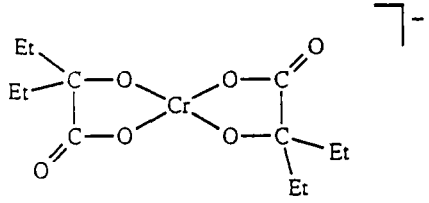

FIG. 2. $[Cr(ehba)_2O]^-$.

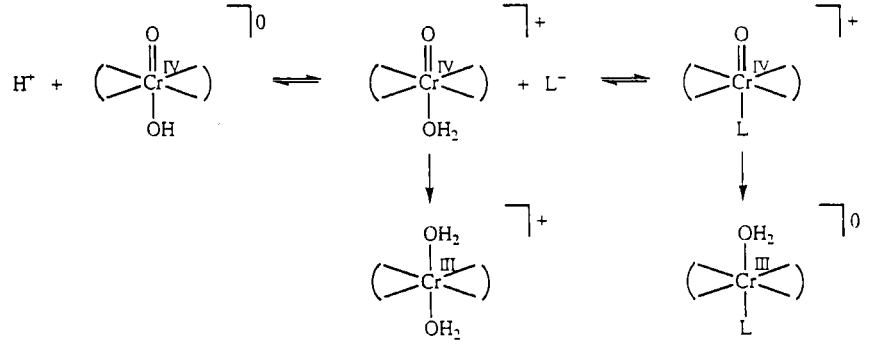

FIG. 3. A possible reaction scheme for chelated Cr(IV) (*21*).

electron reductants shows that chelated Cr(IV) can be detected as a transient. The systems are, however, complicated by further reduction steps. Alternatively, when solutions of Cr(VI) buffered with eaba$^-$ and Heaba are treated with a series of two-electron reductants (As(III) is the most useful), a pink solution with absorbance maxima at 511 (2300) develops. The stability depends on the Cr(VI)/ligand ratio used. At low ligand concentrations, the excess Cr(VI) oxidizes chelated Cr(IV) to $[Cr^{V}(ehba)_2O]^-$, absorption maxima 510 (181), but with excess ligand, the pink Cr(IV) solutions are stable for hours at room temperature and can be used in a variety of redox processes (*21*).

The UV-vis absorbance spectrum of the chelated Cr(IV) product is dependent on pH and ligand concentration, with the latter reflected in ligand-concentration-dependent reduction products (Fig. 3).

One of the difficulties in characterizing the Cr(IV) state is that it is ESR silent, whereas the corresponding Cr(V) oxidation state (Section II,B) gives strong signals (*24*).

Macrocyclic Cr(IV) has been produced by dihalide radical oxidation of the corresponding Cr(III) complex (20) (*25*).

$$[RCr^{III}(L)(H_2O)]^{2+} + \cdot X_2^- \longrightarrow 2X^- + [RCr^{IV}(L)(H_2O)]^{3+} \qquad (20)$$

(R = alkyl; L = 1,4,8,12-tetraazacyclopentadecane).

B. REDUCTION OF CHROMIUM(VI)

The $[Cr^{II}(OH_2)_6]^{2+}$ reduction of Cr(VI) is very rapid and the products (2 M $HClO_4$) are again $[Cr(OH_2)_6]^{3+}$ and $[(H_2O)_4Cr(OH)_2Cr(OH_2)_4]^{4+}$, with 50–70% of the monomer (*10*). A number of mechanisms have been proposed, including (21) and (22) followed by (4).

$$HCr^{VI}O_4^- + [Cr^{II}(OH_2)_6]^{2+} \xrightarrow{-1e} [Cr^{III}(OH_2)_6]^{3+} + Cr^{V} \quad (21)$$

$$HCr^{VI}O_4^- + [Cr^{II}(OH_2)_6]^{2+} \xrightarrow{-2e} 2[(H_2O)_5Cr^{IV}O]^{2+} \quad (22)$$

With H_2O_2, the products (in 2 M $HClO_4$) are $[Cr(OH_2)_6]^{3+}$ (75–93%) and two dark green μ-peroxo–Cr(III) complexes: $[(H_2O)_5CrO_2Cr(OH_2)_5]^{4+}$ (4–5%), absorption maxima at 272(1180), 439(153), 634(202); and a +5 charged species, $[Cr_3(O_2)_2]^{5+}$ (2–17%), absorption maxima 230 (3800), 267 (3170), 433 (360), and 625 (384) (*10*). Earlier work (*26*) suggests that this "trimer" may be $[(H_2O)_5CrO_2Cr(OH_2)_5]^{5+}$, which would be the Cr(III)-bridged equivalent of the superoxo, $[(H_2O)_5CrO_2]^{2+}$. This model, with the +4 charged species as a peroxo and the +5 charged species as a superoxo, has an attractive parallel in Co(III) chemistry with the characterization of $[(NH_3)_5CoO_2Co(NH_3)_5]^{4+}$ (peroxo) and $[(NH_3)_5CoO_2Co(NH_3)_5]^{5+}$ (superoxo) complexes (*27*). The +4 $[Cr(III)]_2$ charged species decomposes spontaneously in acid with a half-life of about 25 min (2 M $HClO_4$, 25°C) to give O_2, $[Cr(OH_2)_6]^{3+}$, and Cr(VI) with isosbestic points at 387 and 326 nm. Thermal acid decomposition of the +5 charged species is slower ($t_{1/2}$ = 90 min, 5 M $HClO_4$, 25°C), and polynuclear Cr(III) species are produced in addition to $[Cr(OH_2)_6]^{3+}$, O_2, and Cr(VI). The observation that Ce(IV) does not react with the +5 charged species (*10*) is further evidence supporting a μ-superoxo formulation.

Numerous attempts have been made to characterize the first products formed in the $H^+/H_2O_2/Cr(VI)$ reaction (*6*). A transient blue complex ("perchromic acid"), which is believed to be $[Cr^{VI}O(O_2)_2(OH_2)]$, absorbance maximum 580(450), by analogy with the structurally characterized $[Cr^{VI}O(O_2)_2(py)]$, rapidly decomposes (seconds).

Rate laws for the formation (23) and decomposition (24) have been determined (*6*).

$$-d[HCrO_4^-]/dt = k[HCrO_4^-][H_2O_2] \quad (23)$$

$$-d[CrO(O_2)_2(OH_2)]/dt = k_1[CrO(O_2)_2(OH_2)][H^+] + k_2[CrOH(O_2)_2(OH_2)][H^+] \quad (24)$$

$k = 1.87 \times 10^4\ M^{-2}\ sec^{-1}$, $k_1 = 0.25\ M^{-1}\ sec^{-1}$, and $k_2 = 1.8\ M^{-1}\ sec^{-1}$ at 25°C.

If the H_2O_2/Cr(VI) reaction solution is alkaline, red-brown salts, absorbance maximum 372 (1600) (*30*), of the tetra(peroxo)chromate(V) anion can be isolated and structurally characterized.

The D_{2d} symmetry of this anion has attracted several theoretical investigations (*6*), and the single unpaired electron makes this species

an ideal candidate for Cr(V) ESR (g = 1.9720) studies (*28*). The rate of decomposition of $[Cr(O_2)_4]^{3-}$ in aqueous alkaline solution (25) has been followed using pH-stat (*29*), spectrophotometric (*30*), and ESR (*31*) techniques. At constant pH, a first-order decay is observed ($t_{1/2} \approx$ 6 min, pH = 9.1, T = 30°C, I = 3 M, $NaClO_4$) with a first-order dependence on $[H^+]$ in the range pH = 7.9–11.8 (*30, 31*) (25).

$$-d[Cr(O_2)_4^{3-}]/dt = k_2[Cr(O_2)_4^{3-}][H^+] \tag{25}$$

In basic solution, the decomposition stoichiometry follows (26), but as the $[H^+]$ increases, more Cr(III) is produced.

$$4[Cr(O_2)_4]^{3-} + 2H_2O \longrightarrow 4CrO_4^{2-} + 4OH^- + 7O_2 \tag{26}$$

It has been proposed (*6*) that the μ-peroxo and μ-superoxo Cr(III) products mentioned previously may be generated via the acid decomposition of $[Cr(O_2)_4]^{3-}$, but there is still a large gap in our knowledge as to the origin of these dimeric Cr(III) peroxos.

At intermediate pH (4–7), the H_2O_2/Cr(VI) reaction forms an unstable violet solution, absorption maximum 540 (510), presumed to be $[Cr^{VI}O(O_2)_2OH]^-$, a deprotonated form of "perchromic acid." This same species can also be produced by adding H_2O_2 to a neutral solution of $[Cr^{V}(O_2)_4]^{3-}$. The rate of formation of $[Cr^{VI}O(O_2)_2(OH)]^-$ (seconds) follows the same rate law (23) and has the same activation parameters as for the formation of blue "perchromic acid" (*6*). The products from the decomposition of $[Cr^{VI}O(O_2)_2(OH)]^-$ do not appear to have been determined.

Chromate- and Cr(VI)-containing compounds have been found to have serious toxic and carcinogenic effects (*28*). It has, however, been reported that Cr(VI) does not react directly with isolated DNA, so reduction products of Cr(VI) are implicated in the carcinogenic process. This has led to a large number of kinetic and product analysis studies involving Cr(VI) and biologically active reducing agents, including ascorbic acid (*32–37*), thiols (*32, 37–41*), alcohols (*42*), sugars and sugar derivatives (*43–45*), glycerophosphates (*46*), and DNA (*47*). There are, in these investigations, an impressive variety of reactant and product variables, with both pH and $[O_2]$ (*33*) being important. Radicals and lower oxidation states of Cr are potential intermediates before the final isolated form of Cr(III) is obtained. Relevant kinetic information can be obtained in the Twigg series "Mechanisms of Inorganic and Organometallic Reactions" (*4*).

One problem in surveying the redox chemistry of Cr(VI) is the seem-

ingly bewildering array of acid dependencies reported by various investigators. In fact, much of the reported data can be rationalized in terms of the known acid–base equilibria associated with the oxidant and the reductant.

For a dibasic acid reductant (e.g., ascorbic acid, H_2A), there will be three potential reductants, H_2A, HA^-, and A^{2-}, (27), (28).

$$H_2A \rightleftharpoons HA^- + H^+ \quad K_1 \tag{27}$$

$$HA^- \rightleftharpoons A^{2-} + H^+ \quad K_2 \tag{28}$$

In the pH range 1–6, there will be two forms of the oxidant, $HCrO_4^-$ and CrO_4^{2-} (see Section II,C, reaction (45)).

This gives six reactant pair combinations, (29)–(34), that have the potential to contribute to the rate law.

$$HA^- + [HCrO_4]^- \xrightarrow{k_1} \text{products} \tag{29}$$

$$HA^- + [CrO_4]^{2-} \xrightarrow{k_2} \text{products} \tag{30}$$

$$H_2A + [HCrO_4]^- \xrightarrow{k_3} \text{products} \tag{31}$$

$$H_2A + [CrO_4]^{2-} \xrightarrow{k_4} \text{products} \tag{32}$$

$$A^{2-} + [HCrO_4]^- \xrightarrow{k_5} \text{products} \tag{33}$$

$$A^{2-} + [CrO_4]^{2-} \xrightarrow{k_6} \text{products} \tag{34}$$

In this set, the k_4 and k_5 paths are indistinguishable from the k_1 and k_2 paths, respectively, and can be eliminated from the mechanistic scheme [the so-called proton ambiguity (2)]. The overall rate law consistent with this modified set, (29), (30), (31), (34), is given in Eq. (35).

$$\text{rate} = (k_1[HCrO_4^-] + k_2[CrO_4^{2-}])[HA^-] + (k_3[HCrO_4^-])[H_2A] + (k_6[CrO_4^{2-}])[A^{2-}] \tag{35}$$

After the relevant substitutions from (27), (28), and (45), (35) transforms to Eq. (36).

$$\text{rate} = \left(\frac{k_6K_1K_2K_c + k_2K_1K_c[H^+] + k_1K_1[H^+]^2 + k_3[H^+]^3}{(K_c + [H^+])(k_1[H^+] + K_1K_2 + [H^+]^2)}\right) \times [Cr(VI)_T][A_T] \tag{36}$$

The best way to follow this analysis is to express (35) in terms of $[CrO_4^{2-}]$ and $[HA^-]$ and then use the mass balance expressions, (37), (38).

$$[CrO_4^{2-}] = [Cr(VI)_T]\left(\frac{K_c}{K_c + [H^+]}\right) \tag{37}$$

$$[HA^-] = [A_T]\left(\frac{K_1[H^+]}{K_1[H^+] + K_1K_2 + [H^+]^2}\right) \tag{38}$$

Equation (36) means that a variety of $[H^+]$ dependence expressions will be observed for different reductants, depending on the magnitudes of K_1, K_2, k_1, k_2, k_3, and k_6. Thus, if K_2 is zero and k_2 and k_3 are small, (36) reduces to (39).

$$\text{rate} = \frac{k_1K_1K_c^{-1}[H^+]}{1 + K_c^{-1}[H^+]} \times [Cr(VI)_T][A_T] \tag{39}$$

Cr(VI) ester formation before electron transfer is a well-accepted first step, and if the ester is reasonably long-lived, saturation kinetics are observed (40).

$$k_{obs} = \frac{a[\text{reductant}][H^+]}{1 + b[\text{reductant}]} \tag{40}$$

Chelated Cr(V) is frequently detected (ESR) as an early reduction product, but care must be taken to distinguish these signals from those produced by organic radicals. Unfortunately, Cr(IV) is much more difficult to detect (some investigators have used NMR methods (*37*)), but Cr(II) can be detected by the formation of $[(H_2O)_5CrO_2]^{2+}$ (*7, 9*).

It has been postulated (*28, 38*) that in the biological situation the first-formed chelated Cr(V) may react with H_2O_2 in a Fenton-type process (40a) to yield ·OH radicals.

$$Cr(V) + H_2O_2 \longrightarrow Cr(VI) + \cdot OH + OH^- \tag{40a}$$

Carcinogenesis could be caused by either Cr(V) or ·OH.

C. The Bichromate(VI) Anion ($HCrO_4^-$)

As mentioned earlier, a variety of pH-dependent Cr(VI) species are available in solution as potential reactants, (41)–(45).

$$H_2Cr_2O_7 \rightleftharpoons HCr_2O_7^- + H^+ \tag{41}$$

$$HCr_2O_7^- \rightleftharpoons Cr_2O_7^{2-} + H^+ \quad (42)$$

$$Cr_2O_7^{2-} + H_2O \rightleftharpoons 2HCrO_4^- \quad (43)$$

$$H_2CrO_4 \rightleftharpoons HCrO_4^- + H^+ \quad (44)$$

$$HCrO_4^- \rightleftharpoons CrO_4^{2-} + H^+ \quad K_c \quad (45)$$

Higher polychromates (e.g., $Cr_3O_{10}^{2-}$) can be isolated in yields up to 45%, under appropriate conditions (*48*). A systematic classification of Cr—O bond lengths has been developed for polychromate anions (Fig. 4), and these bond types have been correlated with the degree of polymerization (*48*).

Equilibrium constants have been measured for (41)–(45) using a variety of techniques: spectrophotometry (*49*), conductivity, ^{17}O-NMR line broadening (*50*), isopiestic measurements, potentiometry, and others (*51*). From these data, speciation distribution estimates have been calculated (*52*). As the equilibrium constants for (41)–(45) are quite sensitive to ionic strength, so are the speciation distributions. Thus, for pH = 1, $Cr(VI)_T = 10^{-2}$ M and T = 25°C, the $[H_2CrO_4]$ is calculated to be 29% at I = 0 and 1% at I = 1.0 M (*52*). Nevertheless, a considerable proportion (~50%) of Cr(VI) in the pH range 1–6 is estimated to be in the $HCrO_4^-$ form.

Consequently, it was surprising that a study of the Raman spectra of Cr(VI) in aqueous acidic solution concluded that only equilibrium (*46*) occurred, and H_2CrO_4, $HCrO_4^-$, and $HCr_2O_7^-$ could not be detected (*53*).

$$2CrO_4^{2-} + 2H^+ \rightleftharpoons Cr_2O_7^{2-} + H_2O \quad (46)$$

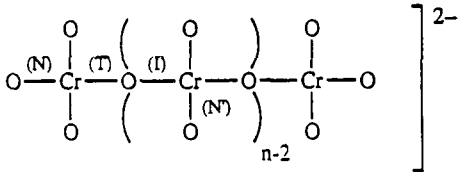

FIG. 4. Classification of Cr—O bonds within $[Cr_nO_{3n+1}]^{2-}$ anions. (T) and (I) are the terminal and inner bridging distances between terminal and inner Cr atoms, respectively. There is no significant difference between Cr—O(N) and Cr—O(N′) distances. For any particular $[Cr_nO_{3n+1}]^{2-}$ anion, the Cr—O bond length increases in the order Cr—O(N) < Cr—O(I) < Cr—O(T), and whereas Cr—O(N) bonds shorten with increasing n, the opposite is found for Cr—O(I) and Cr—O(T) (*48*).

Further high-pressure, high-temperature Raman studies (*51*) confirmed the original data, but not the conclusions. Indeed, Palmer *et al.* (*51*) have convincingly argued for the formation of $HCrO_4^-$ and believe that the symmetrical stretching vibration that should be observed for $HCrO_4^-$ is coincident with the more intense $\nu_s(CrO_3)$ band. It must, however, be admitted that evidence for the existence of the $HCrO_4^-$ ion has hitherto been indirect, and no salts isomorphous with, say, $KHSO_4$ (*54*) have been isolated. This situation has been changed by the report and crystal structure of $[Ph_4P][HCrO_4]$ (*55*) with three Cr—O(N) bonds of 1.56 Å and one Cr—O bond (presumably Cr—OH) of 2.02 Å. (Typical Cr—O(N) bonds in the CrO_4^{2-} anion are 1.65 Å.) Evidence for the existence of the $HCrO_4^-$ anion is now quite conclusive (*50*).

III. Organochromium Compounds

This is a rapidly developing area of Cr chemistry, and the two main classes discussed here are the chromium(0) pentacarbonyl carbenes (*56*) and the chromium(III) alkyls (*57*).

A. Amino Acid Synthesis

The synthesis of unnatural chiral amino acids is a considerable challenge to the organic chemist. One approach is via chiral organochromium(0) carbenes (*56*). The starting material is easily prepared from chromium hexacarbonyl and organolithium reagents (Fig. 5), and the resulting carbenes are air-stable yellow to red solids.

Irradiation of these complexes with visible light results in CO insertion to produce a species with ketene-like properties that can react with olefins, imines and alcohols (Fig. 6). When the photolysis is performed in a CO atmosphere, $Cr(CO)_6$ is regenerated.

To obtain amino acids, amino carbenes (X = NH_2 in Fig. 6) must be used, and if chirality is required, the asymmetry of the new α-carbon center must be controlled. Higedus and co-workers have achieved good stereochemical control by using a chiral oxazolidine chromium carbene.

The resulting product is, however, an *N*-substituted oxazolidine amino acid, but this can easily be removed by either reductive or oxidative (Fig. 7) procedures. These and similar reactions can be used to prepare γ-hydroxy-α-amino acids, arylglycines, α-alkyl-α-amino acids, and a variety of nonproteinogenic dipeptides (Fig. 7). The review by Muzart (*58*) is an excellent source of further information on the use of Cr compounds in organic synthesis.

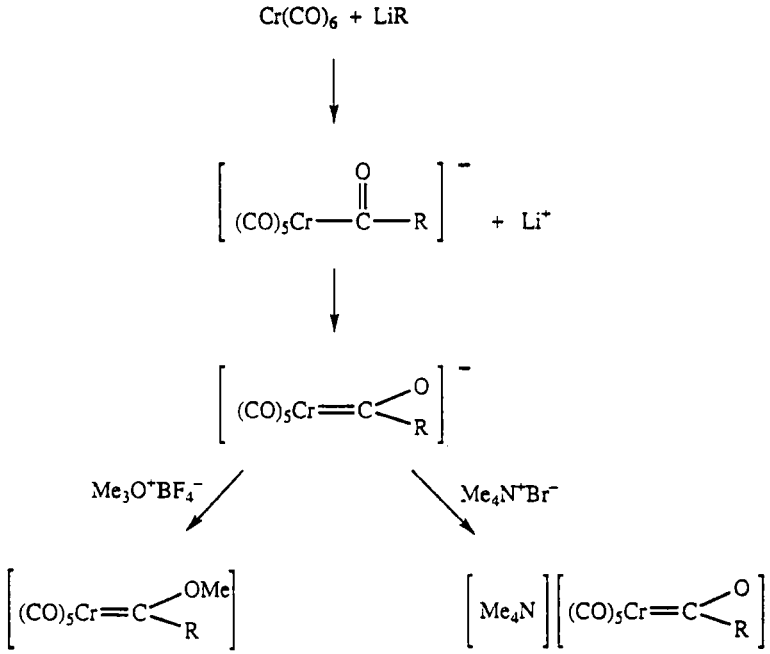

FIG. 5. Synthesis of anionic or neutral organochromium(0) carbenes.

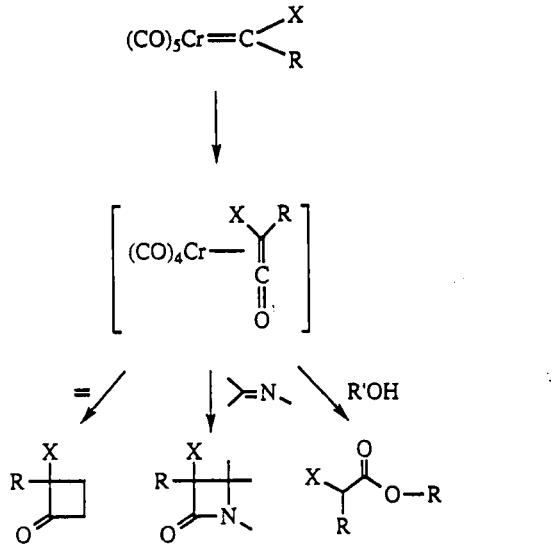

FIG. 6. Photolysis of organochromium(0) carbenes.

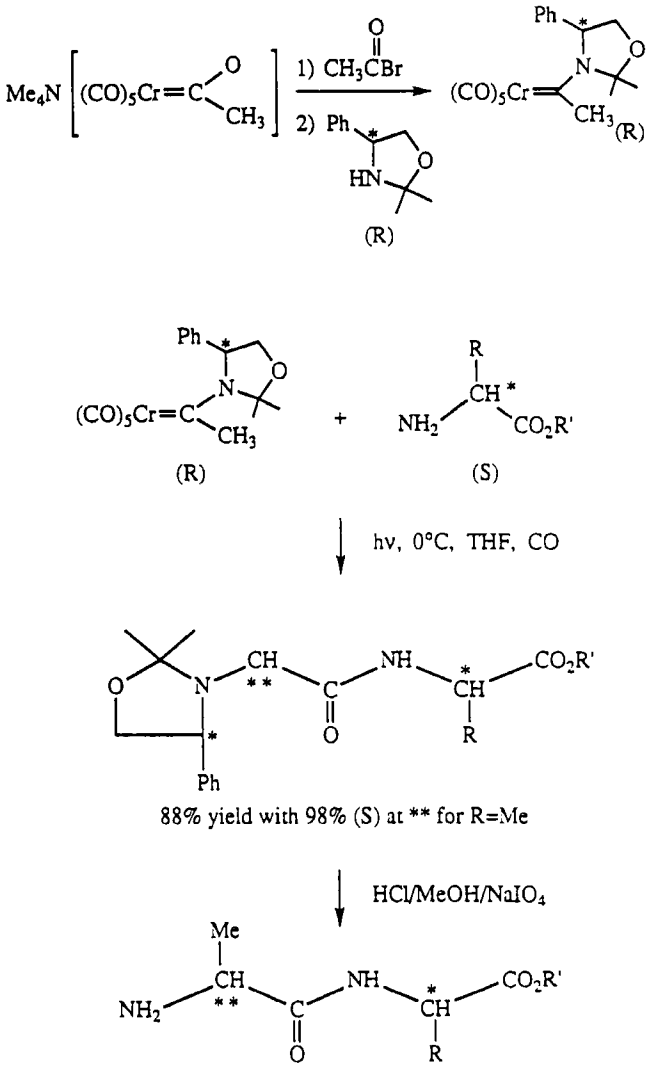

FIG. 7. Synthesis of dipeptides using organochromium(0) carbenes (* indicates known chiral center; **indicates a new chiral center).

B. CHROMIUM(III) ALKYL COMPOUNDS

Cr(III) complexes of the type $[(H_2O)_5CrR]^{2+}$ have been widely investigated in solution (*57*). These orange-colored cations, absorption maxima ~400 (~300), ~280 (~300), ~555 (~25), have a solution stability that is quite dependent on R and undergo a variety of reactions includ-

ing homolysis (49), heterolysis (48) radical transfer, electron transfer (50), substitution, and photolysis.

All known synthetic routes involve $[Cr(OH_2)_6]^{2+}$ and a radical (47). The variation between particular synthetic processes involves the method of radical generation (Fig. 8).

$$[Cr(OH_2)_6]^{2+} + \cdot R \longrightarrow [(H_2O)_5CrR]^{2+} + H_2O \qquad (47)$$

In many cases, the $[(H_2O)_5CrR]^{2+}$ cations can be purified by ion-exchange chromatography, but the rate of thermal heterolysis (48) is acid and anion (*59, 60*) catalyzed.

$$[(H_2O)_5CrR]^{2+} + H_3O^+ \longrightarrow [Cr(OH_2)_6]^{3+} + HR \qquad (48)$$

The loss of the alkyl group is also accelerated by other electrophiles, Hg^{2+} (*61*), HgR^+, and halogens (e.g., Br_2). One point to note with the last reagent is that the products are RX, X^-, and $[Cr(OH_2)_6]^{3+}$. The

1) $[Cr^{II}(OH_2)_6]^{2+} + RX \longrightarrow [Cr^{III}X(OH_2)_5]^{2+} + \bullet R$

2) $[Cr(OH_2)_6]^{2+} + RC(Me)_2OOH \longrightarrow [Cr(OH_2)_6]^{3+} + RC(Me)_2O\bullet$

$RC(Me)_2O\bullet \longrightarrow Me_2CO + \bullet R$

3) $[Cr(OH_2)_6]^{2+} + h\nu \longrightarrow [Cr(OH_2)_6]^{3+} + e^-(aq)$

$e^-(aq) + RBr \longrightarrow Br^- + \bullet R$

4) $[Cr(OH_2)_6]^{2+} + H_2O_2 \longrightarrow [Cr(OH_2)_6]^{3+} + \bullet OH$

$\bullet OH + RH \longrightarrow H_2O + \bullet R$

5) $[Cr(OH_2)_6]^{2+} + [(H_2O)_5CrCHCl_2]^{2+} \longrightarrow [CrCl(OH_2)_5]^{2+} + [(H_2O)_5Cr\dot{C}HCl]^{2+}$

$[Cr(OH_2)_6]^{2+} + [(H_2O)_5Cr\dot{C}HCl]^{2+} \longrightarrow [(H_2O)_5CrCH(Cl)Cr(OH_2)_5]^{4+}$

$\xrightarrow{H^+} [Cr(OH_2)_6]^{3+} + [(H_2O)_5CrCH_2Cl]^{2+}$

FIG. 8. Methods of radical generation for the formation of organochromium(III) alkyls.

absence of $[Cr^{III}X(OH_2)_5]^{2+}$ suggests that a four-centered transition state is not operative. The other major decomposition pathway is homolysis (49), the reverse of (47).

$$[(H_2O)_5CrR]^{2+} + H_2O \longrightarrow [Cr(OH_2)_6]^{2+} + \cdot R \qquad (49)$$

Reaction (49) can be suppressed by addition of $[Cr(OH_2)_6]^{2+}$, or it can be driven at the limiting rate by adding a scavenger to eliminate $[Cr(OH_2)_6]^{2+}$ or ·R. As a consequence, the first-order rate constant for (49) remains independent of the nature and concentration of the scavenger. Thus, these organochromium(III) alkyls can be regarded as a source of "stored free radicals," but practical applications such as polymerization initiation are only in their infancy.

One of the more recent reactions of organochromium(III) alkyls to be studied is oxidation (50) to a Cr(IV) analogue.

$$[(H_2O)_5Cr^{III}R]^{2+} + Ox \longrightarrow [(H_2O)_5Cr^{IV}R]^{3+} + Ox^- \qquad (50)$$

Typical oxidants are $[Ru(bipy)_3]^{3+}$, $[Cr^*(bipy)_3]^{3+}$, $\cdot Br_2$, I_2, and NO^+, and the fate of the Cr(IV) complex is again either heterolysis (51) or homolysis (52).

$$[(H_2O)_5Cr^{IV}R]^{3+} + H_2O \longrightarrow [Cr(OH_2)_6]^{2+} + ROH + H^+ \qquad (51)$$

$$\longrightarrow [Cr(OH_2)_6]^{3+} + \cdot R \qquad (52)$$

The reaction between chromium(III) alkyls and O_2 is quite complicated (*57*) and may involve O_2 insertion in the Cr—C bond to form an alkyl peroxo species, $[(H_2O)_5CrO_2R]^{2+}$, analogous to $[(H_2O)_5CrO_2H]^{2+}$, described in Section II,A.

Although no solid-state information is available for the pentaaquachromium(III) alkyl cations, crystal structures are available for chelated analogues, e.g., $[(H_2O)(2,3,3,3\text{-tet})CrR](ClO_4)_2$, where 2,3,3,3-tet is the N_4 macrocycle, 1,4,8,12-tetraazacyclopentadecane and R is $4\text{-}BrC_6H_4CH_2^-$.

The Cr—C bond exerts a considerable (ca. 0.1 Å) solid-state trans elongation (Table I), and the trans effect is implicated in the enhanced substitution lability of the trans aqua ligand. A variety of chelating systems can be used to form $[L_5CrR]^{2+}$ cations, including diamines (*63*), polyamines, macrocyclic N_4 ligands, acac, bipy, and polycarboxylates such as nta, edta (*64*), and hedtra.

TABLE I

SOLID-STATE TRANS EFFECT $[(L)_5CrC]^{n+}$ COMPLEXES (*57*)

trans Ligand	*cis* Ligand	R	Cr–R (Å)	Cr–X(*trans*) (Å)	Cr–X("normal") (Å)
H_2O	2,3,3,3-tet	$4BrC_6H_4CH_2$–	2.14	2.13	1.95
py	$(acac)_2$	$ClCH_2$–	2.13	2.16	2.10 (*62*)
H_2O	$(acac)_2$	$ClCH_2$–	2.06	2.134	1.95
MeOH	$(acac)_2$	$ClCH_2$–	2.05	2.15	2.00

IV. Polynuclear Chromium(III) Complexes

Most systems considered in this section contain bridging oxo- or hydroxo ligands with water occupying the non-bridging sites, but recent developments in this area also involve ammonia and polyamine ligands (*3, 65*).

The oligomerization process that takes place when $[Cr(OH_2)_6]^{3+}$ solutions are aged have been described by Marty (*66*), and these investigations have been continued by his co-workers (*67, 68*). The multiproduct equilibria that develop depend on Cr:OH ratios, temperature, pH, and time. In some cases, the system may take years to reach equilibrium, and constant pH cannot be used as an indication of attainment of an equilibrium.

Starting with $[Cr(OH_2)_6]^{3+}$, the nature of the "second hydration shell" has been probed with a variety of techniques including IR, XRD, EXAFS, and neutron diffraction (*4*). Surprisingly consistent results have been obtained, with $n = 13 \pm 1$ in $\{[Cr(OH_2)_6]^{3+}\ (H_2O)_n\}$ and a Cr—O distance of 4.02 Å for the water molecules in the second hydration shell.

Aqueous solutions of hydrated Cr(III) salts are acid by hydrolysis (53) ($pK_a = 4.2$) (*69*).

$$[Cr(OH_2)_6]^{3+} \rightleftharpoons [Cr(OH)(OH_2)_5]^{2+} + H^+ \qquad (53)$$

The characteristic light purple color of $[Cr(OH_2)_6]^{3+}$ in chrom alum, $K_2SO_4 \cdot Cr_2(SO_4)_3 \cdot 12H_2O$, absorption maxima 575 (13.2), 408 (15.5), $I = 1.0$ M (*70*), is frequently masked by complex ion formation in other salts, e.g., the green form of $CrCl_3 \cdot 6H_2O$, which contains predominantly *trans*-$[CrCl_2(OH_2)_4]^+$.

Addition of excess base to a solution of $[Cr(OH_2)_6]^{3+}$ at room temperature produces a deep green solution, absorption maxima 588 (~20),

TABLE II

RATE CONSTANTS FOR Cr(III) OLIGOMERIZATION PROCESSES AT 25°C, I = 1.0 M, $NaClO_4$ (*74, 75, 79*)

Reaction	k (M^{-1} sec^{-1})
$monomer^{2+} + monomer^{2+} \longrightarrow dimer$	2
$monomer^{2+} + monomer^{+} \longrightarrow dimer$	3.8×10^3
$monomer^{+} + monomer^{+} \longrightarrow dimer$	1.8×10^4
$monomer^{0} + monomer^{0} \longrightarrow dimer$	2.5×10^4
$monomer^{0} + monomer^{-} \longrightarrow dimer$	3.8×10^3
$monomer^{-} + monomer^{-} \longrightarrow dimer$	1.2×10^2
$dimer^{3+} + dimer^{3+} \longrightarrow tetramer$	2.18
$dimer^{3+} + dimer^{2+} \longrightarrow tetramer$	52
$dimer^{2+} + dimer^{2+} \longrightarrow tetramer$	8.3×10^3

433 (~22) of "chromite" anions (*71*). This contains a complex mixture of hydroxo-bridged Cr(III) polymers as, on acidification of the "chromite" solution, at least 10 different oligomers can be separated by ion-exchange chromatography (*72*). The nature of the species in the alkaline solution is quite speculative, but tetrahedral $[Cr(OH)_4]^-$ is considered unlikely (*71*) and, although the final concentrations of mononuclear species such as $[Cr(OH)_6]^{3-}$ (*73*), $[Cr(OH)_4(OH_2)_2]^-$ (*74*), or $[Cr(OH)_3(OH_2)_3]$ (*74*) are quite low (~10%), they are initially formed in sufficient concentration that the rates of dimerization (Table II) can be measured on the stopped-flow time scale (*74*). The final products are believed (*71*) to be highly condensed polynuclear species such as

TABLE III

DETAILS OF VISIBLE ABSORPTION SPECTRA FOR OLIGOMERIC Cr(III) HYDROXO BRIDGED SPECIES (*70*)

Species[a]	λ_{max} (nm) (ε) (M^{-1} cm^{-1})	λ_{min} (nm) (ε) (M^{-1} cm^{-1})	λ_{max} (nm) (ε) (M^{-1} cm^{-1})
$[Cr_2(OH)_2]^{4+}$	582	490	417
	(17.4)	(5.2)	(20.4)
$[Cr_3(OH)_4]^{5+}$	584	499	425
	(19.2)	(5.5)	(30.5)
$[Cr_4(OH)_6]^{6+}$	580	500	426
	(15.6)	(5.6)	(30.3)
$[Cr_6(OH)_{10}]^{8+}$	585	503	426
	(18.6)	(6.1)	(29.0)

[a] H_2O molecules omitted from formula.

$[Cr_{12}(OH)_{28}(OH_2)_{12}]^{8+}$ that fragment on acidification. What is remarkable is the observation that deprotonation can turn a kinetically inert metal center into an extremely labile one.

Once the solution is acidified, there is a slow, time-dependent cleavage of higher oligomers (nuclearity > 6) into lower oligomers (Table III). One of the more persistent lower oligomers obtained from this procedure is the trimer $[Cr_3(OH)_4(OH_2)_9]^{5+}$, and yields of up to 65% can be obtained. The structure of this species is the subject of some debate, as Marty proposed a "nonclassical" condensed structure as opposed to the more open structures observed with amine ligands (*3*) in the nonbridging positions (Fig. 9).

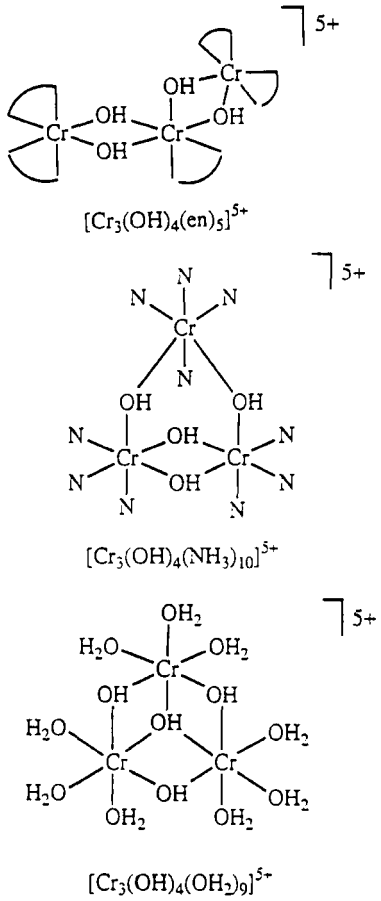

FIG. 9. *Possible structures for* $[Cr_3(OH)_4(L)_n]^{5+}$ *ions (3, 65, 72).*

With lower $[Cr(OH_2)_6]^{3+}$:OH^- ratios (1:≤1) and with a final pH of <5, clear green solutions are formed. The Cr(III) speciation depends on age (*66*), but the initial step, after deprotonation (54), is dimer formation (*75*).

$$[Cr(OH_2)_6]^{3+} + nOH^- \longrightarrow [Cr(OH)_n(OH_2)_{6-n}]^{(3-n)+} \qquad (54)$$

Sequential steps are proposed (*75–77*) with two monomeric units combining to form first a single hydroxo-bridged dimer, which in turn closes to give the double hydroxo-bridged dimer. This latter species $[(H_2O)_4Cr(OH)_2Cr(OH_2)_4]^{4+}$ is one of the major products from the O_2 oxidation of $[Cr(OH_2)_6]^{2+}$ (*11*) (Section I,A), and the crystal structure of the *p*-toluenesulfonate salt has been determined (*78*).

The tetramer is the main polymerization product obtained (21% yield) on addition of hydroxide ion (3 days, 25°C, pH = 3.8) to solutions of the pure dimer (*11, 70, 79*). On acidification, the tetramer splits into $[Cr(OH_2)_6]^{3+}$ and the trimer. Careful investigation of the tetramer showed that two rapidly interconverting species could be detected (Fig. 10). The proposed structure of TC (*80*), with a square pyrimidal tetraco-

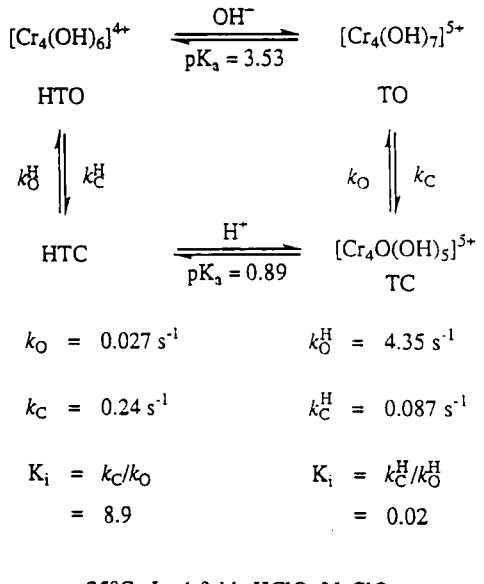

25°C, I = 1.0 *M*, $HClO_4/NaClO_4$

FIG. 10. Interconversions between two hydrolytic chromium(III) tetramers (*75*).

ordinate oxo ligand, is quite controversial (*3*). Unconventional structures are needed, however, to account for the unprecedented lability.

In all these condensation processes there are a number of monomer species, related to one another by acid–base equilibria, that can combine to give the observed product. Thus, all binary combinations of $[Cr(OH_2)_6]^{3+}$, $[Cr(OH)(OH_2)_5]^{2+}$, $[Cr(OH)_2(OH_2)_4]^{+}$, and $[Cr(OH)_3(OH_2)_3]^{0}$ need to be considered (*75*) when forming the hydroxo-bridged dimer. Even though some of the lower-charged species are only present at low concentrations, the reactivity increases with deprotonation. In fact, the oligomerization processes (monomer → dimer; dimer → tetramer) are dominated by six reaction pathways (Table II), and each deprotonation step affords a rate enhancement.

A cyclic, hydrogen-bonded intermediate (Fig. 11) is believed to be a precursor to dimer formation, as there are now a considerable number of solid-state structures of "(hydroxy)(aqua)" complexes that contain this unit (*81–85*).

Before the conclusion of this section, it should also be noted that the alleged oxo-bridged aqua dimer (*86*) $[(H_2O)_5CrOCr(OH_2)_5]^{4+}$, formed from $[Cr(OH_2)_6]^{2+}$ and 1,4-benzoquinone, must now be reformulated as a semiquinone radical-bridged species (*20*).

When solutions of the monomer (*87, 88*), dimer (*78*), or trimer (*72*) are basified to pH = 5–7, precipitates of "active hydroxides" are formed. Immediate removal of the precipitate gives products that are reasonably stable over time and regenerate substantial (90%) amounts of the starting oligomer on acidification. If, however, the precipitate is left in contact with the mother liquor, an "aging" process occurs. Acidification of the aged hydoxides and analysis of the resulting mixtures shows that oligomerization has taken place, the extent depending on the time of aging, the rate of stirring, and the pH of the solution. Thus, aging of the "active trimer hydroxide" at pH = 8, I = 1.0 M ($NaClO_4$), T = 25°C for 30 min gives, on acidification, 40% trimer, 30% hexamer, and 30% higher oligomers (*72*).

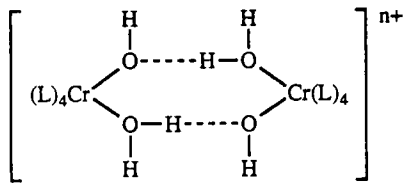

FIG. 11. Bridging of two Cr(III) centers by H-bonded $H_3O_2^-$ groups.

V. Polyaminocarboxylic Ligands

This topic has recently been reviewed (*89*), and only selected aspects are discussed here.

Cr(III) complexes of edta were first described by Schwartzenbach and Biedermann in 1948 (*90*). Since that time, many variations in the design of the potentially hexadentate aminopolycarboxylate ligand have been investigated. Most of these involve changes in the nature of the diamine backbone or changes in the number and length of the carboxylate arms. A variant of this is the introduction of C-branches rather than N-branches (*89*) in the carboxylate arm, and there seems no reason why this could not be extended to C-branches on the diamine backbone (Fig. 12). As the complexity of the ligand increases, so does the potential for geometric and optical isomers in an octahedral Cr(III) complex. Thus, ligand (Z) has two chiral C-centers (*) and two potentially chiral N-centers (**) when coordinated. Also, there are now isomeric possibilities resulting from differing spatial ring arrangements (Fig. 13).

In this area, a unique nomenclature system has gradually developed where differing rings are assigned alphabetical letters. The E-ring contains the diamine backbone, and this effectively defines a meridional plane in the octahedron. Chelate rings within this plane are the G

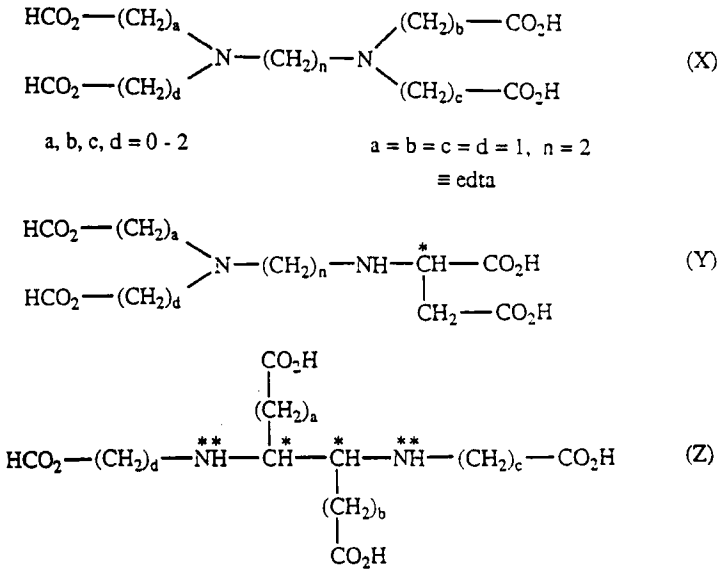

FIG. 12. Diamine polycarboxylate-type ligands.

(girdle) rings. Rings at right angles to this plane are R (relaxed) rings. Although this system is useful to describe ring opening or ring loss processes, it is not often used to describe isomers and becomes quite ambiguous once one arm is lost (*90*). Attempts to rescue the system result in the introduction of a G′ ring, i.e., a ring that once was in the G plane, but is now at right angles to it (Fig. 13). Alternative nomenclature systems (*89, 91*) seem to offer little advantage.

The out-of-plane R rings are believed to be "less strained" than the G or E rings, mainly on the chemical basis that another ligand displaces a G ring more easily.

The structure of $[Cr(edta)]^{n-}$ in aqueous solution is still under active investigation. Two series of salts can be isolated: Rb^+ (*92*) or $K[Cr(edta)] \cdot 2H_2O$ with N_2O_4 hexadentate coordination in the solid state (*93*), and $[Cr(Hedta)(OH_2)]$ (*94, 95*) with one G-ring dechelated and protonated. The system is very labile (rechelation rates exceed stopped-flow measurement), and several acid–base equilibria are involved (Fig. 14).

Anation studies involving $[Cr(Hedta)(OH_2)]$ (*96*) confirm that the coordinated water molecule is exceptionally labile.

Starting with $[Cr(Hedta)(OH_2)]$, alkalimetric titration gives pK_a^1 as 2.10 (*97*), and from $[Cr(edta)]^-$, a similar titration gives $pK_a^2 = 7.42$ (*98*). The questions under debate are (i) what is the coordination number of the edta ligand bound to Cr(III) in the pH range 4–7, and (ii) if the ligand is hexadentate, can a seventh position in the inner coordination sphere be occupied by a water molecule? The latter proposal is not unreasonable, as 7-coordination is observed in the solid-state hexaden-

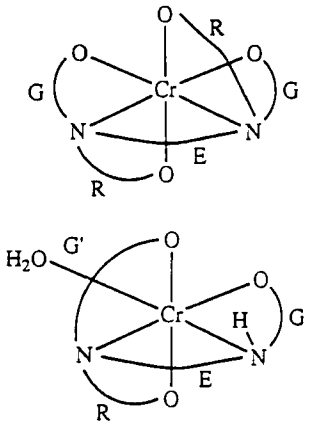

FIG. 13. Chelate ring nomenclature in edta complexes.

tate edta structures of V(III), Mn(II), and Fe(III) (*99*) and is also observed for certain other Cr(III) complexes (*100*).

These questions have been probed using a variety of solution techniques including visible absorption spectra (*101*), chiroptical and MCD spectra (*102*), ^2H NMR spectra (*103*), rapid kinetic measurements (*92*), pH titrations (*98*), molar volumes (*97*), and electrochemical methods (*98, 104*).

The consensus at the moment is that the edta ligand remains hexadentate when bound to Cr(III) in the pH range 3.5–6.5, and a seventh donor site occupied by water is not involved. Increased solution stability of the hexadentate can be achieved by increasing the size of the E ring, for example, in $[Cr(1,3\text{-pdta})]^-$ (propanediaminetetraacetate) and $[Cr(1,4\text{-bdta})]^-$ (butanediaminetetraacetate), and there is no suggestion of 7-coordination in these complexes.

The strain inherent in the five-membered carboxylate rings in hexacoordinated $[Cr(edta)]^-$ has led to an investigation of systems with longer and bifurcated carboxylate arms (*89*), in the hope that the resulting six-membered chelates would be more stable. Increasing the length of the carboxylate arms seems to allow the complex to attain octahedral angles closer to the ideal, but other sources of strain are introduced (*89*). The solution stability of the complex is enhanced, however, and hexadentate [Cr(edtp)] (H_4edtp = ethylenediaminetetrapropionic acid) can be resolved into its enantiomeric forms (*105*).

The strain estimates in these systems have been made on the basis of bond-length and bond-angle distortions (*89*), and it would be interest-

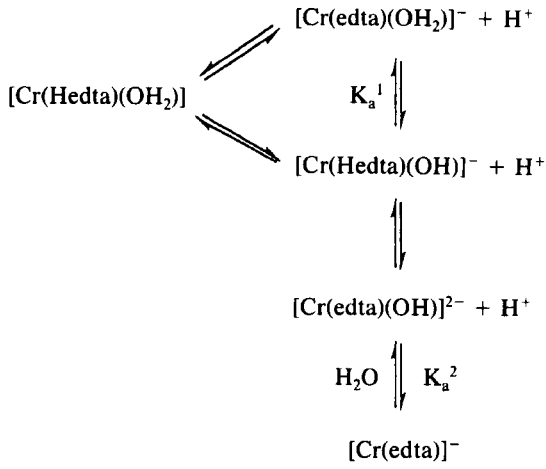

FIG. 14. $[Cr(edta)]^-$ equilibria.

ing to apply full molecular mechanics calculations, to make better allowance for nonbonded interactions.

Nevertheless, these investigations of longer-arm edta analogues have produced some fascinating and entirely unpredicted chemistry. Three isomers of $[Cr(edtp)]^-$, differing only in R-ring conformation, have been isolated in a ratio of 1 : 1 : 40, and the most abundant of these, $[lel_2\Lambda(\delta\delta)]$, dechelates on an H^+-cation exchange resin to give two quinquidentate isomers, stable in basic solution, with configurations shown in Fig. 15.

In aqueous or acid solution, these isomers revert back to the hexaden-

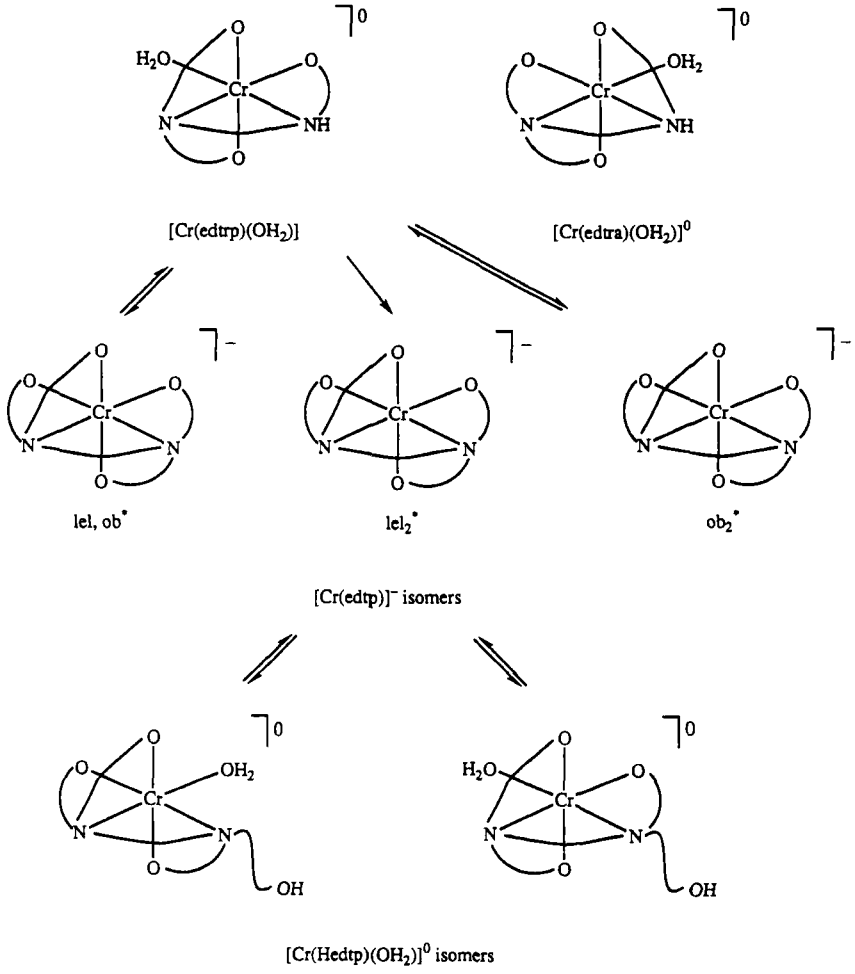

FIG. 15. Reactions of $[Cr(edtp)]^-$ and $[Cr(edtrp)(OH_2)]^0$. * R-ring conformations.

tate form with different rates (*91*). The less abundant $[Cr(edtp)]^-$ isomers, [ob, lel$\Lambda(\delta\lambda)$] and [ob$_2\Lambda(\lambda\lambda)$], both react with C—N bond cleavage to form a "three-carboxylate-armed" chelate $[Cr(edtrp)(OH_2)] \cdot 3H_2O$ (Fig. 15) (H_3edtrp = ethylenediaminetripropionic acid) (*91, 106*). What is quite unprecedented is that this reaction is reversible: treatment of $[Cr(edtrp)(OH_2)]$ with 3-hydroxypropionic acid in aqueous solution results in the formation of the three $[Cr(edtp)]^-$ isomers (*107*), and the new ring is incorporated in the R position. The work described in this section has been supported by the use of E-ring analogues containing chiral centers, which allows CD spectra as an additional probe, and the use of ^2H-labeled ligands, allowing NMR techniques to be used with a paramagnetic metal center.

Attempts to extend the C—N bond formation reaction using $[Cr(edtra)(OH_2)]$ (H_3edtra = ethylenediaminetriacetic acid) were unsuccessful. The structures of the two ethylenediamine triacid complexes are different (*107*) (Fig. 15), and only $[Cr(edtrp)(OH_2)]$ has a "flat" sec-NH proton at the site of dehydration (see Section VI).

VI. Conjugate-Base Mechanism in Reactions of Chromium(III) Amine Complexes

Ammine and amine complexes of Co(III) with suitable anionic leaving groups undergo substitution in protic solvents at rates that are proportional to the concentration of the conjugate base of the solvent (i.e., OH^- in water), and the topic (base hydrolysis) has been extensively reviewed (*5*).

The conjugate-base mechanism, (*55*)–(*57*), originally proposed in 1937 (*108*), is now widely accepted, although there is still some "fine structure" to elucidate.

$$[CoCl(NH_3)_5]^{2+} + OH^- \underset{k_{-1}}{\overset{k_1}{\rightleftharpoons}} [CoCl(NH_3)_4(NH_2)]^+ + H_2O \qquad (55)$$

$$[CoCl(NH_3)_4(NH_2)]^+ \xrightarrow{k_2} [Co(NH_3)_4(NH_2)]^{2+} + Cl^- \qquad (56)$$

$$[Co(NH_3)_4(NH_2)]^{2+} + H_2O \xrightarrow{\text{fast}} [Co(OH)(NH_3)_5]^{2+} \qquad (57)$$

This mechanism implies that OH^- acts as a base rather than a nucleophile, and removes a proton from a coordinated am(m)ine ligand, generating the rate-determining amido conjugate base. Also implicit is a

dissociative process (56) to produce an intermediate of reduced coordination number, which is attacked by the solvent to form the product (57).

The areas of "fine structure" not immediately apparent in this mechanistic scheme are these:

1. Which proton is involved in forming the most reactive conjugate base (e.g., cis or trans to the leaving group)?
2. Are internal proton transfers within the conjugate base possible?
3. What is the "lifetime" of the conjugate base (*109, 110*)?
4. How valid is the mechanism when there are no acidic protons present in the amine ligand?
5. How does the structure of the nonreplaced amine ligands influence the rate of base hydrolysis?

The base hydrolysis of the Cr(III) analogues is generally much slower. Co(III)/Cr(III) rate ratio effects have been discussed by Tobe (*5*), but

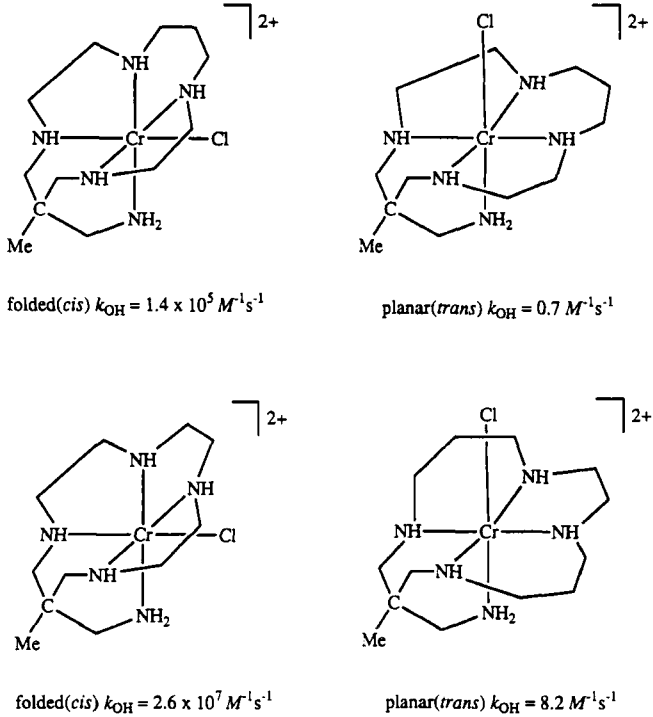

FIG. 16. Structural effects on rate constants (25°C) for base hydrolysis of some $[CrCl(N_5)]^{2+}$ complexes (*111*).

there are now examples where chloropentaaminechromium(III) complexes base hydrolyze up to 10^6 times *faster* than their Co(III) analogues (*111*) (Fig. 16). It is tempting to attribute this rapid rate of base hydrolysis to the presence of a folded macrocyclic ligand, but *cis*-$[CrCl_2(cyclam)]^+$ behaves quite normally.

Other structural features that have acceleratory influences in the base hydrolysis of Co(III) systems are (i) the incorporation of a pyridine ligand in the coordination sphere and (ii) the incorporation of a "flat" secondary nitrogen donor system in the polyamine ligand skeleton (*5*) (structures C and D in Fig. 17).

Do such features influence the rate of base hydrolysis for Cr(III) complexes? Suitable examples have only recently become available (*112*), and the data in Table IV suggest neither of the preceding ligand effects is important. Thus, removal of the "flat" sec-NH proton by methylation only slightly decreases the base hydrolysis rate, [(en)(dpt) vs (en)(Medpt)] and incorporation of a pyridine ligand cis to the leaving group has hardly any influence [(ampy)(2,3-tri) vs (en)(2,3-tri)]. The conclusion reached is that Cr(III) complexes are much less responsive to changes in the nature of the nonreplaced ligands than are Co(III) systems.

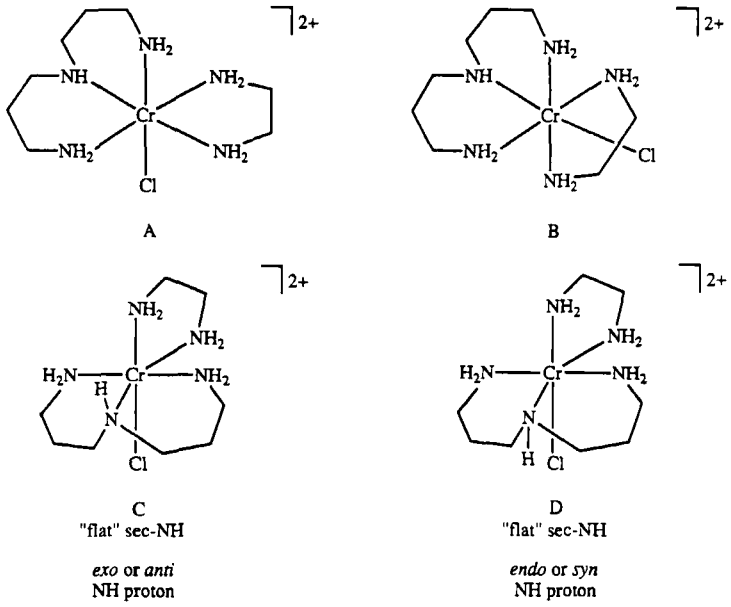

FIG. 17. Possible isomers for $[CrCl(dpt)(en)]^{2+}$.

Activation volumes ($\Delta V^{\#}_{OH}$) for the base hydrolysis processes lie in the range +17 to +35 $cm^3\ mol^{-1}$, increasing with increasing bulk of the nonreplaced ligands (*115*). There is rather more variation in $\Delta V^{\#}_{OH}$ for $[CrCl(N_5)]^{2+}$ than there is for Co(III) [$\Delta V^{\#}_{OH}$(mean) = +30 $cm^3\ mol^{-1}$ for 16 complexes].

The observation that base hydrolysis rates for $[CrCl(N)_5]^{2+}$ are generally much slower than those for Co(III) could be due to the Cr(III) complexes having less acidic protons and thus producing a lower concentration of the conjugate base. Proton exchange rates are a general measure of NH-proton acidity, but no generalizations can yet be made for differences between Cr(III) and Co(III) (*5, 116*). $[M(en)_3]^{3+}$ and $[M(NH_3)_6]^{3+}$ (M = Co, Cr) exchange at comparable rates, but for other ligand systems (cyclam or 3,2,3-tet), the expected decrease for Cr(III) is observed (*116*). It should be remembered, however, that the most acidic NH-proton site may not yield the most reactive conjugate base, and it will require many more investigations and carefully chosen examples to unravel the relative contributions.

Systems that, on first glance, should lead to unambiguous information are those with no acidic protons. There is a surprising lack of modern data on Co(III) complexes, although suitable ligands, shown

TABLE IV

KINETIC PARAMETERS FOR THE BASE HYDROLYSIS OF SELECTED $[CrCl(N)_5]^{2+}$ COMPLEXES AT 25°C, I = 0.1 M

N_5[a]	$10^2\ k_{OH}$ ($M^{-1}\ s^{-1}$)	$\Delta H^{\#}$ (kJ mol^{-1})	$\Delta S^{\#}$ ($JK^{-1}\ mol^{-1}$)	$\Delta V^{\#}$ ($cm^3\ mol^{-1}$)	Ref.
(en)(dpt)	10.5	97	+48	+25.3	*113*
(en)(Medpt)	1.19	105	+44	+30.3	*115*
(en)(2,3-tri)[b]	73.5	108	+113		*113*
(ampy)(2,3-tri)[c]	71.4	108	+110		*119*
(ampy)(dpt)[d]	518	113	+140		*119*
(tn)(dpt)	60.6	108	+105	+25.5	*113*
(Me_2tn)(dpt)	58.6	84.7	+26		*113*

[a] These complexes have the *mer–exo* configuration (*112, 114, 119*) unless otherwise noted (Fig. 17).

[b] The *mer–endo* isomer has also been isolated (*114*).

[c] This isomer has the py end of the 2-aminomethyl pyridine ligand cis to the chloro ligand (*119*).

[d] This isomer has the py end of the 2-aminomethyl pyridine ligand trans to the chloro ligand (*119*).

in Fig. 18, have been designed (*117*). Using tmpa, and a series of μ-oxo-μ-carboxalatodinuclear Cr(III) complexes (Fig. 18), Holwerda and his co-workers (*118*) have found that the rate of base hydrolysis increases with increasing $[OH^-]$. The dependency is not great, as $10^3 k_{obs}$ (60°C, R = CH_3) = 1.05 and 5.80 sec^{-1} in $[H^+] = 10^{-3}$ and $[OH^-]$ = 0.1 M, respectively, and saturation kinetics are observed with all R except R = H.

One important feature of the ligands shown in Fig. 18 is that they both contain the py—CH_2—R functional group. Jackson *et al.* (*117*) have shown that for several Co(III) systems, these $-CH_2-$ protons can exchange in alkaline D_2O at rates comparable to those of base hydrolysis. Consequently, there are three possible mechanisms for the OH^- dependence in these complexes without NH protons: (i) reversible Cr—N bond rupture (*118*); (ii) conjugate base formation at the methylene protons and subsequent electron delocalization through the chelated pyridine ring (*117*); and (iii) direct bimolecular attack.

In the final analysis, it may be that both conjugate base and bimolecular mechanisms are operative in the base hydrolysis of Cr(III) amine complexes (*115*).

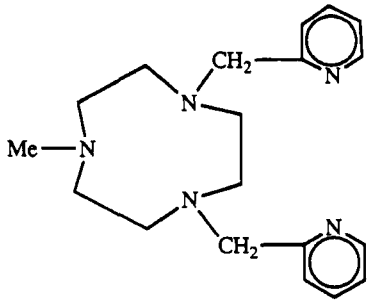

Me(ampy)$_2$tacn

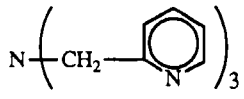

tmpa

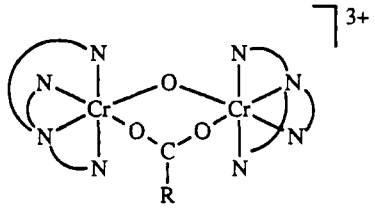

[(tmpa)Cr(μ–O)(μ–O_2CR)Cr(tmpa)]$^{3+}$

FIG. 18. Multidentate ligands with no NH protons, and the tmpa binuclear Cr(III) complex.

REFERENCES

1. See, e.g., Wilkinson, G., Ed. "Comprehensive Coordination Chemistry"; Pergamon Press: Oxford, 1987.
2. Wilkins, R. G. "Kinetics and Mechanism of Reactions of Transition Metal Complexes"; VCH: Weinheim, **1991**, 2nd Ed., p. 75.
3. Springborg, J. *Adv. Inorg. Chem.* **1988,** *32,* 55.
4. House, D. A. In "Mechanisms of Inorganic and Organometallic Reactions"; Twigg, M. V., Ed.; Plenum Press: New York; Vol. 8, Ch. 6, **1994,** 97; see also earlier volumes in this series.
5. Tobe, M. L. In "Comprehensive Coordination Chemistry"; Wilkinson, G., Ed.; Pergamon Press: Oxford, 1987; Vol. 1, p. 281; *Adv. Inorg. Bioinorg. Mech.* **1983,** *2,* 1.
6. Dickman, M. H.; Pope, M. T. *Chem. Rev.* **1994,** *94,* 569.
7. Bakač, A.; Espenson, J. H. *Acc. Chem. Resh.* **1993,** *26,* 519.
8. Bakač, A. *Prog. Inorg. Chem.* **1995,** *43,* 267.
9. Perez-Benito, J. F.; Arias, C.; Lamrhari, D. *New J. Chem.* **1994,** *18,* 663.
10. Adams, A. C.; Crook, J. R.; Bockhoff, F.; King, E. L. *J. Am. Chem. Soc.* **1968,** *90,* 5761.
11. Merakis, T.; Murphy, A.; Spiccia, L.; Beguin, A.; Marty, W. *Helv. Chim. Acta* **1989,** *72,* 993.
12. Kang, C.; Anson, F. C. *Inorg. Chem.* **1994,** *33,* 2624.
13. Scott, S. L.; Bakač, A.; Espenson, J. H. *Inorg. Chem.* **1991,** *30,* 4112.
14. Wang, W-D; Bakač, A.; Espenson, J. H. *Inorg. Chem.* **1993,** *32,* 5034.
15. Fenton, H. J. H. *J. Chem. Soc.* **1894,** 899.
16. Bakač, A.: Espenson, J. H. *Inorg. Chem.* **1983,** *22,* 779.
17. Wang, W-D; Bakač, A.; Espenson, J. H. *Inorg. Chem.* **1993,** *32,* 2005.
18. Gaede, W.; van Eldik, R. *Inorg. Chem.* **1994,** *33,* 2204.
19. Bakač, A.; Espenson, J. H.; Janni, J. A. *J. Chem. Soc. Chem. Commun.* **1994,** 315.
20. Scott, S.; Bakač, A.; Espenson, J. H. *J. Am. Chem. Soc.* **1992,** *114,* 4205.
21. Gould, E. S. *Coord. Chem. Rev.* **1994,** *135/6,* 651.
22. Krumpole, M.; DeBoer, B. B.; Rocek, J. *J. Am. Chem. Soc.* **1978,** *100,* 145: Krumpole, M.; Rocek, J. *J. Am. Chem. Soc.* **1979,** *101,* 3206.
23. Judd, R. J.; Hambley, T. W.; Lay, P. A. *J. Chem. Soc., Dalton Trans.* **1989,** 2205.
24. Farrell, R. P.; Lay, P. A. *Comments Inorg. Chem.* **1992,** *13,* 133.
25. Shi, S. *J. Organomet. Chem.* **1994,** *468,* 139.
26. Ardon, M.; Bleicher, B. *J. Am. Chem. Soc.* **1966,** *88,* 858.
27. Sykes, A. G.; Weil, J. A. *Prog. Inorg. Chem.* **1970,** *13,* 1.
28. Shi, X.; Dalal, N. S. *Environ. Health Perspect. Suppl.* **1994,** *102(Suppl 3),* 231.
29. Quane, D.; Earley, J. E. *J. Am. Chem. Soc.* **1965,** *87,* 3823.
30. Brown, S. B.; Edwards, J. O.; Herman, I. J.; Jones, P.; Mills, J. R.; Earley, J. E. *Inorg. Chem. Acta* **1969,** *3,* 351.
31. Peters, J. W.; Bekowies, P. J.; Winter, A. M.; Pitts, J. N. *J. Am. Chem. Soc.* **1975,** *97,* 3299.
32. Cieslak-Golonka, M.; Raczko, M.; Staszak, Z. *Polyhedron* **1992,** *19,* 2549.
33. Dixon, D. A.; Sadler, N. P.; Dasgupta, T. P. *J. Chem. Soc., Dalton Trans.* **1993,** 3489.
34. Perez-Benito, J. F.; Arias, C. *Int. J. Chim. Kin.* **1993,** *25,* 221.
35. Agrawal, A.; Rao, I.; Sharma, P. D. *Transition Met. Chem.* **1993,** *18,* 191.
36. Stearns, D. M.; Kennedy, L. J.; Coutney, K. D.; Giangrande, P. H.; Phieffer, L. S.; Wetterhahn, K. E. *Biochem.* **1995,** *34,* 910.
37. Moghaddas, S.; Gelerinter, E.; Bose, R. N. *J. Inorg. Biochem.* **1995,** *57,* 135.

38. Shi, X.; Dong, Z.; Dalal, N. S.; Gannett, P. M. *Biochim. Biophys. Acta* **1994,** *65,* 1226.
39. Perez-Benito, J. F.; Lamrhari, D.; Arias, C. *J. Phys. Chem.* **1994,** *98,* 12621.
40. Kortenkamp, A.; O'Brien, P. *Environ. Health Perspect. Suppl.* **1994,** *102(Suppl. 3),* 237.
41. Sala, L. F.; Palopoli, C.; Alba, V.; Signorella, S. R. *Polyhedron* **1993,** *12,* 2227.
42. Perez-Benito, E.; Rodenas, E. *Transition Met. Chem.* **1993,** *18,* 329.
43. Rao, C. P.; Kaiwar, S. P. *Carbohydrate Resh.* **1993,** *244,* 15.
44. Signorella, S. R.; Santoro, M. I.; Mulero, M. N.; Sala, L. F. *Can. J. Chem.* **1994,** *72,* 398.
45. Sen Gupta, K. K.; Tribedi, P. S.; Sen Gupta, S.; Sen, P. K. *Indian J. Chem.* **1993,** *32B,* 546.
46. Sen Gupta, K. K.; Mahapatra, A.; Sanyal, A. *Indian J. Chem.* **1994,** *33A,* 332.
47. Snow, E. T. *Environ. Health Persp. Suppl.* **1994,** *102(Suppl. 3),* 41.
48. Pressprich, M. R.; Willett, R. D.; Poshusta, R. D.; Saunders, S. C.; David H. B.; Gard, G. L. *Inorg. Chem.* **1988,** *27,* 1564.
49. Cieslak-Golonka, M. *Coord. Chem. Rev.* **1991,** *109,* 223.
50. Brasch, N. E.; Buckingham, D. A.; Clark, C. R. *Inorg. Chem.* **1994,** *33,* 2683; *Abstracts of Inorg. React. Mech. Meeting 93,* Frankfurt, **1993,** *12.*
51. Palmer, D. A.; Begun, G. M.; Ward, F. H. *Rev. Sci. Instrum.* **1993,** *64,* 1994.
52. Tong, S-Y; Li, K-A. *Talanta* **1986,** *33,* 775.
53. Michel, G.; Cahay, R. *J. Raman Spectr.* **1986,** *17,* 79.
54. Baran, J. *J. Mol. Struct.* **1988,** *172,* 1.
55. Mukherjee, A. K.; Mukhopadhaya, A.; Mukerjee, M.; Ray, S. *Acta Cryst.* **1994,** *50C,* 1401.
56. Hegedus, L. S. *Acc. Chem. Resh.* **1995,** *28,* 299.
57. Espenson, J. H. *Acc. Chem. Resh.* **1992,** *25,* 222.
58. Muzart, J. *Chem. Rev.* **1992,** *92,* 113.
59. Zhang, Z.; Jordan, R. B. *Inorg. Chem.* **1994,** *33,* 680.
60. Gaede, W.; van Eldik, R. *Inorg. Chim. Acta* **1994,** *215,* 173.
61. Sisley, M. J.; Jordan, R. B. *Inorg. Chem.* **1988,** *27,* 1963.
62. Goher, M. A. S.; Abu-Youssef, M. A. M.; Mautner, F. A. *Z. Naturforsch.* **1992,** *47B,* 139.
63. Grouse, K.; Goh, L. Y. *Inorg. Chem.* **1986,** *25,* 478.
64. Shoji, M.; Shimura, M.; Ogino, H. *Chem. Lett.* **1986,** 995.
65. Anderson, P. *Coord. Chem. Rev.* **1988,** *94,* 47.
66. Stunzi, F.; Spiccia, L.; Rotzinger, F. P.; Marty, W. *Inorg. Chem.* **1989,** *28,* 66.
67. Drljara, A.; Anderson, J. R.; Spiccia, L.; Turney, T. W. *Inorg. Chem.* **1992,** *31,* 4894.
68. Crimp, S. J.; Spiccia, L.; Krouse, H. R.; Swaddle, T. W. *Inorg. Chem.* **1994,** *33,* 465.
69. Pettit, L. D.; Powell, H. K. J. "SC-Database, Stability Constants Database"; IUPAC/ Academic software, **1993.**
70. Stunzi, H.; Marty, W. *Inorg. Chem.* **1983,** *22,* 2145.
71. Bradley, S. M.; Lehr, C. R.; Kydd, R. A. *J. Chem. Soc., Dalton Trans.* **1993,** 2415.
72. Spiccia, L.; Marty, W.; Giovanoli, R. *Inorg. Chem.* **1988,** *27,* 2660.
73. Jacobs, H.; Block, J. Z. *Anorg. Allg. Chem.* **1987,** *546,* 33.
74. Zhao, Z.; Rush, J. D.; Holeman, J.; Bielski, B. H. J. *Radiat. Phys. Chem.* **1995,** *45,* 257.
75. Rotzinger, F. P.; Stunzi, H.; Marty, W. *Inorg. Chem.* **1986,** *25,* 489.
76. Spiccia, L.; Marty, W. *Polyhedron* **1991,** *10,* 619.
77. Merakis, T.; Spiccia, L. *Aust. J. Chem.* **1989,** *42,* 1579.
78. Spiccia, L.; Stoeckli-Evans, H.; Marty, W.; Giovanoli, R. *Inorg. Chem.* **1987,** *26,* 474.

79. Grace, M. R.; Spiccia, L. *Polyhedron* **1991,** *10,* 2389.
80. Stunzi, H.; Rotzinger, F. P.; Marty, W. *Inorg. Chem.* **1984,** *23,* 2160.
81. McKenna, A.; Pennington, W. T.; Fanning, J. C. *Inorg. Chim. Acta* **1991,** *183,* 127.
82. Bossek, U.; Haselherst, G.; Ross, S.; Weighardt, K.; Nuber, B. *J. Chem. Soc., Dalton Trans.* **1994,** 2041.
83. Goodson, D. A.; Glerup, J.; Hodgson, D. J.; Michelsen, K.; Rychlewska, U. *Inorg. Chem.* **1994,** *33,* 359.
84. Andersen, P.; Larsen, S.; Pretzmann, U. *Acta Chem. Scand.* **1993,** *47,* 1147.
85. Ardon, M.; Bino, A.; Michelsen, K. *J. Am. Chem. Soc.* **1987,** *109,* 1986.
86. Spicca, L. *Polyhedron* **1991,** *20,* 1865.
87. Spiccia, L.; Marty, W. *Inorg. Chem.* **1986,** *25,* 255.
88. Spiccia, L. *Inorg. Chem.* **1988,** *27,* 432.
89. Douglas, B. E.; Radanovic, D. J. *Coord. Chem. Rev.* **1993,** *128,* 139.
90. Schwartzenbach, G.; Biedermann, W. *Helv. Chim. Acta* **1948,** *31,* 459.
91. Sakagami, N.; Kaizaki, S. *J. Chem. Soc., Dalton Trans.* **1992,** *187,* 285, 291.
92. Thorneley, R. N. F.; Sykes, A. G.; Gans, P. *J. Chem. Soc. A.* **1971,** 1494.
93. Mizuta, T.; Yamamoto, T.; Shibata, N.; Miyoshi, K. *Inorg. Chim. Acta* **1990,** *169,* 257.
94. Hamm, R. E. *J. Am. Chem. Soc.* **1953,** *75,* 5670; Ogino, H.; Tanaka, N., *Bull. Chem. Soc. Japan* **1968,** *41,* 1622.
95. Gerdom, L. E.; Baenzinger, N. A.; Goff, H. M. *Inorg. Chem.* **1981,** *20,* 1606.
96. Mitra Mustofy, H. G.; De, K.; De, G. S. *Indian J. Sci. Ind. Resh.* **1989,** *48,* 444.
97. Yoshitani, K. *Bull. Chem. Soc. Japan* **1994,** *67,* 2115.
98. Boddin, M.; Meier, R. *Abstracts Inorg. React. Mech. Meeting 93,* P9, OP6, **1993.**
99. Ogino, H.; Nagat, T.; Ogino, K. *Inorg. Chem.* **1989,** *28,* 3656.
100. Bino, A.; Firm, R.; Van Genderen, M. *Inorg. Chim. Acta* **1987,** *127,* 95.
101. Miura, N.; Shimura, M.; Ogino, H. *Bull. Chem. Soc. Japan* **1987,** *60,* 1349.
102. Kaizaki, S.; Mizu-uchi, H. *Inorg. Chem.* **1986,** *25,* 2732.
103. Wheeler, W. D.; Legg, J. I. *Inorg. Chem.* **1984,** *23,* 3798.
104. Hecht, M.; Fawcett, W. R. *J. Phys. Chem.* **1995,** *99,* 1311.
105. Radanovic, D. J.; Djuran, M. I.; Djorovic, M. M.; Douglas, B. E. *Inorg. Chim. Acta* **1988,** *146,* 199; **1991,** *182,* 177.
106. Kaizaki, S.; Hayashi, M. *J. Chem. Soc. Chem. Commun.* **1988,** 613.
107. Sakagami, N.; Kaizaki, S. *J. Chem. Soc. Chem. Commun.* **1993,** 178.
108. Garrick, F. J. *Nature* **1937,** *139,* 507.
109. Rotzinger, F. P.; Weber, J.; Daul, C. *Helv. Chim. Acta* **1991,** *74,* 1247.
110. Rotzinger, F. P. *Inorg. Chem.* **1991,** *30,* 2763.
111. Lawrance, G. A.; Martinez, M.; Skelton, B. W.; White, A. H. *J. Chem. Soc., Dalton Trans.* **1992,** 823.
112. House, D. A.; Robinson, W. T. *Inorg. Chim. Acta* **1988,** *141,* 211.
113. House, D. A. *Inorg. Chem.* **1988,** *27,* 2587.
114. Derwahl, A.; Robinson, W. T.; House, D. A. *Inorg. Chim. Acta* **1996,** *247,* 19.
115. House, D. A.; Bal Reddy, K.; van Eldik, R. *Inorg. Chim. Acta* **1991,** *186,* 5.
116. House, D. A. *Coord. Chem. Rev.* **1992,** *114,* 249.
117. Jackson, W. G.; McKeon, J. A.; Dickie, A. J.; Bhula, R. Abstracts, International Macrocyclic Meeting, Victoria University of Wellington, New Zealand, Jan. 1996, p 20.
118. Tekut, T. F.; Holwerda, R. A. *Inorg. Chem.* **1994,** *33,* 5254.
119. House, D. A.; Schaffner, S.; van Eldik, R.; McAuley, A.; Zhender, M. *Inorg. Chim. Acta* **1994,** *227,* 11.

This Page Intentionally Left Blank

INDEX

A

Q

R

S

This Page Intentionally Left Blank

CONTENTS OF PREVIOUS VOLUMES

ISBN 0-12-023644-3